

24th INTERNATIONAL MULTIDISCIPLINARY SCIENTIFIC GEOCONFERENCE - SGEM 2024

01 – 07 July 2024 - Albena, Bulgaria

CONFERENCE PROCEEDINGS OF SELECTED PAPERS in

WATER RESOURCES. FOREST, MARINE AND OCEAN ECOSYSTEMS

ISSUE 3.1

DISCLAIMER

The **International Multidisciplinary Scientific GeoConference SGEM (Survey, Geology, Ecology, and Management)** serves as a global platform for pioneering research and scientific dialogue across the diverse fields of geosciences. It is dedicated to advancing interdisciplinary solutions for the most pressing environmental challenges of our time — **Global Warming, Climate Change, CO_2 Reduction, Biodiversity Conservation, and the Development of Green Technologies**. By fostering a collaborative exchange of knowledge and **aligning its objectives** with the **United Nations Sustainable Development Goals (SDGs), SGEM aims to inspire scientific excellence and drive sustainable practices toward a greener, more resilient future for our planet.**

Authors are responsible for the content and accuracy of the written papers. Opinions expressed are not meant to represent or reflect the position of the SGEM International Scientific Committee members.

No part of this book may be reproduced or transmitted in any form or by any means, electronic or mechanical, for any purpose, without the express written permission of the SGEM International Scientific Committee on Earth and Planetary Sciences.

Copyright © SGEM WORLD SCIENCE (SWS) Scholarly Society 2024
Haidingergasse 1, C / 1113, Vienna 1030, Austria
Published by STEF92 Technology
Total print: 5000

E-mail: **sgem@sgem.org** | URL: **www.sgem.org**

ISBN 978-619-7603-70-5
ISSN 1314-2704
DOI: 10.5593/sgem2024/3.1

FOREWORD

Dear Readers,
It is our great pleasure to introduce the third issue of the **24th volume of the SGEM GeoConference 2024 Conference Proceedings**, which focuses on **Hydrology and Water Resources, Soils, Forest Ecosystems, and Marine and Ocean Ecosystems**. This issue brings together a diverse collection of research that addresses some of the most critical challenges facing our planet, with an emphasis on sustainable resource management, ecosystem preservation, and environmental resilience.

Addressing Global Challenges Through Multidisciplinary Research
This collection of papers highlights the vital role that water and soil sciences, alongside forest and marine ecosystem studies, play in advancing our understanding of climate change adaptation, food security, and biodiversity conservation. The research presented here aligns with key UN Sustainable Development Goals (SDGs), including **clean water and sanitation (SDG 6), life on land (SDG 15), and life below water (SDG 14).** These studies offer **valuable insights into sustainable practices and innovative solutions for mitigating the environmental impacts of human activities**.

Issue Highlights

- **Hydrology and Water Resources**: This section delves into the management of water systems, with topics ranging from hydrological drought analysis and **flood risk reduction** to innovative approaches for **monitoring water quality** and managing **ecological flows**.
- **Soils**: Research in this section explores the dynamics of **soil ecosystems**, addressing soil degradation, fertility management, and the potential of ecological agriculture in **promoting sustainability and food security**.
- **Forest Ecosystems**: Studies in this section examine the health and productivity of forests, exploring issues like **carbon sequestration**, **biodiversity assessment**, and the impact of **human activities on forest ecosystems.**
- **Marine and Ocean Ecosystems**: The final section investigates the dynamics of marine environments, focusing on **eutrophication, pollutant management**, and the critical role of **marine ecosystems in global climate regulation**.

Rigorous Peer Review and Multidisciplinary Insights
Each paper included in this conference proceedings has undergone a **stringent peer review process, ensuring the highest standards of scientific rigor, originality, and relevance**. The multidisciplinary nature of the research demonstrates the interconnectedness of hydrology, soil science, forest management, and marine ecosystems, emphasizing the need for integrated approaches to solving complex environmental challenges.

A Call for Sustainable Action
This collection of papers serves as a reminder of the urgent need for **sustainable practices to protect and preserve our planet's vital resources**. The findings and insights presented here not only contribute to the academic discourse but also offer

practical solutions for policymakers and practitioners working toward a more sustainable and resilient future.

We would like to extend our heartfelt thanks to all the authors, reviewers, and conference organizers for their invaluable contributions to this volume. It is our hope that these proceedings will inspire further research and collaboration in these crucial fields.

Sincerely,

Prof. Dr. hab. oec. Baiba Rivza
Editor-in-Chief of XXIV SGEM GeoConference Proceedings
Member of the Presidium of the Latvian Academy of Sciences, LATVIA
President of the Latvian Academy of Agricultural and Forestry Sciences
Vice-chair of the Latvian Council of Higher education
President of Latvian universities professors' association
Expert from the European Academy of Sciences Academic Advisory Board (EASAC)

Prof. DSc. Oleksandr Trofymchuk
Editor-in-Chief of XXIV SGEM GeoConference Proceedings
National Academy of Sciences of Ukraine, UKRAINE

CONFERENCE PROCEEDINGS CONTENTS

HYDROLOGY AND WATER RESOURCES

1. COMPARISON OF FIELD AND LABORATORY METHODS FOR THE ASSESSMENT OF SOIL HYDRAULIC CONDUCTIVITY, PhD Stanislav Paseka.....3

2. ABOUT THE APPLICABILITY OF ECOLOGICAL FLOW METHODOLOGY FOR PILOT DRAINAGE AREAS IN DANUBE RIVER BASIN DIRECTORATE IN BULGARIA, Assoc. Prof. Dr. Elena Bojilova, PhD Borislav Vuchkov, PhD Maya Rankova, PhD Plamen Angelov, PhD Radoslava Ivanova.....11

3. ANALYSIS OF WATER RESOURCES IN THE VASLUI HYDROGRAPHIC BASIN, ROMANIA, PhD. eng. Lavinia Tataru, Professor PhD. eng. Florian Stătescu, Lecturer PhD. eng. Nicolae Marcoie.....19

4. ARMA MODELS APPLICATION FOR FORECASTING OF THE RIVER DISCHARGE AND THE HYDROLOGICAL DROUGHT INDEX SRI IN DAMS MANAGEMENT, Assoc. Prof. Dr. Anna Yordanova, Prof. Dr. Irena Ilcheva, Prof. Dr. Elena Bojilova, Prof. Dr. Olga Nitcheva, Dr. Yordan Dimitrov.....27

5. BLACK SEA THERMOHALIN STRATIFICATION: PARTICULARITY AND RECENT CHANGES, PhD Nadezhda Valcheva.....35

6. CATCHMENT ABSTRACTION MANAGEMENT STRATEGY AND ECOLOGICAL FLOW DETERMINATION IN CASE OF NATURA 2000 AREAS, Assoc. Prof. Dr. Irena Ilcheva, Assoc. Prof. Dr. Vesela Zaharieva, Assoc. Prof. Dr. Anna Yordanova, Assoc. Prof. Dr. Snejanka Balabanova……..49

7. CLIMATE ANALYSIS ALONG THE NAVIGATION ROUTES ON THE DANUBE, Prof. Dr. Eng. Ana-Maria Chirosca, Prof. Dr. Liliana Rusu, Eng. Victor Ionut Popa, Prof. Dr. Eugen Rusu……...59

8. COMPARISON OF TWO METHODS FOR ASSESSMENT OF PH-DEPENDING VALUES IN SURFACE WATER, Ing. Viera Kováčová.....67

9. COMPARISON OF THE RESULTS OBTAINED BY THE PROPOSED METHODOLOGY FOR ENVIRONMENTAL RUNOFF WITH THOSE CALCULATED UNDER THE CURRENT REGULATION, PhD Maya Rankova, Assoc. Prof. Elena Bojilova, PhD Plamen Angelov, PhD Borislav Vuchkov, PhD Radoslava Ivanova.....75

10. DROUGHT INDICES AND VIS-BASED CANOPY STATUS OF VINEYARDS, Prof. Dr. Mariam Tsitsagi, Ana Palavandishvili, Zaza Gulashvili.....83

11. FISHER-X: AN ENGINEERING CONCEPT TO MONITOR WATER ENVIRONMENTS USING ROBOTIC BIOMIMICRY, Yury Vasquez-Charcape, Gustavo Jamanca-Lino, David Sanchez-Perez, Bruno Cevallos.....91

12. HYDROECOLOGICAL STATE OF THE SMALL UPLAND ARMENIAN LAKES, Assoc. Prof. Dr. Irina Fedorova, Larisa Ghazaryan, Vsevolod Rudakov, Elizaveta Chezhina, Assoc. Prof. Dr. Grigory Fedorov.....103

13. HYDROLOGICAL DROUGHT FREQUENCY ANALYSIS IN THE YANTRA RIVER DOWNSTREAM, Dr. Yordan Dimitrov.....111

14. HYDROMETEOROLOGICAL DROUGHT IMPACT ON CEREAL PRODUCTION IN NORTHERN BULGARIA, Prof. Dr. Nina Nikolova, PhD Simeon Matev, Prof. Dr. Nelly Hristova, Assoc. Prof. Dr. Kalina Radeva.....121

15. INTEGRATED MODELING OF STAGNATING WATER AND URBAN DRAINAGE SYSTEMS, Assistant Prof. Dr. Marcell Knolmar.....129

16. INTEGRATION OF EROSION CONTROL MEASURES AND TECHNICAL MEASURES TO PROVIDE EFFECTIVE FLOOD RISK REDUCTION FOR SMALL WATERSHEDS, PhD Stanislav Paseka.....137

17. MODELLING OF HYDROMORPHOLOGICAL CHANGES DUE TO THE EFFECT OF FISHING PORT "KARANTINATA", Petya Eftimova, Assoc. Prof. Dr. Nikolay Valchev, PhD Bogdan Prodanov, PhD Nataliya Andreeva, Todor Lambev, Prof. Dr. Lyubomir Dimitrov.....145

18. MODERN METHODS OF DETERMINING OF THE MOMENTS WATER QUALITY. COMPARING THE RESULTS WITH TRADITIONAL METHOD, PhD Plamen Angelov, PhD Maya Rankova, PhD Ress. Borislav Vuchkov.....157

19. PRIMARY STUDIES FOR THE PRESENCE OF OFFSHORE FRESHENED GROUNDWATER IN THE BULGARIAN BLACK SEA SHELF, Assoc. Prof. Dr. Olga Nitcheva.....165

20. RELIABILITY OF PUMPING STATIONS, PhD Eng. Tanya Igneva-Danova.....175

21. RETENTION-BASED SOLUTIONS FOR OUTFALL REDUCTION, Assoc. Prof. Dr. Marcell Knolmar, Sandor Szel.....181

22. THE IMPACT OF WASTEWATER EMISSIONS ON THE HEALTH OF THE POPULATION OF BUKHARA (UZBEKISTAN), Prof. DSc. Alexander Vorobyov, PhD Ress. Kirill Vorobyev, Prof. DSc. Shukhrat Teshaev, Prof. DSc. Zhamaletdin Mamasaidov, Assoc. Prof. Dr. Tatiana Chekushina.....189

SOILS

23. SOIL PROPERTIES OF CHROMIC LUVISOLS FROM KREMIKOVTSI AREA IN SOFIA MUNICIPALITY, Prof. Dr. Toma Shishkov, Assoc. Prof. Dr. Emil Dimitrov..... 197

24. DEGRADED SOILS OF THE MOST BASIN AND THE POSSIBILITIES OF THEIR LOCATION, CLASSIFICATION AND RECLAMATION, PhD Michal Rehor, Eng. Pavel Schmidt, Eng. Radka Duzekova, Assoc. Prof. Petr Vrablik.....205

25. DETECTION OF AGATE-LIKE SOIL COVER STRUCTURES USING NEURAL NETWORK FILTERING OF BIG REMOTE SENSING DATA, PhD Polina Koroleva, PhD Dmitry Rukhovich, Alexey Rukhovich, Galina Chernousenko.....213

26. ECOLOGICAL AGRICULTURE AS A SOCIAL COMPONENT OF ENVIRONMENTAL SUSTAINABILITY AND FOOD SAFETY, Prof. DSc. Roman Oleksenko, Prof. DSc. Valentyna Voronkova, Prof. DSc. Vitalina Nikitenko, Prof. DSc. Natalya Metelenko, Assoc. Prof. Liudmyla Holovii.....221

27. EFFECTS OF ORGANIC FERTILIZER APPLICATION ON AMERICAN CRANBERRY CULTIVATION – MINERAL NUTRITION STATUS, PLANT VITALITY AND POSSIBLE ENVIRONMENTAL ASPECTS, PhD Andis Karlsons, PhD Anita Osvalde, Msc. Laura Abolina.....229

28. FOREST SOILS FROM SREDNA GORA MOUNTAIN IN BULGARIA, Prof. Dr. Toma Shishkov, Assoc. Prof. Dr. Emil Dimitrov, Prof. Dr. Ekaterina Filcheva,.....237

29. LOCAL SOURCE OF PHOSPHORUS FROM SEED PRODUCTION WASTE, Ing. Antonín Kintl, Ing. Igor Huňady, Ing. Julie Sobotková, Ing. Martin Brtnický, Ing. Jakub Elbl, Ph.D.....245

30. MICROMORPHOLOGICAL FEATURES OF SALT-AFFECTED SOILS FROM THE BAIKAL REGION OF RUSSIA, PhD Irina Yamnova, PhD Galina Chernousenko.....253

31. MULTITEMPORAL SPECTRAL CHARACTERISTICS OF INTRAFIELD SOIL FERTILITY HETEROGENITY ZONES OF NORTHERN KAZAKHSTAN ARABLE LANDS, Vasily Rashkovich, PhD Dmitry Rukhovich, Dmitri Borschev..... 261

32. PHYTOSTABLIZATION OF SULPHIDE MINE TAILINGS Ph.D. candidate Raghad Soufan, Prof. Dr. Antoine Karam, Prof. Dr. Ahmed Aajjane 269

33. QUALITY OF POST-HARVEST RESIDUES WHEN GROWING MAIZE IN THE SYSTEM OF MIXED CROPPING, Ing. Antonin Kintl, Ing. Julie Sobotkova, Ing. Jakub Elbl, Ing. Martin Brtnicky, Ing. Igor Hunady.....277

34. SEASONAL DYNAMICS IN THE MICROBIOLOGICAL STATUS OF FOREST SOILS FROM THE TERRITORY OF VITOSHA NATURE PARK, PhD Bilyana Grigorova-Pesheva, PhD Boyka Malcheva, PhD Biser Hristov.....285

35. SELECTION OF CASE STUDY AREAS OF THE MOST BASIN FOR SOLVING RECLAMATION ISSUES OF EUROPEAN PROJECT REECOL, RNDr. PhD Michal Rehor, Eng. Pavel Schmidt, Eng. Radka Duzekova, Assoc. prof. Frantisek Helebrant 293

36. SOIL PROTECTION AGAINST SOIL EROSION BY USING ANTI-EROSION METHODS IN THE HILL AREA OF BUZAU, ROMANIA, Assoc. Prof. Dr. Radu Alexandra Teodora, PhD Burcea Mariana.....301

37. SPECTRAL CHARACTERISTICS OF GROUPS AND TYPES OF LANDS, CONSTRUCTED BY AVERAGIN LONG-TERM SERIES OF VEGETATION INDECES, Dmitry Borshchev, PhD Dmitry Rukhovich, Vasily Rashkovich 313

38. TEMPORAL VARIATIONS IN GREENHOUSE GAS EMISSIONS FROM AGRICULTURAL SOILS, PhD Kristine Valujeva, Jovita Pilecka-Ulcugaceva, Kristaps Siltumens, Olga Skiste, PhD Inga Grinfelde.....321

39. STATISTICAL AND CHEMICAL ANALYSIS OF SOIL POLLUTION FROM KOSHTOVA LANDFILL MITROVICE – KOSOVO, MSc. Bahri Sinani, Prof. Dr. Blazo Boev, Prof. Dr. Arianit Reka, Prof. Dr. Ivan Boev, Berat Sinani, MSc. Elida Lecaj, MSc. Adelina Haskaj 329

FOREST ECOSYSTEMS

40. A COMPARATIVE STUDY OF CARBON SEQUESTRATION IN DIFFERENT TYPES OF FOREST, PhD Nodar Khujadze, Prof. DSc. Lia Matchavariani.....339

41. BIOMETRIC MEASUREMENTS AND DEMOGRAPHIC STRUCTURE OF DUCKS HUNTED ON LAKE ENGURE IN THE PERIOD 1993-2022, Dr. Linards Sisenis, Prof. Irina Pilvere, Bc. Toms Endzins, PhD Baiba Jansone, Dr. Oskars Keiss 347

42. ASSESSMENT OF THE QUALITY AND PRODUCTIVITY OF LODGEPOLE PINE GROWN IN THE WESTERN PART OF LATVIA, Prof. Linards Sisenis, Prof. Irina Pilvere, PhD Baiba Jansone, Dr. Dace Brizga, Mg. Edgars Dubrovskis.....357

43. FIRE SAFETY IN PEAT EXTRACTION SITES IN LATVIA, Assoc. Prof. Dace Brizga, Mg. silv. Edgars Dubrovskis, Prof. Dr. Olga Miezite, Prof. Dr. Linards Sisenis, Mg. Kristine Kirsbauma.....367

44. MACROMYCETES OF BEECH FOREST IN MTIRALA NATIONAL PARK, GEORGIA, Assoc. Prof. Dr. Inga Diasamidze, PhD Gia Bolkvadze, Assoc. Prof. Dr. Natela Varshanidze, Assoc. Prof. Nana Zarnadze, Nino Varshanidze.....375

45. NATURAL REGENERATION OF PINUS SYLVESTRIS L. FROM SEED TREES IN POOR MINERAL SOILS, Prof. Dr. Olga Miezite, Mg. silv. Edgars Dubrovskis, Dr. Dace Brizga, Mg. Aija Berzina.....383

46. STOCHASTIC SIMULATION OF SELF-THINNING, Prof. Dr. Petras Rupsys 393

47. TAXONOMIC AND ECOLOGICAL STRUCTURE OF FREE-LIVING AND PLANT PARASITIC NEMATODES IN POTATO FIELDS IN KHULO (AJARA, EASTERN GEORGIA), Assoc. Prof. Dr. Lali Jgenti, Prof. Dr. Eka Tskitishvili, Tengiz Vadatchkoria 401

48. THE CHANGES OF FOREST GROUND VEGETATION CAUSED BY GRAZING, LATVIA, Prof. Inga Straupe, Bac. silv. Alise Dimane.....409

49. THE EFFECT OF TRAIL PATHS IN GRASSLAND ECOSYSTEMS USING A SWOT-AHP HYBRID METHOD, PhD Aimilia Lempesi, Christodoulos Daoutis.....417

MARINE AND OCEAN ECOSYSTEMS

50. ROLE OF UNACCOUNTED SOURCES OF TOTAL NITROGEN AND PHOSPHORUS IN THE NEVA BAY ANTHROPOGENIC EUTROPHICATION, Assoc. Prof. Dr. Victor Tretyakov, Stepan Klubov, Prof. DSc. Vasiliy Dmitriev, Anna Nikulina 427

SECTION

HYDROLOGY AND WATER RESOURCES

COMPARISON OF FIELD AND LABORATORY METHODS FOR THE ASSESSMENT OF SOIL HYDRAULIC CONDUCTIVITY

Ing. Stanislav Paseka, Ph.D.[1]

[1] Brno University of Technology, Faculty of Civil Engineering, Institute of Landscape Water Management, **Czech Republic**

ABSTRACT

Hydraulic conductivity (K_S) is a critical parameter used in soil and land research, essential for accurate hydrological modelling. This study endeavours to compare assessments of K_S across designated sites near the Czech Republic - Poland border using a range of measurement techniques, with the aim of establishing their reliability and variability for modelling applications. The investigation spans the determination of permeability from grain size curves, K_S estimation via field infiltration tests employing the double-ring method, and laboratory K_S determination using a constant head permeameter.

The findings reveal that the double-ring method for the determination of K_S produces results akin to laboratory measurements conducted with the permeameter, showing consistency between the field and laboratory approaches. However, it is notable that the permeameter exhibits significant variability, particularly as the depth varies. Moreover, noteworthy disparities emerge between K_S and permeability estimates, underscoring the need for careful consideration in the interpretation of these parameters.

Considering these results, it seems advisable to give precedence to field-based evaluations of K_S for immediate assessments, as they provide valuable insights into real conditions. Conversely, for long-term assessments, the utilization of laboratory derived K_S values may be more suitable, given their potential for stability over time. Nonetheless, the study emphasizes the necessity for further research to minimize the uncertainties and refine model inputs. Ultimately, this study underscores the intricate nature of hydraulic conductivity in soils and the imperative for comprehensive research to further develop water management models.

Keywords: saturated hydraulic conductivity, double ring infiltrometer, permeameter, permeability, Philip equation

INTRODUCTION

Hydraulic conductivity (K_S) is one of the fundamental inputs to simulation models employed in soil and land research. It is the paramount hydraulic parameter for soil-related flow and transport phenomena, yet the results from various methods of measurement exhibit variability under field conditions. Overall, K_S proves to be highly variable, as demonstrated by many studies [1].

K_S can be determined by direct measurement or can be derived indirectly, for example, from pedotransfer functions [2]. In paper [1] four methods for the measurement of K_S were compared for different field conditions: Guelph Permeameter (GP), Velocity Permeameter (VP), Disk Permeameter (DP), and Double-Tube Method (DTM) at four

depths and five locations on glacial-till soil. The results showed variability in the Ks values between methods. GP yielded the lowest values, due to the small sample size, while DP and DTM provided higher K_S values with less variability. The measurements of K_S were most similar between the VP and laboratory method. In paper [3] field experiments compared K_S measured using four methods: Double Ring Infiltrometer (RI), Rainfall Simulator (RS), Guelph Permeameter (GP), and Guelph Infiltrometer (GI). The results showed that Ks values from RI and GP were similar but lower than those from RS and GI. The GP and GI methods produced greater variability in the measurement of Ks and required more measurements to achieve comparable precision to the RI and RS methods.

The aim of the study is to determine the hydraulic conductivity, K_S, at selected sites on the border between the Czech Republic and Poland using various measurement techniques. Through a comparison of the hydraulic conductivities the aim is to assess the reliability and variability of these inputs for hydrological modelling. The measurements will focus on (I) a determination of permeability from the soil grain size curve, (II) an estimate of the *Ks* from infiltration measurements using the double-ring method, and (III) laboratory determination of *Ks* using a constant-head permeameter.

MATERIALS AND METHODS

A. Determination of Permeability from Grain Size Curve

To determine permeability, disturbed soil samples were collected from the specified sites as shown in Figure 1. Grain size analysis, also known as granulometric analysis, expresses the percentage by weight of the fraction of individual particle sizes in soil. [4] This analysis involves a determination of the weight of each fraction of finer particles, which are then converted to percentages relative to the weight of the dry sample. The results are represented on a graph as a grain size curve, which shows the percentage weight of each fraction on a graph with a horizontal logarithmic scale (grain size) and vertical linear scale (percentage of particles passing through sieves of specific sizes).



Fig. 1 Sampling of disturbed soil samples

The proportion of particles larger than 0.063 mm was determined by sieving through a standard sieve set. The size of particles smaller than 0.063 mm was indirectly determined based on their variable sedimentation rate in suspension, using the Casagrande hydrometer method.

Permeability was determined based on the grain size curve using the Mallet – Pacquant method. Specifically, the permeability was determined for the particle diameter that corresponded to 20% pass through on the grain size curve, denoted as d20 [5].

B. Determination of K_S from infiltration measurements using the double-ring method

Measurement by the double-ring method, also known as infiltration testing, for an approximate determination of K_S, is based on two measuring cylinders and is conducted directly in the field. The inner cylinder monitors the cumulative infiltration over time, while the outer cylinder ensures a vertical flow within the inner cylinder, which is particularly relevant for more permeable soils. Both cylinders are embedded to a sufficient depth in the substrate, which is properly prepared to avoid interference from vegetation as shown in Figure 2.

A brief outline of the measurement procedure is as follows: water is poured into the inner cylinder (up to a mark) of a known volume and simultaneously into the outer cylinder, at the same water level; as the water level drops in the inner cylinder, a known quantity of water is replenished and the time and volume are recorded; measurements are taken from the start of infiltration until the relative stabilization of the infiltration rate.



Fig. 2 Sample measurement using the double-ring method, also known as infiltration testing

Based on these measurements, K_S can be evaluated, for example, using the Philip equation, where Equation 1 shows a system of two equations with two unknowns, in summarised form. [6]

$$\begin{aligned} S\sum_{i=1}^{m} t + A\sum_{i=1}^{m} t^{3/2} &= \sum_{i=1}^{m} I.t^{1/2} \\ S\sum_{i=1}^{m} t^{3/2} + A\sum_{i=1}^{m} t^{2} &= \sum_{i=1}^{m} I.t \end{aligned} \tag{1}$$

where S is sorptivity, A is a parameter related to the rate dimension, t is time, and I is the cumulative infiltration.

Alternatively, through the use of the three-parameter Philip equation, where equation 2 represents a system of three equations with three unknowns in a summarised form. [6]

$$\begin{aligned} C_1 \sum_{i=1}^{m} t_i + C_2 \sum_{i=1}^{m} {t_i}^{3/2} + C_3 \sum_{i=1}^{m} {t_i}^{2} &= \sum_{i=1}^{m} I_i {t_i}^{1/2} \\ C_1 \sum_{i=1}^{m} {t_i}^{3/2} + C_2 \sum_{i=1}^{m} {t_i}^{2} + C_3 \sum_{i=1}^{m} {t_i}^{5/2} &= \sum_{i=1}^{m} I_i t_i \\ C_1 \sum_{i=1}^{m} {t_i}^{2} + C_2 \sum_{i=1}^{m} {t_i}^{5/2} + C_3 \sum_{i=1}^{m} {t_i}^{3} &= \sum_{i=1}^{m} I_i {t_i}^{3/2} \end{aligned} \quad (2)$$

where C_1 is estimate of sorptivity, and C_2 and C_3 are parameters of the levelling process.

For the Philip equation, the parameters S and A were determined from a system of two equations with two unknowns using Gaussian elimination, and K_S was calculated according to equation 3:

$$Ks = \frac{A}{m} \quad (3)$$

where m is a constant with a value of 2/3.

For the three-parameter Philip-type equation, the parameters C_1, C_2, and C_3 were determined from a system of three equations with three unknowns using Gaussian elimination, and the saturated hydraulic conductivity was calculated according to equation 4:

$$Ks = (3C_1C_3)^{\frac{1}{2}} + C_2 \quad (4)$$

C. Determination of K_S in the laboratory using a constant head permeameter

For the laboratory determination of K_S, undisturbed soil samples, taken near the infiltration experiments, were used as shown in Figure 3. The samples were measured in a constant head permeameter.



Fig. 3 Undisturbed soil samples were collected for analysis with a constant head permeameter

A constant head permeameter is a device used to determine saturated hydraulic conductivity. It allows the simultaneous measurement of up to ten samples with closed water circulation. The difference (head) in water level is measured using a micrometre with light signalling of the level. [7]

Before the samples are inserted into the permeameter, it is necessary to saturate the collected soil samples so that all the pores are filled with water. Once the maximum capillary capacity is reached, the samples are placed into the permeameter, where they continue to saturate through the flow of water through the permeameter.

The value of the coefficient K_S is calculated from the steady flow rate (q) through the sample over time (t) according to equation 5:

$$Ks = \left(\frac{q}{S}\right)\left(\frac{l}{H}\right) \tag{5}$$

where q is the steady flow rate equal to V/t, V is the volume of water that passed over time t [$cm^3.s^{-1}$], S is the area of the Kopecký cylinder [cm^2], l is the height of the Kopecký cylinder [cm] and H is the constant difference in water levels before and after the sample [cm].

CASE STUDY

Sampling and infiltration measurements were conducted in the cadastral area of Krásné Loučky – Krnov. Specifically, at four sites southwest and northwest of the built-up area of Krásné Loučky near the border between the Czech Republic and Poland.

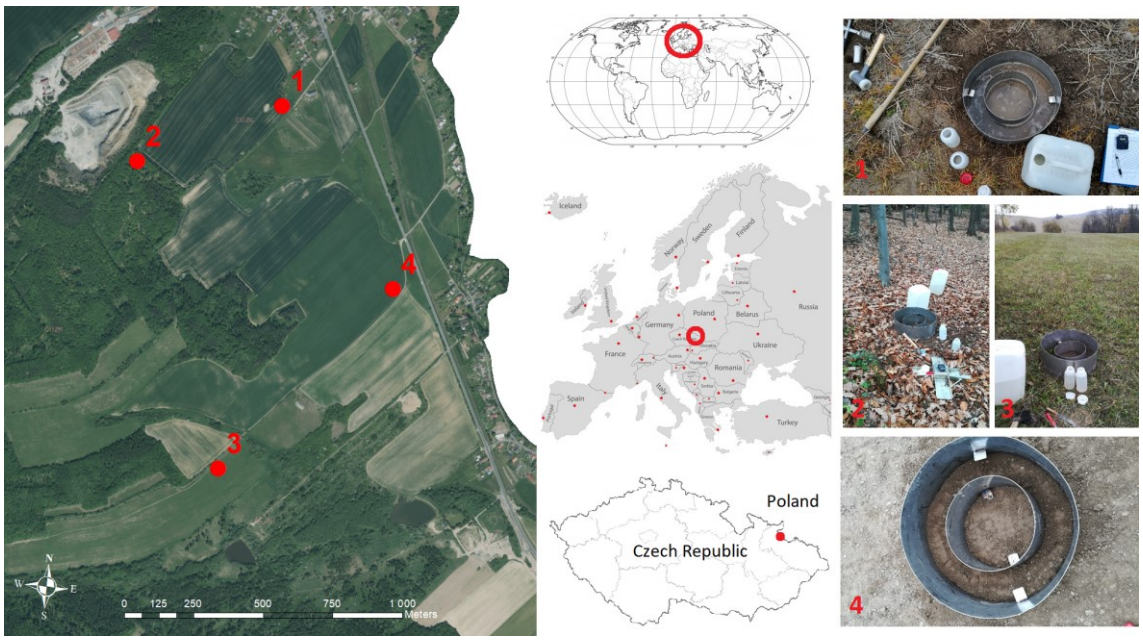


Fig. 4 Sampling and measurement site location

Locations 1 to 4 were chosen to represent the terrain as accurately as possible for the rainfall-runoff model in the given watershed. All locations are shown in Figure 4. Location 1 contained remnants of the corn harvest, with very crumbly soil. Location 2 was a forested area with very low moisture during measurements. Location 3 was a meadow, and location 4 was freshly sown with grain, but the substrate was highly compacted. All surfaces were cleaned before any measurements to ensure that only soil infiltration was measured. Measurements at these locations took place in the autumn of 2022.

During the double-ring method measurements, a disturbed soil sample was collected near the measurement site from depths of 0-10 cm (labelled A) and 20-30 cm (labelled B) to determine the grain size curve and moisture content by [8]. Additionally, an undisturbed soil sample was collected in close proximity and at the same depths for the laboratory determination of K_S, again at depths A and B.

RESULTS

A. Determination of permeability k from the grain size curve

Grain size determination was conducted according to [4], and permeability was determined from the grain size curves using the Mallet-Pacquant method. Broken up samples, intended for grain size determination, from two depths were always mixed, and rough estimates of permeability *k* are provided in Table 1 below.

Tab. 1 Permeability results *k* based on the grain size curve

Location	1	2	3	4
Permeability *k* [m s^{-1}]	2,9E-7	<3,0E-8	5,7E-8	1,5E-7

B. Determination of K_S from infiltration measurements using the double-ring method

Table 2, contains the calculated estimates of *Ks* according to the Philip equation, equations 1 and 3, the three-parameter Philip equation and equations 2 and 4.

Tab. 2 Results of *Ks* based on infiltration measurements using the double-ring method

Location	1	2	3	4
Ks (eq3) [m s^{-1}]	1,18E-4	9,94E-5	4,28E-6	8,26E-8
Ks (eq4) [m s^{-1}]	8,36E-5	6,61E-5	4,15E-6	8,82E-7
Ks average [m s^{-1}]	1,0E-4	8,3E-5	4,2E-6	4,8E-7

C. Determination of K_S in the laboratory using a constant head permeameter

After saturation, the flow through the individual Kopecký cylinders were measured, and the calculations were performed according to equation 5. The following table presents the estimates of K_S from laboratory measurements using a constant head permeameter. The calculation of K_S (A) corresponds to a sampling depth of 0-10 cm, and K_S (B) corresponds to a sampling depth of 20-30 cm.

Tab. 3 Results of K_S based on laboratory measurements in a constant head permeameter are shown below

Location	1	2	3	4
Ks (A) [m s^{-1}]	7,37E-6	4,64E-5	1,23E-5	1,37E-6
Ks (B) [m s^{-1}]	5,85E-7	5,79E-8	2,72E-9	1,30E-5
Ks average [m s^{-1}]	4,0E-6	2,3E-5	6,2E-6	7,2E-6

SUMMARY OF RESULTS AND DISCUSSION

The permeability coefficient *k* and saturated hydraulic conductivity K_S values were obtained for 4 sites in the Krásné Loučky – Krnov area. The individual results are summarized in the following table for all four of the locations tested.

Tab. 4 Summary of k and *Ks* results

Location	1	2	3	4
k [m s^{-1}]	2,9E-7	<3,0E-8	5,7E-8	1,5E-7
Ks (double-ring) [m s^{-1}]	1,0E-4	8,3E-5	4,2E-6	4,8E-7
Ks (permeameter) [m s^{-1}]	4,0E-6	2,3E-5	6,2E-6	7,2E-6
Ks (average) [m s^{-1}]	5,2E-5	5,3E-5	5,2E-6	3,8E-6

In the final Table 4, significant differences can be observed among the various approaches in estimating K_S as well as between K_S and *k*.

The initial estimation of *k*, which characterizes soil properties, is based solely on grain size analysis, which does not reflect current moisture content, bulk density, compaction, etc. These results are particularly irrelevant, especially at site 2 (forest), where soil infiltration was extremely high. For the remaining field sites (sites 1 and 4), the results are very similar in magnitude despite significantly different levels of infiltration for both locations. The lowest permeability was observed for site 3, a meadow.

Conversely, field determination of K_S, which characterizes the relationship between water and soil, through infiltration using the double-ring method, reflects current conditions and the results of water infiltration rates into the soil. Here, the highest K_S values are found at site 1 (post-harvest field) and 2 (forest), while lower values are observed at site 3 (meadow) and the lowest at site 4 (field with significant compaction).

Laboratory determination of K_S showed variability depending on the sampling depth, as seen in Table 3. For instance, at site 3, the difference in K_S between the upper layer (0-10 cm) and the deeper layer (20-30 cm) differed by 4 orders of magnitude. Further analysis would benefit from considering the level between 10-20 cm. The average results indicated that sites 1(very crumbly soil) and 2 (forest) had the highest K_S, while the remaining sites showed similar results on the order of 10^{-6} m s^{-1}.

It can be observed that there is not as significant a difference between field-determined Ks and laboratory-determined K_S. Conversely, a more pronounced difference in results is seen between K_S and *k*. These findings can be beneficial not only for rainfall-runoff models and mathematical groundwater models but also for testing input uncertainties in water management solutions for reservoirs, as demonstrated in articles [9] and [10].

CONCLUSION

Regarding averaging of the field and laboratory methods to determine *Ks*, it can be stated that all the examined soils in the given locality fall within the range of 10^{-5} m s^{-1} to 10^{-6} m s^{-1}, which puts them in the category of permeable soils. However, the individual *Ks* results indicate that some values, primarily those obtained in locations 2 and 3, as well as location 4, range from 10^{-8} m s^{-1} to 10^{-9} m s^{-1}, which is characteristic of poorly permeable to impermeable soils.

For immediate assessments, it is likely preferable to obtain *Ks* through the field measurement method using the double-ring infiltrometer. Conversely, for long-term evaluation, it would be better to conduct multiple tests throughout the year in the given locality to minimize the influence of weather on the soil. From a long-term perspective, it is more appropriate to consider the hydraulic conductivity *Ks* from laboratory measurements, where a more stable development of results over the year is expected

(due to the long-term saturation of samples under laboratory conditions). Here, characteristics such as soil porosity, compaction, etc., will influence the outcome. Alternatively, the use of an average value of *Ks* from both methods could be considered.

Rough estimates of permeability *k* from the grain size distribution curve should remain near constant throughout the year, as grain size undergoes minimal changes under constant conditions. However, this rough estimate of *k* is likely the least accurate.

This study confirms that hydraulic conductivity is a complex hydraulic characteristic of soil influenced by many factors. Therefore, further research in this area is essential, comparing the results with indirect estimates using pedotransfer functions, as hydraulic conductivity is a key parameter in the development of mathematical models for water management.

ACKNOWLEDGEMENTS

This paper was funded by "Innovative measurement and modelling in water management for the sustainability of water resources", research project number FAST-S-24-8540.

REFERENCES

[1] Mohanty B. P., Kanwar, R. S., Everts C. J. Comparison of Saturated Hydraulic Conductivity Measurement Methods for a Glacial-Till Soil. Soil Science Society of America Journal. 1994 Volume 58. no. 3.

[2] Attila Nemes, Walter J. Rawls, Yakov A. Pachepsky. Influence of Organic Matter on the Estimation of Saturated Hydraulic Conductivity. Soil Science Society of America Journal. 2005. Volume 69, Issue 4.

[3] R. K. Gupta, R. P. Rudra, W. T. Dickinson, N. K. Patni, G. J. Wall. Comparison of Saturated Hydraulic Conductivity Measured by Various Field Methods. 1993. Transactions of the ASAE. 36(1).

[4] Standard: ČSN EN ISO 17892-4 Geotechnický průzkum a zkoušení – Laboratorní zkoušky zemin – Část 4: Stanovení zrnitosti.

[5] Mallet, C., and Pacquant, J. Earth dams. Editions Eyrolles, 1951. Paris, 1–345.

[6] Philip, J. R. The theory of infiltration: 4. Sorptivity and algebraic infiltration equations Soil Science. 1957. 84, 257-264.

[7] Laboratory permeameters – User manual. Eijkelkamp Soil & Water, Netherlands, 2017.

[8] Standard: ČSN EN ISO 17892-1 Geotechnický průzkum a zkoušení – Laboratorní zkoušky zemin – Část 1: Stanovení vlhkosti.

[9] Paseka, S., Marton, D. The Impact of the Uncertain Input Data of Multi-Purpose Reservoir Volumes under Hydrological Extremes. Water, 2021, 13(10).

[10] Marton, D., Paseka, S. Uncertainty Impact on Water Management Analysis of Open Water Reservoir. Environments, 2017, 4(1).

ABOUT THE APPLICABILITY OF ECOLOGICAL FLOW METHODOLOGY FOR PILOT DRAINAGE AREAS IN DANUBE RIVER BASIN DIRECTORATE IN BULGARIA

Assoc. Prof. Dr. Elena Bojilova[1]

PhD Borislav Vuchkov[2]

Dr. Maya Rankova[3]

Dr. Plamen Angelov[4]

PhD Radoslava Ivanova[5]

[1] National Institute of Meteorology and Hydrology, **Bulgaria**

ABSTRACT

The research uses monthly water flow in river watersheds within Danube's river basin – Ogosta, Iskar, Yantra and Rusenski Lom rivers, as pilot basins. The water flow indicators describe river flow regime and hydrological streamflow characteristics. Our article describes the determination of environmental flow limits on surface water abstractions in Bulgaria. Monthly river flow is characterized by annual variability due to climate factors and anthropogenic impacts. Furthermore information from hydrometric stations often cannot be used directly and the important tasks of hydrological research is to transfer information from observed river sections to unobserved ones based on the recorded flows from the monitoring network. During the analysis we established spatial relationships between the river flow indicators and the selected physical parameters describing the basin.

Registered flow data in the river gauging stations are executed for the 1981-2019 study period. The main flow indicators are being calculated. For the selected period, there are complete time series of monthly data for most of the stations in the country, ensuring comparability of the results. The regional regression analysis is applied. Three spatial relationships are obtained for three water seasons: high water season, medium water season and low water season.

The paper is illustrated with maps and graphics of the hydrological zones and regional relationships in the selected river systems. The established relationships give the possibilities to interpolate and extrapolate in reasonable range. The reported results are needed for decision makers at different level.

Keywords: water runoff volume per second, river flow per unit area, ecological flow per unit area

INTRODUCTION

Ecological flow assessments typically consider various components of flow, including magnitude (volume of water), timing (seasonal patterns), duration (length of time water is present), frequency (how often certain flow conditions occur) etc. Understanding

these components helps in evaluating their ecological significance and identifying flow requirements for different species and habitats [13], [7].

The different hydrological conditions throughout Bulgaria mean that different catchment basins have their highest and lowest flows at different times of the year. To be applicable to all catchments, the seasonal approach to runoff thresholds should be based on "runoff seasons" rather than calendar seasons. For example, instead of setting a 'winter' runoff threshold, we should consider thresholds for the 'high runoff season' - ie. the months with the highest average runoff when this may be during the year.

The research uses monthly water flow in river watersheds within Danube's river basin – Ogosta river and rivers west of Ogosta river was selected as a pilot basins. These rivers are formed in the conditions of a moderate continental climate with decreasing air temperature and increasing precipitation amounts from the plain to the high mountain part of the river basin and an increase in the degree of forestation in the same direction [4], [5]. We observed the hydraulic connection between the river and underground waters in the lower reaches of the main river and feeding of the karst waters with river waters in the middle reaches of the Ogosta River [10]. Runoff-forming factors determine the appearance in the studied catchment of spring high water, summer-autumn low water and a transitional phase in the autumn months, with runoff maximum in May and runoff minimum in August.

The narrowest and lowest part of the Danube plain is the western one [3]. The study includes the river basins west of Ogosta and the Ogosta river basin, with a large part of them forming their outflow in the North-western part of Bulgaria between the Western Stara Planina, the Timok river and the Iskar river [11]. The most important rivers west of the Ogosta River are: Erma, Nishava, Topolovets, Voinishka, Vidbol, Archar, Skomlya, Lom, Tsibritsa and Ogosta itself. With the exception of the Nishava river and the Erma river, all others discharged into the Danube river. Our article describes the determination of environmental flow limits on surface water abstractions in Bulgaria.

MATERIALS AND METHODS

The relationship between ecological sensitivity to river runoff is very complex [1], [2], [3]. The methods and practices for ensuring the ecological conditions in the river basins on the territory of Bulgaria are defined in Art. 116, Art. 117, Art. 135 and Art. 188 of the Water Act [9]. The methodology for calculating the minimum permissible runoff in rivers is approved by Order No. RD - 1383/18.11.2003 - "ensuring a runoff equal to 10 per cent of the average multi-year water quantity, determined on the basis of information from a representative period, such as water quantity cannot be less than the minimum monthly average water quantity with a guarantee of 95% for the corresponding point in an undisturbed regime" (in l/s or m^3/s).

Each river water body is assigned to one of 14 river types (World Bank, 2022), an approach that determines the sensitivity of runoff to river type. It can therefore be used to provide an overall macro-scale sensitivity assessment for all water bodies as part of a common runoff approach for Bulgaria.

Once the river typology has been determined to provide a solid basis for determining sensitivity [12], [10], consideration should be given to appropriate runoff sensitivity categories to be added. On the one hand, the purpose of the sensitivity

typology is to provide a distinction between different levels of sensitivity to river runoff – therefore, it is necessary to have a sufficient number of categories to allow this distinction. On the other hand, the presence of too many categories complicates the methodology. As a starting point, three levels of sensitivity provide a reasonable balance between these two positions - high, medium and low sensitivity.

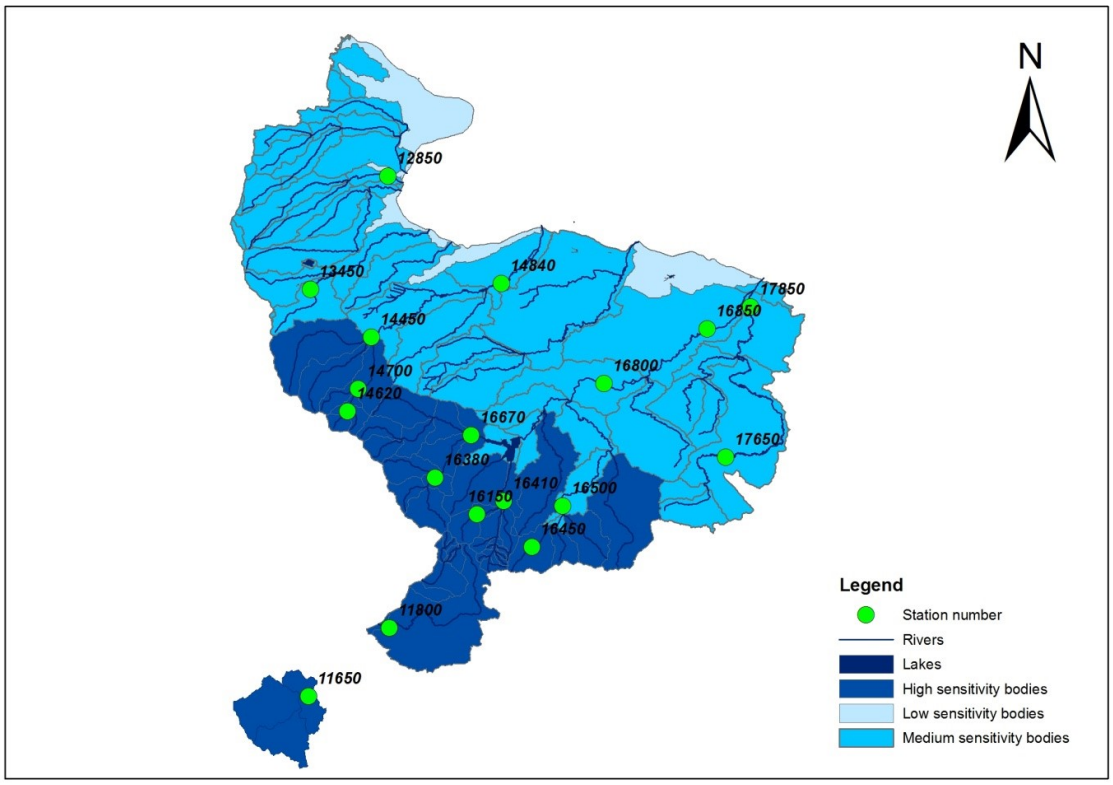


Figura 1. Scheme of the drainage basin of Ogosta river basin and rivers west from Ogosta river with indicated sensitivity water bodies

Ecological flow methodologies recognize the importance of flow variability, including both low-flow periods during droughts and high-flow events during floods. Maintaining natural flow variability helps sustain diverse habitats and species adapted to different flow conditions [6], [7].

RESULTS and DISCUSSION

The use of three runoff seasons – high, medium and low flow seasons – ensures that flow variability is incorporated into the ecological runoff approach. To determine the months that fall within each runoff season, average monthly runoffs are calculated and sorted from highest to lowest. The four months with the highest average runoff form the high runoff season, the next four months form the average runoff season, and the lowest four months form the low runoff season. Seasons are not necessarily made up of chronological months [1], [8].

Ecological runoff is applied in each stream season using the mean runoff to the current minimum residual runoff approach. The National institute of meteorology and hydrology (NIMH) monitoring network in the Ogosta river basin and rivers west of Ogosta includes 17 hydro meteorological stations (HMS).

https://doi.org/10.5593/sgem2024/3.1/s12.02

Table 1. Analysed hydrometric stations within Ogosta river basin and rivers west of Ogosta river.

River	Station number	Location	Drainage area (F, km^2)
Erma	11650	Trun town	367.713
Nishava	11800	Kalotina village	277.598
Voinishka	12850	Tarniane village	261.143
Veshtitska	13450	Veshtitsa village	85.908
Stakaevska	14450	Falkovets village	328.923
Lom	14620	Gorni Lom village	20.238
Lom	14840	Vasilovtsi village	1037.035
Berkovska	16150	Begovitsa district	46.288
Dalgodelska	16380	Govejda village	125.018
Barzia	16410	Balabanitsa village	173.035
Botunia	16450	Varshets village	20.83
Botunia	16500	Stoianovo village	237.968
Ogosta	16670	Gavril Genovo	521.273
Ogosta	16800	Kobiliak village	2241.383
Ogosta	16850	Butan village	3000.743
Skat	17650	Nivianin village	252.523
Skat	17850	Mizia	1058.563

After a hydrological analysis of the homogeneity of the hydrometric stations along the Ogosta river and the rivers west of it, 4 regions were formed. The regions are the same for the three types of water seasons.

Region 1: Rivers with watersheds south of Stara Planina and Veshtitska river (Salashka) and their tributaries. Hydrometric stations used are: HMS № 11650 Erma - Trun, HMS № 11800 Nishava – Kalotina village, HMS № 13450 Veshtitska reka - Veshtitsa village.

Region 2. The foothills, with a relatively low altitude and watersheds entirely or mostly plains. Stations used are: HMS № 12850 Voinishka reka - Tarniane village, HMS № 17650 Skat - Nivianin village, HMS № 17850 Skat - Mizia.

Region 3. Lom River. Stations used: HMS № 14450 Stakaevska reka - Falkovets village, HMS № 14620 Lom (Burza Reka) - Gorni Lom village, HMS № 14840 Lom - village Vassilovtsi.

Region 4. Ogosta River and its tributaries. Stations used: HMS № 16150 Berkovska reka - Begovitsa district, HMS № 16380 Dalgodelska Ogosta - Govejda village, HMS № 16410 Burzia - Balabanitsa village, HMS № 16450 Botunia (Stara reka) at Varshets village, HMS № 16500 Botunia - Stoianovo village, HMS № 16670 Ogosta - Gavril Genovo village, HMS № 16800 Ogosta - Kobiliak village, HMS № 16850 Ogosta - Mizia.

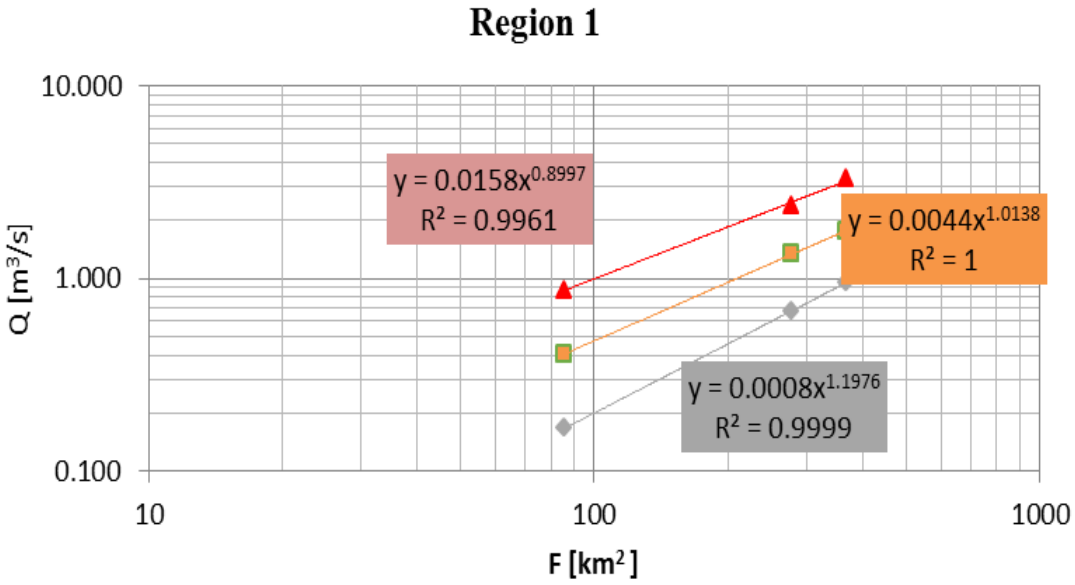


Figure 2. Relation between high, medium and low flow season discharge (m^3/s) and drainage area (F, km^2)

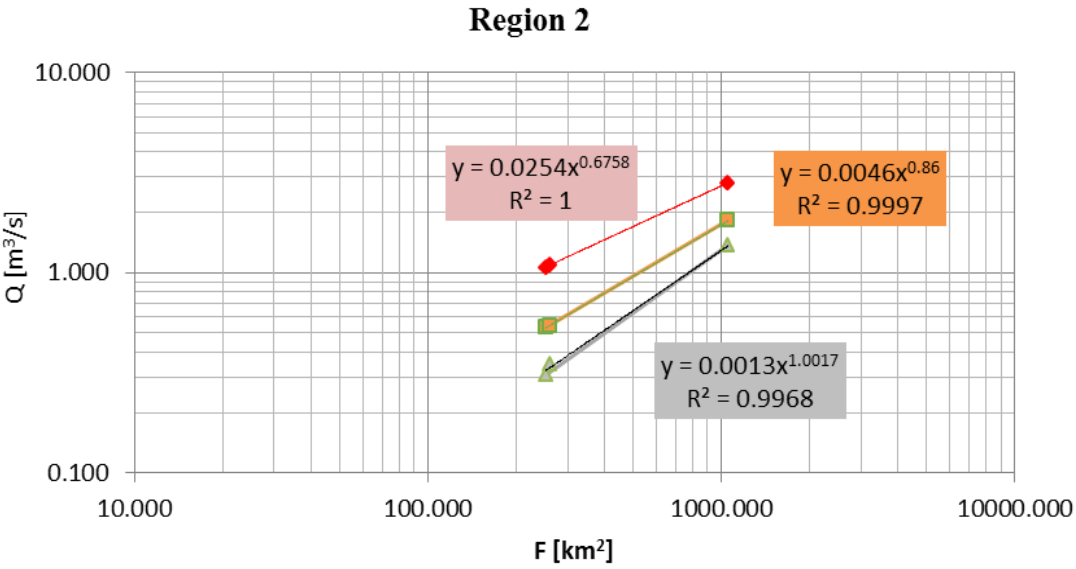


Figure 3. Relation between high, medium and low flow season discharge (m^3/s) and drainage area (F, km^2)

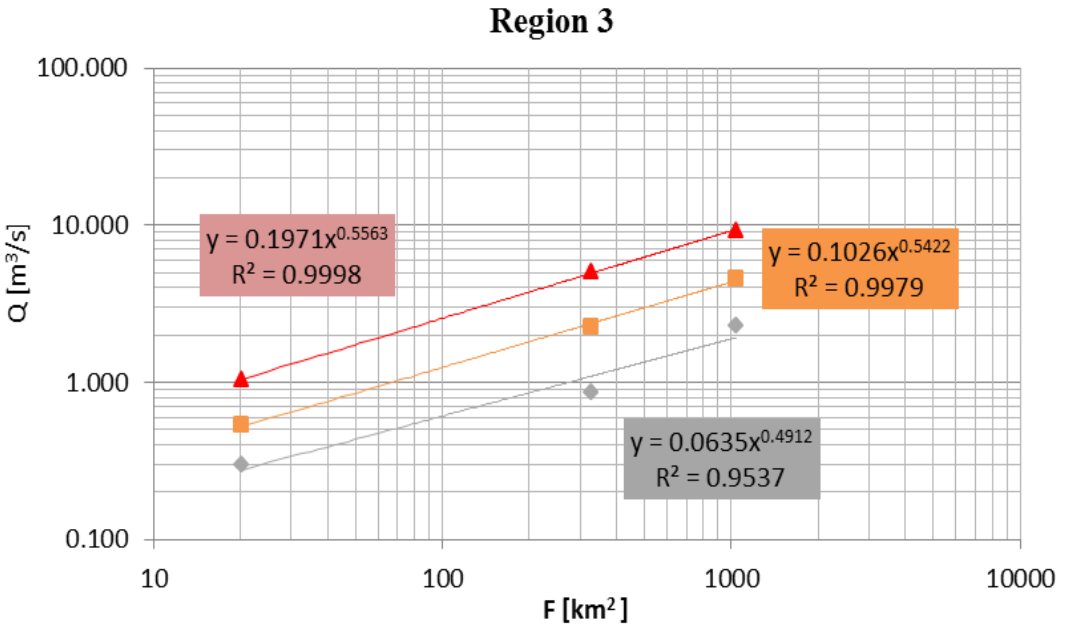


Figure 4. Relation between high, medium and low flow season discharge (m^3/s) and drainage area (F, km^2)

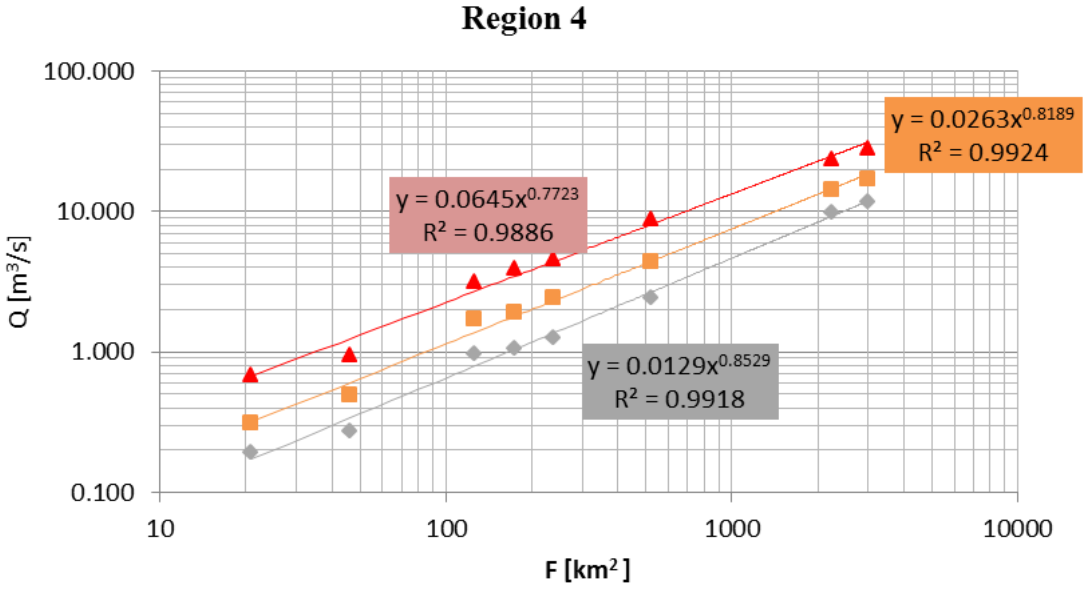


Figure 5. Relation between high, medium and low flow season discharge (m^3/s) and drainage area (F, km^2)

CONCLUSION

The survey of the selected catchment area of the Ogosta River and rivers west of Ogosta aims to assess the characteristics and indicators of the river runoff. Preserving ecological flow is fundamental for sustaining healthy freshwater ecosystems and the myriad benefits they provide to both human societies and the natural world. Effective management strategies that prioritize ecological integrity, stakeholder engagement, and

adaptive governance are essential for ensuring the resilience and sustainability of water systems in the face of growing environmental pressures.

Natural flow regimes exhibit variability over different temporal scales, from daily fluctuations to seasonal patterns and long-term trends. Maintaining this variability is essential for supporting diverse habitats and species adapted to specific flow conditions. Maintaining natural flow variability through flow management strategies can help sustain ecosystem health and resilience.

The presented research used monthly water flow in river watersheds within Danube's river basin – Ogosta rivers and rivers west of Ogosta river as pilot basins. The article described the determination of environmental flow limits on surface water abstractions in Bulgaria. During the analysis we established spatial relationships between the river flow indicators and the selected physical parameters describing the basin. The regional regression analysis was applied. Three spatial relationships were obtained for three water seasons: high water season, medium water season and low water season. The established relationships give the possibilities to interpolate and extrapolate in reasonable range. The reported results are needed for decision makers at different level.

ACKNOWLEDGEMENTS

The paper is based on research project "Determination of the hydrological characteristics according to a developed methodology for determining the ecological runoff for the conditions of Bulgaria and comparison with the values according to the current regulations" with project leader prof. Plamen Ninov. The authors wish to acknowledge the supervision of Eng. Kamelia Krumova for the research concerning Ogosta river basin.

REFERENCES

[1] Bozhilova E.K., Application of Methodology for Ecological Flow for Yantra River Basin in Bulgaria, Journal of Balkan Ecology, Vol. 27, № 1, ISSN 1311-0527 (Print) ISSN 2815-3758 (Online), pp 67-78, 2024

[2] Chilikova-Lubomirova M., 2015. Monitoring of the Ecological River Flow in Conditions of Climate Change, Drought and Water Scarcity Conditions, Bulgarian Academy of Sciences, Vol. 3–4, Problems of Geography, Bulgaria, 2015.

[3] Dimitrov Y., Yordanova A., Trends assessment of meteorological factors, river flow and droughts in North-western Bulgaria, E-book with full paper from XXVII Conference of The Danubian Countries, pp 321-330. Bulgaria, ISBN 978-654-90537-2-2, 2017.

[4] Dimitrov Y., Ilcheva I., Application of an Indicator System for Integrated Space-time Analysis and Drought Management in North-western Bulgaria, XXIX Conference of the Danubian Countries, The Czech Republic, Conference Proceedings with Full Papers, ISBN 978-80-7653-031-7, pp 172–180, 2021.

[5] Ilcheva I., Yordanova A., Nikolova K., Estimation of the Impact of Climate and Land Use Changes on the Availability of Water Resources and Drought Risk, International Multidisciplinary Scientific Geo-conference SGEM 2019, Bulgaria, pp 193-200, 2019.

[6] Hristova N., Seymenov K., Annual Flow Dynamics in Large and Small Drainage Basins in Northern Bulgaria during the Last Two Decades, Socio-Brains, ISSN 2367-5721, issue 54, pp 123-131, 2019.

[7] Hristova, N. 2011. Hydrological regime in Bulgaria according to the monthly maxima and minima of runoff. – Fourth International Scientific Conference „Water – problems and solutions", FMNS–2011, 08–11.06.2011, Blagoevgrad, 627–632.

[8] Ninov, Pl., Karagiozova, Tz., Rankova, M. 2017. Water Resources Determination of Surface Water Bodies at the Bulgarian basin of the Lower Danube, Journal of the Geographical Institute "Jovan Cvijić" SASA, Vol. 67, No 1

[9] Ninov P., Karagiozova T., Monitoring and Investigation of Intermittent Rivers in Bulgaria, E-book of the 28th Conference of the Danubian Countries, Ukraine, pp 6-14, 2019.

[10] Technical Report, Ecological Flow in the Implementation of the Water Framework Directive (086). Guidance Document 31, 2015.

[11] Vasileva T., An Assessment of Potential Ground Water Recharge Zones in Bulgaria, Geological Balcanica, vol. 48(1), Bulgaria, pp 43-61. 2019.

[12] World Bank. Delivering the Water Framework Directive in Bulgaria: Developing a Flows Approach WSP, WSP Environment & Infrastructure Solutions UK Limited, 2022.

[13] Yordanova A., Ilcheva I., Bocheva L., Malcheva K., Lubenova K., Analysis of Hydrological Drought Indices and their Relationship with Meteorological Factors and River Basin Specifics, International Multidisciplinary Scientific Geo-conference SGEM, 10.5593/sgem2022/3.1/s12.05, (3.1), Bulgaria, pp 57-64, 2022.

ANALYSIS OF WATER RESOURCES IN THE VASLUI HYDROGRAPHIC BASIN, ROMANIA

PhD. eng. Lavinia Tataru[1]

Professor PhD. eng. Florian Stătescu[1]

Lecturer PhD. eng. Nicolae Marcoie[1]

[1] "Gheorghe Asachi" Technical University of Iași, Faculty of Hydrotechnical Engineering, Geodesy and Environmental Engineering, **Romania**

ABSTRACT

Surface water resources are already being utilized at maximum capacity and the trend is unlikely to change. This situation has led to increasing concerns regarding the sustainable use of this resource, with continuous efforts being made to reduce water pollution.

In this context, the analysis of surface water quality is essential for protecting human health, the environment and the economy, providing significant opportunities for improving the quality of life and conserving natural resources.

This paper presents the results of a study aimed at identifying the degree of pollution of the Vaslui River water in Romania, in four monitoring sections using the *Water Quality Index* (WQI). It simplifies the classification of water quality parameters by including multiple parameters in a single mathematical equation and provides a unique value reflecting the overall state of water quality. The water samples were analyzed for a series of water quality parameters. Statistical analyses were performed to determine the mean values and ranges of variation of the studied indicators.

Water quality parameters were studied in correlation with the recorded flows on the Vaslui River. For this purpose, monthly average flows measured in the upstream sections before the Solesti reservoir were considered.

The obtained results indicate the necessity of adopting a Plan of Measures, both to improve the current quality and to prevent further degradation of water quality. The decrease in water quality is associated with the level of urbanization and human activities in the research area.

Keywords: Water Quality Index, Vaslui River, Pollution Sources, Statistical Analysis.

INTRODUCTION

In recent years, research on water quality in lakes and rivers has been a topic of interest in Romania, with numerous scientific papers published in this field, featuring various approaches and analysis methods.

Some authors argue that the main factors contributing to the degradation of water quality are natural factors (sedimentation, soil erosion, rainfall runoff) and anthropogenic factors (domestic, agricultural, and industrial activities). Anthropogenic factors are often the

main cause of surface water pollution, such as untreated wastewater, waste deposits, and industries [1, 2].

Being a universal solvent, water easily becomes polluted through the dissolution of chemical substances, with water quality influenced by natural phenomena, social contexts, or economic conditions [3, 4].

The Vaslui River is facing severe ecological degradation due to agriculture and urban agglomerations.

In recent decades, this hydrographic basin has undergone substantial changes resulting from land use. In the study area, agricultural lands predominate, with strong soil erosion phenomena observed along the hillsides and in the riverbed [5, 6].

This paper aims to analyze the spatial variation of water quality parameters and evaluate the water quality of the Vaslui River in four monitoring sections for the year 2021 using a Water Quality Index (WQI). Potential sources of pollution are also analyzed. This study adds to current knowledge and will assist local authorities in decision-making and the development of watershed management plans.

Numerous county-level studies have been conducted covering various research areas, but not specifically addressing surface water quality for the Vaslui River [7]. Therefore, research on assessing WQI for the Vaslui River is a relevant topic.

MATERIALS AND METHODS

VASLUI RIVER BASIN

The hydrographic basin of the Vaslui River (Figure 1) is located in the Northeast Region of Romania, being one of the regions with limited water resources, unevenly distributed in space and time. The Vaslui River is a left tributary of the Bârlad River, with a length of 81 km and a surface area of 692 km^2. It is an intermittent watercourse, with a multiannual average flow of 1 m^3/s (31.56 million m^3/year), and precipitation ranges between 450-550 mm/year. The area is predominantly hilly and plateaued, with maximum altitudes of 500 m, and geologically, sands, gravels, and clay deposits are present [4, 5, 6, 8].

The monitoring network comprises four sections where physico-chemical parameters have been monitored: S-1 upstream of the Poieni locality, S-2 Solești reservoir, S-3 Muntenii de Sus, and S-4 downstream of the Vaslui municipality. Hydrological regime monitoring is carried out by measuring flow rates at two hydrometric stations, Satu Nou and Codăești, located upstream, and one hydrometric station located downstream of the Solești reservoir [6, 8].

The physico-chemical parameters analyzed include: Temperature (T), Dissolved Oxygen (DO), Biological Oxygen Demand (BOD), Total Nitrogen (TN), Total Phosphorus (TP), Calcium (Ca), Magnesium (Mg), Detergents, Total Phenols.

Administrative management is conducted at the county level by the Prut-Bârlad Basin Water Administration, and locally by the Vaslui Water Management System (SGA Vaslui) [6].

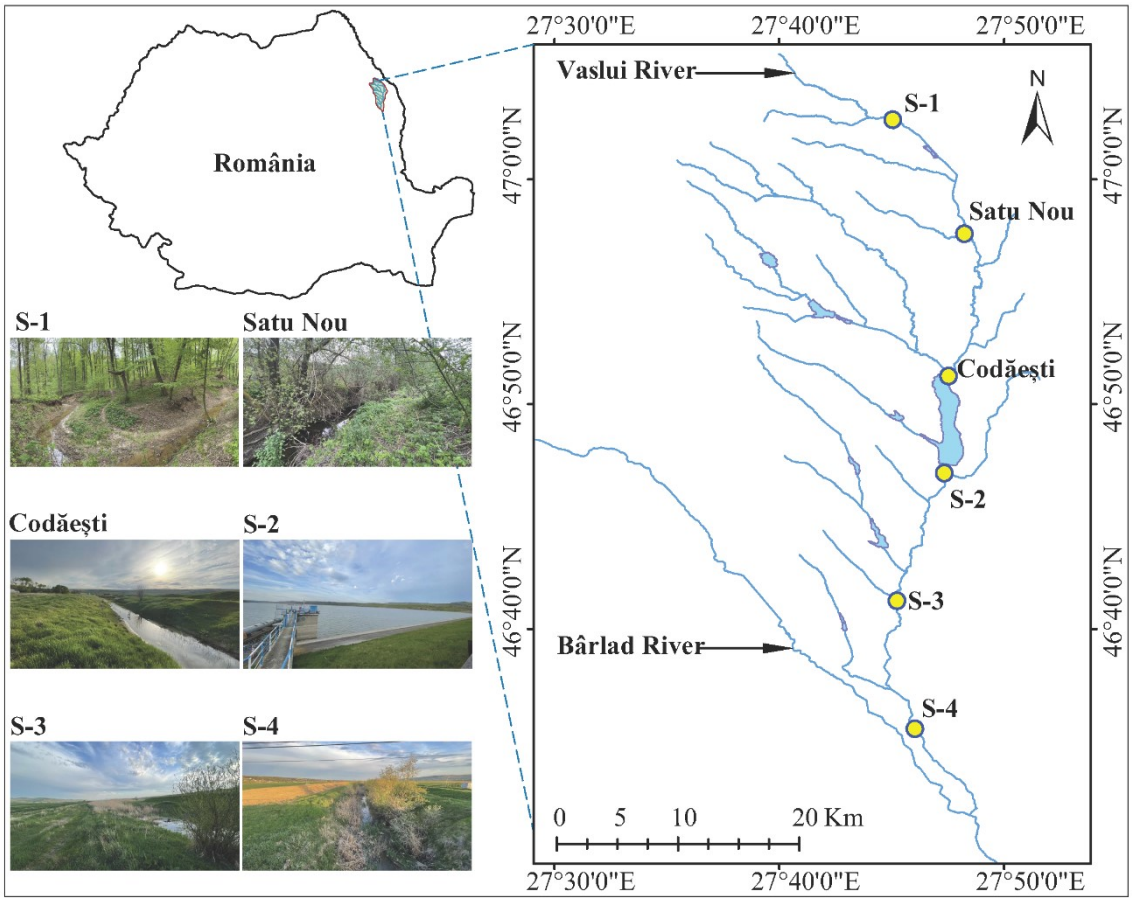


Figure 1. The hydrographic basin of the Vaslui River and monitoring sections

WQI CALCULATION

The calculation of the WQI provides a comprehensive assessment of river water quality and involves the use of a mathematical equation that combines data from multiple water quality parameters, resulting in a single value that classifies surface water quality [1, 9, 10, 11].

This study adopts the calculation method based on arithmetic weighting used by Frîncu [12]. WQI is calculated using Equation 1, where Q_i is calculated using Equation 2, and W_i is calculated using Equation 3:

$$WQI = \frac{\sum Q_i \times W_i}{\sum W_i} \quad (1) \qquad Q_i = 100 \times \frac{V_i - V_0}{S_i - V_0} \quad (2) \qquad W_i = \frac{K}{S_i} \quad (3)$$

where V_i is the determined concentration of parameter i, V_0 is the ideal concentration of parameter i, K is a proportionality constant, and S_i is the recommended standard limit value for parameter i.

To fulfill the objectives of Directive 2000/60/EC of the European Parliament and of the Council of 23 October 2000 establishing a framework for community action in the field of water policy, water bodies should be at least in the second class of quality [6, 7]. Thus, for the calculation of WQI, the limit values for S_i have been taken from national legislation for the second class of quality.

The intervals for classifying water quality based on WQI values are as follows: 0-25 excellent, 26-50 good, 51-75 moderate, 76-100 poor, and greater than 100 very poor [12].

RESULTS

For the efficient management of water resources, it is necessary to analyze river flow. Generally, flows are influenced by changes in precipitation, as well as by anthropogenic activities, such as draining or filling maneuvers at the Solești reservoir [5, 8]. The Vaslui River, being an intermittent water body, considers the phenomenon of drying up as a natural occurrence [6].

Figure 2 presents the average annual flows measured at the Codăești hydrometric station with values ranging from 0.085-0.571 m^3/s, at the Satu Nou hydrometric station with values ranging from 0.012-0.196 m^3/s, and at the Solești hydrometric station with values ranging from 0.002-0.176 m^3/s. At these stations, maximum flows were recorded in 2017, while minimum flows were recorded in 2020.

According to Jora and Românescu [8], the reduced flows observed downstream are due to the Solești reservoir, which redistributes the flow carried by the Vaslui River and its tributaries over time, depending on socio-economic requirements.

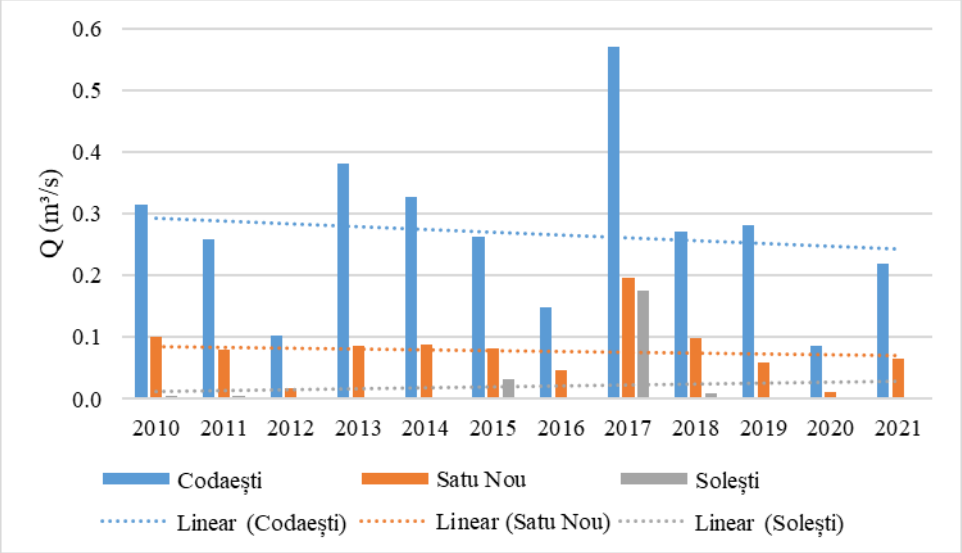


Figure 2. Multiannual variation of average annual flows measured at hydrometric stations

To determine if the correlation between physico-chemical parameters is statistically significant, the Pearson correlation matrix was applied (Figure 3). The greater the absolute value, the stronger the correlation between parameters. For example, a correlation coefficient greater than 0.75 (or less than -0.75) represents a strong correlation [2, 3, 10, 12]. Thus, we observe the strongest correlations between pH and T, DO, and Ca; between DO and BOD; between TP and TN and BOD; between Detergents and Total Phenols, BOD, TN, and TP; between Total Phenols and TN.

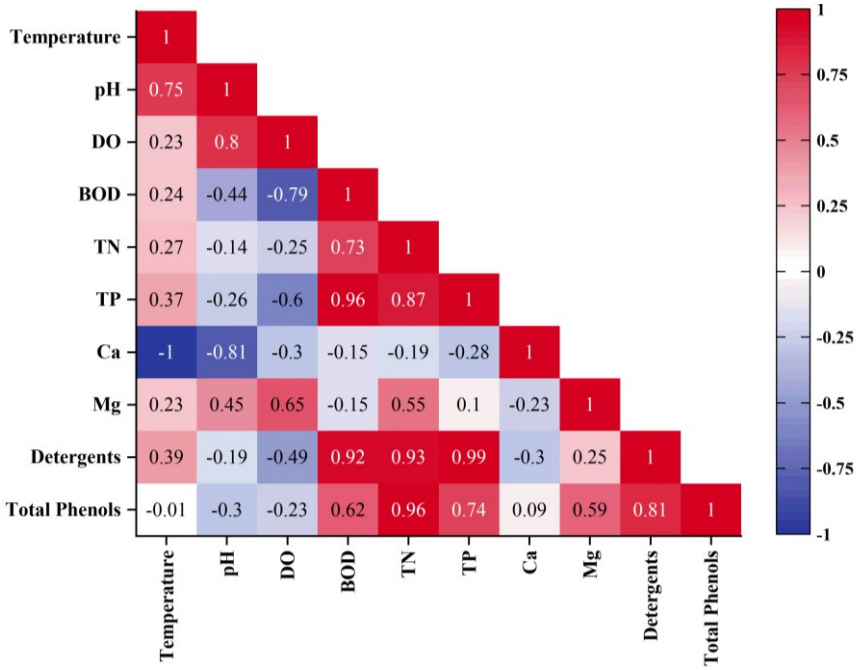
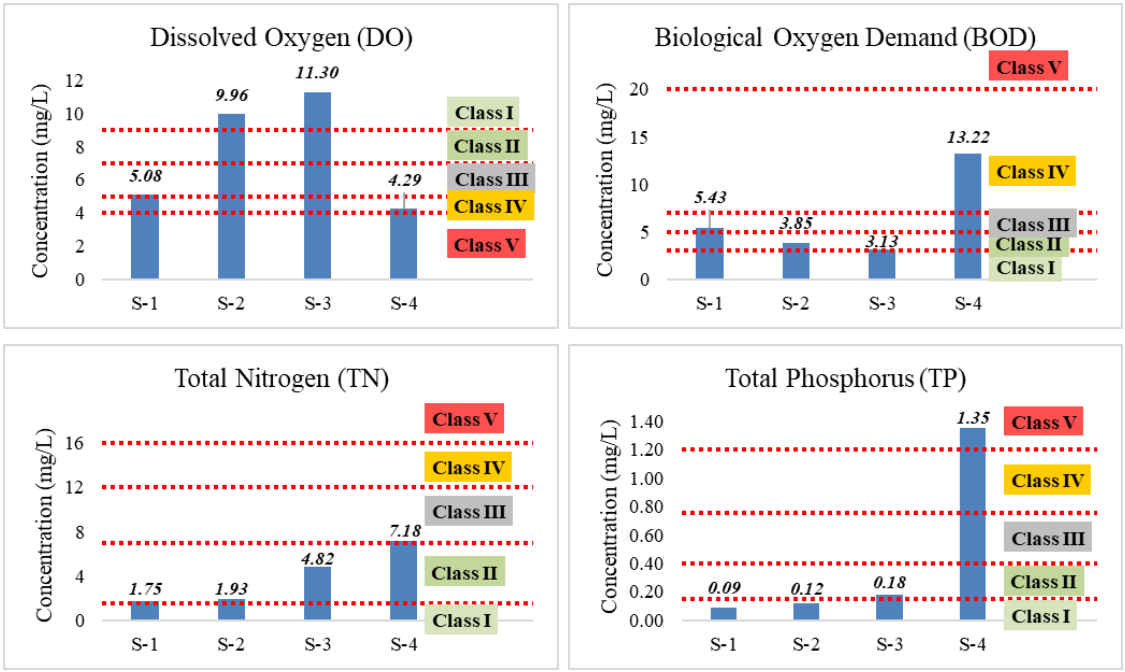


Figure 3. Pearson correlation coefficients for water quality parameters in the Vaslui River

In accordance with the provisions of the Regulation on the classification of surface water quality for the purpose of determining the ecological status of water bodies [13], the limit values of parameters for the five classes of water quality are presented in Figure 4.



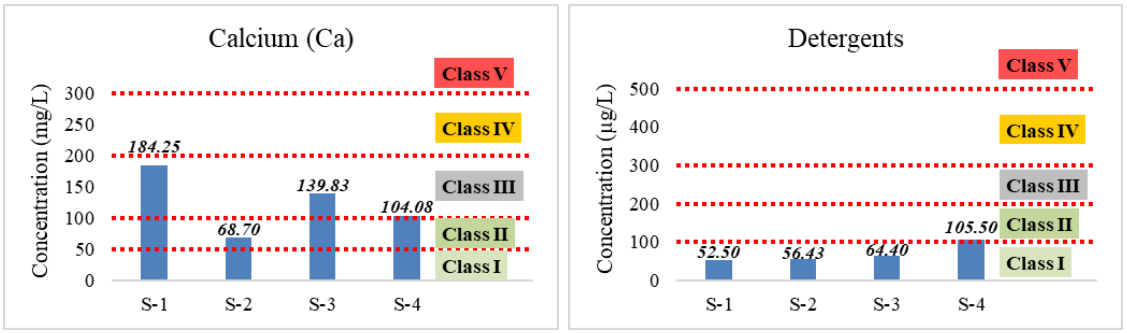


Figure 4. Classification and spatial variation of water quality parameters for monitored sections in the Vaslui River

It can be observed that there are few indicators falling into class I (clean water), while the majority of indicators fall into class II and III, but there are also indicators classified in class IV and V, especially in the monitoring section of Vaslui municipality (S-4). This means that the Vaslui River is classified as having poor water quality and needs rapid improvement.

The spatial variations of WQI in the Vaslui River are presented in Figure 5. The water quality in the Vaslui River has been classified as good in S-1, moderate in S-2 and S-3, while in S-4, the water is classified as very poor.

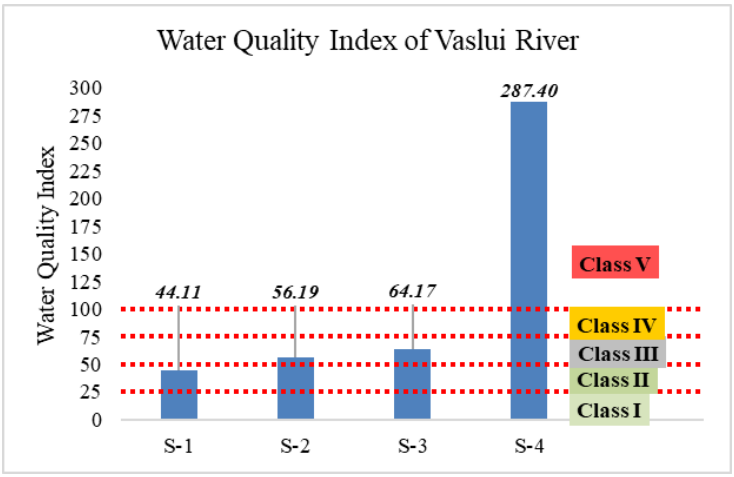


Figure 5. Spatial variation of Water Quality Index (WQI) in the Vaslui River

DISCUSSION

In the hydrographic basin of the Vaslui River, a number of 11 larger agglomerations of over 2,000 equivalent inhabitants without wastewater treatment plants, one agglomeration of over 10,000 equivalent inhabitants with a mechanical-biological (secondary) treatment plant, and one agglomeration of over 15,000 equivalent inhabitants with a mechanical-biological treatment plant with advanced removal of nitrogen and phosphorus (tertiary) have been identified. These are considered significant point sources of pollution. Diffuse sources of pollution come from agricultural activities (arable land and pastures), and pollutants reach water bodies through surface runoff or percolation.

The lack or inadequacy of wastewater treatment leads to water pollution, as urban wastewater contains suspended matter, organic substances, nutrients, heavy metals, detergents, etc. [6]. These are the most significant factors contributing to the deterioration of water quality.

Although there are difficulties in implementing the integrated water resources management process, the water quality of the Vaslui River has improved recently due to increased connection of the population to sewage networks and modernization of wastewater treatment plants, resulting in reductions in the effects of point source pollution from urban agglomerations, as well as a reduction in the application of organic and chemical fertilizers in agricultural land [4, 6, 7].

The Pearson correlation analysis showed strong positive correlations, such as pH with T (0.75), DO (0.8), and Ca (-0.81); between DO and BOD (-0.79); between TP and TN (0.87) and BOD (0.96); between Ca and pH (-0.81) and T (-1.00); between Detergents and Total Phenols (0.81), BOD (0.92), TN (0.93), and TP (0.99); between Total Phenols and TN (0.96).

Approximately 30% of all calculated correlations were negligible (from -0.25 to 0.25). On the other hand, about 30% of the calculated correlations were strong positive and negative correlations (greater than 0.75 or less than -0.79). The remaining 40% were moderate correlations (0.27 and 0.74; -0.26 and -0.6).

The study results show that the water of the Vaslui River gradually deteriorates from the source to the mouth and can be classified based on WQI as having good quality in the Poieni section, moderate quality in the Solești Reservoir and Muntenii de Sus sections, while in the Vaslui section, the water is classified as very poor.

CONCLUSION

Given the large number of parameters monitored, in this study, we evaluated the water quality of the Vaslui River using a quality index that provides information on the degree of pollution in different monitoring sections, based on the annual average values of selected parameters.

The water quality of the Vaslui River showed clear spatial variations. The analysis of the parameters highlighted values ranging from class I to class V quality, depending on the monitoring sections. This suggests that the river is facing various environmental pressures, especially pollution from municipal sources.

The results contribute to increasing the understanding of surface water conditions, but knowledge needs to be continuously enriched. Improving knowledge and increasing the exchange of information between the scientific community and decision-makers in the water sector lead to more informed and responsible decision-making, resulting in more sustainable and balanced management of water resources, benefiting both the environment and the human communities dependent on these resources.

The study could be enhanced by adding additional monitoring sections, including analysis of indicators for the tributaries of the Vaslui River, and developing a model focused on estimating WQI to improve watershed management practices.

REFERENCES

[1] Kujiek D.C., Sahile Z. A., Water quality assessment of Elgo river in Ethiopia using CCME, WQI and IWQI for domestic and agricultural usage, Heliyon, vol.10/issue 1, e23234, 2024.

[2] Shanmugasundharam A., Akhina S. N., Adhithya R. P., Satheesh Herbert Singh D., Krishnakumar S., Water quality index (WQI), multivariate statistical and GIS for assessment of surface water quality of Karamana river estuary, west coast of India, Total Environment Research Themes, vol. 6, 2023.

[3] Ravi N.K., Kumar P., Varma K., Tripathi P., Gautam S. K., Ram K., Kumar M., Tripathi V., Application of water quality index (WQI) and statistical techniques to assess water quality for drinking, irrigation, and industrial purposes of the Ghaghara River, India, Total Environment Research Themes, vol. 6, 2023.

[4] Gavrilescu D., Teodosiu C., David M., Environmental assessment of wastewater discharges at river basin level by means of waste absorption footprint, Sustainable Production and Consumption, vol. 21, pp 33-46, 2020.

[5] Croitoru A.E., Minea I., The impact of climate changes on rivers discharge in Eastern Romania, Theoretical and Applied Climatology, vol. 120, pp 563-573, 2015. https://doi.org/10.1007/s00704-014-1194-z.

[6] Ministerul Mediului, Apelor și Pădurilor, Administrația Națională „Apele Române", Planul de management actualizat al spațiului hidrografic Prut-Bârlad, 2021.

[7] Teodosiu C., Robu B., Cojocariu C., Barjoveanu G., Environmental impact and risk quantification based on selected water quality indicators, Natural Hazards, vol. 75/suppl 1, pp 89-105, 2015.

[8] Jora I., Romanescu G., .Influenţa activităţilor antropice asupra regimului hidrologic al râului Vaslui, Resursele de apă din România. Vulnerabilitate la activităţile antropice, Targoviste – Romania, 2010. ISBN: 978-606-8042-65-7

[9] Azha S.F., Sidek L. M., Ahmad Z., Zhang J., Basri H., Zawawi M. H., Noh N. M., Ahmed A. N., Enhancing river health monitoring: Developing a reliable predictive model and mitigation plan, Ecological Indicators, vol. 156, 2023.

[10] Qi J., Yang L., Liu E., A holistic framework of water quality evaluation using water quality index (WQI) in the Yihe River (China), Environmental Science and Pollution Research, vol. 29, pp 80937-80951, 2022.

[11] Kwon H.G., Jo C. D., Water quality assessment of the Nam River, Korea, using multivariate statistical analysis and WQI, International Journal of Environmental Science and Technology, vol. 20, pp 2487-2502, 2023.

[12] Frîncu R.M, Evoluția principalilor parametri fizico-chimici de calitate a apei din Dunăre pe teritoriul României în perioada 1996-2017, Teză de doctorat, București, 2020.

[13] ORDIN nr. 161 din 16 februarie 2006 pentru aprobarea Normativului privind clasificarea calității apelor de suprafață în vederea stabilirii stării ecologice a corpurilor de apă.

ARMA MODELS APPLICATION FOR FORECASTING OF THE RIVER DISCHARGE AND THE HYDROLOGICAL DROUGHT INDEX SRI IN DAMS MANAGEMENT

Assoc. Prof. Dr. Anna Yordanova[1]

Assoc. Prof. Dr. Irena Ilcheva[1]

Assoc. Prof. Dr. Elena Bojilova[1]

Assoc. Prof. Dr. Olga Nitcheva[2]

Chief Assistant Dr. Yordan Dimitrov[1]

[1, 2, 3, 5] National Institute of Meteorology and Hydrology, **Republic of Bulgaria**
[4] Bulgrian Academy of Sciences, Institute of Mechanics, **Republic of Bulgaria**

ABSTRACT

Reproducing the hydrological process of river runoff is a fundamental part of water resources planning and management. Finding a mathematical model to reproduce the runoff time series aims not only to extract maximum information from the limited available data, but also to extrapolate into the future by representatively generating the historical runoff process. Almost all management decisions are based on forecasts. Our present is characterized by the increasingly frequent occurrence of hydrometeorological processes that lead to flash floods and critical droughts. The river runoff, as the main element of water management systems, must be as well analyzed and substantiated as possible, so that its estimated values are of acceptable accuracy for practical application of water management. There are two forecasting approaches: real-time forecasting and observational time series forecasting. A stochastic method used in the second approach is presented here. The method uses the most applied class of models for forecasting time series - the ARMA models. Their application in forecasting one of the main indicators of the hydrological drought occurrence is shown. This is the SRI index, i.e. the standardized normal value from the probability distribution of the monthly river runoff observations. River runoff is a non-stationary process and ARIMAs are those ARMA models that transform, by differentiation, river runoff time series into stationary ones. The method is applied for a 43-year period of monthly river runoff observations on the tributary of the Ogosta river. With an ARIMA model is forecasted the runoff for the next few months and with it the SRI index monthly values are estimated. The accuracy of the results is investigated. The developed method makes it possible to predict hydrological drought and can be used in optimizing the regimes of dams with hydropower, irrigation water supply and environmental purposes.

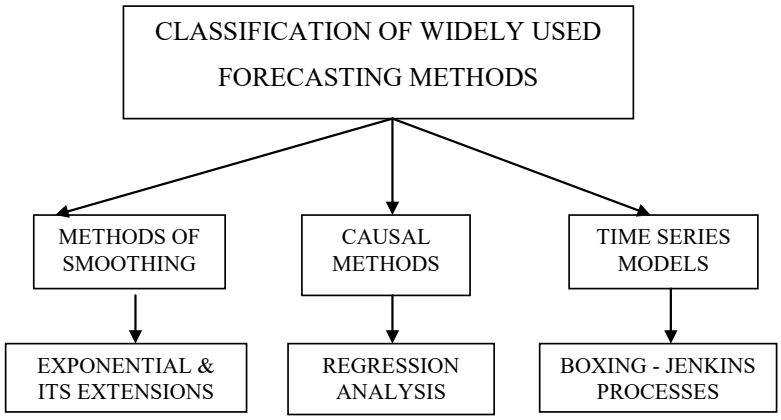
Keywords: hydrologic drought, forecasting, ARMA, SRI, river runoff

INTRODUCTION

The improvement of the methods and means for assessing the multi-year runoff fluctuations and its forecasting is required by the imposed higher requirements for the adequacy of the basic hydrological information, by the high degree of water use, which adversely affects the natural conditions, as well and from the warning of the world's scientists about global climate change, which adversely affects the water quantity and quality. Without representative hydrological information, it is impossible to carry out modern water management studies for rational use of water resources and obtaining an optimal economic, social and ecological effect.

1. MATERIALS AND METHODS

The main forecasting methods are classified by Prof. Clifford Hurwich[1] (scheme 1).



Scheme 1. Classification of the main forecasting methods

Exponential smoothing is a type of weighted moving average model that allows for the inclusion of a trend. It gives greater weight to the meanings of the random process from a more recent point in time compared to those from a more distant past point in time. Causal methods are based on a known or established relationship between the process to be forecasted and other internal or external factors.

The most widely applied class of time series forecasting models are ARMA models[2],[3],[4],[5]. Their application in forecasting one of the main indicators that determine the occurrence of hydrological drought is shown. This is the SRI index, i.e. the standardized normal value from the probability distribution of the series of river runoff observations. River runoff is a non-stationary process. ARIMAs are that subclass of ARMA models that transform, by differencing, river runoff time series into "stationary" ones.
The ARIMA model, which best models the given river runoff is specified, based on the observations. With this model the outflow is predicted for the next few months and from the obtained values, the estimated monthly values of the SRI index are calculated (figure 1).

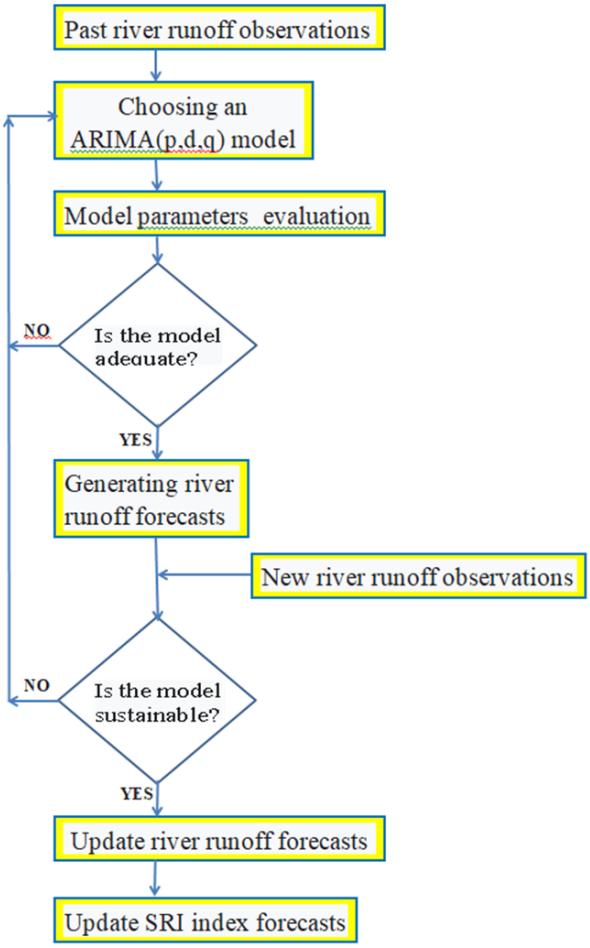


Fig.1 Scheme of the SRI forecasting process

The mathematical expression of the ARIMA(p,d,q) model with **p** number of autoregressive parameters, **q** number of moving average parameters and **d** number of differencing for the time series of observations of the river discharge $\boldsymbol{x_t}$ is as follows:

$$z_t = \sum_{j=1}^{p} \phi_j z_{t-j} + \varepsilon_t - \sum_{j=1}^{q} \theta_j \varepsilon_{t-j}$$

where at d=1, i.e. 1st order difference, each $z_t = x_t - x_{t-1}$.
In the case of periodic series, such as the monthly runoff $\boldsymbol{x_t}$ with a periodicity of 12 months, then their differentiation from the first order looks like: $z_t = x_t - x_{t-12}$. Second order differentiation (d=2) is accordingly:

$$u_t = z_t - z_{t-12} = (x_t - x_{t-12}) - (x_{t-12} - x_{t-24}) = x_t - 2.x_{t-12} + x_{t-24}$$

Therefore, for the ARIMA(p,d,q) model, (p+q+2) number of parameters must be estimated, namely:

$$\overline{z}, \phi_1, \ldots, \phi_p, \varepsilon_1, \varepsilon_2, \ldots, \varepsilon_q, \sigma_\varepsilon^2$$

The ARIMA(p,d,q) model combines two models: the autoregressive (short memory model) and the moving average (long memory model).

https://doi.org/10.5593/sgem2024/3.1/s12.04

Accuracy of results

Fisher's test [6] is recommended as a strict criterion for a good approximation of forecasted values compared to observed ones for the river runoff. In practice, it is used when sample sizes are small. The application of this test requires:

a. the observations in the two samples are random and independent;
b. the distributions of the two populations to be approximately normal.

Let :

- σ_1^2 and σ_2^2 are population variances of the two samples;
- S_1^2 and S_2^2 are the estimates of the variances of the two samples;
- ν1 and ν2 are the number of members of the first and second samples, respectively;

The hypotheses are defined accordingly:

1. The null hypothesis states that there is no statistically significant difference between the variances of the two populations.

$$H_o : \quad \sigma_1^2 = \sigma_2^2$$

2. In the general case, the alternative hypothesis states that there is a statistically significant difference between the variances of the two populations.

$$H_1 : \quad \sigma_1^2 \neq \sigma_2^2$$

To test the hypotheses in this case, the F-distribution (also known as the Fisher distribution of the probability - Fig.1) is used.

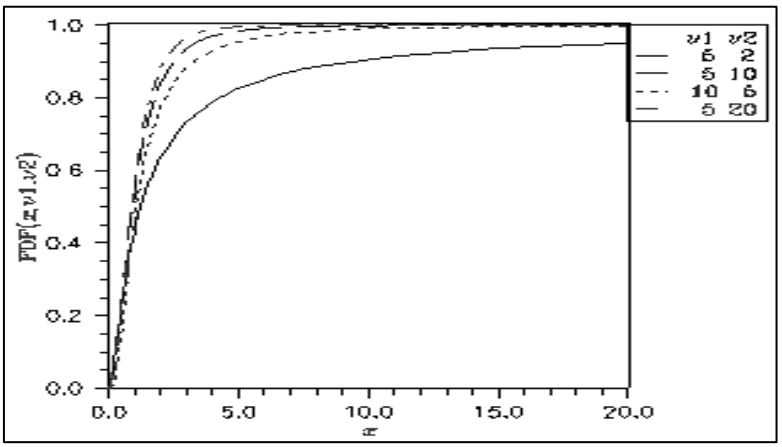


Fig.1 Fisher distribution of the probability

The distribution has three parameters: ν_1 – degree of freedom of the numerator; ν_2 – degree of freedom of the denominator in empirical characterization and degree of significance α.

The empirical characteristic F calculated for the two compared samples is determined by equation:

$$F = \begin{cases} S_1^2 / S_2^2 & , npu\ S_1^2 > S_2^2 \\ S_2^2 / S_1^2 & , npu\ S_1^2 < S_2^2 \end{cases}$$

The null hypothesis is not rejected if the empirical characteristic F is less than or equal to the theoretical one $F = (\alpha, \nu_1, \nu_2)$, i.e.:

$F \leq F(\alpha, \nu_1, \nu_2)$, where $\alpha = 0{,}01$ (1% possibility for error).

2. RESULTS

A 43-year mouthly series of runoff observations at the Botunya River, a tributary of the Ogosta River, are used[7]. The ARIMA(2,2,2) model is determined, as the best adequate model for the time series (Fig. 2).
With the help of this model, the monthly runoff for one year ahead is forecasted (Fig.3). The monthly SRI index is calculated based on the forecasted monthly runoff and it is compared with the SRI, calculated based on the observed runoff data (Fig. 4).

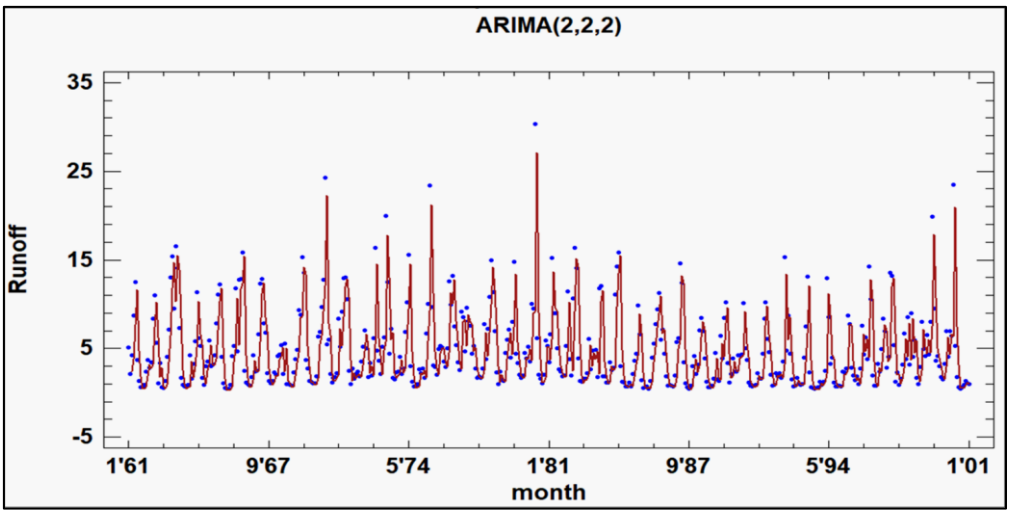


Fig. 2 River runoff hydrograph for 1961-2003
● observed runoff; ▬ modelled runoff

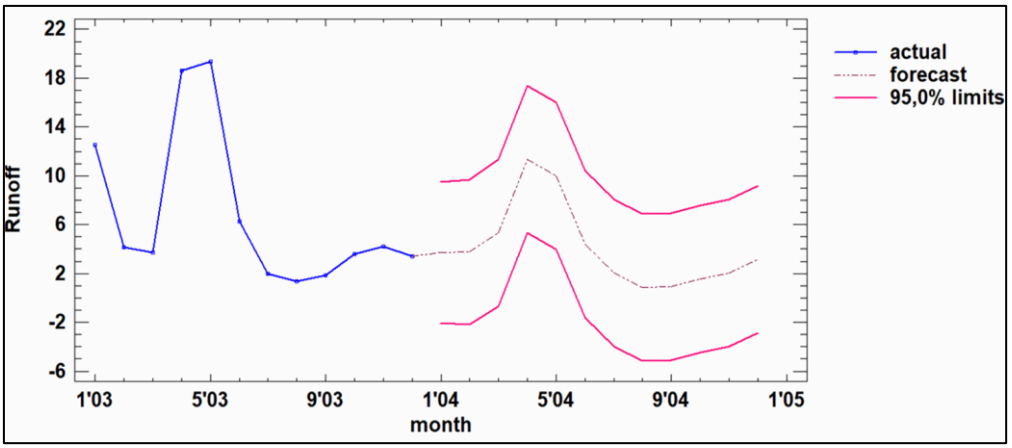


Fig.3 Hydrograph for forecasted river runoff in 2004
observed runoff; forecasted runoff

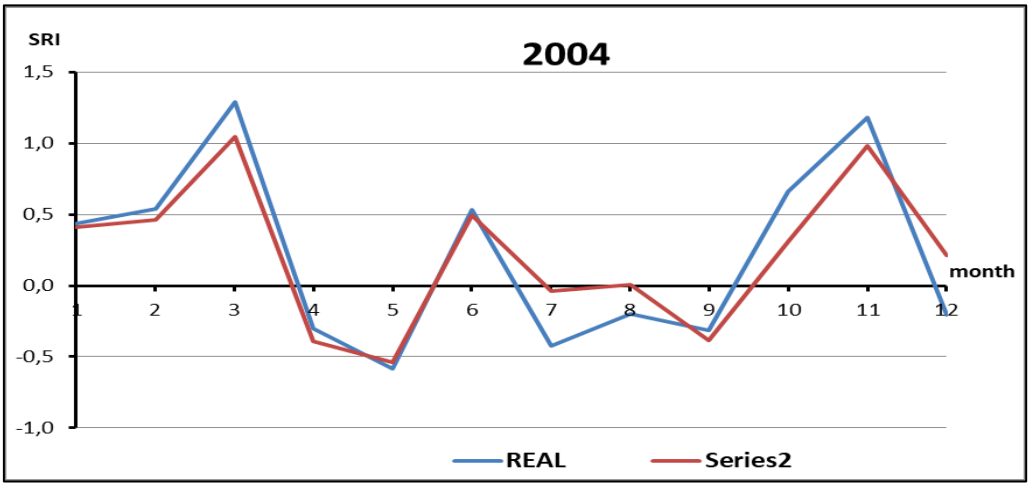


Fig.4 Hydrograph for SRI in 2004
observed runoff; forecasted runoff

The calculated monthly SRI index from the observed and forecasted river runoff values are given in a table 1.

Table 1 Real and forecast monthly SRI index

SRI	Jan	Feb	Mar	Apr	May	Jun	Jul	Aug	Sep	Oct	Nov	Dec
real	0,44	0,54	1,29	-0,30	-0,58	0,53	-0,42	-0,20	-0,31	0,66	1,18	-0,20
forecaste	0,41	0,46	1,05	-0,39	-0,54	0,49	-0,04	0,00	-0,39	0,31	0,98	0,21

In Fisher's test, the obtained characteristics of degrees and deviations are:

$\nu_1=12$ $\nu_2=12$

$S_1^2 = 0,41$ $S_2^2 = 0,26$

$$F = {S_1^2}/{S_2^2} = 1{,}56$$

From table 2 for the theoretical value is obtained: $F_{(1\%,12,12)} = 4{,}16$

Table 2 Theoretical *F*-distribution for α=0,01

υ_1 υ_2 =	1	2	3	4	5	6	7	8	9	10	11	12
1	4052.18	4999.50	5403.35	5624.58	5763.65	5858.99	5928.36	5981.07	6022.47	6055.85	6083.32	6106.32
2	98.50	99.00	99.17	99.25	99.30	99.33	99.36	99.37	99.39	99.40	99.41	99.42
3	34.12	30.82	29.46	28.71	28.24	27.91	27.67	27.49	27.35	27.23	27.13	27.05
4	21.20	18.00	16.69	15.98	15.52	15.21	14.98	14.80	14.66	14.55	14.45	14.37
5	16.26	13.27	12.06	11.39	10.97	10.67	10.46	10.29	10.16	10.05	9.96	9.89
6	13.75	10.92	9.78	9.15	8.75	8.47	8.26	8.10	7.98	7.87	7.79	7.72
7	12.25	9.55	8.45	7.85	7.46	7.19	6.99	6.84	6.72	6.62	6.54	6.47
8	11.26	8.65	7.59	7.01	6.63	6.37	6.18	6.03	5.91	5.81	5.73	5.67
9	10.56	8.02	6.99	6.42	6.06	5.80	5.61	5.47	5.35	5.26	5.18	5.11
10	10.04	7.56	6.55	5.99	5.64	5.39	5.20	5.06	4.94	4.85	4.77	4.71
11	9.65	7.21	6.22	5.67	5.32	5.07	4.89	4.74	4.63	4.54	4.46	4.40
12	9.33	6.93	5.95	5.41	5.06	4.82	4.64	4.50	4.39	4.30	4.22	4.16

Consequently the empirical $F < F_{(1\%,12,12)}$ and therefore the null hypothesis is NOT rejected, i.e. there is no statistically significant difference between the variances of the forecasted and observed SRI index samples.

The results show that the method is suitable for the river runoff and SRI index forecasting and will find wide application in the researches for regime optimization of the water management systems with ecological purpose in conditions of hydrological drought.

3. CONCLUSIONS

The management of river basins and dams under droughts sets new tasks for scientists related to the River Basin Management Plans (RBMPs), Drought Risk Management Plans, and the programme of measures[8],[9],[10]. The responsible institutions (Ministry of Environment and Water, Basin Directorates - BD, National Institute of Meteorology and Hydrology - NIMH) should solve tasks such as:

- Construction of early warning systems, systems for monitoring and forecasting of precipitation and river runoff, incl. operation of dams;
- Adaptation to climate change;
- Improving the flow regime, etc.

The main objective of the Water Framework Directive (WFD) is to achieve good ecological status. In support of these goals, NIMH is developing new approaches, models, indicator systems, early warning and decision support systems.

A methodology, which determines the monthly forecasts of the main for the hydrological drought SRI index, is presented. A moving average autoregression model is used to monthly time series modelling for the river runoff of a given site. The representativeness of the results is shown through the Fischer test.

SRI's monthly forecast is an important step in any study of hydrological drought. This approach is not difficult and can be applied to the SRI index also, as well as to other indices that are presented with monthly time series.

4. ACKNOWLEDGEMENTS

Thanks to the Ministry of Environment and Water for the support and to the experts from Executive Forest Agency, Forest Research Institute and NIMH, we work with to assess climate changes and water resources.

REFERENCES

[1] Hurvich, C. M., and Tsai, C.L., Regression and time series model selection in small samples, Biometrika 76, 1989.
[2] Box,G., Jenkins, G.: Time series analysis-forecasting and control. Revised edition, Holden-Day, 1976.
[3] Chang, Dayly Precipitation Modelling by Diiscrete Autoregressive Moving Avarege Processes, v.20,No.5 , 1984.
[4] Joseph, E.S., Some Applications of Statistic Hydrological Models. Proc. Int. Symp. on Modeling Techniques in Water Resources Systems, Canada,1972.
[5] Salas, J.D.,D.C. Boes, ARMA Modeling of Seasonal Hydrologic Series. J. Hyd. Div., ASCE, 1980.
[6] Storm, R., P. Muller, P. Neumann, Tables of Mathematical Statistics, M., "Finance and Statistics",1982.
[7] Dimitrov Y. "Application of the hydrological indices in determining the types of drought in the river Botunya", Journal of Meteorology and Hydrology,19/1 p.88–96, 2015.
[8] Monzonís, M., et al., A review of water scarcity and drought indexes in water resources planning and management, Journal of Hydrology, 2015.
[9] Ortega-Gomes,T., et al., Improvement of the drought indicators system in the Jucar River Basin, Spain, Science of the Total Environment, 2018.
[10] Rossi, G., Cancelliere, A., Managing Drought risk in water suplly systems in Europe: a Review. International Journal of Water Resources Development, 2012.

BLACK SEA THERMOHALIN STRATIFICATION: PARTICULARITY AND RECENT CHANGES

Dr. Nadezhda Valcheva[1]

[1]Institute of Oceanology – Bulgarian Academy of Sciences, **Bulgaria**

ABSTRACT

The Black Sea hydrological regime is impacted by external factors, which exerts effect on the sea surface in the process of interaction with the atmosphere and those confined to the lateral borders. The most pronounced features of the Black Sea thermohaline structure are large vertical contrasts in salinity (5 psu), temperature (20°C) and density (7 kg m^{-3}); well-defined vertical asymmetry; existence of a cold intermediate layer during the warm half of the year with an absolute vertical temperature minimum, below which temperature inversion takes place; major contribution of salinity to density stratification. In view of the accelerated climate change, it is particularly important to consider the state and modification of the thermohaline balance, because it gives indications about the phase of basin evolution and climate change impact on the stability of stratification and associated risks. Therefore, the goal of the present study is to summarize the contemporary knowledge of the thermohaline structure and to illustrate the changes that have occurred during the period 1993-2022.

Keywords: temperature, salinity, cold intermediate layer, water masses, climate change

INTRODUCTION

The Black Sea is an elliptical semi-enclosed basin with a unique thermohaline stratification. Its hydrological regime is formed due to the impact of external factors. They can be divided into two groups: factors excreting effect on the surface of the sea in the process of its interaction with the atmosphere (heat, humidity, salts and gases), and factors confined to the lateral borders (river inflow, water exchange, the associated heat and salt exchange through the straits, the topography). Interannual mean fields of temperature and salinity show the integral, long-term effect of each of these factors [1].

The monotonous Black Sea waters haline stratification is marked by one maximum of the vertical salinity gradients – the permanent halocline. The total external salt balance and the global mixing processes control the existence of this main halocline. On the other hand, the depth of Bosphorus Strait and basin shape also limits its depth [2]. It is also associated with the depth of autumn-winter convection [3]. Thus, the permanent halocline is located between 55–60 m and 100–110 m [1]. The flux of salts carried by the Bosphorus lower (bottom) current on the one hand, and the large river inflow and precipitation on the other, are the external factors causing the existence of the halocline.

The non-monotonic thermal stratification is defined by haline stratification [4]. It is characterized by a minimum in the upper part of the main halocline. There are two maxima of vertical temperature gradients. The largest negative gradient is in the layer of seasonal thermocline. It forms in summer because of heating and wind mixing in the surface layer. The seasonal thermocline has a crucial influence at a depth of 20–30 m. At

the end of autumn, it is eroded, and in winter, it disappears because of the intense convection. The second maximum of vertical positive gradients is in the region of the main (permanent) thermocline, which is located in the lower part of the main halocline. This creates conditions for a sharp density increase, which impedes water exchange between the surface fresher water masses and the denser layers lying below them. Hence, the Black Sea is conditionally divided into two layers – a relatively thin surface layer and an order of magnitude deeper layer – which differ significantly in terms of hydrochemical properties and dynamic regime. Between the two thermoclines are located the waters of the cold intermediate layer, which forms mainly in the western part of the Black Sea [5].

Depending on the nature of steady perennial spatial inhomogeneities and the presence of seasonal temperature fluctuations, the water column in the Black Sea can be divided into three layers. The active layer is the most variable, and its lower limit can be taken to be 200 m. In the limits of the 200–500 m layer, stable vertical and horizontal gradients are observed. At a depth greater than 500 m, there are no sustained horizontal changes. From a climatic point of view, only an increase in the water temperature at depth is found here, which is associated with adiabatic heating [3].

The Black Sea active layer on its own can be divided into two sublayers according to the mechanism of enthalpy change. The first one, in which the vertical heat exchange prevails, includes the upper mixed layer and the seasonal thermocline. The second is represented by the cold intermediate layer, whose enthalpy changes (especially in winter) due to the advection transfer. They spread parallel to the isopycnic surfaces in the upper layers of the permanent halocline [5]. Long-term changes in temperature and salinity fields in the Black Sea serve as a reliable indicator of regional climate changes. Therefore, the goal of the present study is to summarise the contemporary knowledge of the thermohaline structure and based on the author's own investigations to illustrate the changes that have occurred in the last two decades.

MATERIALS AND METHODS

The present study is focused on the western Black Sea and covers the entire water column. Regarding the cold intermediate layer, data for the entire Black Sea basin where it can be fully observed (both upper and lower limit present), typically at depths of more than 200 m, were used. In this case, the basin is divided into 5 subregions to distinguish between areas of specific mesoscale dynamics as indicated in Fig. 3. Four were delimited within the anticyclonic periphery – western (1), northern (2), eastern (3) and southern (4); and one comprising the cyclonic interior (5), confined approximately by the 1400-m isobath.

The studied period encompasses 30 years (1993–2022). An assessment is performed for two timespans: successive months of June-July-August-September and January-February-March roughly corresponding to summer and winter, respectively.

Data in use consist of temperature and salinity profiles originating from both *in-situ* shipboard and Argo profiling floats observations. Additionally, a dataset originating from expendable bathythermograph (XBT) casts was employed [6]. More than 10 000 profiles have been processed, 47% of which represent shipboard observations and 51% are data derived from Argo floats (starting from 2005). Concerning sea surface temperature, monthly global binned MODIS/AQUA Level 3 standard mapped night-time images at 4 km horizontal resolution were used as described in [7].

The study region comprises areas with varied hydrological features – nearshore, shelf, open sea (continental slope) – which were sampled with different temporal frequency and spatial density. Therefore, the interpolation grid resolution is a key element to properly estimate the regional thermohaline regime. From statistical point of view, a higher reliability can be achieved using as large as possible data volumes, while from dynamical point, processes' scales are of utmost importance. Hence, grid resolution should be consistent with the number and density of sampling station and quantity of data collated, on one hand, and typical mesoscale processes, on the other. From the hydrodynamic point of view, the intrinsic scale of Rossby deformation radius is leading in this study. It is reported to be 20-30 km in open areas and about several kilometers near the shore [8]. Thus, the climate fields of temperature and salinity were obtained by data interpolation onto a regular grid of 1/8° horizontal resolution employing the objective analysis [9]. The depth is resolved at each meter. Several features were examined such as typical temperature, salinity; depth and thickness of layers defining the thermo-haline stratification in the basin. Additionally, the indications supporting climate change impact are pointed out.

RESULTS AND DISCUSSION

Thermal stratification

Sea surface temperature (SST) is the temperature of the extremely thin (about 10 μm) interface between the ocean and the overlying atmosphere, which controls heat and gas exchange and responds most quickly to the atmospheric impacts. This is the reason why SST experiences a significant spatial and temporal (interannual, seasonal, and synoptic) variability [10]. Moreover, the spatial variations of SST can be used as an indicator of the large- and mesoscale dynamics of the waters in the Black Sea and an impact on the temperature of the cold intermediate layer.

During the 20th century, the Black Sea surface temperature had been constantly increasing due to climate change. Analysis of SST data covering the period 1982–2015 showed that SST had increased with a rate of 0.64°C per decade thus conforming to the worst climate change scenario. Thus, by the end of 21century, the relative increase of the average SST was predicted to be 5.1°C [11]. Moreover, the large area-dependent differences could exist between the SST and air temperature, creating an important eddy-dominated component of the ocean-atmospheric heat exchange [12].

To examine winter and summer dynamics of the SST in the western part of the Black Sea, data for the period 2003–2019 have been analysed. The winter climatic SST distribution reveals the main features of typical seasonal dynamics, namely presence of narrow frontal zone of sharp horizontal gradients between coastal and inner shelf waters, on one hand, and outer shelf and deep basin, on the other, defined between 6.8 and 7.6°C isotherms; colder coastal waters of temperatures lower than 6.2°C; and vast area of quasi uniform open sea waters of temperatures about 8°C (Fig. 1). The front is determined by intensification of the large-scale circulation. As a result, the flow of Rim current is strongly pressed against the basin lateral boundary and both intense mixing of surface waters and restricted water exchange with the northwestern shelf are observed.

In summer, the relatively cooler waters in the northernmost part of the domain are marked by temperatures lower than 24.1°C. Farther within the western shelf, these waters are being transformed while their impact can be traced along the entire shelf curve. The

frontal zone is less discernible and considerably wider with respect to winter, which is determined by the weakening and instability of the large-scale circulation (lower Rim current velocity) and existence of quasi-stable (recurrent) anticyclonic eddies (Fig. 1). For example, the Burgas eddy is visible on the SST climatic distribution on the coastal side of the Rim current in both seasons marked by temperatures higher than 24.3°C in summer and lower than 6°C in winter, that is being slightly warmer and cooler, respectively, with respect to the surrounding waters. The same is valid for the Kaliakra eddy that contains cooler waters in both seasons – less than 6.4°C in winter and 24.0°C in summer. Thus, the summer circulation pattern allows for horizontal water exchange between the periphery of the large-scale gyres and the shelf. The process of entrainment of warmer open seawaters (SST>24.5°C) in the shelf and nearshore zone, which are being spread to the north, is particularly visible in the middle and southern part of the western Black Sea. The summer SSTs increase from northwest to southeast as the spatial temperature variability ranges in less than 0.7°C, i.e. three to four times smaller compared to the winter (2.6°C).

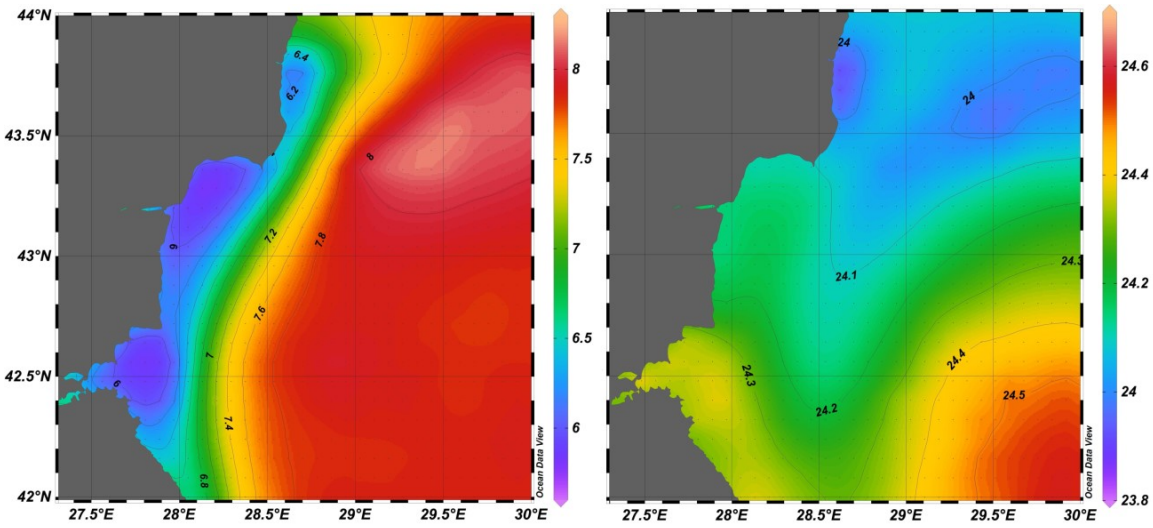


Figure 1. Spatial distribution of the sea surface temperature (°C) in winter (left) and summer (right) in the western Black Sea for the period 2003–2019

Atmospheric warming of the sea surface and winter SST can be used as an indicator of the cooling intensity. With this respect, the warmest winters were those of 2007, 2009-2010, 2014, 2016 and 2020 (SST maxima of 7.9–8.7°C) and the coolest once were in 2006, 2012 and 2017 (4.3–4.8°C). Over the past 20 years, both winter and summer SSTs exhibit increasing long-term trends; there is almost uniform increase of the winter SSTs of 0.6–0.7°C per decade for all zonal areas, while the summer ones tend to vary in somewhat wider range 0.5–0.7°C per decade, with the warming of coastal waters being more pronounced.

The ocean mixed layer defines a vertically quasi-homogeneous surface region of temperature, salinity, or density, which directly interacts with the overlying atmosphere. Atmosphere-ocean interaction, therefore, can be modulated by the ocean mixed layer, whose depth is determined by wind driven mechanical stirring, surface buoyancy forcing, such as heat or freshwater flux, or ocean circulation changes [13]. Changes in the mixed layer depth influence the variability of the SST and oceanic uptake of atmospheric CO_2. On the other hand, they can affect primary production and timing of autumn and spring

phytoplankton blooms by altering nutrients supply and light conditions, thus affecting biological productivity in the Black Sea and subsequently higher trophic levels [14].

In the Black Sea, the mixed layer depth is distinguished with great seasonal dynamics. It rarely exceeds 50 m during winter; while, in summer, it is relatively thin (15–20 m) due to the low intensity of hydrodynamic processes, in contrast to the cooling during winter convection. Due to the variation of the depths in the coastal zone and the dome-like spread of isopycnal surfaces, the depth of the surface mixed layer also varies in space (Fig. 2). The temperature in the layer varies from 27°C in August to 19°C in September. Over the past 20 years, there has been an increasing trend in surface mixed layer temperature, with two periods of gradual increase are identified being 1997–2007 and 2008–2016, which suggests a quasi-decadal scale of change. The amplitude of the changes increases from the north (0.53°C per decade) to the south (0.97°C per decade); hence, in the southern regions the increase in temperature is more notable.

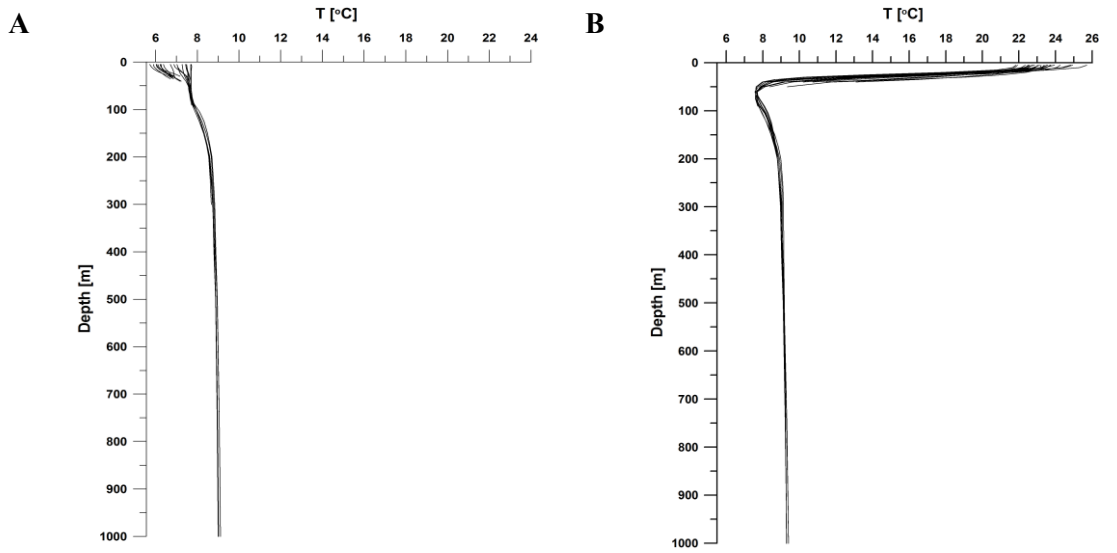


Figure 2. Climatic temperature profiles representative for 1993-2010 in the layer 0–1000 m: winter (A) and summer (B)

Below this relatively homogeneous surface water stratum, the seasonal thermocline lays. It represents a transition layer between the warm surface waters and the colder waters in the rest of the water column. Its formation begins in the end of March and beginning of April with the sea surface warming, which penetrates to depth due to the vertical water exchange. In August, the position of the seasonal thermocline approximately corresponds to 20 m depth. In the western part of the Black Sea, it is located 5–7 m deeper compared to the southern one, i.e. at a depth of about 25 m in the coastal area and 15 m in the open sea. This layer is associated with strong vertical gradient in the seasonal thermocline and is about 10 m thick due to the deviation from the horizontal position related also to presence of large horizontal gradient. The temperature in this layer decreases by 12–15°C and salinity increases with about 0.5 psu, while the density jumps from 12.0 to 14.0 kg/m^3. In the coastal and shelf areas, the temperature drops by 3–4°C reaching 9°C at the bottom.

One of the features of a fundamental importance is the Cold Intermediate Layer (CIL), which represent the interface between surface and deep Black Sea waters. Its lower boundary corresponds to the permanent pycnocline, while in the second half year (from June to December) the layer's upper boundary is limited by the seasonal thermocline.

Traditionally confined by the 8°C isotherm, the CIL contains water with the lowest temperatures along the entire column, including those of the upper pycnocline [15, 16].

It has been established that the CIL is formed both in the centres of cyclonic gyres and by extreme cooling of waters in the northwestern shelf and continental slope [3, 17], which are afterwards advected throughout the Black Sea between depths of approximately 50–100 m through the cyclonic circulation dominated by the Rim Current. Baroclinic eddies formed on both sides of the Rim Current play an important role in the horizontal exchange of heat and salt [18]. The depth of temperature minimum – cold intermediate layer core – can sink down to more than 110 m in anticyclonic edge and rise to 30 m in cyclonic centre [19] with respect to average values of 60–90 m for the continental slope.

The cold intermediate layer thickness interannual variability reveals a steady decreasing trend. It was found to grow thinner as its thickness dropped by more than half during the study period, from hundred in the beginning to several tens of meters depending on the basin subregion. More specifically, in summer, the thickness changed from 95–125 m in 1993 to 45–55 m in 2018 in the anticyclonic periphery, and between 73 and 38 m, respectively, in the basin interior (Fig. 3A).

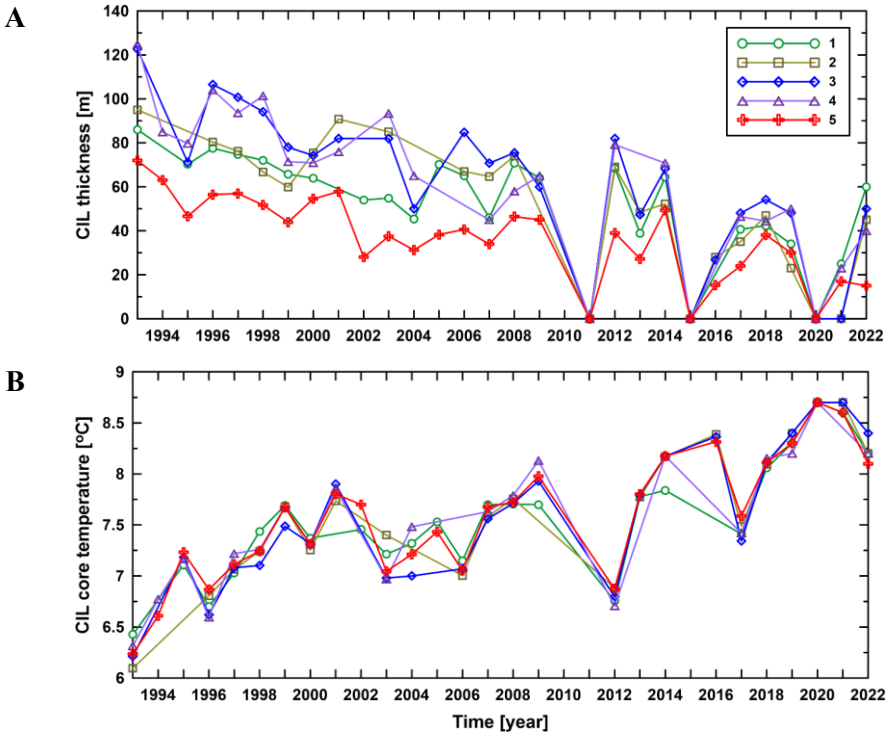


Figure 3. Interannual variability of the cold intermediate layer thickness (A) and core temperature (B) averaged over summer

Ever since 1995, the intensity of the cold intermediate layer replenishment has been reducing and according to [20] it was weaker than the climatic mean. Several exceptions were noted in 2003, 2004, and 2006, which corresponds to the mean climatic conditions and more intense winter cooling [21]. The result shown in Fig. 3 supports this finding. Later, following a sequence of not particularly cold winters, bringing forth a weak ventilation of the active layer, the cold intermediate layer disappeared in 2011, 2015–2016, and most recently in 2020-2021.

Nevertheless, it appears that the thickness decrease (so as the layer shrinking) is not an irreversible process since because of the 2012 winter cooling, in only a year timespan, the cold intermediate layer grew thicker being renewed to reach the levels of the 2003–2006. A frail recovery was also observed in 2022.

Evidently, the occurrence of severe winter cooling with consequent intensification of vertical and horizontal mixing leads to pycnocline deepening so as to a more effective cold layer replenishment. Thus, in 2017 and 2018 a slight recovery has also been observed since the thickness drop in 2016. A summarized time series of all vertical profiles for the western part of the Black Sea, regardless of their specific geographical location, is presented in Fig. 4, which clearly shows the trend of CIL thickness decrease and its disappearance since 2000.

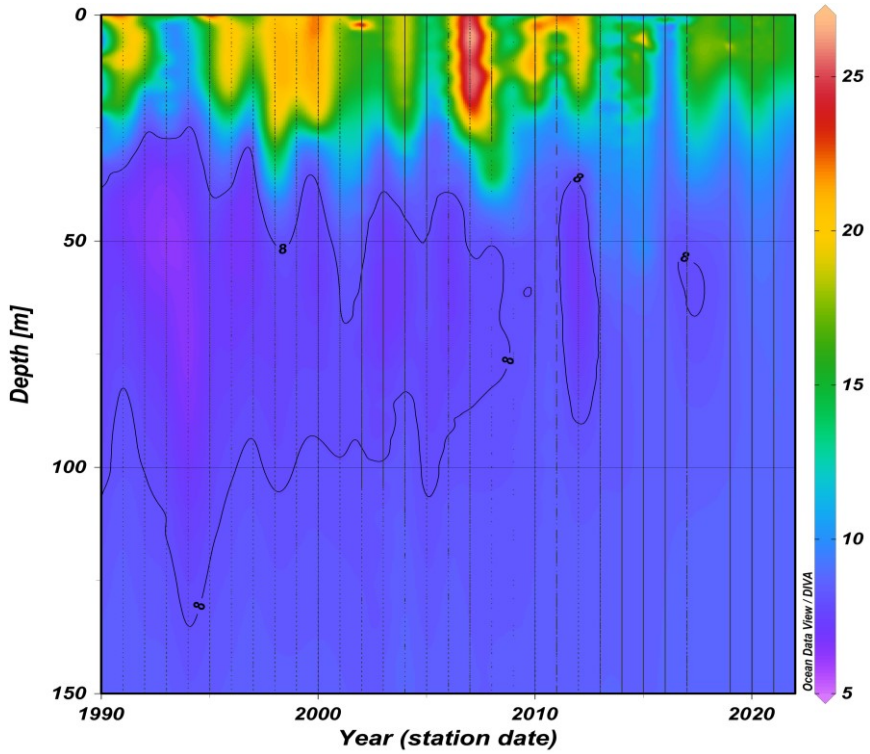


Figure 4. Hovmoller diagram showing interannual variability of the water temperature in the surface 0-200 m. The black contour denotes isotherm 8°C

Together with the decrease of cold intermediate layer thickness, the temperature in its core has been constantly growing higher from 6.3°C in 1993 to 8.2°C observed in 2014–2016 and 8.6 in 2020–2021, i.e. during periods in which the layer was disrupted (Fig 3B). The cold intermediate layer recovery in 2003, 2006 and 2012 was accompanied by lowering of the core temperature down to about 7°C, which was the level in the late 1990s. The maximum cooling with 1.13°C was observed in 2012. Although presence of CIL was observed in 2022, the temperature variation within the layer was so small – only 0.2–0.3°C – hence, it could be considered as a weak sign of recuperation but not as a renewal of the layer.

The process of increased warming of the Black Sea surface waters for the past 10–15 years has led to alteration of isotherm surfaces marking out the cold intermediate layer limits. Historically defined by the isotherm 8°C, since 2007 it has been gradually shifting towards higher values to reach 8.4°C during the period preceding the 2012 cooling. After

the latest marked recovery in 2012, this temperature was increasing again and in recent years, it has been set in the range of 8.5–8.6°C.

The Black Sea permanent thermo-halocline (pycnocline) is a layer of about 100 m thickness separating relatively warm, more saline, anoxic, and homogeneous water mass of the lower layer from the water of the less saline, oxygenated, highly variable and relatively thin upper layer. Entering the through the Bosporus, the Marmara Sea waters spread like a plume and following the bottom and underwater canyons mix with the waters of the Black Sea. Being denser, these waters penetrate below the permanent pycnocline, thus ensuring ventilation of the Black Sea deep layers. They are also the main source of salt and heat. Since the heat flow in the pycnocline layer is always directed towards the surface, any cooling or warming at a certain depth leads to an increase or decrease in the ventilation rate. The analysis of regional distribution of physicochemical properties during the winter months shows that the lower part of the pycnocline is continuously ventilated by isopycnic movement of waters penetrating through the Bosphorus, while the effective ventilation of its upper part is an episodic process (once every few years) in response to extreme winter surface cooling. The latter mechanism takes place in the parts of the basin with prevailing cyclonic circulation and is intensified with strengthening of the general circulation [22, 23].

In the deep-water part of the Black Sea, the temperature increases monotonically due to inflow of warmer (13–16°C) Marmara Sea waters. The hyper adiabatic temperature inversion in the deep layers, where the temperature reaches 9°C, is also related to the geothermal heat flow from the bottom of the Black Sea.

Haline stratification

Seasonal variability of salinity in the surface layer is related to the amount of river inflow, superimposing the influence of atmospheric precipitation, evaporation, and the intensity of mixing with the underlying layers. Because of the cyclonic nature of the general circulation, waters of lower salinity entering from the large rivers mouth spread in the form of a plume. Minimum salinity is observed at the mouth of the Danube River, where waters with a salinity of 13 psu are constantly present. As they move to the south, they are transformed, and in the Cape Kaliakra area, the salinity increases to 16–17 psu.

Maximum salt content in the surface layer is observed in February and March. This is related to the intensification of the wind stirring and convection, causing the surface 50–60 m layer to be practically isohaline. In coastal water areas, the average surface salinity is 16.5–16.8 psu, while it rises to 17.2–17.5 psu in the shelf. Continuing its increase, the salinity reaches 17.7–18 in the open sea (Fig. 5A). The above results in higher vertical gradient (0.02–0.03 psu m^{-1}) observed in the coastal and shelf waters compared to the open sea (0.01 psu m^{-1}).

The spring warming of surface waters slows down the convection, which leads to the intensification of horizontal diffusion. At the same time, the quasi-stationary salinity fronts are strengthened, especially in the northwestern areas. The increasing river inflow causes surface waters in the western shelf to be freshened up to 15.5 psu. Due to the surface mixing, a seasonal halocline is often formed ay about 20 m depth, which is observed all over the coastal and shelf areas. In the open sea areas, the salinity is around 18.2–18.4 psu (Fig. 5A).

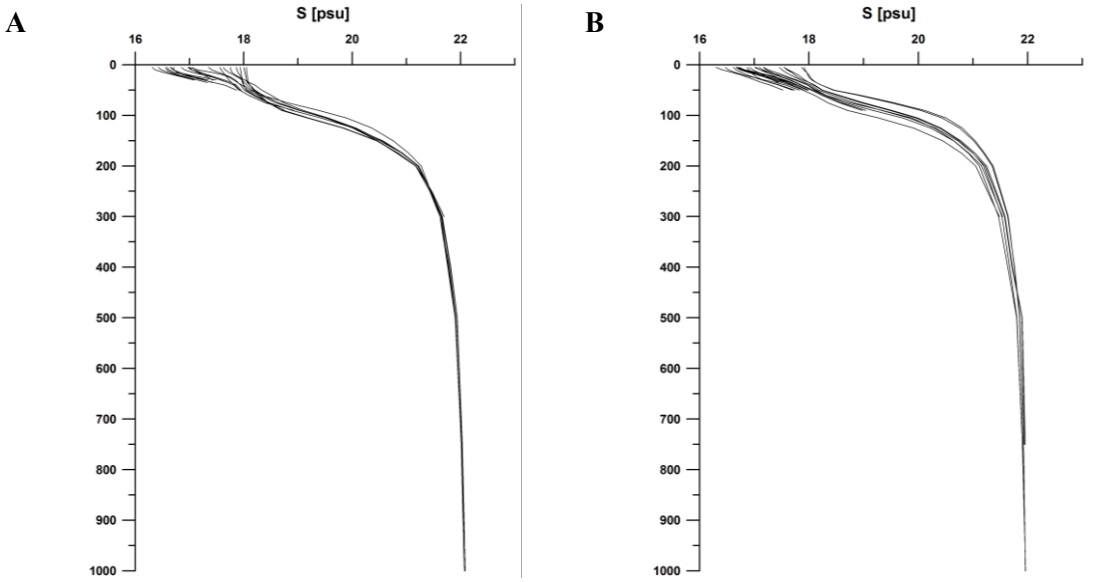


Figure 5. Climatic salinity profiles representative for 1993-2010 in the layer 0–1000 m: winter (A) and summer (B)

The transformation of salinity field in summer is determined by the gradual extension of freshening zone at the expense of diffusion. The excessive heating of waters in shallow areas leads to a greater evaporation and increase in salinity to about 17 psu. Due to the limitation posed by the coastal orography, locally formed waters are observed in bays and adjacent narrow coastal areas where the salinity is greater than 17 psu. The salinity increases southward varying between 16.7–16.9 psu in the northern part and 17.1–17.3 psu in the southern part of the western shelf. In open sea (cyclonic) areas, the average surface salinity increases and varies within 17.5–17.97 psu (Fig. 5 B).

Salinity gradually increases in the deeper layers until the permanent halocline where it is marked by isohaline 18.5 psu. Its upper limit is located at different depths – from 75 m on the shelf to 50 m in the open sea. The specific markers of winter stratification, such as the depth and thickness of the layer of permanent halocline, are about 120 m and 185–195 m, respectively. They experience weak zonal variations within 5–10 m but are located at a shallower depth compared to summer due to the sharpening of the dome-like stratification resulting from the more intense circulation. Thus, zonal variations in the thickness of the permanent halocline are from 130 m on the shelf to 110 m in the open sea. The maximum depth changes from 200 m to 160 m accordingly. The average salinity in the layer increases from 19.6 to 20.3 psu. The lower part of the halocline promotes a stable density stratification. Below the halocline, salinity increases monotonically to the bottom and at 1500 m reaches 22.3 psu.

Water masses

The structure of waters in the western Black Sea is defined by the presence of four types of water masses – shallow (surface), subsurface, intermediate and deep. This structure shows up well in temperature-salinity diagrams, also known as T-S curves (Fig. 6). The area can be divided into three meridional parts according to their specific features: coastal, shelf and open sea. In the coastal part, two water masses are observed in summer – shallow and subsurface, and in winter – only one. The shelf also includes the intermediate, and a smaller or larger part of the deep-water mass. To reveal the climate change impact, two periods were considered 1993-2010 and 2011-2022.

The summer T-S curve exhibits the typical *L*-shape, which defines a mixing triangle (Fig. 6A, C). This means that three water masses are present: subsurface, intermediate and deep-water. The surface is located at the top of the T-S curves and is not included into the mixing triangle. The well-pronounced *L*-shape indicates little or no mixing between them, which is due to the strong summer stratification.

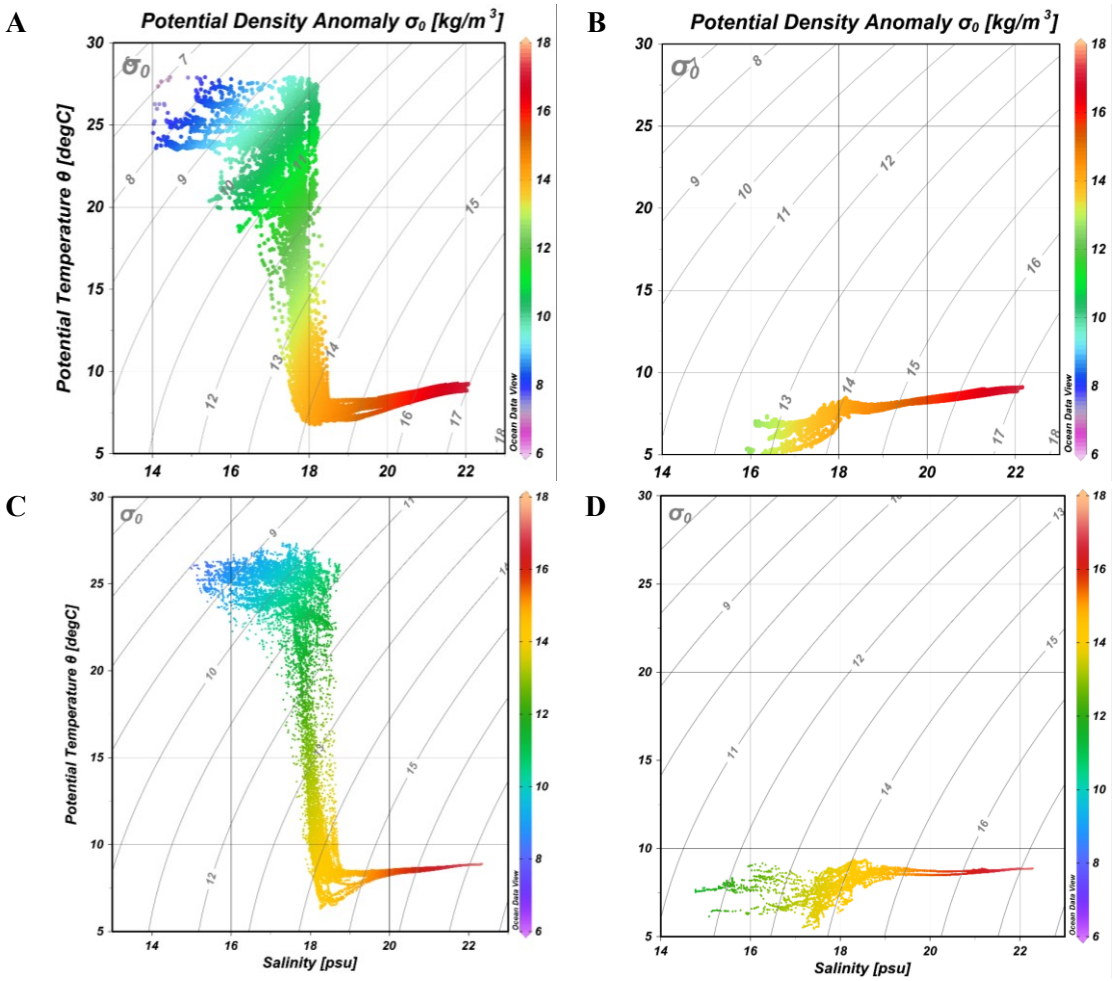


Figure 6. T-S diagrams of water masses in the western Black Sea relevant for periods 1993-2010 (A, B) and 2011-2022 (C, D): summer (A, C) and winter (B, D)

In winter, due to the cooling of the surface layer, the T-S curve has a close to linear shape (Fig. 6 B, D). The presence of a surface water mass in the upper 50 m, formed due to the cooling and convection processes, makes the curve shape more complex. This mass is distinguished with uniform temperature and very weak salinity fluctuations (i.e. isothermal and quasi-isohaline). Additionally, the intermediate and deep-water masses are observed. The curve shape indicates a more active mixing between the shallow and subsurface water masses, which even merge into a single water mass.

The summer T-S diagram suggests that the highest variability is observed in the surface 50–60 m layer. The largest volume of shallow (surface) water mass is detected in the bays and coastal waters, incorporating almost the entire water column. Its existence is determined by the presence of fresher (the lowest salinity of 14–16 psu) and warmer (23–27°C) waters. The boundary between shallow and subsurface water masses is located at

15 m with T-S index (22.5; 17.3) relevant for 1993-2010 and (24.6; 17.4) for 2011-2022. Hence, the mixed layer temperature increased with more than 2°C on the average.

The subsurface water mass comprises mainly the waters in the thermocline and is also widely distributed. Its volume decreases during the transition to deep waters, which is related to the shallower depths of thermocline. The limit between subsurface and intermediate water masses is located at a depth of 25–30 m and has T-S index (14.7; 17.8) relevant for 1993-2010 and (15.1, 18.0) for 2011-2022, which also indicates a rise of temperature.

The intermediate water mass consists of the waters of the cold intermediate layer with an absolute temperature minimum and salinity above 18.0 psu. The presence of this layer prevents mixing between the surface and deep-water masses in summer. The core of the intermediate water table is located at a depth of 50-75 m and has a T-S index (7.5; 18.5) for 1993-2010. As commented above, the core temperature increased drastically during the last decade while salinity remained stable. This find expression in the average index of (8.3; 18.5). The well-defined deep-sea mass is observed only in the open sea. It borders the intermediate one at about 120 m depth and is characterized by T-S index (8.2; 20.0) for 1993-2010. The temperature increase can be traced to these depths as the index is (8.4, 20.0).

In winter, the surface and subsurface water masses actively mix between each other and form one water mass spreading to a depth of about 30 m in cyclonic and 50–55 m in anticyclonic areas. The T-S index of this boundary is (7.7; 18.0) relevant for 1993-2010 and (8.0, 18.0) for 2011-2022. This mass covers the entire water column in the coastal areas. Due to the erosion of the cold intermediate layer, which is rarely observed during the last ten years, the surface water mass increases its volume at the expense of the intermediate one. On the other hand, the deepening of the latter is observed and the corresponding boundary with the deep-water mass is located at 120–130 m depth having the T-S index (8.3; 20.0) for 1993-2010 and (8.5; 20.0) for 2011-2022. The index value almost corresponds to the summer one, which indicates the weak exchange between the intermediate and deep-water masses. The results obtained also point out to a temperature increase.

CONCLUSION

The present study did an attempt to summarize the contemporary knowledge of the thermohaline structure in the Black Sea and by employing a large amount of temperature and salinity data to outline the changes that have occurred during the period 1993-2022. During the 20th century, the Black Sea surface temperature had been constantly increasing due to the atmospheric warming, which can be considered a climate change impact. The process can be traced over the entire active 150 m layer. Over the past 20 years, both winter and summer sea surface temperature exhibit increasing long-term trends – 0.6–0.7°C per decade on the entire western basin, while the summer ones tend to vary in the range 0.5–0.7°C per decade as the warming of coastal waters was more pronounced. The same is valid for the mixed layer as the amplitude of the changes increases from the north (0.53°C per decade) to the south (0.97°C per decade).

One of the features of a fundamental importance is the cold intermediate layer. Here, the most alarming changes occurred, leading to its disruption affecting the thermal balance. The layer thickness shows a steady decreasing trend as it dropped by more than half

during the study period, from hundred in the beginning to several tens of meters depending on the basin region. The intensity of the cold intermediate layer replenishment has been reducing since 1995. Presence of warm winters, bringing forth a weak ventilation of the active layer, caused its disappearance in 2011, 2015–2016, and most recently in 2020-2021. Together with the decrease of cold intermediate layer thickness, the temperature in its core has been constantly growing higher from 6.3°C in 1993 to 8.2°C observed in 2014–2016 and 8.6 in 2020–2021. This finding is supported by the changing characteristic of water masses. On this background, the haline stratification appears to be stable thus contributing to the thermohaline balance.

ACKNOWLEDGEMENTS

This work has been carried out in the framework of the National Science Program "Environmental Protection and Reduction of Risks of Adverse Events and Natural Disasters", approved by the Resolution of the Council of Ministers № 577/17.08.2018 and supported by the Ministry of Education and Science (MES) of Bulgaria (Agreement № Д01-27/06.02.2024).

REFERENCES

[1] Гидрометеорология и гидрохимия морей СССР (Альтман, Э. Н., Ворник, В. И., Ред.), Том IV: Черное море, Гидрометеоиздат, Санкт-Петербург, 430, 1991;

[2] Korotaev G., Oguz T., Riser S., Intermediate and deep currents of the Black Sea obtained from autonomous profiling floats, Deep Sea Research Part II: Topical Studies in Oceanography, vol. 53, pp 1901-1910, 2006;

[3] Stanev E.V., Bowman M.J., Peneva E.L., Staneva J.V., Control of Black Sea intermediate water mass formation by dynamics and topography: Comparison of numerical simulations, surveys and satellite data, Journal of Marine Research, vol. 61, pp 59-99, 2003;

[4] Oguz T., Aubrey D.G, Latun V.S., Demirov, E, Koeshnikov L., Sur H.I., Diaconu V.S, Besiktepe S., Duman M., Limeburner R., Eremeev V., Mesoscale circulation and thermohaline structure of the Black Sea observed during HydroBlack ’91, Deep Sea Research Part I, vol. 41, Issue 4, pp 603–628, 1994;

[5] Блатов А.С., Булгаков Н.П., Иванов В.А., Косарев А.Н., Тужилкин В.С., Изменчивость гидрофизических полей Черного моря, Гидрометиздат, Ленинград, 240, 1984;

[6] Valcheva N., Valchev N., An evaluation of temperature and depth accuracy of Sippican T-6 and T-10 Expendable bathythermographs (XBT) in the western Black Sea, Proc. of 12th Int. Conf. on “Marine Sciences and Technologies - Black Sea’2014”, Bulgaria, 2014, pp 183-188;

[7] Valcheva N, Slabakova V., Winter and summer variability and trends of MODIS derived sea surface temperatures for the western Black Sea, Proceeding of 1st Int. Conf. on Environmental Protection and disaster RISKs – Part One, Az-buki National Publishing House, 2020, pp 8-20;

[8] Stanev E., Rachev N., Numerical study on the planetary Rossby modes in the Black Sea, Journal of Marine Systems, vol. 21, 283-306, 1999;

[9] Barnes S.L., A technique for maximizing details in numerical weather-map analysis, Journal of Applied Meteorology, vol. 3, No. 4, 396-409, 1964;

[10] Ginzburg A.I., Kostianoy A.G., Sheremet N.A., Sea surface temperature variability. The Black Sea Environment. The Handbook of Environmental Chemistry. Vol. 5: Water Pollution, Part 5/Q, Kostianoy A.G. and Kosarev A.N., (Eds.). Springer-Verlag Berlin Heidelberg, 255-276, 2008;

[11] Sakalii A., Başusta, N., Sea surface temperature change in the Black Sea under climate change: A simulation of the sea surface temperature up to 2100, International Journal of Climatology; vol. 38, Issue13, pp 4687-4698, 2018;

[12] Stanev E.V., Staneva J.V., The sensitivity of the heat exchange at sea surface to meso and sub-basin scale eddies: Model study for the Black Sea, Dynamics of Atmospheres and Oceans, vol. 33, Issue 3, pp 163–189, 2001;

[13] Jang C.J.,Park J., Park T., Yoo S., Response of the ocean mixed layer depth to global warming and its impact on primary production: a case for the North Pacific Ocean, ICES Journal of Marine Science, pp 996–1007, 2011;

[14] Oguz T., Ducklow H.W., Malanotte-Rizzoli P., Modeling distinct vertical biogeo-chemical structure of the Black Sea: Dynamical coupling of the oxic, suboxic, and anoxic layer. Global Biogeochem. Cycles, vol. 14, pp 1331-1352, 2000;

[15] Oguz, T., Besiktepe, S., Observations on the Rim Current structure, CIW formation and transport in the Western Black Sea. Deep Sea Research, Part I: Oceanographic Research Papers, vol. 46, Issue 10, 1pp 733–1753, 1999;

[16] Ivanov L.I., Backhaus J.O., Özsoy E., Wehde H., Convection in the Black Sea during cold winters, Journal of Marine Systems, vol. 31, pp 65–76, 2001;

[17] Ivanov L.I., Besiktepe S.T., Özsoy E., Sensitivity to Change: Black Sea, Baltic Sea and North Sea, The Black Sea cold intermediate layer, Kluwer Academic Publisher, pp 253–264, 1997;

[18] Kubryakov, A.A., Stanichny S.V., Seasonal and interannual variability of the Black Sea eddies and its dependence on characteristics of the large-scale circulation. Deep Sea Research Part I: Oceanographic Research Papers, vol. 97, 8pp 0–91, 2015;

[19] Zatsepin A.G., Ginzburg A.I., Kostianoy A.G., Kremenetskiy V.V., Stanichny S.V., Poulain P., Observation of Black Sea mesoscale eddies and associated horizontal mixing, Journal of Geophysical Research: Oceans, vol. 108, Issue C8, pp 1-27, 2003;

[20] Belokopytov V., Interannual variations of the renewal of waters of the cold intermediate layer in the black sea for the last decades, Physical Oceanography, vol. 20, pp 347–355, 2011;

[21] Piotukh V.B., Zatsepin A.G., Kazmin A.S., Yakubenko V.G., Impact of the winter cooling on the variability of the thermohaline characteristics of the active layer in the Black Sea. Oceanology, vol. 51, pp 221–230, 2011;

[22] Ovchinnikov I.M., To the question of cold intermediate layer formation in the Black Sea, DAN SSSR 279, pp 986-988, 1984;

[23] Ivanov L.I., Besiktepe S., Black Sea Cold Intermediate Water Mass Volumetric Structure and its Variability. In: Oceanic Fronts and Related Phenomena. Konstantin Fedorov memorial Symposium. St. Petersburg, Pushkin, 1998.

CATCHMENT ABSTRACTION MANAGEMENT STRATEGY AND ECOLOGICAL FLOW DETERMINATION IN CASE OF NATURA 2000 AREAS

Assoc. Prof. Dr. Irena Ilcheva[1]

Assoc. Prof. Dr. Vesela Zaharieva[2]

Assoc. Prof. Dr. Anna Yordanova[1]

Assoc. Prof. Dr. Snejanka Balabanova[1]

[1] National Institute of Meteorology and Hydrology, **Bulgaria**
[2] University of Architecture, Civil Engineering and Geodesy, **Bulgaria**

ABSTRACT

A classical approach to the assessment of the available water resources for different users, including environmental, in Europe is the Catchment Abstraction Management Strategy (CAMS). An assessment has to be made of the extent, to which natural runoff regime could be changed without affecting the sustainable functioning of the environment. The aim of the Restoring Sustainable Abstraction (RSA) is to identify over-abstraction in rivers and wetland sites and make the abstraction sustainable again. In this regard, the report presents an innovative approach for the integrated assessment and management of the water and natural resources (water ecosystems, wetlands, forest, etc.) in cases of Natura 2000 areas (on the example of Vitosha Nature Park, Sanitary Protection Zones of the Struma River Basin, etc.). In the methodology, the ecosystems are also part of the measures. Some measures (such as to restore water regime of the peatlands) are non-traditional measures for RSA and supply-side drought measure. This is a step towards improving the CAMS approach. The main stages of the improved methodology are: Modeling and assessment of climate factors and trends; Water balance modeling; Assessment of water consumption and the environmental needs; Ecological flow assessment and RSA; Simulation modeling and CAMS; Monitoring and adaptive management. A methodology and a mathematical model for determination the ecological flow in Bulgaria which is a necessary condition for achieving a good ecological status are proposed. As an object of research macrozoobentos ecosystem are considered. Emphasis is given to the places of water abstraction, water transfer, rivers at risk of not achieving good ecological potential (hot spots). Measures with synergistic effects are recommended – to protect ecosystems, for flood risk prevention, etc. The results and applications in practice are related to the Vitosha Nature Park Management Plan, Program of Measures, for the goals of WFD and Natura 2000 and supports the MoEW and Basin Directorates in determining the ecological flow and implementation the Eflow concept in Bulgaria.

Keywords: ecological flow, macrozoobentos ecosystem, water balance modeling, Catchment abstraction management strategy, Natura 2000

INTRODUCTION

The environment and ecosystems are affected by human activity and land use changes, climate changes and extreme events (intense rainfall, floods, drought, etc.), invasive species, etc. Water resources are subject to water abstraction, water transfer, hydromorphological alterations, etc. All these factors are a risk to ecosystems, but also a risk to the drinking water supply, to the economy, etc. A classical approach to the assessment of the available water resources for different users, including environmental, in Europe is the Catchment Abstraction Management Strategy (CAMS) [8], [10]. An assessment has to be made of the extent, to which natural runoff regime could be changed without affecting the sustainable functioning of the environment [11]. The aim of the Restoring Sustainable Abstraction (RSA) is to identify over-abstraction in rivers, wetland sites and to make the abstraction sustainable again [10]. Natura 2000 is a network of protected areas that aims to protect the valuable habitats. The specificity of Natura 2000 areas, water protection zones, etc., requires new, non-traditional approaches to the assessment of water resources and ecosystems.

MATERIALS AND METHODS

In this regard, an innovative approach for the integrated assessment and management of the water and natural resources (water ecosystems, wetlands, etc.) in cases of Natura 2000 areas is developed and applied [3], [4], [8]. In the methodology, not only the assessment of the available water resources and the review of water rights are measures, but the ecosystems and their functions are also part of the measures. Some measures (such as water regime restitution of the peatlands, integrated management of the water and forest in the Sanitary Protection Zones) are non-traditional measures for RSA and supply-side drought measure [9]. This is a step towards improving the CAMS approach. The main stages of the improved methodology are:

1. *First stage*. Modeling and assessment of the climate factors, scenarios and trends.
2. *Second stage*. Water balance modeling. Evaluation of the trends in water resource alterations, incl. under different scenarios of climate change or drought.
3. *Third stage*. Developing a calculation scheme of the Water Management System. Assessment of water consumption and the environmental needs.
4. *Fourth stage*. Ecological flow assessment and RSA. A methodology and a mathematical model for determination the ecological flow in Bulgaria which is a necessary condition for achieving a good ecological status are proposed. As an object of research macrozoobentos ecosystem are considered.
5. *Fifth stage*. Simulation modeling and CAMS. Evaluation of water shortage and risk of water resources and water supply. At this stage juxtaposition is made of the available water resources and the current and future water consumption. The main tasks and expected results from this stage are:
   - Development of CAMS and measures for sustainable water abstraction (RSA)
   - Identification of HMWB and regulated rivers. Mitigating measures;
   - Development of water scarcity and drought management plans/measures. Climate change and drought projection;
   - Floods – risk factors and preventive measures. Measures with synergistic effects;
   - Development of measures for the purposes of Natura 2000, protected zones
   - Integrated vulnerability assessment with consideration of the taken measures
   - Identification of “critical issues and areas” (the so-called “hot spots”) and etc.

6. *Sixth stage*. Analysis and formation of measures, monitoring and adaptive water management for WFD and Natura 2000 objectives.

The methodology for minimum ecological flow assessment and for RSA

According to the Guidance No. 31, ecological flow (e-flow) is considered within the context of the Water Framework Directive (WFD) as "a hydrological regime consistent with the achievement of the environmental objectives of the WFD in natural surface water bodies as mentioned in Article 4 (1). Most of methods for determination of the ecological flow are based on the main hypothesis, which states that the fluctuations of the river runoff are the most important abiotic factor, determining the quality of living environment, a decisive factor for development of a biocoenosis. For CAMS and RSA, a methodology and a mathematical model for determination the ecological flow in Bulgaria which is a necessary condition for achieving a good ecological status are proposed [11]. As an object of research macrozoobentos ecosystem are considered.

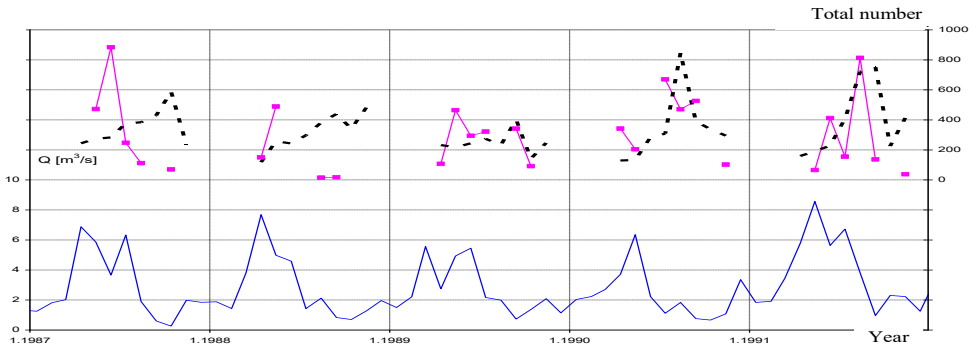


Fig.1. Comparison of the hydrographs of observed (rose) and modeled (blue) total number [11]

The assessment of impact on the river ecosystem is determined by the scheme:

- The development of the zoobenthos is modeled in natural flow regime (undisturbed conditions), including periods of low and high waters. The obtained modeling series for the total number are called standard regime and serves as comparison basis at the determination of the ecological flow.
- Models for different scenarios of zoobentos development are worked out.
- A comparison with the standard regime is done using Fisher criterion, for assessment of the importance of zoobenthos cenosis variations for different scenarios. A variant is selected where the river ecosystem is consistent with undisturbed conditions.

APPLICATION IN PRACTIS AND RESULTS

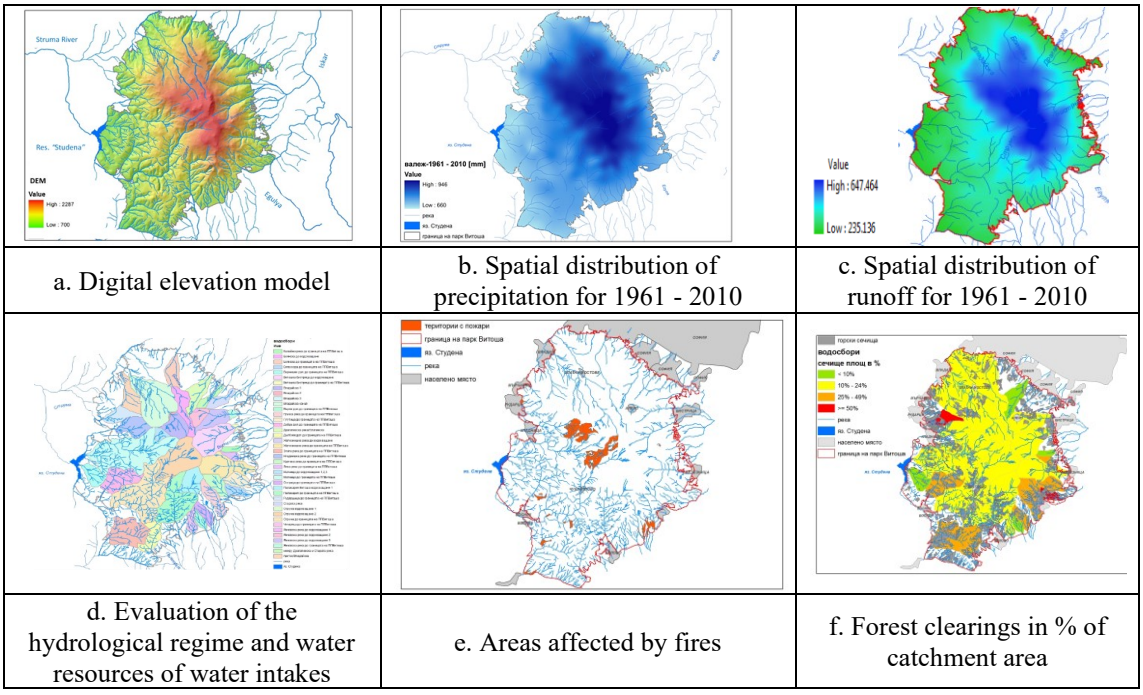
The methodology for integrated assessment is applied in practice for Vitosha Nature Park (NP) (the results support the Vitosha NP Management Plan), as a part of international projects for Executive Forest Agency (EFA) for integrated analysis of water and forest resources under climate change (Struma and Kamchia River Basins), for some new analyzes in support of the Ministry of Environment and Water (MOEW), etc. [3], [4], [8], [9]. The methodology for ecological flow assessment is applied also for more than 80 river sections on the territory of the Republic of Bulgaria, for the purposes of environmental impact assessment (EIA), etc. [11].

https://doi.org/10.5593/sgem2024/3.1/s12.06

Vitosha Nature Park is part of European ecological network Natura 2000. The territory of the Vitosha NP includes zones with special status: sanitary protection zones and reserves. There are the "Torfeno Branishte" and "Bistrishko Branishte" reserves [3].

As a first stage**,** all factors forming the local climate are analyzed for the purposes of the water balance (precipitation, temperatures, etc.), trends and climate changes – Fig.2.b.

Vitosha is rich in water resources. The more significant rivers are: Struma, Vladaya, Boyana, Dragalevska, Bistritsa, Palakaria, etc. ***In the second stage***, the water balance model is developed for different periods (1961-1990, 1961-2010, etc.) and the natural runoff for all river catchments, as well as for all major water intakes and water balance points, is evaluated – Fig. 2.c. and Fig. 2.d.



a. Digital elevation model	b. Spatial distribution of precipitation for 1961 - 2010	c. Spatial distribution of runoff for 1961 - 2010
d. Evaluation of the hydrological regime and water resources of water intakes	e. Areas affected by fires	f. Forest clearings in % of catchment area

Fig. 2 The integrated assessment of the water and natural resources in cases of Natura 2000 [3]

The development of the calculation scheme is a start point for the simulation modeling. ***In the third stage*** are identified all water users, water transfer from/to other watersheds, water supply systems, water infrastructure, approved water rights, etc. The specificity of protected areas is taken into account. A new approach has been developed for the identification and assessment of tourist water supply groups. The main anthropogenic factors are: the collecting channels of Vladaya, Palakaria, the water intakes of the Vladaya, Boyana, Zheleznitsa, Vitosha Bistritsa, Yanchovska Rivers, the water intakes of the Struma, Rudarshtnitsa etc. (for water supply of the town of Pernik, Rudartsi, Dragichevo, etc.).

Ecological flow assessment and Restoring Sustainable Abstraction

The fourth stage is the main one. For the Restoring Sustainable Abstraction and CAMS realization, the ecological flow is assessed on the basis of the new hydrological information. The ecological water quantities are assessed in some basic points of the

Vitosha NP [3], [11]. Emphasis is given to the places of water abstraction, water transfer, rivers at risk of not achieving good ecological potential ("hot spots").

The monthly runoff distribution below water intake of the Vladaya River in natural and disturbed conditions is given on Fig.3. For each variant model investigations of zoobenthos development are carried out. The obtained results are presented on Fig. 4. The monthly changes of Fisher criterion are given which estimates the cenosis state in disturbed conditions towards to natural runoff state – Fig. 5. The results show that the increase in the minimum allowed outflow does not substantially change the status of the cenosis. This is due to the severely reduced river flow during high water due to the high level of construction. The prescriptions for RSA and CAMS are given:

- It is proposed to accept a ecological flow 0,050 m3/s – water intake of the Vladaya River, Vladaya collecting channel.
- In the months of April and May, 5-10 days to be provided, in which the catchments not to work, so that the rivers run through the entire natural flow to improve the status of the cenosis during the spring high water.

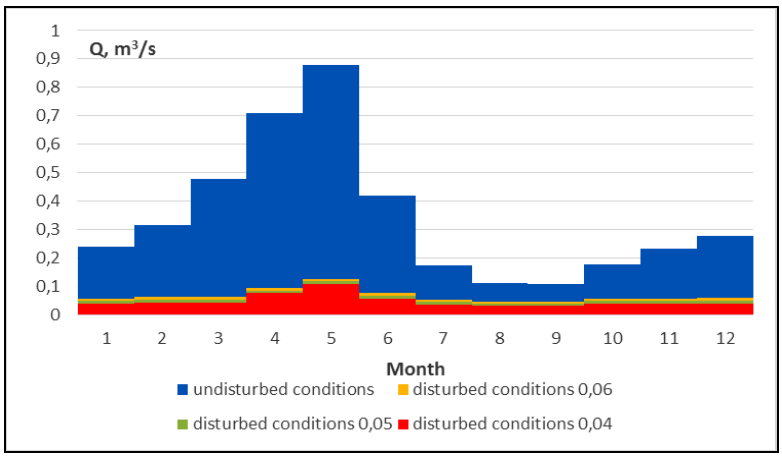


Fig. 3 The monthly runoff distribution in natural and disturbed conditions [11]

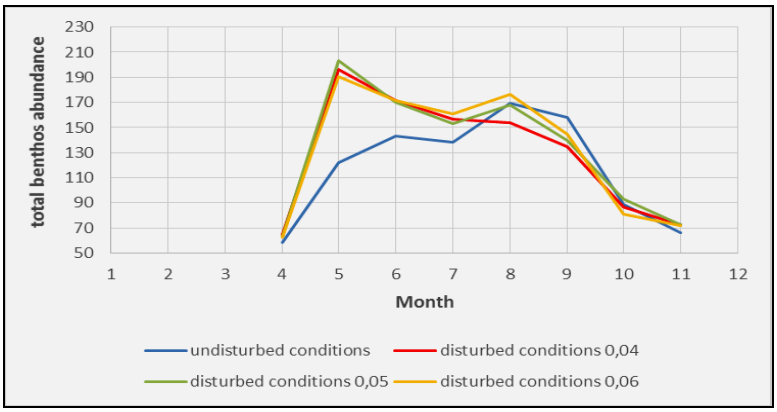


Fig. 4 Model investigations of zoobenthos development [11]

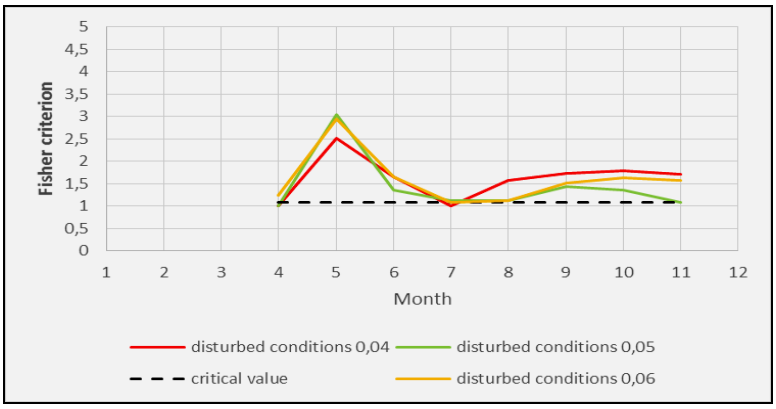


Fig. 5 The monthly changes of Fisher criterion [11]

The results for the Palakaria catchments are similar.

The increase of ecological flow for the Boyana River (Kameno Zdanie water intake) does not significantly change the status of the cenosis during summer low water, but it improves its condition during spring high water. It is proposed to accept an e-flow 0,010 m^3/s. For Zheleznitsa, Vitosha Bistritsa and Yanchovska rivers it is proposed an ecological flow, according Water Law. Some results from modelled ecological flow after up-to-date assessment are given in Table 1. A comparative analysis is carried out.

Table 1. Some results from modelled ecological flow and MAF from the permits issued

Location of water abstraction, water intake	Location of water use	Minimum acceptable flow from the permits issued, m^3/s	Proposed ecological flow and up-to-date assessment, m^3/s
Vladaya river, water intake Vladaya collecting channel	Water transfer from Iskar to Struma River Basin and Studena Reservoir	0,020	0,050
Boyana River, Kameno Zdanie water intake	Tourist centers, tourist water supply groups	0,010	0,010
water intake of the Zheleznitsa River	Sofia water supply in emergency situations	0,010	0,013
water intake of the Yanchovska River	Sofia water supply in emergency situations	0,010	0,011
water intake of the Vitosha Bistritsa River	Sofia water supply in emergency situations	0,010	0,015

The fifth stage is applied iteratively for scenario analysis and CAMS. A simulation model has been elaborated to assess the vulnerability of water resources and water supply under various scenarios: scenarios for the resource, including "drought" scenarios, different alternative water supply schemes, "with" or "without" water transfer, various management decisions and measures [3]. Climate changes are analyzed. The results from simulation modeling show that water supply is ensured close to the normative probability, but permanent small deficits occur basically in the settlements of the so-called Vitosha group. Water shortage is observed also for the tourist centers and the highest priority user – the ecological runoff. The deficits are aggravated during periods of prolonged drought and climate change, and part of the rivers and gullies even dry up. As a result the critical sections and "hot spots" are specified (Vladaya, Rudarshtitsa rivers, etc.) – Table 2.

Table 2. Results from the simulation modeling, Variant (maximum) - ecological runoff

River Assessment point	E- flow	Probability of exceedance (PE) %			Reliability index
		by volume	by years	by months	
Vladaya river 1 – after water intakes	Vl R_1	97,52	65,79	94,30	0,354
Vladaya river 2 – Vladaya channel	Vl R_2	98,20	78,95	95,61	0,253
Boyana river – after Boyana HPS	Bo R_1	99,89	97,37	99,56	0,005
Palakariya – Palakariya channel	Pal R	99,51	89,47	98,25	0,057
Rudarshtitsa – Vladaya channel	Ru R_1	74,86	2,63	50,44	7,682
Kladnishka - Vladaya channel	Kl R_1	94,85	36,84	86,84	0,887
Struma river – under res. ”Studena”	St R_1	100,0	100,0	100,00	0,000

Floods-risk factors are also analyzed (deforestation, erosion, forest fires, etc.) – Fig.2e and Fig. 2f. Evaluation of high water is developed.

In the sixth stage the measures, monitoring and adaptive management are defined. The measures for integrated water and ecosystem (forest ecosystems, peatlands, etc.) management are proposed. As a result of approach, measures with synergistic effects are recommended – not only to protect water quantity and quality, but also for flood risk prevention, erosion control, increasing water retention capacity, etc. The measures (included in the Programme of Measures of the RBMP) have been applied to achieve the WFD objectives: optimal water allocation of the water resources management systems, reservoirs and collecting derivations for ecological flow and water supply provision; environmental flow releases from reservoir and applying the concept of “compensation” during prolonged drought, etc.

For the purposes of the MoEW, an up-to-date assessment of the minimum acceptable flow (MAF) from the 52 complex and significant dams from Appendix 1 of the WL is carried out [4]. In the regulated rivers, the MAF is for the purpose of water ecosystems, groundwater and drinking water supply, wetlands and Nature 2000 areas. For example, Koprinka and Zhrebchevo reservoirs provide greater ecological quantities, not only ecological runoff, but also feed groundwater and contribute to the protection of longose forests along the Tundzha River [4], [5]. The identification of the most vulnerable areas is also useful [6]. It is recommended that any change of the MAF, including according to the new hydrological approaches [1], [2], must to be expedient and with accordance to the good practices for e-flow evaluating in Bulgaria [4], [11]. Environmental flow from dams for WFD, needed to be assessed through local model studies (assessment of impact on the river ecosystem) or a combined approach and monitoring [1], [11].

CONCLUSION AND RECOMENDATIONS

Climate factors are already exerting negative pressure on water resources, society, natural ecosystems and their ecosystem services. An innovative approach for the integrated assessment and management of the water and natural resources (water ecosystems, wetlands, etc.) in cases of Natura 2000 areas is developed and applied. The developed methodology contributes to the goals achieving of the WFD, according to Art. 4 (1), even to a greater extent: "the standards and objectives for protected areas, including relevant Natura 2000 sites designated under the Birds and Habitats Directives”. Actually, the development realizes the CAMS and Drought Management Plan, by the example of the UK, taking into account the protected areas, Natura 2000 and the ensuring of e-flow. On the basis of the available water resources, Water Companies develop their Strategic Plans, environmental monitoring and update their

water use permits. On the other hand, in the context of Article 1 of (Directive 92/43/EEC on the conservation of natural habitats and of wild fauna and flora), conservation means a series of measures, required for conservation or restoration of natural habitats. Some measures (such as to restore water regime of the peatlands) are non-traditional measures for RSA and supply-side drought measure.

The methodology for ecological flow assessment is applied for more than 80 river sections on the territory of the Republic of Bulgaria, for the purposes of environmental impact assessment (EIA), etc. The application of the methodology implements the main three stages, according to Guidance No. 31 of the WFD [7]:

1. The first step of the analysis is to identify the pressures on the hydrologic regime that are most likely to result in a change in ecological status. As it is indicated in Annex II, point 1.4 of the WFD, this assessment should start with an inventory of the river basin: all significant water abstractions; regulation of river flow, water transfer.

2. The WFD recognizes the importance of the runoff regime for the status of aquatic ecosystems. Analysis of the impact of hydrological changes can be supported by statistical analysis of available hydrological data in an existing and undisturbed state.

3. The assessment of the significance of hydrological changes and the extent to which the pressure affects biological communities and is likely to prevent the achievement of good ecological status or specific requirements of protected areas.

The results and applications in practice are related to the Vitosha Nature Park Management Plan, Program of Measures, for the goals of WFD and Natura 2000 and supports the MoEW and Basin Directorates in the ecological flow determining and in the Eflow concept implementation in Bulgaria.

ACKNOWLEDGEMENTS

The research is part of the research projects carried out with the support of the Agreements with the MOEW, Vitosha NP, Executive Forest Agency and Forest Research Institute.

REFERENCES

[1] Approach to eflows in Bulgaria, Draft Report, Wood Group UK Limited, 2022

[2] Bojilova, E., Methodology for ecological flow applied to Tundza watershed in Bulgaria, Journal of Balkan Ecology, Vol.27, № 1, ISSN 1311-0527, 79-88, 2024

[3] Development of Water Balance for the Territory of the Vitosha Nature Park 2014. Project financed by OP "Environment 2007 – 2013", National Institute of Meteorology and Hydrology, Contract with the Vitosha NP. Project leader - Ilcheva, I.

[4] Determination of the minimum acceptable flow in the river beds after the complex dams according to the current Water Law, MoEW, 2022, Project leader – Ilcheva, I.

[5] Droumeva-Antonova, G., Groundwater and protected areas of dense forests along Tundzha River, Science & Technologies, Volume VI, Number 2, pp 37 – 43, 2016

[6] Droumeva-Antonova, G., K. Nacheva, Research of the drought severity for porouse groundwater, SocioBrains, issue 41, 230-236, ISSN: 2367-5721, pp 230-235, 2018

[7] Guidance No. 31, Ecological flows in the implementation of the WFD, 2015

[8] Ilcheva, I., A.Yordanova, V. Rainova, Water resource balance for Vitosha Nature Park and adaptive management under conditions of climate change, European Journal of Geography, Volume 10, Number 3:56-72, ISSN 1792-1341, pp 56-72, 2019

[9] Marinov, I., Velizarova, E., Niagolov, I., Nikolova, K., Ilcheva, I., Zlatanov, T., Mirchev, P., Zaharieva, V., Yordanova, A., Nikolov, I., Pavlova, E. and Mitev, S., Climate changes and their influence on forest ecosystems and water resources in the catchment area of the Struma River watershed, ISBN: 978-954-395-081-2, 2012

[10] Managing water abstractions, Environmental Agency, UK, 2013

[11] Zaharieva, V., Environmental Runoff Assessment Approach EFLOW, ISBN 978-619-188-371-4, 2020

CLIMATE ANALYSIS ALONG THE NAVIGATION ROUTES ON THE DANUBE

Ass. Prof. Dr. Eng. Ana-Maria Chirosca

Prof. Dr. Liliana Rusu

Eng. Victor-Ionut Popa

Prof. Dr. Eugen Rusu

[1]"Dunarea de Jos" University of Galati, Faculty of Engineering, Department Mechanical Engineering, Galati, Romania

ABSTRACT

The Danube has been a traditional trade route in Europe since ancient times. Transport on the Danube has many economic and environmental advantages. By using the river as a transport route, logistics costs can be reduced, and delivery times optimized. Another feature of the Danube is its connection to the North Sea and maritime transport via the Rhine-Main-Danube Canal. In addition, waterborne transport produces less carbon dioxide than road or rail transport, helping to reduce environmental impact and promote sustainable development. The study of the wind climate of the Danube is particularly important for transport and navigation on this waterway, allowing ship operators to use this information to optimize their routes and plan their voyages with maximum efficiency and safety for both cargo and crew. A statistical analysis of vessel traffic for the period 1990 - 2020 was carried out and cargo types and vessel types were characterized. Also, cargo quantities and vessel capacity were analyzed in terms of both imports and exports. Thus, this paper presents a study of the river from an economic, statistical, and climatic point of view.

Keywords: Danube, climate changes, wind climate, freight transportation

INTRODUCTION

The Danube is one of the largest waterways in Europe. The river has a long history and has had a major impact on the economic and cultural development of the regions through which it flows, being considered one of the most important transport arteries in the world [1]. The Danube in the European economy is seen as a strategic corridor and border route, known, and appreciated for its value since ancient times.

The economic importance of this river has an impact on several branches of industry, the most important being the transport of goods and people, followed by energy production, water supply, and fishing.

Nowadays, freight transport is the major economical use of the Danube. Major ports include cities such as Izmail, Ukraine, Galati, Ruse, Budapest, Vienna, Regensburg, and Germany. Since World War II, navigation has been improved by dredging and building a series of canals, whilst traffic on the river has increased at an accelerated rate. The main shipping channels connected to the river are the Danube-Black Sea Canal, which

starts in Cernovada and stretches to the Black Sea, and the Rhine-Main-Danube Canal which connects the Danube to the North Sea [2].

This paper aims to investigate navigation areas along the Danube and identify dangerous areas on the waterway by optimizing navigation routes and ensuring safe transport. The study is also enriched with a statistical analysis of navigation on the Danube for the period 1990 - 2020 concerning the volumes of cargo transported and the capacity of the vessels transited.

The findings were correlated with a climatic study of wind conditions on the Danube for the same period, using the latest data from the European Centre for Medium-Range Weather Forecasts [3] (ECMWF).

NAVIGATION ON THE DANUBE

The Danube, illustrated in Figure 1, has the highest flow in Europe [4] and its main tributaries are the Sava, Tisa, Inn, Drava, and Siret. The Tisa is the tributary with the longest length, 966 km, and only 16 km behind comes the Prut. Along its course, the river splits into several branches.

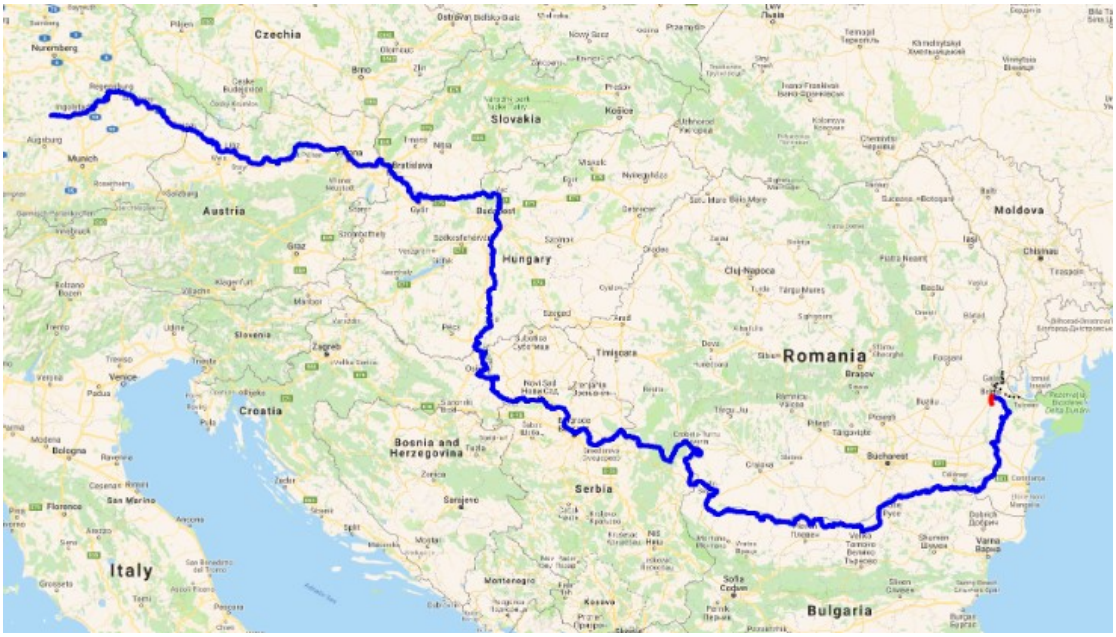


Figure 1. The course of the Danube

The main feature of navigation on the Danube is the ability to transport large quantities of cargo at a much lower cost than other transport methods. Other benefits of this method of transport are its environmental friendliness, the level of safety, and the availability of the trips, which can occur constantly, except in bad weather conditions.

The disadvantages of navigation on the Danube are the speed of transport, the port infrastructure that needs to be optimized according to market requirements, and the connection between routes, some of which need to be intermediated with other transport methods [2]. Unfortunately, shipping on the Danube presents several difficulties for sailors, regardless of their training and experience, and is sometimes impossible to cross due to low water levels in dry seasons and extreme weather conditions. Hazard zones include areas of unstable difficulty (changes in the channel direction, variable depth,

and width depending on water level) and areas of fixed difficulty (no significant changes occur, the difficulty remains constant, and crossing these sectors imposes countermeasures and restrictions) [5].

Crossing the Luta becomes a dangerous section when the water level is low, so it becomes dangerous to pass through and there is a risk of ending up with the convoy on land. Every year the navigable channel can change due to silting, and depending on the water level and currents, a new path is formed which all ships will then cross.

The Tulcea crossing has a degree of difficulty due to currents. Lack of attention and experience leads to the deviation of the ship's route towards the Chilia arm, but by increasing engine power it is possible to pass without problems. This passage does not face water level problems, instead, it may encounter high wind speeds or fog.

Another sector that faces problems when the water level is low is the Topalu - Capidava area, and due to the water level, the width of the fairway is reduced. In this sector, ships are forced to stop unless they receive permission from the control port in Cernavodă, which imposes a certain draught for passage. The same situation is found on the Parjoaia - Cernavoda sector, except that when it is blocked, ships can detour around areas on the Borcea arm.

Low water level is not always a problem, for example, in the sector crossing Harsova there is a rock in the fairway, which when the water level is high is no longer visible, and there is a risk of hitting the convoy and causing damage on board.

A waterfall effect is formed in the Bala - Borcea area, this passage is very difficult when the water level is low, and the more the water level varies, the more this effect is felt on the Borcea arm. Some of the smaller vessels cross this sector upstream with only one barge to avoid this effect, while larger vessels can cross with 2 or 4 barges.

The crossing near the Novi Sad bridge is considered a dangerous area because the Serbian authorities between km 1250 and km 1260 require the convoy to be uncoupled and pass with a maximum of 2 barges. During these maneuvers, especially when transporting rolled products and grain, there is a risk of cargo being stolen. The Novi Sad and Smederevo area is the most famous on the Danube for this piracy.

The next three sectors, the Apatin curves, the Baja area (and the Venek - Gonyu curves) are difficult to cross because of the sharp and dangerous curves, and these areas are generally only traveled during the day in conditions of maximum visibility.

STATISTICAL ANALYSIS OF SHIPS AND GOODS TRANSPORTED

The Danube was and is an important route for the transport of goods [6-7]. A variety of goods, including raw materials, agricultural products, fuel, and other general cargo are transported on the river by cargo ships and barges. A study of traffic on the Danube for the period 1990 - 2020, in terms of cargo transported based on information provided by ACN [8] has been carried out. The volume of cargo was analyzed according to the direction of transport, internal or external, but total quantities were also presented, as can be seen in Figure 2.

During the years under investigation, 354,167,329 tonnes of goods were transported, of which 63% were transported internally and 37% internally. Freight transport has a largely upward trend, with small exceptions, as freight volumes increase from year to

year. At the same time, according to the results, at the beginning of the period studied, the volume of goods transited externally was much lower than that of internal goods, but as the years went by, a balance was reached between them. In recent years, exports have exceeded imports.

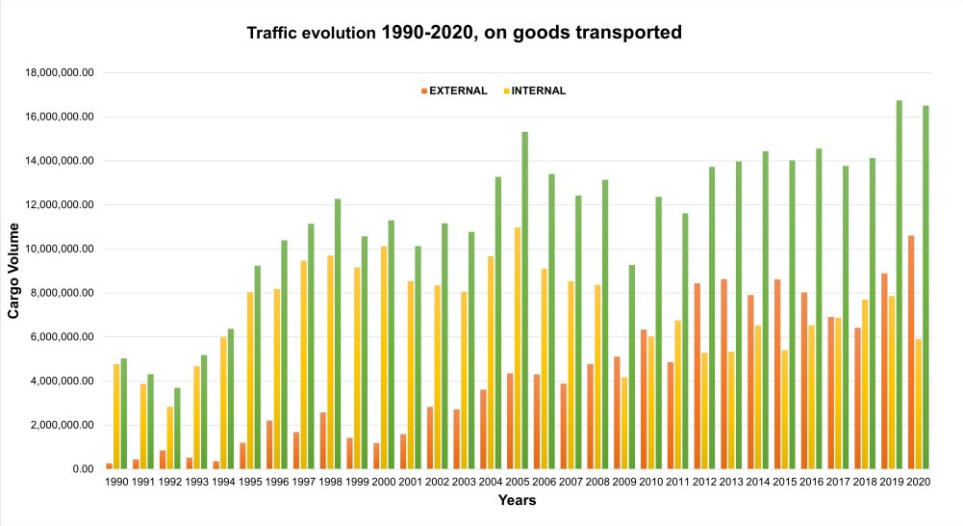


Figure 2. Evolution of traffic for the period 1990-2020 in terms of goods transported

The types of vessels used for the transport of goods on the Danube can be classified according to their characteristics and the type of goods transported [9][10]. Analogous to the analysis of vessel traffic on cargo transported, an analysis of vessel capacity for the period 1990 - 2020 has been carried out, shown in Figure 3 from three perspectives, external, internal, and total. As with freight volumes, the same upward trend can be seen in ship traffic.

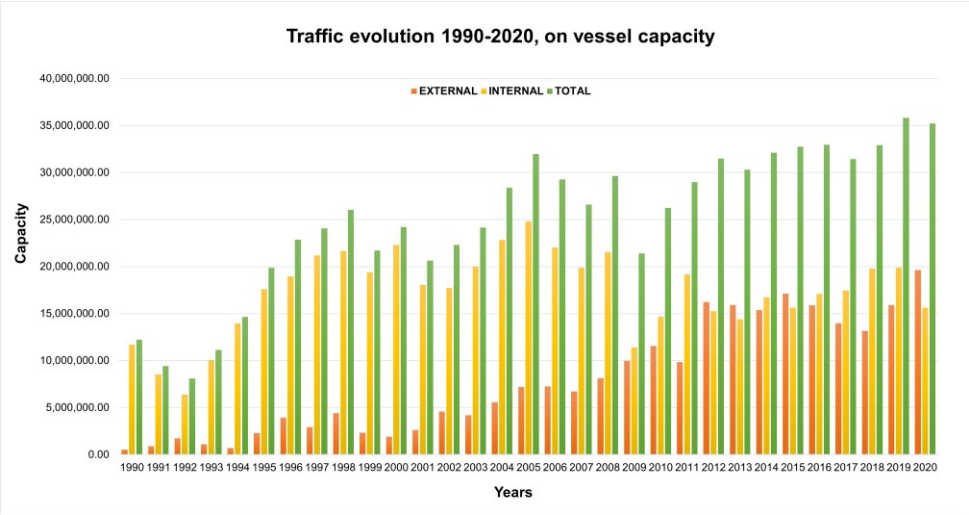


Figure 3. Evolution of traffic for the period 1990-2020 on vessel capacity

WIND CLIMATE

Wind is a key factor in navigation and has a major impact on the safety of ships and crews. Studying the wind climate of the Danube helps to understand wind characteristics, including wind direction and variation. This enables seafarers and ship

operators to take weather conditions into account when planning and executing voyages and to better decide on speed, manoeuvres, and navigation routes.

Wind speed analysis was carried out based on data extracted every 3 hours for wind speed components at 10 meters, using the latest data from the European Centre for Medium-Range Weather Forecasts (ECMWF). The wind climate data used for the period 1990-2020 were extracted from the 5th generation ERA5 database [11] provided by the Copernicus Climate Change Service (C3S). These represent the new generation of reanalysis databases for global climate and weather, with improved resolution compared to the previous generation, ERA-Interim [12], as well as better consistency of sea surface temperature and sea ice, better representation of tropical cyclones, and more. An analysis of some significant meteorological and hydrological processes along the Lower Danube was made in [13].

Various categories of cargo are transported on the Danube, from minerals, coal, limestone, grain, fertilizers, and rolled products to components and equipment. These cargoes follow both internal and international routes to all the countries crossed by the river, such as Germany, Austria, Hungary, Croatia, Serbia, Bulgaria, Moldova, and Ukraine. Thus, for the transport of phosphate, one of the main routes is Agigea - Pischelsdorf, illustrated in Figure 4, which covers several secondary routes for various types of cargo.

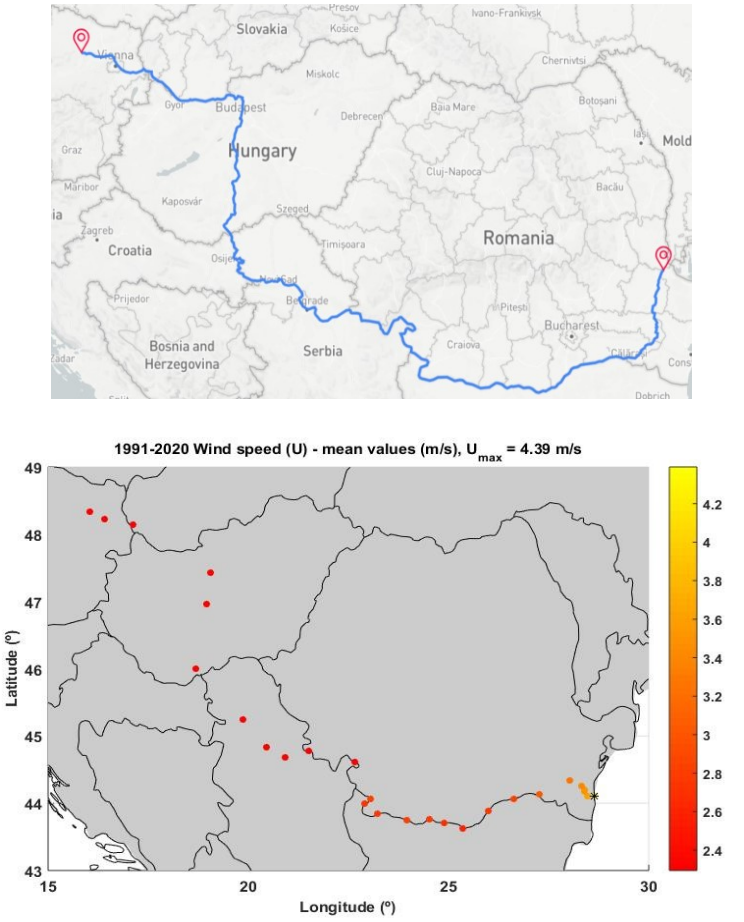


Figure 4. Agigea - Pischelsdorf

https://doi.org/10.5593/sgem2024/3.1/s12.07

Grains are transported on a wide range of routes, such as Ismail - Agigea, Braila - Agigea, Galati - Agigea, Giurgiu - Agigea, and others. Analogous to the main phosphate transport routes, the most important routes for cereals arrive in Agigea, hence the highest wind speeds are also recorded in the Agigea - Medgidia area. The conflict situation between Russia and Ukraine has directly affected this category of goods for which Ukraine is one of the world's exporters, and the blockade of the Black Sea ports has led to an increase in global food prices.

The Ismail - Agigea route, shown in Figure 5, is also particularly important for the transport of cast iron, ilmenite, and tiles, and the Csepel - Agigea route is also known for the transport of scrap iron.

Salt is an indispensable mineral in the food industry, but it is also used in other industries such as the chemical industry, the textile industry, the construction industry, and many others. On the Danube, this mineral is most frequently transported on the Galati - Ismail route. In terms of wind climate, the average wind speed for the period 1991 - 2020 is 3.3 m/s on this route. The highest values are recorded in Galati and Grindu, and the lowest values are recorded in Ismail and Tulcea.

On the Galati - Vienna, Galati - Agigea, and Galati - Tulcea routes, rolled products are frequently transported. The highest wind speeds are found on the Galați - Agigea route, which is also known for the transport of coal and ore.

Brick is one of the many building materials that are transported on the Danube, and the main route for this type of cargo is Novi Sad - Giurgiu and Vukovar - Giurgiu. Compared to the other routes, these routes are easier to cross in terms of wind climate, where we encounter maximum average wind speeds of 2.8 m/s.

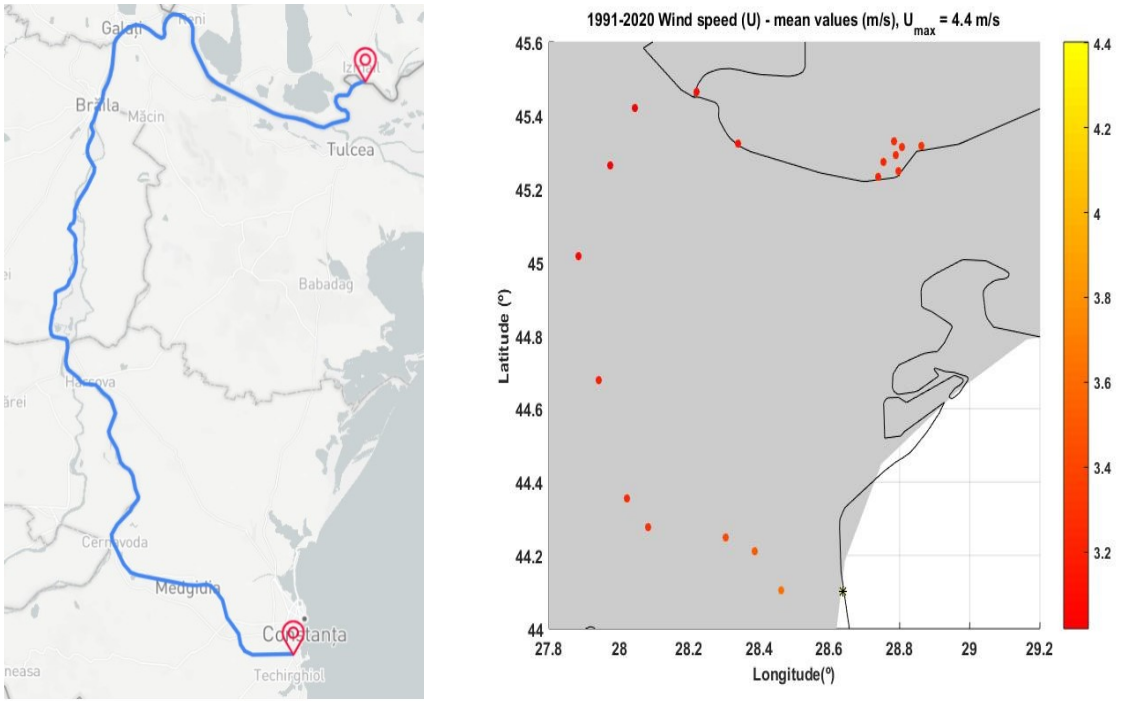


Figure 5. Ismail - Agigea

CONCLUSION

Inland waterway transport has developed into a complex and constantly evolving activity due to the increasing market demands, but also because of the many advantages it offers and the cost-effective service prices.

Transport on the Danube has broad prospects and great development opportunities. Projects to modernize and expand river infrastructure, such as building new locks and improving waterways, will help shift goods and passengers more efficiently and sustainably. The development of ship technology, such as low-emission inland vessels and autonomous ships, will bring further improvements to the Danube transport sector.

By studying the wind climate, prevailing wind zones and periods can be determined, allowing ship operators to use this information to optimize routes and plan their operations for maximum efficiency. The study of wind climate is also essential for developing the Danube port infrastructure. Knowing the direction and speed of the wind helps to properly design breakwaters and other port structures, ensuring that they can withstand weather conditions and providing a safe environment for ship operations and cargo handling.

A valuable resource for Europe, therefore, the Danube provides a vital link for transporting goods and passengers between regions, and water transport is the most advantageous method of transport.

ACKNOWLEDGEMENTS

This work was carried out in the framework of the research projects: the Horizon Europe Project HORIZON-CL5-2021-D6-01, ID 101069941 — PLOTO – „Deployment and Assessment of Predictive modeling, environmentally sustainable and emerging digital technologies and tools for improving the resilience of IWW against Climate change and other extremes” and CLIMEWAR (CLimate change IMpact Evaluation on future WAve conditions at Regional scale for the Black and Mediterranean seas marine system), supported by the Romanian Executive Agency for Higher Education, Research, Development and Innovation Funding – UEFISCDI, grant number PN-III-P4-PCE-2021-0015.

REFERENCES

[1] Z. R. Radmilovic, V. Masas, Role of Danube Inland Navigation in Europe, International Journal for Traffic and Transport Engineering, 2011, 1(1): 28 – 40

[2] Chirosca A.-M., Vazdoaga I., Popa V.-I., Rusu L., The economic importance of navigation along The Danube-Black Sea Channel, International Multidisciplinary Scientific GeoConference Surveying Geology and Mining Ecology Management, SGEM, 21 (3.1), 2021, pp. 297 - 305, Doi: 10.5593/sgem2021/3.1/s12.45

[3] ECMWF Reanalysis v5 (ERA5). Available online: https://www.ecmwf.int/en/forecasts/dataset/ecmwf-reanalysis-v5 (accessed on 20 March 2024)

[4] Constantin Sava, The importance of the Rhine-Main-Danube, transport corridor. Its impact on the Central and East European countries, with an emphasis on Romania. World Maritime University Dissertations, General Maritime Administration & Environment Protection, Swede, 1997, https://commons.wmu.se/all_dissertations/926/

[5] Vâzdoaga I., Chirosca A.-M., Popa V.-I., Rusu L., Extreme phenomena on Danube hydrodynamics and the influence on the navigation conditions, International Multidisciplinary Scientific GeoConference Surveying Geology and Mining Ecology Management, SGEM, August (3.1), 2020, pp. 123 - 130, 2020, Doi: 10.5593/sgem2020/3.1/s12.016

[6] Andrej Dávid, Emilia Madudová, The Danube river and its importance on the Danube countries in cargo transport, Transportation Research Procedia, Volume 40, 2019, Pages 1010-1016, ISSN 2352-1465, Doi: 10.1016/j.trpro.2019.07.141.

[7] Mako, P.; Dávid, A.; Böhm, P.; Savu, S. Sustainable Transport in the Danube Region. Sustainability 2021, 13, 6797, Doi: 10.3390/su13126797

[8] Administația Canalelor Navigabile, ACN: https://www.acn.ro/index.php/ro/ accessed in May 2023

[9] Interreg Danube Transnational Programme, Overview Vessel Types on the Danube, http://www.interreg-danube.eu/approved-projects/danube-skills, accessed in May 2023

[10] Cosmin Katona, Alecu Toma, The cargo evolution transportation on Romanian Waterways Cernavodă – Agigea and Poarta Albă – Midia Năvodari, "Mircea cel Batran" Naval Academy Scientific Bulletin, Volume XVIII – 2015 – Issue 1

[11] ECMWF Reanalysis v5 (ERA5). Available online: https://www.ecmwf.int/en/forecasts/dataset/ecmwf-reanalysis-v5 (accessed on 12 July 2023)

[12] Dee, D.P.; Uppala, S.M.; Simmons, A.J.; Berrisford, P.; Poli, P.; Kobayashi, S.; Andrae, U.; A, M.; Balmaseda; Balsamo, G.; Bauer, P.; et al. The ERA-Interim reanalysis: Configuration and performance of the data assimilation system. Q. J. R. Meteorol. Soc. 2011, 137, 553–597.

[13] Răileanu, A.B., Rusu, L. and Rusu, E., An Evaluation of the Dynamics of Some Meteorological and Hydrological Processes along the Lower Danube. Sustainability, 2023, 15(7), p.6087, Doi: 10.3390/su15076087

COMPARISON OF TWO METHODS FOR ASSESSMENT OF PH-DEPENDING VALUES IN SURFACE WATER

Ing. Viera Kováčová
[1] Institute of Hydrogy Slovak Akademy of Science, v.v.i., **Slovakia**

ABSTRACT

The recent advances in current status and major mechanisms of water quality worsening, assessment of evaluation criteria and the influencing factors were reviewed. The changes in the atmosphere, the periodicity of the occurrence of extreme hydrological situations has been increasing in recent years. In the natural conditions of Slovakia, periods without rain are lengthening and the incidence of precipitation of extreme intensity and abundance is increasing. Hydrological extremes are generally manifested in the form of floods and droughts. The increased incidence of drought is a new phenomenon. The analysis was conducted using a long series pH and temperature measurements.

The pH, temperature and conductivity are the most important water quality parameters. Their time-series were used for investigation of pH with regard to the place of collection and seasonal cycle. The pH ranged from 5 to 9, i.e. predominantly in the alkaline area. Average value of pH in the monitored period 2010-2020 was 7.56, One of the most important tools for evaluating water quality and character in a catchment is a detailed knowledge of the ranges and trends in pollution of natural water. This requires water accounting be conducted at the regional scale.

Keywords: surface water, quality parameters, pH

INTRODUCTION

Climate change in resent years causes environmental deterioration. The anthropogenic activity have an impact on the components of the hydrological regime of rivers, potentially leading to negative effects on the quantity and quality of water [1], [2]. In terms of climatic situations, the Žitný ostrov belongs to a very warm and very dry agroclimatic area whith winter. Moisture conditions of the territory are deficient. The climatic indicators of irrigation, and precipitacion stating the difference of potential vapour, the deficiency of rainfalls achieves here as much 200 mm within summer months.

The relationship between the quality and quantity of water also deserves attention. Much less attention is paid to the long-term pH and water temperature behaviour in natural streams and rivers. Lack of suitable data hinders such studies few analyses of detailed pH and water temperature records covering [3].

The pH and water temperature time series were used on investigation of pH with regard to the place of collection and seasonal cycle. The impact of rising air temperatures on

water temperature is critical for protecting water resources and ensuring water quality. Comprehensive analysis of the development of the quantity and quality regime of water in streams and their mutual relationship in selected Danube basin of Slovakia.

According [4], [5] irrigation is usually required for agriculture in regions where water is in limited supply due to the lack of precipitation during some part of the growing season. The agrochemicals can have detrimental effects to the receiving environments, causing changes in water quality, habitat and species composition

The well-water quality of Danube river basin indicated that inorganic chemical quality of water is very good. The correlation between pH and other parameters is significantly positive for each season studied. Fresh water resources are renewable, but limited in quantity and variable in time and place. The concerned territory of the Žitný ostrov is situated between Bratislava and Komárno surrounded by the Danube river and the branch of the Small Danube (*Fig. 1*).

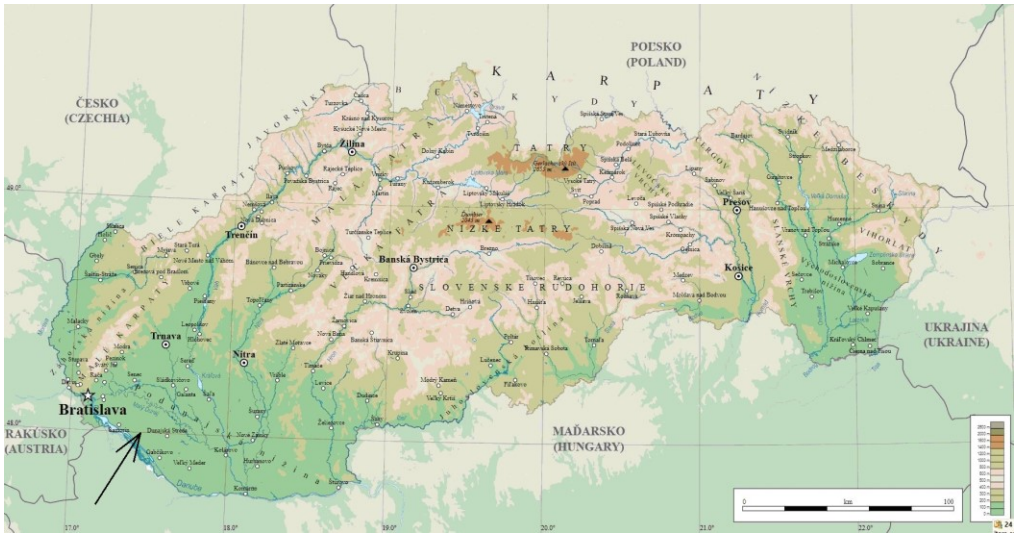


Fig. 1. The map of interest area on the South part of Danube Lowland.

In terms of geomorphology, this territory can be characterised as a young riverside plain with a vere low denivellisation of the surface with an overall inclination from nort-west to south-east, break up the island in transvelsal as well as in longitudinal directions in to different geomorphologic areas. In the sense of transversal division, we recognice the upper, the middle and the lower parts of the Žitný ostrov. Within transversal division, we distinguish the Pleistocene core, late Holocene aggradation walls and early Holocene depressions.

The early Holocene depressions occurs as large lowerings in the they middle and lower parts of this territory. This part of the Žitný ostrov is created by river gravels. The surface layer is built up by Holocene marsh loamy clay sediments rich in humus. In terms of the scope and frequency of data collection on surface water, the monitoring involves one-off determinantion as as well as those repeated within long run [6].

The process of creation of chemism in groundwaters is affected by primary and secondary factors. From among the primary factors the folloving ones are of determining significance chemical composition of the Danubian water, composition of precipitation waters as well as mineralogical composition of Quaternary sediments.

[7] has demonstrated control of some of undesirable chemical constituents in surface water. He states that correlations and multiple linear regressions were used to develop models relating well water chemical quality parameters to a set of independent chemical variables. Irrigation is usually required for agriculture in regions where water is in limited supply due to the lack of precipitation during some part of the growing season. Seasonal evaluation of hydro-geo-chemical parameters using correlation and regression analysis was calculated [8].

In addition to primary composition of infiltrating waters, mainly the process of dissolving carbonates and that of decomposition of minerals have been aplied here. These factors reflecting towards formation of calcium-magnesium-bicarbonate chemism on the groudwater. Secondary or antropogeneous factors influence the quality of groudwater adversely effecting mainly towards an increase of the conponents as SO_4^{2-}, Cl^-, NO_3^- and foreign matters. Influencing the quality of groundwater through anthropogeneous activities predominantly occures at its surface or its upper zone. [9] states, that the one of the most important tools for evaluating water quality and character in a catchment is a detailed knowledge of the ranges and trends in pollution of natural water. Water deterioration has become a environmental problem in recent years, and understanding the mechanisms of water pollutation will help for prevention, remediation of water pollution [10].

Although measurements are simple, effective assessment requires intensive measurement of the parameter in a reliable and consistent manner with respect to location, time and hydrological condition. It was found out [11] that increased agricultural activity leads on average to higher contamination. Temperature, pH and conductivity are the three important factors to induce algal bloom.

The comprehensive set of data acquired within 10 years monitoring was partly assessed in the previous characterizing natural conditions of the conconred territory as well as bassic pedogenetic, physical and chemical features of the locations monitored. The change in pH is directly related to the availability and assesment of nutrients from solution. High pH values promote the growth of phytoplankton [12]. Impact of vegetation on flow in a lowland area during the growing season were investigated by [13], [14.]. Vegetation growing in the water along watercourses has been the subject of several studies since it was recognized that it could have a significant impact on the water flow.
The variation of pH, temperature and conductivity affect the vegetation and algal bloom growth. The important condition for this.is that temperature increases and conductivity decreases faster than ever in short time. Statistical analysis shows that the influence of temperature on algal growth rate is the largest, followed by their interaction.

MATERIALS AND METHODS

For the evaluation of the water quality we went out from the data obtained on Institute of Hydrology Slovak Academy of Sciences. [15] states, that one of the most important tools for evaluating water quality in a catchment is a detailed knowledge of the ranges and trends in a pollution of natural water. Žitný ostrov is one of the most productive agricultural areas of Slovakia, situated on the Danube Lowland. Under its surface is the richest water reservoir of Slovakia drinking water. For this reason, it is very important to deal with quantity and quality of water resources in this region [16]. The channel network at the Žitný Ostrov area was built up for drainage and also to provide irrigation

water. There are three main channels of this network: Chotárny channel – is the P1M water body type (partial river-basin Váh, code SKW0029), Gabčíkovo-Topoľníky channel – is the P1M water body type (partial river-basin Váh, code SKW0023), Komárňanský channel – is the P1M water body type (partial river-basin Váh, code SKV0226). Was carrying out the measurements in the period 2010–2020. We take samples once per month for chosen indicators of water quality assessment from the same sampling sites. By the evaluation of the obtained results we used statistical methods [17].

Water quality was evaluated by the comparison of the characteristic values for chosen indicators Three profiles were monitored in each main channel, i.e. total of 9 measurements each month in time period 2010–2020. A total of 648 samples were investigated. Profiles with an assumed higher pollution value were selected by previous observation. In-situ measurements were carried out to evaluate the quality of surface water on Žitný ostrov territory. For each locality, the quality in selected indicators was separately evaluated using the YSI multiparametric probe. The samples provide a wide range of pH and temperature.
Important was to evaluate pollution state of surface water in Žitný ostrov channel network following the assessment physical-chemical and microbiological indicators in monitored period 2010–2020 [18].
Nine surface-water sites were monitored at least every month describe the sample collection and list all surface-water analyses from 2010 through 2020. Water samples were collected, when the pH, temperature, specific conductance and dissolved oxygen concentration had stabilised. Surface water samples were filtered through a 1 mm membrane filter and stored in polyethylene bottles. Preliminary experiments on sampling methodology found significant results between the pH sampling place and the sampling time (1-12 month) [19]. Changes in freshwater biological communities as a response to pollution have long been recognised. Mostly research has focused on impairment to water quality resulting from pollution of either a physical, chemical and biological nature [20].

RESULTS

The objective of this study was to characterize the reactions slightly alkaline water that has contaminated the alluvial aquifer and stream. This contribution analysed pollution problem, factors affecting this process, its consequences and possibilities of prevention. Important was to evaluate pollution state of surface water in Žitný ostrov channel network following the assessment physical-chemical and microbiological indicators in monitored period 2010–2020.
pH can be measured easily in situ by a portable water quality checker (YSI Multiparametric probe). pH was established in 648 samples collected from Žitný ostrov area. These data are extremely variable in content, reliability and periodicity of sampling. The data were sorted into useable tables, and their statistical distribution was examined. The median value of pH were between 5 and 9 with normal variability ranging, whit 7,59 average value.

Chemical and biological processes taking place in the surface water can significantly affect pH of the water. We observed regularity in the seasonal dynamics and in sampling location. pH-place depending had a greater influence on the pH-time

depending, than the seasonal dynamics (*Fig.2,3*). High pH values promote the growth of phytoplankton and result in bloom.

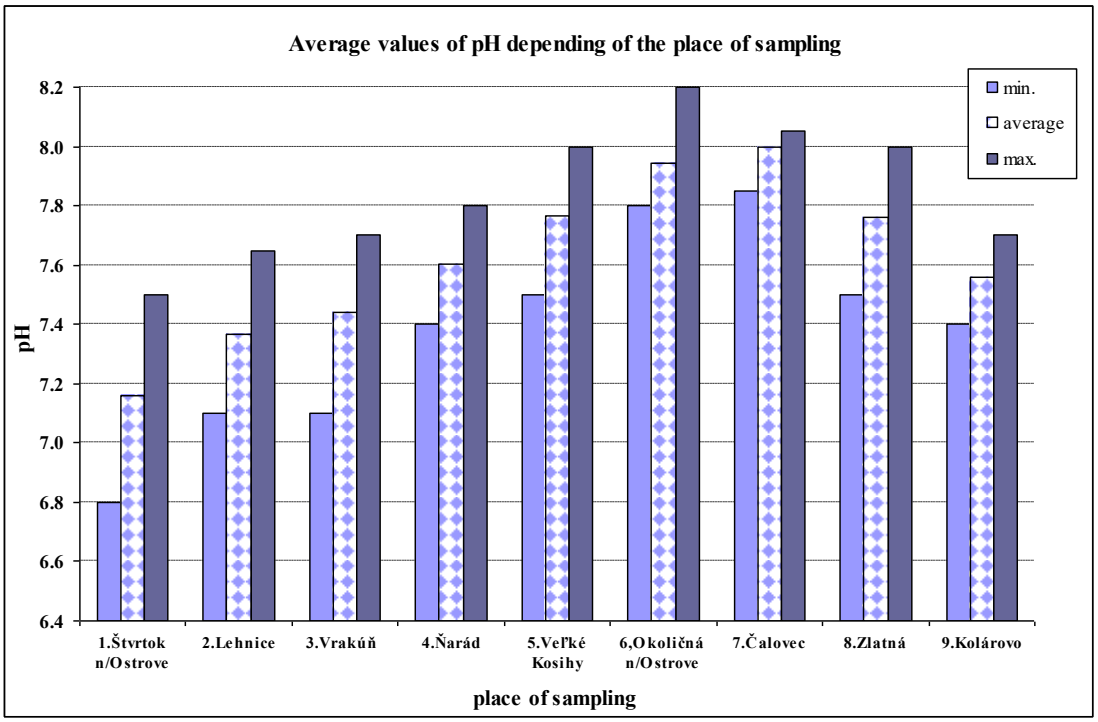


Fig. 2 Average pH values depending on the sampling place. As an exampl we present profile Komárňanský channel (Okoličná na Ostrove).

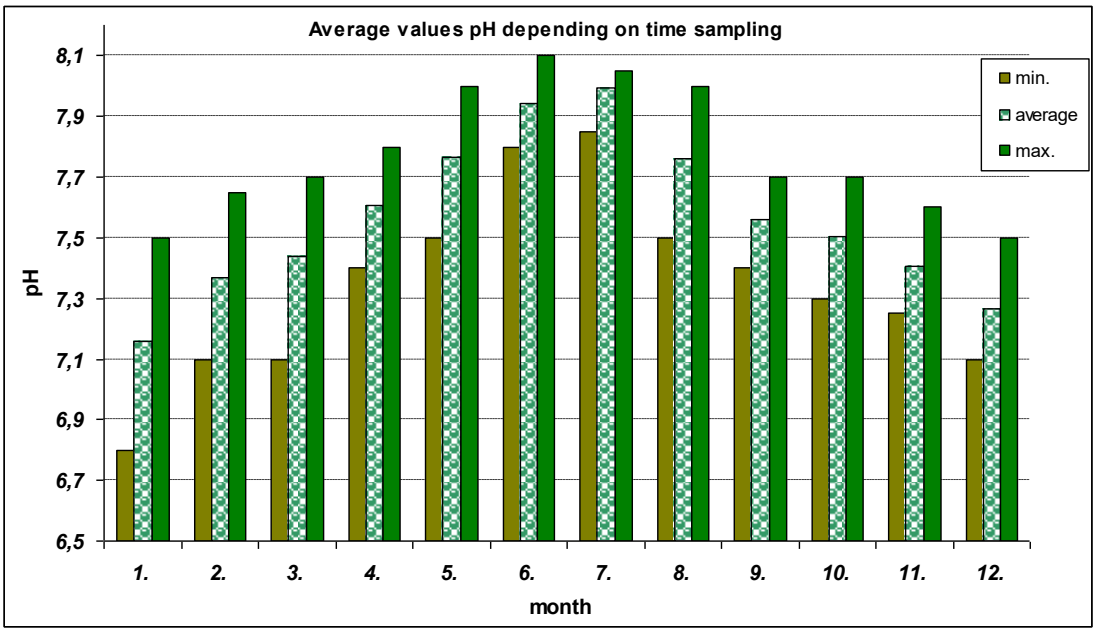


Fig. 3 Average pH values depending on the sampling time (1-12month). As an exsaple we present profile Komárňanský channel, (Okoličná na Ostrove).

https://doi.org/10.5593/sgem2024/3.1/s12.08

Monitoring of surface water bodies has been provided in terms of requirements for fresh water. Directive for water quality are in No. 1, Part A and E of NV 269/2010 determined as annual average and highest permissible concentrations. With regards of international and national legislative for the ecological status, ecological potential, chemical status assessment the biological quality elements (phytoplankton, phytobenthos and water macrophytes, benthic invertebrates, fish), supporting physical-chemical and hydro-morphological quality elemnts as well as the specific substances have been investigated.

DISCUSSION

The main purpose of this paper was to provide a brief review on recent state of water pollution in Žitný ostrov channel network and understanding the mechanisms of water worsening. Irrigation is usually required for agriculture in regions where water is in limited supply due to the lack of precipitation during some part of the growing season. The agrochemicals can have detrimental effects to the receiving environments, causing changes in water quality.

The variation of pH, temperature and conductivity also affect vegetation and algal bloom growth. These processes are important condition for them. Temperature increases and conductivity decreases faster than ever in short time. Statistical analysis shows that the influence of pH and temperature on algal growth rate is the largest, followed by their interaction.

Water deterioration has become a environmental problem in recent years, and understanding the mechanisms of water pollutation will help for prevention, remediation of water pollution. Recent advances in current status and major mechanisms of water pollution, assessment, evaluation criteria, and the influencing factors were reviewed. Comprehensive analysis of the regime development for water quantity and quality in streams and their mutual relationship in selected basins of Slovakia.

This contribution analysed pollution problem, factors affecting this process, its consequences and possibilities of prevention. Important was to evaluate pollution state of surface water in Žitný ostrov channel network following the assessment physical-chemical and microbiological indicators in monitored period 2010–2020. The well-water quality parameters of Danube River basin indicated that inorganic chemical quality of water is excellent. The correlation between pH and other parameters is significantly positive for each season studied. We observed regularity in the seasonal dynamics of pH. The sampling location had a greater influence on the pH, than the seasonal dynamics.

Correlation and multiple linear regression were used for relating the given well-water chemical quality parameters to a set of independent chemical variables. to study the relationship between two hydrologic variables and also investigate the dependence between successive values of a series of hydrologic data.

CONCLUSION

Water quality assessment is important for environmental protection. Mechanisms and assessment of water pollution investigated. Water pollution has become (an) the environmental problem in recent years and understanding the mechanisms of water pollution will help in the prevention and remediation of water pollution. Recent

advances in the current status and major water pollution mechanisms, assessments, assessment criteria, and influencing factors are reviewed.

This contribution analysed pollution problem, factors affecting this process, its consequences and possibilities of prevention. Important was to evaluate pollution state of surface water in Žitný ostrov channel network following the assessment physical-chemical and microbiological indicators in monitored period 2010–2020.
The comprehensive set of data acquired within 10 years monitoring was partly assessed in the previous characterizing natural conditions of the conconred territory as well as bassic pedogenetic, physical and chemical features of the locations monitored. High pH values promote the growth of phytoplankton and result in bloom. The change in pH is directly related to reduction of water quality. Hydrological extremes are generally manifested in the form of floods and droughts. The increased incidence of drought is a new phenomenon resulting from a change in climatic conditions.

ACKNOWLEDGEMENTS

This contribution was supported by project *VEGA 2/0028/23* Seasonal variations of hydrodynamic and morphological parameters in lowland vegetated rivers.

REFERENCES

[1] Climate Atlas of Slovakia, Slovak Hydrometeorological Institute (SHMÚ), Bratislava, 2015, ISBN 978-80-88907-90-9.
[2] Pekárová P., Bajtek Z., Pekár J., Výleta R., Bonacci O., Miklánek P., Belz J., U., Gorbachova L. Monthly stream temperatures along the Danube River: Statistical analysis and predictive modelling with incremental climate change scenarios. In Journal of Hydrology and Hydromechanics, 2023, vol. 71, no. 4, p. 382-398, 2022ISSN 1338-4333.
[3] Bačová Mitková V., Investigation of water temperature changes in the Hron River in the context of expected climate change. In Acta Hydrologica Slovaca, 2023, vol. 24, no. 1, p. 52-62. (2022: 0.159 - SJR, Q4 - SJR). ISSN 2644-4690.
[4] McCleskey R. B.,, Nordstrom K.., Ryan J.N., Electrical conductivity method for natural waters. Applied Geochemistry 26, S227–S229, 2011.
[5] Cook, F.J., Nihal S., Jayawardane N.S., Rassam D.W., Christen, W.H. Hornbuckle J.W., Stirzaker R.J., Keith L. Bristow K.L.,Tapas K. Biswas T.K. The state of measuring, diagnosing, ameliorating and managing solute effects in irrigated systems., CRC for Irrigation Futures 2006,p.1- 38.
[6] Fulajtár, E., Čurlík, J. Barančíková G. Sedláková, B. Šurina, B.: Impact of the Gabčíkovo hydropower structure on the agricultural soils. VUPÚ Bratislava, 1997, p. 179.
[7] Raju N., J. Seasonal evaluation of hydro-geo-chemical parameters using correlation and regression analysis. Page 820-826 Current Science, Vol.91, No.6, 2009.
[8] Hem D., Study and interpretation of the chemical characteristics of natural water U.S. Geol. Surv. Water Suppl. Pap. 2254 1–263, 1985.
[9] McNeal B.L. Oster J. Hatcher J. Calculation of electrical conductivity from solution composition data as and aid to in-situ estimation of soil salinity. Soil Sci. 110. 405.- 414, 1970.

[10] Marandi M., Polikarpus A., Jõeleht: A new approach for describing the relationship between electrical conductivity and major anion concentration in natural waters Appl. Geochemistry 38 103–109, 2013.
[11] Rathore S., S., Chandravanshi P., Jaiswal K. Eutrophication: Impacts of Excess Nutrients Inpucts on Aquatic Ecosystem. Journal of Agriculture and Veterinary Science, Vol. 9, 89–96. . 2016.
[12] Hubert E., Wolkersdorfer Ch., Establishing a conversion factor between electrical conductivity and total dissolved solids in waters. Water SA Vol.41, No.4, 2015.
[13] Schùgerl R., Velísková Y., Sokáč M., Dulovičová R., Kováčová V., Influence of aquatic vegetation on quantitative and qualitative characteristics in lowland rivers]. Bratislava : VEDA, 2022. 118 s. ISBN 978-80-224-1994-9 Typ: AAB
[14] Velísková, Y., Dulovičová, R., Schügerl, R. 2017: Impact of vegetation on flow in a lowland stream during the growing season. Biologia 72/8, 840–846, DOI: 10.1515/biolog-2017-0095.
[15] Sokáč, M., Velísková, Y., Impact of Combined Sewer Overflows Events on Recipient Water Quality. In Cost-efficient Wastewater Treatment Technologies : Natural Systems. vol. 117. - Berlin ; Heidelberg : Springer, 2023, p. 241-271. (2022):
[16] Dulovičová R., Schűgerl R., Velísková Y. Hydraulic conductivity of saturated bed silts in Chotárny channel, Žitný ostrov area, Slovakia. In Acta Hydrologica Slovaca, vol. 23, no. 2, p. 180-189, 2022.
[17] Koczka Bara M., Velísková Y., Dulovičová R., Schügerl R., Influence of surface water level fluctuation and riverbed sediment deposits on groundwater regime. Journal of Hydrology and Hydromechan., vol. 62, no. 3, 177–185, 2014. DOI: http://dx.doi.org/10.2478/johh-2014-0030.
[18] Makovinská I., Velická Z., Hlúbiková D., Baláži P., Tóthová L: Methodology of monitoring and evaluation of surface water bodies of Slovakia VÚVH, 179 p, 2015 ISBN 978–80-89740–024.
[19] Directive of Government SR No. 269/2010 for accomplish suitable state of water. Governmmet of Slovak republic, Part 106/2010, validity of directive 2010.
[20] Pärn J., Pinay G., Mander U: Indicators of nutrients transport from agricultural catchments under temperature climate: A review. Ecological Indicators, 22, 4–15, 2012.

COMPARISON OF THE RESULTS OBTAINED BY THE PROPOSED METHODOLOGY FOR ENVIRONMENTAL RUNOFF WITH THOSE CALCULATED UNDER THE CURRENT REGULATION

Dr. Maya Rankova[1]

Assoc. Prof. Dr. Elena Bojilova[2]

Dr. Plamen Angelov[3]

PhD Borislav Vuchkov[4]

PhD Radoslava Ivanova[5]

[1] National Institute of Meteorology and Hydrology, **Bulgaria**

ABSTRACT

In climate change, drought, and water scarcity, the natural functioning of river systems largely depends on the proper distribution of water resources. Accurate determination of hydrological characteristics is essential for the sustainable management of water resources and provides information on the status and potential of water systems. Water management must be implemented in such a way as to meet the needs of man and the economy. At the same time, measures are taken to protect the quantitative characteristics of the aquatic environment. This means that water consumption must not exceed a particular limit value of the river flow - the ecological river flow. The development set determines the hydrological characteristics according to the methodology developed for determining the environmental flow for Bulgarian conditions and comparing it with the value according to the current regulation. The results obtained make it possible to make adequate management decisions, guaranteeing the maintenance of sufficient water in rivers and water ecosystems. The current regulation uses average annual and minimum average monthly water quantities. In our presented Methodology, the estimates are based on average monthly values grouped by three types of water content. It is recommended to work with a hydrological approach and standard statistical methods for calculating ecological flow, which requires a minimum of hydro-ecological information and enables the development of a national strategy.

Keywords: Ecological river runoff, regional relation, hydrological characteristics

INTRODUCTION

There is a regulation that provides minimum permissible discharge in rivers. This discharge equals 10 percent of the average multi-year water quantity, determined based on information from a representative period. This water quantity cannot be less than the minimum monthly average water quantity with a guarantee of 95 percent for the corresponding point under undisturbed mode. Understanding and managing the complexities of the relationship between ecological sensitivity and river runoff is crucial for the sustainable management of freshwater ecosystems and the services they provide to human societies. *[2].*

https://doi.org/10.5593/sgem2024/3.1/s12.09

In 2023, the Methodology for Ecological river flow was provided to the MoES (Ministry of Environment and Water), which determined three water thresholds at a given sensitivity for the respective area.

In NIMH, the values according to the existing regulations were compared to those obtained according to the proposed Methodology. After a thorough analysis, it was concluded that a hydrological approach and standard statistical methods are appropriate for Bulgaria's conditions to calculate the ecological flow.

MATERIALS AND METHODS

A detailed analysis of the basin of the Iskar River is made. Regional relations of 10% of the average multi-year water quantity and the minimum average monthly water quantity at 95% security are developed according to the regulation in force until now, and the regional relations for the three types of water according to the proposed methodology - high water season, medium water season and low water season. In a joint project with the MoEW, three water thresholds with set sensitivity to different areas have been defined. The methods and practices for ensuring the ecological conditions in the river basins on the territory of Bulgaria are defined in Art. 116, Art. 117, Art. 135, and Art. 188 of the Water Act *[8].*

The sensitivity thresholds to changes in the hydrological regime are based on the river type and the application site. Those thresholds are divided into high, medium, and low. They correspond to the months with the highest average river discharge values during the year. River flow disturbances that impact water levels must be taken into account.

The work is based on generalized regional relations and detailed hydrological analysis for points with different discharge-forming characteristics. Different rivers exhibit varying hydrological characteristics based on flow regime, discharge variability, and response to precipitation events. Classifying rivers based on their hydrological behavior (e.g., perennial vs. intermittent, flashy vs. stable flow) can help identify their sensitivity to changes in river flow. *[9].*

The developed methodology and the applied verification methods guarantee the currently valid legal requirements for ensuring the minimum permissible river flow in the rivers. Iskar River (fig 1) is formed in a moderate continental climate with decreasing air temperature, increasing precipitation from the plain to the high mountain part of the river basin, and an increase in the degree of forestation in the same direction. *[3],[4].* Higher mountain precipitation leads to more river flow, resulting in rivers with more variable flow regimes, particularly during spring snowmelt or heavy rainfall events. If the test is not passed, the initially selected parameters should be increased until the statutory minimums are reached. Based on three flow seasons, the recommended seasonal approach for determining the ecological flow thresholds is the most suitable for Bulgaria. This approach protects hydrologic regime variability for ecological river flow while avoiding unnecessary complexity in estimation.*[1]*

Ecological river flow methodologies assess and manage water discharge in rivers and streams to maintain or restore environmental health and functions. These methodologies consider the natural flow regimes of water bodies and aim to balance human water needs with the requirements of aquatic ecosystems. The application of river flow calculated at specific points to the relevant categories of the surface water bodies is below. [6].

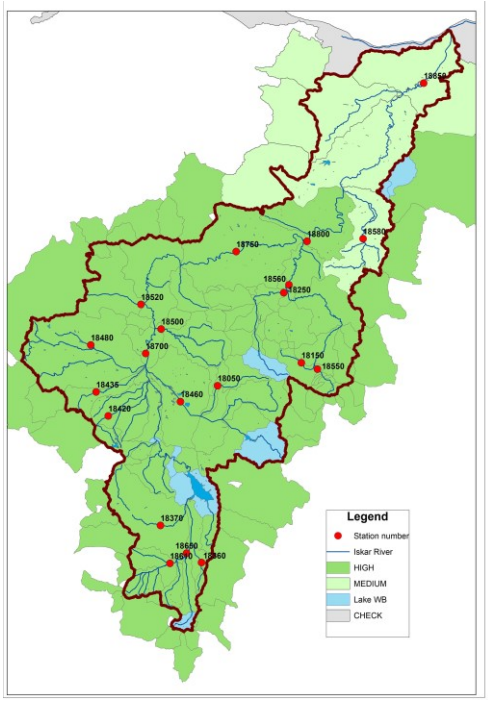


Figure 1. Scheme of the drainage basin of Iskar River basin with indicated sensitivity water bodies

RESULTS AND DISCUSSION

Multi-year average monthly water quantities have been determined, which reflect the formed discharge to the respective creation. It is important to note that various anthropogenic impacts affect the measurements in the existing hydrometric stations. For the present study, the data from 20 hydrometric stations (HMS) were used, which, in terms of area, cover the entire watershed, and their density in the upper and middle part of the watershed is more significant compared to that in the lower flat part. *[7].*

Data from all stations were used for the study. The hydrological characteristics in any number of points were determined according to a developed methodology for determining the ecological river runoff for DRBD (Danube River Basin Directorate). They were compared with the values obtained according to the regulations currently in force with data for the reference period 1981-2019.

When determining the regional relation on water content, the methodology's recommendations were followed, as in most cases, the months with the same water content are not chronological.*[1], [5].*

The regions formed for the three water types—low, medium, and high—are the same. Due to the specificity of some sections, the method of regionalization, analogy, and transfer of the module of the outflow from a place with an observation hydrometric station (HMS) to the corresponding point is applied.

After a hydrological analysis of the homogeneity of the sections in the Iskar river basin, four regions were formed: individual areas, the same for the three water types, and four

others by analogy and transfer of information of the outflow module from a place with monitoring HMS to the corresponding point. Eight regions were established (Fig. 2 ÷ Fig. 5).

Table 1. Analyzed hydrometric stations within the Iskar River basin.

River	Station number HMS №	Location	Drainage area (F, km²)
Matica	18050	Eleshnica	97.198
Suha	18150	Boikovec	25.568
Bebresh	18250	Svode	495.068
Musalenska Bistrica	18360	Borovec	19.380
Palakaria	18370	Reliovo	277.963
Vladaiska	18420	Sofia	49.473
Bankenska	18435	Bankia	53.948
Leskovska	18460	Peturch	842.938
Blato	18480	Peturch	97.978
Batulia	18500	Batulia	251.443
Iskrecka	18520	Svoge	276.623
Malusk Iskar	18550	Etropole	54.590
Malusk Iskar	18560	Svode	1171.615
Panega	18580	Petrevene	180.390
Iskar	18610	Govedarci	43.9
Iskar	18650	Beli Iskar	329.473
Iskar	18700	Novi Iskar	3550.253
Iskar	18750	Reburkovo	4797.473
Iskar	18800	Roman	6522.738
Iskar	18850	Orehovica	8312.118

Region 1 (fig.2): *Musalenska Bistrica river* – HMS №. 18360, starting from the highest massif of the Rila, which divides the Iskar region from the Maritsa region, and HMS №. 18650 on the Iskar River near the village of Beli Iskar. To confirm the dependence, the closed HMS №. 18610 on the river Iskar (Cherni Iskar) near Govedartsi was also used.

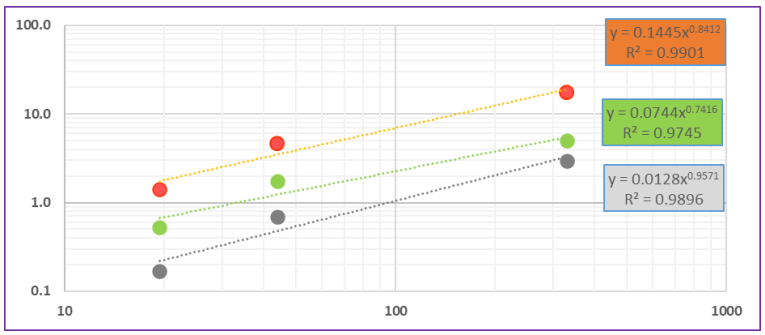


Figure 2. Relation between high, medium, and low flow season discharge (m^3/s) and drainage area (F, km^2)

Region 2: *Palakaria River*. Due to the specifics of the catchment area, the average multi-year water quantity is determined by transferring the river flow related to HMS № 18370 - Palakaria River near the village of Reliovo.

Region 3 (fig.3): *Tributaries of the Iskar River from the Pancharevo dam to Rebarkovo.* The Sofia basin is a catchment basin in which surface and underground waters are formed. The entire valley is drained by the river Iskar and its tributaries - Lesnovska, Perlovska, Vladaiska, Bankenska, Blato, etc. Characteristic features of the regime of the rivers here are the large overflows that cause flooding in agricultural and residential areas. Form a common regional dependence, including the data of 7 hydrometric stations, namely: № 18050 - Matitca (Eleshnitsa) near the village of Yordankino, № 18420 - Vladaiska - Sofia, Kniazhevo quarter, № 18435 - Bankenska near Bankia, № 18480 - Blato near the town of Petarch, № 18500 - Batuliyska near the village of Batulia, № 18520 - Iskretska near Svoge and № 18700 - Iskar near Novi Iskar (Kurilo).

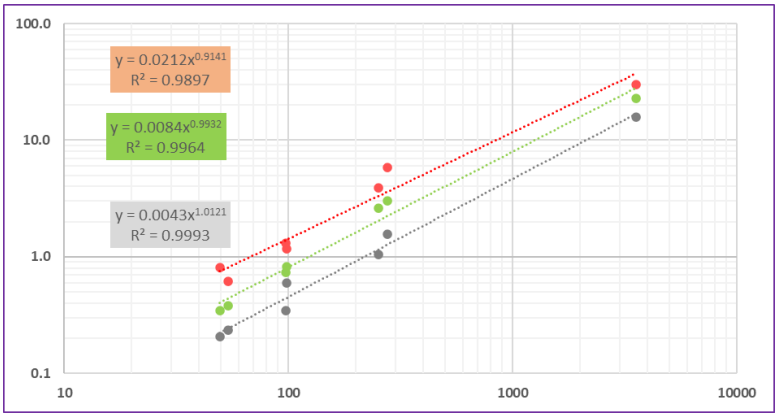


Figure 3. Relation between high, medium, and low flow season discharge (m^3/s) and drainage area (F, km^2)

Region 4: *Lesnovska river* after Ognyanovo Dam - Due to the specifics of the catchment area and the influence of the Ognyanovo Dam, the average multi-year water quantity in the lower part of the river is determined by transferring the river flow related to HMS № 18460 - Lesnovska river near the village of Petarch.

Region 5 (fig.4): *Malak Iskar River covers the riverbed of the Malak Iskar River*. The data from the following hydrometric stations were used: № 18150 - Suha River near the village of Boykovets, № 18250 - Bebresh near the town of Svode, № 18550 - Maluk Iskar near Etropole, № 18560 - Malak Iskar near the town of Svode, № 18800 - Iskar near Roman.

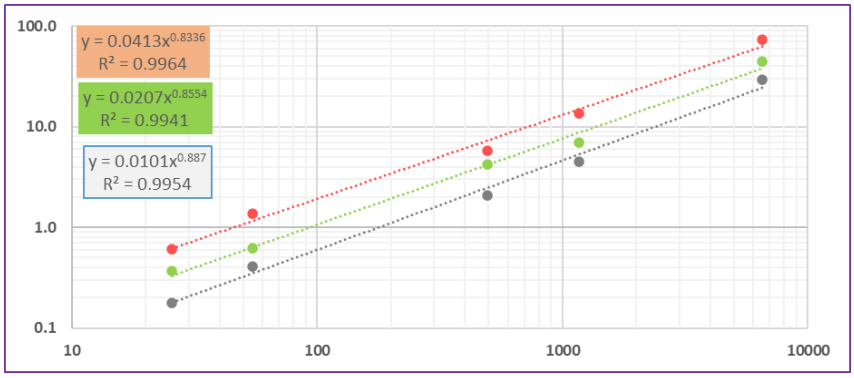


Figure 4. Relation between high, medium, and low flow season discharge (m^3/s) and drainage area (F, km^2)

Region 6: *Panega River* originates from the largest spring in Northern Bulgaria. It is near the river Vit and takes part of its waters underground, so the catchment area is significantly larger than the orographic one. These specific features of the river set it apart with an independent regional relation. Due to the specificity of the river flow formation (karst feeding) and its disturbance, it is determined by transferring the river flow of HMS № 18580 - Panega village of Petrevene.

Region 7 (fig. 5): *The main river* – Iskar, from the Pancharevo dam to the mouth. The main river after the Pancharevo dam unites the waters and, accordingly, the characteristics of its tributaries. The downstream shows values of a gradual decrease in the module of the maximum outflow depending on the area. The data from the following hydrometric stations were used: № 18700 - Iskar near Novi Iskar (Kurilo), № 18750 Iskar near the village of Rebarkovo, № 18800 Iskar near Roman, № 18850 - Iskar near the town of Orehovitsa, № 18650 on the Iskar river near the village of Beli Iskar and the closed hydrometric station № 18610 on the river Iskar (Cherni Iskar) near the town of Govedartsi.

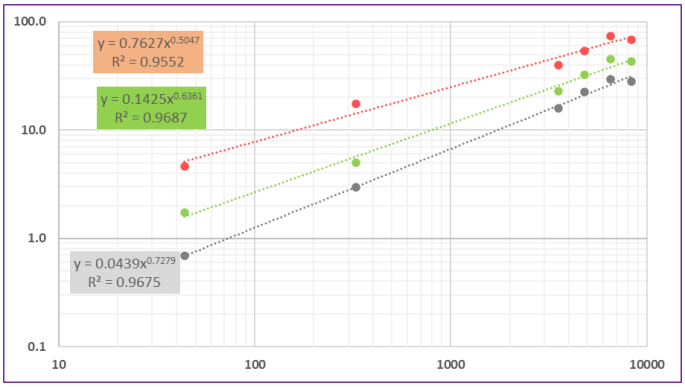


Figure 5 Relation between high, medium, and low flow season discharge (m^3/s) and drainage area (F, km^2)

Region 8: *Gostilya River* – Due to the lack of monitoring and a suitable analog station in the Iskar River catchment, a comparative analysis was performed to determine the outflow of the non-monitored Gostilya River. An analog station was selected in the Skat River catchment—HMS № 17650 near the village of Nivianin. The method of analogy was used.

CONCLUSION

The NIMH surface water monitoring network consists of 197 unevenly located hydrometric stations. Due to their unequal location in different basins, observations from hydrometric stations cannot be used directly in most cases. Calculating environmental river flow can require extensive data collection and analysis of various factors. However, it is an essential step in understanding the impact of humans and other factors on the environment and how measures can be taken to protect nature.

Water management must be implemented to meet the needs of man and the economy while protecting the quantitative characteristics of the aquatic environment. This means that water consumption must not exceed a particular limit value of river flow—the ecological river flow. When evaluating the regional dependencies for the three water types, the data for the points monitored by NIMH and their catchment area were used.

The watershed of the Iskur River was shown as a pilot study to present the new methodology. Eight homogeneous regions were formed, and results were presented and discussed. In the presented method, the estimates are based on average monthly values grouped by three types of water content. It is recommended to work with a hydrological approach and standard statistical methods for calculating ecological river flow, which requires a minimum of hydro-ecological information and enables the development of a national strategy.

ACKNOWLEDGEMENTS

The paper is based on the research project “Determination of the hydrological characteristics according to a developed methodology for determining the ecological flow for the conditions of Bulgaria and comparison with the values according to the current regulations” with project leader Prof. Plamen Ninov. The author wishes to acknowledge Eng. Kamelia Krumova supervised the research concerning the Iskar River basin.

REFERENCES

[1] Bozhilova E.K., Application of Methodology for Ecological Flow for Yantra River Basin in Bulgaria, Journal of Balkan Ecology, Vol. 27, № 1, ISSN 1311-0527 (Print) ISSN 2815-3758 (Online), pp 67-78, 2024

[2] Dimitrov Y., Yordanova A., Trends assessment of meteorological factors, river flow and droughts in North-western Bulgaria, E-book with full paper from XXVII Conference of The Danubian Countries, pp 321-330. Bulgaria, ISBN 978-654-90537-2-2, 2017.

[3] Dimitrov Y., Ilcheva I., Application of an Indicator System for Integrated Space-time Analysis and Drought Management in North-western Bulgaria, XXIX Conference of the Danubian Countries, The Czech Republic, Conference Proceedings with Full Papers, ISBN 978-80-7653-031-7, pp 172–180, 2021.

[4] Ilcheva I., Yordanova A., Nikolova K., Estimation of the Impact of Climate and Land Use Changes on the Availability of Water Resources and Drought Risk, International Multidisciplinary Scientific Geo-conference SGEM 2019, Bulgaria, pp 193-200, 2019.

[5] Ninov, Pl., Karagiozova, Tz., Rankova, M. 2017. Water Resources Determination of Surface Water Bodies at the Bulgarian basin of the Lower Danube, Journal of the Geographical Institute “Jovan Cvijić” SASA, Vol. 67, No 1

[6] Hristova N., Seymenov K., Annual Flow Dynamics in Large and Small Drainage Basins in Northern Bulgaria during the Last Two Decades, Socio-Brains, ISSN 2367-5721, issue 54, pp 123-131, 2019.

[7] Balabanova Sn., Operational system for streamflow forecasting in the Iskar river basin based on Artificial Neural Networks, INHGA - Scientific Conference/Bucharest, November 10-11, 2014, ISBN 978-973-0-18825-7, p. 159-166

[8] Ninov P., Karagiozova T., Monitoring and Investigation of Intermittent Rivers in Bulgaria, E-book of the 28th Conference of the Danubian Countries, Ukraine, pp 6-14, 2019.

[9] World Bank. Delivering the Water Framework Directive in Bulgaria: Developing a Flows Approach WSP, WSP Environment & Infrastructure Solutions UK Limited, 2022.

DROUGHT INDICES AND VIS-BASED CANOPY STATUS OF VINEYARDS

Prof. Dr. Mariam Tsitsagi[1]

MS. Ana Palavandishvili[1]

MS. Zaza Gulashvili[1]

[1] TSU, Vakhushti Bagrationi Institute of Geography, **Georgia**

ABSTRACT

The study aims to evaluate how droughts impact irrigated and non-irrigated vineyards by analysing the relationship between short-term drought and vegetation indices to identify areas irrigated from unofficial sources. The re-search area includes vineyards in Telavi municipality (eastern Georgia). RStudio was used to calculate SPI and SPEI (1- month and 3-month timescales) and EDI (daily) to measure the severity of the meteorological drought. The 27-year (1993–2020) data from a weather station in the study area included daily temperature and precipitation. Water stress in crops using Sentinel 2-based NDVI and NDMI data from April 1 to August 31, 2020, was estimated in ArcMap 10.8. For accuracy assessment, data from the vineyard cadaster (2020) and Georgian amelioration were used. The study's findings indicate that based on the SPI and SPEI (1-month and 3-month) values, the growing season of 2020 experienced a near-normal (-1–1) condition. In June, there is a reported moderate drought (SPI_1=- 1.3, SPEI_1=-1.6), and in July, the 3-month data shows a value of -1.1 for SPEI_3. According to daily EDI measurements, the number of drought days is highest in June and early July. Because of the climatic conditions in the research area, irrigation is re- quired for the agricultural parcels. The Georgian irrigation system is the country's primary source of irrigation water. According to official sources, 589 hectares of vineyards out of a total of 6936 hectares receive irrigation. Examining the irrigated parcels' vegetation indices showed that, despite the dry days, the NDVI and NDMI values remained stable, while in some parcels, the values decreased significantly after the dry days. Identified areas include those that receive water from a variety of sources, as well as those that lack both official and unofficial irrigation sources. The findings indicated that 5.3% (337 ha) of vineyards lack an alternate water source, whereas 94.7% (6010 ha) receive water supply during periods of drought. Additional data analysis showed that the majority of such parcels are adjacent to rivers and provide water supplies on their own. The findings ensure that we can accurately evaluate irrigation patterns using drought and Sentinel-based vegetation indices.

Keywords: Drought, SPI, SPEI, NDVI, NDMI

INTRODUCTION

Currently, societies deal with various natural hazards, with drought being one of the most severe in many regions. Generally, it is classified into meteorological, agricultural, hydrological, socio-economic [1] and ecological droughts [2]. It is

generally accepted that extreme climate events such as droughts have significantly increased in frequency and severity since the 1970s [3] and will become more common worldwide [2]. Economic losses by global meteorological disasters accounted for 85% of all-natural disasters, among which droughts were responsible for more than 50% of all meteorological disasters [3]. The rapid increase in population and socio-economic needs has increased the pressure on the agricultural sector. Climate change will add to the increasing demand for water. More severe and more frequent droughts will increase water shortages in the agricultural sector, a significant consumer of water, especially in the semi-arid and arid regions. Accordingly, drought research is vital for countries or regions with a strong focus on agricultural production.

Much research in recent years focused on meteorological drought. It is defined as a lack of precipitation over a region for some time [1] and is well monitored using indices such as the Standard Precipitation Index (SPI) [4], the Standard Precipitation Evapotranspiration Index (SPEI) [5], and the Effective Drought Index (EDI) [6], among others.

The World Meteorological Organization recommends that the SPI should be used by all National Meteorological and Hydrological Services worldwide to characterize meteorological droughts [7]. Because it is calculated only based on precipitation data and does not consider parameters such as evaporation, a new index SPEI has been created where potential evapotranspiration (PET) is considered as well. Similar to the SPI, it can be calculated for periods of 1-24 months. The EDI also relies on precipitation data similar to SPI; both SPI or EDI do not consider other parameters such as vegetation, temperature, and soil moisture, while SPEI includes temperature. EDI can be calculated on both daily and monthly timescales.

Meteorological droughts, among other processes, affect hydrological and agricultural droughts. An abnormal decrease in precipitation causes agricultural drought, which is influenced comprehensively by land surface temperature, evapotranspiration, soil properties, and physiological or ecological characteristics of the crop [3]. Agricultural drought is a considerably complex phenomenon and is affected by meteorological droughts due to soil properties, the presence of groundwater, and irrigation. Generally, drought can be monitored through either ground observations or re-mote sensing. Ground observation is a direct and accurate method for drought monitoring, but it is challenging to obtain sufficient spatial information for regional monitoring. It is also quite labour- and cost-intensive [8], especially when assessing agricultural drought. On the other hand, assessing of agricultural droughts only by meteorological drought indices is ineffective. It is commonly accepted that dry conditions occur only during a particular part of the hydrological cycle and often do not even show simultaneous water deficits in soil moisture, streamflow, reservoir storage, and groundwater [9]. Accordingly, remote sensing-based indices are preferable for agricultural drought monitoring [10]. It represents a fast and economical method for drought monitoring but needs to develop a practical approach for the study region [8]. Recent advances in the remote sensing of microwave e land emissivity indicate that there are opportunities to quantify surface soil moisture and vegetation water content [11].

The territory of Eastern Georgia is characterized by solid droughts, which in turn

affect the crop, and all which is reflected in the economic situation. For Georgia, the agricultural sector is an important part of the economy, in which wine-making occupies a leading place. Proper supply of irrigation water and determination of losses remain a challenge in the country. The aim of the research is to determine the water status in the vineyards of east Georgia (Telavi municipality) by using drought indices and vegetation indices (VIs) to determine unofficial irrigation.

MATERIALS AND METHODS

Telavi municipality (E 045°31'N41°56') located in eastern Georgia has moderate humid climate with moderately cold winter and hot summer, precipitation with two minimum per year. Drought is expected mainly during the spring, summer, and autumn seasons. During winter, due to frequent cyclonic and frontal periods, the dry day duration is shorter. Data on the vineyards in the study area were obtained from the cadastre of vineyards in the country (2020). The data on the official irrigation areas in the municipality are obtained from the Georgian Amelioration (GA). Daily precipitation and temperature data (1993-2020) from the weather station provided by the National Environment Agency (NEA), Georgia, was used in this study.

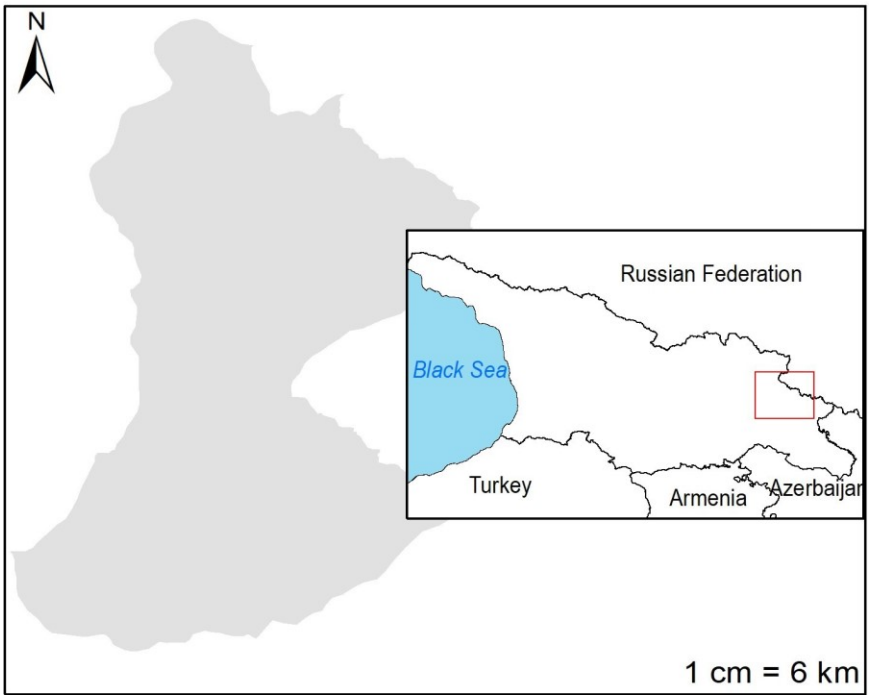


Fig. 1. Study area-Telavi municipality

The study used three indices to assess meteorological droughts: SPI, SPEI, and EDI, and two Sentinel 2-based indices (Normalized Difference Vegetation Index (NDVI) and Normalized Difference Moisture Index (NDMI)) to assess agriculture drought. The Copernicus Sentinel-2 mission is based on a constellation of two identical satellites in the same orbit. Each satellite carries an innovative wide swath high-resolution (10m) multispectral imager with 13 spectral bands for a new perspective of our land and vegetation.

The R package-SPEI [12] was used to calculate SPI and SPEI for 1 and 3 months. EDI was calculated according to [6] at daily timescales (365 days). Drought indices

have the same threshold: extremely wet (>2), severe wet (1.5-2), moderate wet (1-1.5), near normal (-1-1), moderate dry (-1.5- -1), severe dry (-2- -1.5). VIs were calculated in Arcmap 10.8 with equations (1) and (2), where NIR is near infrared (band 8), R is red (band 4) and SWIR is shortwave infrared (band 11).

$$(NIR - R)/(NIR + R) \quad (1)$$

$$(NIR - SWIR)/(NIR + SWIR) \quad (1)$$

Both VIs values range from +1.0 to -1.0. Areas of barren rock, sand, or snow usually show very low NDVI values (for example, 0.1 or less). Sparse vegetation such as shrubs and grasslands or senescing crops may result in moderate NDVI values (approximately 0.2 to 0.5). High NDVI values (approximately 0.6 to 0.9) correspond to dense vegetation. While the lowest values of NDMI indicate low vegetation water content, and the highest ones correspond to high water content. For the irrigated areas, we calculated the average values of the VIs (April-August as growing season) and compared them with the values of the official non-irrigated areas. Parcels with a Pearson correlation of
0.5 and above were identified as irrigated (in this case from unofficial sources).

RESULTS

According to the data obtained from official sources, only 589 ha (8.5%) of the 6936 ha of vineyards in Telavi municipality are irrigated by GA based on the official agreement. The aim of the study was to determine those parcels that do not receive irrigation water from the official source (GA) using drought indices and VIs. Although we used a 28- year period of data to calculate the drought indices, only the situation of 2020 is considered in this particular research.

The analysis of the drought indices showed that although the EDI daily data shows a moderately dry period in the study area from the second decade of May onwards, and in July it turns into a severe dry condition, the long-term indices do not confirm this (Fig. 2). Based on the SPI and SPEI (1-month and 3-month) values, the growing season of 2020 experienced a near-normal (-1–1) condition. In June, there is a reported moderate drought (SPI_1=-1.3, SPEI_1=-1.6), and in July, the 3-month data shows a value of -1.1 for SPEI_3.

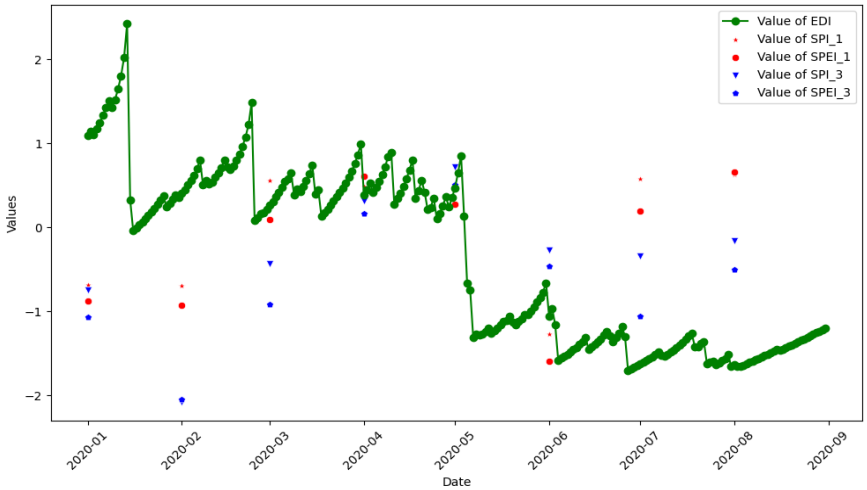


Fig. 2. Drought indices during the growing season.

Figure 3 shows the average values of NDVI (Fig. 3a) and NDVMI (Fig. 3b) of official irrigation parcels during the growing season. Both indices react almost the same, namely in April and May there are relatively low (0-0.3) NDVI values, and in June and July, despite relatively dry conditions (Fig. 2), VIs values do not decrease sharply. NDVMI values also range between 0-0.2 in June and July, indicating low water stress. Figure 2 presents the values of VIs of officially non-irrigated parcels and their relation to the average values of irrigated parcels. Officially, 6,347.7 ha (91.5%) of the parcels are not irrigated, totaling 14,599 parcels.

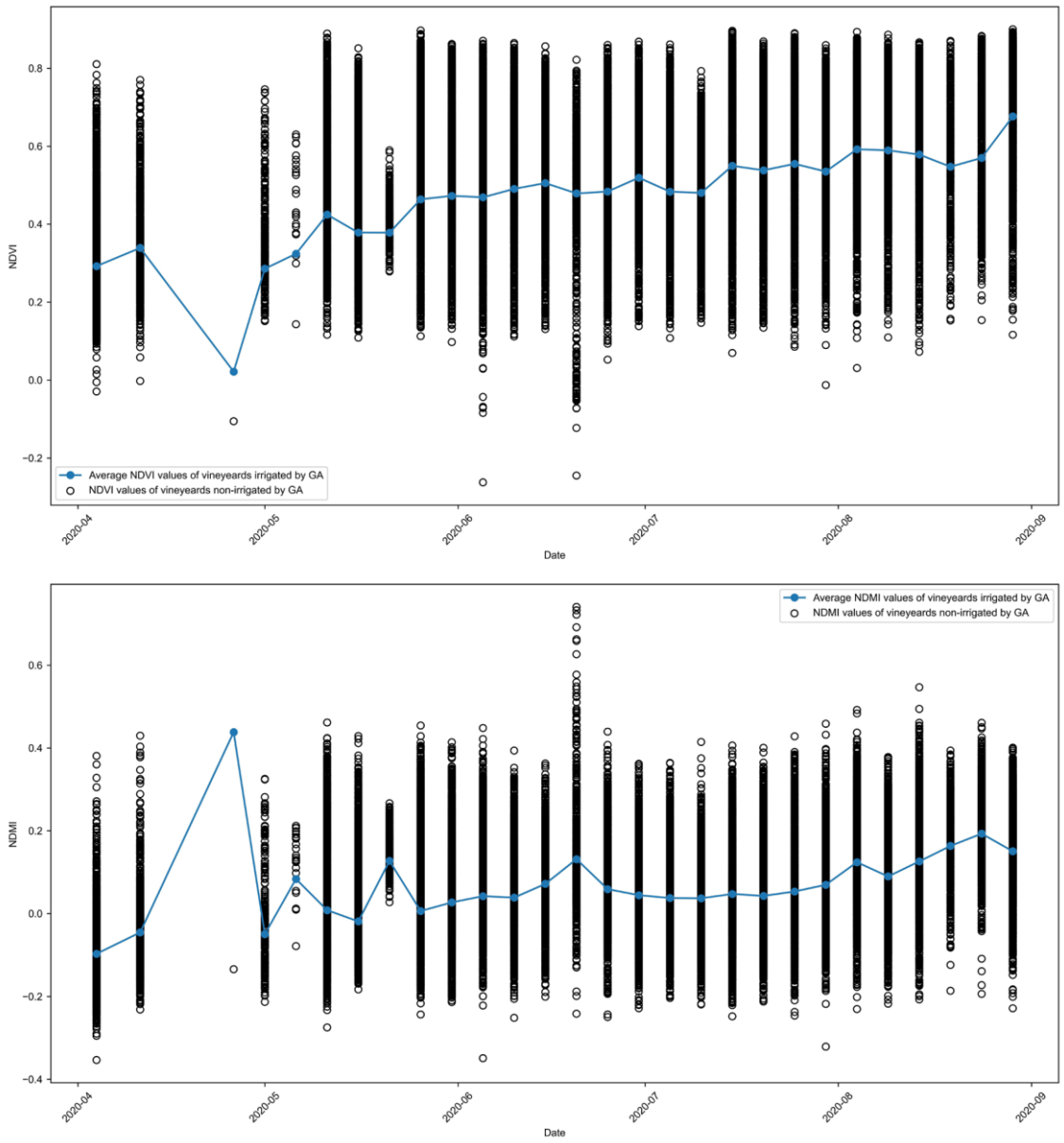


Fig. 3. The relationship between Vis values of officially irrigate and non-irrigated parcels during growing season.

As mentioned above, parcels with a Pearson correlation of 0.5 and above were identified as informally irrigated (i.e., parcels that have access to irrigation water

without a contract with the GA), while parcels with a low correlation were identified as non-irrigated. In this case, the correlation with both indices is taken into account, i.e., passes that had a correlation index of 0.5 or more in the case of both indices. Correlation of VIs on irrigated and non-irrigated parcels confirmed that approximately 48.3% of parcels (officially non-irrigated) (3348 ha) have a high correlation with the average indicator of irrigated parcels, while 43.2% (2999 ha) react differently to drought and the values of both indices decrease, i.e., suffers from water shortage.

DISCUSSION

In general, the use of long-term indices to observe agricultural droughts is more effective. It was found that in the same meteorological drought conditions vineyards and orchards are less sensitive to drought compared to arable lands

According to the results of the research, 2020 was not marked by a drought, although the agricultural drought is a phenomenon that is insufficient to be discussed as of one year. That is why 28 years of data were used in the study. Previous studies confirm that Kakheti (the region where Telavi Municipality is located) is particularly vulnerable to droughts [13]. In general, SPI is characterized by relatively extreme indicators, both positive and negative, in the short-term evaluation. The same is confirmed by the study by [14], where the results show that the longer the time scale the smaller the weight of the monthly value in the case of both indices.

The study confirmed that despite the very small officially irrigated areas (only 8.5% of the total area of vineyards), quite large areas of vineyards (48.3% of non-irrigated vineyards) receive water from alternative sources. Additional spatial analysis showed that this picture may be caused by several circumstances: 1. The mentioned parcels are located near the river and naturally it is not difficult to deal with drought; 2. In addition to the parcels officially contracted by GA, the result of irrigation itself is reflected on the neighbouring parcels as well; 3. Based on the topographical features, the parcels on the plain benefit from the irrigation water by themselves.

CONCLUSION

The aim of the study was to evaluate how drought indices can be used for agricultural monitoring. Analysis of three different timescales (daily, 1-month, 3-month) indices of meteorological drought (EDI, SPI, SPEI) and VIs used in the study showed that EDI data accurately reflects instantaneous drought and agricultural drought response in most cases. Therefore, based on EDI data, it is possible to determine at an early stage whether moisture deficit will be created for agricultural lands. The results obtained on the other hand assured us that the use of long-term indices in the observation of agricultural droughts is more advantageous to capture a complete picture. Effective use of irrigation water in Telavi municipality is one of the main challenges of the agricultural sector. The use of VIs in the assessment of agricultural droughts is a practical tool that we can effectively use for the efficient use of irrigation water. The example of Telavi municipality showed that the area of parcels receiving water from alternative sources exceeds the official users of GA. The research has some limitations, for example, high fragmentation of parcels (6936.8 hectares of vineyards in Telavi municipality are divided into 15148 parcels). In this

case, even if one owner has a contract with GA, the positive result will be reflected on neighbouring parcels as well. The same natural regularity is due to the relief, in the lowland parcels the water stress from the irrigation parcels on the slopes is automatically regulated.

In the future, the use of detailed RS images will improve the accuracy of the results and provide more detailed data that will help us allocate irrigation water more efficiently.

ACKNOWLEDGEMENTS

The authors are grateful to the Georgian National Environment Agency (NEA) for providing the meteorological data. This work was supported by the Shota Rustaveli National Science Foundation of Georgia (SRNSFG) [FR-21–13962].

REFERENCES

[1] Mishra, A. K., Singh, V. P.: A review of drought concepts. Journal of Hydrology 391(1–2) (2010).

[2] Yihdego, Y., Vaheddoost, B., Al-Weshah, R. A.: Drought indices and indicators revisited. In Arabian Journal of Geosciences 12(3), (2019).

[3] Liu, X., Zhu, X., Pan, Y., Li, S., Liu, Y., Ma, Y.: Agricultural drought monitoring: Pro-gress, challenges, and prospects. Journal of Geographical Sciences 26(6), (2016).

[4] McKee, T. B., Nolan, J., & Kleist, J. (1993). The relationship of drought frequency and duration to time scales. Preprints, Eighth Conf. on Applied Climatology, Amer. Meteor, Soc., January.

[5] Vicente-Serrano, S. M., Beguería, S., & López-Moreno, J. I. (2010). A multiscalar drought index sensitive to global warming: The standardized precipitation evapotranspiration index. Journal of Climate, 23(7). https://doi.org/10.1175/2009JCLI2909.1

[6] Byun, H. R., Wilhite, D. A.: Objective quantification of drought severity and duration. Journal of Climate 12(9), (1999).

[7] Copernicus European Drought Observatory (EDO): https://edo.jrc.ec.europa.eu/

[8] Gao, M., Qin, Z., Zhang, H., Lu, L., Zhou, X., Yang, X.: Remote sensing of agro-droughts in Guangdong Province of China using MODIS satellite data. Sensors 8(8), (2008).

[9] Vicente-Serrano, S. M., Beguería, S., Lorenzo-Lacruz, J., Camarero, J. J., López-Moreno, J. I., Azorin-Molina, C., Revuelto, J., Morán-Tejeda, E., Sanchez-Lorenzo, A.: Performance of drought indices for ecological, agricultural, and hydrological applications. Earth Interactions 16(10), (2012).

[10] Aswathi, P. V., Nikam, B. R., Chouksey, A., Aggarwal, S. P.: Assessment and monitoring of agricultural droughts in Maharashtra using meteorological and remote

sensing based indi-ces. ISPRS Annals of the Photogrammetry, Remote Sensing and Spatial Information Sci-ences 4(5), (2018).

[11] AghaKouchak, A., Farahmand, A., Melton, F. S., Teixeira, J., Anderson, M. C., Wardlow, B. D., Hain, C. R.: Remote sensing of drought: Progress, challenges and opportunities. In Reviews of Geophysics 53(2), (2015).

[12] Santiago Beguería., Sergio M. Vicente-Serrano.: SPEI: Calculation of the Standardized Precipitation-Evapotranspiration Index. R package version 1.7. (2017).

[13] Tatishvili, M., Palavandishvili, A., Tsitsagi, M., Suknidze, N. (2023). The Big Data for Drought Monitoring in Georgia. In: Geibel, R.C., Machavariani, S. (eds) Chances and Challenges of Digital Management. ISPC 2022. Springer Proceedings in Business and Economics. Springer, Cham. https://doi.org/10.1007/978-3-031-45601-5_13

[14] Labudová, L., Labuda, M., & Takáč, J. (2017). Comparison of SPI and SPEI applicability for drought impact assessment on crop production in the Danubian Lowland and the East Slovakian Lowland. Theoretical and Applied Climatology, 128(1–2). https://doi.org/10.1007/s00704-016-1870-2

FISHER-X: AN ENGINEERING CONCEPT TO MONITOR WATER ENVIRONMENTS USING ROBOTIC BIOMIMICRY

Yury Vasquez-Charcape[1]
Gustavo Jamanca-Lino[2]
David Sanchez-Perez[3]
Bruno Cevallos[4]

[1]Universidad Nacional de Moquegua, **Peru**
[2]Universidad Privada del Norte, **Peru**
[3]Universidad Peruana de Ciencias Aplicadas, **Peru**
[4]Universidad Científica del Sur, **Peru**

ABSTRACT

Human activities have significantly impacted aquatic ecosystems worldwide, especially in developing countries. Acid mine drainage from mineral extraction and wastewater containing xenobiotics pose substantial threats for lakes and marine ecosystems, introducing heavy metals and increasing antibiotic resistance in pathogenic microbes. Despite the urgent need for effective solutions, many environmental liabilities remain without an adequate mapping unmapped or remediation plan, exacerbating risks for environmental health. To address these challenges, our team proposes FISHER-X, a biomimetic robot inspired by the hadal snailfish *Pseudoliparis swirei*. This innovative technological tool is designed to support integrative studies and monitor water bodies near industrial facilities, particularly mining units. FISHER-X's proposed capabilities make it a suitable tool for assessing polluted and hazardous environments. This paper presents the conceptual design of FISHER-X, including fundamental equations for engineering design, motion mechanisms based on computational simulation, and a proposed validation test. Potential applications extend beyond conventional environmental monitoring, such as habitability surveys, life detection, and physicochemical characterization and mapping of aquatic environments on Earth and beyond.

Keywords: underwater robot, water pollution, acid mine drainage, bioinspiration, undulatory motion, FISHER-X.

INTRODUCTION

In recent years, anthropogenic industrial activities have caused significant pollution in many aquatic ecosystems. In Peru, an emerging country in Latin America, one of the major environmental concerns is acid mine drainage (AMD). This issue affects rivers and lakes, which provide essential services to rural communities. To address this issue, the authors propose the development of FISHER-X [1], illustrated in Figure 1. The concept aims to enhance the monitoring and diagnostic capabilities of water bodies through holistic and continuous real-time monitoring. It focuses on areas near mining activities to measure and control pollution, as well as on remote natural areas, to gather valuable scientific data.

Since the early designs of Leonardo da Vinci, machines have supported underwater exploration, today expanding human capacity to perform activities in previously inaccessible places [2]. Bioinspired robots, which use pneumatic actuators, cables, and "shape memory" alloys, mimic the natural movement of soft-tissue gelatinous animals, such as fish, cnidarians, and cephalopod mollusks [2-5]. Indeed, bioinspired soft robotic designs have improved adaptability and versatility for challenging tasks in unpredictable environments [6-7].

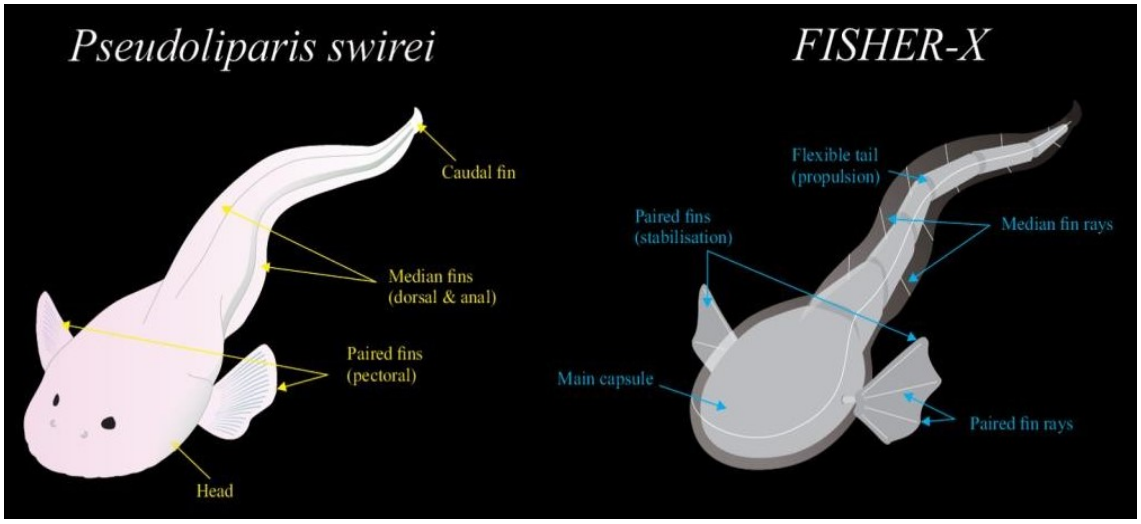


Figure 1. FISHER-X bioinspired design concept. Design made by the authors.

The FISHER-X project started in 2021 as a system projected for astrobiological purposes. Currently, the terrestrial application is in conceptual phase (TRL-2). It aims to develop and implement a monitoring system with minimal environmental impact and disturbance for the living species in water bodies. Initial results from FISHER-X have already been presented at conferences in Paris [1] and Canada, and the team is receiving support and mentoring from the peruvian mining sector through the Perumin Hub Bootcamp: "*Jóvenes que transforman*". The paper introduces the conceptual design of FISHER-X, encompassing fundamental equations for engineering design, motion mechanisms, computational simulations, and a proposed validation test.

MATERIALS AND METHODS

Need analysis and objectives definition

This article outlines the methodological aspects of the initial phase of conceptual design. The design of FISHER-X uses the ISO/IEC 15288 model ("Systems Engineering-System Life Cycle Processes") which involves eight stages and 25 main processes. For FISHER-X design, the methodology includes A) Needs analysis based on a systematic review of 180 indexed articles, already published in a previous article [1]. B) Definition of the objectives, covering performance, cost and lifespan. C) Analysis of alternatives, based on 13 systems proposed to explore the extreme environments on oceanic worlds. D) Conceptual design, modeling and simulation. The results section details the system operation strategy, application of mathematical models for the oscillatory wave movement of the fish body, modelled in Matlab, as well as SolidWorks kinematic simulations for the innovative dorsal fin mechanism.

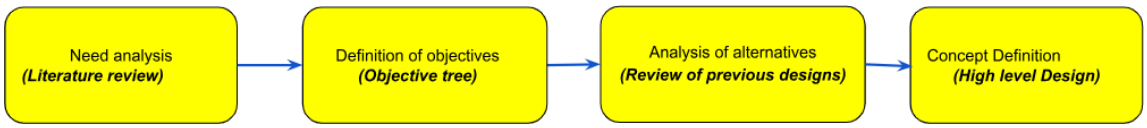


Figure 2. Methodological sequence.

Definition of objectives: A system for environmental monitoring

Industrial activities are prone to contaminating water bodies unintentionally and, in most cases, due to the inefficiency of the contingency strategy. A prime example is acid mine drainage affecting rural Peruvian lakes like Junín and Titicaca. This drainage results from metal sulfides, primarily pyrite or arsenopyrite, reacting with raining water and oxygen. These conditions produce acid water streams with low pH (<3.0) and high concentrations of metal ions such as iron, zinc, and arsenic, far beyond the maximum allowable concentration. Artisanal and informal mining units discharge these toxic drainages directly into rivers without any remediation process, either intentionally or accidentally. Additionally, wastewater introduces a wide variety of xenobiotics, altering the ecosystem, reportedly affecting microbial resistance and increasing health risks [8-9]. These polluted environments become unsuitable for human activities, including agriculture, farming and basic services. In this context, a mobile sensor is required to support integrative studies to address environmental issues associated with industrial operations. Figure 3 represents a real example of this environmental issue.



Figure 3. Acid mine drainage stream from an abandoned artisanal mining unit, located in Peru [10].

Definition of objectives: Science data acquisition

The Earth's Ocean encompasses a wide range of environments where a probe would be invaluable for exploration and prospecting activities [11]. A mobile sensor could facilitate the biological and marine science analysis of various aspects, from deep-sea minerals and geochemistry to non-human communication in marine mammals [12] as well as the biodiversity in marine environments, and conservation sites along the Peruvian- Chilean trench, such as the Nazca Ridge and the Salas y Gómez Ridge [13-14].

Definition of objectives: Ocean worlds exploration

Exploration technologies for Earth's deep sea and polar regions can be applied to study habitability and detect life on ocean worlds within the solar system [15-18]. Besides the Earth, over a dozen potential ocean worlds exist in our solar system, from Mars to icy moons of Jupiter and Saturn, and trans-Neptunian bodies [1]. NASA's Europa Clipper and ESA's JUICE missions are scheduled this decade to explore Europa and prepare for future robotic landing missions.

On this context, the team decided to design a suitable system for three scenarios: unexplored oceanic environments on Earth, industrial-contaminated rivers and lakes, and extraterrestrial oceans. Key scientific data to collect includes: pressure (essential for hydraulic stresses and environmental evaluation); temperature, (to predict convective currents and determine conditions for physicochemical or biological activities); pH, (acidity or alkalinity, essential to determine the ionic state of the metals dissolved) ; and oxidation-reduction potential (ORP), to complement the information provided by the pH, evaluate the thermodynamics feasibility of chemical reactions and the bioavailability of contaminants [19]. All these parameters are crucial for comprehensive environmental assessments and study the aquatic ecosystems in various scenarios. Figure 4 summarizes the needs analysis information.

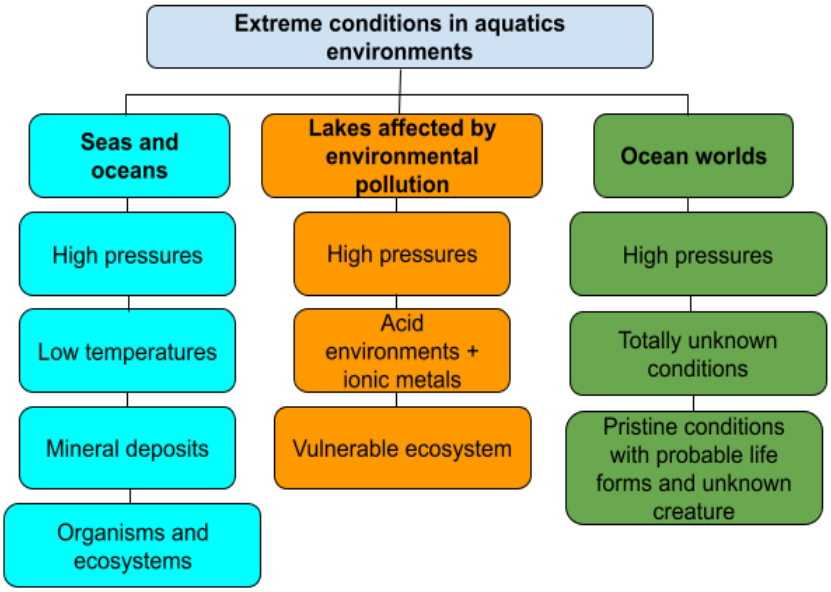


Figure 4. Need analysis of extreme conditions in aquatic environments.

Analysis of alternatives

Scientific studies in the deep sea, subglacial environments, and submerged caves have provided relevant information to astrobiological research proposed to be carried out in ocean worlds. In fact, in recent decades, multiple concepts have been proposed for aquatic exploration of ocean worlds [1, 20-21]. The FISHER-X concept was developed from analyzing the most advanced robots designed, tested, or proposed for exploring extreme aquatic environments on Earth and beyond, as shown in Table 1.

Table 1: List of system concepts proposed for oceanic world exploration [1]

Concept	Ocean World	Developer
Titan Submarine	Titan	Nasa - JPL, NIAC
ShapeShifter	Titan	Nasa - JPL, NIAC
EELS	Enceladus	Nasa - JPL
EnEx-IceMole	Enceladus	German Aerospace Center, German FH AUAS, NASA - JPL
BRUIE	Europa &Enceladus	Stone Aerospace/NASA ASTEP
Endurance	Europa &Enceladus	Stone Aerospace/NASA ASTEP
DEPTHX	Europa	Stone Aerospace/NASA ASTEP
ARTEMIS	Europa	Stone Aerospace
SUNFISH (R)	Icy Moons	Nasa - JPL
SLUSH	Europa	

MARUM	Europa	German Aerospace Center
Icefin	Europa	NASA - PSTAR
DeepLeng	Europa	German Research Center
SWIM	Europa	for Artificial Intelligence
		Nasa - JPL, NIAC

Conceptual design

The project's inspiration is derived from fish capable of swimming at great depths, pressures and the absence of light, without disturbing the aquatic environment. FISHER-X was inspired by hadal snailfish locomotion, which minimizes environmental disturbance during swimming and hunting [1]. Our team considered the biological entity to be used as inspiration, adapting the physical structure of the design by defining dimensions of its components that are linked to each other through kinematic pairs. We decided to use kinematic pairs of restricted rotation and oscillation, with a degree of freedom that allows us to provide a movement that simulates the fin as well as the movement of the robot's body. Because the robot's structure is inspired by snailfish morphology, it comprises three main elements: the main capsule, the tail, and fins. The main capsule contains the power supply and payload instruments, the pectoral fins include the mechanism to precise movement control. The tail houses dorsal and ventral fins is segmented to facilitate oscillating movement. The tail determines the robot's movement. All fins include radial arms internally, to enable undulating motion, stabilizing the robot during navigation activities. Next, we proceed to the physical and mathematical analysis by MATLAB of the movement complemented with a virtual design in CAD program that allow movement simulations.

RESULTS

Design and biomechanics modeling

FISHER-X requires sub-carangiform locomotion and in general undulatory locomotion fulfills this requirement. The waveform describing the sub-carangiform fish's geometry is possible due to a slight modification of the proposals developed by [22], which were later adopted by [23-24]. The fundamental equation is presented as follows:

$$y_{body(x,y)} = [C_1X + C_2X^2].\sin(K_x + 2\pi M_i) \qquad Eq\ (1)$$

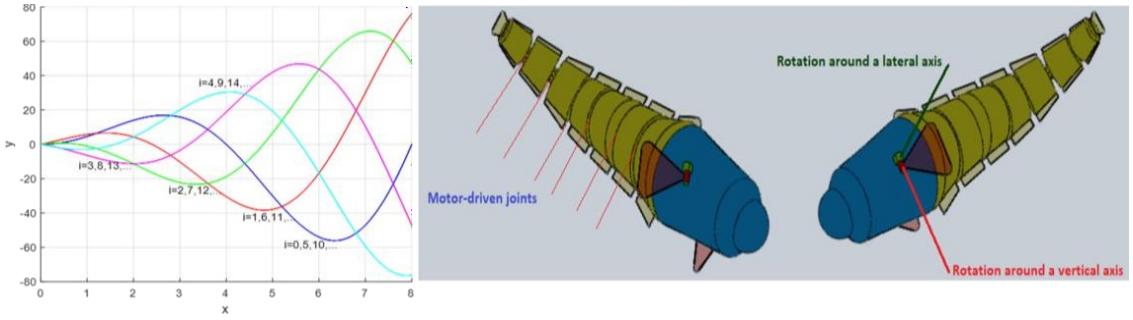


Figure 5. (Left) Body waveform at different instants "i". (Middle) Static image of dynamic simulation during the wave movement of the fish body. (Right) Static image of dynamics simulation during fin movements, created by SolidWorks Premium 2020.

The transverse displacement of the body "y_{body}" is expressed in terms of the position

along the axial coordinate "x". The traveling wave is expressed as the superposition of a linear and quadratic wave oscillating sinusoidally. This function depends on the horizontal coordinate along the fish's body "x" and the temporal condition characterized by each instant "i".C_1 represents the linear wave's amplitude, while C_2 is the quadratic wave's amplitude. At the same time, "k" denotes the body wave number, given by k=2π/λ, where λ is the body wavelength. In addition, the body wave frequency is expressed as 2/M, where M is the body wave resolution, constrained by the motors' maximum oscillation frequency. The figure illustrates a superimposed graph of the body waveforms that can be described by equation (1) for different instants "i," with the following parameter values: C_1 = 6; C_2 = 0.5; λ = 8; 0 ≤ x ≤ λ; M = 5; 0 ≤ i ≤ 2M.

During its undulatory motion, *Pseudoliparis swirei* extends the posterior part of its body near the tail to a greater extent, allowing it to propel itself more easily. The reference [24] proposed a simplified propulsion model for carangiform fish, utilizing body segments and joints to emulate an undulatory motion along the axial axis. Coincidentally with this proposal, FISHER-X team simulated the wave movement along the fish body, inserting virtual motors with partial oscillating rotation whose lateral displacement amplitude is programmable. The results of this simulation are illustrated in Figure 5. The undulatory movements of the dorsal and ventral fins approximate a simple sine wave. Indeed, this movement is fully explained in a previous paper [26], where it was proposed that the oscillations of the fin rays can be expressed by:

$$\Theta_i(t) = Asin[2\pi ft - (i-1)\theta_0\ ] + \theta_b; \qquad \text{i=1 : n} \qquad \textit{Eq (2)}$$

Where "A" is the maximum amplitude, "f" is the frequency of the wave, "θo" is the phase angle between adjacent fins, "θb" is the angular deflection between the horizontal plane and the rays of the fins. The reference [25] uses the previous value to give an undulatory movement of the fins in a horizontal plane. The aforementioned background has allowed the implementation of robot prototypes with two pectoral fins and a caudal fin, as is the case published on [26]. The pendulum harmonic motion is easy to replicate, but in real-life conditions, we observe that the fish can rotate its fin in relation to both a horizontal and vertical axis. This greater mobility has been made possible in the design and simulation, by inserting a double articulation into the virtual fish fin. The oscillatory motion, a recurring movement, has been achieved through a mechanism created and designed by Prof. Yury Vásquez.

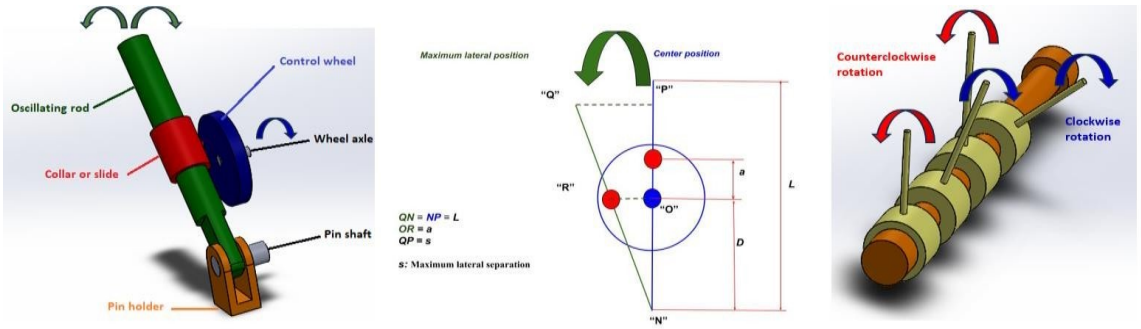


Figure 6. (Left) Mechanism designed to convert a rotary movement into an oscillating movement, by SolidWorks Premium 2020. (Medium): Simplified diagram of the oscillating mechanism, to establish the kinematics equations. (Right) Mimicry of the ribs that move the dorsal fins, allowing a wave movement.

Regarding Figure 6, the "D" axis allows the rotation of the drive wheel "C" (linked to a continuous rotation motor). In this way, an oscillatory motion is transmitted to the rod "B" which is connected to the collar or slider "A". The oscillating rod rotates on the pin of the "E" axis held by the respective support "F". We show a graphic and calculations that allow determining the separation where the support center of the collar or slider "a" is located, based on the separation between the center of the drive wheel and the fixed support point of the oscillating bar "D", the maximum lateral separation to be obtained at the free end of the oscillating bar "s", and its length "L".” Based on Figure 6, similarities can be established between the triangles "NQP" and "NRO", from Equation 3 & 4. These mathematical constraints guide the implementation of the physical model. For example, the ribs of the dorsal fin are discretized into four bars with alternating rotational configurations. This imitates the wave and sinusoidal movement of the fins. All the ribs will be connected to a flexible membrane to achieve this effect.

$$\frac{a}{D} = \frac{s}{\sqrt{L^2 + s^2}} \qquad Eq(3)$$

$$\frac{a}{D} = \frac{s}{\sqrt{L^2 + s^2}} = \frac{sD}{\sqrt{(L+s)(L-s)}} \qquad Eq(4)$$

Sequence of operation - strategy

FISHER-X is designed, considering a two-part control system: an action module and the actual control system. This setup monitors physicochemical parameters via sensors, manages movement through a sub-carangiform module, and administers initial navigation via the control system. The implementation of an autonomous navigation system will use SLAM (Simultaneous Localization and Mapping) in a second phase (TRL 3-4). It is planned to design a model with an intermediate-level monitoring system with a ground-based command and control center. The command center will communicate with the FISHER- X control module through a Raspberry Pi CPU that will have the AUV navigation algorithm and the PID controller [20]. In addition to data acquisition, navigation also requires automated decision-making capabilities and the ability to deal with unexpected situations. Initially, the plan is to use the command-and-control center for manual movement, allowing the bio-inspired design to move in the required direction and to evaluate its behavior in all types of environments and depths. Figure 7 describes the data module.

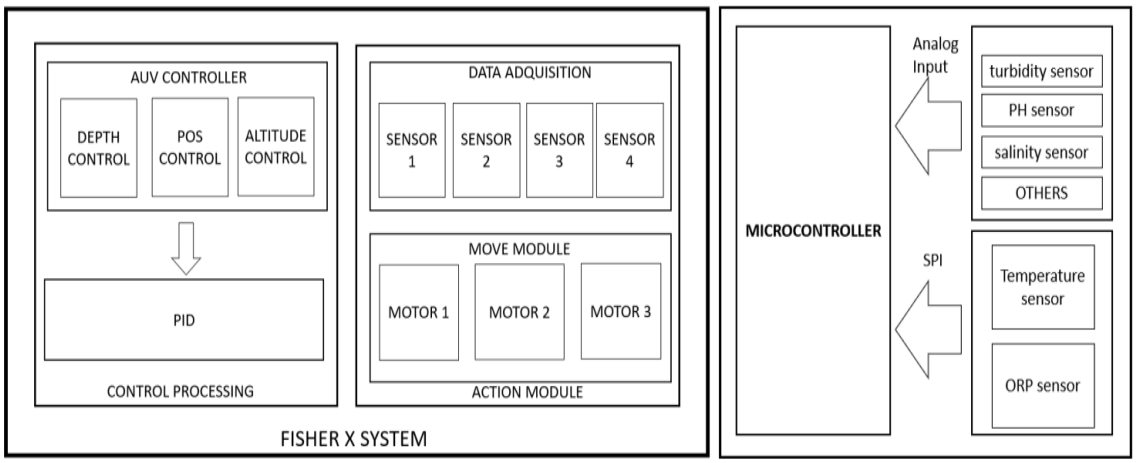


Figure 7. FISHER X Data module schematic.

The process of conceiving a bio-inspired design to meet our purpose of exploring aquatic environments requires the following steps to achieve the conceptual design, explained by Figure 7. In terms of operations, the bio-inspired prototype consists of two fundamental modules: the action module and the control module. The action module includes two submodules: the data acquisition submodule, which has sensors to evaluate the environment where the probe is navigating, and the movement submodule. The data acquisition module's sensors monitor physicochemical parameters such as temperature, ORP, conductivity, pH, among others. These sensors will communicate with the action module's central brain using protocols like analog inputs or the microcontroller's SPI inputs, which will allow higher data transmission speeds to expand the use of sensors, only if it is required [19]. The movement module will have a master microcontroller to execute the actions determined by the control system. This microcontroller will send the necessary data to actuators, such as PWM signals to control their speed or ENABLE/DISABLE signals to perform the bio-inspired model's movement. The motion module is described in Figure 8.

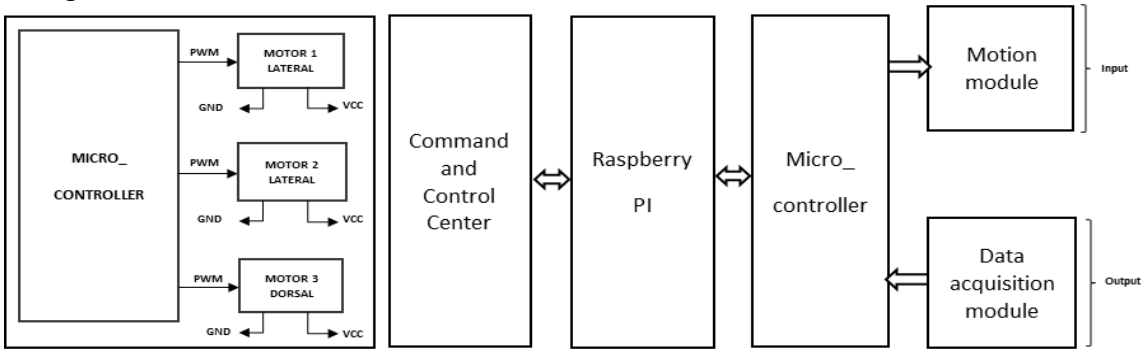


Figure 8. Movement Module connection schematic.

DISCUSSION

The exploration of aqueous environments under extreme conditions requires the use of numerous models and technologies, evaluated in controlled or natural environments depending on their application. On Earth, conventional water monitoring uses static sensors with online information at specific points or is controlled manually by technicians who take samples at different time intervals. Conversely, FISHER-X is a mobile robotic system which depends on the efficiency of their swimming movement to remotely gather real time data and into an extensive area. Based on the provided mathematical model of transverse motion [22], the dynamic simulation of the fish's undulatory movement was achieved using kinematic pairs and virtual oscillatory motors by SolidWorks Premium 2020.

The FISHER-X approach was selected from several published spin-off concepts and designs transferable from the study of ocean worlds, as it is presented in Table 1. Mimicking the undulatory motion of fins led to the design of an innovative mechanism. The desired maximum lateral displacement at the end of an oscillatory rod defines the eccentricity on the driving rotary disc. Equations 1 and 2 describe the relationship between the mechanism's main dimensions. For a next stage, the aim is to complement the navigation system avoiding human intervention by applying simultaneous localization and mapping (SLAM) techniques, thus adjusting the vehicle's trajectory to behave adaptively while communicating remotely with the control center [21]. In addition, structural analysis and modeling is crucial. Given the intended application in deep water exploration, careful

considerations are related to the hydraulic pressures and potential deformations on the robot's components. To meet this requirement, a material selection, optimization of component sizes using Finite Element Model (FEM) techniques and shaping designs, are necessary to minimize stress concentrations that could lead to operational failures and meet the lifespan expectations.

Subsequent steps involve simulating the robot's interaction with the fluid environment. This simulation allows for the visualization of trajectories and the evaluation of the system into a fluid, considering the velocity of surrounding currents to optimize performance. Successful execution of this stage will rely on Computational Fluid Dynamics (CFD) simulations, which will provide insights into enhancing the robot's operational efficiency and adaptability across various aquatic conditions.

CONCLUSION

This article presented the development of a bioinspired model “FISHER X”, based on the design of the snail fish, which will be used for underwater exploration tasks in inaccessible places and with minimal environmental impact. Being used to monitor parameters in acid mine drainage (ADM) and later used for space aplications. This design is in the conceptual phase (TRL-2) with as its main function the adaptation of temperature, salinity, conductivity, pH sensors, among others, using AUV navigation algorithms combined with SLAM simultaneous localization and mapping, for greater autonomy of the robot, to In turn, as part of the conceptual design and obtaining the subcarangiform locomotion, studies were complemented by the replication of the structural part using dynamic simulations in SolidWorks Premium 2020, managing to obtain the physical model that imitates the wave and sinusoidal movement of the fins. Finally, FISHER-X is a good example of dual use technology or spin-off, which means that concepts created for space exploration can be adapted to solve current problems on Earth.

ACKNOWLEDGEMENTS

The team recognizes the intellectual contributions of Arturo Alvarez Flores & Jose Napan in the creation of the concept, as it is reflected in the first publication of FISHER-X [1]. This paper was developed under the support of the ARIES Peruvian research group, a multidisciplinary team who are working on systems engineering for planetary exploration and environmental technologies. Finally, thanks to the Department of Research, Innovation, and Social Responsibility at the Universidad Privada del Norte, Peru; for the support received for the participation in SGEM 2024

REFERENCES

[1] B. Cevallos, G. Jamanca-Lino, J. L. N. Herrera, A. Flores, and &. Y. Vasquez, “FISHER-X: A Bioinspired Robotic Alternative for The Exploration of the Oceanic Environment on a Jupiter’s Moon,” in Proceedings of the International Astronautical Congress, IAC, 2021.

[2] L. Lapierre, Underwater Robots Part I: Current Systems and Problem Pose, in: A. Lazinica (Eds), Mobile Robots Towards New Applications, InTech, 2006, pp. 784

[3] R. Salazar, V. Fuentes, A. Abdelkefi, Classification of biological and bioinspired aquatic systems: A review, Ocean Engineering 148 (2018) 75-114.

[4] L. Ren, B. Li, G. Wei, K. Wang, Z. Song, Y. Wei, L. Ren, Q. Liu, Biology and bioinspiration of soft robotics: Actuation, sensing, and system integration, iScience 24 (2021), 103075.

[5] S. Fu, F. Wei, C. Yin, L. Yao, Y. Wang, Biomimetic soft micro-swimmers: from actuation mechanisms to applications, Biomedical Microdevices 23 (2021) 1-13.

[6] M. Calisti, G. Picardi, C. Laschi, Fundamentals of soft robot locomotion, Journal of The Royal Society Interface 14 (2017) 20170101.

[7] J. Fang, Y. Zhuang, K. Liu, Z. Chen, Z. Liu, T. Kong, J. Xu, C. Qi, A Shift from Efficiency to Adaptability: Recent Progress in Biomimetic Interactive Soft Robotics in Wet Environments, Advanced Science 9 (2022) 2104347

[8] J Paredes, A. Sanchez, K. Ordoñez, M. Palo, Caracterización de Microplásticos en los Recursos Hidrobiológicos del Lago Titicaca.

[9] F.Z. Vilca, N.C. Galarza, J.R. Tejedo, W.A.Z. Cuba, C.N.C. Quiróz, V.L. Tornisielo, Occurrence of residues of veterinary antibiotics in water, sediment and trout tissue (Oncorhynchus mykiss) in the southern area of Lake Titicaca, Peru, Journal of Great Lakes Research 47 (2021) 1219-1227

[10] H. Vargas, G. Jamanca Lino, and Y. Vasquez, "Heterogeneous UV/TiO2 photocatalysis applied to the removal of arsenic from acid mine drainage," in Proceedings of the 21th LACCEI International Multi-Conference for Engineering, Education and Technology (LACCEI 2023): "Leadership in Education and Innovation in Engineering in the Framework of Global Transformations: Integration and Alliances for Integral Development," 2023.

[11] J. Aguzzi, D. Chatzievangelou, S. Marini, E. Fanelli, R. Danovaro, S. Flögel, N. Lebris, F. Juanes, F.C. De Leo, J. Del Rio, L. Thomsen, C. Costa, G. Riccobene, C. Tamburini, D. Lefevre, C. Gojak, P.M. Poulain, P. Favali, A. Griffa, A. Purser, D. Cline,

D. Edgington, J. Navarro, S. Stefanni, S. D'Hondt, I.G. Priede, R. Rountree, J.B. Company, New hightech flexible networks for the monitoring of deep-sea ecosystems, Environmental Science & Technology 53 (2019) 6616-6631.

[12] J. Andreas, G. Beguš, M. M. Bronstein, R Diamant, D. Delaney, S. Gero, S. Goldwasser, D. F. Gruber, S. Haas, P. Malkin, N. Pavlov, R. Payne, G. Petri, D. Russ, P. Sharma, D. Tchernov, P. Tonnesen, A. Torralba, D. Vogt & Wood, Towards Understanding the Communication in Sperm Whales, iScience (2022).

[13] A.M. Friedlander, W. Goodell, J. Giddens, E.E. Easton, D. Wagner, Deep-sea biodiversity at the extremes of the Salas y Gómez and Nazca ridges with implications for conservation, PloS one 16 (2021) e0253213.

[14] S.M. MacKenzie, N. Neveu, A.F. Davila, J.I. Lunine, K.L. Craft, M.L. Cable, C.M. Phillips-Lander, J.D. Hofgartner, J.L. Eigenbrode, J.H. Waite Jr, C.R. Glein, R. Gold, P.J. Greenauer, K. Kirby, C. Bradburne, S.P. Kounaves, M.J. Malaska, F. Postberg, S.P. Kounaves, M.J. Malaska, F. Postberg, G.W. Patterson, C. Porco, J.I. Núñez, C. German,

J.A. Huber, C.P. McKay, J.P. de Vera, J.R. Brucato, L.J. Spilker, The Enceladus Orbilander Mission Concept: Balancing Return and Resources in the Search for Life, The Planetary Science Journal 2 (2021) 77.

[15] J.W. Sahl, N. Fairfield, J.K. Harris, D. Wettergreen, W.C. Stone, J.R. Spear, Novel

microbial diversity retrieved by autonomous robotic exploration of the world's deepest vertical phreatic sinkhole, Astrobiology 10 (2010) 201-213.

[16] W. Stone, K. Richmond, C. Flesher, B. Hogan, V. Siegel, Sub-ice Autonomous Underwater Vehicle Architectures for Ocean World Exploration and Life Search, Outer Solar System (2018) 429-541.

[17] J. Aguzzi, S. Flögel, S. Marini, L. Thomsen, J. Albiez, P. Weiss, G. Picardi, M. Calisti, S. Stefanni, L. Mirimin, F. Vecchi, C. Laschi, A. Branch, E.B. Clark, B. Foing,

A. Wedler, D. Chatzievangelou, M. Tangherlini, A. Purser, L. Dartnell, R. Danovaro, Developing technological synergies between deep-sea and space research, Elem Sci Anth 10 (2022) 00064.

[18] J.I. Lunine, Ocean worlds exploration, Acta Astronautica 131 (2017) 123-130.

[19] Conejeros Molina, Alvaro, Hueichaqueo Pichunman, Camilo, Martinez-Jimenez, Boris L., & PlaceresRemior, Arley. (2021). Monitoreo de calidad del agua en sistema de agua potable rural. Ingeniería Electrónica, Automática y Comunicaciones, 42(3), 60-70. Epub 11 de diciembre de 2021.

[20] S. Cao, H. -l. Xu, Q. -y. Jia and G. Chen, "Design of portable AUV remote control device based on MOOS-IvP," 2016 IEEE International Conference on Cyber Technology in Automation, Control, and Intelligent Systems (CYBER), Chengdu, China, 2016, pp. 25-28, doi: 10.1109/CYBER.2016.7574789.

[21] M. Rahmati, S. Karten and D. Pompili, "SLAM-based Underwater Adaptive Sampling Using Autonomous Vehicles," OCEANS 2018 MTS/IEEE Charleston, Charleston, SC, USA, 2018, pp. 1-7, doi: 10.1109/OCEANS.2018.8604552.

[22] Lighthill, M. J. (1960). Note on the swimming of slender fish. Journal of Fluid Mechanics, 9(2), 305–317. https://doi.org/10.1017/s0022112060001110

[23] Barrett, D., Grosenbaugh, M., & Triantafyllou, M. (2002). The optimal control of a flexible hull robotic undersea vehicle propelled by an oscillating foil. Proceedings of Symposium on Autonomous Underwater Vehicle Technology.

[24] Yu, J., Wang, S., & Tan, M. (2005). A simplified propulsive model of bio-mimetic robot fish and its realization. Robotica, 23(1), 101–107. https://doi.org/10.1017/s0263574704000426

[25] Liu, L., Li, Y., Wang, Y., & Ma, X. (2020). Design and preliminary evaluation of A biomimetic underwater robot with undulating fin propulsion. IOP conference series. Materials science and engineering, 790(1), 012160. https://doi.org/10.1088/1757-899x/790/1/012160

[26] Zhong, Y., Li, Z., & Du, R. (2018). Robot fish with two-DOF pectoral fins and a wire-driven caudal fin. Advanced Robotics: The International Journal of the Robotics Society of Japan, 32(1), 25–36. https://doi.org/10.1080/01691864.2017.1392344

HYDROECOLOGICAL STATE OF THE SMALL UPLAND ARMENIAN LAKES

Assoc. Prof. Dr. Irina Fedorova[1]
Larisa Ghazaryan[1]
Vsevolod Rudakov[1]
Elizaveta Chezhina[2]
Assoc. Prof. Dr. Grigory Fedorov[1]
[1]Institute of Botany after A.Takhtadjan of the National Academia of Sciences, **Republic of Armenia**
[2]Saint Petersburg State University, **Russian Federation**

ABSTRACT

During summer-autumn 2023 hydrophysical, hydrochemical, and hydrobiological measurements had been done on six small upland Armenian lakes. For the first time colored dissolved organic matter (CDOM) and methane (CH_4) – emission were observed.

Studied lakes are on 1479-3312 m a.s., has maximal depth up to 12 m with groundwater springs input. Anoxic conditions were noticed on the lake bottom in August but changed to oxygen in October. Conductivity range was 0-231 µS cm^{-1}, TDS - 3-102 mg l^{-1}, pH – 6.4-9.4 for surfaces of all lakes. Main part of nutrients was silicates Si, phosphates PO_4 and ammonium NH_4. CH_4 flux was quite high – reached 13 gCH_4 m^{-2} d^{-1}. Colored dissolved organic matter changes in 12 times range for the lakes, shows allochthonous and autochthonous source of organic matter, ecosystems have low ability to photo degradation.

Ecosystems of lakes depends on altitudes. Thus, pelagic zooplankton of Shushanalich (1552 m a.s.) presented Rotifera, Cladocera and Cyclopoida mostly, whereas Lessing lake (3312 m a.s.) had only Copepoda (Calanus sp.). Numerous diatoms were in plankton and sediments.

Keywords: alpine lakes, Armenia, ecosystems, hydrochemistry

INTRODUCTION

Studies of Armenian lakes mostly focused on the Lake Sevan. It is the biggest and deepest alpine lake with unique history and ecosystem. There are several small upland lakes in Armenia as well: in 1963 according to Sadovskiy, there were 194 lakes [1], but Boynagryan in 2022 detects just 120 lakes [2]. Desertification due to climate warming and agriculture intensification during last century [3] are main reasons of small Armenian lakes disappearance. Irregular seasonal distribution of water resources demands a reservoirs creation in the upland and, consequently, some lakes turned to water-storage object and lost their unique ecosystems.

The first mention of the specifics of the Armenian lakes and water resources can be attributed to the works of beginning of XX century: geologist Paffengolts [4] and results of Levinsong-Lessing's expedition. However, the most part of information was just about ground water and large Sevan lake. Later the Limnological station was created on Sevan lake, therefor hydrobiological and hydrochemical measurements started but reports about studies of the small upland lakes could be found just after 1930-40-th. Thus, in Boynagryan [5] bathymetry and chemical composition of small upland lakes was provided. Only during the era of irrigation in Armenia, (30-70-th of last century) small highland lakes were studied as a source of water and subject to reservoir construction. After huge gap of studies in the end of last century and beginning XXI century new sporadic information (but in higher scientific level) can be found not earlier than last 10-15 years.

Current bathymetry, paleogeographical studies, and hydrochemistry of small Kari, Umroy, Akna and Sev alpine lakes presented in Sapelko et al. [6]. Spatial-temporal change of hydrochemical parameters of Shushanalich lake last summer-autumn presented in Ghazaryan et al. [7].

Estimations of greenhouse gases emission from water objects were published by Karakhanian et al., [8] according to measurements of CH4 on 3 points of Sevan lake in 1999. Later [9] observation were done for ebbulation methane flux on Sevan shoreline. Measurements from small upland lakes surface have not been done. Results presented here are the pilot ones.

Stable water isotopes were well studied in groundwater of Ararat Valley in October and December 2019 [10] and were compared to Ankara and Tbilisi isotope ration of precipitation. There were not found any information about stable water isotopes in small upland lakes of Armenia before our research that give some problems to the results interpretation but reach information about environment of alpine region of Lesser Caucasus.

Hydrobiological features and regime are mostly investigated for the Sevan lake because it is the main and biggest aquatic object in Armenia. Studies was started one century ago on the new Limnological station and have been successfully prolonged up to now. Gevorgyan et al. [11], Krylov et al., [12], and Hayrapetyan et al. [13]. The first fully overview of plankton community in small alpine Armenian lakes were introduced in Meshkova's book [1].

This study shows the first results of beginning of the small Armenian upland lakes monitoring. The main target is inventory of small lakes and overview the current ecosystem specific in compare to former studies.

MATERIALS AND METHODS

Six small Alpine lakes of Lesser Caucasus were chosen for investigation (table 1). Elevation of lakes vary from 1479 to 3312 m a.s. Most of lakes have significant percentage of area covered by macrophytes. Studies had been done during July-October 2023 in Armenia. Measurements on Shushanalich (Urasar lake) lake and Parz liman performed 3 and 2 times correspondingly in different months that allow to show seasonal values of hydrochemical futures.

The biggest and deepest of studied lakes is Akna lich, the highest – Lessing lake. Relict lakes of Lori province (Shushanalich, Parz liman and Horse liman) were in the list of Ramsar convention due to their unique wetlands vegetation, water regime and fauna [14]. Main part of these lakes covered by lilies *Nymphaea alba.* Margalich lake aquatic vegetation has endemic fern *Thelypteris palustris* Schott (CR).

Table 1. Coordinates and morphometric parameters of studied lakes

Название озер	Northern latithaude	Eastern longitude	Altitude, m	Maximal depth, m	Lake surface square, sq m / lake surface without macrophytes, %
Margalich	39,595	45,521	2000	9	11 900 / 98%
Akna lich	40,2833	44,915	3041	12	385 407 / 99%
Shushanalich	41,024	44,304	1552	8,5	75 429 / 20%
Parz liman	41,050	44,309	1479	5,3	89 884 / 28%
Lessing lake	40,525	44,236	3312	1,5	14 200 / 100%
Horse liman	41,04218	44,327	1499	6	11 000/ 34%

Following hydrochemical parameters were observed by portable instruments: water temperature, pH, dissolved oxygen, redox potential, conductivity, total dissolved salinity (TDS). “OHAUS” meters and “Expert” loggers were used. Nutrients (PO_4, NO_2, NO_3, Si, NH_4) were analysed in a field laboratory in the same day after sampling by a photometer “Expert-003”. Samples for cations composition were fixed by 1-3 µl of 65% HNO_3 and stored together with anions samples in the dark at 4°C.

Diffusion methane flux from lakes’ surface was measured by portative SPD203 gas analyzer of Sanpometer Company with thin boundary layer method. Camera had a volume 0.04 m^3, exposition for measurements – 4-10 minutes. Temporary variability of CH_4 flux received in Shushanalich: measurements had been repeated during the day in August and October.

Coordinates of objects received by GAMIN GPS map 62s, a depth – by GARMIN map 421s echo sounder. Hydrobiological samples taken plankton net of mesh size 100 µm, analyses of plankton were done by Optica C-B18+ microscope (Italy) with fixed by formaldehyde immediately after sampling.

Hydrochemical and stable isotope $\delta^{18}O$, $\delta^{2}H$ composition of water samples analysed in Resource Centre of St. Petersburg State University. Stable water isotopes (in per mil ‰) ratio were expressed using the conventional δ notation relative to Vienna Standard Mean Ocean Water (V-SMOW). CDOM and cDOM absorption were done in Otto-Schmidt Laboratory in Arctic and Antarctic Research Institute.

https://doi.org/10.5593/sgem2024/3.1/s12.13

RESULTS

Hydrochemical measurements on lakes show quite similar values for all parameters; seasonal variability and effect of lake elevation could be additional environment factors that lead to different amounts.

Conductivity range was 0-231 µS cm^{-1}, TDS - 3-102 mg l^{-1}, pH – 6.4-9.4 for surfaces of the lakes. Color of water was not higher than 30.4 degree (Pt/Co **scale** or Apha-Hazen **Scale)**; turbidity reached just 5.1 turbidity formazine units.

Type of **water composition** is hydrocarbonate-calcium and presented on the Piper plot (figure 1). Hydrochemical ratio of ions was similar for all lakes except Parz liman. Parz liman had ration of ions like ($HCO3^{-}$+$SO4^{2-}$)<(Ca^{2+}+Mg^{2+}) but other lakes had more hydro carbonates than water hardness $HCO3^{-}$ > (Ca2+ + Mg2+).

Nutrient and oxygen content. Average content of oxygen ranged from 3.8 to 5.7 mg l^{-1} (36-86%) on the surface of all studied lake. Anoxic conditions was noticed on the bottom of Shushanalich in August (O_2 value was less 1 mg l^{-1}, Eh was -130 mV) but changed to oxygen regime in October. Main part of nutrients was silicates Si (0.02-3.7 mg l^{-1}), phosphates PO_4 (0.04-2.1 mg l^{-1}) and ammonium NH_4 (0.02-1.6 mg l^{-1}). The highest nutrients concentration observed in Margalich, the most oligotrophic lake – upland Akna lich.

The average diffusion **methane flux** for all studied small lakes was 6.5 g CH_4*m^2*day^{-1} with variations for each objects and season. Thus, the average values of CH_4 flux were 10.1 gCH_4*m^{-2}*day^{-1} for the Margalich on July 2023; 6.1 gCH4*m-2*day-1 for Akna lich on August; 2.1-6.5 gCH_4*m^{-2}*day^{-1} for Parz liman on October. For Shushanalich in August, the average flux at different hours per a day was 4.3-12.8 gCH_4*m^{-2}*day^{-1}, in October it's ranged from 0.8 to 5.8 gCH_4*m^{-2}*day^{-1}, i.e. decreased by more than 2 times. During the day CH_4 flux has a sinusoidal function with high emission in day and small - in night. In Autumn the function attenuated. The most significant CH_4 flux reached 13 gCH_4 m^{-2} d^{-1}.

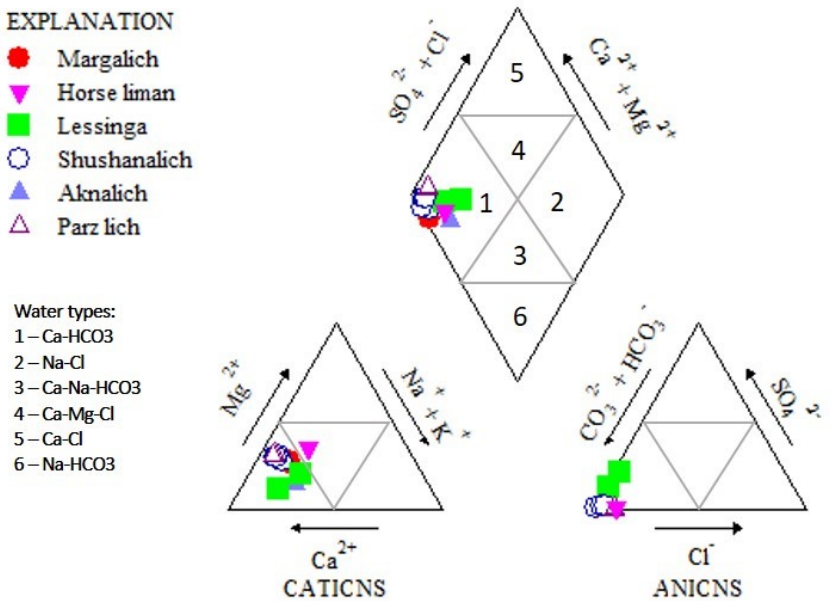


Figure 1. Piper plot of lakes' hydrochemical types

Colored dissolved organic matter (CDOM) and the spectral shape is essential to determine the influence of the CDOM absorption to the whole underwater light field (e.g.. light availability for phytoplankton, transparency and euphotic depths). The largest number of CDOM at a wavelength of 440 nm, therefore, the largest number of DOC (dissolved organic carbon), was found in the Shushanalich (1.89 nm^{-1}), and the lowest - in oligotrophic and the least overgrowth Akna Lich (0.15 nm^{-1}). The DOC amount in these lakes varies significantly, by 12 times. According to the spectral slope S value, autochthonous origin of CDOM predominates in lakes Akna lich, Horse liman, and Shushanalich (in Autumn) rather allochthonous - in Margalich, Lessing lake, Parz liman, and Shushanalich (in Summer). The angle of inclination S indicates also about predominantof fulvic acids in the first group of lakes and humic acids – in the second, on the contrary. The index of phytodegradation (Sr<1.2) in all the studied lakes indicates "fresh" organic matter in lakes and humic acid-rich terrestrial organic substances. No lake have the specific process of photodegradation.

Stable water isotopes has huge variation of value $\delta^{18}O$ from -10.59 to +1.39‰, range of $\delta^{2}H$ are - 70.2 ÷ +1.1‰. Lori's Plateau Parz liman and Horse liman lakes have positive value of $\delta^{18}O$ (1.20÷1.39‰) and using the conventional δ notation relative to Vienna Standard Mean Ocean Water (V-SMOW) (0.5÷1.1‰). Isotopes magnitude of Shushanalich that situated close to above mention lakes is -1.04÷ -0.49‰ for δ18O and ratio -11.9 to -9‰ for δ2H. Three of these lakes have elevation 1479-1552 m above a sea. The heaviest isotopic content has Margalich (-10.59‰ $\delta^{18}O$ and -68.52‰ $\delta^{2}H$), satiated on the 2000 m a.s. Meaning of Akna lich (3041 m a.s.) and Lessing (3312 m a.s.) lakes are between Shishanalich and Margalich lakes' values.

Ecosystems of studied lakes depends on altitudes and environment conditions of a lake catchment. Pelagic zooplankton of Shushanalich (1552 m a.s.) presented by Rotifera, Cladocera and Cyclopoida mostly, rather Lessing lake (3312 m a.s.) had only Copepoda (Calanus sp.). Rotifera largely contributed to the zooplankton abundance of Lori province lakes. *Asplanchna sp.* and *Keratella cochlearis* dominated in term of Rotifera abundance with *Polyarthra sp.* in minor amount; *Daphnia pulex, Allonella excisa* and *Daphnia magna* prevalenced of Cladocera and *Eucyclops macruroides* - of Cyclopoida as well as *Diaptomus castor* and nauplii of Copepoda. Zooplankton of Lessing lake was poore, only *Calanus* sp. of Calanoida were found.

Research shows that among the modern diatoms of Shushanalich lake of Lori province, representatives of the genera *Navicula, Nitzschia, Cyclotella, Pinnularia, Gomphonema and Tabellaria* are the most common, bulk of which live in the sediments. Their abundance in the plankton is significantly reduced and were absent in some cases. The species composition is dominated by *Gomphonema acuminatum, Gomphonema constrictum, Tabellaria fenestrata and Pinnularia major.*

DISCUSSION

Hydrochemistry. Hydrochemical parameters detected in our study are similar to reported previously for other lakes [6]: neutral or light alkaline pH, not high salinity (conductivity) and nutrients concentration. However, studied lakes in our investigation had higher amplitude of parameters because of their wider type range. In [6] investigated lakes were mountain oligotrophic lakes Kari, Umroy and Aknalich while we measured relict meso- and eutrophic lakes as well. Sapelko et al. [6] and co-authors noticed the high concentration of total phosphorus for Sev eutrophic lake and low

dissolved oxygen concentration for Kari and Sev lake. Marked differences between hydrochemical parameters of the lakes can be explained by various seasons of measurements and environment of catchments.

CH_4 flux. The methane fluxes from the surface of the small Armenian lakes studied in summer 2023 turned out to be within the limits previously measured by other authors. In the article Karakhanyan et al. [8], the values of the methane flux measured from the end of August to mid-October 1999 from the Lake Sevan surface varied from 100 to 700 $gCH_4*m^{-2}*day^{-1}$. In our case, the maximum values are in the middle of August 2023 and amount to 16.2 g $CH_4*m^{-2}*day^{-1}$ for Shushanalich. The independently obtained values of CH_4 flux show a greater emission value than the average values indicated for this ecoclimatic region.

CDOM and absorption illustrate an origin of organic matter, their age and ability of lakes to eutrophication. So, parameter Sr<1.2 on the Margalich bottom reflect additional influx of groundwater to the lake but Sr value shows "fresh" organic meter in the lake. Autochtonous sedimentation in Parz liman, Horse liman, and Shushanalich supported by spectral slope S and agree to relict origin of Lori's Plateau lakes [14] in spite of lotic lakes Akha lich and Margalich have predominant allochtonous organic matter due to significant additional income of snowpatch melting and ground water correspondingly.

Stable water isotope ratio shows water sources for studied lakes. Thus, Parz liman, Horse liman, and Shushanalich lakes have mostly atmospheric source due to slightly below the Global Meteoric Water Line (GMWL, Craig (1961) [15]) values. According to investigations of groundwater based and environmental tracers [16] the precipitation samples in Artashat (Ararat valley) had ration from −22.45 to 4.54‰ for δ18O and from −173.5 to 37.2‰ for δ2 H. From one hand, other lakes have atmospheric water source as well but with addition transformations. For example, Margalich has partly groundwater income that could be noticed in temperature profiling as well: a temperature on the lake surface was 24.3°C and only 14.2°C - on the depth of 6 m, which can be effect of groundwater springs on the bottom. From another hand, isotopically lighter precipitation at greater elevation, that were noticed for the central Anatolian Plateau: −2.6 to −2.9‰ $\delta^{18}O$ per km [16], did not were found in our studies. Thus, Lessing Lake has the highest elevation than Akna lich but lighter ration of stable water isotopes. It could be an uncertainty of different regions comparison (Ararat valley is southern and lower part of Armenia than studied lakes' areas) or lack of data and necessity of additional dating in future.

Zooplankton abundance of small Armenian lakes, that studied by Meshkova [1] during 1938-1966 and other researchers, included investigation of Cladocera in general. Rotifera, Copepoda and Calanoida were introduced latter as well. Our studies fulfill in main list of biodiversity of aquatic ecosystems but we received new species that did not marked before in small lakes. The abundance of Sevan Lake is more variable [11, 12] but small aquatic ponds have a little bit other specific sue to their environment.

CONCLUSION

Results of the investigation of six small alpine lakes of Armenia are the first step to start the monitoring of aquatic ecosystems of local relict and unique waterbodies on the modern scientific level. Our results have yet show similarities with previous researches of last century with some new specific of hydrochemical and hydrobiological features.

Continuation of monitoring, enlarging the number of study sites and lakes inventory, will allow to enrich our knowledge about all small alpine lakes of Lesser Caucasus. The new obtained data concerning several actual parameters like CDOM, CH_4 flux, and stable water isotopes content is the basis for the modeling and forecasting of environment change of the region under climate warming. The first observations of CH_4 flux made by the authors on small Armenia lakes will help to further assessment the contribution of reservoirs to greenhouse gas emission and plan to reduce the carbon footprint during lake remediation, if necessary. Stable water isotopes content show the necessity of additional monitoring of precipitation all year round especially in highlands because the lack of baseline for estimation and comparison. Understanding of hydrological regime and water sources of small lakes will also improve with bigger massive of data. CDOM parameter with additional DOC (dissolved organic carbon) measurements give greater information about aquatic ecosystems. Finally, monitoring of Armenian small lakes will bring us closer to understanding nature and the ongoing changes in the lakes of the entire Caucasus.

ACKNOWLEDGEMENTS

The work is supported by the Ministry of Education, Science, Culture and Sports of Armenia (project – 23IRF-1E02). Authors thanks Resource Centres (Methods for the analysis of the composition of a substance and X-ray diffraction research methods) of St. Petersburg State University for hydrochemical and isotopic analyses of water samples and OSL in Arctic and Antarctic Research Institute for CDOM results. Individual thanks to G. Nigamatzyanova and L. Hambaryan for help in interpretation of zooplankton and diatom analysis results correspondingly.

REFERENCES

[1] Meshkova T.M. Zooplankton of lakes, ponds and reservoirs of Armenia. Publishing House of the Academy of Sciences of the Armenian SSR. Yerevan, 1968, 108 p. (in Russian) https://books.google.ru/books?id=WUM_AAAAYAAJ

[2] Boynagryan, V. R. (2022). The latest data on a number of high-altitude lakes of Armenia. Proceedings of the YSU C: Geological and Geographical Sciences, 56(1(257), pp.37–46. https://doi.org/10.46991/PYSU:C/2022.56.1.037

[3] Aslanyan N., Harutyunyan D. (2020) Armenia's 4th National Communication on Climate Change. UNDP Armenia, Yerevan, Armenia, 213 pp Environmental Value, Landscape and Biological Diversity of the Lori Plateau Lakes and Watershed (Lori Region, Republic of Armenia». Final Report of the Rufford foundation grant. Project No. 31363-1 Yerevan, Armenia, January 2022. 75 p.

[4] Paffengolts K. N. The basin of Lake Gokcha (Sevan): (geological essay) / Proceedings of the All-Union Geological Exploration Association NKTP USSR ; issue 219, Geological and Petroleum Publishing House, 1934. 104 p.

[5] Boynagryan V.R. Geomorphology of Armenian Plateau. YSU. 2016, 650 p.

[6] Sapelko Tatyana V., Boynagryan Vladimir R., Naumenko Mikhail A., Sevastyanov Dmitry V., Gabrielyan Ivan G., Piloyan Artak S., Margaryan Liana A., Aleksandrin

Mikhail Yu,. Terekhov Anton V (2019) First Multy-Proxy Studies Of High-Mountain Lakes In Armenia: Preliminary Results. Geography, Environment, Sustainability, Vol.12, No 4, p. 272-284. DOI-10.24057/2071-9388-2019-87

[7] Ghazaryan L.G., Gambaryan L.R., Fedorova I. V., Fedorov G. B. The first results of hydroecological studies of the high-altitude lake Shushanalich (Republic of Armenia). Materials of the reports of the international scientific conference in memory of the outstanding Russian scientist Yuri Borisovich Vinogradov [Electronic resource]; St. Petersburg, 2023 / edited by O. M. Makarieva, P. A. Nikitina. — St. Petersburg: Publishing House of the VVM, 2023. pp.224-228. (in Russian) http://elibrary.ru/download/elibrary_60063700_16027047.pdf

[8] Karakhanian A., Tozalakyan P., Grillot J.C., Philip H., Melkonyan D., Paronyan P., S. Arakelyan. Tectonic impact on the Lake Sevan environment (Armenia). Environmental Geology 40 (3), 2001, P.279-288

[9] Avagyan, A., Sahakyan, L., Meliksetian, K., Karakhanyan, A., Lavrushin, V., Atalyan, T., Hovakimyan, H., Avagyan, S., Tozalakyan, P., Shalaeva, E., Chatainger, C., Sokolov, S., Sahakov, A., Alaverdyan, G., 2020. New evidences of Holocene tectonic and volcanic activity of the western part of Lake Sevan (Armenia). Geological Quarterly, 64 (2): 288–303, doi:10.7306/gq.1530

[10] Schubert Michael, Michelsen Nils, Schmidt Axel, Eichenauer Laura, Knoeller Kay, Arakelyan Alexander, Harutyunyan Lilith, Schüth Christoph. Age and origin of groundwater resources in the Ararat Valley, Armenia: a baseline study applying hydrogeochemistry and environmental tracers. Hydrogeology Journal https://doi.org/10.1007/s10040-021-02390-4

[11] Gevorgyan G, von Tuempling W, Shahnazaryan G, et al. Lake-wide assessment of trace elements in surface sediments and water of Lake Sevan. J. Limnol. 2022;81(s1):2096

[12] Krylov A. V., Hayrapetyan A. O., Kosolapov D. B., Sakharova E. G., Kosolapova N. G., Sabitova R. Z., Malin M. I., Malina I. P., Gerasimov Yu. V., Hovsepyan A. A., Gambaryan L. R., [13] Hayrapetyan A, Gevorgyan G, Schultze M, Shikhani M, Khachikyan T, Krylov A, Rinke K. Contemporary community composition, spatial distribution patterns, and biodiversity characteristics of zooplankton in large alpine Lake Sevan, Armenia. J. Limnol. 2022;81(s1):2150. DOI: 10.4081/jlimnol.2022.2150

[14] Environmental Value, Landscape and Biological Diversity of the Lori Plateau Lakes and Watershed (Lori Region, Republic of Armenia». Final Report of the Rufford foundation grant. Project No. 31363-1 Yerevan, Armenia, January 2022. 75 p.

[15] Craig H. (1961) Isotopic variations in meteoric waters. Science 133:1702–1703. https://doi.org/10.1126/science.133.3465.1702

[16] Schemmel F., Mikes T., Rojay B., Mulch A. (2013) The impact of topography on isotopes in precipitation across the central Anatolian plateau (Turkey). Am J Sci 313(2):61–80. https://doi.org/10.2475/02. 2013.01

HYDROLOGICAL DROUGHT FREQUENCY ANALYSIS IN THE YANTRA RIVER DOWNSTREAM

Chief Assist. Dr. Yordan Dimitrov[1]

[1] National Institute of Meteorology and Hydrology - Department of Hydrology, Blvd. 66 Tsarigradsko Shose - 1784 Sofia, **Bulgaria**

ABSTRACT

Hydrological droughts are formed by different processes, but how strong and heterogeneous they are, leading to different manifestation and characteristics of the droughts. Droughts have no distinct starting date, but different methods gives a course of action that may help to identify dry signals and possible drought conditions for early warning. We choose hydrological drought indices that are applicable for Bulgarian conditions. Using statistical methods, minimum flow, deficits and spatial characteristics can be evaluate, as well as identifying vulnerable river catchments and regions or affected areas and intensity they suffer, or is it a prolonged drought in terms of EU Directive. By doing that evaluation, more effective adaptation and mitigation schemes can be recommend to benefit hydrological drought management and maps creation for highlight regional variations and similarities in low flow regimes, drought hazards, vulnerability, and risk for local communities and stakeholders (for recovery measures). A classification based on these drivers, advances river scientist also. The central region of our investigation is Yantra river basin, especially the lower reaches, north of Veliko Turnovo heights and before flow contribute to Danube.

Keywords: hydrological drought, index, threshold, deficit, early warning

INTRODUCTION

Droughts are natural, temporary state of reduction in available water resources as a result of a systematic decrease in precipitation, compared to a certain norm, extending in a long-term aspect over a large geographical area. It is the result of rainfall that is persistently and consistently below average. That is known as meteorological drought, and may turn into hydrological and agrometeorological drought.

A hydrological drought is regional phenomenon that develops slowly. Dry periods and droughts are concepts describing a phenomenon that does not have an exact starting date and time of occurrence and does not have a precisely defined territorial extent, which is why it is necessary to adopt criteria to establish if/since when a territory experiences this phenomenon and to what extent [1].

Hydrological droughts occur both in the traditionally wet and dry periods of the year and can have different effects in different directions. The following types of hydrological drought are observed: Deficiency droughts and Minimum runoff droughts. The term "Water scarcity" is apart from drought and can arise from poor water quality and mismanagement.

The fundamental characteristics and frequencies, that distinguish one drought period from another are: intensity, magnitude, seasonality, frequency, rate of change and spatial extend that defines the drought depth, importance, severity, duration and etc.

Hydrological drought should not be confused with aridity, which is a permanent feature of arid climates, nor with water scarcity, which implies a long-term imbalance of available water resources and needs. Drought research suffers from the lack of consistent methods for drought analysis. The first step in drought analysis would be to define the drought event.

If dry weather continues and water supply problems develop, the dry period may turn into drought. When managing water resources in the conditions of drought, it is necessary to know the direction in the development of the period with outflow below the norms, as well as the trends of climate change, the potential for the development of hydrological drought and whether the phenomenon is progressing [2]. Hydrological analyses of drought, in terms of water flow deficits, are studies of a season or longer periods of time and in a regional context. However, short-term deficits (shorter than a month or season) can also be defined as droughts and treated at a fixed point in space [3]. Usage of Drought Intensity-Duration-Frequency curves (IDF) based on deficit in precipitation and streamflow for water resources management developed by [4], helps to assess how associated deficits vary in a given catchment at different return periods although they have similar drought intensity in the drought index. [5] use the copula method for IDF analysis and modelling of the joint distribution of drought duration and drought severity. Some authors, identify the long-term climatic trends and the magnitude of those trends and analyse drought duration, frequency, and severity [6].

MATERIALS AND METHODS

The derivation of the hydrological drought characteristics is based on methods of established low flow and deficit characteristics and their frequency. The methods used are applicable for observed and simulated time series of streamflow or groundwater. A certain record length is required to obtain stable and reliable results. Percentiles and the Flow Duration Curve (FDC) and Partial Duration Curve (PDC) methods are used as low flow indices, by producing information about the river regime, and as threshold levels. The FDC can be based on daily, monthly and other time interval. For perennial rivers the percentiles will never be zero.

Threshold level method is a hydrological drought definition method. It derives time series of drought deficit characteristics such as deficit duration and the deficit volume. The time interval and the threshold level is decided by the purpose of the study and hydrological regime of the river. Other drought deficit indices can be derived from the time series of drought deficit characteristics. The "threshold level" method is the most commonly applied quantitative method for hydrological drought, where it is essential to determine the beginning and end of drought. The threshold can be fixed or variable during the year [1].

The threshold is considered fixed if a constant value is used for the entire time series. If the threshold is derived from the watercourse FDC, this means that the entire observation period (or a predetermined period) is used in its derivation. When summer and winter drought are studied separately or by hydrological season, the threshold can also be fixed, but based only on runoff data from the respective studied seasons.

A variable threshold is a threshold that changes throughout the year, for example using a seasonal, monthly or daily variable threshold level. A daily variable threshold level can

be defined as an exceedance probability of the 365 daily FDC. To increase the sampling range and smooth the threshold, daily exceedances can be calculated from all flows that occur within n-day window. For example, applying a 10-day window, the flow exceedance on 1 May would be calculated from all discharges recorded between 26 April and 5 May in each year of the period of record. That approach has been adapted to detect deviations of water quantities during seasons of both high and low runoffs. Periods of lower than normal water quantities during high runoff seasons can be important for later drought development. Periods of relatively low runoff during the high runoff season or, for example, due to a delayed high waters from snowmelt, are generally not always considered as drought.

Therefore, events defined by the varying threshold, should be called runoff deficits or anomalies, rather than watercourse droughts. The problem of droughts lasting longer becomes more severe as the threshold levels increase, and care should be taken when choosing a relatively high threshold. The usage of a daily time resolution introduces two special problems, namely the dependence between drought and the presence of small, short (minor) droughts. During a prolonged dry period, it is often observed that the flow exceeds the threshold level for a short period of time, and thus a large drought is divided into several small droughts, which are, however, interdependent. To avoid these problems, which could bias the modelling of extreme values, the sequential definition of drought events should include some kind of pooling to define an independent sequence of drought thresholds (e.g., a moving average procedure, a sliding window is recommended).

To reduce the problem of minor droughts, a minimum drought duration may be required, which removes droughts of duration less than the specified number of days (here D_{min} is set to five days). The time between events criterion is used to combine dependent droughts that are separated by a short period of runoff above the threshold. If the time between two droughts is less than a critical duration, T_{min}, the two events are merged. In this example, T_{min} is equal to two days.

The threshold level is obtained as a value from the FDC and it is determined as an exceedance percentile. In this study Q70, Q75 and Q90 as daily threshold values are used.

Because there is not universal indicator for assessing the vulnerability and magnitude of drought periods and their consequences, the system of indices and complex indices method has been used [7], [8]. Complex indices are based on water balance calculations and describe the whole spectrum of wetness conditions from wet to dry.

The frequency analysis is one of the most common applications of statistics within hydrology. It involves definition of hydrological event, and extreme characteristics to be studied; selection of the extreme events and probability distribution to describe the data; estimation of the parameters of the distribution and estimation of extreme events or design values for a given problem.

The issue of climate change has raised the question of whether the frequency of extreme events might increase as a result of an intensified hydrological cycle. Independent of the origin of the change, there is a need to check whether there is any tendency for the frequency or severity of the studied events to increase or decrease during the observation period.

Many of the hydrological phenomena studied using frequency analysis are regional in nature and there is a tendency for extreme values to occur simultaneously at several sites. This is reflected in a spatial correlation between the observation series. One of the main purposes of frequency analyses is to find the most suitable probability distribution to describe the data. The occurrence and spatiotemporal evolution of drought is important for developing measures for drought mitigation and management.

The aim of that study is to present several applications of frequency analysis to time series of hydrological drought characteristics to demonstrate the procedures and international experience.

Yantra river spring is situated in Shipka range in Central Stara Planina Mountain above town of Gabrovo. The length of the river is 285.5 km with watershed area of 7861.6 km^2. Its major tributaries are river Lefedja from east and river Rositsa from west. They flow into Yantra north of Veliko Tarnovo heights. About 20 km after that is situated the Hydro Monitoring Station (HMS) No 23850 Yantra – village Karantsi, with the highest flow from the entire system, south-west of Byala (fig. 1.). Another used data are from HMS No 23650 Yantra – Gabrovo, No 23700 Yantra – Veliko Tarnovo, No 23500 Rositsa – Sevlievo, No 23400 Dzhulunica – Dzhulunica and No 23150 Golyama – Strazhica. In total 46 years of daily streamflow records are available covering the period 1974 to 2019 and they were used for fundamental statistics extraction and the drought events definition.

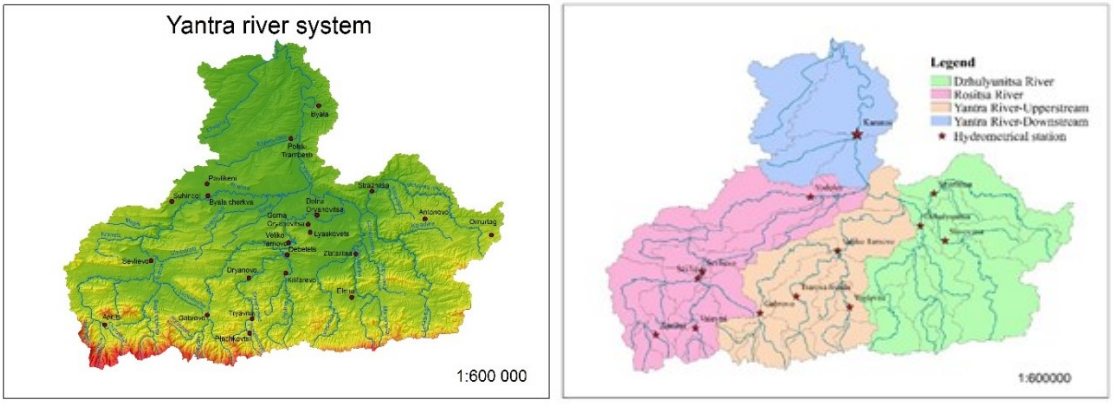


Fig.1. Maps of Yantra river basin hydrography and sub-basins

RESULTS

Average river runoff at HMS No 23850 Yantra – Karantsi is 45.284 m^3/s with minimum average annual runoff 9.911 m^3/s for year 1994 and maximum average annual runoff 128 m^3/s for year 2005. The absolute minimum flow (Fig. 2) is 1.299 m^3/s from 30 Sept. 1985. 50 % of the annual minimum runoff is less than 12.500 m^3/s.

Streamflow drought events were derived from the daily flow series Q_{70} threshold level. The variable daily threshold values chosen are with 20 days' smoothness. Using that extracted daily thresholds, we found 128 hydrological drought cases for the period 1974-2019.

A histogram of the values is shown on Fig. 3, from where we can conclude that more of the observed drought periods are less than 40 days' longer. From the plot we can identify minor drought, as well as long duration multi seasonal hydrological droughts, more than four months duration (red colour bars).

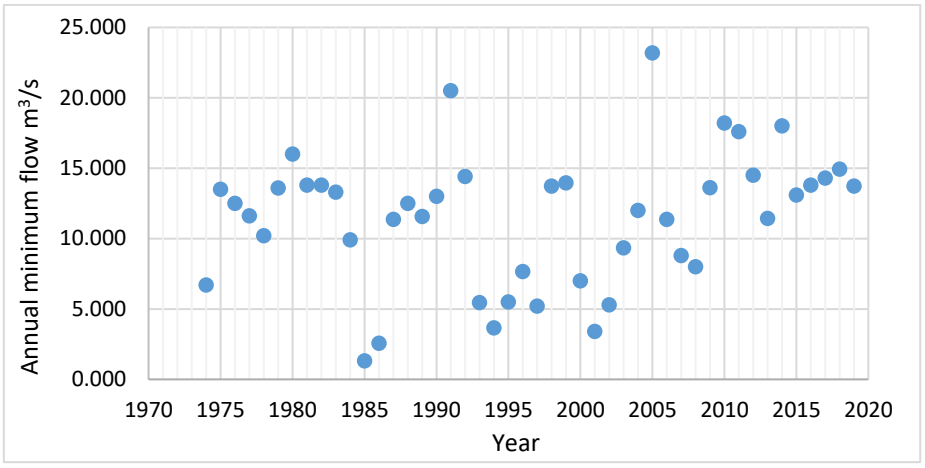


Fig. 2. Time series of annual minimum 1-day flow AM (1) at HMS 23850 Karantsi

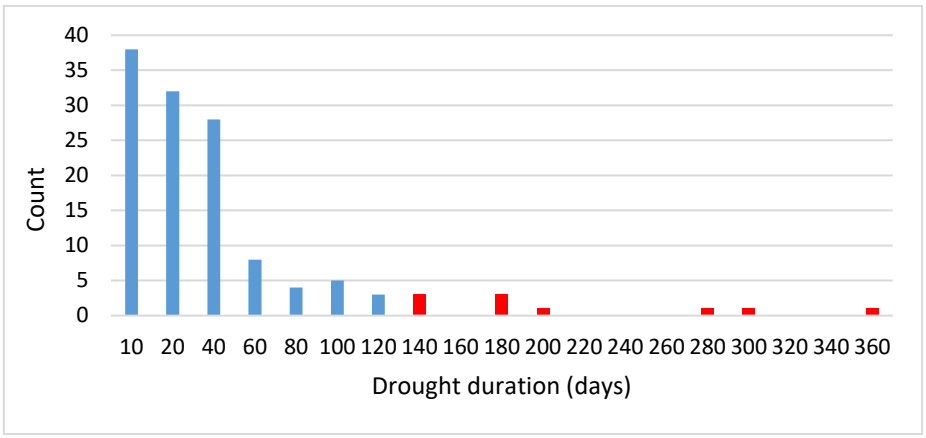


Fig. 3. Hydrological drought events duration histogram for HMS 23850 Karantsi

Deficit volume of the drought event is a characteristic that shows us that more of 20 events has deficit from -8 to -16 m^3/s per day and in some years we have more than one of that extreme values (Fig. 4).

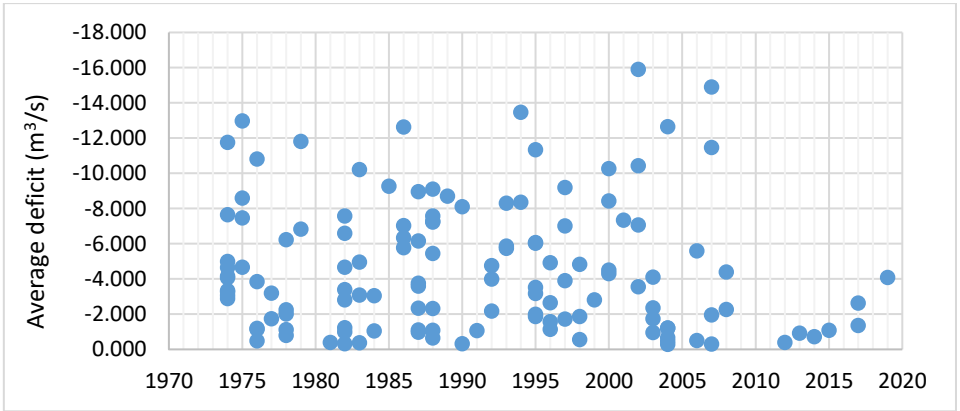


Fig. 4. Average deficit volume per drought event at HMS 23850 Karantsi

Some of the minor hydrological droughts, can have very low deficits, as well as the longest drought, less than -20 minimal daily deficit (in red zone) (Fig. 5) with Exceedance probability colour code system (Table 1) for HMS 23850 Karantsi.

https://doi.org/10.5593/sgem2024/3.1/s12.14

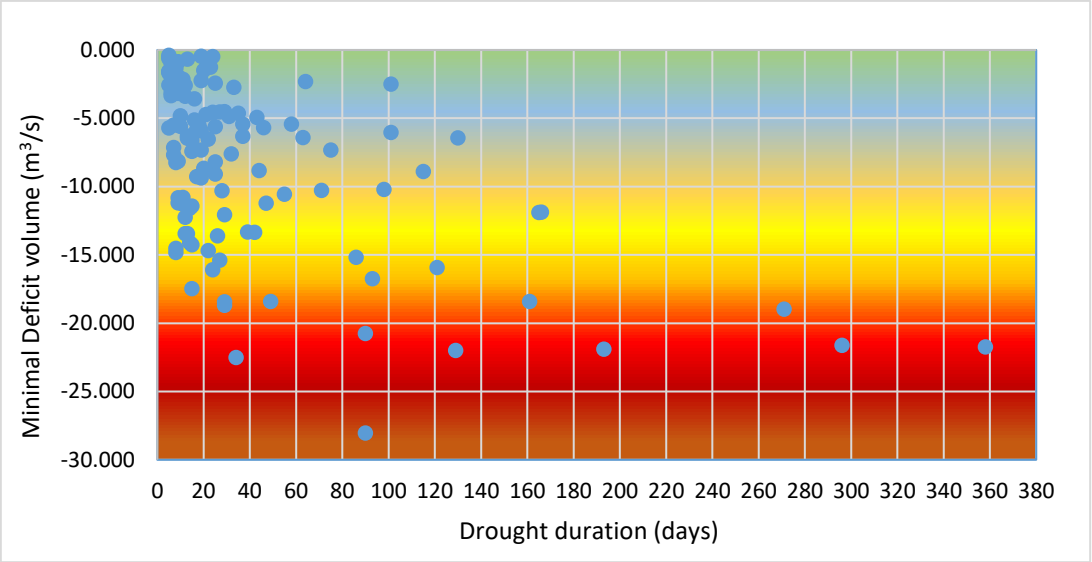


Fig. 5. Scatter plot of Minimal deficit volume and Drought duration at HMS 23850 Karantsi

From fig. 6 one can see that real duration (without few days above daily Q_{70} threshold level) of the droughts is till 350 days' in one single event, but we have years with five and more 20-30 days' drought duration. Subsequently the return period in years for a given event can be calculated.

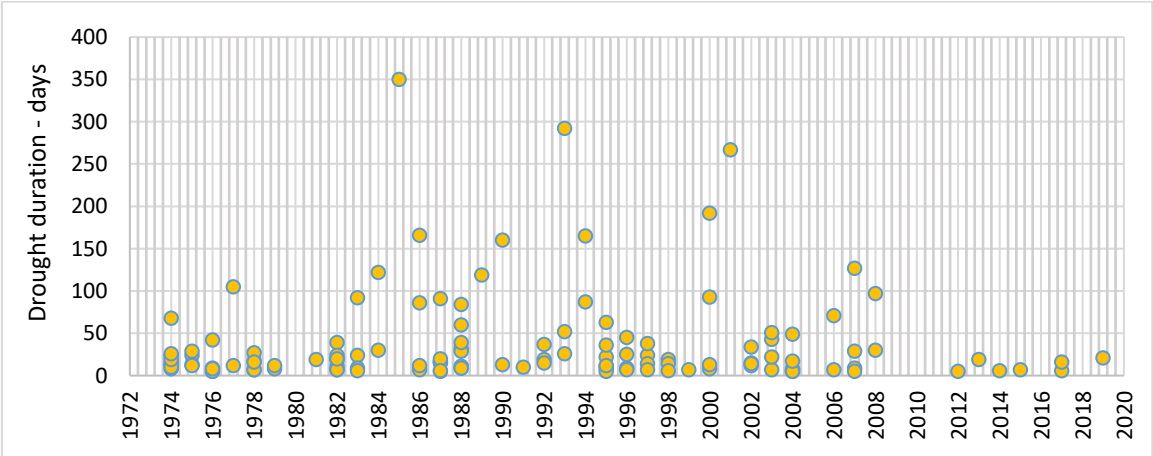


Fig. 6. Real duration of the hydrological drought spells at 23850 Karantsi

Flow duration curves for the separate years (Fig. 7) shows that 1994, 2001, 1993 and 1990 has the lowest flow in different part of the curve. At river Dzhulunitsa the maximum year flow for dry years can be a little more than the driest conditions in the wet years.

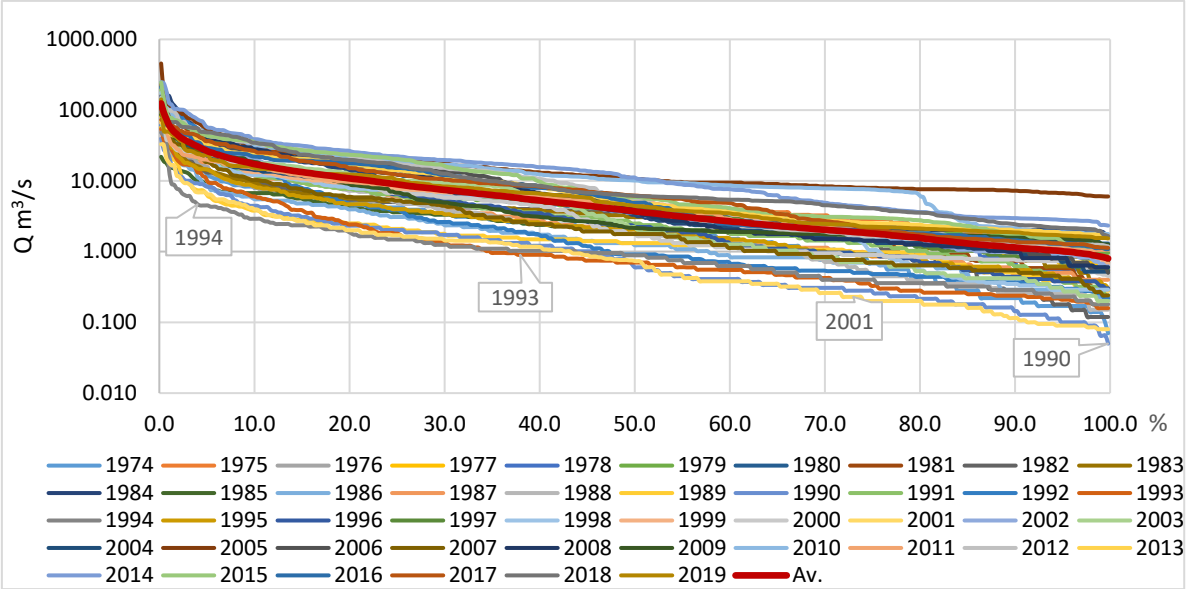


Fig. 7. Flow Duration curves by years – HMS 23400 Dzhulunica

As only events below the Q_{70} (or Q_{75}, Q_{90} etc.) percentile are selected, it might happen that the flow never becomes less than the threshold in a year (non-drought year). We observe years with no dry days under threshold (Fig.8), with just one year for HMS 23500 Rositsa, with shorter droughts and seven years, like the case with HMS 23150 Strajica, but with the longest droughts there as well. That means that areas enter a dry phase slowly, than recover the water storage slower, with comparison to the other tributaries. That requires a special development of the system of codes for all separate HMS separately (Table 1), where possible, or using regionalization methods in unexplored watersheds.

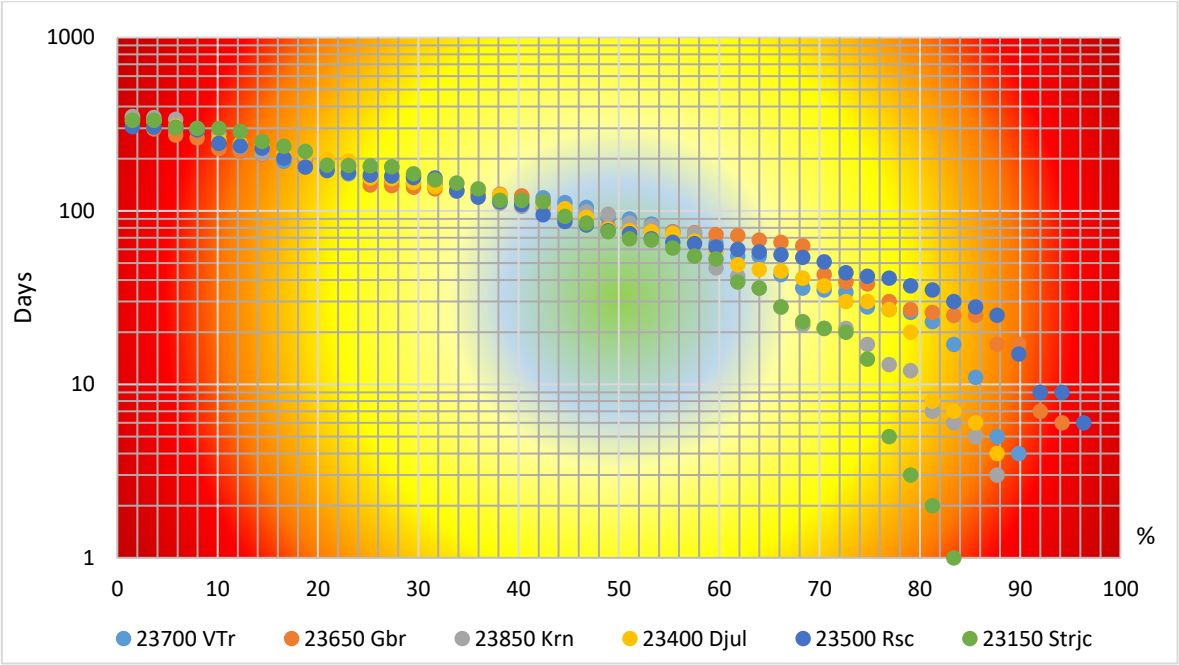


Fig. 8. Frequency of dry days per year with runoff below Q_{70} in different parts of the Yantra river catchment.

Table.1. Exceedance probability with 10 threshold levels colour code and Drought Early Warning codes with thresholds for duration, extracted particularly for HMS23850 Karantsi.

Probability %	100-90	90-80	80-70	70-60	60-50	50-40	40-30	30-20	20-10	10-
Duration	1 - 2	3 -7	8 - 21	22 - 47	48 - 96	97 - 106	107-159	160-195	196-235	235-

DISCUSSION

Based on that drought characteristics distribution graphs, we can derive thresholds for every single drought characteristic and can be used for example for Drought Early Warning system (Table 2.), evaluation of dry signals, drought magnitude and severity forecasting, regional frequency analysis and perform severity area frequency curves.

Table 2. Dry signals and hydrological drought development in the Yantra river main course and its sub-catchments. The segment embrace the period (26.04.2002 – 20.05.2002) and starting date of Drought N102 for HMS 23850 Karantsi – 16th of May, with red code deficit from 19th of May 2002.

	HMS	Rosica	Gabrovo	V. Tarnovo	Karantsi	Dzhulunitsa	Strazhica
	No	23500	23650	23700	23850	23400	23150
Year	Date						
2002	26.Apr	11.913	0.073	4.560	19.352	3.357	0.663
2002	27.Apr	4.537	-0.151	3.571	17.571	2.185	1.167
2002	28.Apr	3.240	-0.151	2.628	15.969	1.532	0.575
2002	29.Apr	2.049	-0.339	1.153	10.120	0.895	0.391
2002	30.Apr	1.518	-0.077	0.208	8.701	0.065	0.200
2002	1.May	3.429	-0.021	0.126	7.401	-0.044	0.217
2002	2.May	2.901	-0.187	0.004	7.058	-0.414	0.227
2002	3.May	2.366	-0.356	-0.174	9.358	-1.013	0.041
2002	4.May	2.439	-0.540	-1.072	9.892	-1.136	0.051
2002	5.May	1.931	-0.504	-1.741	11.521	-1.364	0.065
2002	6.May	1.962	-0.682	-2.161	12.726	-1.432	0.077
2002	7.May	1.455	-0.639	-2.137	11.972	-1.477	-0.098
2002	8.May	1.506	-0.827	-2.530	10.248	-1.600	-0.006
2002	9.May	1.025	-0.789	-2.298	11.480	-1.671	-0.264
2002	10.May	0.600	-0.763	-2.514	11.893	-1.738	-0.398
2002	11.May	0.182	-0.968	-2.676	11.712	-1.804	-0.382
2002	12.May	-0.226	-0.951	-2.847	10.774	-1.863	-0.442
2002	13.May	-0.970	-0.946	-2.846	10.961	-1.948	-0.433
2002	14.May	-1.247	-0.940	-2.827	9.209	-1.992	-0.438
2002	15.May	-1.235	-1.147	-3.021	9.034	-2.000	-0.441
2002	16.May	-1.478	-1.133	-2.771	-0.209	-2.021	-0.442
2002	17.May	-1.947	-1.117	-2.749	-12.089	-1.982	-0.365
2002	18.May	-2.118	-1.078	-2.724	-13.512	-1.943	-0.355
2002	19.May	-2.320	-1.041	-3.341	-14.261	-1.917	-0.430
2002	20.May	-2.056	-0.364	-3.517	-14.178	-1.846	-0.363

CONCLUSION

There are hundreds of dry periods, but not all are droughts, "flash droughts" or "prolonged droughts". It should have a substantiation reason for Hydrological Drought Declaration process. Short-term droughts, less than 10 days, occurring in a certain vegetation or biotic period, also can be dangerous. The 1-day time scale illustrates, that often more than one smaller drought is combined to form a single large drought. The depiction of water deficits also reveals how a deficit rapidly accumulated followed by a lull and then a second drought phase before any real recovery was achieved. Accumulated water deficit is another application to use in defining the magnitude of drought if the initiation is identified.

The choice here to use Q_{70} threshold as a measure is based on the logic that the manifestation of that flow longer, means that the drought persists without a water recharge and the worse will be the magnitude, as evaporation continues to occur. This is particularly important to end-users and decision-makers to act against the drought quickly and precisely in a more physically understandable manner. Probability of future dry periods, based on the past can be calculated for all time scales, such that estimates can be provided of the probabilities to emerge from drought. Such estimates are particularly useful, when they indicate that drought is not likely to end soon and the impacts must be minimized. Further research goal will be trend analysis and the relationship between meteorological and hydrological drought characteristics investigation.

ACKNOWLEDGEMENTS

The author would like to acknowledge National Institute of Meteorology and Hydrology, for granted daily hydrological data.

REFERENCES

[1] Tallaksen, L.M., van Lanen H. A. J. (Eds.) 2004. Hydrological Drought. Processes and Estimation Methods for Streamflow and Groundwater. Hydrology and Environmental Hydraulics WIMEK. Development of Water Science, Vol. 48 Elsevier.

[2] Smakhtin, V. Y. 2001. Low Flow Hydrology: a Review. J. Hydrology 240, 147-186.

[3] Zelenhasic, E., Salvai A. 1987. A Method of Streamflow Drought Analysis. Water Resources Restoration 23 (1), 156-168.

[4] Cavus Y., Stahl K. Aksoy H. 2023. Drought intensity-duration-frequency curves based on deficit in precipitation and streamflow for water resources management. Hydrology and Earth System Sciences https://doi.org/10.5194/hess-2023-107

[5] Kwak J., Kim Y.S., Lee J.S., Ki H.S. 2012. Drought Severity-Duration-Frequency Analysis of Hydrological Drought Based on Copula Theory. Hydrology Days 2012 Department of Civil Engineering, Inha University, South Korea

[6] Abara M., Komariah, Budiastuti S. 2020. Drought Frequency, Severity, and Duration Monitoring Based on Climate Change in Southern and Southeastern Ethiopia. IOP Conf. Ser.: Earth Environ. Sci. 477 012011

[7] Rossi, G. 2011. Drought Risk for Water Supply Systems Based on Low-flow Regionalisation. – Ph.D. Thesis, Department of Architecture, Civil Engineering and

Environmental Sciences University of Braunschweig, Institute of Technology and University of Florence and Faculty of Engineering.

[8] Ilcheva, I., Dimitrov Y., Yordanova A., Ljubenova K., Drumeva G. 2022. Approach and Indicator System for Prolonged Drought Identification in Bulgaria. – Bulgarian Journal of Meteorology and Hydrology, 26(2), 10-21.

HYDROMETEOROLOGICAL DROUGHT IMPACT ON CEREAL PRODUCTION IN NORTHERN BULGARIA

Prof. Dr. Nina Nikolova[1]

Dr. Simeon Matev[1]

Prof. Dr. Neli Hristova[2]

Assoc. Prof. Dr Kalina Radeva[1]

[1] Sofia University "St. Kliment Ohridski", Faculty of Geology and Geography, **Bulgaria**
[2] Climate, Atmosphere and Water Research Institute – BAS, **Bulgaria**

ABSTRACT

On the background of regional climate changes, an increase in the frequency and intensity of extreme droughts has been observed in many regions of Europe in recent years, and this trend is expected to continue in the future. While common in southern Europe, including Bulgaria, drought can adversely affect human life and economic activities. Extreme droughts lead to water scarcity, restricting the availability of irrigation water for agricultural purposes. In the regions where irrigation is vital for sustaining crop production, diminished water availability can result in crop failures and economic losses.

This study aims to contribute to understanding the climate-water-food nexus by assessing the impact of drought on the main cereal crops in Bulgaria, namely maize, wheat, and barley. The analysis incorporates climatic data (air temperature and precipitation), hydrological data (streamflow), and statistical data on crop yields. Drought indices such as Standardized Precipitation Evapotranspiration Index (SPEI), Standardized Precipitation Index (SPI), and Streamflow Drought Index (SDI) were calculated at different timescales (from 1 to 12 months) to identify drought periods. A significant decrease in yields is observed during dry years. Correlation analysis shows a clear link between drought in warm months and maize production, while the winter drought is more crucial for wheat and barley.

Keywords: Bulgaria, water scarcity, drought, agriculture, drought indices, adaptation

INTRODUCTION

Drought is one of the most destructive hydrometeorological hazards, adversely impacting natural ecosystems, natural resources, agricultural development, and society [1]. The severity of drought stress is unpredictable as it depends on many factors such as the occurrence and distribution of rainfall, evaporative demands, and moisture-storing capacity of soils [2]. There is no general concept of drought due to the ambiguity of the process and the evolution of droughts and their multifaceted and various impacts on the environment. Drought generally can be characterized as an irregular, longer period of below-normal water availability, including surface, ground, or atmospheric water. Meteorological drought occurs due to the lack of precipitation over some prolonged period (less than 75% of normal), and hydrological drought occurs when water levels in aquifers, lakes, and rivers drop below the required level for operational and ecological purposes [1]. These types of droughts could propagate into agricultural drought which

https://doi.org/10.5593/sgem2024/3.1/s12.15

occurs due to the lack of water at various stages of crop development to support production [3].

Climate change and extreme weather events directly affect global food production, causing yield loss to a large extent [4]. At the same time, food demand is expected to double by 2050 [5]. It is important to understand the relationship between rainfall, temperature, and streamflow. Their interactions can significantly reduce cereal production during drought and water deficit conditions.[6]. Therefore, quantifying drought hazards and impacts on crops is important for sustainable agricultural management and developing appropriate drought mitigation strategies.

Drought has been a notable characteristic in Bulgaria in recent years, particularly during the second half of the 20th century (the 1980s and early 1990s) and at the beginning of the 21st century [7, 8]. However, the last decade of the 21st century has seen an increase in the number of severe droughts, with significant events recorded in 2012, 2016, 2017, 2018, 2020, and 2021 [8, 9, 10]. This presents a significant challenge for agriculture in Bulgaria, affecting food security and water supply. This study aims to assess the impact of meteorological and hydrological drought on the primary cereal crops in North Bulgaria, one of the country's key agricultural regions. By calculation of meteorological (Standardized Precipitation Index–SPI and Standardized Precipitation Evapotranspiration Index–SPEI) and hydrological (Streamflow Drought Index–SDI) drought indices and analyses of yields of maize, barley and wheat the paper contributes to the understanding of the dynamic of climate-water-food nexus with climate change.

MATERIALS AND METHODS

The studied area covers one of the main agricultural areas of Bulgaria, including the Danube Plain and the Fore-Balkan. The region experiences a typical continental climate characterized by significant droughts, especially during summer, and is particularly vulnerable to climate change and related hydrometeorological extremes. The analysis is based on monthly air temperature and precipitation data collected from seven meteorological stations and streamflow data from four stream gauging stations, covering the period from 1961 to 2020. (Figure 1.). The selection of stations and the investigated period were determined based on data availability and accessibility. To analyze drought impact on cereal production the statistical data for the yield of wheat, barley and maize for Vidin, Pleven and Lovech districts (NUTS-3) were used.

Hydrological and meteorological drought occurrence, frequency and severity were determined by the following drought indices: Streamflow Drought Index (SDI) for analysis of hydrological drought and Standardized Precipitation Index (SPI) and Standardized Precipitation Evapotranspiration Index (SPEI) for study of meteorological drought. The SPI and SDI were computed according to the methodology developed by [11]. The SPI (SDI) values represent the standardized series of precipitation (streamflow) data, that have been transformed to fit a gamma distribution. Positive indices values indicate precipitation (streamflow) levels above the long-term average, while negative values signify precipitation (streamflow) levels below the long-term average. SPI Generator program (Version 1.7.5; National Drought Mitigation Center) was used for SPI and SDI calculation. SDI was calculated as SPI but instead of monthly precipitation monthly streamflow data were used as input data.

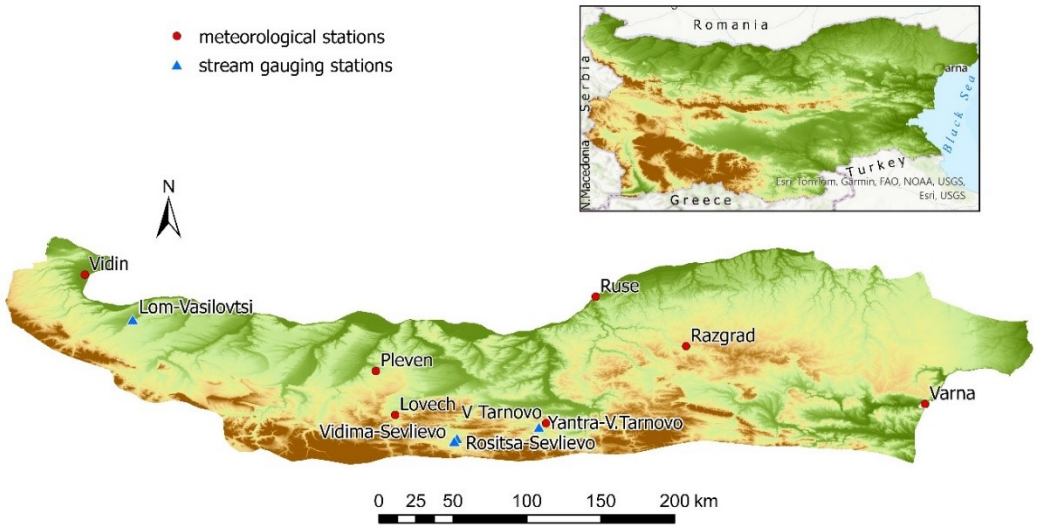


Figure 1. Study area and location of meteorological and stream gauging stations

The SPI, computed based solely on precipitation data, does not consider air temperature's effect on drought. To overcome this limitation, we computed the Standardized Precipitation Evapotranspiration Index (SPEI) as described by Vicente-Serrano et al. [12]. SPEI, representing the difference between cumulative precipitation and potential evapotranspiration, is a valuable tool for detecting increased drought severity due to rising temperatures. SPEI is widely recommended for studying drought impact on agriculture. [13,14].

This study analyses the three drought types: moderate (–1 ≥SPI;SDI;SPEI >–1.50), severe (–1.50≥SPI;SDI;SPEI>–2) and extreme (SPI;SDI;SPEI≤–2.00). SPI calculated on a timescale from 1 to 12 (SPI-x, where x is from 1 to 12) and SPEI on timescales 1, 3, and 6 were used for meteorological drought assessment. Hydrological drought was analysed using SDI-1. Based on SPI-1 and SDI-1 we analysed the drought frequency, maximum continuous duration of drought (D), drought magnitude (DM), and average drought intensity (ADI). According to [15], drought duration was defined as the period beginning when the SPI drops to –1 or lower and ending when the SPI returns to 0 or a positive value. *DM* was calculated by the following formula [11]:

$$DM = -\left(\sum_{i=j}^{x} SPI_{ij}\right)$$

where j is the first month when *SPI* becomes equal to or less than –1 and x is the last consecutive month with a negative *SPI* value [11].

Average drought intensity over the duration (ADI) is determined as a relation between drought magnitude (DM) and drought duration (D) as follows [8]:

$$ADI = \frac{DM}{D}$$

Correlation analysis between SPI-x and SDI-1 was conducted to study the propagation of meteorological to hydrological drought. The impact on cereal production was evaluated by correlating wheat, barley, and maize yields with seasonal SPEI. Pearson correlation

coefficients were calculated, and statistical significance was assessed using a T-test at the 0.05 level.

RESULTS

Hydrological and meteorological drought characteristics

The results from the analyses of SPI-1 and SDI-1 show that the maximum drought duration for hydrological and meteorological droughts was observed mainly in the 80s and early 90s (Table 1). The longest duration of the meteorological drought was between seven and 10 months, while much longer drought periods were found for hydrological drought, with a maximum duration of 15 to 24 months.

Table 1. Drought duration (D), magnitude (DM), and average drought intensity (ADI), according to SPI-1 and SDI-1

	Start	End	D, months	Average D, months	Peak	DM	ADI
Stream gauging stations							
Lom - Traykovo	Nov 1992	Jun 1994	20	5.8	-1.88	21.78	-1.09
Yantra - VT	Feb 1989	Nov 1990	22	6.0	-1.88	19.29	-0.88
Rositsa - Sevlievo	Jul 1984	Jun 1986	24	4.8	-1.72	27.03	-1.13
Vidima - Sevlievo	Nov 1984	Feb 1986	15	4.4	-1.49	15.28	-1.02
Meteorological stations							
Vidin	Oct 2001	May 2002	8	2.3	-2.37	8.77	-1.1
Pleven	Aug 1992	Apr 1993	9	2.0	-1.88	7.9	-0.88
Lovech	Oct 1984	Jul 1985	10	2.0	-1.41	7.1	-0.71
Veliko Tarnovo	Feb 1990	Aug 1990	7	2.0	-2.46	6.17	-0.88
Ruse	Nov 1982	May 1983	7	1.9	-1.74	6.39	-0.91
Razgr	Aug 1993	Feb 1994	7	2.2	-2.53	6.67	-0.95
Varna	Aug 2019	Feb 2020	7	2.2	-2.37	5.27	-0.75

The average meteorological drought duration for the investigated period is around 2 months while the average duration for the hydrological drought varies between 4.4 and 6 months. Although the lowest SPI values (peak) indicate severe and extreme drought, the average intensity of droughts has been much lower (moderate and even mild drought, with conditions close to normal - SPI between -1 and 0). This analysis shows that Rositsa-Sevlievo and Vidin are the stations with the most significant recorded changes in their respective categories.

Hydrological drought typically lags behind meteorological drought because it takes longer for precipitation deficits to translate into reduced water availability in these sources. The correlation analysis between SPIx and SDI-1 for nearby meteorological and stream gauging stations shows the highest Pearson correlation coefficients for SPI-3 to SPI-6, with statistically significant values between 0.59 and 0.67. This indicates that the

transition from meteorological to hydrological drought typically takes 3 to 6 months, depending on climate conditions.

The analyses of meteorological drought using the SPEI indicate a rise in dry events (Figure 2), compared to drought detected with SPEI which is correlated with increasing air temperatures. The geographical location of station Varna on the Black Sea coast probably affects the occurrence of dry events determined by SPEI – due to the cooling influence of the sea in summer, the temperatures here are not very high and even with lower rainfall, the drought is not very pronounced.

According to SPIE-1, moderate drought conditions are observed to be the most frequent type of drought, with severe and extreme droughts occurring less frequently (Figure 3). A comparative analysis of two distinct 30-year periods, 1961-1990 and 1991-2020, reveals a notable increase in the occurrence of all drought categories during the latter period.

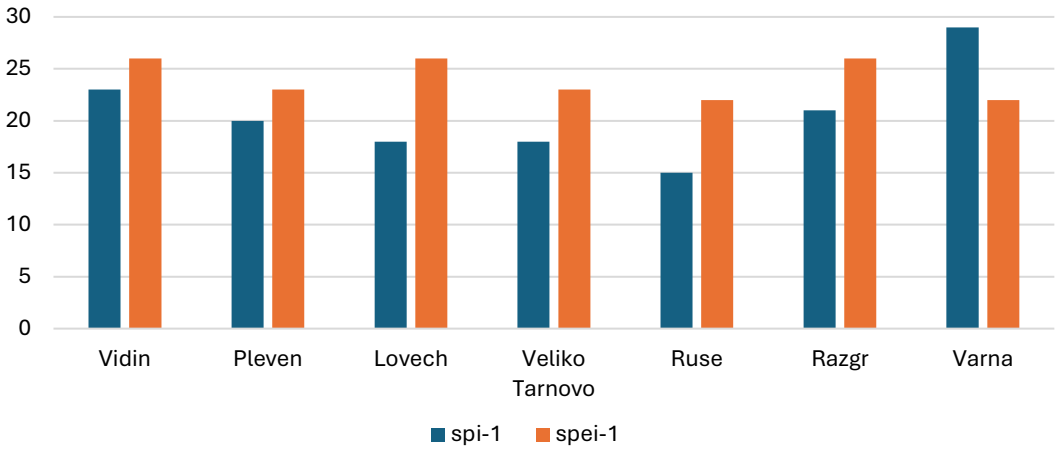


Figure 2. Number of dry events lasting at least 3 months, according to SPI-1 and SPEI-1

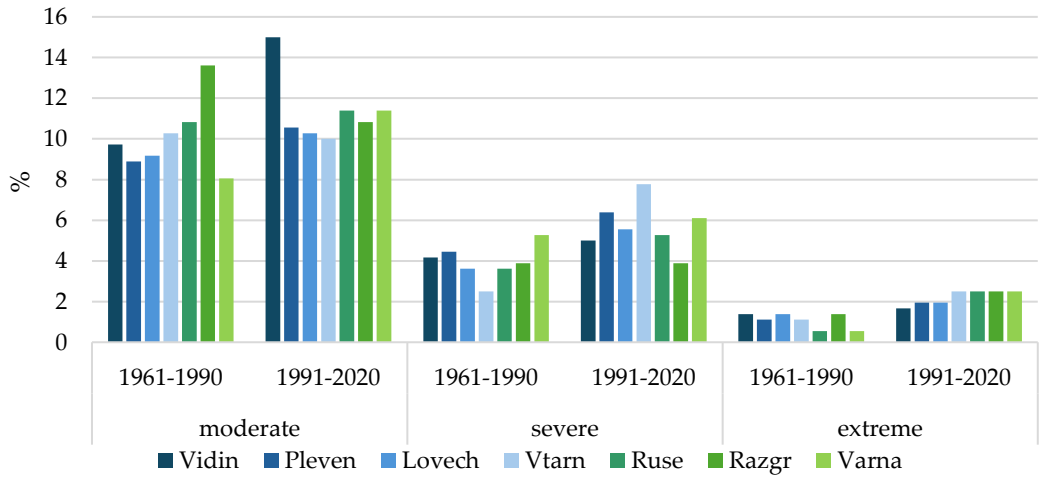


Figure 3. The number of dry months of varying drought intensity as a percentage of the total number of months over the 30 years (according to SPEI-1).

https://doi.org/10.5593/sgem2024/3.1/s12.15

The data indicates that the frequency of moderate droughts has the most significant rise among the different classes of drought over these decades. This trend suggests a shift in climate patterns leading to more frequent drought events in recent years.

Drought impact on cereal production

The initial impacts of drought are related to reduced soil moisture, reduced water supply for plants, and decreased streamflow. Average maize and barley yield data for North Bulgaria from 2001 to 2021 reveal a notable decline during the dry years of 2007 and 2012. In contrast, an uptick in yields was observed in the wet years of 2010, 2014, and 2017. Wheat yield data demonstrate a similar pattern, although with comparatively smaller fluctuations between dry and wet years. Correlation analysis between yield data and seasonal SPEI values reveals the strongest positive relationship for maize during spring, summer, and the warm half-year (April-September), Table 2. The results show that an increase in the severity of drought during the warm months leads to a decrease in maize yields while wetting conditions in winter have a greater effect on wheat and barley yields.

Table. 2. Correlation between seasonal SPEI and yields of selected crops for the period 2008-2020 by districts (NUTS-3)

	Winter	**Spring**	**Summer**	**Autumn**	**Apr-Oct**
			wheat		
Vidin	-0.68	0.31	0.21	0.06	0.27
Pleven	-0.67	0.44	-0.06	0.14	0.13
Lovech	-0.70	0.37	0.26	0.15	0.41
			winter barley		
Vidin	-0.48	0.16	0.22	-0.03	0.14
Pleven	-0.62	0.15	0.13	0.24	0.23
Lovech	-0.76	0.27	0.22	0.13	0.37
			maize		
Vidin	-0.43	0.61	0.68	0.09	0.59
Pleven	-0.24	0.45	0.69	0.11	0.70
Lovech	-0.26	0.43	0.86	0.18	0.72

** for Vidin the period is 2011-2020*

DISCUSSION

Hydrological drought stands out from meteorological drought mainly because it persists over longer periods, often spanning months or even years, and exhibits a more pronounced impact on water resources due to its greater magnitude. Drought's impact on cereal production encompasses various aspects, including yield reduction, quality deterioration, economic losses, and food security concerns. Drought conditions adversely affect cereal crops such as wheat, barley, and maize by causing moisture stress, hindering plant growth and development, and compromising overall crop health. Drought-induced heat stress during critical growth stages can further exacerbate yield losses and diminish grain quality. Additionally, water scarcity impacts irrigation systems, exacerbating crop water stress and reducing yields. The severity and duration of hydrological drought depend on the intensity and persistence of meteorological drought. Extended periods of meteorological drought can exacerbate hydrological drought conditions. Furthermore,

food security is threatened as cereal crops serve as staple food sources for millions worldwide. Adaptation strategies such as drought-resistant crop varieties, improved water management practices, and timely drought monitoring and early warning systems are essential to mitigate the adverse effects of drought on cereal production and ensure food security in vulnerable regions.

CONCLUSION

The study's results indicate a notable increase in drought frequency during the period 1991-2020 compared to 1961-1990. Furthermore, the average and maximum durations of hydrological droughts are significantly longer than those of meteorological droughts. A key factor contributing to the increased frequency and extended duration of drought events is the rise in air temperature, which exacerbates drought conditions.

Droughts present significant challenges to agriculture in Bulgaria, impacting food security and water supply. The analysis of the influence of hydrometeorological drought on cereal production in North Bulgaria, reveals significant correlations between drought conditions and reduced yields of main cereal crops and maize in particular. This relationship emphasizes the need for effective drought management strategies and adaptive agricultural practices to mitigate the negative consequences on cereal production.

Future research will focus on developing predictive models for drought impact and exploring innovative agricultural techniques to adapt to the increasing frequency and intensity of drought events caused by climate change.

ACKNOWLEDGEMENTS

This study has been carried out in the framework of the project “The Nexus Approach in Agriculture. The water-food nexus in the context of climate change”, supported by the Ministry of Education and Science (MES) of Bulgaria (Agreement № КП-06-КОСТ-2/17.05.2022 and is based upon work from COST Action NEXUSNET, CA20138, supported by COST (European Cooperation in Science and Technology).

REFERENCES

[1] van Loon, A. F. Hydrological drought explained. WIREs Water, 2(4), 359-392. 2015/ https://doi.org/10.1002/wat2.1085

[2] Wery, J., Silim, S. N., Knights, E. J., Malhotra, R. S., & Cousin, R. Screening techniques and sources of tolerance to extremes of moisture and air temperature in cool season food legumes. In Expanding the production and use of cool season food legumes (pp. 439–456). 1994. Springer

[3] Martínez-Fernández, J., González-Zamora, Á., Sánchez, N., & Gumuzzio, A. A soil water-based index as a suitable agricultural drought indicator. Journal of Hydrology, 522, 265-273. 2015. https://doi.org/10.1016/j.jhydrol.2014.12.051

[4] Dasgupta, S. and Robinson, E. J. Z. Attributing changes in food insecurity to a changing climate, Scientific Reports 12 (1), p. 4709. 2022. https://doi.org/10.1038/s41598-022-08696-x

[5] Leng, G. and Hall, J. Crop Yield Sensitivity of Global Major Agricultural Countries to Droughts and the Projected Changes in the Future. Science of the Total Environment, 654, 811-821. 2019. https://doi.org/10.1016/j.scitotenv.2018.10.434

[6] Matiu, M., Ankerst, D.P., Menzel, A. Interactions between temperature and drought in global and regional crop yield variability during 1961–2014. *PLoS ONE.* 12: e0178339. 2017. doi: 10.1371/journal.pone.0178339

[7] Petkova, B.; Kuzmova, K.; Berova, M. The main abiotic stress factors limiting crop cultivation and production in Bulgaria. Climate changes, drought, water deficit and heat stress. Agricultural Sciences/Agrarni Nauki, 11(26). 2019.

[8] Radeva, K., Nikolova, N. Hydrometeorological Drought Hazard and Vulnerability Assessment for Northern Bulgaria, Geographica Pannonica, Volume 24, Issue 2, 112–123. 2020.

[9] Stoyanova, R.; Nikolova, N. Meteorological drought in Southwest Bulgaria during the period 1961–2020. Journal of the Geographical Institute "Jovan Cvijić" SASA, 72(3), 243–255. 2022. https://doi.org/10.2298/IJGI2203243S

[10] Evgeniev, R.; Malcheva, K.; Marinova, T.; Chervenkov, H.; Bocheva, L. Assessment of drought in Bulgaria in recent years through the standardized precipitation index, ,245-252. 2023. 10.5593/sgem2023/4.1/s19.31

[11] McKee, T. B., Doesken, N. J., & Kleist, J. The Relationship of Drought Frequency and Duration to Time Scales. In *Proceedings of the 8th Conference on Applied Climatology*. Vol. 17, No. 22, pp. 179-183. 1993.

[12] Vicente-Serrano, S. M., Beguería, S., & López-Moreno,J. I. A multiscalar drought index sensitive to global warming: the standardized precipitation evapotranspiration index. Journal of Climate, 23 (7),1696-1718. 2010.

[13] Bezdan, J.; Bezdan, A.; Blagojević, B.; Mesaroš, M.; Pejić, B.; Vranešević, M.; Pavić, D.; Nikolić-Đorić, E. SPEI-Based Approach to Agricultural Drought Monitoring in Vojvodina Region. *Water*, *11*, 1481, 2019. https://doi.org/10.3390/w11071481

[14] Li, L.; Zhao, L.; Li, Y. Spatiotemporal Characteristics of Meteorological and Agricultural Droughts in China: Change Patterns and Causes. *Agriculture*, *13*, 265. 2023 https://doi.org/10.3390/agriculture13020265.

[15] World Meteorological Organization & Global Water Partnership. H*andbook of Drought Indicators and Indices* (M. Svoboda & B. A. Fuchs). 2016. https://library.wmo.int/doc_num.php?explnum_id=3057

INTEGRATED MODELING OF STAGNATING WATER AND URBAN DRAINAGE SYSTEMS

Assistant Prof. Dr. Marcell Knolmar[1]
[1] Budapest University of Technology and Economics, **Hungary**

ABSTRACT

The drainage challenges of a large settlement encompass both urban areas and adjacent agricultural and industrial zones. Surface runoff from increasingly impermeable subcatchments flows into the underground gravitational closed conduits drainage network of the settlement during rapid storm events, a phenomenon effectively modeled using hydrodynamic simulation tools such as SWMM. Meanwhile, excess precipitation water that fails to infiltrate the soil accumulates predominantly on agricultural lands outside the settlement, necessitating drainage through gravitational open channels. Typically, pumping stations are deployed to provide the requisite external energy. Steady flow simulation models like HEC-RAS are applied to accurately simulate water flow in open channels during longer water stagnation periods.

Integrating the drainage systems of urban runoff and stagnant water is essential for capturing dynamic events effectively. This integration involves coupling unsteady models like HEC-RAS with hydrodynamic urban SWMM simulations. The resulting integrated model enables comprehensive simulation of the entire drainage network, facilitating predictions of system capacity during storm events, including periods of water stagnation.

Keywords: HEC-RAS, SWMM, stagnating water, urban drainage, coupling models

INTRODUCTION

Traditionally, urban and land drainage models have been handled separately. Urban runoff, generated by storm events on predominantly impervious surfaces, is typically conveyed in closed conduits. Real storm events entail dynamic loads, with precipitation-generated waves moving through the drainage system over a few hours. This runoff can be effectively simulated and assessed through unsteady analysis. Conversely, stagnant water collected on pervious lands is usually drained in open channels. The flow in these channels is generally steady, with minimal variation over time for extended periods, typically changing on a daily scale.

The application of various specialized models reveals slight variations in flow principles. Attempting to solve the drainage simulation of the entire area using a single model requires compromises. However, integrating specialized models into an integrated simulation system offers an applicable solution for dynamically simulating the entire drainage network.

https://doi.org/10.5593/sgem2024/3.1/s12.16

In the chosen case study area, we aimed to validate the application of the integrated model in simulating the dynamic effects of a storm event.

MATERIALS AND METHODS

Urban runoff simulations often rely on hydrodynamic models, with the EPA Storm Water Management Model (SWMM) being widely acknowledged as a useful tool for simulating the quality of runoff from urban areas [1].

Similarly, tools like HEC-RAS are commonly used for analyzing river and channel flow, assessing flood risks, and conducting flash flood simulations [2] [3]. These tools are also applicable to simulating floods in agricultural areas [4] and irrigation channels [5].

However, while there is some existing research that touches on similar topics, this paper offers a comprehensive analysis of integrated modeling solutions for both urban and rural channels, filling a gap in the current literature.

The drainage area is situated to the north of a major Hungarian city. To the east of the area lies a large river (Tisza) flowing from north to south, serving as the receiving water body. Within the area, there are both natural watercourses and artificial channels designed to collect and convey surface runoff and stagnant water (Fig. 1).

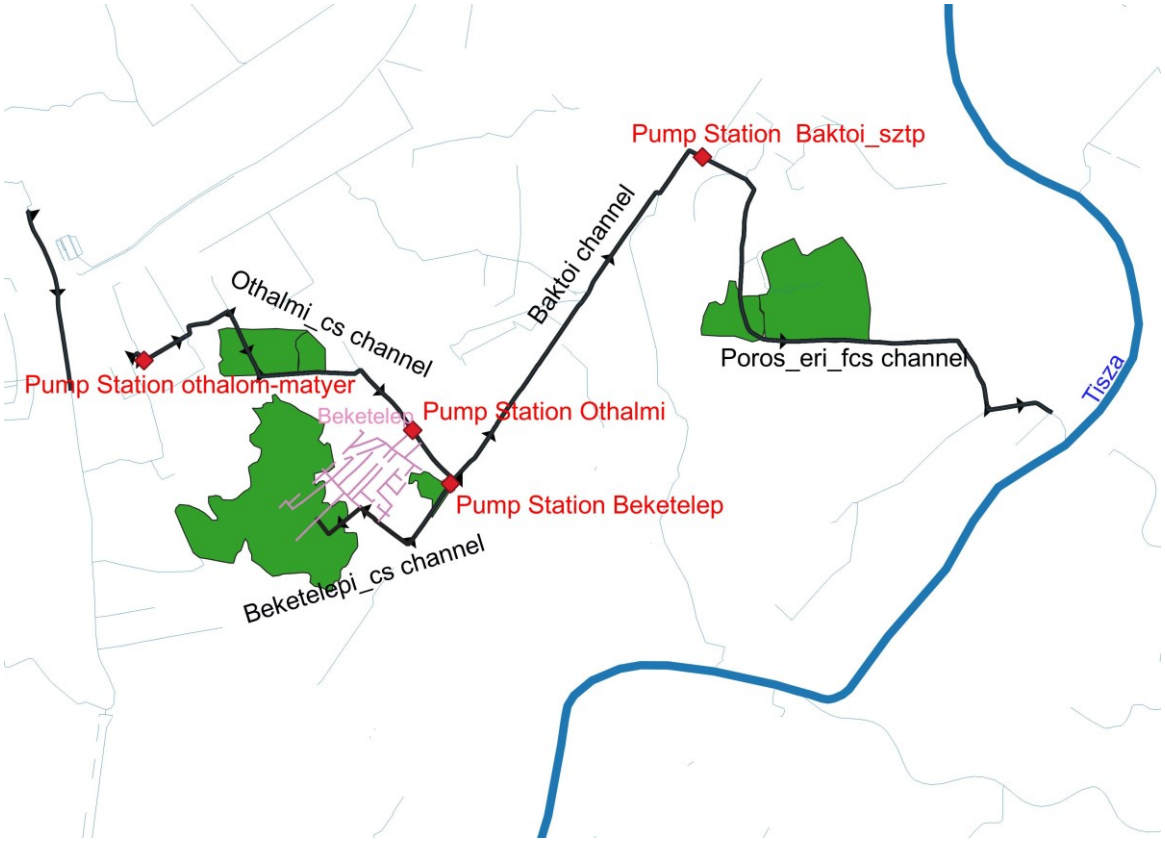


Fig. 1 Drainage area: black-artificial channel, red-pumping station, green-rural catchment, pink-urban drainage system, blue-natural watercourse

In our integrated environment, we have devised a methodology for merging the following one-dimensional models to address this intricate challenge:

HEC-RAS (Hydrologic Engineering Center's River Analysis System) is a widely used hydraulic modeling software developed by the U.S. Army Corps of Engineers [6]. It is designed for analyzing water flow and sediment transport in rivers, channels, and floodplains. HEC-RAS utilizes one-dimensional steady and unsteady flow equations to simulate water surface profiles and flow velocities under various hydraulic conditions. The software allows users to model complex river systems, evaluate flood risk, design bridges and culverts, and assess the impact of hydraulic structures on water flow.

SSA (Storm Sewer Analysis) [7] is a component of the SWMM software package developed by the U.S. Environmental Protection Agency (EPA) [8]. SSA focuses specifically on simulating stormwater drainage systems, including storm sewers, culverts, and other conveyance structures. It employs one-dimensional flow equations to model the movement of stormwater through the drainage network under various rainfall conditions.

Our developments were based on a steady flow HEC-RAS model prepared for the drainage system of a suburban area. The steady flow model was including the present and planned drainage system, the present and planned pump stations and flow control structures, the present loads and loads of the future development areas.

Due to the need to achieve stability in the new integrated model, several adjustments were required, including refining the initial water levels and modifying the calculation time step.

To attain a quasi-permanent state before time-varying precipitation events, we began with the results of a 24-hour run with base loads and also utilized a restart file to provide realistic initial flow conditions. Within 24 hours, the quasi-permanent state was established across the entire system due to the influence of the base loads. In the integrated model, we adopted the base loads of the 4 natural watercourses.

We imposed surface runoff generated from rainfall events onto the quasi-permanent state established by the base loads. In the model, we examined the impact of rainfall loads with a return period of 10 years and a duration of 10 minutes, based on data from the national meteorological station recorded for the last 25 years.

We developed the hydrodynamic model of the drainage system for Beketelep utilizing the SWMM (SSA) software, corresponding to the load generated from the Beketelep urban stormwater drainage system (Fig. 2). The flow curves illustrate the typical outflow pattern from an urban catchment.

The runoff from rainfall occurring in the southern and central parts of Beketelep's urban area is directed towards the Beketelepi channel, while the northern part is connected to the Othalmi channel.

https://doi.org/10.5593/sgem2024/3.1/s12.16

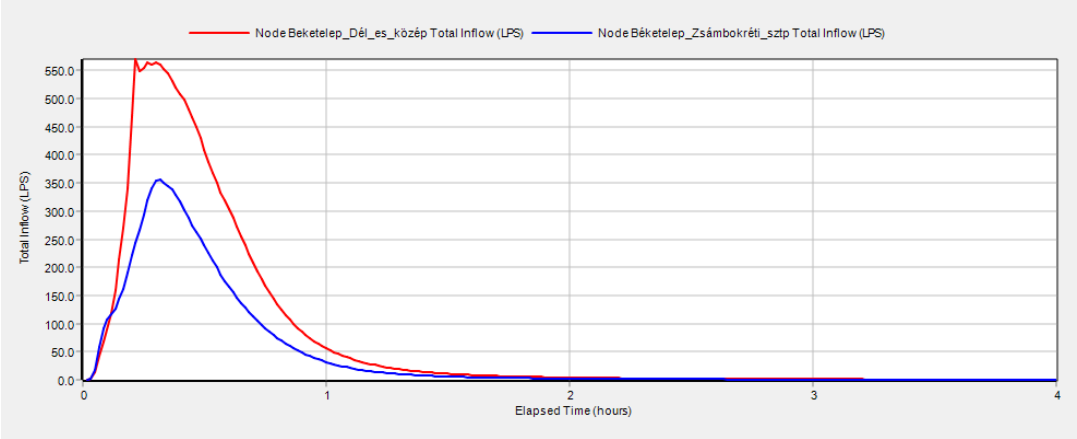


Fig. 2 The flow rates from the Beketelep drainage network: southern and central parts (red line), northern part (blue line).

Surface runoff watersheds could be delineated (Fig. 1) for integration into the canal system, among which at Beketelep includes the runoff from covered areas such as supermarket parking lots.

The flow rates from the rural rainwater catchments were calculated using SWMM (SSA) simulation.

In development areas and where rainwater is otherwise pumped, we specified a constant load lasting for several hours.

The total volume of water from Beketelep and another smaller urban catchment was calculated using the SWMM (SSA) model, while the loads from development areas were specified based on the "Steady" model.

RESULTS

The simulation begins at 24:00 with the onset of rainfall at all watershed points in the drainage network. From the specified 13 loading points, runoff generates flood waves. Fig. 3 - Fig. 5 depict longitudinal sections of the channels. Along with the channel bottom elevations (Ground), characteristic water levels are also illustrated at the left bank (LOB) and right bank (ROB). The bottom line represents the "established" initial water level (WS 01JAN2018 0000), the middle line indicates the formation of flood waves (WS 02JAN2018 0015 and WS 02JAN2018 0050), and the top line represents the envelope of maximum water levels (WS MAX WS).

Fig. 3 shows the generation of peak flow resulting from the dynamic precipitation loads in the Othalmi channel. However the banks of the channel is safely high enough.

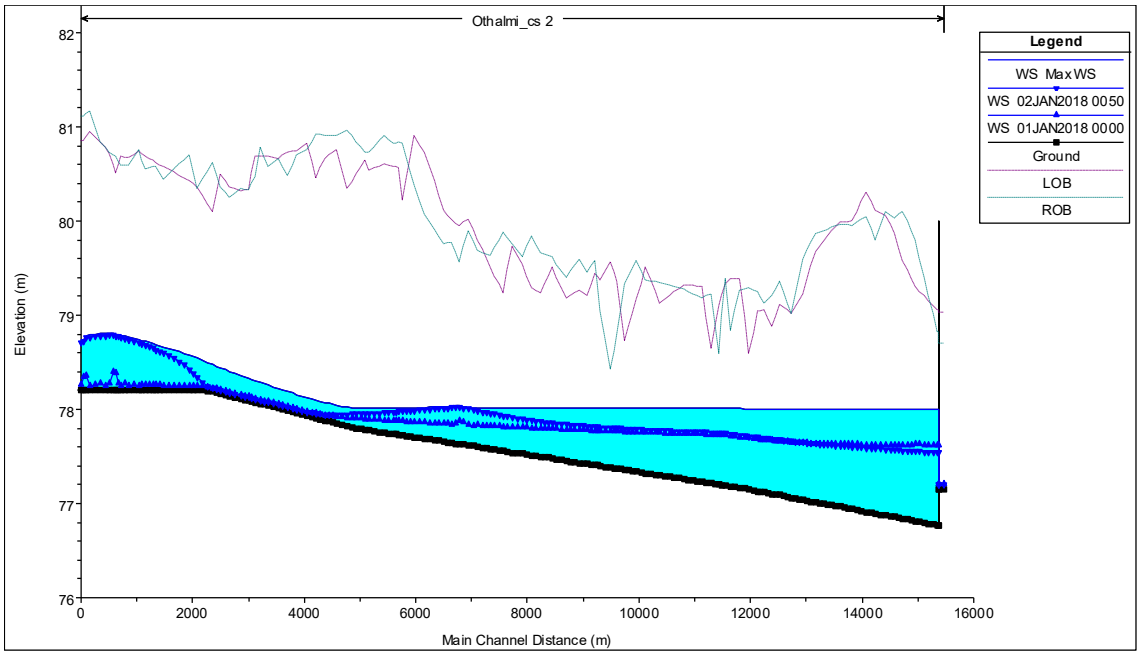


Fig. 3 Initial water levels, onset of flood waves, and maximum water levels on the upper section (above the pumping station) of the Öthalmi channel

In the Beketelepi channel (Fig. 4), steady flow conditions are controlled. However, the flood wave originating from the urban outlets exceeds the height of the levees. The computational algorithm of HEC-RAS employs a vertical "wall" if one end of the cross-section is lower than the computed water level, preventing overflow. Realistic adjustments to the cross-sectional surface only resulted in minor changes compared to the automatic corrections by HEC-RAS.

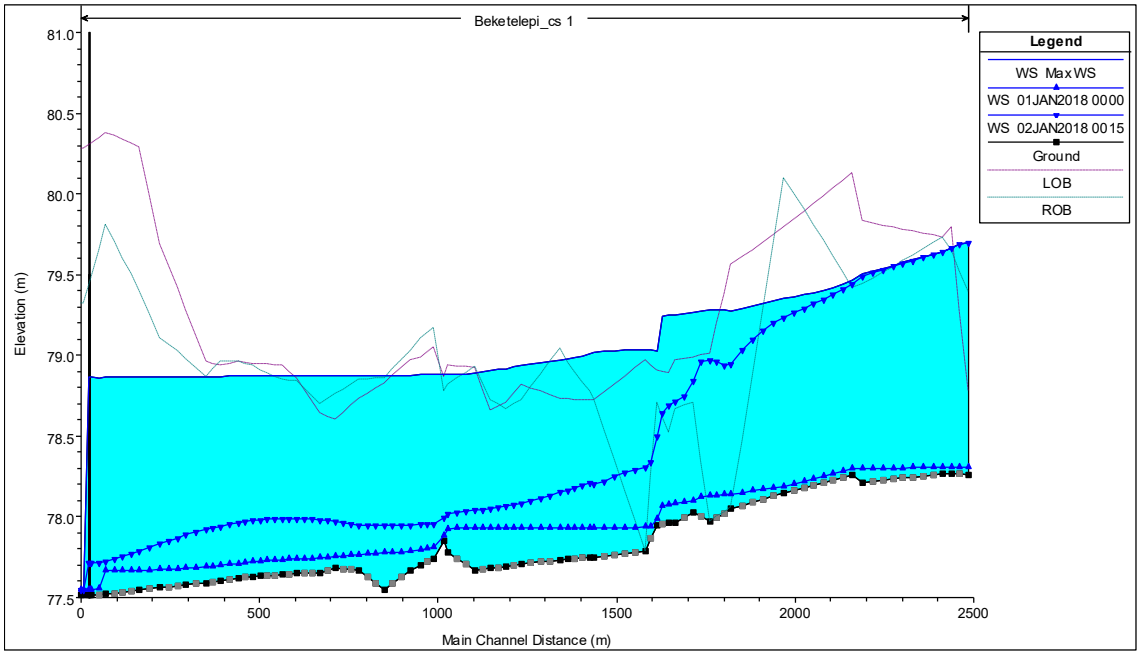


Fig. 4 Initial water levels, onset of flood waves, and maximum water levels on the upper section (above the pumping station) of the Beketelepi channel

https://doi.org/10.5593/sgem2024/3.1/s12.16

In the lowest sections of the drainage system, the flood wave flattens out, and the water levels remain within the acceptable range (Fig. 5).

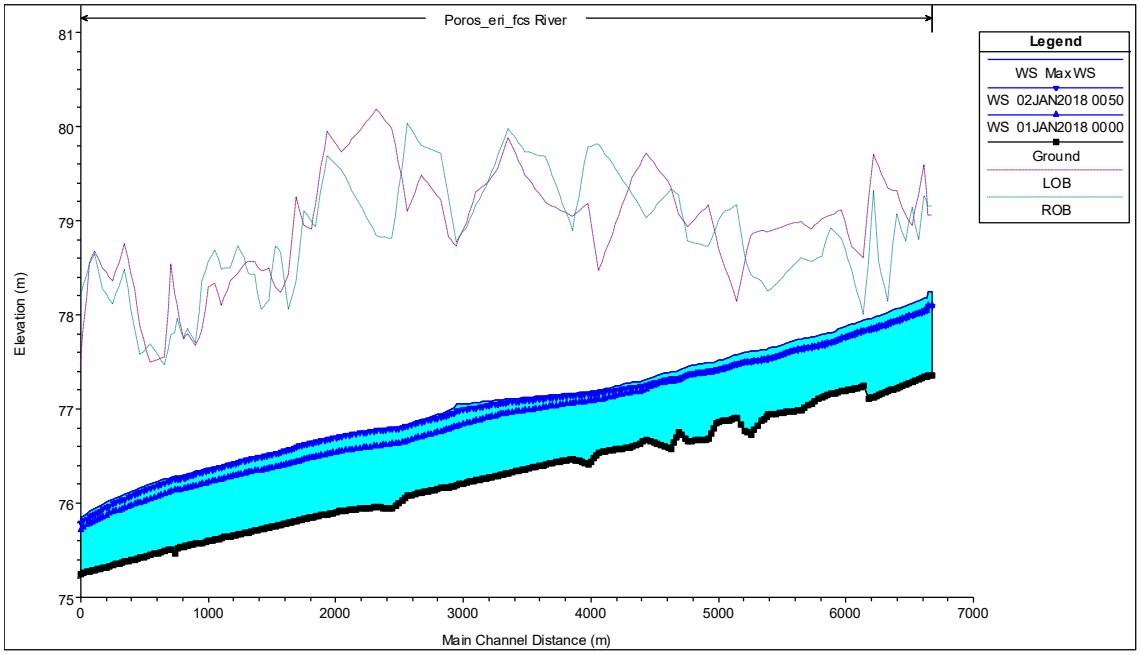


Fig. 5 Initial water levels, onset of flood waves, and maximum water levels on the Poros_eri channel.

The othalom-matyer pumping station does not start operating at such water levels. The other three pumping stations operate continuously based on the specified Q-H curves (Fig. 6, Fig. 7, Fig. 8).

The wave reaching the pumping stations after normal operation hours (beyond 24:00) is exerting additional load, causing the pumps to operate at higher capacities. While two of the pumping stations (Fig. 6 and Fig. 8) are handling this situation effectively, the Beketelep pumping station (Fig, 7) is operating at its maximum capacity.

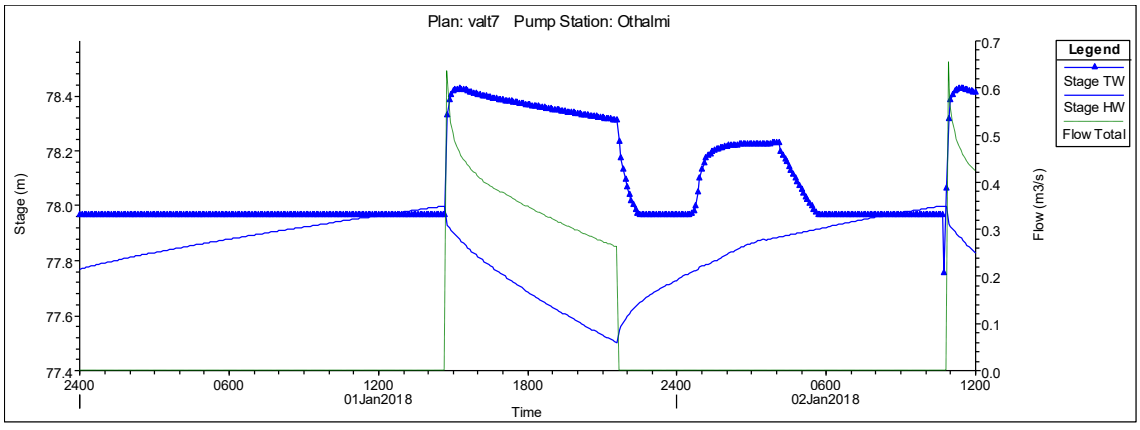


Fig. 6 Flood stage (Stage HW), upstream stage (Stage TW), and total flow (Flow Total) at the Othalmi pumping station.

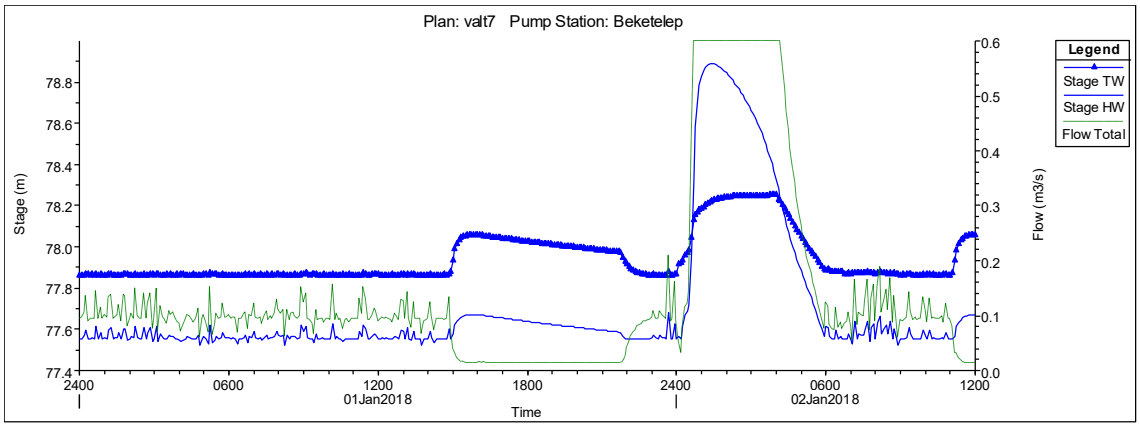


Fig. 7 Flood stage (Stage HW), upstream stage (Stage TW), and total flow (Flow Total) at the Beketelep pumping station.

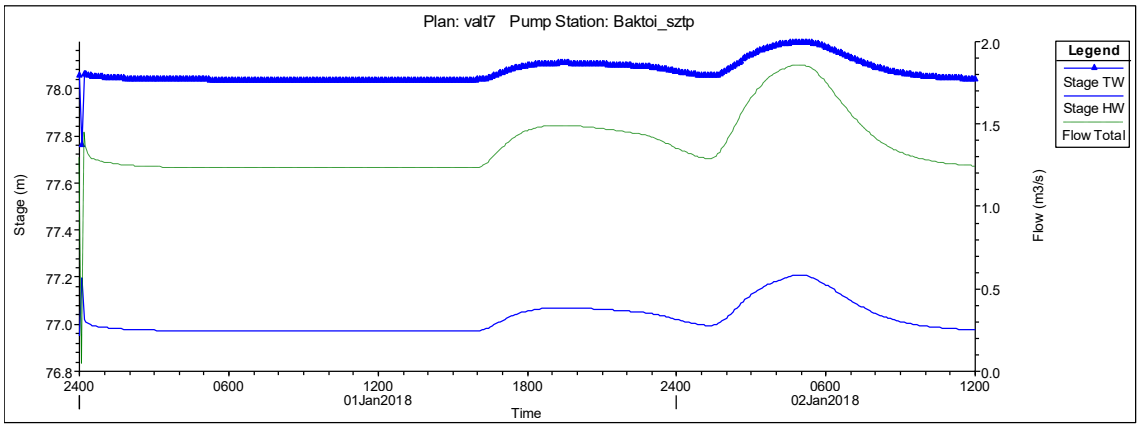


Fig. 8 Flood stage (Stage HW), upstream stage (Stage TW), and total flow (Flow Total) at the Baktoi pumping station.

DISCUSSION

As expected, the variability of precipitation over time leads to notably distinct flow patterns within drainage channels compared to constant loads, as evidenced by the steady flow model. It was anticipated that sections of channels receiving runoff from urban areas would encounter capacity issues. This is not only due to the additional volume stemming from these catchments but also because their temporal runoff, influenced by a high ratio of impervious surfaces, imposes peak loads on the receiving channels.

Our computation of rainfall runoff utilized the most precise and detailed theoretical models available, implemented through advanced software tools. The application of dynamic computation is also expected to yield different results compared to steady calculations.

CONCLUSION

Based on the executed dynamic simulations the majority of the examined stormwater channels, including Othalmi, Baktoi, and Poroseri, along with the planned pumping stations, exhibit sufficient capacity to accommodate rainfall runoff. The integrated

https://doi.org/10.5593/sgem2024/3.1/s12.16

drainage system could effectively manage even the peak waves generated by the specified dynamic loads in the unsteady model.

However, concerns arise regarding the capacity of the Beketelepi channel, which is expected to be insufficient to handle the drainage from Beketelep and additional urban rainfall. One potential investment could involve increasing the height of levees along critical sections of the channel. Another option would be to install pumps with a higher maximum flow rate at the Beketelep pumping station.

The accuracy of our calculations is influenced by the delineation and parameterization of watersheds, based on the most comprehensive datasets accessible. It's worth noting that the boundaries and characteristics of surface runoff watersheds evolve over time, allowing for model refinement to accurately reflect these changes.

The developed integrated model has the capability to manage the dynamic impacts of a storm event on both urban and rural areas. The unsteady model can effectively simulate the open channel flows and the operation of pumping stations.

ACKNOWLEDGEMENTS

The research presented in this article was carried out with the support of the RRF-2.3.1-21-2022-00008 project, by the National Research, Development and Innovation Office.

REFERENCES

[1] Marko I., Wittmanova R., Skultetyova I., Sutus M., Simulation of urban surface runoff using SWMM model, International Multidisciplinary Scientific GeoConference SGEM, Bulgaria, vol. 20/issue 1.3, 2023.

[2] Stoyanova V., Flood hazard mapping to protect important habitats, International Multidisciplinary Scientific GeoConference SGEM, Bulgaria, vol. 23/issue 3.2, 2023.

[3] Uhrova M., Krecek J., Pazourkova E., Vrtiska J., Dendrogeomorphic analysis of flash floods in a small forest catchment, International Multidisciplinary Scientific GeoConference SGEM, Bulgaria, vol. 23/issue 3.2, 2023.

[4] Banescu A., Georgescu L. P., Iticescu C., Rusu E, Analysis of the flood risk agriculturals enclosures from the Danube delta using 2D modeling, Case study Pardina enclosure, International Multidisciplinary Scientific GeoConference SGEM, Bulgaria, vol. 19/issue 3.1, 2019.

[5] Kurniawan B., Sasmita F. S., Alviana S., Application of Hec-Ras Technology to irrigation and water building in agricultural businesses, INCITEST IOP Conf. Series: Materials Science and Engineering, Indonesia, vol. 879, 2020.

[6] HEC-RAS River Analysis System Hydraulic Reference Manual, US Army Corps of Engineers, Hydrologic Engenering Center, Version 5.0.7, United States, 2019.

[7] Storm and Sanitary Analysis (SSA), User’s Guide, Autodesk, United States, 2019.

[8] Rossman L.A., Storm Water Management Model, User’s Manual, Version 5.0, U.S. Environmental Protection Agency, United States, 2010.

INTEGRATION OF EROSION CONTROL MEASURES AND TECHNICAL MEASURES TO PROVIDE EFFECTIVE FLOOD RISK REDUCTION FOR SMALL WATERSHEDS

Ing. Stanislav Paseka, Ph.D.[1]

[1] Brno University of Technology, Faculty of Civil Engineering, Institute of Landscape Water Management, **Czech Republic**

ABSTRACT

The article examines the effectiveness of measures to reduce flood risk in small watersheds in the Czech Republic. Currently, there is a search for integrated approaches that combine cost-effective erosion control measures (ECMs), in the form of organizational and agrotechnical changes, with more expensive technical measures (TMs) in the form of infiltration trenches and dry reservoirs. To achieve this goal, the critical drainage profile of a small village in the Olomouc region, at the interface between rural and urban areas, was studied.

The study utilized a combination of ECMs and TMs to reduce the flood risk. The results were evaluated using the DesQ-MaxQ hydrological model and the TRANSFORM_WAVE simulation model. The synergistic integration of inexpensive ECMs with more expensive TMs led to significant reductions in peak flows, confirming their key role in enhancing flood resilience. The study showed that the standalone use of a single type of measure may not be sufficient for provide flood protection.

The findings underscore the need for a comprehensive approach to address flood risk in various geographic and environmental conditions. In the future, it will be essential to consider the unique challenges and characteristics of individual locations and tailor strategies to each of their specific needs. It is also important to carefully consider the cost of TMs compared to cheaper ECMs. Such an approach can contribute to the development of sustainable and effective measures for flood protection.

Keywords: erosion control measures, technical measures, hydrological modelling, flood transformation, curve number

INTRODUCTION

Floods are natural disasters triggered by an accumulation of water that is greater than the normal capacity of the area. Flash floods, arising from intense, short-term rainfall, typically impact a limited area, the surplus precipitation that the ground is unable to absorb leads to runoff.

When the runoff volume exceeds the capacity of the existing infrastructure, such as culverts, bridges, or other critical structures, water overflows and causes flooding.

Flash floods pose a direct threat to residents' lives, particularly those who reside near or below critical infrastructure. Additionally, floods cause substantial financial loss, this includes damage to the affected individuals and the expense incurred by authorities for the restoration of flood-affected areas.

https://doi.org/10.5593/sgem2024/3.1/s12.17

In many studies, climate change, as well as human activity, has been found to contribute to changes in runoff. Specifically, in [1,2,3] it was found, by using Curve Number (CN) methods, that changes in land use, such as the conversion of agricultural land to impervious surfaces or urbanization, can increase runoff depth. However, through the conversion of agricultural land or impervious surfaces to grass or forest, projects that involve the restoration of vegetation, can reduce runoff depths.

Surface runoff on a watershed is calculated using the CN runoff method to calculate peak flows. The model provides results which are relatively easily attainable which provide an estimate of direct runoff caused by intense rainfall on areas smaller than 10 km^2. The model was developed in 1954 by the United States Department of Agriculture (USDA) and Soil Conservation Services (SCS). Thanks to its straightforward nature and comprehensive documentation, this technique is commonly used across the globe, adopted by countless engineers and practitioners across various hydrological projects. Its widespread acceptance can be attributed to it being both simple and effective, supported by readily available and well-documented environmental data. Moreover, it effectively addresses the various factors that influence the generation of runoff, consolidating them into a single parameter, CN [4].

The main intent of the paper is to propose and assess the effectiveness of two approaches to reduce flood risk: lower cost erosion control measures (ECMs) and more expensive technical measures (TMs). The evaluation of the impact of each measure on flooding is considered when applied to the critical drainage profile of the municipality of Hlinsko in the Olomouc Region, Czech Republic.

MATERIALS AND METHODS

- ***Curve number (CN)***

The CN method is widely used in hydrologic design and environmental impact analysis to generate the direct runoff from intense flash rainfall. The core of the method is a simple hyperbolic equation (1) [6]

$$Q = \frac{(P - I_a)^2}{(P - I_a + S)}; P \geq I_a \quad (1)$$

in which Q is the direct runoff depth, P is the rainfall depth, S is a storage index extracted from the land conditions, and Ia is the initial abstraction, or the rainfall prior to the onset of direct runoff.

When all the above are expressed in millimetres, then the curve number, CN, is a transformation of S via equation 2:

$$CN = 25{,}4\frac{1000}{25{,}4 + S} \quad (2)$$

An important simplification of this method is an assumption for the initial abstraction, Ia = 0,2S (the storage coefficient). Using this in place of Ia in equation 1 leads to the simplified and widely used form shown in equation 3.

$$Q = \frac{(P - 0.2\,S)^2}{(P + 0.8\,S)};\ P \geq 0.2\,S \tag{3}$$

CN also serves as an indicator of the likelihood of the type of runoff. The higher the value of CN, the more likely it is to be surface runoff. CN values are determined by the soil hydrological characteristics, degree of vegetation cover, extent of impermeable surfaces, interception capabilities, and surface retention capacity. The volume of direct runoff is estimated based on the assumption that the ratio of runoff volume to total volume of rainfall is equal to the ratio of retained water volume during runoff to the maximum possible retention. Runoff begins after the initial loss, which includes any reduction caused by interception capacities, infiltration, and surface retention. This initial loss has been set to 20% of the maximum retention.

The hydrological model DesQ–MaxQ was used. This model is designed to determine the design characteristics of flood waves in ungauged profiles, for small watersheds triggered by heavy rainfall and to calculate the influence on maximum flows and flood volumes of changes in the watershed characteristics based on changes in CN [5].

- ***Dry reservoir simulation model***

The TRANSFORM_WAVE simulation model was created by the author to modify flood discharges - for dry reservoir designs. For the first time, the model was applied to the optimization of a resilient design for a multi-purpose reservoir under the uncertain conditions of climate change [7]. Within the model, flood discharge transformation occurs through mathematical adjustments derived from the original Klemeš graphical method [8]. This method, rooted in the first-order differential equation for reservoirs, illustrates the correlation between the water inflow and outflow from the reservoir over time and the volume of water in the reservoir.

The primary inputs required for the Klemeš method include the flood hydrograph, parameters related to the bottom of the reservoir and the emergency spillway, and the curve that represents flooded volumes to allow the construction of the transformation curve. This transformation curve describes the cumulative outflow from the reservoir in relation to its capacity. It defines the potential outflow of the reservoir and is dependent on its volume. To ascertain this curve, the capacities of the bottom outlets (O_B) and the emergency spillway (Q_{ES}) are determined through the use of the respective equations (4) and (5) [9].

$$O_B = \mu\,S\,\sqrt{2\,g\,h_w} \tag{3}$$

$$Q_{ES} = m\,b\,\sqrt{2\,g}\,h_{es}^{3/2} \tag{4}$$

where μ is the outflow coefficient (-), S is the outlet area (bottom outlets) (m^2), g is acceleration due to gravity ($m\ s^{-2}$), h_w is the height of the water above the bottom outlets (m), m is the overflow coefficient (-), b is the width of the emergency spillway (m) and h_{es} is the height of water above the spillway (m).

Additionally, use of the Klemeš method is crucial for the determination of the reduction angle α, which reflects the relationship between flow magnitude, time, and the area enclosed by the inflow and outflow. This graph is constructed step by step over different

https://doi.org/10.5593/sgem2024/3.1/s12.17

time intervals, utilizing the transformation curve and α, firstly during the rise in water level and then the fall due to flood water discharge. A more detailed description is given in article [10].

CASE STUDY

The critical drainage profile near the village of Hlinsko (Olomouc Region) in the Czech Republic was selected for the study and is shown in Figure 1. The contributing area covers 0,495 km^2, with a stream length of 1,23 km. The average elevation is 328,6 meters above sea level, with an average slope of 8,73%. Sixty-eight percent of the contributing area is used as arable land, while the remainder is predominantly forested. The runoff from the contributing area is directed into a drainage ditch, which then transitions into a pipeline. The pipeline continues through gardens adjacent to residential homes and discharges beneath the local road into the river that flows through the town. The pipeline, at the transition from the rural to urban area, has a diameter of DN600 and an approximate slope of 8%, with a capacity of approximately 2,1 m^3s^{-1}, which is significantly inadequate (a lack of capacity).

Within this specific critical drainage profile, sections within the watershed were identified along with proposed technical measures as part of a bachelor's thesis [11]. Additionally, erosion control measures were proposed through changes in crop rotation to mitigate flow and damage over the given profile.

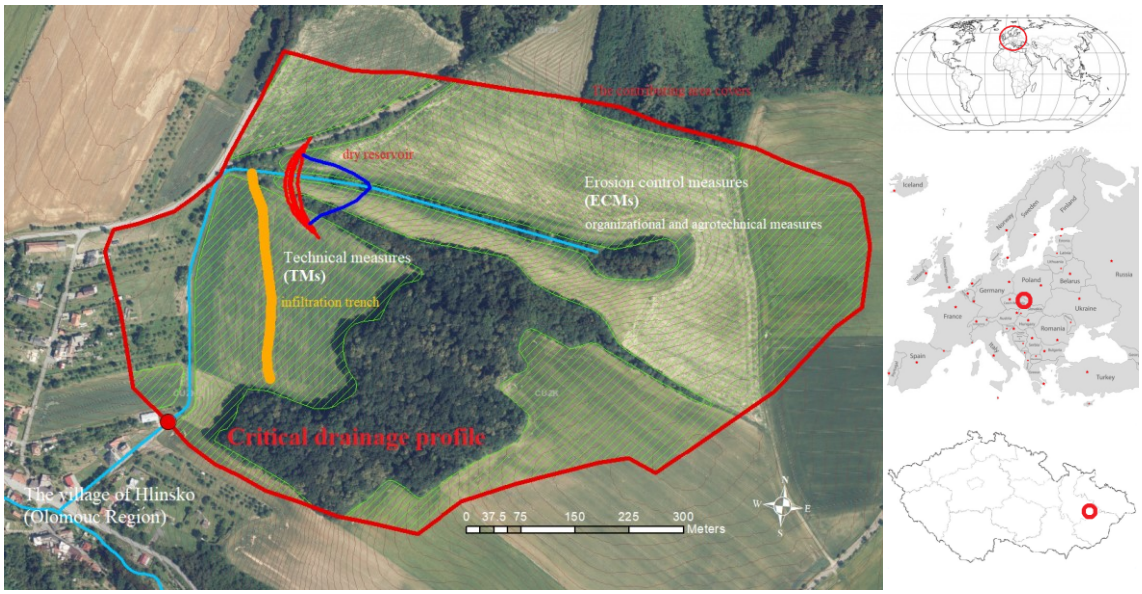


Fig. 1 Critical drainage profile.

DESIGNS, CALCULATIONS AND RESULTS

The CN of the current arrangement was calculated, along with peak flows and volumes, for hundred–year (Q_{100}) and fifty-year floods (Q_{50}). The total design rainfall was determined using the maximum rainfall intensities over a 24–hour period with the assumed frequency of occurrence as recorded at the nearest gauge station. The CN value is approximately 84,9. The peak flows for Q_{100} are 5,18 m^3s^{-1} with a flood volume (V_{100}) of 14.100 m^3, and for Q_{50}, the flow is 3,99 m^3s^{-1} with a volume (V_{50}) of 12.300 m^3.

These results demonstrate that the existing culvert is significantly undersized, thus control measures are required in the upstream watershed. In this case, enlarging the culvert is not feasible as it traverses privately owned gardens and is relatively long. Therefore, two alternatives were proposed within the watershed. The first alternative involves less costly ECMs and the second includes more expensive TMs.

1) The ECMs were implemented in the arable land of the watershed. Specifically, organizational and agrotechnical measures were developed, including the identification of an exclusion area where erosion-prone crops would not be grown and areas of permanent grassland. These practices were discussed with a local farmer, whose specialization in cattle breeding facilitated the expansion of grassland areas without significant cost and immediate implementation was practically feasible. Following this measure, not only was the water erosion in the watershed reduced to an acceptable level, but there was also a decrease in the average CN value to 79,35, resulting in a reduction in the Q_{100} peak flow to 3,32 m^3s^{-1} and the Q_{50} peak flow to 2,55 m^3s^{-1}. However, it was evident that these measures were insufficient considering the maximum capacity of the culvert.
2) Infiltration trench and a dry reservoir were proposed as TMs. The infiltration trench with a zero longitudinal slope was designed for a hundred-year event. The volume of the trench corresponds to the runoff volume for the design rainfall from the adjacent watershed area. The infiltration trench was designed according to recommended technical parameters based on the digital terrain model. Therefore, there is a high probability that it will be implemented. In addition, a grassland strip, 10 meters wide, was proposed above the trench.

   The dry reservoir was designed for a suitable location according to the digital terrain model and the valley profile. The complete design of a homogeneous dam and structures was carried out according to the relevant standards [12,13] to produce a real transformation of the flood wave. The downstream outlet structure (restriction) was carefully adjusted to allow safe drainage (discharge from the reservoir into the critical drainage profile), and the safety features were designed for a hundred-year event, consistent with the approach used for the infiltration trench. The hundred-year event volume was determined in a similar way to that used for the infiltration trench.

   The resultant flood transformation from the proposed reservoir, for the Q_{100} and Q_{50} events are shown in Figure 2. From the course of the transformed flood, it is evident that the dry reservoir alone is adequate for a fifty-year event (the safe discharge level was not exceeded = there was no overflow of the safety spillway crest).

https://doi.org/10.5593/sgem2024/3.1/s12.17

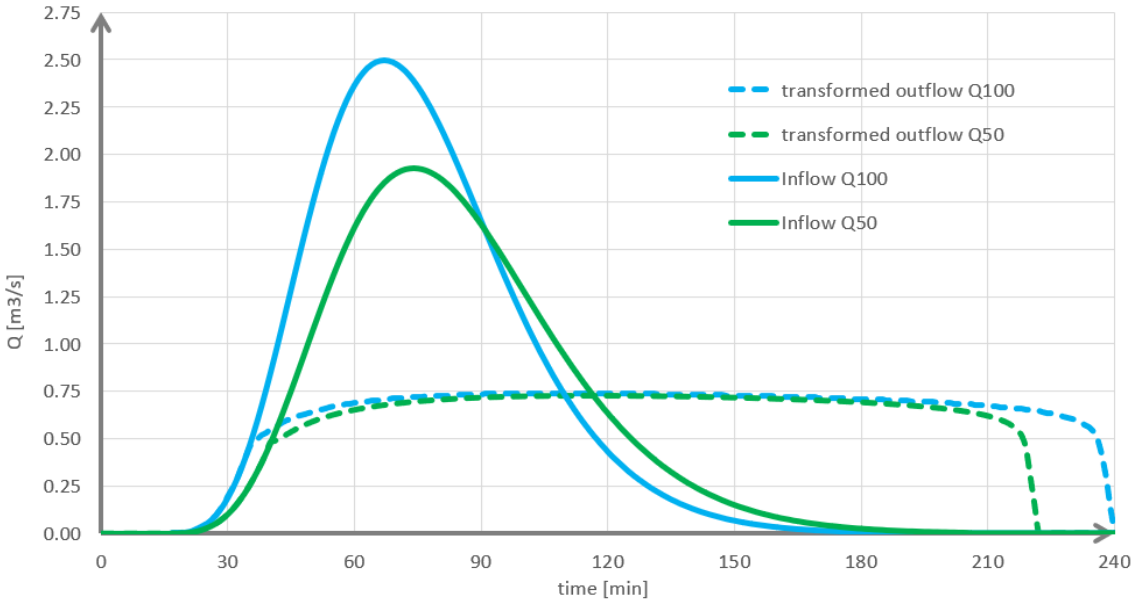


Fig. 2 Transformation of the Q_{100} (blue) and Q_{50} (green) flood waves with the dry reservoir design.

The two TMs combined resulted in a reduction of the Q_{100} peak flow to 2,30 m^3s^{-1} and the Q_{50} peak flow to 1,91 m^3s^{-1}. These measures provided an adequate reduction in flow through the culvert for the fifty-year event but were still insufficient for a hundred-year event. Therefore, Variant 3 was also considered as a combination of both alternatives.

3) The combined effect of the ECMs and TMs resulted in a reduction in the Q_{100} peak flow to 1,87 m^3s^{-1} and the Q_{50} peak flow to 1,69 m^3s^{-1}. This combination of measures was sufficient to reduce the maximum flow rate below the maximum capacity of the culvert for both the hundred-year and fifty-year events.

SUMMARY OF THE RESULTS AND DISCUSSION

To mitigate both the flood and erosion risks, two approaches were proposed: lower cost ECMs and more expensive TMs. The ECMs were applied to arable land and included organizational and agrotechnical measures, which led to a significant reduction in erosion and flow rates. The TMs included infiltration trench and a dry reservoir, which together resulted in a reduction in peak flow. The specific decreases in peak flows are shown in Table 1.

Tab. 1 Reductions (acute state) in the Q_{100} and Q_{50} peak flows [m^3/s] after the proposed measures for all combination (variant 3)

[m^3/s]	acute state	1) ECMs	2) TMs	3) ECMs + TMs
Q100	5,18	3,32	2,30	1,87
Q50	3,99	2,55	1,91	1,69

From Table 1, it is evident that neither of the measures alone, ECMs or TMs, met the requirements for a hundred-year event in the critical drainage profile, and the more expensive TMs were only able to mitigate the impact of a fifty-year event. The

combination of the ECMs and TMs achieved the best results, producing a sufficient reduction in the peak flow from hundred-year and fifty-year events. This combination of measures should significantly reduce the risk of flooding and protect residents and property in the affected area. However, this combination is also the most expensive solution, both in terms of the acquisition costs for the technical measures, which could run to millions of euros, and in terms of compliance with the proposed organizational and agrotechnical measures on the agricultural land.

For the variant 3 that combines both the ECMs and TMs the water inflows into the critical drainage profile during Q_{100} and Q_{50} events are shown in Figure 3. There is a significant reduction in the original inflow from 5,18 m^3s^{-1} (Q_{100}) and 3,99 m^3s^{-1} (Q_{50}).

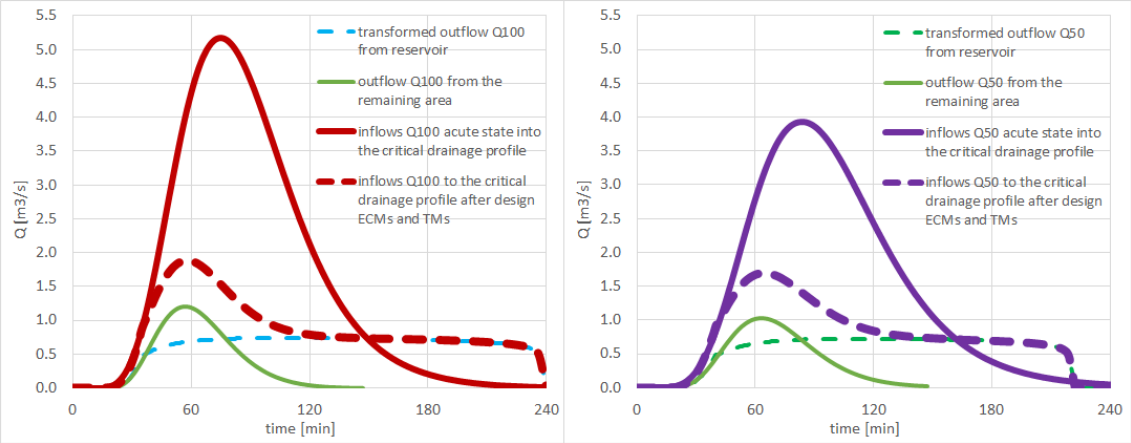


Fig. 3 Water inflows into the critical drainage profile during Q_{100} (left) and Q_{50} (right) events after the implementation of the ECMs and TMs.

CONCLUSION

The study unequivocally demonstrates that a synergistic integration of cost-effective erosion control measures (ECMs) in the form of organizational and agrotechnical measures with sophisticated technical measures (TMs) produces the most efficacious strategy in the mitigation of flood risk. These combined measures yield a reduction in peak flow, underscoring their pivotal role in bolstering flood resilience. It is foreseeable that future attempts to manage floods within small watersheds within the Czech Republic will necessitate a context-specific blend of strategies, as each scenario presents its unique challenges and considerations. The findings underscore the inadequacy of the reliance on a singular approach, emphasizing the imperative for a holistic exploration and experimentation to devise robust, sustainable solutions tailored to diverse geographic and environmental contexts.

Land use planning and land management play a crucial role in reducing flood risk. Changes in agricultural practices and landscape modification can significantly influence flood risk in any region.

Importantly, when flood protection measures are evaluated, it is crucial that both the financial implications of implementation and the intrinsic value of the protected area be considered. While high-cost technical interventions may prove to be effective, a very careful evaluation is needed to compare their exorbitant costs to lower cost erosion control measures.

https://doi.org/10.5593/sgem2024/3.1/s12.17

ACKNOWLEDGEMENTS

This paper was funded by "Innovative measurement and modelling in water management for the sustainability of water resources", research project number FAST-S-24-8540.

REFERENCES

[1] Li, Y.; Liu, C.; Zhang, D.; Liang, K.; Li, X.; Dong, G. Reduced Runoff due to Anthropogenic Intervention in the Loess Plateau, China. Water 2016, 8, 458

[2] Zhang, Y.; Xia, J.; Yu, J.; Randall, M.; Zhang, Y.; Zhao, T.; Pan, X.; Zhai, X.; Shao, Q. Simulation and Assessment of Urbanization Impacts on Runoff Metrics: Insights from Landuse Changes. J. Hydrol. 2018, 560, 247–258

[3] Li, C.; Liu, M.; Hu, Y.; Shi, T.; Qu, X.; Walter, M.T. Effects of Urbanization on Direct Runoff Characteristics in Urban Functional Zones. Sci. Total Environ. 2018, 643, 301–311

[4] Ponce, V.M.; Hawkins, R.H. Runoff Curve Number: Has It Reached Maturity? J. Hydrol. Eng. 1996, 1, 11–19

[5] Software DesQ – MaxQ. Calculation of maximum flows in small watersheds, on-line: www.desq-maxq.cz

[6] Hawkins, R.H.; Khojeini, A.V. Initial Abstraction and Loss in the Curve Number Method. Hydrology and Water Resources in Arizona and the Southwest 2000, 30, 29–35

[7] Paseka, S., Kapelan, Z., Marton, D. Multi-Objective Optimization of Resilient Design of the Multipurpose Reservoir in Conditions of Uncertain Climate Change. Water 2018, 10, 1110

[8] Klemeš, V. A simplified solution of the flood-routing problem. Vodohospod. Časopis 1960, 8, 317–326

[9] Jandora, J., Šulc, J. Hydraulics (MODUL 01); Education Tutorial, Faculty of Civil Engineering, Brno University of Technology: Brno, Czech Republic, 2006

[10] Paseka, S., Marton, D. The Impact of the Uncertain Input Data of Multi-Purpose Reservoir Volumes under Hydrological Extremes. Water 2021, 13, 1389

[11] Špaček, S. Study of landscape measures in the Hlinsko near Přerov cadastral area. Brno, 2022. Bachelor thesis. Brno University of Technology, Faculty of Civil Engineering, Institute of Landscape Water Management

[12] Standard: ČSN 75 2410 Malé vodní nádrže, 2011

[13] Standard: TNV 75 2415 Suché nádrže, 2013

MODELLING OF HYDROMORPHOLOGICAL CHANGES DUE TO THE EFFECT OF FISHING PORT "KARANTINATA"

Petya Eftimova[1]
Assoc. Prof. Dr. Nikolay Valchev[1]
Dr. Bogdan Prodanov[1]
Dr. Nataliya Andreeva[1]
Todor Lambev[1]
Prof. Dr. Lyubomir Dimitrov[1]
[1]Institute of Oceanology – Bulgarian Academy of Sciences, Varna, **Bulgaria**

ABSTRACT

Presence of coastal structures usually causes significant impacts to adjacent shores, especially when they are composed of sand. Many times, these impacts are associated with inappropriate design due to inadequate consideration of hydromorphological processes and system interactions. As a result, excessive erosion and/or deposition of sediment is observed, which implies costly, and in some cases, continuous maintenance. The study presents an assessment and gives explanation of significant changes in the morphology of Asparuhovo Beach (Varna Bay, Bulgarian Black Sea coast) occurred immediately after the construction of the fishing port "Karantinata". In only two-year period, the beach adjacent to the facility increased several times in width, significant amount of sediments accumulated on the submerged slope in front of the port entrance, silting it up to such an extent that only the smallest vessels can access the port. The study elucidates the pattern of hydrodynamic and morphodynamic regime in the area influenced by the port, allowing the prediction of future changes in the hydromorphology of Asparuhovo Beach.

Keywords: coastal system, beach evolution, coastal (processes) modelling, port siltation

INTRODUCTION

Coastal regions have important social and economic relevance and are vulnerable to anthropogenic impacts. Port and marina development are among the main economic activities [1] and generally require the design of coastal structures such as breakwaters, jetties, seawalls and bulkheads. While these interventions should ensure that the adjacent areas are not affected, some of them frequently have adverse effects [2] by changing the local flow and wave conditions and alteration of the sediment transport [3]. The increasing levels of anthropogenic pressure on the dynamics of coastal systems are of great importance for coastal sciences and highlight the requirement for sustainable coastal management. Hence, the most important point is to consider the broad environmental impacts associated with interventions on coastline and morpho-sedimentary processes [4].

In this context, the study presents an assessment of impacts on hydromorphological regime associated with fishing port development. It explains the reason for the rapid morphological changes in the area influenced by fishing port "Karantinata", which is

associated with the modification of hydrodynamic and sedimentation regime. The assessment was performed by means of hydrodynamic and morphodynamic modelling, and geospatial morphological analysis based on satellite images, past and present field observations describing the settings before and after the port construction.

MATERIALS AND METHODS

Study area

The study area spans over the southernmost part of the Varna Bay where Asparuhovo Beach and recently constructed fishing port "Karantinata" are located. This coastal sector is approximately 1300 m long, stretching from I-shaped groin at the navigational channel to the fishing port (**Error! Reference source not found.**). The area is characterized by a beach-dune system bordered by the port quay wall. The beach consists of course- to medium-grained sand (0.19 mm ≤ D50 ≤ 0.61 mm), transitioning to fine sand (0.138 mm ≤ D_{50} ≤ 0.21 mm) at backshore **Error! Reference source not found.**.

In the southernmost part of the Varna Bay underwater coastal slope, the geomorphological conditions are characterized by a gently sloping accumulative slope extending to a depth of 11 m and a distance of 1 300 m from the shoreline. From the morphological point of view, the seabed of Varna Bay can be divided into four relatively independent subzones. *Active Subzone*: Located at depths from 0 to 5–6 m, this subzone is subjected to significant wave action and is characterized by various morphological forms such as abrasion-structural terraces and rocky outcrops. *Steady Subzone*: Spanning depths from 6 to 12–15 m, this subzone is characterized by milder slopes and accumulative forms covered with medium-grained sands and shells. *Non-active Subzone*: Represented by a gently sloping accumulative platform with clayey and sandy deposits, this subzone extends between depths of 12 and 18 meters. *Anthropogenic Subzone*: This subzone includes artificial structures such as navigational canals, ports and shore protection structures **Error! Reference source not found.**.



Figure 1. Location of the study site: satellite image of Asparuhovo Beach and fishing port “Karantinata”

Geospatial analysis

To monitor coastal zone processes over the years, periodic remote sensing and field surveys were conducted, including multi-beam and single-beam bathymetry, photogrammetric surveys using unmanned aerial systems, and geodetic GNSS-RTK measurements for high-accuracy control points and validation. Single and multi-beam bathymetric surveys were conducted at various intervals during 2013–2022. The objective was to monitor changes in the topographic characteristics of the seabed and underwater landforms. The generated bathymetric models have varying resolutions, ranging from 0.5 m to 5 m (Fig. 2). The accuracy of Digital Surface Models (DSM) and Orthophotomaps (OM) is a primary goal in the proposed methodology, necessitating the use of reference and control geodetic points. Control measurements were conducted using the HiTarget V90Plus RTK GPS receiver, which provided high coordinate accuracy through a certified RTK network in Bulgaria. The achieved horizontal accuracy is 2 cm and the height accuracy – 3 cm, thus ensuring high spatial reliability of the surveys.

Important digital products for subsequent interpretative analysis of the geomorphological spatial pattern includes digital surface model of 6 cm/pixel resolution and orthophotomosaic of 3 cm/pixel resolution. The high-resolution detection of beach features is crucial for understanding short-term geomorphic evolution. After mapping the landforms, a statistical analysis of the shoreline position for different time series was performed. ArcGIS 10.8 software with the add-in Digital Shoreline Analysis System (DSAS v5.0) was used [6].

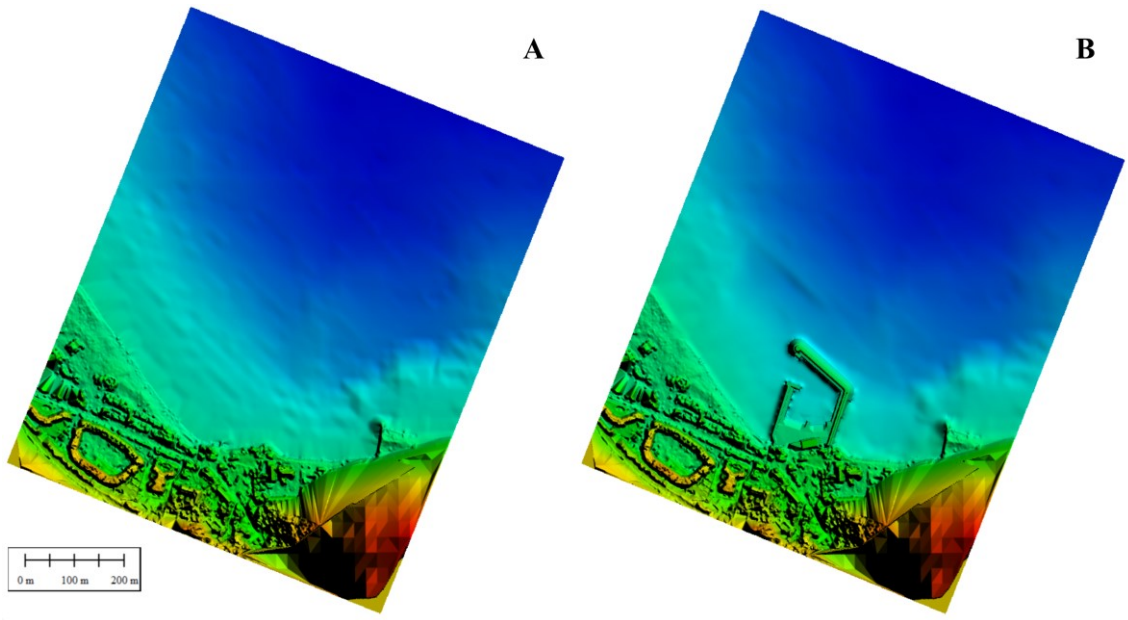


Figure 2. Digital elevation models for the situation before (A) and after (B) construction of the fishing port

Boundary conditions

Wave climate data was derived for a location in front of the Asparuhovo Beach at 8 m depth from a wave model hindcast data set covering 1949–2018 [7]. For the present

study, typical seasonal instead the extreme conditions were considered since they, having a higher probability of occurrence, better determine the prevailing hydrodynamic fields. The 97th quantile (Q97) was selected as representative of typical seasonal conditions, according to which the significant wave height, peak period and mean direction of wave propagation were computed and complemented with the corresponding water levels [8]. For all seasons, the predominant waves propagated from east-northeast. The wave parameters and water levels relevant for summer and winter forcing used as boundary conditions in the model simulations are presented in Table 1.

Table 1. Wave parameters and water levels for typical summer and winter forcing used as boundary conditions in model runs

Season	H_s [m]	T_p [s]	D_m [deg]	Water level [m]	Duration [h]
Winter	1.81	8.2	67.5 (ENE)	0.25	12
Summer	0.79	6	67.5 (ENE)	0.08	12

where: H_s – significant wave height [m], T_p – peak wave period [s], D_m – mean wave direction

Model set-up

The aim of modelling effort was to clarify the change in processes leading to the port siltation. 2DH morphodynamic model XBeach [9] was employed to simulate the hydrodynamic and morphodynamic processes in the model domain. It was calibrated and validated for the Bulgarian coast [10]. The study is carried out considering the situation before and after the fishing port construction in order to detect specific coastal impact. Both typical seasonal wave conditions and related surges were reconstructed in terms of boundary conditions (Table 1).

The model grid used is a regular equidistant grid of 1m resolution, resulting in 809 295 grid cells, that allows a very good representation of individual waves transformation, local flows and adequate sediment transports. The model domain outlined in Fig.2 has 990m x 820m size and expands to depth of 8 m.

The model was run in non-hydrostatic mode allowing calculation of individual waves. Cyclic lateral boundaries for the flow and waves were applied in the modelling simulations. The presence of hard structures as the port facility itself, coastal structures, roads, buildings and the rocky formations located within the model domain were reflected in the model. The bed friction was addressed using different Manning coefficients for the sandy bottom slopes and for hard structures. The same conditions were applied for the port facility pre- and post-construction phases. The simulations aim to outline the distinctive hydro- and morphodynamic regimes in representative seasonal hydrodynamic conditions.

RESULTS & DISCUSSION

Geospatial analysis

The geospatial morphological analysis shows that the beach was in equilibrium state before the construction. After the modification, abrupt changes in the beach morphology occurred, especially at the western side of the port, which resulted in a process of slow

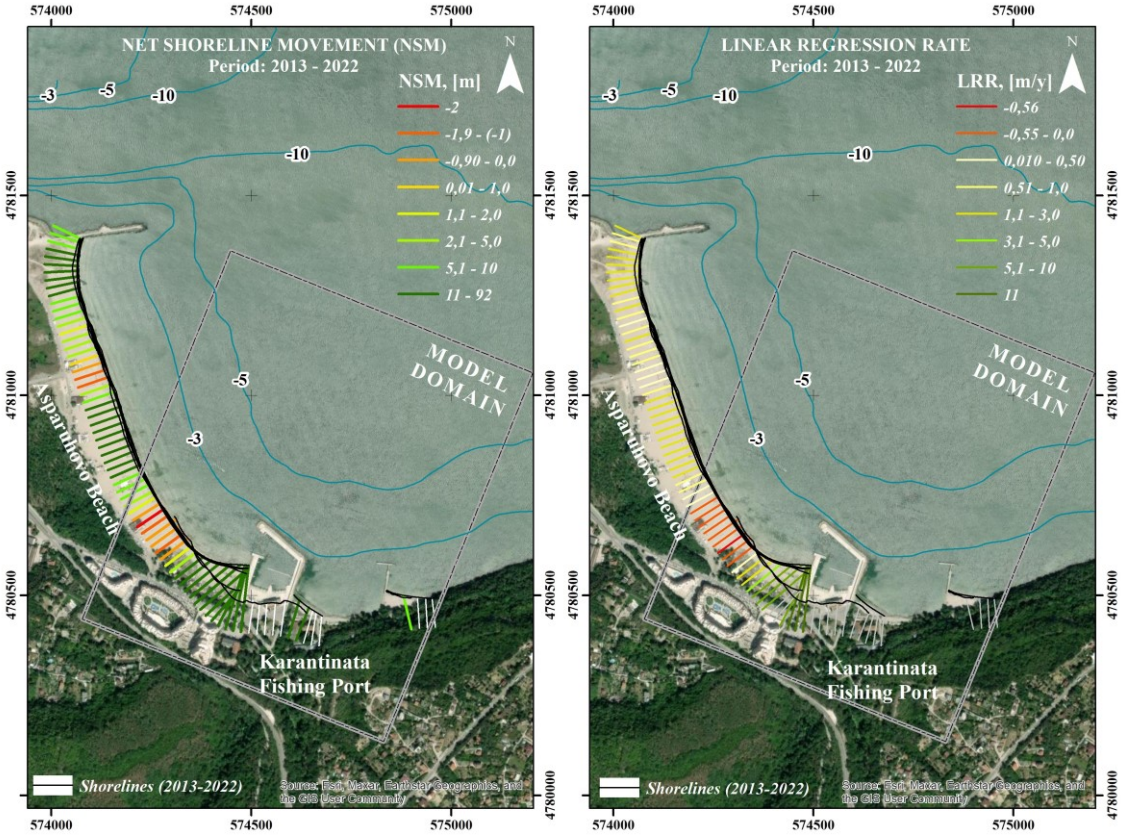


Figure 3. Net shoreline movement (left) and linear shoreline regression rate per year (right) for 2013–2022, measured shorelines and position of model domain

beach evolution. The net shoreline movement computed for 2103–2022 reveals a presence of alternating stretches of erosion and deposition as the largest erosion takes place next to the area of accumulation near the port (Fig. 4, left). Overall net shoreline movement analysis shows that the accumulation prevails over erosion. On the other hand, the linear regression rate computed for the same period shows stable shoreline position in the larger part of the Asparuhovo Beach. The most significant change is detected in the area adjacent to the port presented by stretches of shoreline retreat and advance. On this basis, the extent of model domain was set up. At present, the shoreline seems to be close to equilibrium state. Based on geospatial analysis it was calculated that the beach area was 9.44 ha in 2013, while in 2022, it was 10.604 ha. If we consider the net change of beach area for the studied period, it turns out that the beach increased with 12.3% on the account of hydromorphological changes occurs after the port construction.

Hydrodynamic and morphodynamic modelling studies

Wave transformation

The sea surface state reflecting wave group envelope and sea level fluctuations represents the wave field transformation in the study area (Fig. 4). Clearly, for both winter and summer conditions, the facility causes refraction of wave fronts in the wave shadow zone. Wave diffraction at the port entrance as well as non-linear interactions, e.g. agitation, can also be observed. Besides, a reduction in wave run-up is noticeable close to the facility.

https://doi.org/10.5593/sgem2024/3.1/s12.18

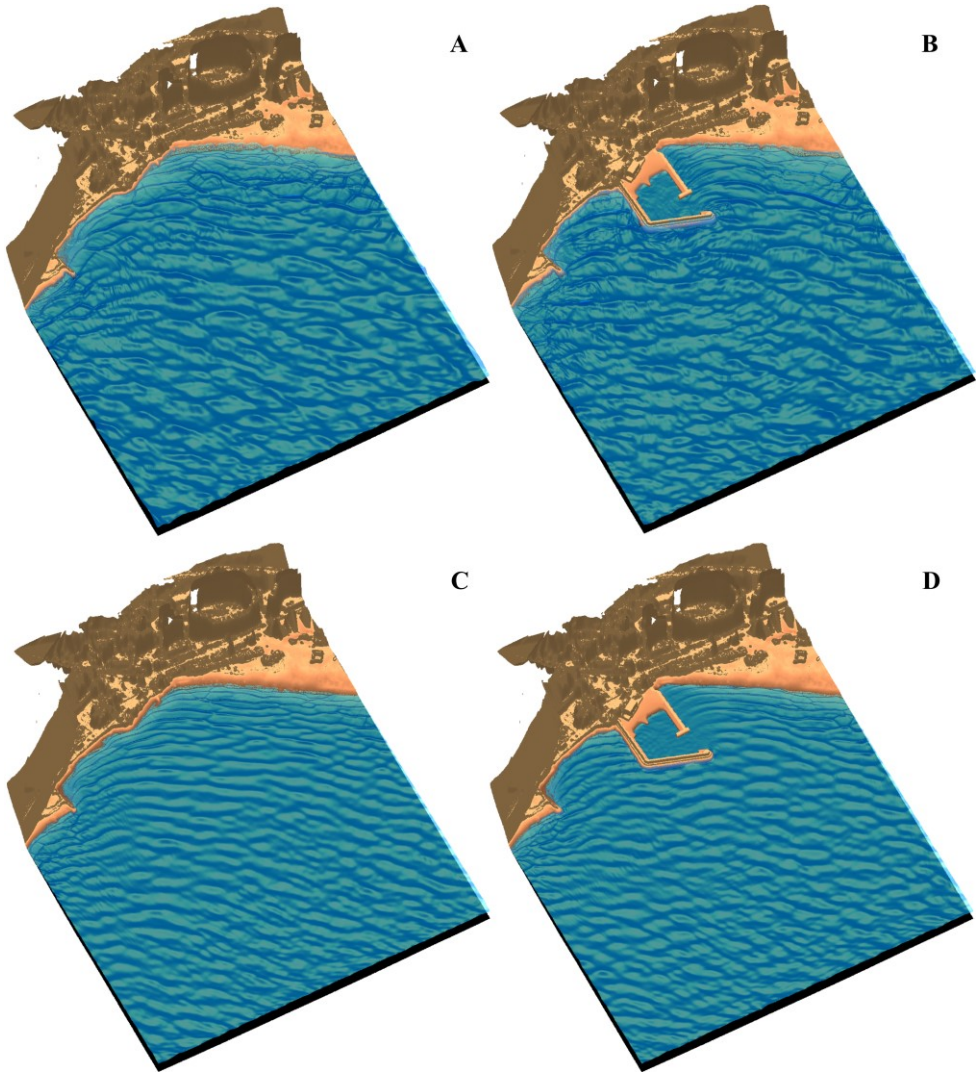


Figure 4. Simultaneous picture of sea surface during winter conditions (pre- and post-construction: A and B) and summer conditions (pre- and post- construction: C and D)

Wave flow

The wave flow pattern before the port construction shows that the main stream is directed westward along the coast (Fig. 5 A, C). While in winter, it is significantly more intense and propagates up to 2–3 m depth, in summer, this zone extends up to 1–2 m depth. In winter, the flow can be observed along almost the entire model domain as it slows down near the western boundary. In summer conditions, the wave flow is weaker, which results in speed decrease and meandering. This phenomenon correlates well with the presence of crescent underwater bars observed in several satellite images. The intense wave flow in the eastern and central part of the domain explains the lack of sedimentation observed before the port construction.

The model results show that the construction of the port facility caused significant changes in the hydrodynamic regime (Fig. 5 B, D). Its presence causes the main flow to deviate towards the sea, propagating in the 4–5 m deep area and forms a couple of secondary circulation cells on both sides of the facility. A general decrease in the wave flow velocity is observed as it becomes highly inhomogeneous.

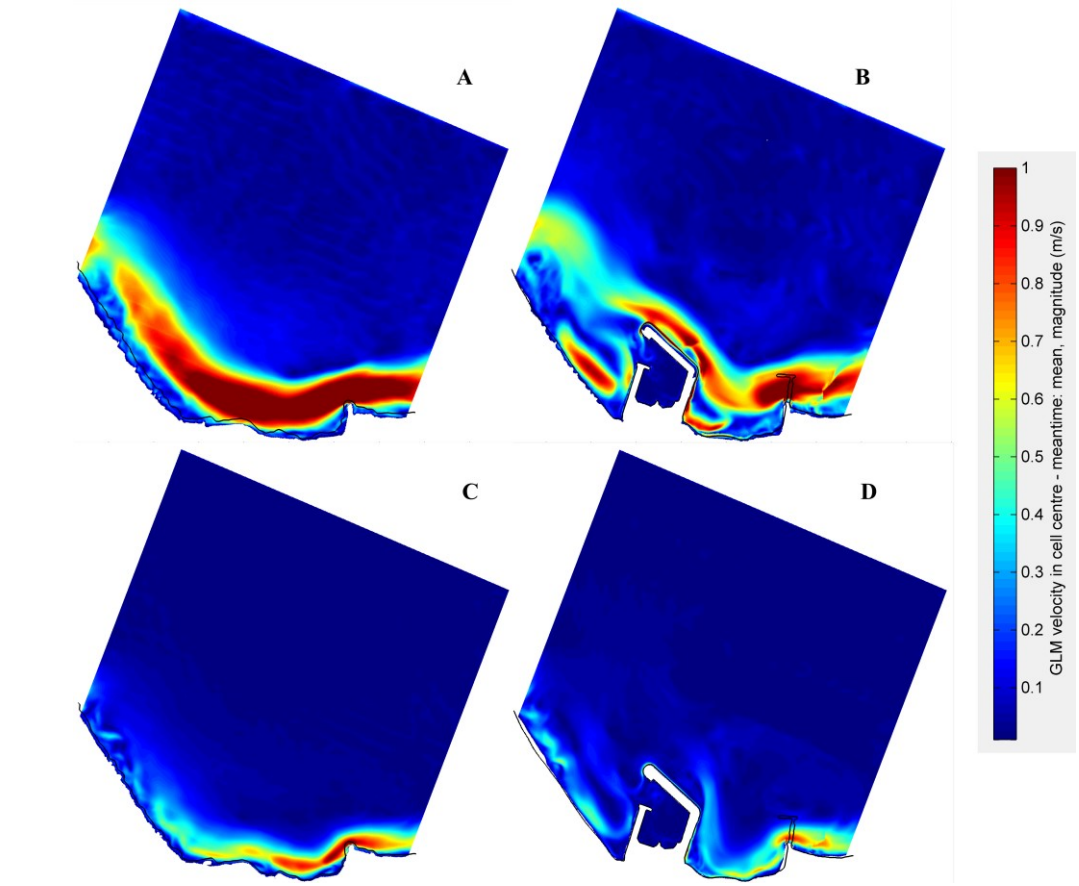


Figure 5. Wave flows pattern observed during winter conditions (pre- and post-construction: A and B) and summer conditions (pre- and post- construction: C and D)

Regarding the newly formed circulation cells after the port construction, the general circulation pattern is similar for both seasons but significant differences in intensity and location of the cells is noticeable depending on the relevant conditions (Fig. 6 B, D). In winter, the current flowing along the frontal part of the eastern port breakwater bifurcates, and the larger stream forms a cyclonic circulation cell to the left of the port with significant nearshore velocities in southeast direction and relatively lower velocities along the pier in the direction of port entrance. This circulation cell strongly correlates with the observed intense sedimentation immediately after the facility construction. The second less intense stream propagates in deeper waters.

Another small cyclonic eddy is observed to the right side of facility, which is most intensive while flowing shoreward along the breakwater and parallel to the shore. Here, sedimentation is also observed but, due to the smaller sediment volume availability, it is not significant. In summer conditions, the similar circulation pattern is observed but much less intense. The cell located in the port left side is flatter in shape and expands over a narrower area near the shoreline. The intensity is greater along the shoreline where the flow becomes unstable, and meanders. Attached to this eddy is another slow speed anticyclonic cell located just before the port entrance. It is vaguely noticeable also in winter conditions as the energy of the larger one covers it up. Eventually, the two flows merge with one another and form a common stream propagating to the northwest. The cell to the port right side is much less pronounced and keeps position in closer

https://doi.org/10.5593/sgem2024/3.1/s12.18

proximity to the breakwater, whereas the alongshore westward stream largely dominates the circulation pattern.

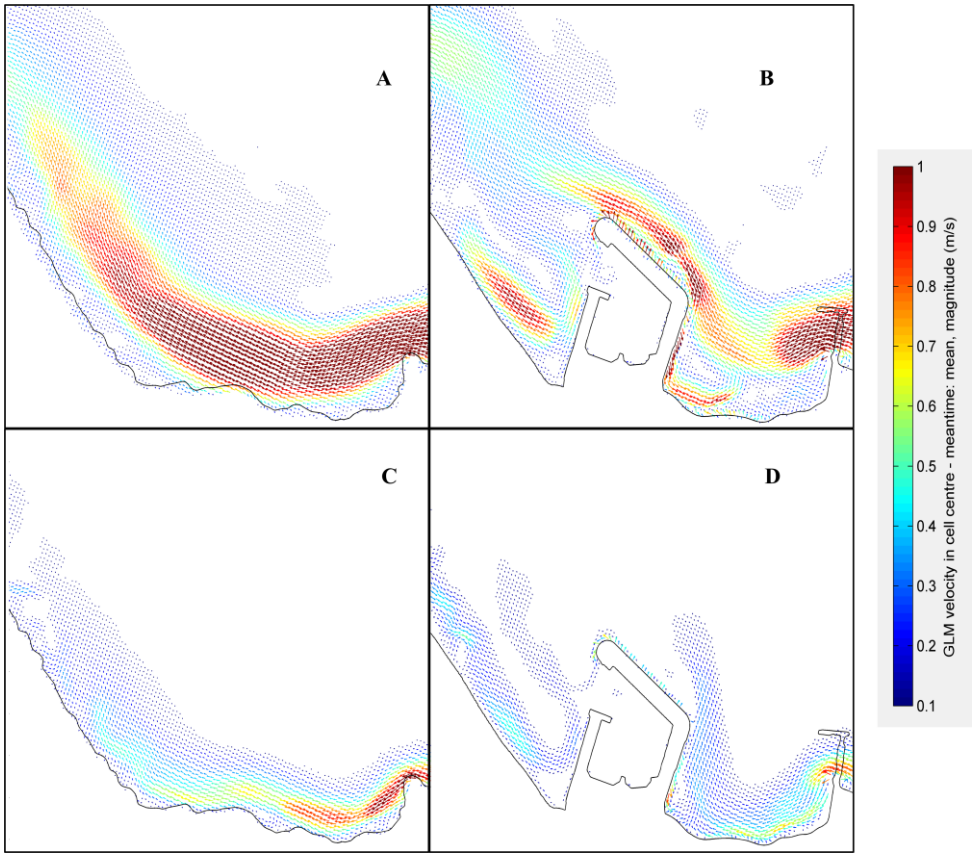


Figure 6. Vectors of wave flow velocities observed during winter conditions (pre- and post- construction: A and B) and summer conditions (pre- and post- construction: C and D)

Sedimentation erosion pattern

The change in morphology occurs due to the sediment transport – bedload and suspended, which in turn depends on the currents in the water column and near the bottom, as well as on the sediment availability. The sedimentation-erosion pattern resulting from the modeled seasonal conditions shows a considerable difference for different seasons, as for winter conditions the extent of morphodynamic changes is significantly larger (Fig. 7). This is explained by the difference in wave properties: in winter, apart from occurrence of higher waves, the longer period infragravity waves reach larger amplitudes. This phenomenon mainly determines the aerial and submerged beach erosion, and therefore the processes of sedimentation. The general pattern within the shoreline area for all considered situations shows erosion of the beach front and sedimentation on the underwater slope, which is influenced by the flows and bottom forms distribution.

The model results show that the port construction significantly changes the morphodynamic pattern especially for winter type conditions (Fig. 7 A, B). A large accumulation zone is observed to the left side of the port, in the wave shadow of the

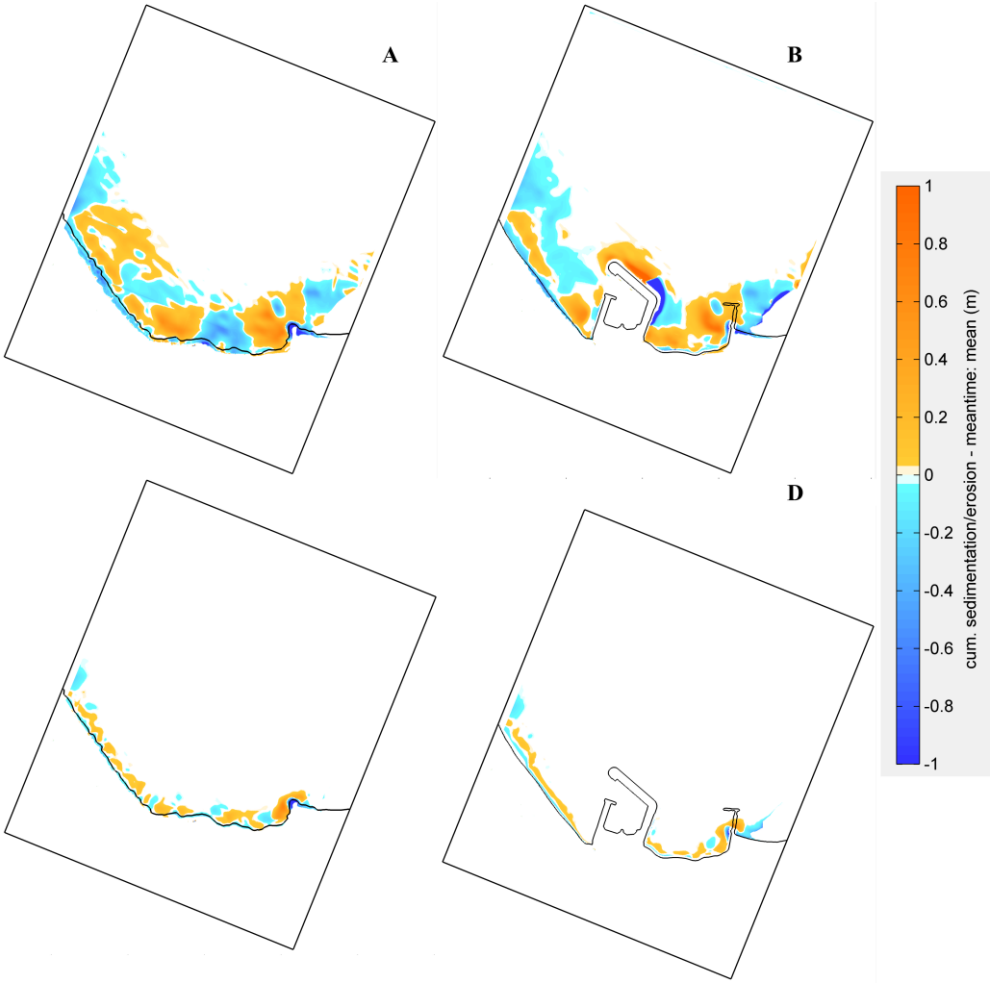


Figure 7. Sedimentation – erosion pattern calculated for winter (pre- and post-construction: A and B) and summer conditions (pre- and post- construction: C and D)

facility. This is attributed to the effect of the circulation cell acting there, leading to decrease of wave flow velocities and subsequent sediment deposition. Such accumulation was observed on the site immediately after the port construction, which was extremely intense in the beginning. As a result of this change in the longshore sediment transport, an area of the surface layer erosion is formed in the west of the facility at depths of approx. 2 to 4m. The second accumulation zone, also observed in place, is located to the right side of port. It is connected to the seaward erosion zone, in the corner of the eastern breakwater. Hence, this morphodynamic pattern is modified by the local circulation cell taking place due to the influence of the facility. The third accumulation zone is located along the frontal part of the eastern breakwater. It is attributed to the severe erosion at the corner of the breakwater, caused by the wave flow intensification. In summer conditions, the effect on the morphodynamic regime is minor due to smaller rates of erosion and accumulation (Fig. 7 C, D).

It should be noted that the change in the hydrodynamic regime is representative over a longer period, although it is expected to change to some extent over time due to changes in bottom morphology. The modelled morphodynamic erosion-accumulation pattern is indicative and gives a notion about the overall trend of morphodynamic changes. Nevertheless, it is representative only of the wave event that is modelled, albeit typical

https://doi.org/10.5593/sgem2024/3.1/s12.18

for the season. The long-term evolution of the beach is a consequence of the effect of different wave conditions combined with the action of factors such as surges, sea level rise, etc.

CONCLUSION

The study presented an assessment of impacts on hydromorphological regime associated with a fishing port construction. It explained the reason for the rapid morphological changes in the area influenced by fishing port "Karantinata", which is associated with the modification of hydrodynamic and sedimentation regime. The assessment was done through hydrodynamic and morphodynamic modelling as well as geospatial morphological analysis based on satellite images, past and present field observations, which describe the settings before and after the port construction.

The analysis of hydrodynamic and morphodynamic modelling shows that the general pattern of wave flow and associated suspended and bedload sediment fluxes are significantly modified by the port presence. The new elements of hydrodynamic regime are two circulation cells of a cyclonic type formed at both sides of the port. The first one formed westward of the port is causing an excessive accumulation of sediments in the area. The second one, at the eastern side of the port, provokes sediment accumulation and moderate increase of beach width.

The geospatial analysis shows 12.3% of net increase in beach area for the studied period (2013–2022). This could be attributed to the changed hydrodynamic and morphodynamic regime after the port construction, since the major changes in beach morphology are observed in near proximity to the port. One explanation could be that the diverted towards bigger depths main wave flow entrains sediments that are usually not involved in the longshore flux thus creating conditions for larger sediment supply. After the abrupt changes in beach morphology observed immediately after the port construction, a phase of slower changes took place, which is expected to further pace down in coming years. Presently, a new beach morphology equilibrium is formed, while the siltation of the port entrance is expected to persist until engineering solutions are implemented to solve the problem.

ACKNOWLEDGEMENTS

The study has been performed within the project “Coastal HYdro-Morphological Regime changes in mAn-modified environment – CHYMERA”, funded by Bulgarian National Science Fund under the Ministry of Education and Science of Republic of Bulgaria, Contract No КП-06-Н54/8/01.12.2021.

REFERENCES

[1] Kizielewicz J., Luković T., The Phenomenon of the Marina Development to Support the European Model of Economic Development, Int. J. on Marine Navigation and Safety of Sea Transportation, vol. 7/issue 3, DOI: 10.12716/1001.07.03.19, 2013, pp. 461-466;

[2] Kraus, N.C., 2009. Engineering of tidal inlets and morphologic consequences. In: Kim, Y.C. (Ed.), Handbook of Coastal and Ocean Engineering. World Scientific, Singapore, pp. 867–901;

[3] Dugan J.E., Airoldi L., Chapman M.G., Walker S.J., Schlacher T., Estuarine and coastal structures: Environmental effects. In: Estuarine and Coastal Structures: Environmental Effects, a Focus on Shore and Nearshore Structures. Treatise on Estuarine and Coastal Science, Vol. 8., Elsevier Inc., 2012, http://dx.doi.org/10.1016/B978-0-12-374711-2.00802-0;

[4] Prumm M., Iglesias G., Impacts of port development on estuarine morphodynamics: Ribadeo (Spain), Ocean Coast. Management, 130, http://dx.doi.org/10.1016/j.ocecoaman.2016.05.0032016, pp. 58–72;

[5] Prodanov B., S. Keremedchiev, L. Dimitrov, N. Andreeva. Seabed Morphology of the Varna Bay Coastal Zone, Bulgarian Black Sea. Comptes rendus de l'Academie bulgare des Sciences, Vol 72/issue 8, 2019, pp. 1077-1085. DOI: 10.7546/CRABS.2019.08.10;

[6] Himmelstoss E.A., Henderson R.E., Kratzmann M.G., Farris A.S., Digital Shoreline Analysis System (DSAS) version 5.0 user guide: U.S. Geological Survey Open-File Report 2018–1179, 110, 2018;

[7] Valchev N., Trifonova E., Andreeva N., Past and recent trends in the western Black Sea storminess, Natural Hazards and Earth System Sciences, 12, 2012, pp. 1–17, https://doi.org/10.5194/nhess-12-961-2012;

[8] Deltares. Delft3D-FLOW. Simulation of multi-dimensional hydrodynamic flows and transport phenomena, including sediments, User Manual, Version: 3.15, August, 2018, 710 pp;

[9] Roelvink, D., Reniers, A., van Dongeren, A., van Thiel de Vries, J., McCall, R., Lescinski, J., Modelling storm impacts on beaches, dunes and barrier islands, Coast. Eng. 56, 2009, pp. 1133–1152;

[10] Valchev N., Eftimova P., Andreeva N., Implementation and validation of a multi-domain coastal hazard forecasting system in an open bay, Coastal Engineering, 134, Elsevier, Netherlands, 2018, DOI:https://doi.org/10.1016/j.coastaleng.2017.08.008, pp. 212-228.

MODERN METHODS OF DETERMINING OF THE MOMENTS WATER QUALITY.COMPARING THE RESULTS WITH TRADITIONAL METHOD

Dr. Plamen Angelov [1]

Dr. Maya Rankova[1]

PhD Ress. Borislav Vuchkov[1]

[1] National Institute of Meteorology and Hydrology, **Bulgaria**

ABSTRACT

Hydrometric propeller methods, is device that responds and measuring the velocity of the water current at the point where its sensor axis is located. Mechanical hydrometric propellers are widely used in our country, in which the current causes rotation of a screw vane with an angular velocity proportional to the velocity of the current, in this method the depth of the river profile must be taken into account in order to comply with the measurement condition in 1, 2, or 3 points namely 0.2h, 0.6h and 0.8h, h-depth of flow [2].

In the present topic, a comparison will be made between a hydrometric propeller, a device for measuring speeds and depths based on the principle of magnetic induction. Graphs, tables and conclusions from field measurements will be presented. The device will be compared measures water velocity by using Faraday's principle of magnetic induction. This allows measurement of low velocities without rotating parts. The research will help solve problems during operational work (field work), will aim to show fast, accurate results in determining water quantities, shortening measurement time, using the device at low water levels, at small flows.

Keywords: water flow, quantities, speed, measurement, magnetic induction

INTRODUCTION

The measuring technique today is able to improve the operability, to improve the basic measuring methods, by introducing additional innovative solutions. These solutions are accompanied by assurances that, subject to certain restrictive conditions that cannot always be ensured, the measurement samples are considered completely acceptable to the alternative of the impossibility of carrying out the measurement in another way. Carrying out measurements at certain times of increased water levels or increased water quantities is a task that hydro engineers must use skills and adapt to the situation. One of the few studied in our country are the springs. The springs can be formed in any kind of rock. Small ones are found in many places. The largest springs are formed in limestone and dolomite in the karst topography. A spring is a water resource, the bottom of a dried-up river, now a valley, crossing a flowing underground water body, a water table below which the surface material is saturated with water. A spring is the result of the filling of aquifers to the extent that the water overflows onto the earth's surface. They are very in size from small, flowing only after a lot of rain, to huge basins flowing thousands of litters daily. Systematic work over the years National Institute of Meteorology and Hydrology (NIMH) has proven its expertise and assessment of the

water resources available in the country. All this is the result of persistence and methodical following of the investment policy for equipment rearmament of the highest class, used by developing European countries, superior in quality to the equipment existing until now. The present report is dedicated to some of these issues, mainly innovative will be presented way to determine the amount of water in rivers and springs. The facility was chosen under the condition of increased water levels, River Elechnica, near to city Elin Pelin.

MATERIALS AND METHODS

The measuring device is a two-electrode sensor located on a body, monitored on a bar graphed in meters and centimetres (Fig. 1). The meter is connected to the sensor by means of a cable and a connector. The speed calculations are made in the speed meter by converting the magnetic induction from the sensors. The device is equipped with a power supply and additional outputs for connecting to a computer. The speed data is saved in the device's memory and can be downloaded at any time. A metal cone/ special tools part/is used for mounting the bottom, which is mounted on the end rod. The Model 801 Flow meters are with Display unit that both drives the sensor and provides data display of the measured water velocity. Data is updated at 1 Hz, and may be averaged over any number of seconds from 1 to 600. The display will show real-time speed data at a resolution of 1 mm/s, as well as the result of the data average, and a Standard Deviation figure to give added data confidence. A solid state memory records all results (up to 999 averaged readings), and the data may be downloaded to PC using the RS232 interface.



Figure 1. Model 801 – EM Flow meter

The Model 801 Electromagnetic Flow Meters measure the speed of water in Open Channel environments with exceptional accuracy. This small solid state sensor has been designed specifically for use in open channels where fouling by weed or sewage can be a problem. Experience in electromagnetic technology has ensured that the Model 801 is a high precision instrument which can be relied upon to give accurate readings (±0.5% of reading plus zero stability) over a wide flow range (±5 m/sec) in only 5cm of water. The control display unit provides a choice of averaging modes, standard deviation of the data, and a logging facility. In this connection my colleges and I, we will try to make a

comparison between this instrument and the so used hydrometric propeller with mechanical parts.

The universal current meter OTT C 31 (Fig. 2) is designed to measure the flow rate in combination with hand wading rods or a cable suspended from a bridge or staff bridge. OTT C31 Universal current meters stand of times proven quality, precision and reliability - all over the world for decades.



Figure 2. Model C31, Ott mechanical propeller on the rod.

METHODS

Determining discharge using Current Meters. The most common approach to determining discharge is the so called conventional current-meter method. The method is **based on determining the mean stream flow velocity and flow cross sectional area**; the product of these variables determines the stream discharge. Stream flow discharge is defined as the volume rate of flow of water that includes any substances dissolved or suspended in the water. Discharge is usually expressed in units of cubic per second (m^3/sec). With rare exception, stream discharge is not measured directly, but is computed indirectly from velocity and water level (stage) measurements. If the mean water velocity normal to the direction of flow (V) and the cross-sectional area (A) of water flow is known, then the discharge (Q) can be computed as $Q=VA$. The discharge rating is a relationship between the stage and discharge or between stage, discharge, slope, rate of change of state, or other factors [4].

Two-Point Method- The two point methodology uses velocity observations at 0.2 and 0.8 of the depth below the surface. The average of these two observations is the mean velocity in the vertical. The methodology is generally used by the USGS, and has been shown to give accurate and consistent results. The two-point method results are typically within 1 percent of the true mean vertical velocity [4].

Three-Point Method -The three point method is a combination of the two-point and the six-tenths depth methods and utilizes velocity measurements at 0.2, 0.6 and 0.8 of the depth. The mean velocity is determined by averaging the 0.2 and 0.8 depths; the result is then average with the 0.6 depth observation [5].

We use an approach in which a velocity observation taken in the vertical at 0.6 of the depth below the surface is assumed to be the mean vertical velocity. Observational data

and mathematical models show that a depth of 0.6 gives reliable results in the case of depths up to 60cm. **In our case, the depths will not exceed 60cm.**

Cross midsection method of computing stream discharge using current meter velocity measurements. In this method, the stream cross section is divided into rectangular subsections as shown in Figure 3. At the centre of each of these subsections (called a *vertical*), a depth and velocity measurement is made, and the distance from a datum point on the shore is determined. The total discharge can be determined [5] using the procedure outlines in Figure 4.

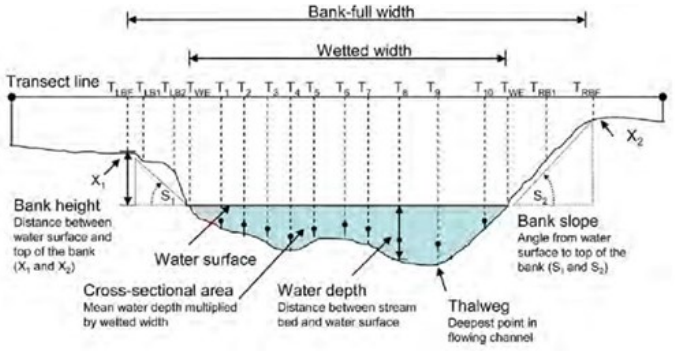


Figure3. Elements of a River section

Determining the mean stream flow velocity and flow cross sectional area; the product of these variables determines the stream discharge. Depth and position measurements are made with simple surveying or sounding equipment. A device known as a current meter (described in a section below) measures the stream velocity.

The National Institute of meteorology and Hydrology currently uses the midsection method of computing stream discharge using current meter velocity measurements. In midsection, the stream cross section is divided into rectangular subsections as shown in Figure 4. At the centre of each of these subsections (called a *vertical*), a depth and velocity measurement is made, and the distance from a datum point on the shore is determined. The total discharge can be determined using the procedure outlines in Figure 4[7],[8] with equations (1) and (2).

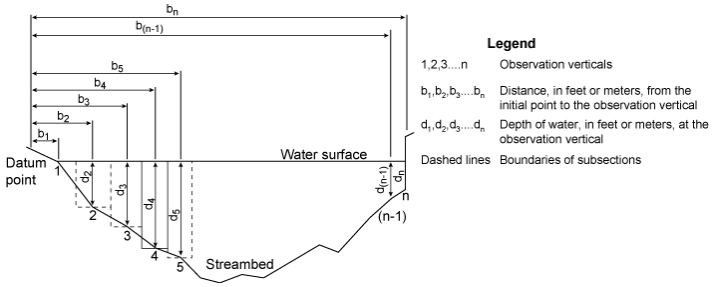


Figure4. The midsection stream cross section

$$Q = \sum_{i}^{n} qi = \sum vi, ai = \sum vi(widi) \quad (1)$$

Where:

Q = total stream discharge; qi = discharge in subsection;

vi = mean flow velocity normal to subsection i;

ai =cross section area of subsection i; wi=width of subsection i;

$$\begin{cases} \frac{b_2 - b_1}{2}; if i = 1; \\ \frac{b_{i+1} - b_{i-1}}{2}; if\ 2 \le i \le n-1 \\ \frac{b_n - b_{n-1}}{2}; if i = n \end{cases} \quad (2)$$

di =depth of subsection i; b_i =distance from shoreline datum to centre of subsection i; n = number of subsections dividing the stream cross section.

RESULTS

Method is consistent with the seasonal flow of the river. In another case, when the river has very large water levels, another method will be used to determine the water quantities without the need for the employee to enter the water. In our hydrometric structure we have measuring bridges from which we make these measurements [1], [2],

There are several basic steps to follow:

- Measurement of the depths in the river profile [4];
- Measurement of the speeds in the verticals more than 7 [3], [4];
-Positioning at the correct -Recording and validating the data.

Depending on the season, a measurement method can be selected.

Measurement: 1 (Table 1)

Table1 The River Eleshnitsa station № 18050 speed-area, calculation of the water quantity using Excel**.** Hydrometric propeller mechanical C31 OTT, Stage is 66cm

Vertical №	Distance, m	Depth, m	Area, m^2	0.6 depth	Velocity (average), m/s	Discharge, m^3/s
Start point 1	7.3	0	0	0	0	0
2	7.5	0.08	0.016	4.8	0.525	0.008400
3	8	0.1	0.050	6	1.129	0.056450
4	8.5	0.17	0.085	10	1.105	0.093925
5	9	0.23	0.115	14	1.455	0.167325
6	9.5	0.49	0.245	30	1.180	0.289100
7	10	0.5	0.250	30	1.199	0.299750
8	10.5	0.52	0.260	31	1.214	0.315640
9	11	0.51	0.255	30	1.181	0.301155
10	11.5	0.52	0.260	30	0.960	0.249600
11	12	0.52	0.260	32	0.932	0.242320
12	12.5	0.53	0.265	30	1.080	0.286200
13	13	0.5	0.250	31	0.830	0.207500
End point 14	13.3	0.47	0.235	28	0.758	0.178130
					Total Q	2.695495

The table 1 shows the number of verticals, initial and final vertical (Fig. 4). The average speeds and depths are shown in each vertical [6]. From the calculations, the result is shown in yellow Total Q = 2.695495 m^3/s

https://doi.org/10.5593/sgem2024/3.1/s12.19

Measurement 2 (Table 2)



Figure 4. Show measures a end point. New Model 801 – EM Flow meter magnetic inductive

It measures an end point to a hydrometric staff gages with innovative equipment of Flow meter magnetic inductive. Table 2 show the number of verticals, initial and final vertical. The average speeds and depths are shown in each vertical. From the calculations, the result is shown in yellow Total Q = 2.716034 m3/s, equation (3) and (4).

Table 2 The River Eleshnitsa station № 18050 speed-area, calculation of the water quantity using Excel. New Model 801 – EM Flow meter magnetic inductive. Stage is: 66cm

Vertical №	Distance, m	Depth, m	Area, m^2	0.6 depth	Velocity (average), m/s	Discharge, m^3/s
Start point 1	7.3	0	0	0	0	0
2	7.5	0.08	0.016	4.8	0.349	0.005584
3	8	0.1	0.05	6	1.179	0.05895
4	8.5	0.17	0.085	10	0.988	0.08398
5	9	0.23	0.115	14	1.356	0.15594
6	9.5	0.49	0.245	30	1.224	0.29988
7	10	0.5	0.25	30	1.356	0.339
8	10.5	0.52	0.26	31	1.207	0.31382
9	11	0.51	0.255	30	1.287	0.328185
10	11.5	0.52	0.26	30	1.036	0.26936
11	12	0.52	0.26	32	0.969	0.25194
12	12.5	0.53	0.265	30	0.927	0.245655
13	13	0.5	0.25	31	0.859	0.21475
End point 14	13.3	0.47	0.235	28	0.634	0.14899
					Total Q	2.716034

DISCUSSION

In various situations of large waves and current speeds, this particular device will not be suitable for this type of measurement. In such a situation of very large currents and

depths, measuring devices such as boats with attached measuring sensors for speed and depth should be used. They exist and are used to measure flow. Field measurement shows very little difference in both measurement methods, leading to the conclusion that we are measuring correctly and the instruments are accurate with minimal deviations.

$$Q = Area * meanVelocity \quad (3)$$

Q = Water quantity [m3/s];

Area=mathematic calculation [m^2];

mean Velocity= is main velocity on The river [m/s];

$$\Delta Q = Q(measurement1) - Q(measurement2); \quad (4)$$

ΔQ = difference between two measurements, $\Delta Q = 0.020539 m^3 / s$.

The measurement took place under bad unfavorable conditions for the person who made the measurement. In different water flow regimes, the water can be fast, with destructive force and in such a case the person cannot measure also, the water is very low temperature in this case. This leads to freezing of the hydrolog.

An advantage of the magnetic inductive method is that it quickly and correctly measures the speed, which can be considered a fast and reliable speed meter, to be used in different situations for small rivers and springs.

Advantage: small and compact, does not need any maintenance.

Advantage: Saves measurement data.

Disadvantage: Cannot be used in swampy rivers due to silt and algae covering the sensors,

CONCLUSION

In various situations of large waves, and the shocks from the field measurement cannot be used, devices, boats are used to measure the flow rate. This field measurement shows a very small difference in the two measurement methods, which leads to the conclusion that, we are measuring correctly, and instruments are accurate.

Regardless of difference construction:

1. The measured water quantities are almost the same with both methods.

2. River depths are measured once without the need for re-measurement with the rod.

3. The positioning of the sensor (speed meter) has a great influence, it must be fixed, perpendicular to the current

4. A plus of the magneto-inductive principle is that there are no rotating parts and no need for calibration.

5. The result written on the display is quickly obtained.

6. It can measure very small depths the magnetic sensor compared to the hydrometric propeller.

https://doi.org/10.5593/sgem2024/3.1/s12.19

7. Can be used to measure the flow rate of springs of very small sizes and depths with depths up to 2 cm, width 1 m.

ACKNOWLEDGEMENTS

The paper is based on research project "Determination of the amount of water in open rivers and canals using the velocity-area method". The purpose of this article is to compare two different measuring devices to see what results they will show. A river with a flat bottom was chosen, but the peculiarity here is when measuring without wading from a bridge and by entering the water (wading). The results are in tables 2, 3, a very small difference. Accuracy of current-meter measurements is 1 present. This once again shows that modern methods are reliable and can be used as correct measuring tools. Thanks to the colleagues who showed patience in the rainy weather during the measurement.

REFERENCES

[1] Monev E S., Engineering Hydrology and Hydraulics - Hydrological and Hydraulic Calculations, Water Supply Equipment, Correction, Drainage, Inspection and Targeting of Overflow Systems. 1998.

[2] Angelov P A., Contemporary Devices for Measurement of Water Discharge in Open Flows. 2017. 44-52,

[3] Marinov, I., Mandanzhiev, D., Gerasimov G., Pechinov, D., Hydrological handbook. Part I. Technica State Publishing House. 415 p. 1979.

[4] Guide to Hydrological Practice, WMO, 168, 1994.

[5] Rantz, S. E., et al., Measurement and Computation of Streamflow. USGS Water Supply Paper 2175. http://water.usgs.gov/pubs/wsp/wsp2175/index.html) 1982.

[6] Carter, R.W. and I.E. Anderson, Accuracy of current-meter measurements. Journal of Civil Engineers, ASCE, v. 89, no. HY4, p. 105-115. 1963.

[7] US Bureau of Reclamation, Water Measurement Manual, Third Edition. (available online at https://www.usbr.gov/tsc/techreferences/mands/wmm),1997.

[8] Young, K.B., A comparative study of mean-section and mid-section methods for computations of discharge measurements. USGS open-file report, 52 p. 1950.

PRIMARY STUDIES FOR THE PRESENCE OF OFFSHORE FRESHENED GROUNDWATER IN THE BULGARIAN BLACK SEA SHELF

Assoc. Prof. Dr. Olga Nitcheva[1]

[1]Institute of Mechanics - Bulgarian Academy of Sciences, **Bulgaria**

ABSTRACT

The groundwaters draining in the continental shelf area can be an unconventional resource of fresh water for drinking, irrigation, and industrial purposes in water-scarce coastal areas. Recently, possible offshore sources of such groundwater in the coastal zone have been subject of increased investigation and description.

The aim of the present research is to identify similar, available for use, potential sources of Offshore Frehsened Groundwater (OFG) in the area of the shelf of the Northern part of the Bulgarian Black Sea coast. In the watershed of this region, which has the least rainfall in the country, there is almost no surface runoff, the rainfall mainly feeds the groundwater.

A hydrogeological analysis of the region was carried out to identify potential submarine sources of fresh groundwater.

40 years ago in that shelf area, on the basis of temperature and mineralization anomalies of the seafloor waters, continental Submarine Groundwater Discharge (SGD) zones were established. The present studies, based on the detection of anomalies in the distribution of bottom and surface sea water temperature in the area, were carried out to confirm the then established data on the availability of potential submarine sources of fresh water.

For this purpose, data from observation obtained by modern high-tech means were used. Sea Surface Temperature (SST) mapping and water contrast plume zones establishment was conducted for Northern Bulgaria by applying a high-resolution satellite product (GHRSST, CNR MED Sea Surface Temperature) from the NASA data-set.

The locations of mapped potential groundwater discharge determined by the present SST study are consistent with those previously estimated.

The study is the basis for further research, local sampling to assess the existence and magnitude of the Offshore Freshened Groundwater (OFG) and its potential utility.

Keywords: Offshore Freshened Groundwater (OFG), Submarine Groundwater Discharge (SGD), Northern Bulgaria Sea shelf, Sea Surface Temperature (SST)

INTRODUCTION

Research related to the study of potential Offshore Freshened Groundwater (OFG), with the aim of supplying water to coastal areas with limited water resources, accompanied by marine intrusion, as well as with onshore groundwater often polluted

by agriculture and industry, has been very popular in recent years [1], [2]. Exploring the potential of OFG in the shelf zones as an unconventional source of potable water is frontier research [3], [4].

Groundwater sources at a distance of 1 km to several tens of km from the coast in the shelf, i.e. in the continuation of aquifers in the sea at a depth of up to 100 m below the sea surface with a salinity below 33 PSU (having mean salinity of 15 PSU) are accepted as OFG and can be used for industrial and domestic purposes [3], [4].

Experimental submarine geological studies to locate Offshore Freshened Groundwater (OFG) are expensive and preliminary studies by other means are mandatory. This necessitates the analysis of hydro-geological submarine data from other sources.

As a first step, a hydro-morpho-geological analysis of the watershed and shelf area should be prepared in order to highlight the fresh water-rich onshore-offshore continuous aquifers. Next is the localization of the sectors in the shelf test section, as close to the coast as possible, for the presence of terrestrial groundwater discharge [5]. Accurate knowledge of nearshore Submarine Groundwater Discharge (SGD) and its investigation is an important task and indicative information on the location and source of potential OFG.

Submarine Groundwater Discharge is usually the subsurface flow coming from the land to the sea through continuous aquifers, under favorable hydro-geological and hydrology conditions, the presence of a hydraulic gradient in rich freshwater aquifers [6], [7], [8].

It is known that the zones (water plumes due to thermal contrast) with differences in the temperature of the water on the sea floor and the temperature of the water on the sea surface (SST) are due to SGD. Commonly, groundwater temperatures show less variability than SST and temperatures distinct from the sea water. That is why, thermally anomalous plumes often occur in coastal areas with SGD [9].

Thus, our main task is to conduct research for the registration of SGD by means of temperature profiling and determining the areas with negative temperature anomalies.

Identification of Submarine Groundwater Discharge at the nearshore scale can be done through in situ experimental work for the sea water temperature detection of the seafloor and mapping of the places with a lower temperature than the background for the area. Another way is to use satellite observations of sea surface temperature and mapping of the sectors with a lower temperature than the background.

The last technique for identifying SGD locations is based on the formation of thermally anomalous plumes due to the thermal differences between groundwater and sea surface water [10], [11].

A global database of 305 Offshore Freshened Groundwater (OFGs), which are located along the continental margins, has been created from the investigations of submarine freshwater horizons conducted so far. These data do not include information on potential sources of OFG in the Bulgarian Black Sea shelf, because such studies have not been done.

The purpose of the present study is identification of the locations of potential OFG zones in the Bulgarian Black Sea shelf from a hydrology and geological point of view. Exploration with the same target were performed in the period 1985-1988 in the northern shelf area of the Bulgarian Black Sea region. Then the presence of SGD areas was registered through a survey on the seabed with special equipment installed on a research vessel for seismoacoustic profiling and determination of anomalies in the temperature and electrical conductivity of seawater. The natural experiment was conducted in the autumn season (October 1986) [12].

In the present study, the SST anomalies are considered for the same region for the month of October of 2020, 2021 and 2022 .

The survey of the SST is prepared by the comprehensive satellite based product, GHRSST (The Group for High Resolution Sea Surface Temperature) - High Resolution and Ultra High Resolution L3S Sea Surface Temperature. GHRSST CNR MED Sea Surface Temperature data are operationally processed in near real time by CNRISMAR-GOS (Italian National Research Council - Institute of Marine Sciences - Group of Satellites Oceanography) [13], [14]. Techniques used to combine SST information collected by infrared sensors mounted on different satellite platforms and covering the southern European seas. There are a number of satellites offering high resolution data for analysis and monitoring of near-Earth space [15], [16], [17].

Such a preliminary survey in search for Offshore Freshened Groundwater (OFGs) in the Bulgarian Black Sea shelf is prepared for the first time. The study is the basis for further research, local sampling for assessment of potential OFG occurrence. It is an exemplary scheme for scientific feasibility studies in locating submarine sectors of aquifers as possible sources of fresh drinking water.

MATERIALS AND METHODS

General information about the Bulgarian Black sea basin.

Bulgaria is an Eastern European country, the climate is moderate-continental, the relief is mostly flat-hilly (200-600m). The territory of the country is 111,000 sq. km, with 32% of the relief being flat (0-200 m), 41% flat-hilly (200-600 m), 15% low-mountain (600-1000 m), 10% mid-mountain (1000-1600m) and 3% is high mountain (1600-2798m), Figure 1. Average annual precipitation is 670 mm. In the Black Sea basin, precipitation is the least, with an average of 400 mm per year in its northern part.

The conceptual geological scheme, Figure 2a, shows the main Bulgarian morphotectonic units: the Moesian platform, the Balkanides and the Moravian-Rhodope massif. To the east towards the sea basin, the upper morphostructures gradually pass into the shelf zone and the continental slope of the Black Sea Basin.

The Bulgarian Black sea watershed has a complicated geological structure. It is developed on the stable Moesian Platform (part of the Eurasian plate) and on the Balkan zone (part of the Alpine-Himalayan orogenik belt).



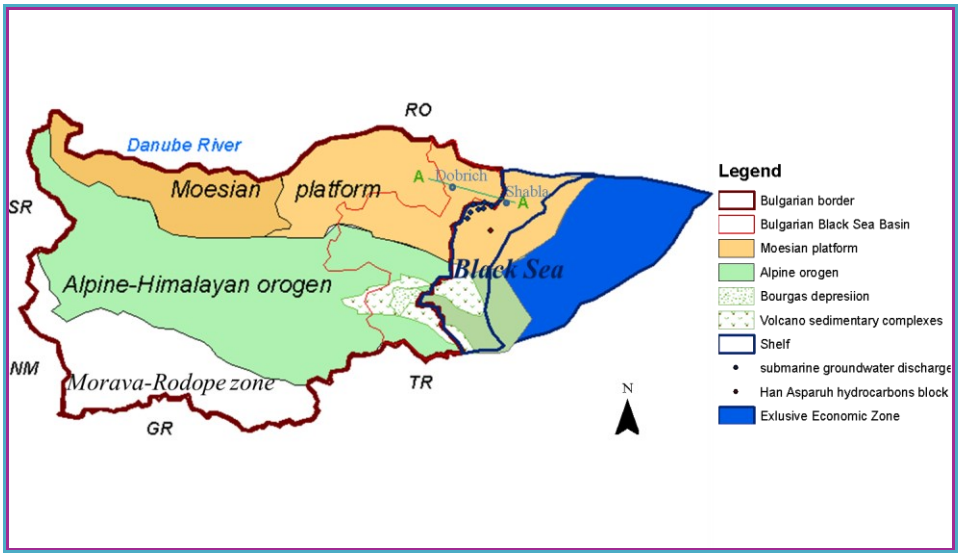
Fig.1. Bulgarian geographic map [18]

The Moesian platform is presented by the primary geological units like the Lom depression (left part of the Moesian platform) and the North Bulgarian High (right part of the Moesian platform), Figure 2a. The relief is smooth, the geological layers are stratified (parallel) covered by loess (60-100m). The porous and karst aquifers prevail.

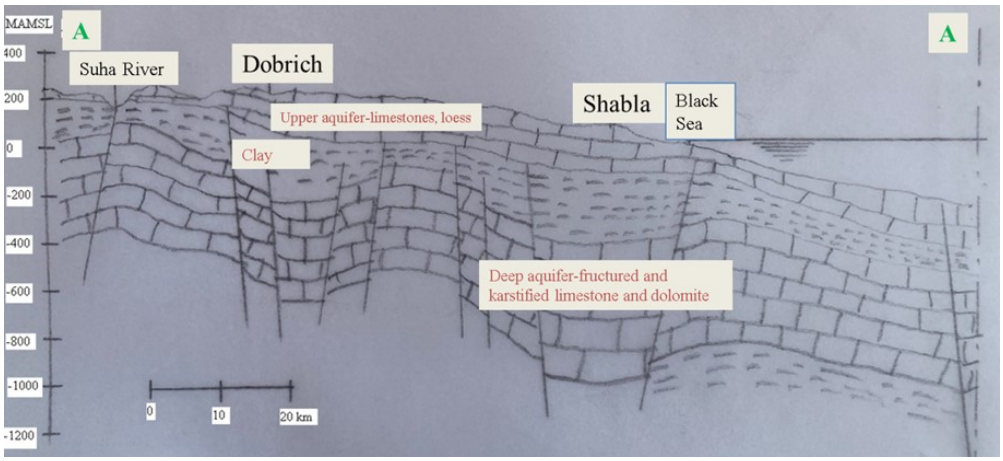
The basement of the study area is formed by layers of the Moesian platform and is represented by Jurassic and Cretaceous units that overlap with Paleozoic rocks. The Moesian Limestone continues seaward as submarine bench, while in the rest of the Bulgarian Black Sea - the Alpine orogen, magmatic rocks continuing submarine to the east as a system of volcanic fissures.

The borders of the Bulgarian shelf from the border with Romania to the border with Turkey reach 90-70 km east from the coast. The average depth is 130 m (in some places it reaches 200 m).

Search and exploration of oil and gas in the Black Sea is carried out on the Northern part of the Bulgarian Black Sea shelf the "Khan Asparuh" block (east of Varna, Figure 2a). They did not so far find industrial accumulations of oil and natural gas, but the explorations continue. If oil and gas extraction begins, it will be detrimental to the submarine groundwater horizons and to the water in our water area.



a) Simplified geology map of the Bulgarian territory, Bulgarian Black Sea Shelf and Exlusive Economic Zone



b) Schematic geological profile A-A, Dobrich-Shabla

Fig.2. Conceptual hydrogeological scheme [19], [20]

In North Eastern part of the country there is no permanent surface run off. The waters of the temporary arising streams enter the karst beds and transforms into groundwater flows. For this reason the groundwater is the only source for water supply in this region. It is done by several hundred meters deep drilling wells. Regardless of the intensive exploitation of the aquifers amounting to 4 m^3/s there still exist reserves for more than 6 m^3/s.

There are two aquifers (Figure 2b), the upper unconfined, consisting of limestones, sands and loess of Miocene age, up to 250 m thick. Underlying is Miocene clay. The deep aquifer of Jurassic age has an average thickness of 400 m, which is higher in the eastern direction. Meteoric recharge is in the area of the city of Dobrich (Figure 2).

In the area of Dobrich the altitude is 220 m, the distance from the city to the sea coast is 30 km, the groundwater flow moves to the east. The average hydraulic gradient is 0.05-1%. Due to the high water-absorbing and water-conducting capacity of the carbonate complex, about 19% of the precipitation infiltrates and there is no surface runoff.

https://doi.org/10.5593/sgem2024/3.1/s12.20

In the upper Sarmatian aquifer there is pollution with nitrates and chlorides. In the deep aquifer in the coastal part the hydrocarbon compounds of H_2S and NH_4 exceed 10 mg/l [20]. It is due to the vertical migration of organic matter from oil and coal deposits and their further degradation.

RESULTS

Based on the gathered data, a map with generalized hydro-geological information was prepared, which is presented in Figure 2a (geological map) and Figure 2b (geological profile) as Conceptual hydro-geological scheme. Figure 2a shows that the Bulgarian Black Sea shelf is made up of two geological structures, the northern - Moesian platform and the southern Alpine shelf. The northern part of the Bulgarian Black Sea basin is represented by a carbonate suite rich in fresh groundwater. The northernmost part - the area of Dobrich-Shabla, which is experiencing a severe freshwater shortage due to over exploitation and saline water intrusion, is the selected onshore study area (Figure 3). In the continuation of this region in the sea, the shelf zone, our efforts are directed to search for potential sources of submarine fresh ground water.

In October 1986, marine hydrogeological studies were carried out in the shelf area 250 km along the coast within a band of 10 km width, of the Northern Bulgarian Black Sea by Russian and Bulgarian hydrogeologists [12]. One of the tasks was thermoprofiling of the water on the seabed with a scientifically equipped ship. As a result of it zones with a reduced temperature, compared to the background, which in October 1986 was 16-18°C, were identified. In Figure 3 and 4, these recorded areas are indicated as Offshore Groundwater Drainage (circles in green), where the measured temperature was 12-14°C. These are the places where fresh groundwater is drained, coming from the land to the sea, whose average annual temperature is of this order. A decrease in salinity to 13-14°/₀₀ was also found in these areas, with the background being 16.5°/₀₀ for this area.

On the other hand, as stated above, zones of submarine groundwater flow are known to lead to sea surface temperature anomalies by causing a thermal contrast with the ambient, seasonally normal sea surface temperature. These areas are captured by satellite sensors.

For this purpose, the ambient surface temperature of the Black Sea was calculated and mapped using publicly available data. SGD potential points are fixed by applying integrated SST data from the NASA, NOAA, ESA and EUMETSAT measurement set (GHRSST, CNR MED Sea Surface Temperature). The data are produced by the satellite radiometers infra-red measurements, their statistical interpolation and validation. The maps are prepared on the basis of gridded (0.01◦x0.01◦) GDS-2.0 daily data for the months of October 2020, 2021 and 2022 for the northern Bulgarian shelf. These represent the SST at a reference depth of 1 meter below the sea surface. These satellite estimates data are analyzed to identify cooling zones and locations where submarine drainage is expected to occur.

In the present study, only the data for the Bulgarian shelf in the Northern Black Sea were used to support the field experiment of the 1980s and to complement the offshore groundwater drainage mapping. The latter is relevant for locating the sites for pre-project geological search for water abstraction of fresh water from submarine aquifers. Figure 3 shows the area for which the locations with temperature anomalies will be studied.



Fig.3. Study area, North Bulgarian Black Sea region

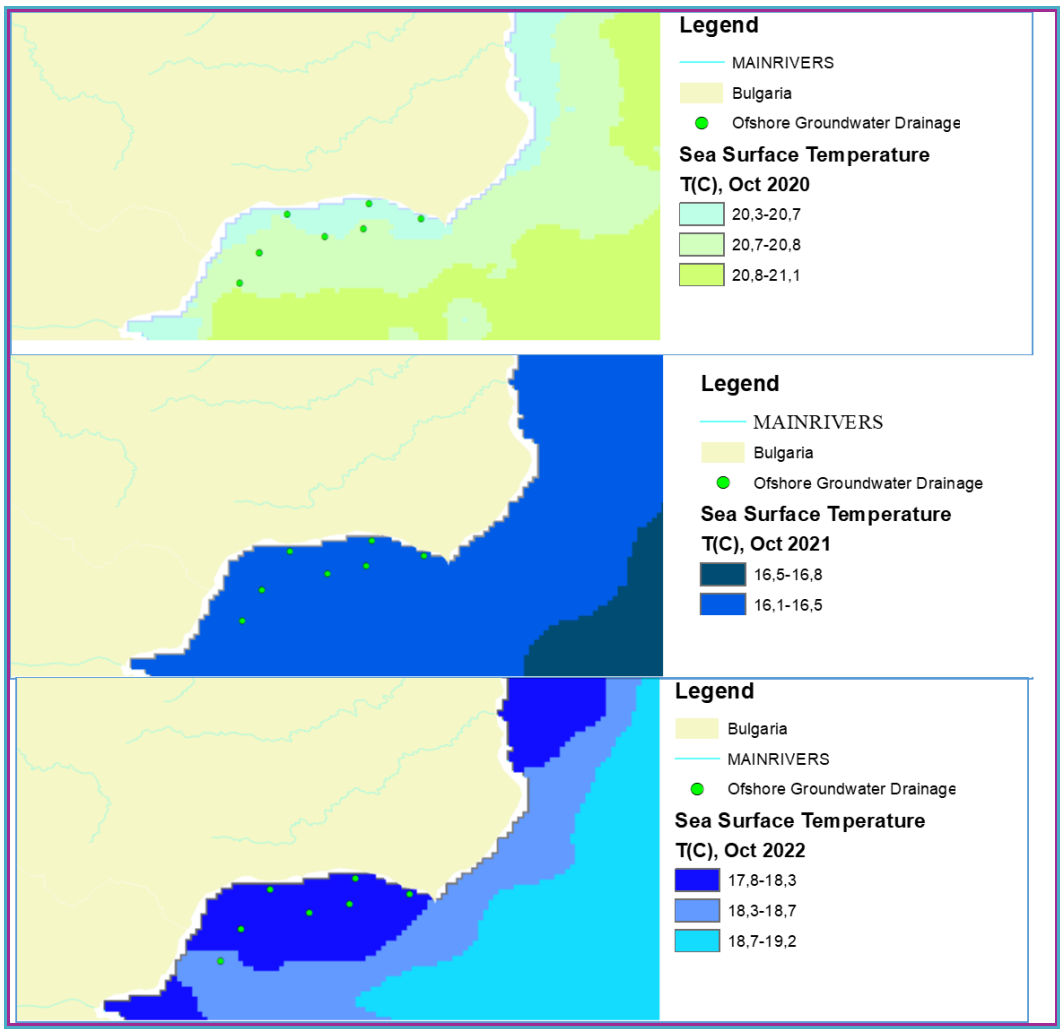


Fig. 4. Monthly average Sea Surface Temperature calculations from satellite-based

GHRSST (the Black Sea (BS), the CNR BS Sea Surface Temperature (SST)) estimates Figure 4 shows the processed results of the daily SST data for obtaining a monthly mean SST value. For the study area, the lowest sea surface temperature was in October 2021 - 16.1 °C, and the highest in October 2020 - 20.8 °C. In all three years, 2020-2021-2022, sectors of negative seafloor temperature anomalies established in 1986

(green circles in Figure 3) are covered by the zones. The satellite-estimated SST is 0.5°C lower than the adjacent sea surface waters.

The seawater temperature anomalies at places on the bottom due to Submarine Groundwater Discharge (SGD) are of the order of 4°C, while at the sea surface they are 0,5°C degrees for the studied area. It is logical and gives reason to confirm the results of the field experiment in 1986 and data from current satellite surveys as complementary and applicable to monitoring and mapping Submarine Groundwater Discharge (SGD) and hence potential Offshore Freshened Groundwater (OFG).

CONCLUSION

The presence of anomalies in the distribution of seasonal Sea Surface Temperature may be a sign of presence of continental groundwater discharges (SGD) on the seabed. The discovery of such non-conventional sources of Offshore Freshened Groundwater (OFG) near the coast are of particular interest for coastal areas with severe water shortage, as is the case in the Northern Bulgarian Black Sea. The article shows how to identify the location of such water sources by evaluating Sea Surface Temperature (SST) anomalies on the Bulgarian Black Sea shelf in the area of Dobrich-Shabla, which is designated for research.

For this purpose, a conceptual hydrogeological scheme has been prepared for the Bulgarian Black Sea watershed. State-of-the-art means of evaluating seawater temperature anomalies to reveal the location of groundwater discharges are described.

The research was carried out using the database developed by the Group for High Resolution Sea Surface Temperature (GHRSST) - the Black Sea, a high-tech product of remote sensing, for recording Sea Surface Temperature. In parallel, the data from scientific experiments for thermal profiling of the area carried out by a specially equipped scientific vessel for monitoring the seabed with negative temperature anomalies in October 1986 were considered.

The results of the two types of assessment of the region with seawater cooling anomalies are comparable and provide a reliable basis for further studies to map the potential OFGs in the area in order to help the water supply of the settlements in the coastal zone.

ACKNOWLEDGEMENTS

This publication is based upon work within the COST Action CA21112 “Offshore freshened groundwater: An unconventional water resource in coastal regions? (OFF-SOURCE)”, supported by COST (European Cooperation in Science and Technology), as well as within the National Science Programme "Environmental Protection and Reduction of Risks of Adverse Events and Natural Disasters", approved by the Resolution of the Council of Ministers № 577/17.08.2018 and supported by the Ministry of Education and Science (MES) of Bulgaria (Agreement № Д01-27/06.02.2024)

REFERENCES

[1] Bakken T., Ruden F., Mangset L.. Submarine Groundwater: A New Concept for the Supply of Drinking Water, Water Resour Manag., 2012; 26(4), pp 1015–26, https://doi.org/10.1007/s11269-011-9806-1.

[2]UN-Water-Analytical-Brief-Unconventional-Water-Resources.pdf , https://www.unwater.org/sites/default/files/app/uploads/2020/06/UN-Water-Analytical-Brief-Unconventional-Water-Resources.pdf.

[3] De Biase M., Chidichimo F., Micallef A., Cohen D., Gable C., Zwinger T. Past and future evolution of the onshore-offshore groundwater system of a carbonate archipelago: The case of the Maltese Islands, central Mediterranean Sea, Front Water, 2023, https://doi.org/10.3389/frwa.2022.1068971.

[4] Micallef A., Person M., Berndt C., Bertoni C., Cohen D., Dugan B., et al. Offshore Freshened Groundwater in Continental Margins, Rev Geophys., 2021, https://doi.org/10.1029/2020RG000706.

[5] Xing Q., Braga F., Tosi L., Lou M., Zaggia L., Teatini P., et al. Detection of Low Salinity Groundwater Seeping into the Eastern Laizhou Bay (China) with the Aid of Landsat Thermal Data, J Coast Res. ,2016, pp 149–56, DOI:10.2112/SI74-014.1.

[6] Satyaji Rao Y., Nayak S., Yenagimath G., Teeparthi V., Kumar S. Assessment of Submarine Groundwater Discharge (SGD) Zones Along the Coastal Tract of Odisha, Coastal, Harbour and Ocean Engineering, Singapore: Springer Nature; 2023, pp 443–53, DOI:10.1007/978-981-19-9913-0_33.

[7] Lino Y., Rajan A., Prabhu S., Udayashankar H., Sudharsanan R., Balakrishna K. Cost-Effective Methodology to Quantify the Submarine Groundwater Discharge from Coastal Unconfined Aquifers, Innovative Trends in Hydrological and Environmental Systems, Singapore: Springer Nature; 2022, pp 697–712, ISSN (Print)2366-2557.

[8] Raju N, Sharma K, Al R. Preliminary investigation of saline water intrusion (SWI) and submarine groundwater discharge (SGD) along the south-eastern coast of Andhra Pradesh, India, using groundwater dynamics, sea surface temperature and field water quality anomalies. Environ Sci Pollut Res. 2022 Nov 11;30:1–19.

[9] Caineta J., Thomas B., Bain D. Submarine groundwater discharge detection through remote sensing: An application of Landsat 7 and 8 in Hawai‘i and Ireland, Remote Sens Environ, 2022, https://doi.org/10.1016/j.rse.2022.113109.

[10] Jou-Claus S., Folch A., Garcia-Orellana J. Applicability of Landsat 8 thermal infrared sensor for identifying submarine groundwater discharge springs in the Mediterranean Sea basin, Hydrol Earth Syst Sci., 2021, DOI:10.5194/hess-2020-569.

[11] Schubert M., Knöller K., Stollberg R., Mallast U., Ruzsa G., Melikadze G. Evidence for Submarine Groundwater Discharge into the Black Sea—Investigation of Two Dissimilar Geographical Settings, Water, 2017, https://doi.org/10.3390/w9070468..

[12] Gasharov S., Messheteli A., Spasov V. Submarine discharge of groundwater in the North-Bulgaria Black Sea shelf. Eng.Geol. and Hydrogeol., Bulgaria, 1992, 23, 35-44. https://igh-bg.com/Vol/Vol_23_1993/Volume_23_1993_Pages_035_044.pdf.

[13] Physical Oceanography Distributed Active Archive Center (PO.DAAC), 2024, Black Sea Ultra High Resolution SST L4 Analysis 0.01 deg Resolution. Available from: https://podaac.jpl.nasa.gov/dataset/OISST_UHR_NRT-GOS-L4-BLK-v2.0.

[14] Buongiorno B., Tronconi C., Pisano A., Santoleri R. High and Ultra-High resolution processing of satellite Sea Surface Temperature data over Southern European Seas in the framework of MyOcean project. Remote Sens Environ., 2013,

[15] Dobreva P., Kartalev M., Shevyrev N., Zastenker G. Comparison of a new magnetosphere-magnetosheath model with Interball-1 magnetosheath plasma measurements, Planetary and Space Science, 53(1-3), pp. 117–125, 2005, DOI:10.1016/j.pss.2004.09.035.

[16] Dobreva P., Kartalev M., Borodkova N., Zastenker G. Comparison of GOES Magnetosphere Magnetic Field Measurements with IMECH Magnetosphere–Magnetosheath Model Predictions, Proc. of the 11th National Congress on Theoretical and Applied Mechanics, 2009, Bulgaria,

[17] Dobreva P., Kartalev M., Borodkova N., Zastenker G. Near-magnetopause magnetosheath in 3D gasdynamic module of the numerical magnetosheath-magnetosphere model, Advances in Space Research, 58(2), pp. 188-195, 2016, https://doi.org/10.1016/j.asr.2015.11.008.

[18] Bulgaria-geographic map-en.svg - Wikipedia, 2013, Available from: https://commons.wikimedia.org/wiki/File:Bulgaria-geographic_map-en.svg.

[19] Antonov Hr, Danchev D (1980) The groundwater in PRB. Technika. Sofia.

[20] Pulido-Bosch A, Lopez-Chicano M, Calaforra JM, Cal Vache ML, Machkova M, Dimitrov D, et al. Groundwater problems in the karstic aquifers of the Dobrich region, northeastern Bulgaria, Hydrol Sci J., 1999, 44(6), pp 913–27.

RELIABILITY OF PUMPING STATIONS

Dr. Eng. Tanya Igneva-Danova[1]

[1] University of Architecture, Civil Engineering and Geodesy, **Bulgaria**

ABSTRACT

In recent years the subject of reliability prediction of complex systems has become more significant because of increasing the criticality of the infrastructure. The present research refers to surveying the operation of pumping stations and problems encountered during the exploitation, as well as developing a reliability assessment methodology. The main causes of damages in pumping stations are analyzed according maintenance data from water supply and sewerage operators. Reliability assessment is based on the determination of the failure rates, as well as the application of fault tree analysis and probability theory. The criticality of the failure rates of specific components can be assessed in the design process in order to optimize reliability. The main benefit of reliability prediction is the ability to make decisions at early stage of planning and design. The proposed methodology may find application in optimization and improving the performance of water supply and sewerage pumping stations.

Keywords: pumping stations, reliability, failure rates, fault tree analysis

INTRODUCTION

Reliability prediction is the process of calculating expected reliability, availability, maintainability and resilience, as well as determining failure rates of system components. It provides a quantitative measurement of how closely the proposed design model meets the project objectives and allows a comparison to be made between different alternative solutions. Determining reliability gives early indications of the system's potential to meet design reliability requirements and also facilitates the estimation of life-cycle costs. It facilitates identifications which components in the design contribute to the main part of the reliability, moreover contributes to achieving desired reliability.

Reliability may be assessed quantitative or qualitative. Quantitative assessment is based on component failure rates that are predicted and compared to the target. Measures are taken to reach this value. Qualitative assessment aims to minimize the occurrence of system failures (e.g. power supply problems, pump failures, electric motor failures, cavitation, water hammer) by implementing a range of protections that are appropriate for the complexity of the system.

MATERIALS AND METHODS

In the present paper reliability is being assessed using the parameter failure rate [1]. Failure rate is defined for a certain period of life time of an element of the technical equipment as the ratio of the total number of failures to the total cumulative observed time. If with λ is denoted failure rate of N elements then:

$$\lambda = \frac{k}{T}$$

where k is the number of failed elements, T is the cumulative time. The cumulative time is given by:

$$T = N.t$$

for the case that each failure is replaced. For the case of non-replacement of each failure element, T is given by:

$$T = (t1 + t2 + t3 + \cdots \ldots . tk + (N - k).t)$$

where $t1, t2$, …., tk is the occurrence of each failure.

Failure rate has the unit of t^{-1} and for the purposes of the present development, a unit of measurement is adopted times per year.

The probability of survival to time t has been defined as the reliability – R(t):

$$R(t) = e^{-\lambda t}$$

Some basic rules are used for assessing the reliability of pumping stations. For serial system of elements, the next formula is used [1]:

$$R_n = \exp\{-(\lambda_a + \lambda_b + \cdots .. + \lambda_n).\mathrm{t}\}$$

In series systems any single failure causes a system failure. Serial elements are considered to be check valves and gate valves.

In systems with N redundant (parallel) elements the next formula is used [1]:

$$R_{system} = 1 - (1 - R_a).(1 - R_b) \ldots (1 - R_n)$$

In system with redundancy all elements may fail except one. Usually in pumping station design pumps are considered to work in parallel. In that case all elements may fail except the last item.

Failures in a pumping station can be both mechanical and electrical, as well as due to hydraulic problems. The generalization of the most frequent failures is based on a survey of the operation of an existing station, as well as the direct collection of information from the operating personnel.

Data collection for reliability assessment is challenging due to the lack of accurate records of failures that occur and their frequency of occurrence. This paper covers data of a water supply pumping station and the observed failure rate of its individual elements over a period of 5 years. The provided failure records are pre-analyzed, eliminating causes of failures that do not involve the main equipment in the pumping station. For example, damages to the lighting system in the building, damages to the ventilation system of the machine room and others are excluded, since these damages do not directly affect the

operation of the facility. Thus, only the part of the data that relates to the direct operation of the pumping station was used.

Some of the failures have no data records because the failures were repaired without a record being kept. In this case, the accident was not considered significant and was therefore not reported. For the current stage of development, it is considered that the available data is sufficient to perform an assessment of the reliability of the pumping station. For a future stage, it is recommended that more accurate records be kept in order to be able to make a full assessment against all pre-selected criteria.

The following table presents the most common possible failures [2] that occur during the operational life of pumping stations (Table 1).

Table 1 Possible failures in pumping stations

	Possible failures
1	Mechanical failure in the pump
2	Engine failure/Insufficient engine power
3	The pump does not create a vacuum
4	Breakdown along the suction pipeline
5	Breakdown along the pressure pipeline in the pumping station
6	Increased suction height
7	Incorrect direction of rotation of the impeller
8	Pump seal failure and leakage
9	Increased manometric height
10	Formation of air pockets in the suction and pressure pipeline
11	Wear of impeller blades
12	Insufficient rotation frequency of the impeller
13	Emergency discharge of water from the pressure pipeline
14	Cavitation regime of the pump
15	Mechanical damage
16	Loosening of pipe fittings in machine room
17	Control and data system problems
18	Power supply problems
19	Failure of water hammer protection
20	Other failures

For pump seal failure, leakage and increased manometric height there usually are no recorded data. Other failures such as formation of air pockets in the suction and pressure pipeline and cavitation regime of the pump are relatively common and the operating personnel takes measures to eliminate the causes at the moment, and this is not documented. The most common failures are due to breakdown along the suction pipeline, as well as a sudden interruption of the power supply, which can lead to water hammer. The next most frequent ones are pump failures, including wear of the impeller vanes, as well as electric motor failures.

The equipment in the pump station selected for the model consists of 3 separate suction pipelines (SP1, SP2, SP3), 3 pumps (P1, P2, P3) with electric motors (E1, E2, E3). Three check valves (CHV1, CHV2, CHV3) and 3 gate valves (GV1, GV2, GV3) are mounted after the pumps. The separate pressure pipes after the pumps are short and that's the reason they are neglected. The joint pressure pipeline (PP) has a water hammer protection (WHP) installed. The electrical power supply (ES1, ES2) is provided by two independent sources, the control system is SCADA (Supervisory Control and Data Acquisition). For the purposes of calculations, damage to auxiliary equipment (e.g. additional drainage pumps, vacuum pumps, etc.) is not considered.

As a first step Fault Tree is used with failure rates for the individual enabling events. Further on is applied FMEA (Failure Mode and Effect Analysis). FMEA consists of defining the overall failure modes and then defining the contribution of each component. Some authors [3] also prefer using that technique. Other authors [4] prefer to use hybrid neural networks genetic algorithm and method of moment for reliability assessment. In the present paper Failure Mode and Effect Analysis is adopted because of the ability to model complex systems with different types of elements and the possibility to use automation of calculations.

Two specific models have been assessed (Mode 1 and Mode 2). Cutset is given to each model. Cutset ranking involves listing in ranked order according to the contribution to top event. For each model the overall failure rate is 50% for pump because defecting of the pump is assumed as a main event. The second most important are failures in the suction pipeline and the electric engine. Damages to check valves and gate valves are determined to be the least serious. The pumping station has the possibility to switch to manual control mode, and this is the reason why SCADA has a weight of 10%.

RESULTS

Automation of calculations enables to consider different scenarios for the contribution of each element to the reliability of the whole system. The results are automatically generated as a file. The following table (Table 2) presents the results of the calculations for the reliability of the pumping station for Mode 1 and Mode 2.

Table 2 Calculated reliability for Mode 1 and Mode 2 models

Pumping station type MODE 1/MODE2		Water supply						
Component name	Component Ref	Failure rate	Total failure rate	Reliability	Failure Mode 1 Factor	Failure Rate Mode 1	Failure Mode 2 Factor	Failure Rate Mode 2
Suction pipeline	SP1	0.1	0.3	0.741	50%	0.15	30%	0.15
Suction pipeline	SP2	0.1	0.3	0.741	50%	0.15	30%	0.15
Suction pipeline	SP3	0.1	0.3	0.741	50%	0.15	30%	0.15
Pump	P1	0.02	0.02	0.980	50%	0.01	50%	0.25
Pump	P2	0.02	0.02	0.980	50%	0.01	50%	0.25

Pump	P3	0.02	0.02	0.980	50%	0.01	50%	0.25
Engine	E1	0.03	0.03	0.970	40%	0.012	50%	0.2
Engine	E2	0.03	0.03	0.970	40%	0.012	50%	0.2
Engine	E3	0.03	0.03	0.970	40%	0.012	50%	0.2
Check valve	CHV1	0.05	0.15	0.861	20%	0.03	50%	0.1
Check valve	CHV2	0.05	0.15	0.861	20%	0.03	20%	0.04
Check valve	CHV3	0.05	0.15	0.861	20%	0.03	20%	0.04
Gate valve	GV1	0.045	0.135	0.874	20%	0.027	20%	0.04
Gate valve	GV2	0.045	0.135	0.874	20%	0.027	20%	0.04
Gate valve	GV3	0.045	0.135	0.874	20%	0.027	20%	0.04
Pressure pipe	PP	0.07	0.07	0.932	40%	0.028	50%	0.2
Water hammer protection	WHP	0.0056	0.0056	0.994	30%	0.0017	20%	0.06
Electrical power supply	ES1	0.1	0.1	0.905	50%	0.05	75%	0.375
Electrical power supply	ES2	0.1	0.1	0.905	50%	0.05	50%	0.25
SCADA	SCD	0.006	0.006	0.994	10%	0.0006	10%	0.01
MODE 1								
Reliability	**0.876**							
MODE 2								
Reliability	**0.889**							

The calculated reliability in the first case is 0.878 and in the second case it is 0.889. In the second case, the reliability of the pumping station is obtained with a higher value due to the assumptions made. In addition, more scenarios can be calculated depending on the objectives of the analysis.

DISCUSSION

The proposed methodology for determining the reliability of pumping stations includes a thorough analysis of the interconnections of individual elements. In this case, data from one pumping station was used, and it was not possible to assess the reliability of the data used in the models more fully. The obtained results show that the applied models allow the evaluation of pumping stations. Also, it is possible to use the methodology in different scenarios depending on the adopted cutsets.

In the future, the operation of more pumping stations shall be analyzed, including those that are due for rehabilitation and equipment replacement. If possible, the replacement of equipment will be connected with calculation of future reliability and investment costs.

CONCLUSION

In this article, a methodology for assessing the reliability of pumping stations is proposed. Data from a test facility operated by a water supply and sewerage operator were used. According to the data collected, there is a lack of sufficient accountability for operational problems. If water supply and sewerage utilities improve reporting, a full and detailed analysis of the reliability of the pumping stations they operate can be progressed. The improvement of the control and management processes of the pumping stations includes the collection of initial information on the condition of the equipment, as well as data on the damage that has occurred for a period of at least 5 years. The proposed methodology for reliability assessment makes it possible to compare the performance of facilities for a certain period back in time. After measures have been taken to reconstruct and install additional protections or duplicate elements, it is possible to determine the new reliability. It is possible already in the design process to determine a level of project reliability and to set certain equipment against it. In this way, it will be possible to plan both construction costs and operating costs.

REFERENCES

[1] Smith D.J., Reliability, Maintainability and Risk: Practical Methods for Engineers, Seventh Edition, ISBN 0 7506 6694 3, Elsevier, UK, 2005;

[2] Slavov M., Arsov R., Draganov D., Kostakeva E., Pumps and pumping stations (in Bulgarian), Technika, Bulgaria, 1989;

[3] Briggs E.K., Hodkiewicz M., Maintenance and reliability of a water pumping station, 9th International Conference of Maintenance Societies, ICOMS-2005, 2005;

[4] Piri J., Pirzadeh B., Keshtegar B., Givehchi M., Reliability analysis of pumping station for sewage network using hybrid neural networks - genetic algorithm and method of moment, Process Safety and Environmental Protection, ISSN 0957-5820, UK, Volume 145, Pages 39-51, January 2021.

RETENTION-BASED SOLUTIONS FOR OUTFALL REDUCTION

Assistant Prof. Dr. Marcell Knolmar[1]

Sandor Szel[2]

[1] Budapest University of Technology and Economics, **Hungary**
[2] VITUKI Hungary Ltd., **Hungary**

ABSTRACT

The discharge emanating from a municipal wastewater treatment plant (WWTP) is a contributing factor to the pollution load within the adjacent natural water body. Generally, effluent constraints can be upheld during periods of dry weather. Nonetheless, instances of surpassing these limitations are common during storm events due to the substantial surge in inflow. The retention of incoming stormwater presents an opportunity to mitigate both quantitative and qualitative concerns. However, the spatial and financial prerequisites for constructing such facilities necessitate comprehensive deliberation.

Hydrodynamic simulations utilizing EPA Storm Water Management Model (SWMM) were conducted for the network model encompassing the catchment area of the WWTP. This aimed to assess the efficacy of retention-based measures implemented at the wastewater treatment facility and its associated catchment, utilizing extensive historical rainfall data. Various strategies, including network extensions such as storage tanks, and leveraging existing infrastructure for inline storage, were scrutinized and compared based on their impact on overflow occurrences.

The findings underscore the considerable reduction in overflow volumes achieved through the proposed solutions. Nonetheless, they also serve to facilitate an estimation of the retention system's influence on water quality within the receiving water body.

Keywords: WWTP, stormwater, retention, inline storage, SWMM

INTRODUCTION

The introduced retention solutions are closely linked to wastewater treatment. Located adjacent to a natural water body, the municipal wastewater treatment plant (WWTP) releases its treated effluent into this specific part of the river. The observed water quality problems in the receiving water body prompted an evaluation of the WWTP and its catchment. The primary goal is to reduce the untreated discharge into the receiving water body. Furthermore, it is important that the solutions implemented do not have a detrimental impact on the urban catchment area.

The entire catchment area of the WWTP exhibits characteristics of a mixed system. In this context, the newly developed areas, approximately 70% of whole catchment function as separate sanitary sewer systems, while the older urban regions operate as a combined system. Stormwater collected from the new areas is directly discharged into the receiving waters. Meanwhile, all wastewater collected, including both sanitary sewage and stormwater, is channeled into the wastewater treatment plant. The WWTP

https://doi.org/10.5593/sgem2024/3.1/s12.22

employs traditional biological treatment methods and typically functions effectively during dry weather conditions. However, during storm events, the combined sewer system carries a significant volume of diluted, mixed rainwater and sanitary sewage. Furthermore, the separated sanitary system also receives stormwater, primarily through street manholes and unauthorized house connections, which include rainwater roof runoff.

The primary overflow structure ("Main CSO") located at the plant's inlet (see Fig. 1) is intended for separating stormwater from sanitary sewage. The design of the fixed weir level was aimed at achieving a 3x dilution value. However, the "rainwater portion" still contains a notable level of contamination. Consequently, the effluent limits are often not met due to the substantial volumes of stormwater that enter the system.

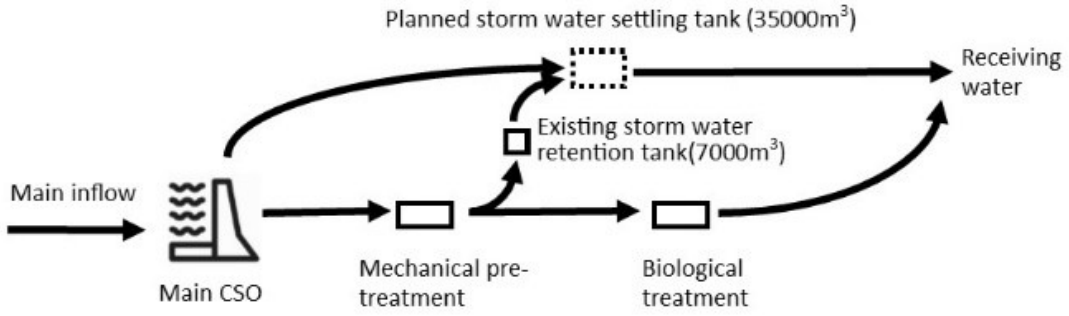


Fig. 1 Schema of the retention system

The proposed stormwater settling tank at the WWTP has a storage capacity of 35,000 m^3. This structure is designed not only for storage but also for settling processes to separate the denser solid particles from the sewage. The separated sanitary portion, which is diverted from the main CSO, proceeds to the biological treatment. After undergoing a preliminary mechanical treatment, a retention tank with an extended capacity of 7,000 m^3 has been in operation recently. The water levels in the retention tank have been engineered to limit the flow to the biological treatment at a specified value. Any surplus water is directed to fill the retention tank. Excess water now flows directly from the retention tank into the receiving water. According to the intended operation, it will flow into the 35,000 m^3 settling tank. The volume of the settling tank was initially determined through manual calculations.

The alternative solution for reducing the effluent at the WWTP is suggested further upstream in the sewer network of the subcatchment. In Fig. 2, which depicts pipe diameters using varying line thickness, you can observe the main collector (D=2.65m) situated in the middle of the combined sewer catchment. operates at nearly 100% capacity. However, there are larger diameter sections, like the "Relief branch" (D=1.65m) that still have capacity. The "Relief branch" operates with a utilization of less than 50%.



Fig. 2 Simulated inline storage system: relief branch (yellow) and weirs (red)

The "Relief branch" appears to be a promising location for inline storage i.e. exploiting the existing inline storage capacity. As shown in the longitudinal profile in Fig. 3, weirs installed on this branch could create a significant storage volume upstream.

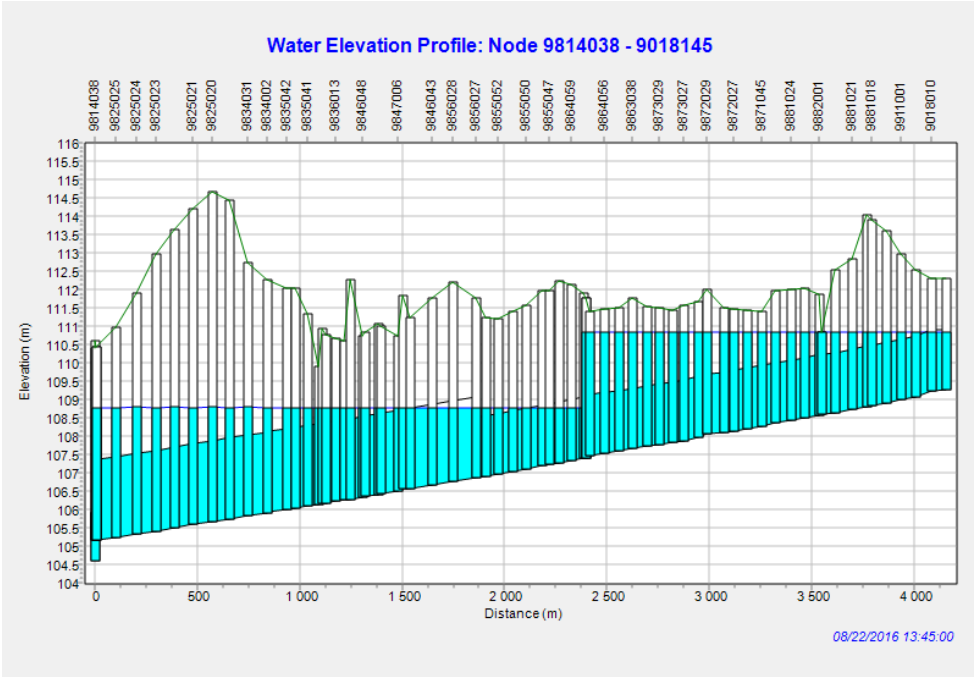


Fig. 3 Longitudinal profile of "Relief branch" with 2 weirs

Of the various attempted versions, the solution depicted in Fig. 2 incorporates weirs at 2 locations in the model. The highlighted section of the "Relief branch" indicates where water levels have risen.

https://doi.org/10.5593/sgem2024/3.1/s12.22

We have incorporated a simplified weir control mechanism into the model to showcase the reservoir's operational efficiency when functioning as a sluice gate:

- The weir closes completely when the water level above the weir rises above the dry weather level (at the beginning of rain event).
- The weir opens completely when the water level above the weir reaches the critical (flooding) level.
- The weir opens a few hours after the rain event.

MATERIALS AND METHODS

Other experiences

Stormwater detention in urban drainage has been the subject of extensive research, particularly concerning issues related to both water quality and quantity [1] [2] [3]. The impact of precipitation on water received at a WWTP was also investigated [4].

Valuable papers released about the impact of water resource management on climate change [5] [3] including recommendations for urban water problems.

Numerous publications [6] [7] have focused on mitigation techniques for urban flooding. Hydrodynamic models are frequently employed for runoff simulations, with the EPA Storm Water Management Model (SWMM) recognized as an effective tool for simulating water quality runoff from urban catchments [7] [8].

Despite some overlapping research, this paper's comprehensive analysis of the retention solutions for a WWTP addresses a gap in the existing body of literature.

Long-term simulations

The subcatchments of the WWTP were delineated using sewer network data. These data, made publicly available for design purposes, were provided by the electronic public work service in the form of shape files.

Rainfall data was obtained from the national meteorological institute, provided at 2km x 2km grid points and hourly resolution. In total, 35 points were selected to capture the spatial variability of rainfall distribution.

The sewer conduits were imported into the SWMM hydrodynamic simulation program [9]. To account for external rainwater entering separate sanitary sewers, small rainwater subcatchments were defined for each manhole. The sizes and other properties of these subcatchments were calibrated using flow measurements at the WWTP during rain events.

For more detailed dynamic analysis of storm events, we employed the SWMM simulation model. Specifically, we chose the dynamic wave model within SWMM, as it can provide the most accurate results by solving the complete Saint-Venant continuity and momentum equations.

Long-term simulations were conducted over a one-year period, utilizing available data on the operation of the WWTP. The model was initially calibrated using available observed daily flow volumes. In this calibrated model, we introduced the extension of the retention tank, the new settling tank, and the inline storage. The simulation results

offered comprehensive insights into the functionality of these newly designed components.

RESULTS

Settling Tank

From the dataset spanning a whole year, we focused on the month with the highest total effluent volume, which was July 2016. Precipitation during this month was exceptionally high, with a total of 140 mm. Consequently, the total overflow during this period was also extraordinary, reaching approximately 678 000 m^3.
Fig. 4 and 5 illustrate the retention effects of the storage tanks. The currently operating smaller retention tank at the WWTP exhibits capability to reduce even smaller rainfall events, whereas the larger settling tank can effectively eliminate them. The settling tank more significantly attenuates the ascending portions of the inflow. To highlight this, the outflow has been placed in front of the main inflow. Additionally, the biologically treated effluent flow approaches the maximum capacity of the plant during these events.

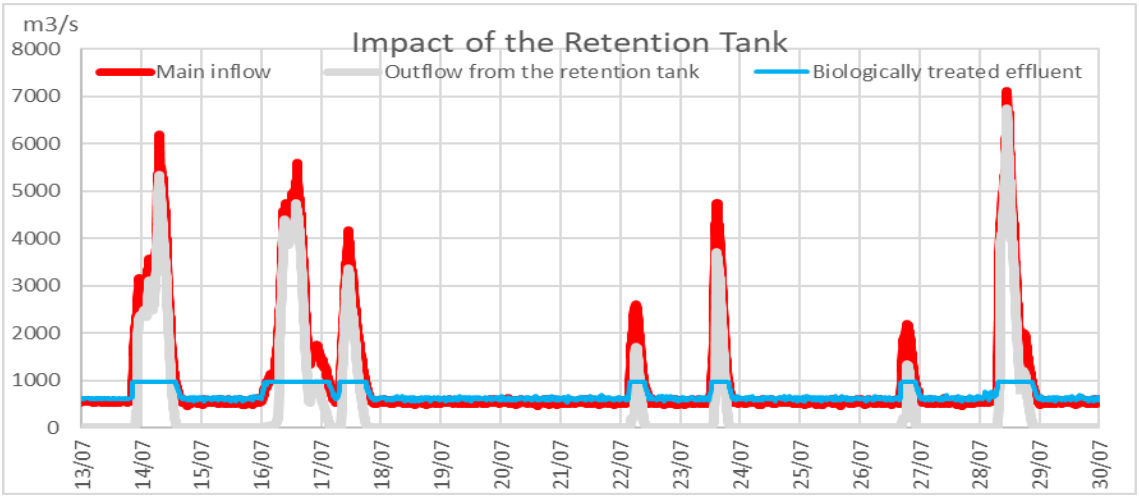


Fig. 4 Impact of the retention tank, July

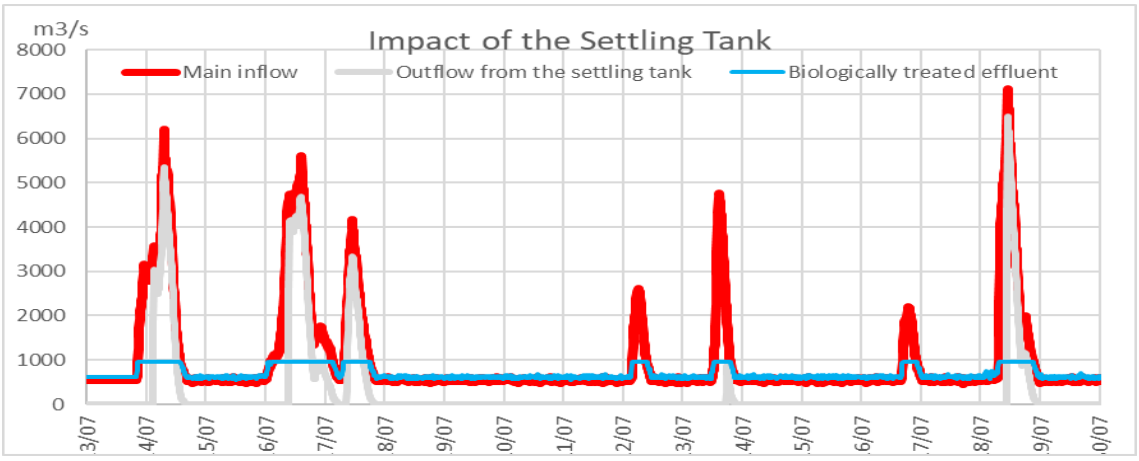


Fig. 5 Impact of the settling tank, July

Inline Storage

From the several simulated versions the selected inline storage is including 2 weirs on the “Relief branch”. One at the lowest point of the "Relief" branch and the other in the middle section (Fig. 2). The resulting water levels along the longitudinal section can be observed on Fig. 3.
In order to demonstrate the effect of inline storage, we selected one high precipitation event with 38mm of rain that occurred on August 22, 2016.
In the flow rate time series (Fig. 6) prepared for the section of the main collector just before the inflow to the wastewater treatment plant, where the effects of the "Relief pipe” storage are already included.

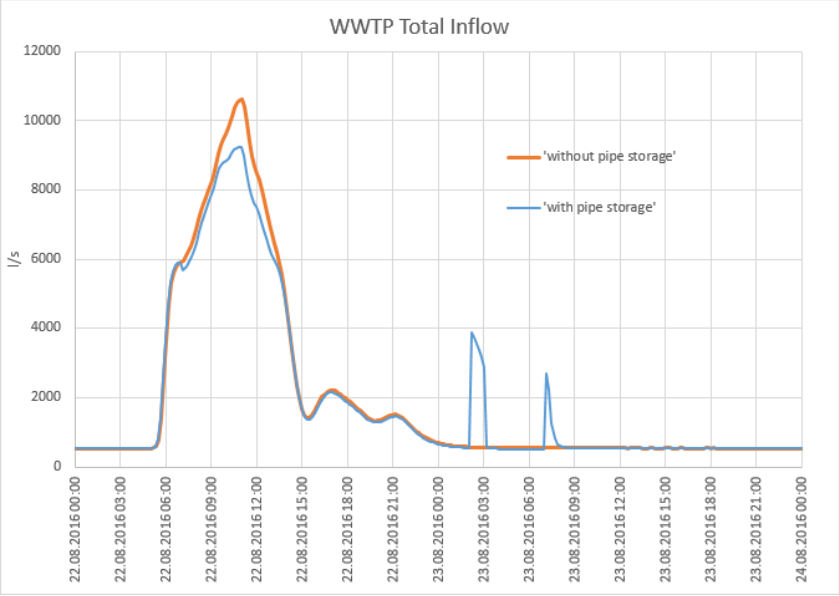


Fig. 6 Inflowing flowrates at the WWTP

It's evident that the peak flow rate, which exceeds 10 000 l/s in the baseline condition, is reduced to only 9 000 l/s, with the peaks observed at 03:00 and 07:00 attributed to the opening of the inline storage weir for the purpose of calculating the volume of stored water.
The discharge volume reduction effect of the 2-weir inline storage is about 13 000 m^3. It is in a similar order of magnitude as the 35 000 m^3 stormwater reservoir of the wastewater treatment plant. Therefore, the solution can significantly reduce peak flow levels, by 10-15%.
The 2-weir version is not causing surface flooding while utilizing the available capacity of the "Relief" branch. In addition to the versions described, we examined several other variations with different locations and weir control strategies. These versions were manually generated based on our hydrodynamic simulation experience. Even more efficient inline storage can be achieved through the application of automated optimization, preferably using some form of artificial intelligence algorithm.

Comparing the Solutions

We carried out a 1-year long simulations for 2016. The reference simulation was done for the 2016 state of the WWTP. Both the 35 000 m^3 settling tank and the inline storage solutions for the possible retention developments were simulated. The overall results of overflows are summarized in Table 1.

Table 1 Overflow volumes with different developments

	Without new developments	With a new 35 000 m³ settling tank	Reduction rate of settling tank, %	With inline storage	Reduction rate of inline storage, %
Overflow volumes, m³	2 687 443	1 632 238	39	2 559 562	5

DISCUSSION

As expected, the settling tank has the potential to diminish the peak intensity of flood waves resulting from storm events. However, the effects of inline storage were less noticeable, given its distinct parameters such as operational methods, volume, and location, which differ significantly from those of conventional storage tanks.

The impact of the simulated solutions on the catchment area may also raise certain inquiries. They align with the sewer service company's requirement to maintain sufficient velocity in the pipe system for self-cleaning. In the case of the settling tank, the entire network remains unchanged. As for the inline storage solution, the velocities in the majority of the network remain unaffected, as the "Relief branch" used for inline storage is situated at the lower part of the network. The natural cleaning function of rainfall continues to operate on the entire catchment surface because the proposed solutions do not reduce surface runoff. The cooling effect of storms during hot periods remains consistent. Furthermore, there is no reduction in infiltration into the ground. The overall effect of the proposed solutions on the entire subcatchment is relatively minor, but the impact on reducing pollution in the receiving water body is significant.

The reduction of the initial part of flood waves is particularly crucial due to the "first flush" phenomenon. At the onset of storm events, the concentrations of various pollutants can rapidly increase. According to published research [8] [10], the maximum pollutant concentration precedes the peak of runoff flow. Our simulations exhibit a symmetrical triangular flow shape, with the peak slightly preceding the midpoint. These findings support other research that suggests around 70-80% of pollutants arrive in the first 50% of the inflow volume. As a result, the pollutant reduction effect of the introduced retention solutions can be even more significant than that of the flow reduction.

CONCLUSION

Based on the retention simulations, it is evident that the operation of both the settling tank and inline storage results in a substantial reduction in outflow load. The differing reduction rates (Table 1) are primarily a consequence of their volumes. The settling tank receives the entire amount from the catchment, while the storage pipe is located upstream on the relief branch. The operation of the inline storage on the existing branch requires much fewer investments than the construction costs of the settling tank.

These storage and settling processes enable more efficient further biological treatment of the reduced flood volumes. Additionally, the quality of the effluent can be further enhanced by removing sedimented sludge from the bottom of the storage spaces.

https://doi.org/10.5593/sgem2024/3.1/s12.22

It is recommended to fine-tune the control strategy for both proposed solutions. Implementing a gradual and delayed opening of weirs can help mitigate the tail of the flood wave. Additionally, a faster emptying of the settling tank can prepare it for the next incoming flood event.

ACKNOWLEDGEMENTS

The research presented in this article was carried out with the support of the RRF-2.3.1-21-2022-00008 project, by the National Research, Development and Innovation Office.

REFERENCES

[1] Klosok-Bazan I., Boguniewicz-Zablocka J., Nowak R., Gono M., Rainwater retention and use as an important element of sustainable water management in urban areas, International Multidisciplinary Scientific GeoConference SGEM, Bulgaria, vol.23/issue 3.1, 2023.

[2] Mourad M., Bertrand-Krajewski J. L., Chebbo G., Design of a retention tank: comparison of stormwater quality models with various levels of complexity. Water Science and Technology, United Kingdom, vol. 54/issue 6-7, pp 231–238, 2006.

[3] Tsakiris, G. P., Loucks D. P., (2023) Adaptive Water Resources Management Under Climate Change: An Introduction, Water Resources Management, Netherlands, vol. 37, pp 2221–2233, 2023.

[4] Yoda T., Effect of precipitation on received water at a sewage treatment plant, International Journal of Environmental Science and Technology, Germany, vol 19/issue 5, pp 3889-3896, 2021.

[5] Bozorg-Haddad O., Climate Change in Sustainable Water Resources Management, Springer Water, Singapore, 2022.

[6] Freni G, Oliveri E., Mitigation of urban flooding: A simplified approach for distributed stormwater management practices selection and planning, Urban Water Journal, United Kingdom, vol.2/issue 4, pp 215-226, 2005.

[7] Safari A., Abbaspour M., Javid A. H., The application of multi-criteria (AHP-PROMETHEE) decision-making methods in selecting and prioritizing the green area irrigation resources, International Journal of Environmental Science and Technology, Germany, vol. 18/issue 5, pp 1135–1146, 2021.

[8] Langeveld J., Daal P. V., Schilperoort R., Nopens I., Flameling T., Weijers S., Empirical Sewer Water Quality Model for Generating Influent Data for WWTP Modelling, Water, Switzerland, vol. 9/issue 491, 2017.

[9] Rossmann L. A., EPA Storm Water Management Model Reference Manual, Volume II – Hydraulics, United States, 2017.

[10] Barco J., Papiri S., Stenstrom M. K., First flush in a combined sewer system, Chemosphere, United Kingdom, vol. 71/issue 5, pp 827-833, 2008.

THE IMPACT OF WASTEWATER EMISSIONS ON THE HEALTH OF THE POPULATION OF BUKHARA (UZBEKISTAN)

Prof. Dr. Alexander Vorobyov [1]

PhD Ress. Kirill Vorobyev [2]

Prof. Dr. Shukhrat Teshaev [3]

Prof. Dr. Zhamaletdin Mamasaidov [4]

Assoc. Prof. Dr. Tatiana Chekushina [5]

[1] Grozny State Petroleum Technical University, **Russian Federation**
[2] RUDN University, **Russian Federation**
[3] Bukhara State Medical Institute, **Uzbekistan**
[4] Ferghana Institute of Public Health, **Uzbekistan**
[5] Institute of Comprehensive Exploitation of Mineral Resources Russian Academy of Sciences, **Russian Federation**

ABSTRACT

Water pollution from untreated wastewater discharge is a major public health concern in the ancient city of Bukhara, Uzbekistan. The city lacks adequate wastewater treatment facilities, leading to the release of contaminated water into the environment. This has resulted in the deterioration of water quality in local water bodies, posing serious risks to human health.

One of the primary sources of pollution is the discharge of domestic and industrial wastewater into the Shavkat aria canal, which flows through the city. The canal water is used for irrigation purposes in surrounding agricultural areas, facilitating the spread of waterborne diseases. Microbiological and chemical analyses have revealed alarmingly high levels of pathogens, heavy metals, and other pollutants in the canal water.

The inadequate wastewater management system has led to an increased incidence of waterborne diseases, such as acute intestinal infections, viral hepatitis A, and typhoid fever, among the local population. Children are particularly vulnerable due to their higher exposure and weaker immune systems.

Addressing this issue requires urgent action, including the construction of modern wastewater treatment facilities, enforcement of environmental regulations, and public awareness campaigns on proper sanitation practices.

Keywords: water pollution, wastewater treatment, public health, environment, Bukhara

INTRODUCTION

Water is a vital resource for humanity. Therefore, access to safe and clean drinking water is a fundamental right for all people, regardless of their nationality, religion, skin color, language or wealth. At the same time, fresh clean water is already a limited

resource that is not provided for many people in many parts of the world. Thus, more than 80% of wastewater generated as a result of man-made human activities is discharged into rivers and oceans without any pre-treatment, which leads to both significant environmental pollution and the emergence of more than 50 types of various human diseases. Moreover, 80% of diseases and 50% of child deaths worldwide are associated with poor drinking water quality.

It is believed that drinking water should contain a minimum amount of some essential minerals (and other components, for example, such as carbonates), but no more. Polluted drinking water and poor sanitary living conditions are usually associated with the occurrence of diseases such as cholera, diarrhea (Campylobacter jejuni bacteria alone is responsible for 4-15% of the spread of diarrhea worldwide, and in general about 2 million people die from this disease annually), dysentery and polio.

MATERIALS AND METHODS

1. Water sampling and analysis:
   - Collect water samples from the Shavkat ariq canal and other local water bodies at multiple locations.
   - Conduct microbiological analyses to determine the presence and levels of pathogens, such as bacteria, viruses, and protozoa.
   - Perform chemical analyses to measure the concentrations of heavy metals, organic pollutants, and other contaminants.
2. Health data collection:
   - Obtain data on the incidence of waterborne diseases, such as acute intestinal infections, viral hepatitis A, and typhoid fever, from local healthcare facilities.
   - Gather demographic and socioeconomic data related to the affected population.
3. Geographic Information System (GIS) mapping:
   - Utilize GIS software to map the spatial distribution of water pollution levels and the incidence of waterborne diseases.
   - Identify hotspots and potential correlations between water pollution and disease prevalence.
4. Community surveys and focus group discussions:
   - Conduct surveys and focus group discussions with local residents to assess their awareness, attitudes, and practices regarding water usage, sanitation, and hygiene.
   - Gather information on the socioeconomic impacts of water pollution and waterborne diseases.

The reasons for the change in the chemical composition of natural waters in the territory of the Bukhara region. Pollution of natural waters is mainly associated with ongoing industrialization (contributing to the supply of arsenic, cadmium and chromium) and agricultural activities (polluting with nitrates, phosphorus compounds, salts, pesticides and pathogens), some natural factors (for example, volcanic activity, etc.), as well as insufficient water supply and treatment facilities (or their poor quality of purification waste water).

The redistribution of various substances with river and man-made runoff is observed all over the world [1-10].

The southern part of the lower reaches of the Zeravshan basin is occupied by irrigated lands of the Bukhara region, the total area of which currently amounts to 275 thousand hectares, the water intake for irrigation is up to 4.8 km^3/year.

The lands of this oasis are irrigated by the waters of the Zeravshan rivers (by gravity, 1.1 km^3/year) and the Amu Darya (supplied by pumps through the Amu–Bukhara Canal, built back in 1965).

At the same time, 225 thousand hectares of lands of the Bukhara region are drained by a specially built collector–drainage network (open trunk and inter–farm collectors – 2,690 km, on–farm collector and drainage network of open and closed type – 4,692 km, as well as vertical drainage wells).

Previously, waste waters (with a volume of 2.61 km^3, containing 9.15 million tons of salts, with a specific average mineralization of 1.70-1.97 g/l, bicarbonate–chloride–sulfate–magnesium–sodium–calcium composition) were diverted to a drainless depression, where on their basis the natural lake Dengizkul was increased (which became man–made), and Currently, they are sent to the Main Water discharge tract and further along the Parsankul discharge are diverted to the Amu Darya River.

As a result, the entire territory of the Bukhara region can be differentiated by the mineralization of the used and drained waters. Water quality is determined by the following main indicators:

- biological impurities (such as bacteria, viruses, parasitic protozoa and phytoplankton);
- mineral impurities that have an indirect effect on human health (such as turbidity – the average turbidity value recommended by WHO should not exceed 5.00 NTU, color, mineralization – the maximum limit prescribed for drinking purposes is 1000 mg/l, some transition metals, ammonium and some dissolved gases);
- mineral impurities that have a significant impact on human health (such as heavy metals, oxidized forms of nitrogen, barium, boron, arsenic, lead, selenium, antimony and fluorine);
- organic impurities: total organic carbon, in all carbonaceous organic substances present in water;
- organic micro-pollutants (pesticides, polychlorinated biphenyls, detergents, hydrocarbons, chlorinated solvents, etc.), as well as new chemicals and compounds that lead to endocrine system disorders (pharmaceutical residues, chemicals, etc.);
- radioactive elements.

The relationship between the composition of waters and the health of the population of the Bukhara region. The World Health Organization (WHO) estimates that up to 80% of all human diseases and ailments in the world are caused by inadequate sanitation, contaminated water or lack thereof.

The different mineralization of natural and man-made waters (in terms of specific content and composition) significantly affects the health of the population of the Bukhara region.

At the same time, it is initially necessary to have up-to-date data on the quantitative and qualitative composition of residents of the Bukhara region. So, as of 2023, the number of permanent residents of the Bukhara region amounted to 2016.6 thousand people. Of

this, the population of the city of Bukhara is 743 thousand people, and the rural population is 1273400 people.

Mortality rates in various localities are also important for analyzing the impact of water composition on the health of the population of the Bukhara region.

Since the death of people in the population occurs for various reasons, it is necessary to take this circumstance into account.

RESULTS

The water analyses revealed alarming levels of pollution in the Shavkat ariq canal and other local water bodies. The microbiological analyses detected high concentrations of fecal coliforms, Escherichia coli, and other enteric pathogens, exceeding the acceptable limits for safe water quality. Chemical analyses found elevated levels of heavy metals, including lead, cadmium, and chromium, as well as organic pollutants, such as pesticides and industrial solvents.

The highest levels of pollution were observed in the sections of the canal passing through densely populated residential areas and industrial zones, where untreated wastewater is directly discharged into the canal. The pollution levels were significantly lower in the upstream sections of the canal, indicating that the primary source of contamination is the discharge of untreated wastewater.

Epidemiological data collected from local healthcare facilities showed a direct correlation between the incidence of waterborne diseases and the proximity to the polluted water bodies. Areas located near the heavily polluted sections of the canal reported higher rates of acute intestinal infections, viral hepatitis A, and typhoid fever, particularly among children.

DISCUSSION

The results of this study clearly demonstrate the severe water pollution crisis in Bukhara, caused by the discharge of untreated wastewater into local water bodies. The high levels of pathogens and chemical pollutants in the water pose a significant risk to public health, particularly for vulnerable populations such as children and the elderly.

The lack of adequate wastewater treatment facilities is the primary driver of this pollution problem. The direct discharge of untreated domestic and industrial wastewater into the Shavkat ariq canal and other water bodies has led to the accumulation of pollutants, rendering the water unsafe for irrigation and other purposes.

The observed correlation between the incidence of waterborne diseases and proximity to polluted water bodies highlights the urgent need for action. Immediate measures must be taken to address this public health crisis and prevent further spread of waterborne diseases

Implementing a comprehensive wastewater treatment system is crucial to mitigate the water pollution problem in Bukhara. This should include the construction of modern wastewater treatment plants, as well as the installation of sewer systems to collect and transport wastewater to these facilities. Additionally, public awareness campaigns and

educational programs should be implemented to promote better sanitation practices and reduce the discharge of untreated wastewater into water bodies.

Furthermore, regular monitoring of water quality and enforcement of environmental regulations are essential to ensure the long-term sustainability of water resources in the region. Collaboration between local authorities, environmental agencies, and the community is vital for the successful implementation of these measures and the restoration of Bukhara's water quality.

CONCLUSION

The impact of wastewater emissions on the health of the population in Bukhara, Uzbekistan, is a pressing concern that requires immediate attention and action. The analysis presented in this article highlights the alarming levels of pollutants found in the local water supply, which significantly contribute to a range of health issues among residents. Chronic exposure to contaminated water has been linked to various ailments, including gastrointestinal diseases, skin conditions, and long-term effects such as reproductive and developmental problems.

The socioeconomic implications of wastewater pollution cannot be overlooked. Many families in Bukhara depend on agriculture and livestock, both of which are adversely affected by polluted water sources. This not only threatens food security but also exacerbates poverty and hinders the overall economic development of the region.

To combat these challenges, it is essential that local authorities, healthcare providers, and environmental agencies collaborate to implement effective wastewater management strategies. This may include improving wastewater treatment facilities, raising public awareness about the dangers of contamination, and encouraging sustainable agricultural practices that minimize runoff.

Robust monitoring systems should be established to regularly assess water quality and health outcomes, ensuring that interventions are effective and timely. By prioritizing the health of the population and the integrity of the environment, Bukhara can pave the way toward a healthier, more sustainable future. Addressing the issue of wastewater emissions is not merely an environmental necessity but a fundamental public health imperative that can lead to improved quality of life for all residents.

ACKNOWLEDGEMENTS

The study was supported by a grant from the Russian Science Foundation № 23-27-00444, https://rscf.ru/project/23-27-00444/, 2023.

REFERENCES

[1] Climate Service Center Germany. 2023 (https://www.climate-service-center.de/products_and_publications/fact_sheets/climate_fact_sheets/index.php.en)

[2] Vorobyov A.E., Ortsukhaeva Z.Sh., Roman A.T. Characteristics of the hydrogeological conditions of the Terek River basin // Proceedings of the International Scientific and practical Conference "Science and education – the leading factor of the

strategy "Kazakhstan – 2030". Part II. Karaganda. 2012. pp. 278-280, ISBN 978-601-296-053-2.

[3] Vorobyov A.E., Tilenova D.K. Hydrochemical study of the territory of Southern Kyrgyzstan // International scientific journal "Sustainable development of mountain territories". - 2010, No. 2. - PP. 39-45, ISSN 1998-4502.

[4] Vorobyov A.E., Tilenova D.K. The hydroecological situation in the river basins of Southern Kyrgyzstan and ways to improve it // Bulletin of the ZabGK, No.6. 2013. pp. 156-163.

[5] Vorobyov A.E., Tilenova D.K. Ion flow of rivers of Southern Kyrgyzstan // Gorny vestnik of Uzbekistan, No. 3 (42). 2010. pp. 120-123, ISSN 2181-7383.

[6] IFC, 2019. Guidance Note 6: Biodiversity conservation and sustainable management of living natural resources, June 27, 2019. International Finance Corporation, World Bank Group. Washington, DC, USA.

[7] Mugue, N. & Karimov, B. 2022. Pseudoscaphirhynchus hermanni. The IUCN Red List of Threatened Species 2022: e.T18600A156719289.

https://dx.doi.org/10.2305/IUCN.UK.2022-1.RLTS.T18600A156719289.en.

[8] Mugue, N. & Karimov, B. 2022. Pseudoscaphirhynchus kaufmanni. The IUCN Red List of Threatened Species 2022: e.T18601A120872031.

https://dx.doi.org/10.2305/IUCN.UK.2022-1.RLTS.T18601A120872031.en

[9] Kozyrev E.N., Rubanovskaya S.G., Vorobyov A.E., Velichko L.N. The use of hydrogeochemical studies for seismic forecasting // Bulletin of MANEB, No.4, 2001. – PP. 17-18, ISSN: 1605-4369.

[10] Shodiev S.R., Chembarisov E.I. Hydrological and hydrochemical features of reservoir waters of the Bukhara region // Economics and Society No.10(101). 2022. pp. 637-641, ISSN 2500-2961, DOI: 10.31862/2500-2961-2022-12-3-334-349.

SECTION SOILS

SOIL PROPERTIES OF CHROMIC LUVISOLS FROM KREMIKOVTSI AREA IN SOFIA MUNICIPALITY

Prof. Dr. Toma Shishkov[1]

Assoc. Prof. Dr. Emil Dimitrov[1]

[1]Institute of Soil Science, Agrotechnologies and Plant Protection "Nikola Poushkarov", Agricultural Academy, **Bulgaria**

ABSTRACT

The result of the survey carried out on the territory of the Sofia-city municipality is presented, in relation to the application of the Program for the protection, sustainable use and restoration of soils as a limited and non-renewable natural resource. The obtained data on the Chomic Luvisols nearby the area of Kremikovtsi debate the basic physical and chemical soil characteristics. The priority task on the soil protection in the region aimed at the sustainable development, restoration and improvement of the soil resource. To fulfill this aim, samples from soil profile and additional sites from arable land were analyzed for texture, content and composition of organic matter, cation exchange capacity, soil bulk and soil particle density, soil moisture content at field sampling, porosity. The intrinsic peculiarity of organic substances is identified and the specific relationship within different fractions of extractable organic carbon. Humic acids are low molecular and with predominance of aliphatic over aromatic moieties in their molecules. The soil is affected by initial acidification but no evidence of destructive process of the soil adsorption complex, as the latter is characterized by high degree of saturation with bases. Chromic Luvisols are less vulnerable to erosion because, despite the low organic matter content, the colloidal clay content is significant.

Keywords: organic matter, physical and chemical properties, sustainability, CEC.

INTRODUCTION

The result of the soil survey carried out on the territory of the Sofia-city municipality is presented, in relation to the application of the Program for the protection, sustainable use and restoration of soils as a limited and non-renewable natural resource. The various aspects of improving soil quality are usually associated with recommendations to promote organic matter conservation practices, sustainable management of soil carbon stocks, conservation of soil functions and maintenance of high productivity [7], [8]. It is necessary to understand the main processes in the soil, induced by threats; to know where these processes occur and how they develop with time; to know the driving forces and pressures behind these processes, as related to cultural, social, economic, ecological or technical, local, regional or global developments; to know the impacts on the ecoservices provided by soils to other environmental compartments and finally to develop operational tools for the mitigation of the threats and impacts [1].

MATERIALS AND METHODS

The region of survey is located to the south of Stara Planina, in so-called Sofia Valley, about 12 km northeast of the Sofia city. The studied Chromic Luvisols [4] or the strongly leached cinnamonic forest soils [11] are localized in the area of Kremikovtsi, nearby the Chelopechene village, in the northwestern part of the Sofia's municipality, being a share of 1500 ha from 24455 ha of the total area occupied by Chromic Luvisols in the municipality. The area is situated in the climatic region of the elevated plains of Western-Central Bulgaria, the latter belongs to the Temperate-continental sub-region of the European-continental climatic region. The average annual air temperature is 10.2 ºC, the average temperature in July is 20.9 ºC and in January is (-1.6 ºC). Generally, the spring is relatively cooler than autumn. The average annual rainfall is 600 mm with maximum 84 mm during May and June and minimum 29 mm in December and January. In the central part of Sofia Valley the terrain is undulating rugged to a high hilly. The former mixed woodlands and scrub have been converted to pastures and arable land. The human influence during recent decades on the soils began with spatial expansion of permanent annual cropping areas, intensively cultivation and technogenic pollution. The soil-forming materials are the Quaternary alluvial-drift and talus-drift sediments (boulders, gravels, sands, clays); the Neocene alternations of clays, sandy clays, and siltstones and partly the Upper Cretaceous marls and marl limestones.

Laboratory methods. Soils from the area of Kremikovtsi were analyzed to determine the organic carbon content and SOM composition by the both, modified Turin's method (dichromate digestion at 125 ºC, 45 min, in presence of Ag_2SO_4 and $(NH_4)_2SO_4$ $FeSO_4$ $6H_2O$ titration, phenyl anthranilyc acid as indicator) and the Kononova-Belchikova's method, respectively [2, 6]. The total soil acidity is determined by the solutions of 1.0 N sodium acetate and 0.2 N potassium maleinate at pH 8.25, the value with maximum saturation of soil colloids with strongly alkaline bases, according to the method of Ganev and Arsova [3]. Particle size distribution was determined by sieving and the pipette method after chemical dispersion of air- dry gridded soil sample (<2 mm) with 25 cm^3 0.4N sodium pyrophosphate ($Na_4P_2O_7$) without preliminary removal of the organic matter and carbonates from the soil sample. Particle-size distribution and textural classes were determined according to Kachinsky method [5] as well USDA [9]. Vertically oriented undisturbed cores were sampled in 100 cm^3 metal cylinders for determination of bulk density ISO11272. Particle density analysis was carried out in water with 100 cm^3 pycnometers. Total porosity (Pt) was calculated using the measured bulk density (Db) and particle density (Ds).

RESULTS

The systematic survey was done on the terrains occupied by Chromic Luvisols for the assessment of soil functions in cropland dominated landscape in the Kremikovtsi area, nearby the Chelopechene village. The number of random samples representing various crop land use was proportional to a combination of techniques was used to gather information as on representative soil profile as well on the spatial area variation of soil properties. The focus of this empirical assessment was conducted with the aim of improving the criteria of potential differences in soil physical, chemical and physico-chemical characteristics in conventional intensive farming. We based the studies on representative analyses on soil texture, content and composition of organic substances,

cation exchange capacity, soil bulk density, soil moisture content at field sampling, soil particle density and porosity.
The studied soil profile is with coordinates N 42.7356911 and E 23.4610481. The soil classification is Strongly leached cinnamonic forest soil, according to the Bulgarian classification [11], or Chromic Luvisol (Endoclayic Epiloamic, Ochric), according to IUSS Working Group WRB [4], manifesting the morphological diagnostic, as follows:



Figure 1. The Chromic Luvisol nearby the Chelopechene village from the area of Kremikovtsi region.

A 0-8 cm. Munsell soil color, dry 7.5YR4/4 (dark brown) and moist 5YR3/2 (dark reddish brown), structure granular, strong pedality grade, aggregates of medium size (2-5mm), moderately developed, consistence hard, no effervescence by HCl, low field packing density <1.40g cm^{-3}, many fine roots <0.5 mm and others 0.5-1.0 mm size , grades into;
A1 8-24cm. Color dry 7.5YR4/4 (dark brown) and wet 5YR3/3 (dark reddish brown), structure subangular blocky of strong pedality grade, with fine size (<5mm diameter), consistence hard, aggregates of medium size (10-20 mm diameter), composed of the fine aggregates and single quartz included; no effervescence by HCl, with medium field packing density 1.40-1.75g cm^{-3}, abundance of fine roots, smooth transition to;
AB 24-42 cm. Color dry 7.5YR4/4 (brown) and wet 5YR3/3 (dark reddish brown), structure subangular blocky, aggregates firm of medium size (10-20 mm diameter), composed of fine aggregates and single quartz, included manganese concretions, no effervescence by HCl, with medium field packing density 1.40-1.75g cm^{-3}, few of fine roots, diffuse boundary and clear transition to;
Bt1 42-60 cm. Color dry 5YR4/8 (yellowish red) and wet 5YR3/3 (dark reddish brown), structure subangular blocky, aggregates firm of medium size (10-20 mm diameter), composed of fine aggregates and single quartz, included manganese concretions, no effervescence by HCl, with high field packing density >1.75g cm^{-3}, diffuse boundary gradual transition to;
Bt2 60-80 cm. Color dry 5YR4/8 (yellowish red) and wet 5YR3/3 (dark reddish brown), structure subangular blocky, aggregates firm of coarse size (20-50 mm diameter), no effervescence by HCl, with high field packing density >1.75g cm^{-3}, gradual transition to;
BC 80-110 cm. Color dry 5YR4/8 (yellowish red) and wet 5YR3/4 (dark reddish brown), structure subangular blocky, aggregates firm of coarse size (20-50 mm diameter), no effervescence by HCl, with high field packing density >1.75g cm^{-3}.

In Europe, there are quite a few soils characterized by a slightly acidic soil reaction and an Argic horizon, and usually these soils belong to the Luvisols group, according to IUSS Working Group WRB [4]. There is the effective saturation with bases, for the separation of the Luvisols group of soils. In the studied soils, the clay minerals are mainly illites/smectites/, which have much higher CEC values of 24 $cmol_c\ kg^{-1}$ in (1M NH_4OAc, pH 7) per kilogram clay fraction.

DISCUSSION

The studied Chromic Luvisols, does not manifested differentiation in the upper soil part, however beneath 40 cm depth the textural differentiation is obvious, confirmed by the data on soil texture (Table 1). The soil textural differentiation is a result of lessivage process, as well as confirming the ongoing process of weathering in situ mostly in the lower part. The texture soil class is defined as sandy clay loam, according to Kachinsky [5]. The distribution of the coarse and fine sand fractions, with particle size (1.0-0.05 mm), prevail in the upper soil part to the depth 42cm, followed by the silt fractions with particle size (0.05-0.001 mm). The clay fraction, with particle size (<0.001 mm), distinctly dominates below 42 cm depth. According to the USDA [9], the predominant fraction of medium sand with particle size (2.0-0.05 mm) is mostly in the upper part to the depth of 42 cm. Downward, in the textural Bt horizons below 42 cm depth, the clay fraction (<0.002 mm) dominates. The content and distribution of the silt fraction is relatively consistent throughout the soil.

Table 1. Particle size distribution (%) and texture classes, according to the Kachinsky (revised method) and USDA texture classes. Abbreviation: *Physical clay, the parameter characterized sum of the particle-size distribution, according Kachinsky [5], $\Sigma < 0.01^* = 0.001 + (0.005\text{-}0.001) + (0.01\text{-}0.005)$

Horizon and depth (cm)	Particle size distribution < 2 mm and fractions (%) after USDA			Texture class after USDA	Size of textural fractions (mm) and their content, (%) of oven dry soil weight, after method of Kachinsky					Texture class after Kachinsky
	Sand 2.0-0.05	Silt 0.05-0.002	Clay < 0.002		1.0-0.25	0.25-0.05	0.05-0.01	<0.001	∑ < 0.01*	
A 0-8	48.0	24.3	27.8	Sandy Clay Loam	26.9	25.0	10.1	21.9	38.0	Sandy Clay Loam
A_1 8-24	46.1	26.9	27.0		29.9	20.0	13.1	21.4	37.0	
AB 24-42	46.0	26.3	27.8		26.5	23.3	12.2	21.9	38.0	
Bt_1 42-60	36.1	21.6	42.3	Clay	20.7	18.8	9.9	35.8	50.6	Clay Loam
Bt_2 60-80	39.8	21.3	38.9	Clay Loam	20.5	22.9	7.7	32.4	48.9	
BC 80-110	40.4	21.1	38.5		23.2	21.7	7.2	31.7	47.9	

Table 2. Measured physical properties, as bulk density (Db), sampling water content (W), particle density (Ds) and total porosity (Pt) in soil horizons of Chromic Luvisol, nearby Chelopechene village, in the Kremikovtsi area.

Horizon and depth (cm)	Core sampl. depth, cm	Bulk density D_b, g.cm^{-3}	St	Particle dencity Ds, g.cm^{-3}	Water content W, %	Total porosity Pt, % vol.
A 0-8	0-5	1.37	0.10	2.64	7.4 ± 0.7	48.3 ± 3.6
A_1 8-24	15-20	1.46	0.05	2.67	9.6 ± 0.7	45.3 ± 1.9
AB 24-42	30-35	1.49	0.12	2.70	13.8 ± 0.7	44.7 ± 4.4
Bt_1 42-60	50-55	1.40	0.08	2.70	18.7 ± 0.3	48.2 ± 3.1
Bt_2 60-80	70-75	1.58	0.01	2.71	19.3 ± 0.7	41.9 ± 0.2
BC 80-110	90-95	1.59	0.02	2.71	14.2 ± 2.1	41.2 ± 0.7

The close relationship of particle density (Ds) with content of soil organic matter is evident in the surface and subsurface humus horizons (Table 2). The manifold relationship of bulk density and organic matter, total porosity, gravimetric and hygroscopic water content is sound and highly dependent.

Table 3. Content and composition of soil organic matter in Chromic Luvisol, nearby Chelopechene village, in Sofia municipality. Notes: (a) % of dry mass; (b) % of total carbon; (org.C) of total humic acids; (C_{ha}) humic acids; (C_{fa}) fulvic acids; (E_4/E_6) optic characteristic, (C_{ha} total) of pyrophosphate extract, (C_{ha} free) of alkali extract.

Horizon and depth, (cm)	Total org. C, %	Organic C, (%) extracted with 0.1M $Na_4P_2O_7$ + 0.1N NaOH			Cha/ Cfa	Organic C, (%) of total Humic acids Fraction		Unextract. org.C, %	C, (%) fulvic acids extract with 0.1 N H_2SO_4	Optic charac-teristic (E_4/E_6) of total humic acids, %	Org. C, (%) NaOH
		Extr. org.C, %	Cha, %	Cfa, %		Free or R_2O_3 bound	Ca bo-und				
A 0-8	1.78	0.40[a] 22.47	0.22 12.26	1.18 10.1[b]	1.22	0.00	100	1.38 77.53	0.06 3.37	3.70	0.23 12.92
A_1 8-24	1.62	0.35 21.60	0.20 12.35	0.15 9.25	1.33	0.00	100	1.27 78.40	0.06 3.70	3.52	0.17 10.49
AB 24-42	1.14	0.29 25.44	0.20 17.54	0.09 7.90	2.22	0.00	100	0.85 74.56	0.05 4.39	3.54	0.14 12.28
Bt_1 42-60	0.88	0.27 30.68	0.27 30.68	0.00	-	0.00	100	0.61 69.32	0.04 4.54	3.44	0.13 14.77
Bt_2 60-80	0.74	0.25[a] 33.78	0.14 18.92	0.11 14.86[b]	1.27	0.00	100	0.49 66.22	0.04 5.41	3.49	0.12 16.22

The amount of total organic carbon (C, %) is an indicator of soil quality and health, while the composition of soil organic matter is an indicator related to the impact of the environment. The amount of total carbon sharply decreases with depth and is two-fold lower in the textural (Bt) horizons comparing to the surface horizons (Table 3). The total amount of organic carbon varies from 1.78 % on the surface to 1.62 % at the depth 8-24 cm. The amount of extractable organic carbon, extracted with 0.1M $Na_4P_2O_7$+0.1M NaOH, is determined of 21.6-22.47 % of the total organic carbon in the humus (A) horizons (0-24 cm depth) and gradually increases to 25.44 % in the transition (AB) horizon (20-35 cm depth). In the textural (Bt) horizons (42-80 cm depth), the extractable organic carbon gradually increases to 30.68-33.78 %. These differences are significant and indicate that organic matter is more strongly bounded with the clay minerals in the upper soil part in the humus horizons. The amount of humic acids, of the total organic carbon, is 12.26-12.35 % in the humus (A) horizons or about 0.2 % of the dry matter, indicating a very low degree of humification process in the soil. The humic acids predominate over the fulvic acids being strongly bounded in complexes with calcium, forming insoluble fragments of microstructure, which amount gradually increased with depth. The ratio Cha/Cfa defines the fulvic-humic type of humus at the surface humus (A) horizons. Downward, this relation alters to humic humus type. The amount of unextractable organic carbon (humin) in the upper soil part being significant 74.5-78.4 % of the total organic carbon, and downward, in the textural (Bt) horizons, this amount decreases to 66.2-69.3 %. The obtained data on the optical characteristic of humic acids, the ratio (E_4/E_6) is almost of similar values throughout the soil claiming to more mature molecular structure (Table 3). The humic acids have been very similar in their molecular weight and structure to those of fulvic ones [10] that are of low molecular weight and with predominance of aliphatic over aromatic moieties in their molecules.

Table 4. Cation exchange capacity (CEC) (meq/100 g soil=cmol/kg^{-1}) and base saturation, (%) after the method of Ganev and Arsova [3]. Notes: ($T_{8.2}$) sum of all cations with acidic functions or total (hydrolytic) acidity; (T_{SA}) cation-exchange capacity of strongly acidic ion-exchanger; (T_A) weakly acidic ion-exchanger of soil

Horizon and depth (cm)	pH H_2O	Exchange cations, (cmol/kg^{-1} of soil)						Exchange cations, $T_{8.2}$ (%)					Base saturation, (%)
		$T_{8.2}$	T_{SA}	T_A	$H_{8.2}$	Ca	Mg	T_{SA}	T_A	$H_{8.2}$	Ca	Mg	
A 0-8	6.7	25.8	23.6	2.2	1.2	21.0	3.0	91.5	8.5	6.9	88.9	12.7	93.0
A_1 8-24	6.7	25.7	23.7	2.0	1.3	20.8	2.9	92.2	7.8	6.6	80.9	11.3	93.4
AB 24-42	6.4	26.2	22.4	3.8	3.1	19.6	2.8	85.5	14.5	11.8	74.8	10.7	88.2
Bt_1 42-60	6.3	25.8	21.7	4.1	3.5	18.7	2.8	84.1	15.9	13.6	72.5	10.8	86.4
Bt_2 60-80	6.4	26.2	22.4	3.8	3.0	19.5	2.8	85.5	14.5	11.5	74.4	12.5	88.5
BC80-110	6.6	24.6	22.9	1.7	1.3	20.0	3.0	93.1	6.9	6.1	87.3	13.1	93.9

According to the quantitative physico-chemical characteristic, after Ganev and Arsova [3], the composition of clay minerals in the Chromic Luvisols is presented by by illite-montmorillonite composition. The moderate colloidal reactivity ($T_{8.2}$=25.8-26.2 cmol/kg^{-1} of soil) is throughout the soil (Table 4). The clay formation *in situ* takes place throughout the soil profile, without differentiation of adsorption structures. The share of strongly acidic (T_{SA}) ion-exchange positions 91.5-92.2 % of ($T_{8.2}$) in upper humus horizons, gradually decreased to 84.1-85.5 % of ($T_{8.2}$) downward the soil, which is evidence of presence there of clay minerals with high isomorphic substitution. There is no occurrence of Al-ions in the adsorption structures. The exchangeable Ca-ions and Mg-ions manifested equal distribution throughout the soil. In the upper part of soil in humus (A) horizons the base saturation is high (93.0 %), below 24 cm depth, slightly decreasing but still is quite high 86.4-88.5 %. The presence of (exch. H8.2=8 % of T8.2) in the upper soil part which slightly increasing downward indicated the occurrence of initial soil acidification process. In the studied Chromic Luvisols the adsorption structures of the strongly acidic positions (T_{SA}) are not affected by the acidification. Mainly the weakly acidic exchange positions of the adsorbent (T_A) have been affected, while strongly acidic exchange positions (T_{SA}) are almost completely saturated with exchange bases, therefore noticeable destructive process in the soil absorption complex is not established.

Table 5. Site localization on the terrain occupied by Chromic Luvisols, in the Kremikovtsi area, nearby Chelopechene village.

Localization of the studied sites	Coordinates of studied sites		Altitude, m	Land cover / Crops
Chelopechene (trial)	42.738568 N	23.468205 E	535	Potatoes
Chelopechene (trial)	42.740505 N	23.470254 E	532	Sunflower
Rudnichna station	42.764505 N	23.491566 E	580	Sunflower
Buhovo	42.757320 N	23.565770 E	699	Maize
Industrial area of Kremikovtsi	42.742466 N	23.555135 E	619	Rape
Kremikovtsi	42.721272 N	23.564559 E	585	Maize
Kremikovtsi	42.7318222 N	23.598103 E	644	Sunflower
Bogrov station	42.719196 N	23.535648 E	550	Wheat
Gorni Bogrov	42.712572 N	23.523237 E	542	Sunflower
Elin Pelin	42.703605 N	23.547237 E	543	Sunflower

Table 6. Particle size distribution (%) to air dry soil and texture classes, according to method of Kachinsky (revised) and USDA. Abbreviation: *Physical clay, the parameter characterized sum of the particle-size distribution, according [9],
$\Sigma < 0.01^* = 0.001 + (0.005\text{-}0.001) + (0.01\text{-}0.005)$

Localization	Particle size distribution <2 mm and fractions (%) after Kachinski						∑ <0.01*
	1.0-0.25	0.25-0.05	0.05-0.01	0.01-0.005	0.005-0.001	<0.001	
Chelopechene (trial)	29.9	14.8	15.2	12.0	4.6	23.5	40.1
Chelopechene (trial)	25.7	13.0	6.1	16.0	10.0	29.2	55.2
Rudnichna station	26.9	21.5	10.1	10.3	4.9	26.3	41.5
Buhovo	36.8	10.9	12.4	4.7	5.4	29.4	39.9
Industrial area of Kremikovtsi	41.2	40.1	3.0	4.9	4.6	6.2	15.7
Kremikovtsi	11.4	9.5	16.2	9.7	5.3	47,9	62.9
Kremikovtsi	10.3	21.1	11.1	13.5	5.3	38.7	57.5
Bogrov station	8.3	16.2	12.0	7.4	5.3	50.8	63.5
Gorni Bogrov	17.3	21.6	6.3	11.1	5.8	37,8	54.8
Elin Pelin	39.7	20.5	4.1	9.3	5.4	21.0	35.7

Table 7. Data on humus content, pH values and nutrient elements availability in the sites of Chromic Luvisols, in the Kremikovtsi area, nearby Chelopechene village.

Localization	pH		∑ N – $NH_4 + NO_3$ mg/kg	P_2O_5 mg/100g	K_2O mg/100g	Organic matter, (%)
	H_2O	KCl				
Chelopechene (trial)	6.6	5.8	9.2	9.5	18.1	1.17
Chelopechene (trial)	6.1	5.2	10.9	1.2	29.6	1.11
Rudnichna station	6.6	5.8	7.5	5.6	10.7	1.09
Buhovo	6.2	5.3	6.5	5.4	16.4	1.53
Industrial area of Kremikovtsi	8.0	7.4	12.3	3.2	15.3	1.67
Kremikovtsi	6.1	5.1	9.8	4.6	12.4	1.42
Kremikovtsi	6.7	5.8	11.3	5.2	16.7	1.49
Bogrov station	6.1	5.3	12.9	7.6	19.4	1.96
Gorni Bogrov	6.9	6.1	10.7	8.9	13.6	1.85
Elin Pelin	6.7	5.8	9.9	7.4	11.8	1.45

The obtained spatial assessment of Chromic Luvisols in the Kremikovtsi area, in Sofia-city municipality is resulting the risk assessment of the soil quality according to the basic studied soil characteristics and grown crop land use (Table 5, 6, 7). Organic carbon stock in surface horizons indicates a low degree of humification in the region. The clay content is mainly represented by mineral colloids. Chromic Luvisols are less vulnerable to erosion because, despite the low organic matter content, the colloidal clay content is significant. Acidification mainly affects weakly acidic exchange positions of the soil adsorbent, which indicates occurence of initial process of soil acidification. From the preliminary soil survey the conclusion is, that the sistematic approach to the sustainable management of the Chromic Luvisols in the region is needed.

CONCLUSION

The obtained data a result of spatial survey of the Chomic Luvisols nearby the area of Kremikovtsi, Sofia-city municipality show the specificity of the environmental conditions and land management on the basic soil characteristics. Carbon stabilization mechanisms are based on the concept of biochemical turnover. The precise

determination of changes in organic carbon stocks and the significance of changes over time and space can only be assessed with limited accuracy, particularly in deep soil horizons. Increasing carbon stocks has the potential to improve soil quality. It is necessary to focus attention on the proper management of soil organic matter, especially with subsequent quantification of the prediction of the role of soils in future climate change. The clay content is mainly represented by mineral colloids. Chromic Luvisols are less vulnerable to erosion because, despite the low organic matter content, the colloidal clay content is significant.

REFERENCES

[1] Blum W.E.H, Land use planning and policy implication: bridging between science, politics and decision making, Developments in soil classification, land use planning and policy implications, Springer, Dordrecht Heidelberg New York London, 2013, pp. 469-481.
[2] Filcheva E., Characteristics of soil organic matter of Bulgarian soils, LAP Lambert Academic Publishing, 2015, pp 178;
[3] Ganev S., Arsova A., Methods for determining the strongly acid and weakly acid cation exchange in soil, Soil Science and Agrochemistry, Bulgaria, vol.15/issue 3, pp 22–33, 1980.
[4] IUSS Working Group WRB, World Reference Base for Soil Resources, International soil classification system for naming soils and creating legends for soil maps, 4th edition. International Union of Soil Sciences (IUSS), Vienna, Austria, 2022, pp 234;
[5] Kachinski N.A., Mechanical and micro-aggregate composition of soil, Methods for it study, Publishing house of Science Academy of USSS, Moscow, 1958, pp 192;
[6] Kononova M.M., Soil organic matter, its nature, origin and role in soil formation and soil fertility, 2nd Eng. Ed., Pergamon Press ING., Elmsfordm M.V., 1966, pp 544;
[7] Lal R., Soil carbon sequestration impacts on global climate change and food security, Science, USA, vol. 304/issue 5677, pp 1623-1627, 2004.
[8] Post W. M., Kwon K. C., Soil carbon sequestration and land use change: processes and potential. Global Change Biology, vol. 6, pp 317–327, 2000.
[9] Soil Survey Staff, Soil Survey Laboratory Information Manual, Soil Survey Investigations Report No. 45, Version 2.0., R. Burt (ed.), U.S. Department of Agriculture, Natural Resources Conservation Service, USA, 2011, pp 506.
[10] Sutton R., Sposito G., Molecular structure in soil humic substances: the new view, Environmental Science and Technology, USA, vol. 39/issue 23, pp 9009-9015, 2006.
[11] Yolevski, M., Ninov, N., Krastanov, S., et al., Brief diagnostic and criterion of the main taxonomic soil divisions in Bulgaria, Precise Classification Scheme, Institute of Soil Science Nikola Poushkarov, Sofia, 1983.

DEGRADED SOILS OF THE MOST BASIN AND THE POSSIBILITIES OF THEIR LOCATION, CLASSIFICATION AND RECLAMATION

RNDr. Michal Řehoř, Ph.D.[1]
Eng. Pavel Schmidt[1]
Eng. Radka Duzekova[1]
Assoc. prof. Petr Vráblik[2]

[1]Brown Coal Research Institute j. s. c., Most, **Czech Republic**
[3]Jan Evangelista Purkyne University, Ústi nad Labem, **Czech Republic**

ABSTRACT

Brown Coal Research Institute j. v. c. (VÚHU) from July 2023, together with scientific teams from several European countries, participates as part of the EU research program in the solution of the REECOL project, which deals with the reclamation of areas affected by mining in European coal basins. This paper includes the results achieved in the preparation of the first sub-research report of the project, which deals with degraded soils. On the basis of archival data and own research, the concept of "soil degradation" was defined for the purposes of the REECOL project solution in the conditions of the Most basin, a set of laboratory analyses of soils suitable for determining the degree of degradation was determined, which will be modified in the course of the next solution in terms of efficiency and financial sustainability. The methodology of research is composed of terrain mapping, sampling and sample analysis realised by accredited test laboratories. The main part of the paper contains a brief description and localization of the areas of degraded soils of the Most Basin. The individual chapters briefly describe the areas affected by various types of degradation and the proposal for their reclamation, one locality is always described in more detail as a case study area. Part of the contribution is a map of areas affected by individual types of soil degradation.

Keywords: soil, reclamation, degradation

1 INTRODUCTION

Brown Coal Research Institute j. s. c. (VÚHU) participates for the first year in the solution of the European project of the Research Fund for Coal and Steel (RFCS) "Ecological rehabilitation and long - term monitoring of post mining areas" (acronym REECOL).

The first research package of the project is WP 3 "Identification of post-mining areas and approaches to ecosystem restoration", which deals with the characterization of different approaches to the reclamation of post-mining areas used in the countries of individual project partners. Currently, the research work of VÚHU focused on the first addressed task of WP 3, which is task T 3.1 "Classification of ecosystem degradation and mapping of degraded land". The output of the T3.1 is this partial research report.

https://doi.org/10.5593/sgem2024/3.1/s13.25

The report deals with the research methodology, the definition of soil parameters important for determining the degree of soil degradation, the results of data summarisation and research work carried out by VÚHU a.s. and the definition of individual degrees of soil degradation. The final part of the report is devoted to a brief description of the identified types of degraded areas.

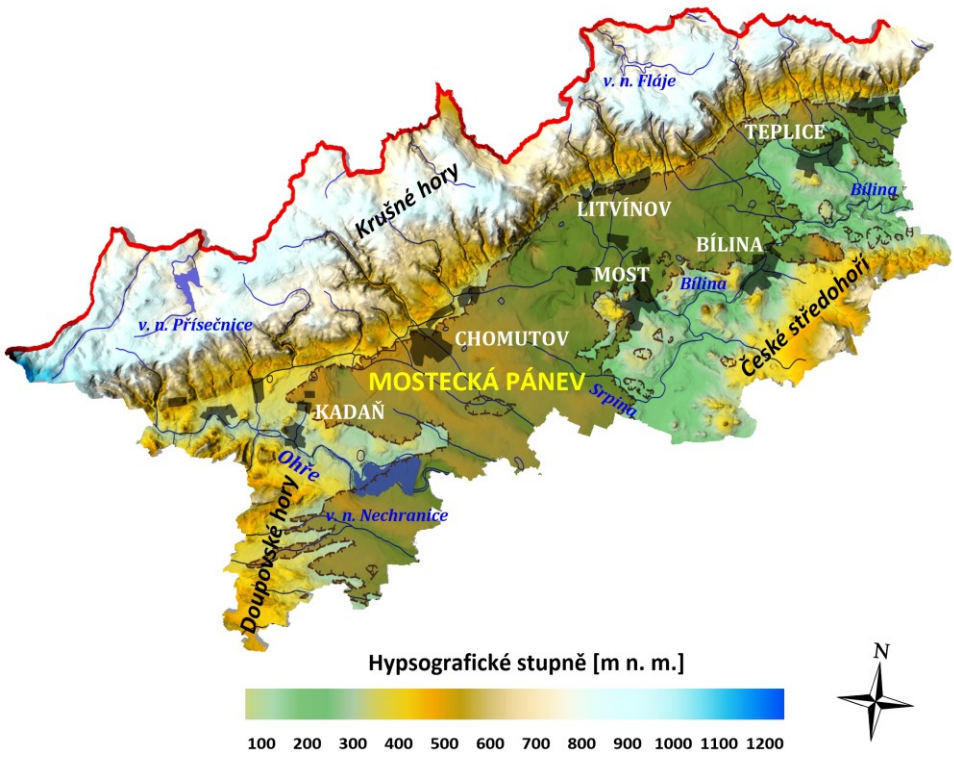


Fig 1: Most Basin situation [4]

2 MATERIALS AND METHODOLOGY

2.1 RESEARCH METHODOLOGY

The first stage of the research was the collection of available data from historical pedological surveys and research. It was primarily VÚHU's own data, as well as available data from stakeholders (mining organizations, regional universities, cooperating organizations dealing with pedological surveys of the region, etc.).

Based on the obtained data, the concept of "soil degradation" was defined for the purposes of the REECOL project in the conditions of the Most Basin, a set of laboratory analysis of soils suitable for determining the degree of degradation was determined, which will be modified in the course of the next solution in terms of efficiency and financial sustainability. Based on the results, individual types of contaminated areas will be briefly characterized, including sub-maps, and each of them will be supported by one location described in more detail.

The selection of laboratory tests and analyses of their results was determined in the range of proven methodologies used in the Most Basin for a long time in reclamation activities [4]. For each sample, granularity determination, evaluation of mineralogical composition on Siemens X-ray diffractometer, determination of soil reaction, determination of CaCO3 content were carried out, determination of the content and

quality of oxidizable carbon and humus, determination of nitrogen content, determination of sorption capacity and determination of the content of acceptable nutrients according to Melich III.

All performed laboratory analyses were carried out by testing laboratories VÚHU and VÚMOP v.v.i. accredited by ČIA according to ČSN EN 150/IEC 17025 based on internal methodological procedures based on the relevant standards [6].

2.2 DEFINITION OF THE CONCEPT OF LAND DEGRADATION FOR PURPOSES OF THE REECOL PROJECT SOLUTION

In the Czech pedological nomenclature, the concept of soil degradation is relatively unambiguously defined as a **process in which the fertility and usability of the soil decreases and its ecological functions are reduced** [3]. Specifically, it is the **compaction of soils** (caused by repeated cultivation of the soil at the same depth and the number of crossings heavy machinery, which leads to a decrease in the porosity and permeability of the soil), **erosion** (a phenomenon in which the soil is disturbed by water, wind, snow), **chemical degradation** (processes by which the soil loses its humus content and the content of nutrients), **excessive fertilization**, **salinization** (caused by irrigating agricultural areas with water that has a high content of dissolved substances), **contamination** (with foreign chemicals or waste), **desertification** (a process in which natural or human causes reduce the biological productivity of dry areas - climate change, deforestation , overgrazing, etc.) [1], [2]. Soil degradation defined in this way is based on the needs and characteristics of agricultural land.

REECOL's research task deals with soils in areas affected by brown coal mining, and these soils are mostly anthropogenic. Therefore, some modification of the above degradation components is necessary. In the case of soils affected by mining in the Most Basin, the following phenomena can be considered as soil degradation:

Contamination

In the conditions of the Most Basin, this is the most significant cause of anthropogenic soil degradation. There are many sources of contamination. The most important ones include:

- soil contamination of the coal seam sediments (increased content of coal mass, sulphur and iron sulphides).
- contamination with risky trace elements (in the conditions of the Most Basin, this is mainly arsenic).
- contamination by coal combustion products (ashes, fly ash, slag, stabilizers, energy gypsum).

Increased content of the sandy component and erosion

The increased content of the sandy component in a number of spoil heap soils of the Most Basin is due to the presence of sand in a number of overburden soils (areas of deltaic sedimentation). A sand content above 50% in the soil leads to low erosion resistance and degradation of soil parameters.

Increased content of the clay component

The increased content of the clay component of the soils in the part of the spoil heap soils of the Most Basin is due to the occurrence of extremely fine-grained clays in the upper part of the tertiary layers. This phenomenon is not common but causes enormous difficulties in forest reclamation.

Chemical degradation

The main soils based on external and internal spoil heaps are sands, kaolinitic clayey sands and kaolinitic - illitic clays. Admixtures in these soils are organic (coal) matter, siderite and pyrite. These rocks are mechanically unstable to wind and water erosion. Due to the ongoing weathering, SO_3 and Al ions acquire an unfavourable, acidic (even toxic) character [5].

Salinization

In the area of the Most Basin, this phenomenon is limited to the area of Doly Nástup Tušimice mining company, where a significant part of the spoil heap soils is made up of homogeneous clays of the Libkovice layers with the occurrence of gypsum. The gypsum occurrence is the cause of an often extremely alkaline soil reaction, which is a fundamental problem in forest reclamation.

Desertification

In the conditions of the Most Basin, it is a problem of dry climatic periods, which can cause drying of exposed localities and major complications in biological reclamation. These problems have already been observed in several locations, but soil degradation cannot yet be established. In the future, attention should be paid to this problem (it is one of the tasks of this project).

3 RESULTS

3.1 PROPOSAL FOR THE CLASSIFICATION OF SOIL DEGRADATION IN THE MOST BASIN

Based on the evaluation of research works, long-term experience with the pedological evaluation of the soils of the Most Basin and new research carried out as part of the REECOL project, the following classification of soil degradation in the Most Basin was proposed.

1st degree of degradation

The soil parameters of the area are degraded compared to the optimal condition, but they do not require reclamation intervention.

2nd degree of degradation

It is not a phytotoxic area, but reclamation of the upper horizon of the terrain can be recommended (suitable application of reclamation additives)

3rd degree of degradation

It is a phytotoxic area and a fundamental modification of the upper horizon of the terrain is necessary (overlaying with suitable reclamation additives).

3.2 SELECTION OF PEDOLOGICAL PARAMETERS AND LIMIT VALUES FOR INDIVIDUAL LEVELS OF DEGRADATION

The selection of laboratory tests and analyses of their results was determined in the range of proven methodologies used in the Most Basin for a long time in reclamation activities [5]. For each sample, granularity determination, evaluation of mineralogical composition on Siemens X-ray diffractometer, determination of soil reaction, determination of $CaCO_3$ content were carried out, determination of the content and quality of C_{ox} carbon and humus, determination of nitrogen content, determination of sorption capacity and determination of the content of acceptable nutrients according to Melich III.

All performed laboratory analyses were carried out by testing laboratories VÚHU and VÚMOP accredited by ČIA according to ČSN EN ISO/IEC 17025 on the basis of internal methodological procedures based on the relevant standards [6].

Determination of limit soil parameters for individual degrees of degradation are shown in the following tables 1 – 4 (selected most important soil parameters.

Table No. 1: Soil granularity evaluation

Content of grain fraction < 0,01 mm (%)	Soil type	Soil evaluation
0 – 10	sandy	light granularity
10 – 20	loam - sandy	light granularity
20 – 30	sandy - loam	middle granularity
30 – 45	loam	middle granularity
45 – 60	clay - loam	fat granularity
60 – 75	clayey	fat granularity
>75	clay	fat granularity

Table No. 2: Soil reaction evaluation (pH)

Soil reaction (pH)	pH_{H20}	pH_{KCl}
very acid	< 4,9	< 4,5
acid	5,0 – 5,9	4,6 - 5,5
lightly acid	6,0 – 6,9	5,6 - 6,5
neutral	7,0	6,6 - 7,2
lightly alkaline	7,1 – 8,0	> 7,2
alkaline	8,1 – 9,4	-
very alkaline	>9,4	-

Table No. 3: Content of pollutants (%)

S %	Coal mass %	Sulphides Fe occurrence
< 0,02	< 0,5	NE
0,02 - 0,06	0,5 – 1,5	ANO
0,06 - 2	1,5 – 4	
> 2	> 4	

Explanations to the tables:

XXX - 1st level of degradation.
XXX - 2nd level of degradation.
XXX - 3rd level of degradation.

Table No. 4: Limit contents of risky trace elements

Soil type	Risky trace element limit content (mg . kg^{-1})										
	As	Be	Cd	Co	Cr	Cu	Ni	Pb	V	Zn	Hg
Lightly soils	15	1,5	0,4	20	55	45	45	55	120	105	0,3
Common soils	20	2	0,5	30	90	60	50	60	130	120	0,3

Limit values according to Decree No. 153/2016 Coll. (Czech Republic)

The limit contents of risky trace elements are based on Decree No. 153/2016, on the determination of the details of the protection of the quality of agricultural land and on the amendment of the Decree No. 13/1994 Coll., which regulates some details of the protection of the agricultural soil fund, where the so-called preventive values of the contents are given of risk elements in agricultural soil determined by the extraction of the *acidum chloronitrosum* (mg.kg-1 dry matter) and are also in full correlation with Decree No. 257/2009 Coll., on the use of sediments on agricultural land [4].

3.3 A BRIEF DESCRIPTION OF THE AREAS OF DEGRADED SOILS IN THE MOST BASIN

Due to limited scope of the paper, only the area where soil degradation is caused by contamination with risky trace elements is given as the example and describes in more detail.

3.3.1 AREAS OF SOILS CONTAMINATED WITH RISKY TRACE ELEMENTS

According to the results of the research works, the main contaminant is arsenic. It occurs to a limited extent on areas contaminated with coal seam soils, where it is bound to the iron sulphides pyrite and marcasite. Increased concentrations of other trace elements (especially cobalt, chromium, copper, vanadium, and nickel) were found on areas reclaimed using bentonite, which is their source. However, the most significant degraded area is the arsenic-contaminated strip of Quaternary soils at the foot of the Krušné Hory Mountains.

Flushes from metamorphizes of the Ore Mountains

It is a discontinuous strip of clayey gravel, clay soils and topsoils under the Krušné Hory Mountains roughly between Klášterec nad Ohří and Litvínov. In this case, the source of degradation is runoff from the metamorphizes of the Krušné Hory Mountains. In certain areas (e.g. the sediments of former Lake Komořany) the content of arsenic, is very difficult to explain in any other way.

This area of degraded soils must be considered during reclamation works in the area of the Nástup Tušimice Mines and the ČSA open pit mine, where it is advisable not to establish agricultural reclamation under the Krušné Hory Mountains (arsenic

contamination was also detected in samples of topsoil). Arsenic-contaminated gravel from the internal dump of the ČSA open pit mine is shown in the following Figure no. 2.



Fig 2: Arsenic-contaminated clay gravel

The following table No. 5 shows the results of analyses of the content of risky trace elements in three samples of clayey gravel.

Table No. 5: Content of risky trace elements in gravel samples

No of sample	Risky trace element content (mg . kg^{-1})										
	As	Be	Cd	Co	Cr	Cu	Ni	Pb	V	Zn	Hg
sample 1	41,5	1,76	0,76	25,4	56,8	95,8	41,7	58,8	82,8	105,5	0,112
sample 2	83,6	1,11	1,75	47,6	56,9	108,3	43,5	67,9	101,6	125,9	0,225
sample 3	53,8	1,23	0,98	37,1	61,2	98,4	46,5	75,5	88,9	115,4	0,211

4 CONCLUSIONS

The partial research report summarizes the current results of VÚHU in solving WP3 (Task 3.1). The first stage of the research devoted to the characteristics of degraded soils in the Most Basin area is evaluated here.

The report describes the methodology of the work, which includes the definition of the concept of soil degradation for the purposes of the project solution, a proposal for the classification of soil degradation in the Most Basin, the methodology of the necessary pedological research and the selection of pedological parameters, including limit values for individual levels of degradation.

https://doi.org/10.5593/sgem2024/3.1/s13.25

The report contains a brief description and localization of areas of degraded soils in the Most Basin. In individual chapters, areas affected by different types of degradation are briefly described, one locality is always described in more detail as a case study area.

The main results of the research so far are, primarily, the first proposal for the classification of the level of soil degradation, determination of limit values of soil parameters for individual levels of degradation, and a brief characterization and localization of areas with different types of soil degradation.

ACKNOWLEDGEMENT

The article was published with the support and co-financing of the EU research program "Ecological rehabilitation and long-term monitoring of post mining areas", project no. 101112657 - REECOL - RFCS-2022.

REFERENCES

[1] BURDA J., HARTVICH F., VALENTA J.; Climate – induced landslide reactivation in the edge of the Most Basin (Czech Republic) – progress towards better landslide prediction Nat. Haz. Earth Syst. Sci., 13, 361-37, 4, 2013, doi:10./nhess-13-361-2013519.

[2] PRACH K., BARTHA S., JOYCE, C., PYŠEK P.: The role of spontaneous vegetation succession in ecosystem restoration: a perspective

Appl. Veg. Sci. 4 (2001), p. 111–114.

[3] TOMÁŠEK M.: Soils of the Czech Republic.

Czech geological service, ISBN 978-80-7075688-1, Prague 2007

[4] ŘEHOŘ M.; JAROLIMOVÁ M.; ŽIŽKA L.; VRÁBLÍK P.; VRÁBLÍKOVÁ J.; The Results of the Long-Term Research on the Development of Anthropomorphic Soil in the Reclaimed and Successive Areas of the Most Basin in Czech Republic.

Journal of Mining Science, 53(4), 778-788, DOI 10.1134/S1062739117042777, 2018, ISSN 1573-8736.

[5] VOJAR J., DOLEŽALOVÁ J., SOLSKÝ M: Utilization of succession areas during reclamation of areas affected by mining

Journal Nature Conservation, 5/2012, Care of nature and landscape, printed version in pdf

[6] Testing Laboratory No 1078: Internal methodological regulations of testing laboratory VÚHU Most, IMR of testing laboratory

DETECTION OF AGATE-LIKE SOIL COVER STRUCTURES USING NEURAL NETWORK FILTERING OF BIG REMOTE SENSING DATA

Polina Koroleva

Dr. Dmitry Rukhovich

Alexey Rukhovich

Galina Chernousenko

Dokuchaev Soil Science Institute, **Russia**

ABSTRACT

Agate-like soil cover structures (ASCS) of leached chernozems are common in some regions of Russia with a total area of 425 242 km^2 (the republics of Tatarstan and Bashkortostan, Orenburg, Samara, and Ulyanovsk regions). The term "agate-like structures" was proposed due to the fact that on remote sensing data they resemble a section of the Timan agate. The structures are formed on loamy and clayey Quaternary sediments with a thickness of 0.5-5 m, overlying Permian sediments (bedrock). It is possible to identify the location of agate-like structures within the framework of the theory of multi-temporal soil line and neural network filtering of big remote sensing data. The distribution of different crop productivity spatially coincides with the ASCS and is determined by the contrasting properties of the soil cover. The degree of influence of ASCS varies for different crops. The maximum differences in yield across ASCS fertility zones were noted for sunflower. The ratio of the yield of the low fertility zone to the high fertility zone within one agricultural field was one to five. The minimum ratio was noted for peas and was four to five. ASCS require specialized agricultural technologies within the framework of precision farming systems.

Keywords: digital soil mapping, remote sensing data, neural network, multi-temporal soil line, productivity of crops

INTRODUCTION

The development of precision farming since 1989 [1, 2] makes the development of mapping the soil cover structure (SCS) and the development of the doctrine of SCS relevant [3]. Back in 1895 V.V. Dokuchaev separated geography and topography of soils, i.e. general patterns of soil cover (SC) distribution and detailed variations of soil combinations in a large scale [4]. Practical large-scale soil cartography developed decades later. The introduction of the terms pedon and polypedon [5, 6] caused criticism from the point of view of the possibility of SC mapping and practical identification of SC [7]. Similar Russian terms "soil individual" [8] and "elementary soil area" [3] had a greater practical and cartographic focus, which no longer required large-scale soil [9] and agrochemical [10] surveys, but detailed mapping on scales more precisely than 1:10 000. The supply of large-scale soil maps for agricultural lands in Russia is great [11]. By the mid-80s of the last century, all arable lands of the USSR were provided with soil maps at scales of 1:10 000 and 1:25 000. But not all soil maps were created taking into

account the identification of SCS. More detailed soil mapping was and still is in the nature of surveying in key areas, i.e. has a very small distribution area.

Classical large-scale soil mapping of the USSR did not have a clear intra-field focus [12], because all recommendations for agricultural use were given for the entire agricultural field [13]. The term “stable intra-field heterogeneity” (SIFH) [12] or "intra-field heterogeneity" [14-16] began to be used specifically in connection with precision farming.

There are various methods for recognizing the causes of soil cover heterogeneity, which can be grouped according to the basic principles of the study: traditional field studies; modeling based on the processing of digital terrain models and climate data; processing of remote sensing data (RSD). When processing RSD, individual images, intra-annual series, and multi-temporal (long-term) series can be used. When indicating different soils and their spatial heterogeneity, both vegetation indices (VIs), which most often reflect vegetation cover, and bare soil surface (BSS) are used.

Previously, it was not possible to reveal agate-like soil cover structures (ASCS) using traditional methods, modeling methods, and methods of processing individual remote sensing scenes. ASCSs are not displayed either on large-scale soil maps of the study area [17] or in descriptions of soils of the Republic of Tatarstan [18,19]. For cartographic work with ASCS, new methods of mapping SIFH over large areas and based on new materials and new methods of their processing were required [20]. For updating soil maps [12] and compiling maps of types of soil degradation [20], it is possible to apply methods for processing big remote sensing data and neural networks. The criterion for the quality of new methods remains the analysis of soil characteristics obtained during field surveys.

Aims of the work:

1. Identify specific agate-like soil cover structures (ASCS) and establish their impact on agricultural productivity.

2. Show high accuracy of detection of ASCS for use in precision farming systems.

STUDY OBJECT, METHODS AND MATERIALS

Study area

ASCS are widespread in some regions of Russia with a total area of 425 242 km^2 (the republics of Tatarstan and Bashkortostan, Orenburg, Samara, Ulyanovsk regions). The object of study is located in the forest-steppe zone on the border of the Republic of Tatarstan and the Samara region (Fig. 1) - the Bugulma-Belebeevskaya Upland. The sum of active temperatures is 2175 °C, the humidification coefficient is 0.84. Arable lands on typical and leached chernozems were studied.

Methods

1. Neural network filtering of big remote sensing data (BRSD).

1.1. Neural network filtering of remote sensing scene / agricultural field combinations - selection of suitable for VIs calculations.

1.2. Recognition of BSS in each remote sensing scene for multi-temporal soil line (MSL) calculations.

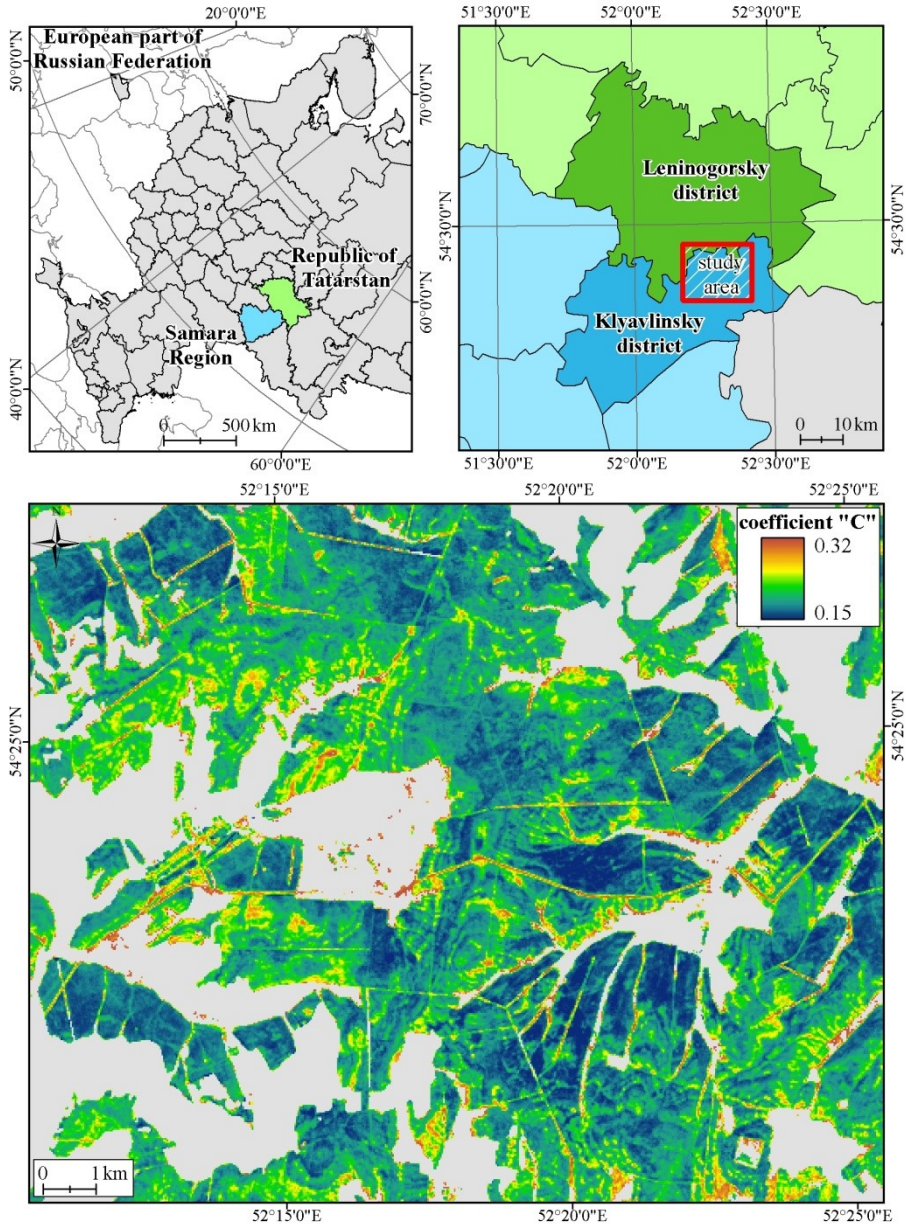


Figure 1. Location of study area and the map of the "C" coefficient of MSL

2. Generation of maps of stable intra-field heterogeneity of soil fertility based on averaging of multi-temporal VIs series.

3. Calculation of MSL coefficients and generation of maps of the coefficient "C" of MSL [20].

4. Field soil surveys based on maps of intra-field heterogeneity and the "C" coefficient. During field surveys, soil pits were made and samples were taken for laboratory measurements of the soil organic matter content (SOM) and carbonates. The degree of rockiness of the arable horizon was also visually determined.

5. Yield measurements by fertility zones. The measurements were carried out on the basis of a map of stable intra-field heterogeneity of soil fertility.

Materials

Archives of Landsat 4-8 from 1984 to the present were used to calculate the SIFH map and the MSL "C" coefficient map. Atmospheric correction was carried out using the ATCOR module of the ERDAS Imagine software package.

RESULTS

BSS map - MSL "C" coefficient map.

Figure 1 shows a fragment of the map of the “C” coefficient of MSL for the part of Leninogorsky district of the Republic of Tatarstan and Klyavlinsky district of Samara region. The fragment covers an area of 3 500 hectares, in which ring-shaped structures of alternating changes in multi-temporal spectral brightness of the BSS are visible. It is difficult to trace the breadth of distribution of the phenomenon in individual remote sensing images (Fig. 2). It is important to understand that the ring structures characteristic of this region are widespread and consist of the same spectral elements.

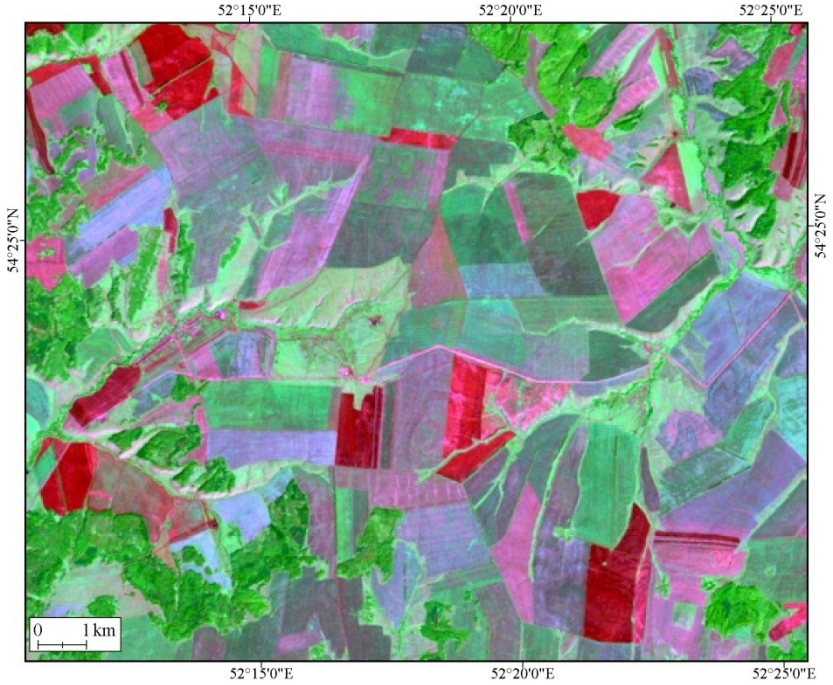


Figure 2. Landsat 5 image, 30 August 1994

The darker rings (shades of blue) in Figure 1 represent more humified thick leached chernozems. Lighter (brown and yellow shades) are carbonate stony chernozems with an incomplete or shortened profile.

The SIFH map.

Figure 3 shows the SIFH map - the averaging map of multi-temporal VIs maps. Zones of low fertility are shown in red, zones of medium fertility are shown in yellow, and zones of high fertility are shown in green. The SCS in Figures 1, 3, 4 is identical. Thick, rich in humus leached chernozems with low reflectivity are the most fertile areas of fields and ASCS. Rocky shortened carbonate chernozems have the lowest fertility. If the coefficient “C” map of the MSL reflects the alternation of spectral characteristics of the BSS, then the SIFH map reflects the alternation of areas with different productivity of agricultural land.

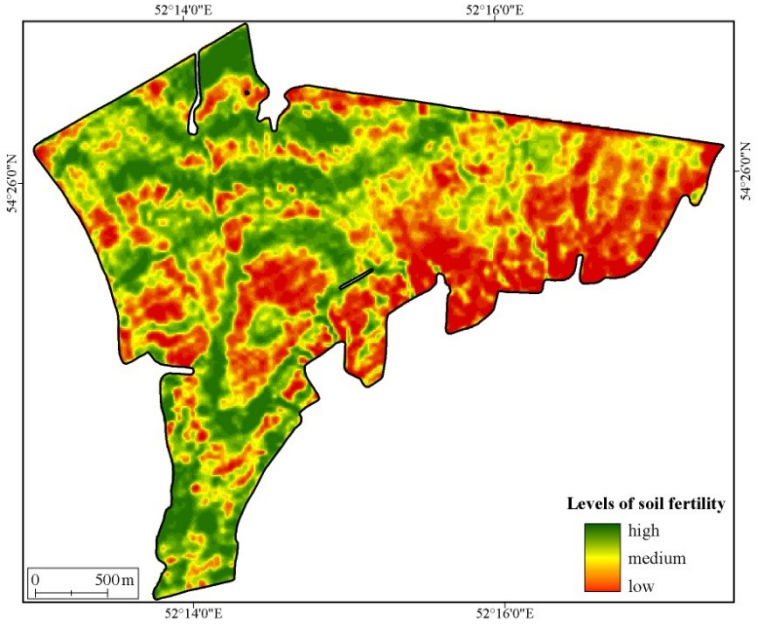


Figure 3. The map of stable intra-field heterogeneity of soil fertility

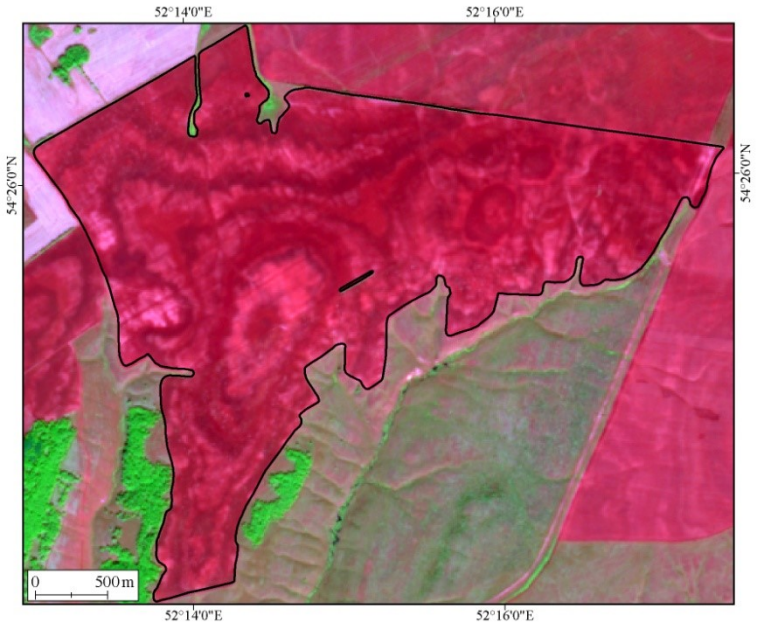


Figure 4. Sentinel image, 9 May 2020

Fertility.

The fertility zones of the SIFH map are related to the thickness of the soil profile and the degree of rockiness. But these factors affect different crops differently. With a shallow, highly branched root system, a thickness of 30-50 cm is sufficient for the normal growing of oats, spring wheat and peas. A decrease in fertility for these crops is determined by a smaller supply of moisture in the red zones of reduced fertility, because the moisture reserve is formed in the clayey and loamy stratum. The yield ratio of spring wheat and peas in the red zone to the green zone is only four to five.

https://doi.org/10.5593/sgem2024/3.1/s13.26

With taproot systems, the underlayment of dense rocks, even at a depth of 1 m, greatly influences the formation of the crop. When the soil profile thickness is less than 50 cm, the yield decreases sharply. For sunflower, the yield ratio of the red and green zones is one to five.

DISCUSSION

The term "agate-like structures" of the soil cover.

The term “agate-like structures” was proposed in connection with the characteristic BSS pattern on the synthesized pseudo-color remote sensing images (Fig. 4). The figure shows a synthesis of SWIR, NIR, and GREEN spectral bands. The image pattern resembles a section of Timan agate. As on a cut of agate, ring-shaped formations of the same genesis and with similar chemical characteristics alternate.

Genesis.

Leached chernozem is formed on Quaternary clayey and loamy sediments throughout the study area. Quaternary sediments are underlain by layered Permian sediments. The layers consist of dense carbonate formations and red-colored loose sediments. The humus profile of leached chernozems does not depend on the depth of the underlying Permian sediments and consists of horizons A and AB with a total thickness of 40-50 cm. The shortening of the profile occurs due to the reduction or absence of horizons B and C, i.e. organogenic horizons lie directly on the underlying rock - horizon D.

With some degradation of the soil cover of the arable land, the D horizon may be involved in the arable horizon and the leached chernozem becomes rocky and carbonate. Leached chernozems with a thickness of organogenic horizons more than 50 cm have low reflectivity. This is due to the low carbonate content, high humus content and large moisture reserves. Reflectivity increases with decreasing of thickness and increasing of carbonate content, and then with the appearance of rockiness. The maximum brightness is recorded when the arable horizon is the most rocky.

Precision farming.

The application of mineral fertilizers cannot affect the contrast of ASCS. Chemicalization agents cannot reduce the negative impact of the underlying dense rocks on the formation of the root system or on the thickness of the loamy layer that retains moisture. Consequently, applying the same doses of fertilizers on average across the agricultural field leads to overconsumption of fertilizers in some elements of the ASCS (zones of low fertility) and a severe shortage of nutrients in others (zones of high fertility). Of course, this is typical if the fertilizer application rate was calculated based on gross measurements of the yield from the entire field. That is, if doses of fertilizers should compensate the removal of nutrients with the crop.

When drawing up task maps for the variable rate application of fertilizers for each crop, it is possible to calculate how much fertilizer doses can be reduced in the red zones without reducing the yield. The released doses of fertilizers can be transferred to areas of increased fertility. At the same time, the total consumption of fertilizers on the field remains unchanged.

With variable rate application of fertilizers while maintaining the same yield in the red zone, it was possible to change the ratio of yield in the red and green zones. For

sunflower the resulting ratio was one to seven, and for spring wheat and peas two to three. Variable rate application of fertilizers makes it possible to more fully use the productivity of individual elements of ASCS, which increases the overall yield (gross yields).

CONCLUSION

The map of agate-like soil cover structures is a consequence of remote sensing archives reaching the state of big data and the development of neural network methods for processing remote sensing data. More than a thousand Landsat scenes were filtered for each pixel of the agricultural field. Remote sensing data fragments that are suitable for VIs calculation or assessing the spectral characteristics of the bare soil surface were selected. Filtered tens and hundreds of remote sensing data scenes are convolved into a single indicator in the form of maps of stable intra-field heterogeneity of soil fertility for VIs or a map of the "C" coefficient of a multi-temporal soil line for BSS. Both maps allow mapping the distribution of ASCS.

ASCS are formed on Quaternary sediments with a thickness of 0.5 to 5 m, underlain by dense Permian sediments. The different thicknesses of Quaternary sediments lead to the formation of leached chernozems of varying thickness and rockiness. In the ASCS, thick leached chernozems and shortened stony carbonate chernozems alternate in a ring shape over several tens of meters. Shortened chernozems can have a full profile of organic horizons (A and AB).

The achieved accuracy of detection (mapping) of ASCS allows to create task maps for precision farming systems. Precision farming in the form of variable rate application of fertilizers and seeds allows to increase gross yields from each agricultural field without increasing the cost of fertilizers.

ACKNOWLEDGEMENTS

This work was supported in the framework of state assignment FGUR-2022-0009

REFERENCES

[1] Haneklaus S., Lilienthal H., Schnug E. 25 years Precision Agriculture in Germany – a retrospective. Proceedings of the 13th International Conference on Precision Agriculture : July 31 – August 3, 2016, St. Louis, Missouri, USA, 2016.

[2] Kukutai A. Can Digital Farming Deliver on its Promise. 2016. URL: http://www.agnewscenter.com/archives.cfm?news=9903

[3] Fridland V.M. Structure of the soil mantle, Geoderma, vol. 12, pp. 35-42, 1974. DOI: 10.1016/0016-7061(74)90036-6

[4] Skryabina O.A. The structure of the soil cover, methods of its study. Perm, Perm State Agricultural Academy, 206 p, 2007.

[5] Smith G.D. A new classification scheme, progress report. Transactions of 7th International congress of soil science, Madison, WI, vol. 4, pp. 150-111, 1960.

[6] Johnson W.M. The pedon and polypedon. Soil Science Society of America, Proceedings, vol. 27, pp. 212-215, 1963.

[7] Webster, R. Fundamental objections to the 7th Approximation. Journal of Soil Science, vol. 19/ issue 2, pp 354–366, 1968. DOI: 10.1111/j.1365-2389.1968.tb01546.x

[8] Kozlovsky F.I. Soil individual and methods for its determination. Patterns of spatial variation in soil properties and information and statistical methods for their study. Nauka, Moscow, pp. 42-59, 1970.

[9] Ischenko T.A. All-Union instruction on soil surveys and the compilation of large-scale soil land use maps. Kolos, Moscow, 1973.

[10] Maksimov P.G., Florinsky M.A. Guidelines for conducting a comprehensive agrochemical survey of soils on agricultural land. TsNTIPR, Moscow, 1994. URL: https://files.stroyinf.ru/Data2/1/4293736/4293736617.pdf?ysclid=lsztcn25o122621490

[11] Simakova M.S. Soil maps. Cartographic knowledge of Russia (topographic and thematic maps). Publishing house of the Institute of Geography of the Russian Academy of Sciences, Moscow, pp. 113-133, 1999.

[12] Kulyanitsa A.L., Rukhovich D.I., Koroleva P.V., Vilchevskaya E.V., Kalinina N.V. Analysis of the informativity of big satellite precision-farming data processing for correcting large-scale soil maps. Eurasian Soil Science, vol. 53/ issue 12, pp 1709–1725, 2020. DOI: 10.1134/S1064229320110083.

[13] Kiryushin V. I. The management of soil fertility and productivity of agrocenoses in adaptive-landscape farming systems. Eurasian Soil Science, vol. 52/ issue 9,pp 1137-1145, – 2019. DOI: 10.1134/S1064229319070068.

[14] Yakusheva O.I. The influence of intra-field soil heterogeneity and the level of intensification of agricultural technologies on the yield of spring wheat. PhD dissertation of agricultural sciences, 2013.

[15] Belik A.V. Intra-field variation in the fertility of forest-steppe chernozems of the Central Chernozem Region and the yield of agricultural crops. PhD dissertation of biological sciences, 2008.

[16] Belousov A.A., Belousova E.N. The influence of intra-field heterogeneity of soil fertility on the choice of elements of the field experiment methodology. Vestnik KrasSAU, issue 6, pp 30-37, 2013.

[17] Soil Map of the Collective Farm Udarnik, Klyavlinsky district, Samara Region, Scale 1:25000, Roskomzem RosNIIzemproekt VolgoNIIgiprozem, 1995.

[18] Ivanov D.V., Alexandrova A.B., Grigoryan B.R., Kulagina V.I. Rare and endangered soils of the Republic of Tatarstan. Georesursy, vol. 5/ issue 41, 2011.

[19] Nomenclature and taxonomy of the main soil types in the Republic of Tatarstan. Shinkarev A.A., Gusarov A.V., Giniyatullin K.G., Melnikov L.V., Latypov M.K. (comp.), Kazan State University Publishing House, Kazan, 2008.

[20] Rukhovich D.I., Koroleva P.V., Rukhovich D.D., Rukhovich A.D., 2022. Recognition of the bare soil using deep machine learning methods to create maps of arable soil degradation based on the analysis of multi-temporal remote sensing data. Remote Sensing, vol. 14/ issue 9, 2224, 2022. DOI: 10.3390/rs14092224.

ECOLOGICAL AGRICULTURE AS A SOCIAL COMPONENT OF ENVIRONMENTAL SUSTAINABILITY AND FOOD SAFETY

Doctor of Philosophy (D.Sc.), Professor Roman Oleksenko[1]
Doctor of Philosophy (D.Sc.), Professor Valentyna Voronkova[2]
Doctor of Philosophy (D.Sc.), Professor Vitalina Nikitenko[2]
Doctor of Economic (D.Sc.), Professor NatalyaMetelenko[2]
PhD in law, Associate Professor Liudmyla Holovii[3]
[1]Volodymyr Vynnychenko Central Ukrainian State University, **Ukraine**
[2]Zaporozhzhia National University, Zaporizhzhia, **Ukraine**
[3]National University of Life and Environmental Sciences of Ukraine, **Ukraine**

ABSTRACT

The research is aimed at identifying the conditions for the formation of the ecological agriculture concept aimed at creating a sustainable, environmentally friendly and efficient agricultural production system. The main idea is to use natural processes and resources to ensure a harvest while maintaining the environmental balance. Ecological farming can be an important step towards sustainable agriculture and environmental sustainability, but it requires a balance between positive and challenging aspects, as well as additional research and innovation to achieve optimal results. The study used methods of system analysis and synthesis, Agile methodology, axiological, synergistic, ecological and humanistic methods and approaches, which allowed us to reveal new directions for improving ecological agriculture (agriculture) as a social factor of environmental sustainability and food security. With this approach, it is possible to combat environmental problems more effectively and develop sustainable approaches to the use of the planet's resources. The main task of implementing digital ecology is to create conditions for the transition to an open, healthy and safe digital ecology, which represents the intended transition to eco-civilisation. The conditions for the formation of an effective mechanism for the ecological development of a secure digital ecosystem are revealed. Digital ecology is one of the key areas aimed at preserving the environment and ensuring the long-term viability of our planet as an eco-civilisation.

Keywords: ecological agriculture, agriculture, environmental sustainability, food security, ecological farming.

INTRODUCTION

Ecological agriculture first emerged in Europe in 1924 and gained traction in Switzerland, the UK and Japan in the 1930s and 1940s. In the 1960s, many farms in Europe turned to organic agriculture. In the late 1970s, Southeast Asia began to explore organic agriculture. Choosing the path of sustainable development has become a common choice for agricultural development in all countries of the world. Today, with the development of society and the integration of world cultures, ecological agriculture, the most human-centric industry, has sparked a wave of rapidly rising waves of ecological agriculture. The concept of ecological agriculture was first introduced in the book Ecological Agriculture, co-authored by Geoffrey McNeely and Sarah Sherr in 2003. Agroecologists study ecological agriculture as a factor of synergy, environmental

sustainability and food security. These attributes use the natural sciences to understand elements of agricultural ecosystems, such as soil properties and plant-insect interactions, and the social sciences to understand the impact of farming practices on rural communities. Economic constraints on production methods or cultural factors determine farming practices. The most common definition of the term can be found in Dalgaard et al. who define agroecology as the study of the interactions between plants, animals, humans and the environment in agricultural systems. Agroecology is interdisciplinary in nature and includes elements of agronomy, ecology, sociology, economics and related disciplines. In this context, the environmental part of agroecology includes social, cultural and economic contexts. The definition has also been expanded, but with a greater emphasis on the conceptual food system. Different definitions of the term "agroecology" can be distinguished, first of all, by defining the specifics of the term "ecology" and possible connotations of the term. Agroecology is defined as the study of the relationship between crops and the environment. This definition refers to the ecological part of agroecology as the natural environment. According to this definition, agroecology studies various relations of agriculture - from soil health, water quality, air quality, fauna, flora and microfauna, and surrounding flora to environmental toxins and other anti-crisis factors [10]. Agroecology is an approach to landscape management aimed at achieving three goals: 1) conservation of biodiversity and sustainable ecosystem services; 2) sufficient food production; 3) provision of livelihoods in rural areas. Agroecology as a concept of ecological agriculture emerged in the 21st century. Humans have an unprecedented demand for limited land and want to increase global food production by 50-100% to improve the quality of life of millions of poor people while protecting wild biodiversity and ecosystem services that support human life. If these needs are to be met simultaneously, the solution must be to create a system of land use in the same geographical space. This is how the term "ecological agriculture" was born [2].

The purpose of the study: development of conditions for the implementation of ecological agriculture as a social factor of environmental stability and food security.

Objectives of the study: 1) to formulate the concept of "ecological agriculture" as a realisation of the Millennium Development Goals; 2) to identify the essence and directions of development of ecological agriculture as a component of environmental sustainability and food security.

MATERIALS AND METHODS

The study used the methods of system analysis and synthesis, Agile methodology,[1] axiological, synergistic, ecological and humanistic methods and approaches, which allowed us to reveal new directions for improving ecological agriculture as a social factor of environmental sustainability and food security. With this approach, it is possible to combat environmental problems more effectively and develop sustainable approaches to the use of the planet's resources. The method of modelling and analysing data on the relationships between various aspects of organic agriculture and its impact on social development, environmental sustainability and food security plays a major role. The cross-cultural method allows comparing approaches and outcomes of organic agriculture in different countries or regions to identify effective strategies and best practices. The use of a systems approach to analyse the interrelationships between the components of organic agriculture allows for the consideration of environmental, economic and social aspects. Studying the impact of agriculture on biodiversity allows

us to determine the species composition and diversity in different agroecosystems. The analysis of the role of new technologies and innovations in the development of organic agriculture and their impact on environmental sustainability and food security allowed us to combine these methods to obtain a comprehensive understanding and in-depth analysis of the topic of organic agriculture and its social impact. The combination of these methods allowed us to get a comprehensive view of the topic and highlight various aspects of organic agriculture as a social factor for ensuring environmental sustainability and food security [3].

RESULTS

The study focuses on the formation of the concept of "ecological agriculture" as a means of implementing the Millennium Development Goals; ecological agriculture as a component of environmental sustainability and food security.

1.The concept of 'ecological agriculture' as a means of implementing the Millennium Development Goals

In recent years, "ecological agriculture" has been developing as a comprehensive approach to the use of agricultural land and biological conservation in the spirit of shared prosperity and coexistence. The values of ecological agriculture have much in common with existing concepts such as permaculture, permaculture, agroecology, natural resource management, organic agriculture, agroforestry, conservation agriculture, protected area management, etc. In fact, the landscape of ecological agriculture is made up of the above characteristics. Ecological agriculture focuses on how to plan and manage land use in rural areas.

Table 1 The latest principles and approaches of the ecological agriculture concept

Principle or approach	Content of the principle or approach to the concept of ecological agriculture
Maintaining soil fertility	Using methods that maintain and improve soil structure and fertility, such as composting, green manuring and crop rotation.
Biodiversity	Creating natural habitats and areas to promote plant and animal diversity. Avoiding the use of chemical pesticides and herbicides that may have a negative impact on the ecosystem.
Preservation of water resources	Use of efficient irrigation methods, reduction of groundwater and surface water pollution, and application of agricultural techniques to prevent erosion.
Promoting health	Growing food without the use of harmful chemicals that can affect product quality and safety.
Using renewable resources	Reducing dependence on unsustainable use of natural resources and promoting the use of alternative energy sources.
Organic agriculture	This approach is based on organic methods and practices that eliminate the use of synthetic chemical fertilisers and pesticides. Instead, natural fertilisers, composting, crop rotation and other methods of preserving soil fertility are used.
Permaculture	This concept, which is based on the creation of sustainable and efficient growing systems that rely on natural ecosystems, includes the development of design that promotes the use of resources efficiently and as close to natural processes as possible.
Biodynamic	This approach considers the farm as a living organism, where

agriculture	specific practices are used to preserve soil fertility and create harmony with nature, including an astrological calendar and specific methods of supporting biological processes.
Agroecology	This approach emphasises the study and use of natural ecological processes to increase yields and support sustainable development, and seeks to create farming systems that take into account ecological interactions and impacts.

Ecological agriculture extends beyond the management of individual farms and studies and plans for the interactions between different land uses from a broader landscape perspective. In addition, it can fully interpret the dynamics of wildlife and plant populations within the landscape and the basic functions of hydrological watersheds. Furthermore, compared to the short-term dimension of a phenomenon, if ecological agriculture operates over a longer period of time, synergistic effects will be more evident, so ecological agriculture advocates usually conduct analyses over a longer period of time than usual. time. Ecological agriculture focuses on the needs and opportunities for mutual cooperation between nature conservation, agricultural production and rural life. In part, agroecology research and monitoring often aims to identify these synergies. The management of ecological agricultural landscapes should rely on the support of different stakeholders at the landscape scale to work together to achieve different environmental and socio-economic goals, and to develop appropriate methods to achieve a win-win situation for conservation, production and life. Ecological agriculture emphasises the importance of ecosystem services in supporting sustainable agricultural production, the conservation of local biodiversity and the concept of ecosystems [3]. By developing farming methods that are both environmentally friendly and improve the livelihoods of agricultural residents, conservationists can effectively harness the benefits of nature reserve conservation. It is only by increasing their productive asset base and encouraging long-term landscape planning that they can improve their quality of life and the health and diversity of ecosystems. Conservationists who ignore the importance of agricultural land for the conservation of natural lands and those who argue that arable land can only be maintained. There is no help and benefit in this area in the case of living agricultural scientists, both factions are biased. Faced with the situation of population growth and relative reduction of cultivated land, rural actors have started to carry out communication activities on officially protected nature reserves, and the end result for this landscape has been good, bad or mutually beneficial, all depending on whether there is a well-thought-out land management plan. Human agricultural activity has had a profound impact on the Earth. Almost a third of the world's land area is heavily affected by cultivated land and pasture. Even the deposit is part of the agricultural cycle and even becomes part of gardens, pastures or forestry [4]. Furthermore, most of the world's 100,000 territories also include large areas of agricultural land, and more than half of these species-rich areas are home to large numbers of people whose livelihoods depend on agriculture, forestry, livestock and fisheries. The intensive practices of modern agriculture often threaten wildlife species and the natural ecosystem services on which people, animals and plants depend. More than 70% of freshwater is used by humans to irrigate crops, which seriously affects the hydrological cycle of the ecosystem. In addition, fertilisers, pesticides and agricultural waste also threaten the biological environment and protected areas downstream. Ploughing and clearing of agricultural land reduces food sources and habitats for organisms, and fishing without consideration of sustainability will lead to

the consumption of freshwater and marine fish stocks. In addition, the planting and sale of certain individual crops reduces the diversity of agricultural products, and the planting of a variety of fruits, vegetables and grains is no longer possible. As the demand for global agricultural production increases, it is essential to use agricultural landscape management to increase productivity and promote biodiversity conservation [5]. Wildlife diversity depends on agricultural producers to sustain the environment. Agricultural production also requires the maintenance of a healthy and diverse ecosystem. The Millennium Development Goals are about reducing poverty, and agroecological strategies are essential to achieving the Millennium Development Goals, especially those related to poverty and hunger, water and sanitation, and a sustainable environment. The Millennium Development Goals cannot be achieved without protecting the livelihoods and incomes of poor rural families, and protecting biodiversity and ecosystem services to sustain them in the long term. An important opportunity to achieve the Millennium Development Goals is to invest in local land management, including the management of ecological agriculture strategies that can promote synergies between rural livelihoods, a sustainable environment and food security. The decline and fragility of ecosystem services are barriers to achieving the Millennium Development Goals, a major cause of poverty that will worsen over the next 50 years. Negative interactions with other ecosystem services can be reduced and positive synergies can be created to maintain or improve ecosystem services in agricultural areas. While there is currently a horizontal communication mechanism between different departments, the prioritisation and investment plans for rural development, agriculture and biodiversity are still handled separately and there is still a lack of linkages between agriculture and biodiversity in the same area [6]. All stakeholders need to have a mentality of following the environment, life and production and communicate multilaterally to reach an agreement that takes into account the three above.

2. Organic farming as a component of environmental sustainability and food security

Ecological agriculture as a component of environmental sustainability and food security is not only about the diversity of agricultural systems, but also about the mosaic and full use of different landscapes, including forests, human settlements, coasts and waters. How to define the relationship between nature reserves and agricultural production areas and how to increase synergies between them are key points to consider in ecological agriculture [7]. Ecological farming (organic farming) is a system of agriculture that seeks to grow food without the use of a wide range of chemical fertilisers and pesticides, while conserving natural resources and maintaining ecological balance. It can have a positive impact on environmental sustainability and food security, but it also comes with challenges.

Table 2. Positive and negative effects of organic farming functions

Function	Positive effects	Negative consequences
Preservation of soil and water resources:	Ecological farming helps to preserve soil and maintain its fertility, emphasising the use of organic fertilisers and composts rather than harmful chemicals. It also helps to avoid contamination	1. Ecological farming can be accompanied by lower yields per unit area compared to intensive methods.

	of water sources from chemicals used in farming.	
Health promotion	Organically grown food usually contains fewer chemical residues, which can be beneficial for human health.	Growing organic products can be more costly, as it requires more manual labour and fewer effective (but more expensive) plant protection methods.
Preserving biodiversity	Avoiding the use of chemical pesticides and growth regulators helps to preserve biodiversity, as it has less harmful effects on natural predators, insects and other organisms.	Refusal of chemical pesticides can lead to increased losses from pests and diseases, especially in the context of epidemics.
Improving soil quality	The use of organic methods helps to improve soil structure, increase its organic carbon content and maintain biological activity.	Some crops may be more vulnerable to pests and diseases in an organic farming system, which may limit their cultivation
Promoting environmental health:	Avoiding the use of chemicals helps to prevent pollution of soil, water, air and the environment in general, reducing the impact of human activity on nature	Organic farming requires detailed planning, careful monitoring of plants and pest and disease control, which can be time-consuming.
Increase the content of organic carbon in soil	Ecological farming contributes to the accumulation of organic carbon in the soil, which can contribute to the fight against climate change by reducing greenhouse gas emissions.	Low resilience to high humidity and weather extremes: organic farms can be vulnerable to weather extremes such as heavy rain or droughts because they do not use synthetic protection measures.
Supporting the development of small farms	Organic farming can be more accessible to small farms and rural communities, providing them with the opportunity to grow food without the high costs of chemicals.	Limited resources for scaling up: Growing organic crops may require a larger land area compared to intensive methods, which can be a limitation for large-scale production.
Challenges with the system integration	The introduction of organic farming into existing agricultural systems may require changes in practices and adjustments to all elements of the system.	Low yields in the first period of transition: During the transition from intensive methods to ecological farming, there may be a period of time when yields may be lower due to ecosystem adaptation.

The effects and benefits of organic farming can vary depending on specific conditions, region, crop type, available resources and technological development. Organic farming can be an important tool in achieving sustainable development, but its success requires careful planning, training and innovation to overcome the challenges it may encounter. Thus, an important feature of ecological agriculture is that every land manager and

operator must communicate and cooperate with each other, because ecological agriculture cannot rely on individuals to implement it, but must rely on the cooperation of all land-related stakeholders [8]. A landscape is a group of ecosystems consisting of local topography, vegetation, land use, and human settlements. The goal of ecological agriculture is to maintain biodiversity and ecosystem services, sustainable agricultural production, and improve the livelihoods of local people. land. It should be linked to a specific landscape scale. To have a significant impact, all elements of the landscape must be considered as a whole. How a landscape is defined depends on local conditions. It can be defined by nature, history, cultural practices, activities and values, or it can be defined by incorporating several of these features at the same time.

3.Ecological agricultural practices.

As global agriculture requires the implementation of the concept of ecological agriculture, agricultural producers and society must work together to promote it. In this regard, it is even more important that farmers consistently protect the biodiversity that provides them with their livelihoods. Based on past experience, there are some incentives to persuade farmers and their communities to continue to maintain the agro-ecological landscape. The inhabitants of each agricultural community play the role of the primary custodian of its ecosystem and biodiversity [9]. They rely on the land and natural resources to uphold an ethic of conservation, as agricultural production depends on some degree of ecosystem services and wild plants also provide fodder for livestock. Fuel, medicines, soil nutrients and sources of building materials for farmers are also important elements of culture, faith and the human spirit. Ecological farming practices can reduce farmers' production costs, increase/maintain stable yields, or improve product quality. For example, crop and pasture rotation systems used in Europe, the United States and Zimbabwe can significantly reduce daily production costs compared to livestock production, as well as reduce land degradation and increase wildlife habitat. To preserve their livelihoods, cultural, spiritual and aesthetic values, rural communities typically actively conserve local biodiversity and ecosystem services. For example, farmers in western Kenya mobilise everyone to protect threatened forest areas within and outside the community for local water resources and medicinal plants. In West Africa, "sacred groves" (sacred groves) have been preserved because of religious beliefs, and virgin forests are still fully intact. Farmers can look for opportunities to increase their income from market channels that support environmentally friendly agricultural products. Currently, there are more than 80 environmental certification schemes, and farmers who ensure environmentally friendly operations can earn a higher than usual income from the crops they grow. In supporting this idea of sustainable agriculture and integrated farming systems, he demonstrates his point of view by focusing on the economics of the system, the environmental impact, and the ethics and values of agriculture.

CONCLUSION

Ecological agriculture aims to mobilise local communities to become the main leaders of ecological agriculture in terms of policy advocacy or organisational change. Global food production is facing the consequences of urbanisation, climate change and conventional farming methods, which are causing various problems such as deteriorating agricultural production conditions, food security crisis, ageing rural populations and economic depression. However, traditional agricultural methods of

extensive use of chemical fertilisers and pesticides have led to the loss of biodiversity and degradation of ecosystem services, and competition between agricultural and domestic and industrial water will become more severe in the future. To enhance the sustainability of the agricultural production environment, the international community continues to call for the development of farmland production and use patterns towards environmentally friendly and ecologically sound sustainable agriculture, and a variety of environmentally friendly farming methods have emerged accordingly.

REFERENCES

[1] Voronkova, V., Nikitenko, V., Oleksenko, R., Andriukaitiene, R., Kharchenko, J., Kliuienko, E. (2023). Digital technology evolution of the industrial revolution from 4g to 5g in the context of the challenges of digital globalization. *TEM Journal,* 12(2), 732-742.

[2] Böck, K., Muhar, S., Muhar, A., Polt, R. (2015). The ecosystem services concept: gaps between science and practice in river landscape management. *GAIA-Ecological Perspectives for Science and Society*, 24(1), 32-40.

[3] Voronkova, V., Nikitenko, V., Oleksenko, R., Andriukaitiene, R., Polysaiev, O. (2023). Environmental crisis overcoming as a factor for achieving economic sustainability in the context of the European green course. *Cuestiones Políticas*, 41(77), 612-629.

[4] Nikitenko, V., Voronkova, V., Oleksenko, R., Matviienko, H., Butkevych, O. (2023). Sustainable agricultural development paradigm formation in the context of managerial experie nce of industrialized countries. *Revista de la universidad del ZULIA.* 3ª época. Año 14(39). 81-97.

[5] Lavrov, V., Grabovska, T., Ternowyi, Yu. (2019). Methodology, mechanisms and tools for substantiation of socio-ecological and economic benefits from the implementation of organic production. Monografia viacerých autorov: Geomanagement in organic agriculture. Vydavateľ: Európsky inštitút ďalšieho vzdelávania. Podhajska, Slovensko. 125–149.

[6] Patyka, V., Kalinichenko, A. (2020). Agricultural microbiology as the basis of organic farming. Biodiversity of Ukraine in the context of modern natural environmental conditions: materials of the International Scientific and Practical Conference (Ternopil, 04-05 June, 2020) [ed. by V. Cherniak (ed.) and others]; Ternopil OKIPPO. Ternopil: TOCIPPO Publishing Centre. 37-39

[7] Ponisio, L. C., M'Gonigle, L. K., Mace, K. C., Palomino, J., De Valpine, P., Kremen, C. (2015). Diversification practices reduce the organic to conventional yield gap. *Proceedings of the Royal Society B: Biological Sciences*, 282(1799), 20141396.

[8] Organisation of the territory of agricultural enterprises: agro-landscape aspect: monograph (2020) / N. M. Stupen, N. E. Stoyko, O. R. Baran, O. I. Stupen. Lviv: Galician Publishing Union LLC. 172 p.

[9] Stupen, M., Stupen, R., Ryzhok, Z., Stupen, O. (2019). Methodological foundations of the organisation and protection of lands in the context of the balanced nature use. Management, *Economic Engineering in Agriculture and Rural Development*, 19(1), 565-571.

[10] Oleksenko, R., Kolokolchykova, I., Syzonenko, O. (2019). Ukraine in the Context of the World Organic Production of Agricultural Products. In *Modern Development Paths of Agricultural Production: Trends and Innovations* (pp. 507-514). Cham: Springer International Publishing.

EFFECTS OF ORGANIC FERTILIZER APPLICATION ON AMERICAN CRANBERRY CULTIVATION – MINERAL NUTRITION STATUS, PLANT VITALITY AND POSSIBLE ENVIRONMENTAL ASPECTS

Dr. Andis Karlsons

Dr. Anita Osvalde

Msc. Laura Abolina

Institute of Biology, University of Latvia, **Latvia**

ABSTRACT

The cultivation of American cranberries (*Vaccinium macrocarpon* Aiton) with organic fertilizers is becoming more common in the world. With 180 ha of producing plantings and 376 tonnes of yearly production, Latvia is one of the largest cranberry producers in the world. The lack of knowledge on fertilization management can be an obstacle to a successful transition to organic farming. The objective of this study was to test the effect of organic fertilizer of animal origin on cranberry mineral nutrition status, plant vitality, vegetative growth and berry yield. Field experiments on cranberry cultivar Bergman were conducted during 2022-2023 in a commercial plantation established on cutover peat bog in Latvia. In the spring of both experimental years, cranberries received five levels (1, 2, 3, 4, and 5 t ha^{-1}) of certified pelleted organic fertilizer FERTIPLUS (4-3-3-65 OM). Two control treatments – without fertilizer and conventional fertilizer with Novatec Classic (12-8-16+3+TE) – were also established. The results showed that even the highest doses of organic fertilizer added in 2022 did not affect the nutrient content in the peat in 2023 at the beginning of vegetation, thus indicating a high release of plant-available nutrients in the first year. Nutrient release process occurred over a longer period than from conventional fertilizer, reaching maximum in August. Adjustment of the organic fertilization strategy is needed to account for the slow release pattern and synchronize with the cranberry growth phases. Thus, organic fertilizer can be successfully incorporated into the American cranberry fertilization plan for plantations in peat bogs with the optimal dose of 2-3 t ha^{-1}.

Keywords: cranberry bog, plant analysis, soil testing, upright length, SPAD

INTRODUCTION

American cranberries (*Vaccinium macrocarpon* Ait.) are grown in acidic (pH 4.0-5.0) sandy or peaty soils with low nutrient availability [1]. Cranberry cultivation requires abundant water resources. Due to these environmental conditions, there are relatively limited places where this berry crop can be mass-produced [2]. Cultivation of cranberries without the use of synthetic fertilizers and chemical plant protection products is becoming more common in the world. Organic production has developed most extensively in Canada and the United States – the largest cranberry-growing countries in the world [3], [4]. One of the main problems organic cranberry growers face, in addition to fighting pests, weeds and diseases [5], is yield reductions of 50% or

more compared to conventional production [6]. Shortcomings in organic fertilization can significantly decrease berry yield as compared to conventionally grown berries.

With 180 ha of producing plantings established in extracted peat bogs and 376 tonnes of yearly production, Latvia is one of the largest cranberry producers in the world [7]. Although the market for organic produce is growing, the lack of knowledge on fertilization management can be an obstacle to a successful transition to organic farming. The information on organic cranberry cultivation in sphagnum peat bogs is particularly limited and incomplete.

Organic fertilizers are characterized by slow-release components, contrary to the fast effect most conventional fertilizers provide. They are also highly dependent on climatic conditions – temperature and precipitation or irrigation. Therefore, managing organic fertilization timing and rates can be challenging to achieve high berry yield and quality. Although cranberries were found to be most responsive to nitrogen fertilization compared to other nutrients, over-fertilization is associated with excessive vegetative growth, which increases the plant's susceptibility to diseases, spring frosts, makes harvesting difficult and can have adverse effects in subsequent years [8]. Thus, one of the main aims in organic cranberry cultivation is providing adequate nitrogen fertilization throughout the growing season. Cranberry fertilization is usually based on tissue and soil nutrient tests [9], as well as on upright growth parameters [10]. However, decisions on site-specific fertilization rates and sources should also be based on local climatic conditions and the trade-off between berry yield and quality.

The objective of this study was to test the effect of organic fertilizer of animal origin on cranberry mineral nutrition status, plant vitality, vegetative growth and berry yield. The results will be important for developing a fertilization system that would be appropriate for organic cultivation of cranberries in peat soils in Latvia, as well as in similar soil and climatic conditions.

MATERIALS AND METHODS

Field experiment site and design. The field trial was arranged in 2022 on a cranberry production farm (57°34′N, 22°69′E, hemiboreal climatic zone) located in a cutover peat bog (Talsi Municipality, Latvia) to investigate the effect of increasing organic fertilizer rates on cranberry nutrient status, plant vitality, vegetative growth and yield. The experiment comprised 7 treatments in a randomized block design with three replications for each treatment. A set of 50 m^2 plots (5x10 m) were established on the existing commercial stand of cranberry cultivar 'Bergman'. Cranberries received five levels (1, 2, 3, 4, and 5 t ha^{-1} designated as treatments F1, F2, F3, F4 and F5) of certified pelleted organic fertilizer FERTIPLUS (4-3-3-65 OM). Two control treatments were established: one without fertilizer (K0) and another with conventional fertilizer (KNPK) – with 250 kg ha^{-1} Novatec Classic (12-8-16+3+TE), containing nitrification inhibitor. At the end of May 2022, the entire dose of fertilizer was applied uniformly by hand on each plot. The same fertilization scheme was repeated in May 2023.

Meteorological data was retrieved from the closest meteorological station in Stende for the vegetation period of 2023 [11].

Determination of the nutrient status of cranberries and plant measurements were carried out in the second year of the experiment – 2023. Peat and cranberry upright tips were sampled monthly for nutrient analysis – peat samples from May (before applying

fertilizer) to September, plant samples from June to September. The length of the cranberry uprights was measured at the end of September. Chlorophyll content (in SPAD values) in cranberry leaves was measured monthly from July to October with a portable chlorophyll meter SPAD 502 (Minolta, Warrington, UK).

Berries were harvested by hand in four 1.0 m^2 sub-plots per plot in mid-October and weighed to calculate average berry mass (g) and yield (t ha^{-1}) for each treatment.

Laboratory analysis. Peat samples (0-20 cm) collected from each plot were air-dried and sieved through 2-mm sieve. Plant available nutrients (N, P, K, Ca, Mg, S, Fe, Mn, Zn, Cu, Mo, and B) were extracted with 1 M HCl (soil: extraction solution ratio 1:5 v/v). Soil pH was detected in 1 M KCl (soil: extraction solution ratio 1:2.5 v/v), electrical conductivity (EC) in distilled water extract (soil: distilled water ratio 1:5 v/v). For the determination of K, P, Ca, Mg, Fe, Cu, Zn, Mn, Mo and B, plant material was dried to constant weight, ground and samples were dry-ashed in concentrated HNO_3 vapours and re-dissolved in 3% HCl. For detection of total N, wet digestion was done in conc. H_2SO_4, for S – in conc. HNO_3. K, Ca, Mg, Fe, Mn, Cu and Zn for peat and plant samples were quantified with microwave plasma atomic emission spectrometer (MP-AES) Agilent 420. The N, P, Mo and B contents were determined by colorimetry, S by turbidimetry with a spectrophotometer JENWAY 6300.

Statistical analysis was performed using MS Excel 2016. A one-way ANOVA with post hoc Tukey HSD test were conducted to determine statistically significant differences ($p < 0.05$) between fertilizer treatments for SPAD indices and cranberry upright tip length.

RESULTS AND DISCUSSION

To characterize the effect of organic fertilizer rates, the concentration of 12 essential nutrients available to the plant was determined in peat samples and their compliance with the sufficiency guidelines [12] was evaluated. The results showed that even the highest doses of organic fertilizers incorporated in the previous year (2022) did not affect the content of nutrients in the peat at the beginning of the next year's vegetation in May 2023 (Figure 1). Also, at the end of the season 2023, the significant effect of the fertilizer applied in the current year was no longer detectable in the peat and the concentrations of N, P, and K for all treatments were close to unfertilized control. This indicates a high release of plant-available nutrients in the year of fertilizer application. The dynamics of nutrient concentrations in the peat were influenced by both the type of fertilizer and the amount of precipitation in a month during the season. The total precipitation in the study region in June 2023 was only 4.5 mm, which is 94% below the monthly norm (70.1 mm) [11]. Therefore, in June, neither the complex fertilizer nor the pelleted organic fertilizer dissolved and affected the content of nutrients in the peat (Figure 1). After precipitation normalized in July (74.3 mm), N, P and K were immediately released from conventional fertilizer, and release rates tended to decrease as the season progressed. The nutrient release process from organic fertilizer was slower, occurred over a longer period and reached its maximum in August, which was warm (mean temperature 17.9 °C) and rich in precipitation (153.5 mm). This contributed to the mineralization of organic matter and nutrient release. During these peak periods, conventional fertilization and the highest rates of organic fertilizer (F3, F4, F5) provided the minimum required N level in the peat.

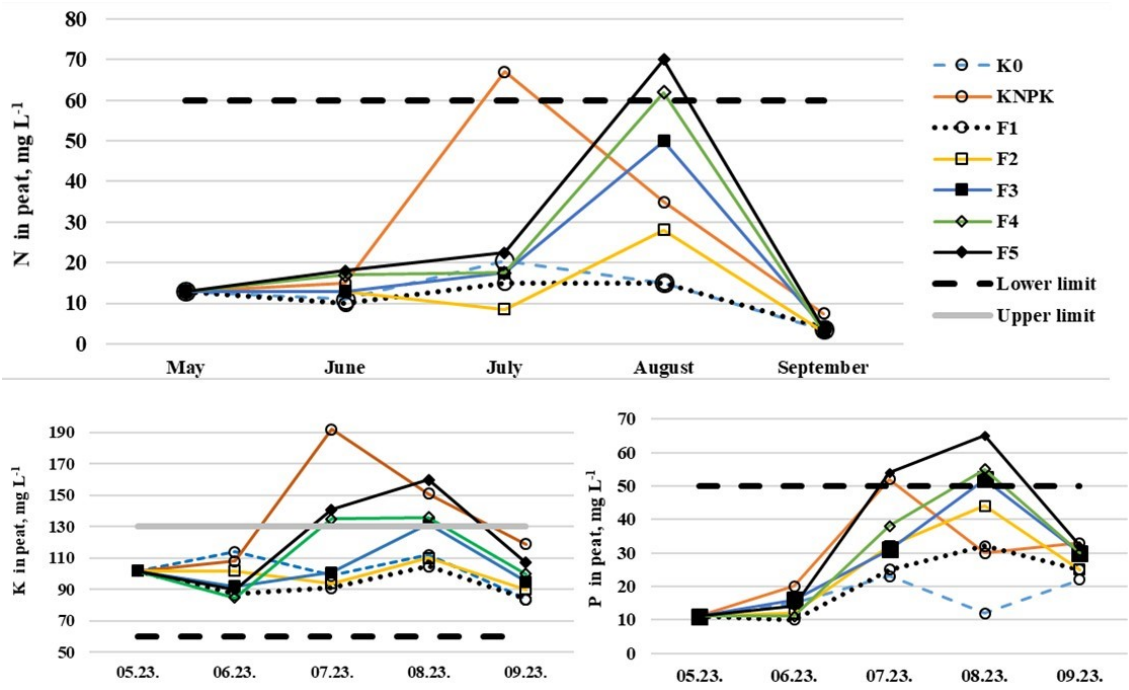


Figure 1. Plant available concentrations of N, P and K in cranberry peat in 1M HCl extraction (mg L^{-1}). K0 – control, KNPK – conventional fertilization, F1-F5 – organic fertilizer from 1 to 5 t ha^{-1}.

Cranberries primarily use N during three stages: early season leaf production, fruit set and filling, and bud set [8]. In our study, the conventional fertilizer better ensured the cranberry stand during the fruit setting period in July, while the organic fertilizer during the fruit filling and floral bud formation in August which usually occur simultaneously. We conclude that organic fertilizers applied in appropriate doses could meet the requirements of plant growth and fruit formation in the most active part of the growing season. Higher levels of plant-available N later in the growing season are considered to favour fall fruit types to support berry production [13]. Similar trends to N were also found for K and P supply in peat during the season, however, the level of K in July was assessed as overabundant in the case of conventional fertilization.

There were no significant differences in the concentrations of other nutrients in the peat between the treatments at specific sampling times. However, in July and August, the Mg, S, Mn, and Zn concentrations were higher for the conventional fertilizer application (KNPK) and the highest levels of organic fertilizer (F4 and F5). The rate and mean concentrations of nutrient, pH and EC levels in peat during the season from June to September 2023 are shown in Table 1. The experimental field had a low supply of S, Cu and B in the peat. The deficit of these nutrients is generally characteristic of cranberry plantations in Latvia [14].

The results of the field experiment showed differences in the effect of organic and conventional fertilizers on the concentration of N and P in cranberry leaf tissue (Fig. 2). Conventional fertilization provided sufficient N supply throughout the season, except in June, when due to drought, the fertilizer was not dissolved and the N concentration was only 0.85%, which was lower than the recommended 1.2-1.5% N for cranberry tissue in June [8]. Influenced by the highest doses of organic fertilizer (F3-F5), the N content in

cranberry tissues increased steadily, reaching the highest values in September: 1.10-1.25%.

Table 1. The rate and mean concentrations of nutrients in peat and cranberry tissue from June to September 2023.

	Peat (mg L^{-1} in 1M HCl extraction)			Plant tissue (Ca, Mg, S in %, micronutrients in mg kg^{-1})		
	Range	Mean±SE	Sufficiency range*	Range	Mean±SE	Sufficiency range**
Ca	479-1173	690.08±30.94	400-1000	0.65-0.92	0.75±0.01	0.5-1.0
Mg	90-169	117.13±4.27	80-200	0.16-0.32	0.21±0.01	0.15-0.40
S	4.4-32	15.31±1.62	40-80	0.08-0.14	0.11±0.003	0.10-0.30
Fe	48-69	58.21±1.14	60-200	23.0-53.0	45.32±1.18	60-200
Mn	0.65-3.67	1.24±0.13	2.0-8.0	31.0-94.4	54.79±2.41	25-120
Zn	2.54-4.87	3.38±0.14	2.0-8.0	17.0-28.0	20.33±0.62	20-100
Cu	0.25-0.88	0.43±0.03	4.0-10.0	2.40-4.12	2.96±0.12	5.0-10.0
Mo	0.02-0.03	0.022±0.001	0.05-0.4	0.20-0.55	0.34±0.02	0.5-5
B	0.1-0.8	0.28±0.03	0.8-1.5	8.0-25.0	17.79±0.69	20-60
pH_{KCl}	2.83-3.39	3.02±0.02	4.0-5.0			
$EC_{mS/cm}$	0.24-1.1	0.46±0.05	0.6-1.2			

*Nutrient sufficiency range in peat (1M HCl extraction) for American cranberries [12].
**Nutrient sufficiency range in plant tissue for American cranberries [9].

Since the N supply from organic fertilizers is modulated by temperature and moisture level [15], it is difficult to regulate the availability of N (both the amount and synchronization with the growth stages). Our study showed N deficiency in cranberry tissues in early summer and relatively high concentrations in autumn if N is released from fertilizer later in the season. Close monitoring of N supply is recommended if N in cranberry tissue is > 1.1% from mid-August [8], mainly to avoid excessive vegetative growth. Seasonal upright growth length significantly increased using the higher organic fertilizer levels (F3, F4, F5), while 5 t ha^{-1} resulted in overgrowth when the mean upright length reached 77 cm (Fig. 3). Optimum new upright length for the 'Bergman'-like cultivar 'Early Black' has been reported to be 55-65 mm [10]. Cranberry stands with excessive vegetative biomass were associated with increased plant susceptibility to diseases and difficult harvest [1]. A non-destructive method to assess the N status of cranberry plants is the determination of leaf chlorophyll using SPAD readings. 25-35 SPAD units were set as the standard range for the cultivar "Early Black" from June to August [10]. Our study results showed the highest chlorophyll content in cranberry leaves in July for treatment KNPK and in August for treatments F4 and F5 (Fig. 4), which coincides with trends in the dynamics of nutrient release from conventional and organic fertilizers. Although the chlorophyll content gradually decreased towards autumn for all treatments, organic fertilizers at rates of 3-5 t ha^{-1} provided significantly higher values also in September and October.

Similar to N, the supply of P in June was generally low; however, in the organic fertilizer treatments F3-F5, the P content in the leaves was slightly higher and reached the minimum recommended in June (0.15-0.19% P). This could be explained by the effect of the previous year's fertilization. The nutrient carryover effect was demonstrated in fertilization trials, where the next year's cranberry yield and leaf composition depended on the fertilizer used in the previous year [4]. During the further course of the

season, no differences were found in the P accumulation pattern – cranberries effectively absorbed the available P from the peat and the P content in cranberry leaves was more dependent on the fertilizer dose. In the case of F5, the content of P reached 0.25% in July and August, exceeding the recommended 0.10-0.20% optimum.

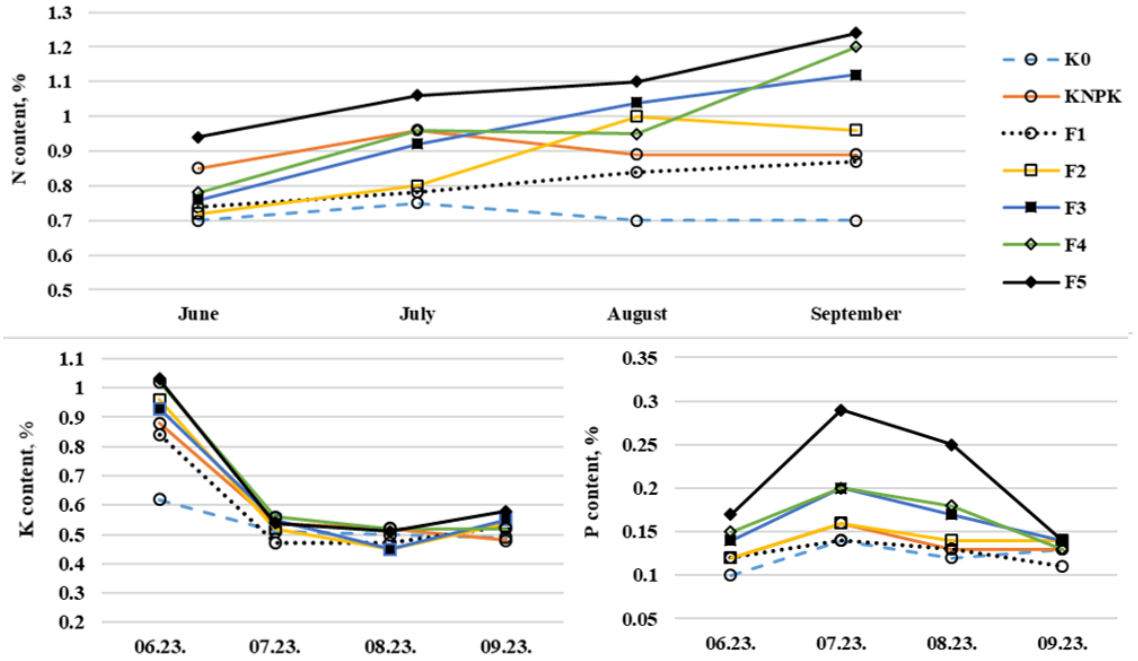


Figure 2. Concentrations of N, P and K in cranberry leaves (mg kg^{-1}). K0 – control, KNPK – conventional fertilization, F1-F5 – organic fertilizer from 1 to 5 t ha^{-1}.

Similar to peat, cranberry tissue K content was optimal for all treatments, including the non-fertilized control, throughout the season. The dynamics of changes in K content depended more on the physiological age of the tissues – the highest levels were typical for young tissues, the lowest – for older ones towards autumn. These data suggest that additional K fertilizer should be limited in cranberry bogs. Our previous studies also showed optimal to high K status for cranberries cultivated in peat bogs in Latvia [14].

There were no significant differences in the concentrations of other nutrients in cranberry tissue between the variants at the sampling times. The rate and mean concentrations of nutrients in cranberry tissue during the season from June to September 2023 are shown in Table 1. Although micronutrients such as Cu, Zn, Fe, and Mn are highly available in acidic soils, most of the tested samples were deficient in Fe and Cu, indicating the need for micronutrient fertilization.

The cranberry plantation suffered significantly from the spring and early summer frosts in 2023. Although sprinkler systems were used to protect flower buds from frost damage, temperatures were extremely cold. Even at the beginning of June, records for daily minimum air temperature were set in Latvia (-2.4 °C in Stende) [11]. Therefore, there was a heterogeneous density of berries in the plots, and the yield achieved (2.9-3.6 t ha^{-1}) did not differ significantly between the treatments. Research should be continued to assess the effect of organic fertilizers on cranberry yield and quality.

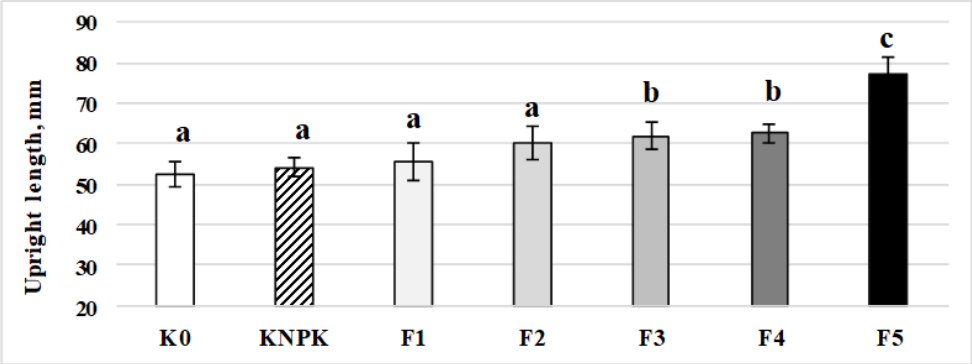


Figure 3. Length of American cranberry uprights (mm) in September 2023. *Treatments with different letters significantly differed from control ($p < 0.05$).

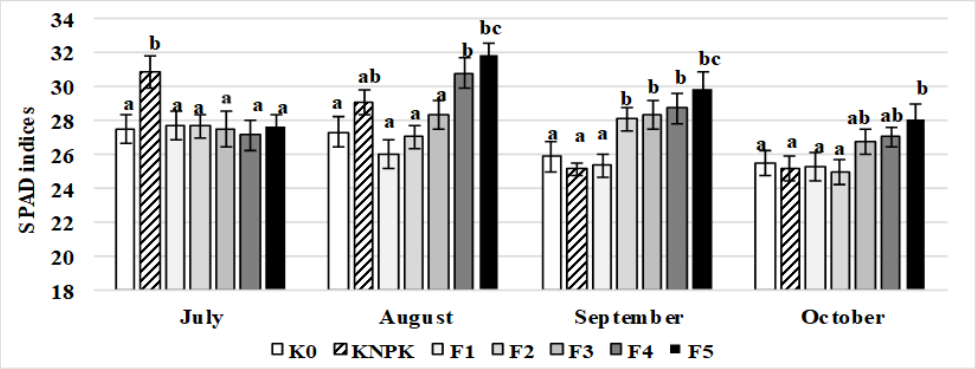


Figure 4. SPAD indices in cranberry leaves. Values with different letters in bars for each sampling time were significantly different ($p < 0.05$).

CONCLUSION

The results indicated a high release of plant-available nutrients from the organic fertilizer of animal origin (FERTIPLUS) during the year of its application in peat soil. The dynamics of nutrient concentrations in the growing medium were significantly influenced by monthly precipitation during the season. Our study found that conventional fertilization better supplied the cranberry stand with N, P and K during the fruit set period in July, while organic fertilization during fruit filling and flower bud formation in August, which usually occur simultaneously. As an autumn-producing berry, cranberries could benefit from a slower nutrient release pattern. Differences in the dynamics of N content in cranberry tissues during the season under organic and conventional fertilization were also found. As the nutrients from organic fertilizer were released over a longer period, the N content in the cranberry tissues increased continuously and the highest values (1.10-1.25%) were reached in September. The authors conclude that organic fertilizer can be successfully incorporated into the American cranberry fertilization plan for plantations in peat bogs with the optimal dose of 2-3 t ha^{-1}. Lower doses did not provide a sufficient mineral nutrition regime, while higher doses caused overgrowth of uprights, with potential disease risks and difficult harvesting. Further research is needed to adjust the fertilization strategy using micronutrient fertilizers and different types of organic fertilizers, possibly earlier in the spring to better synchronize nutrient release with the cranberry growth phases. Since the nutrient levels recommended for cranberries in the peat were not exceeded in any of the

treatments during the vegetation period, the application of organic fertilizer can be considered environmentally safe. Additional studies with other cultivars under local soil and climatic conditions should be considered to complement the results of this research.

REFERENCES

[1] Sandler H.A., DeMoranville C. (eds.), Cranberry production: A guide for Massachusetts. University of Massachusetts Publication CP-08, USA, 198 pp, 2008.

[2] Kennedy C.D., Jeranyama P., Alverson N., Agricultural water requirements for commercial production of cranberries, Can. J. Soil Sci., vol. 97/issue 1, pp 38-45, 2016.

[3] Jamaly R., Parent S.É., Parent L.E., Fertilization and soil nutrients impact differentially cranberry yield and quality in Eastern Canada, Horticulturae, vol. 7, 191, 2021.

[4] Parent L.E., Jamaly R., Atucha A., Parent J.E, Workmaster B.A., Ziadi N., Parent S.É., Current and next-year cranberry yields predicted from local features and carryover effects, PLoS One, vol. 16/issue 5, e0250575, pp 1-16, 2021.

[5] Ben-Zvi Y., Rodriguez-Saona C., Advances in cranberry insect pest management: A literature synthesis, Frontiers in Agronomy, vol. 5, 1006106, pp 1-15, 2023.

[6] Zeldin E., Overview of organic cranberry production, University of Wisconsin-Madison, Center for Integrated Agricultural Systems, 2005.

[7] FAOSTAT, https://www.fao.org/faostat/en/#data/QCL, 2023.

[8] DeMoranville C.J., Ghantous K., 2018–2020 Chart Book: Nutrition management, cranberry chart book – Management Guide 263, University of Massachusetts, USA, pp 63-77, 2018.

[9] Hart J.M., Strik B.C., DeMoranville C., Davenport J.R., Roper T., Cranberries. A nutrient management guide for south coastal Oregon, Oregon State University Extension Service EM8672, 52 pp, 2015.

[10] Davenport J., DeMoranville C.J., Hart J., Roper T., Nitrogen for bearing cranberries in North America, Oregon State University Extension Service EM 8741, 18 pp, 2000.

[11] LVGMC, https://data.gov.lv/dati/lv/dataset/menesu-statistika, 2023.

[12] Nollendorfs V., Plant nutrition levels for American cranberries, Latvian cranberry growers' association, Annual of Cranberry Growers, Latvia, pp. 53-57, 1998, (Latvian).

[13] Strik B.C., A review of optimal systems for organic production of blueberry and blackberry for fresh and processed markets in the northwestern United States, Scientia Horticulturae, vol. 208, pp 92-103, 2016.

[14] Karlsons A., Osvalde A., Nutrient status of the American cranberry in Latvia (2005-2016), Agronomy Research, vol. 15/issue 1, pp 196-204, 2017.

[15] Uddin S., Islam M.R., Jahangir M.M.R., Rahman M.M., Hassan S., Hassan M.M. Abo-Shosha A.A., Ahmed A.F., Rahman M.M., Nitrogen release in soils amended with different organic and inorganic fertilizers under contrasting moisture regimes: A laboratory incubation study, Agronomy, vol. 11, 2163, 2021.

FOREST SOILS FROM SREDNA GORA MOUNTAIN IN BULGARIA

Prof. Dr. Toma Shishkov[1],

Assoc. Prof. Dr. Emil Dimitrov[1]

Prof. Dr. Ekaterina Filcheva[1],

[1] Institute of Soil Science, Agrotechnologies and Plant Protection "Nikola Poushkarov", Agricultural Academy, **Bulgaria**

ABSTRACT

The soils from the central part of Sredna Gora Mountain in Bulgaria were studied aiming to establish the occurrence of contemporal soil forming processes occured in the forest ecosystem. Soils were analyzed to determine the carbon content, the soil organic matter composition and the total soil acidity. The precise soil classification based on the detail morphological diagnostic was carried out. The ecological conditions in forest ecosystem determine the mode of humic substances in the studies soils. Soils are characterized with low degree of humification and considerable amount of organic matter only on the soil surface. Generally, large proportion of absorbed nutrients is returned annually to the soil and is reabsorbed after biological breakdown of litter. Forest soils considerably differ by the soil organic matter (SOM) composition. The quantity and quality of humic substances is linked to the important soil functions. Humic acids are mainly in the upper part in the first soil and fulvic acids dominated in the lower part of profile. Humic acids in the second soil are bounded with calcium and composing humic type of humus. In the shallow soil, formed on the hard rock, the fulvic acids dominate that composing the fulvic type of humus. In the studied forest ecosystem the advanced natural soil acidification occurs mainly in the most upper part of soils.

Keywords: forest ecosystem, humic substances, SOM composition, CEC.

INTRODUCTION

In the recent decades, there has been growing interest in the role of forests ecosystems in climate change mitigation, in the context of the Kyoto Protocol, which Article 3.3 targets principally the uptake of carbon in the forest biomass. Analysis of the range of organic carbon stocks is crucial as soil is most vulnerable to the lost of ecological functions. One of the promising ways is to encourage sequestation of carbon applied to natural forests and grasslands ecosystems. The quantity and quality of humic substances is linked to the important soil functions, including nutrient mineralization, aggregate stability, permeability to air, water retention, infiltration, and other [13]. Soil organic carbon is an essential indicator of soil health and to the ability of soil to function effectively as a component of healfy ecosystem [11].

MATERIALS AND METHODS

The terrain in the central part of Sredna Gora Mountain is characterized as a high hilly to mountainous, rugged. The major woodlands biomes include temperate deciduous and

https://doi.org/10.5593/sgem2024/3.1/s13.29

mixed forests and scrub presented by oak, beech, hornbeam, pine, birch, ash, maple, basswood. The studied area is reffered to the Sub-Balkan's mountainous climatic region with the average annual temperature 10 ºC, there in July the average temperature is 20.6 ºC and in January is (-1.1 ºC). The mean annual rainfall is 600 mm.
Profile 1 is located in the dense beech forest at the altitude 1025 meter and coordinates N 42º32"21.8' and E 023º50"30'. Parent rock is Pre-Cambrian, Lower Archean-Proterozoic laminated gneiss. Soil is classified as Dystric Cambisol (Siltic, Humic) after IUSS Working Group WRB [8], with soil morphology (Figure 1), as follows:



Ah 0-7 cm, Munsell color dry 10YR4/3 (brown) and 10YR3/3 wet (dark brown), structure granular, very friable, with aggregate of fine size (1-2 mm), weakly developed, packing density was low < 1.40 g cm^{-3}, many fine roots < 0.5 mm and others, grades into;
A 7-27 cm, color dry 10YR5/3 (brown) and wet10YR4/2 (dark grayish brown), structure granular, friable, aggregates of medium size (2-5 mm), moderately developed, with low packing density <1.40 g cm^{-3}, few of fine roots, and smooth transition to;
AB 27-60 cm, color dry 10YR6/3 (pale brown) and wet 10YR4/3 (brown), structure granular, firm, aggregates of coarse size (5-10 mm), strongly developed, with low packing density <1.40 g cm^{-3}, few of coarse roots, diffuse boundary and transition to;
Bw 60-120 cm, color dry 10YR6/4 (light yellowish brown) and wet 10YR4/4 (dark yellowish brown), structure subangular blocky, friable, aggregates of fine size (5-10 mm), strongly developed, with low packing density <1.40 g cm^{-3},
BC120-170cm, color dry10YR6/6 (brownish yellow), wet10YR5/8 (yellowish brown), structure single grain and massive.

Figure 1. Morphology of Dystric Cambisol (Siltic, Humic) of Sredna Gora Mountain

Profile 2 is located in the oak forest at the altitude 535 meter and coordinates N 42º30"32.2' and E 024º02"39.2'. Parent rock is Paleozoic, Upper Eocene quartz diorites. Soil is classified as Epidystric Cambisol (Siltic) after IUSS Working Group WRB [8], with soil morphology (Figure 2), as follows:



Ah 0-6 cm, color dry 10YR5/3 (brown) and wet 10YR3/3 (dark brown), structure granular, firm, with aggregate of medium size (2-5 mm), moderately developed, with low packing density <1.40 g cm^{-3}, few of fine roots, clear transition to;
B1 6-30 cm, color dry 10YR6/4 (light yellowish brown) and wet 10YR4/4 (dark yellowish brown), structure subangular blocky, firm, aggregates of fine size (5-10 mm), strongly developed, with medium packing density 1.40-1.75 g cm^{-3}, many roots (1-2 mm) diameter, grades into;
B2 30-65 cm, color dry 10YR6/4 (light yellowish brown) and wet 10YR4/4 (dark yellowish brown), structure subangular blocky, firm, aggregates of fine size (5-10 mm), strongly developed, with medium packing density 1.40-1.75 g cm^{-3}, many coarse roots, grades into;
Bw 65-110 cm, color dry 7.5YR5/4 (brown) and wet 7.5YR4/4 (dark brown), structure subangular blocky, firm, aggregates of medium size (10-20 mm),), strongly developed, with medium packing density 1.40-1.75 g cm^{-3}.

Figure 2. Morphology of Epidystric Cambisol (Siltic) of Sredna Gora Mountain

The shallow profile 3 is located in the pine forest at the altitude 725 meter and coordinates N 42º31”01’ and E 024º08”38.5’, with soil morphology: AC horizon 0-10 cm, color 10YR 6/3 (dry) and 10YR 4/2 (moist), single grain friable structure, many roots and stones, classified as Eutric Skeletic Litic Leptosol (Humic) [8].

Laboratory methods. Soils from the forest ecosystem were analyzed to determine the carbon content and SOM composition by the both, modified Turin’s method (dichromate digestion at 125 ºC, 45 min, in presence of Ag_2SO_4 and $(NH_4)_2$ SO_4 $FeSO_4$ $6H_2O$ titration, phenyl anthranilyc acid as indicator) and Kononova-Belchikova’s method, respectively [3], [10].

Particle size distribution was determined by sieving and the pipette method after chemical dispersion of air- dry gridded soil sample (<2 mm) with 25 cm^3 0.4N sodium pyrophosphate ($Na_4P_2O_7$) without preliminary removal of the organic matter and carbonates from the soil sample. Particle-size distribution and textural classes were determined according to Kachinsky method [9] as well USDA [14].

The total soil acidity is determined by the solutions of 1.0 N sodium acetate and 0.2 N potassium maleinate at pH 8.25, the maximum saturation of soil colloids with strongly alkaline bases, according to the method of Ganev and Arsova [6].

RESULTS

Forest soils are that have developed underneath forest vegetation, being an integral part in the global carbon cycle [5]. Soil development beneath forest ecosystems is influenced by a number of factors, which include the forest vegetation, rock material and topography, climate, organism influence, and the amount of time that these factors have been influencing soil development [1].

Forest soils can be highly variable from site to site that vary predictably across the landscape within a climatically homogeneous region but that they all have in common is that they support a forest ecosystem despite their inherent low fertility [7]. In the studied region generally forest soils are mildly acidic, large proportion of absorbed nutrients is returned annually to the soil and is reabsorbed after biological breakdown of litter. The role of subsoil horizons in the nutrient uptake is more important in case of pronounced weathering forest soils where nutrient depletion occuring deeper in the soil. All these factors combined together can result in soils with different physical, chemical, and biological properties that are unique to particular conditions and provide the framework for ecological functions of forest soils. Meanwhile, the soil-site studies have done little to resolve these relationships, most likely due to the highly empirical nature of the studies [2].

DISCUSSION

The studied forest soils are non-differentiated, which is confirmed by the data of texture (Table 1). The texture soil class in profile 1 is defined as sandy clay loam and in profile 2 as sandy loam according to method of Kachinski [9]. Coarse sand fraction with particle size (1.0-0.25 mm) dominated, followed by the fine sand fraction with particle size (0.25-0.05 mm). The initial formation of textural differentiation was recognized at the depth 65-110 cm in profile 2, confirming the ongoing process of weathering *in situ* in the lower soil part. Same trend in the distribution of sand, silt and clay fractions was established according USDA [14], where the predominant fraction of medium sand was with particle size (2.0-0.05 mm) followed by silt (0.05-0.002 mm).

The balance of humification and mineralization processes in the forest ecosystem takes place generally at the surface. Presence of mobile and aggressive humic substances occurred with depth in forest soils. Soils are characterized with typical distribution of organic carbon in the mountain forest ecosystems (Table 2). The evaluation of the total organic carbon content is according to Filcheva [4].

The surface horizons (Ah) can be defined as with very high amount of organic carbon content, respectively 7.5 % in profile 1 and high 4.6 % in profile 2. Organic carbon content is fourfold lover in the sub-surface horizons compared to the surface (Figure 3), or is 1.8 % in (Ah) horizon in profile 1 and 1.2 % in (B1) horizon in profile 2. Downward, at the depth of 60-65 cm the amount of organic carbon gradually decreases to 1.2 % in profile 1 and 0.7 % in profile 2. The lower part of soils is with very low content of organic carbon 0.45 % in profile 1 and 0.39 % in profile 2.

In the surface (Ah) horizons data of the amount of organic carbon, extractable with 0.1M $Na_4P_2O_7$ + 0.1M NaOH, corresponded to the data of extractable one in alkali extract with NaOH. This relation is due to the fact, that 87-100 % of humic acids in the surface (Ah) horizons are “free” or none complexed, the specific feature for the most soils from forest ecosystems in Bulgaria. Otherwise, humic acids that are bounded with sesquioxides have been identified within the fraction extracted with NaOH. In the surface (Ah) horizons the low degree of humification takes place, which varied from 16.5% (of the total organic carbon) in profile 1 and is only 10 % in profile 2. Humic acids slightly prevailed over the fulvic acids. In the sub-surface (B1) horizon (profile 2), at the depth 6-30 cm the humic acids are totally Ca-complexed. The fulvic acids entirely dominated below the depth of 27-30 cm in the both soil profiles. The fraction of aggressive fulvic acids (extracted with 0.1N H_2SO_4) is very low 1-2 % in the surface horizons and gradually increased to 4-5 % with depth.

Table 1. Particle size distribution (%) and soil texture classes, according to method of Kachinsky (revised) [9] and USDA [14]. Abbreviation: *Physical clay, the parameter characterized sum of the particle-size distribution, according to Kachinsky [9],
$\Sigma < 0.01^* = 0.001 + (0.005\text{-}0.001) + (0.01\text{-}0.005)$

Horizon and depth (cm)	Particle size distribution <2 mm and fractions (%) after USDA			Texture class after USDA	Size of textural fractions (mm) and their content, (%) of oven dry soil weight, after method of Kachinsky					Texture class after Kachinsky
	Sand 2.0-0.05	Silt 0.05-0.002	Clay < 0.002		1.0-0.25	0.25-0.05	0.01-0.005	<0.001	∑ < 0.01*	
Profile 1 Dystric Cambisol (Siltic, Humic), after IUSS Working Group WRB [8]										
Ah 0-7	53.2	30.1	16.7	Sandy loam	30.9	26.5	18.1	11.0	37.7	Sandy clay loam
A 7-27	54.8	30.1	15.1		34.5	24.5	17.6	10.3	34.7	
AB 27-60	53.5	29.5	17.0		42.4	15.3	13.2	11.4	33.0	
Bw 60-120	57.7	26.0	16.3		40.8	21.3	4.3	10.2	24.1	
BC 120-170	64.0	21.0	15.0		41.6	27.0	10.3	10.8	26.5	
Profile 2 Epidystric Cambisol (Siltic), after IUSS Working Group WRB [8]										
Ah 0-6	59.6	27.1	13.4	Sandy loam	47.4	16.6	9.8	9.3	24.2	Sandy loam
B1 6-30	53.7	30.0	16.2		37.4	20.5	10.1	10.6	29.3	
B2 30-65	58.4	26.5	15.1		47.5	15.3	9.8	9.7	27.5	
Bw 65-110	56.6	23.1	20.3	Sandy clay loam	45.0	15.9	8.2	14.8	31.0	Sandy clay
Profile 3 Eutric Skeletic Litic Leptosol (Humic), after IUSS Working Group WRB [8]										
AC 0-10	61.5	25.0	13.5	Sandy loam	51.7	14.3	13.1	9.5	27.6	Sandy loam

In the shallow soil (profile 3), the content of organic carbon is high 3.8 % in the surface (AC) horizon, the humification is low with domination of fulvic acids.
The ratio Cha/Cfa defined the humic-fulvic type of humus at the surface (Ah) horizons in profile 1 and 2 and is of fulvic type in profile 3. Downward, this relation altering, thus in (Ah) horizon in profile 1 to the depth of 27 cm the humus type is of fulvic-humic, and in (B1) horizon in profile 2 to the depth of 30 cm is the humic one, due to the dominance of humic acids complexed with calcium forming insoluble fragments.
It has to be underlined that the content of unextractable organic carbon (%) is very high downward the profiles 1 and 2, which confirmed strong bound of soil organic matter with clay minerals. This content is relatively lower in the surface horizons of profile 1 and 3. The optic characteristic, ratio (E_4/E_6) of the total and "free" humic acids, is almost of similar values in the surface (Ah) horizons in the studied soils (Table 2). The humic acids have been very similar in their molecular weight and structure to those of fulvic ones [12] that are of low molecular weight and with predominance of aliphatic over aromatic moieties in their molecules. Comparatively more mature structure of humic acids is identified in the sub-surface horizons.

Table 2. Content and composition of soil organic matter SOM in the forest soils from the central part of Sredna Gora Mountain. Abbreviation: (a) – % of dry mass; (b) - % of total carbon; (org.C) – of total humic acids; (C_{ha}) – humic acids; (C_{fa}) – fulvic acids; (E_4/E_6) optic characteristic, (C_{ha} total) - of pyrophosphate extract, (C_{ha} free) – of alkali extract.

Horizon and depth, (cm)	Total org. C, %	Organic C, (%) extracted with 0.1M $Na_4P_2O_7$ + 0.1N NaOH			Cha/ Cfa	Organic C, (%) of total humic acids		Unextract. org.C, %	C, (%) fulvic acids extract with 0.1 N H_2SO_4	Optic characteristic (E_4/E_6)		Org. C, (%) NaOH
		Org. C, %	Cha, %	Cfa, %		Free or R_2O_3 bound	Ca bo-und			Total humic acids, %	Free humic acids, %	
Profile 1. Dystric Cambisol (Siltic, Humic), after IUSS Working Group WRB [8]												
Ah 0-7	7.53	2.40[a] 31.87	1.24 16.47	1.16 15.40[b]	1.07	100	0.00	5.33 68.13	0.16 2.12	5.37	5.03	2.29 30.41
A 7-27	1.82	0.30 16.48	0.19 10.44	0.11 6.04	1.73	100	0.00	1.52 83.52	0.04 2.20	4.29	3.52	0.28 15.38
AB 27-60	1.21	0.17 14.05	0.00	0.17 14.05	-	0.00	0.00	1.04 85.95	0.04 3.31	-	-	0.14 11.57
Bw 60-120	0.94	1.12 12.77	0.00	0.12 12.77	-	0.00	0.00	0.82 87.23	0.04 4.25	-	-	0.09 9.57
Profile 2. Epidystric Cambisol (Siltic), after IUSS Working Group WRB [8]												
Ah 0-6	4.66	0.88[a] 18.88	0.47 10.08	0.41 8.80[b]	1.15	0.41 87.23	0.06 12.8	3.78 81.12	0.05 1.07	5.24	5.00	0.77 16.52
B1 6-30	1.20	0.33 27.50	0.24 20.00	0.09 7.50	2.67	0.00	100	0.87 72.50	0.04 3.33	3.78	-	0.20 16.67
B2 30-65	0.69	0.11 15.94	0.00	0.11 15.94	-	0.00	0.00	0.58 84.06	0.04 5.80	-	-	0.05 7.25
Profile 3. Eutric Skeletic Litic Leptosol (Humic), after IUSS Working Group WRB [8]												
AC 0-10	3.84	1.29[a] 33.59	0.47 12.24	0.82 21.35[b]	0.57	0.36 76.68	0.11 23.4	2.55 66.41	0.10 2.60	4.44	4.62	1.22 31.77

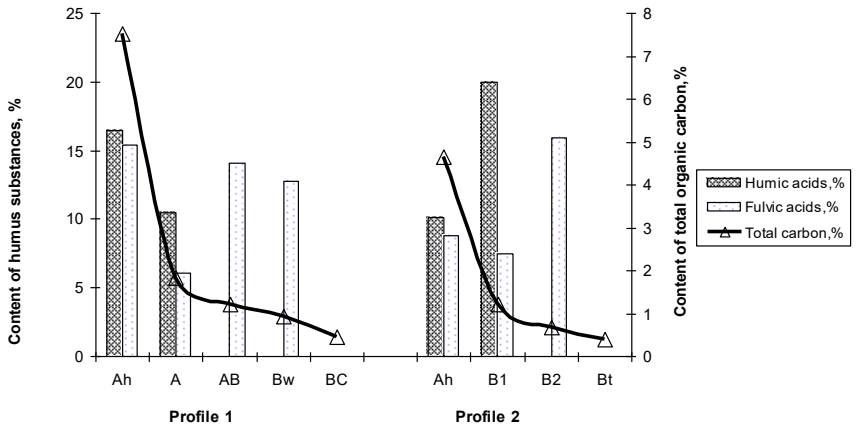


Figure 3. Content of total organic carbon and humic substances in the forest soils from central part of Sredna Gora Mountain.

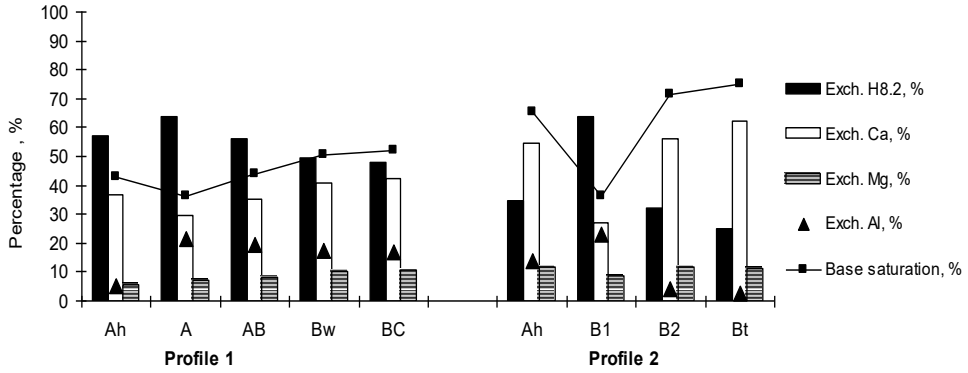


Figure 4. Base saturation, total (hydrolytic) acidity and content of exchangeable ions Ca, Mg, Al in the forest soils from central part of Sredna Gora Mountain.

The quantitative physico-chemical diagnostic is according to the assessment of ion exchange values after Ganev and Arsova [6]. The composition of clay minerals in profile 1 is presented dominated by illite, and in profile 2 by illite-montmorillonite composition. In profile 1 the moderate colloidal reactivity ($T_{8.2}$=32.5 cmol/kg^{-1} of soil) is only in the surface (Ah) horizon 0-7 cm depth, downward it sharply decreased to $T_{8.2}$=22-24 cmol/kg^{-1} of soil (Table 3). The clay formation *in situ* takes place in all parts in the soil profile, without differentiation of adsorption structures. The share of strongly acidic (T_{SA}) ion-exchange positions gradually increased from 48.3 % of ($T_{8.2}$) at the surface to 69.1 % of ($T_{8.2}$) in the lower soil part of profile 1.

In profile 2 the colloidal reactivity is low throughout the soil, the share of strongly acidic (T_{SA}) ion-exchange positions is 80.7 % of ($T_{8.2}$) at the surface (Ah) horizon then sharply decreased to 59.0 % of ($T_{8.2}$) below in (B1) horizon, and these again sharply increased to 71-77 % of ($T_{8.2}$) in (B2 and Bw) horizons, confirming presence of the clay minerals with high isomorphic substitution where.

The Ca-ions leaching and increasing of exchangeable Al ions is manifested as a contemporary process in the studied forest soils. In the upper part of profile 1 in (Ah and A) horizons the base saturation is very low (36-43 %), which slightly increased to

50-52 % below 60 cm depth (Figure 4). The base saturation is 65 % at the surface (Ah) horizon of profile 2, sharply decreasing to 36 % below in (B1) horizon, and again sharply increasing to 71.5-75.0 % in (B2 and Bw) horizons. Occurrence of (exch. $H_{8.2}$=63.6 % of $T_{8.2}$) and the appearance of (exch. Al+H=21.3-22.7 % of $T_{8.2}$) in the upper part of studied forest soils to the depth 27-30 cm have indicated the advanced soil acidification process. In the studied forest soils both the weakly acidic (T_A) as well as the strongly acidic (T_{SA}) positions of soil adsorbent have been affected by the acidification, which indicates the presence of destructive process in the soil absorbing complex.

Table 3. Cation exchange capacity (CEC) (meq/100 g soil=cmol/kg^{-1}) and base saturation, (%) after the method of Ganev and Arsova [6].

Abbreviation: ($T_{8.2}$) sum of all cations with acidic functions or total (hydrolytic) acidity; (T_{SA}) cation-exchange capacity of strongly acidic ion-exchanger; (T_A) weakly acidic ion-exchanger of soil

Horizon and depth (cm)	pH H_2O	Exchange cations, (cmol/kg of soil)					Exchange cations, $T_{8.2}$ (%)						Base saturation, (%)
		$T_{8.2}$	T_{SA}	T_A	$H_{8.2}$	Al+H	T_{SA}	T_A	$H_{8.2}$	Al+H	Ca	Mg	
Profile 1 Dystric Cambisol (Siltic, Humic), after IUSS Working Group WRB [8]													
Ah 0-7	4.4	32.5	15.7	16.8	18.5	1.7	48.31	51.69	56.92	5.23	36.92	5.54	43.08
A 7-27	4.1	22.0	12.8	9.2	14.0	4.7	58.18	41.82	63.64	21.36	29.55	7.27	36.36
AB 27-60	4.15	24.0	15.2	8.8	13.5	4.6	63.33	36.67	56.25	19.17	35.42	8.33	43.75
Bw 60-120	4.2	28.0	19.0	9.0	13.8	4.8	67.86	32.14	49.29	17.14	41.07	10.0	50.71
BC120-170	4.2	28.5	19.7	8.8	13.6	4.8	69.12	30.88	47.72	16.84	42.11	10.53	52.28
Profile 2 Epidystric Cambisol (Siltic), after IUSS Working Group WRB [8]													
Ah 0-6	5.05	26.0	21.0	5.0	9.0	3.6	80.77	19.23	34.62	13.85	54.62	11.54	65.38
B1 6-30	4.0	22.0	13.0	9.0	14.0	5.0	59.09	40.91	63.64	22.73	27.27	8.64	36.36
B2 30-65	4.85	22.5	16.1	6.4	7.2	0.9	71.56	28.44	32.00	4.00	56.00	11.56	71.56
Bw 65-110	5.15	25.6	19.9	3.7	6.4	0.6	77.73	22.27	25.00	2.34	62.50	11.33	75.00
Profile 3 Eutric Skeletic Litic Leptosol (Humic), after IUSS Working Group WRB [8]													
AC 0-10	5.4	25.0	18.9	6.1	6.6	0.4	75.60	24.40	26.40	1.60	63.20	12.0	73.60

CONCLUSION

The ecological conditions of forest ecosystem determine the mode of humic substances in the studies soils from central part of Sredna Gora mountain. The forest soils are characterized with low degree of humification, the content of humic substances is high only on the soil surface, which sharply decreases with depth. The studied forest soils differ by their composition of soil organic matter. In the first profile the humic acids are ”free” or sesquioxide complexes in the upper part and being entirely presented by the fulvic acids in the soil lower part. In the second profile the humic acids are bounded with calcium. In the shallow soil formed on the hard rock the fulvic acids prevail. The occurrence of the contemporary process of soil acidification affects forest soils in the region.

REFERENCES

[1] Brady N.C., Weil R.R., The nature and properties of soils, Prentice Hall: Upper Saddle River, New Jersey, USA, 1996, pp 740;

[2] Carmean W.H., Forest site quality evaluation in the United States, Advances in Agronomy, ELSEVIER, vol. 27, 1975, pp 209-269; DOI.org/10.1016/S0065-2113(08)70011-7

[3] Filcheva E., Tsadilas C. Influence of Cliniptilolite and compost on soil properties, Commun. of Soil Science and Plant Analysis, UK, vol. 33/issue 3-4, pp 595-607, 2002.

[4] Filcheva E., Characteristics of soil organic matter of Bulgarian soils, LAP Lambert Academic Publishing, 2015, pp 178;

[5] Fisher R.F., Binkley D., Ecology and Management of Forest Soils, John Wiley & Sons Inc., New York, USA, 2000, pp 489;

[6] Ganev S., Arsova A., Methods for determining the strongly acid and weakly acid cation exchange in soil, Soil Science and Agrochemistry, Bulgaria, vol.15/issue 3, pp 22–33, 1980.

[7] Homann P.S., Bormann B.T., Boyle J.R., Detecting treatment differences in soil carbon and nitrogen resulting from forest manipulations, Soil Science Society of America Journal, USA, vol. 65/issue 2, pp 463–469, 2001. DOI.org/10.2136/sssaj2001.652463x

[8] IUSS Working Group WRB, World Reference Base for Soil Resources, International soil classification system for naming soils and creating legends for soil maps, 4th edition. International Union of Soil Sciences (IUSS), Vienna, Austria, 2022, pp 234;

[9] Kachinski N.A., Mechanical and micro-aggregate composition of soil, Methods for it study, Publishing house of Science Academy of USSS, Moscow, 1958, pp 192;

[10] Kononova M.M., Soil organic matter, its nature, origin and role in soil formation and soil fertility, 2nd Eng. Ed., Pergamon Press ING., Elmsfordm M.V., 1966, pp 544;

[11] Schoenholtz S.H., Miegroet H.V., Burger J.A., A review of chemical and physical properties as indicators of forest soil quality: challenges and opportunities, Forest Ecology and Management, ELSEVIER, vol. 138/issue 1-3, pp 335-356, 2000. DOI.org/10.1016/S0378-1127(00)00423-0

[12] Sutton R., Sposito G., Molecular structure in soil humic substances: the new view, Environmental Science and Technology, USA, vol. 39/issue 23, pp 9009-9015, 2006. DOI: 10.1021/es050778q

[13] Tate R.L., Soil organic matter: biological and ecological effects. Wiley Interscience, New York, 1987, pp 291;

[14] Soil Survey Staff, Soil Survey Laboratory Information Manual, Soil Survey Investigations Report No. 45, Version 2.0., R. Burt (ed.), U.S. Department of Agriculture, Natural Resources Conservation Service, 2011, pp 506.

LOCAL SOURCE OF PHOSPHORUS FROM SEED PRODUCTION WASTE

Ing. Antonín Kintl[1]

Ing. Igor Huňady[1]

Ing. Julie Sobotková[1]

Ing. Martin Brtnický[2]

Ing. Jakub Elbl, Ph.D.[1,3]

[1] Agricultural Research Ltd., Zahradní 1, 664 41, Troubsko, **Czech Republic**
[2] Department of Agrochemistry, Soil Science, Microbiology and Plant Nutrition, Faculty of Agronomy, Mendel University in Brno, Zemědělská 1, 613 00 Brno, **Czech Republic**
[3] Department of Agrosystems and Bioclimatology, Faculty of Agronomy, Mendel University in Brno, Zemědělská 1, 613 00 Brno, **Czech Republic**

ABSTRACT

The presented paper focuses the issue of finding new sources of phosphorus fertilizers to be used in conventional agriculture. Various types of pellets for heating purposes were tested. Based on the determination of phosphorus (P) content in ash obtained from the combustion of pellets produced from plant waste generated during the production of seed materials, it was found out that getting P from this ash is more effective than getting P from the ash of wooden pellets that are commonly used as fuel in households. With the declared average consumption of wooden pellets by one household living in a family house, which is on average 5 tons for the heating season, one dose of 43 kg P required to fertilize 1 hectare of soil before sowing winter rape would be represented by ash from 50 tons of wooden pellets consumed by ten households, while using pellets made from the plant waste, e.g. from white sweet clover, would need only 7.5 tons of ash which is produced by 1.36 households at the consumption of 5 tons of these pellets for the heating season. Using ash from the combustion of pellets made of plant waste can be a practical contribution to improved cycling of phosphorus in agricultural ecosystems because the sources of phosphorus fertilizers may be depleted in the near future.

Keywords: fertilization, phosphorus, plant waste, pellets, ash

INTRODUCTION

Phosphorus is a limiting factor which is important in sustainable agriculture [1] and plays a role of key element that cannot be substituted by any other substance. It is a part of basic structure of life on earth since its very beginning. Phosphorus also plays an important role in cellular breathing and photosynthesis. This is why its supply should be appropriate for biomass formation [2]. The amount of phosphorus in soils is insufficient all around the word and a concentration of phosphorus available to plants is not higher than 10 μM even in fertile soils [3]. This indispensable nutrient is released for the main crop from parent rocks and through the decomposition of organic residues; in concentrations over 3 mg g^{-1} it is mineralized [4]. Sources of phosphorus are limited

worldwide while the price of commercial phosphorus fertilizers has been continually increasing [1]. The element is of key importance for economy of agriculture as well as for ensuring food products in the European Union and in the world [5]. As the availability of phosphate reserves is globally decreasing, it is necessary to look for other sources of phosphorus [6]. During the application of phosphate fertilizer, phosphorus may precipitate and the fertilizer usability may be thus impaired. Usability of phosphorus in the application of phosphorus fertilizers is therefore relatively low. In acidic soils, phosphorus becomes precipitated with Al^{3+} and Fe^{3+} ions and in alkaline soils with Ca^{2+} and Mg^{2+} ions [7]. Phosphorus is taken up by plants through phosphate transport proteins in roots as phosphate ions $H_2PO_4^{2-}$ and H_2PO_4, when pH is below 7.2 [8].

The aim of this research was to verify a possibility of using ash from pellets made of waste generated in the production of seed and from other materials used as fuel in heating households for the fertilization of farmlands with phosphorus as a substitution for commercial phosphorus fertilizers.

MATERIALS AND METHODS

In the presented experiment, we tested pellets made of plant material produced as waste during the purification of seed from various crops or as secondary products in consumption of various organic substances (coffee grounds, biochar, digestate). A closely unspecified mixture of waste produced at processing seeds of various crops the precise composition of which was impossible to determine was designated as non-specific waste (Tab. 1). Waste used for the manufacture of agro-pellets originated from the production of seeds in the company Agricultural Research, Ltd., Zahradní 1, 664 41 Troubsko, Czech Republic. The material was moistened to 10-12% and then pellets were made on the press JGD 200 (Green Energy Machinery s.r.o., Vazová 2451, 688 01 Uherský Brod, Czech Republic); the resulting pellets were 8 mm in diameter. Pellet samples were homogenized and subjected to analyses for the determination of phosphorus (P) content. Methodology of phosphorus determination based on methodological procedures et the Browman [9] is described in detail in Kintl et al. [10].

RESULTS AND DISCUSSION

The highest P content was found in the dry matter of pellets made from biochar (0.63 $\%_{DM}$) and in the digestate (0.89 $\%_{DM}$) (Tab. 1). The lowest P content was observed in the dry matter of pellets containing coffee grounds (0.15 $\%_{DM}$) and wood (0.08 $\%_{DM}$).

Tab. 1: P content in dry matter of pellets ($\%_{DM}$).

AGRO-PELLETS	P (% DM)
Digestate	0.89
Biochar	0.63
White sweet clover (*Melilotus albus*)	0.58
Non-specific waste 01	0.52
White sweet clover (*Melilotus albus*)-pods rough after scrubber	0.50
Clover ´Pramedi´ (*Trifolium pratense* x *T. medium*)	0.50
Mustard (*Sinapis alba*)-debris	0.50

Non-specific waste 02	0.49
White sweet clover (*Melilotus albus*)-pods fine after scrubber	0.48
Camelina sativa	0.41
Alfalfa (*Medicago sativa*) 1	0.36
Clover incarnate	0.33
Non-specific waste 04	0.28
Barley chaff	0.27
Non-specific waste 03	0.23
Black medick (*Medicago lupulina*)-pods	0.21
Coffee grounds	0.15
Wooden pellets	0.08

The content of phosphorus (P) in 18 ash samples from pellets of different composition ranged from 14.73 (non-specific plant waste 03) to 132.03 g/kg of ash (non-specific plant waste 01) (Fig. 1). In pellets with the known species composition, the lowest content of P was recorded in the ash of pellets from the empty pods of *Medicago lupulina* (21.47 g/kg) and biochar (28.89 g/kg). The highest P content in pellets with the known species composition was recorded in the ash from pellets produced of white sweet clover (*Melilotus albus*) (95.63 g/kg) and from wooden pellets (107.16 g/kg).

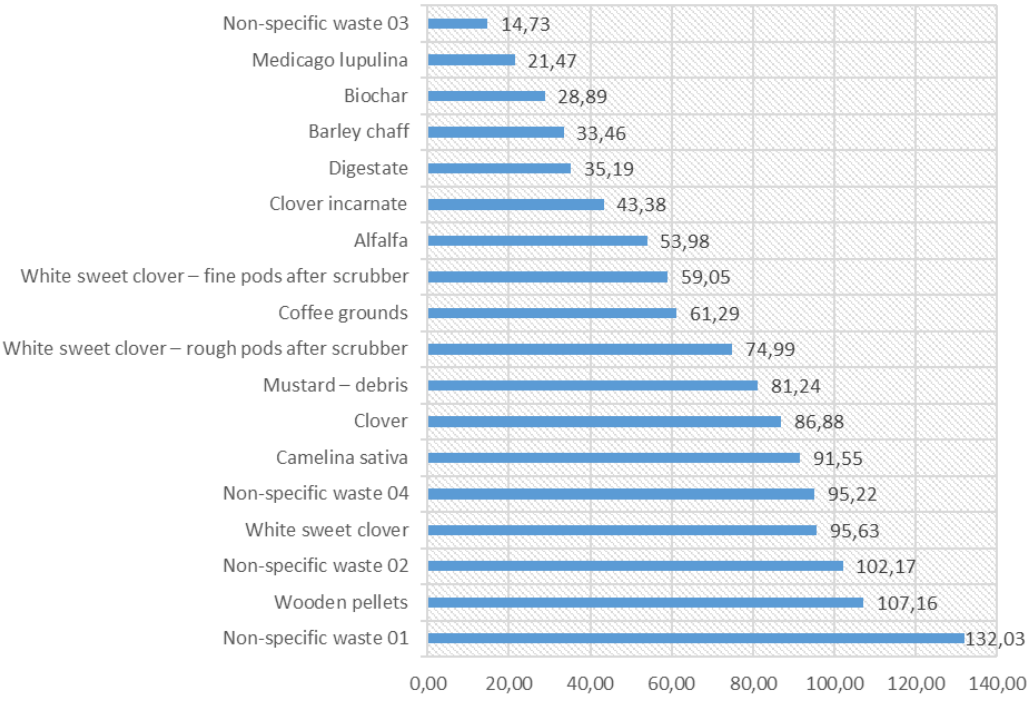


Fig. 1: P content in the ash of pellets (g/kg).

Sumara et al. [11] inform that the content of phosphorus in wooden pellets is 0.7 g P·kg^{-1}. The authors maintain that the content of phosphorus, potassium, calcium and magnesium in ash and in flue ash from the combustion of wooden pellets confirms the use of this material for soil fertilization. However, regarding the low content of

nitrogen, which is comparable to the content of nitrogen in the soil, the material cannot be considered to be a fertilizers supplying the macro-element into the soil. Thus, we have to assume that for a better usability of nutrients contained in ash, the ash from the combustion of pellets should be added further organic matter, for example a mixture with industrial compost.

Results of the study published by Schiemenz and Eichler-Lobermann [12] show that the fertilization effect of ash from fresh biomass was comparable to that of highly soluble triple superphosphate (TSP). The authors further inform that on average of all crops, the highest P uptake (86.7 mg pot^{-1}) was recorded after the application of rapeseed meal ash and the lowest P uptake (66.6 mg pot^{-1}) in the untreated control. Contents of readily biologically available P in the soil significantly increased after the P supply regardless of this being supplied with ash or with highly soluble TSP. According to the authors [12], effects of fertilization with water-soluble P depended also on the cultivated crops; the treatment with ash led to the greatest increase of soil P in combination with growing buckwheat. After the harvest of buckwheat, the content of water-soluble P was 8.0 mg kg^{-1} in control and between 13.9 mg kg^{-1} and 15.7 mg kg^{-1} after treatment with ash in cereals and rapeseed meal, respectively. A certain role in the experiments could be presumably played also by the content of nitrogen in the soil or in plant residues, which could have positively influence the availability of P in the soil.

Based on their research, Schiemenz et al. [13] report that the highest content of P P (10.5 %) was measured in grain ash and the lowest content of P was measured in straw (1 %).

Fig. 2 shows how much of ash is required to obtain 1 kg P in dependence on the composition of pellets. From this point of view, the lowest amount of ash for obtaining 1 kg P is needed when burning pellets made of non-specific plant waste 01 and 02 - (7.57 kg and 9.79 kg of ash, respectively).

In pellets with the known species composition, 1 kg of phosphorus requires 9.33 kg of ash from wooden pellets and (or?) 10.46 kg of ash from pellets made of white sweet clover waste (10.46 kg)?.

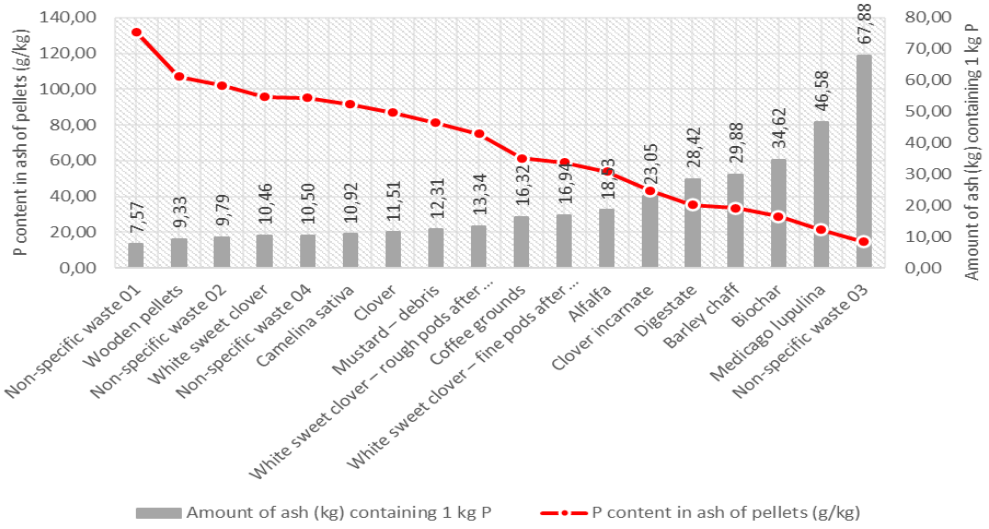


Fig. 2: Amount of ash (kg) obtained from burning pellets made of different materials, which is needed to gain 1 kg of phosphorus.

If we model-calculate an average yield of winter rape seeds to be 4 t/ha and an average export of P to be 36 kg/ha, then a necessary P dose before sowing with a low or satisfying soil P content will be about 43 kg P [14]. This means that the fertilization of winter rape with a P dose required before sowing will be 0.401 t/ha of ash obtained from burning 50.1 t of wooden pellets (Fig. 3) or 0.450 t/ha of ash obtained from burning 7.5 t of pellets made from the waste of white sweet clover.

It is stated [15] that the average consumption of households living in family houses and heating with wooden pellets is 5 t of pellets for a heating season. Fig. 3 shows the dry matter of pellets of different compositions, P content P (kg) in 5 t of pellets, and what amount of pellets has to be burnt to obtain a dose of 43 kg P. The smallest amount of pellets (4.83 t) for obtaining ash with the content of 43 kg P can be get by burning pellets made of digestate with a very low dry matter content (7.4 %) and biochar (6.8 t) with a dry matter of 69.2 %. In pellets made of materials obtained as waste from plant production with the content of dry matter ranging from 84.8 % (clover incarnate) to 90.3 % (non-specific waste of plant origin) a dose of 43 kg P required to burn from 8.2 t (non-specific plant waste 02) to 20.2 t (*Medicago lupulina*) of pellets.

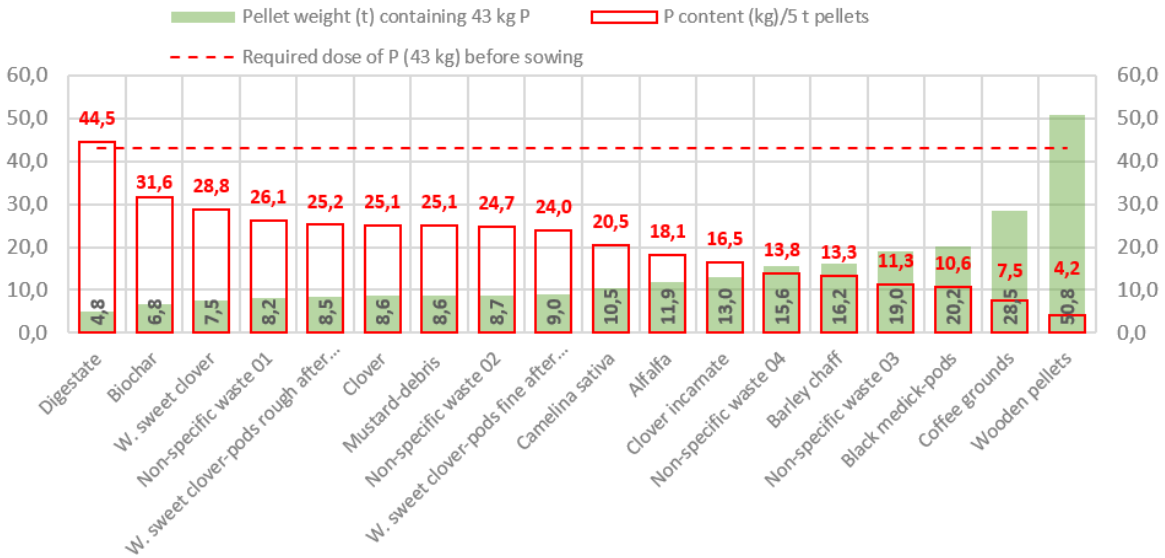


Fig. 3: Content of P (kg) in 5 tons of pellets of different composition and weight of pellets (t) containing 43 kg P.

Tab. 2 shows a potential number of households needed to obtain a dose of 43 kg P/ha when using pellets of different composition, which had in previous periods average consumption 5 t of wooden pellets per heating season. It follows from the Tab. 2 that the mentioned P dose can be obtained with using digestate pellets the production of ash in one household and in 1.36 household with using pellets from white sweet clover. When heating with wooden pellets, the production of ash containing 43 kg P needs 10 households (Tab. 2) with a consumption exceeding 50 t of pellets (Fig. 3).

Tab. 2: Number of households with a consumption of 5 tons of wooden pellets per heating season, needed to obtain a dose of 43 kg P/ha when using pellets from waste generated in production of seeds and other materials.

Composition of pellets	**Number of households**
Digestate	0.97
Biochar	1.36
White sweet clover (*Melilotus albus*)	1.49
Non-specific waste 01	1.64
White sweet clover (*Melilotus albus*)-rough pods after scrubber	1.71
Clover ´Pramedi´ (*Trifolium pratense* x *T. medium*)	1.71
Mustard (*Sinapis alba*)-debris	1.72
Non-specific waste 02	1.74
White sweet clover (*Melilotus albus*)-fine pods after scrubber	1.79
Camelina sativa	2.10
Alfalfa (*Medicago sativa*) 1	2.38
Clover incarnate	2.61
Non-specific waste 04	3.11
Barley chaff	3.23
Non-specific waste 03	3.80
Black medick (*Medicago lupulina*)-pods	4.04
Coffee grounds	5.70
Wooden pellets	10.16

CONCLUSION

Using ash from burning pellets made from plant waste generated during the production of seeds and used as fuel to heat households for the fertilization of farmlands with phosphorus is one of possibilities how to replace commercial phosphorus fertilizers. The reason is not only a potentially lower price and lower carbon footprint as transport of fertilizers over long distances will not be necessary but also the fact that global phosphorus reserves are gradually decreasing. Farmers will have to face a difficult challenge – to look for new, alternative resources, particularly in the form of raw materials originating from waste management: sludge from waste water treatment plants, industrial composts, ash from plants burning plant biomass etc.

Based on the determination of P content in pellets of different composition and in their ash, it was found out that getting phosphorus from ash obtained from burning pellets is more effective than from ash of wooden pellets which are commonly used as fuel. With the declared average consumption of wooden pellets in one household, which is 5 tons per heating season, the phosphorus dose of 43 kg needed to fertilize 1 hectare of soil before sowing rape would require the application of ash from 50 tons of wooden pellets consumed by ten households while the use of pellets made from the waste of white

sweet clover only 7.5 tons of ash would be required, which is produced by 1.36 household consuming 5 tons of these pellets per heating season. From this point of view, using ash from the combustion of pellets made of plant waste can be a significant contribution to improve the cycling of phosphorus in agricultural ecosystems. A challenge for further research remains to investigate potential risks, e.g. the content of heavy metals in ash.

ACKNOWLEDGEMENTS

The result was obtained within the framework of institutional support MZE-RO1724.

REFERENCES

[1] Eichler-Löbermann B., Köhne S., Kowalski B., Schnug E., Effect of Catch Cropping on Phosphorus Bioavailability in Comparison to Organic and Inorganic Fertilization, Journal of Plant Nutrition, vol. 31/issue 4, pp 659-676, 2008. doi: 10.1080/01904160801926517

[2] Whitelaw M.A., Growth Promotion of Plants Inoculated with Phosphate-Solubilizing Fungi, Advances in Agronomy, vol. 69, pp 99-151, 2000. doi:10.1016/S0065-2113(08)60948-7

[3] Gyaneshwar P., Naresh Kumar G., Parekh L. J., Poole P. S., Role of soil microorganisms in improving P nutrition of plants, Plant and Soil, vol. 245, pp 83-93, 2002. doi: 10.1023/A:1020663916259

[4] Damon P.M., Bowden B., Rose T., Rengel Z., Crop residue contributions to phosphorus pools in agricultural soils: A review, Soil Biology and Biochemistry, vol. 74, pp 127-137, 2014. doi:10.1016/j.soilbio.2014.03.003

[5] Cordell D., White S., Life's Bottleneck: Sustaining the World's Phosphorus for a Food Secure Future, Annual Review of Environment and Resources, vol. 39, pp 161-188, 2014. doi:10.1146/annurev-environ-010213-113300

[6] Wells D.E., Beasley J.S., Bush E.W., Gaston L.A., Poultry Litter Ash Rate and Placement Affect Phosphorus Dissolution in a Horticultural Substrate, Journal of Environmental Horticulture, vol. 35/issue 3, pp 117-127, 2017. doi:10.24266/0738-2898-35.3.117

[7] Hinsinger P., Bioavailability of soil inorganic P in the rhizosphere as affected by root-induced chemical changes: a review, Plant and Soil, vol. 237, pp 173-195, 2001.

[8] Raghothama K.G., Phosphate Acquisition, Annual Review of Plant Biology, vol. 50, pp 665–693, 1999. doi:10.1146/annurev.arplant.50.1.665

[9] Bowman R.A., A rapid plant digestion method for analysis of ρ and certain cations by inductively coupled plasma emission spectrometry, Communications in Soil Science and Plant Analysis, vol. 20/issue 5-6, pp 539–533, 1989. doi:10.1080/00103628909368099

[10] Kintl A., Huňady I., Ondrisková V., Hammerschmiedt T., Brtnický M., Vejražka K., Kubíková Z., Elbl J., Influence of Boron and Drought Simulation on Germinability and Hardseededness of Black Medick Seeds (*Medicago lupulina* L.), Journal of Plant Growth Regulation, vol. 42, pp 1704-1719, 2022. doi:10.1007/s00344-022-10652-y

[11] Sumara A., Stankowski S., Gibczyńska M., Jurgiel-Małecka G., ASSESSMENT OF THE USE FOR FERTILISATION PURPOSES INCINERATION ASH PELLETS USING GASIFICATION BURNER LESTER. Ecological Engineering & Environmental Technology, vol. 50, pp 139-144, 2016. doi:10.12912/23920629/65497

[12] Schiemenz K., Eichler-Lobermann B., Biomass ashes and their phosphorus fertilizing effect on different crops, Nutrient Cycling in Agroecosystems, vol. 87, pp 471-482, 2010. doi.10.1007/s10705-010-9353-9.

[13] Schiemenz K., Kern J., Paulsen H.-M., Bachmann S., Eichler-Löbermann B., Phosphorus Fertilizing Effects of Biomass Ashes., Recycling of Biomass Ashes, pp 17-31, 2011. doi:10.1007/978-3-642-19354-5_2

[14] Černý et al., 2020 NENAŠLA JSEM CELOU CITACI V SEZNAMU LITERATURY

[15] Glavonjic Branko & Oblak, Leon & Čomić, Dragan & Lazerevic, Aleksandra & Kalem, Miljan. (2017). Wood fuels consumption in households in Bosnia and Herzegovina. Thermal Science. 21. 34-34, 2017. doi.10.2298/TSCI170102034G TO SI JEŠTĚ UPRAV PODLE

MICROMORPHOLOGICAL FEATURES OF SALT-AFFECTED SOILS FROM THE BAIKAL REGION OF RUSSIA

Dr. Irina A. Yamnova
Dr. Galina I. Chernousenko
Federal Research Center V.V. Dokuchaev Soil Science Institute, Moscow, **Russia**

ABSTRACT

Micromorphological features of salt-affected soils in the Cis-Baikal and Trans-Baikal regions (south of East Siberia, Russia) are considered. When studying morphogenesis of these soils, pedofeatures of soluble salts and gypsum serve as indicators of modern and former stages of soil formation. Comparative-geographical, micromorphological, and chemical methods have been applied to study soil salinization. Chemical analyses attest to the presence of gypsum and soluble salts in solonchaks of both regions. However, they do not allow us to judge the direction of modern soil salinization processes. Micromorphological method makes it possible to specify the genesis of salt pedofeatures. When comparing microfabrics of solonchaks in the Cis-Baikal and Trans-Baikal regions, the features attesting to their different geneses have been identified. Thus, in the solonchak from the Priolkhonye area (Cis-Baikal region), gypsum pedofeatures were formed during previous stages of soil formation and are now subjected to destruction. At the same time, the accumulation of soluble salts is still active in this soil. Analysis of the microstructure of the soil profile of the meadow-marsh saline soil of Transbaikalia showed the presence of both processes currently underway - both gypsum formation and salt accumulation in the soil profile.

Keywords: microstructure, soil salinization, new salt formations, gypsum, Baikal and Transbaikalia regions

INTRODUCTION

Saline soils, which were the object of our study, are distributed in intermontane basins of the Baikal region. Saline soils are found in young Cenozoic basins of the Baikal type, which have been formed in the rift regime since the Pliocene [11] and in the more open Mesozoic basins of the Western rift zone [10]. The formation of rift basins occurred in an extension regime initiated by a hot mantle plume [10]. Intermontane basins differ in their morphology and in the association of saline soils with particular landforms. The climate of the deep closed Cenozoic basins of the rift zone (Priolkhonye area) promotes the advancement of steppe landscapes and, accordingly, saline soils to the north. The distribution of saline soils in the Priolkhonye area is limited to a narrow strip in the intermontane basin stretching east of the Baikal Ridge through the Priolkhonye area and Olkhon Island.

The eastern part is represented by the middle mountains of Transbaikalia. In this area, wider, more open, and therefore more windy Mesozoic intermontane depressions of the Transbaikal type are present. Steppes and dry steppes and, consequently, the accompanying saline soils, are formed here in more southern latitudes. The distribution and chemistry of saline soils in the Cis-Baikal and Trans-Baikal areas were described in a number of works [3, 5, 6, 14, 16, 17]. Morphological (and micromorphological)

features of gypsum in soils were discussed in the works [1, 12, 13, 15]. However, the features of the microstructure of saline soils in the studied areas were not considered in these works.

OBJECTS AND METHODS

The chemical and morphological features of solonchaks are considered by the example of soils profiles 2 and 3 (Cis-Olkhon area) and 6 (Gusinoozersk Basin, Trans-Baikal region) (Fig. 1). The solonchaks of both study areas are represented by hydromorphic soils occupying geochemically subordinate landforms: lakeside lows and river valleys. Solonchaks in the Priolkhonye area were studied around Tazheran salt lakes with the sulfate–sodium salinity, often with a large proportion of chlorides, the presence of gypsum, and trace amounts of soda in some of them. Solonchaks of the Gusinoozersk Basin are characterized by the sulfate–sodium–magnesium salinity; gypsum is present in groundwater and soils [3].



Figure 1. Study areas in the Cis-Baikal (pits 2 and 3) and Trans-Baikal (pit 6) regions.

Traditional chemical methods for studying saline soils (analysis of soil water extract 1:5; contents of gypsum and carbonates) were supplemented with micromorphological description of thin sections using optical microscopes Olympus BH-2 and Nikon E-200; visualization and micromorphometric measurements were performed using DiaMorph software; images of thin sections were obtained using an Epson perfection 2450 Photo scanner and a Nikon E 45004 digital camera.

RESULTS

The analysis of water extracts from saline soils showed the redominance of sodium and magnesium among cations and of sulfate among anions in both regions. Soda was diagnosed in a number of profiles studied in the Priolkhonye area. Among sulfate-saline soils, in which toxic alkalinity appeared, there were gypsum-bearing soils. In this case, toxic alkalinity was associated with magnesium bicarbonate.

Figure 2a shows the salt profile of a crusty sulfate solonchak with toxic alkalinity (pit 2 of the Priolkhonye area). The soil is very strongly saline from the surface to a depth of 86 cm. The salt content exceeds 1% in the surface layer and reaches 13% in the crust. In the upper horizons of the maximum accumulation of salts, the magnesium–sodium sulfate salts predominate with toxic alkalinity caused by magnesium bicarbonate; gypsum is absent. Below 20 cm, sulfate salinity with toxic alkalinity determined by

soda predominates; below 86 cm, the salinity degree decreases from very strong to strong (Fig. 2b).

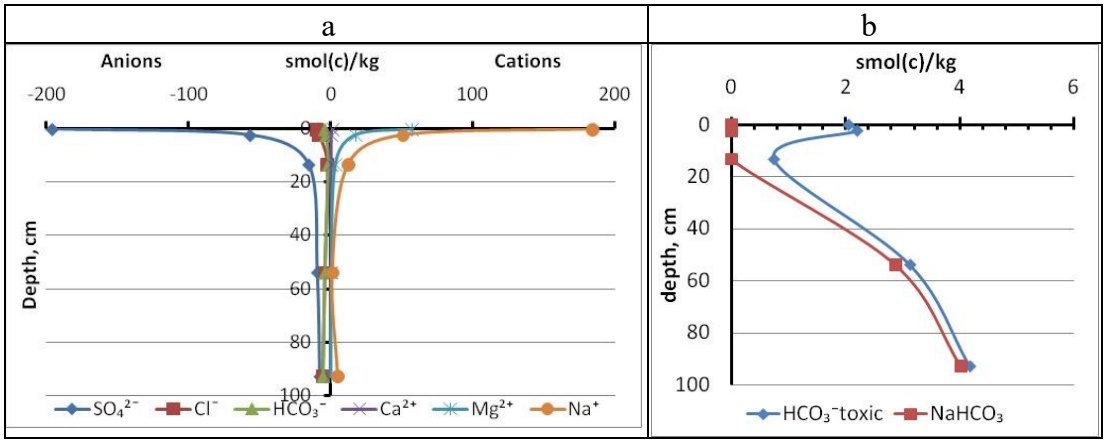


Figure 2. Salt composition of sulfate solonchak (a) and toxic alkalinity (b) (pit 2, Priolkhonye area, Cis-Baikal region).

In thin sections, in plasmic sandy material of the crusty solonchak of pit 2, the presence of dolomite fragments is diagnosed (Fig. 3a).

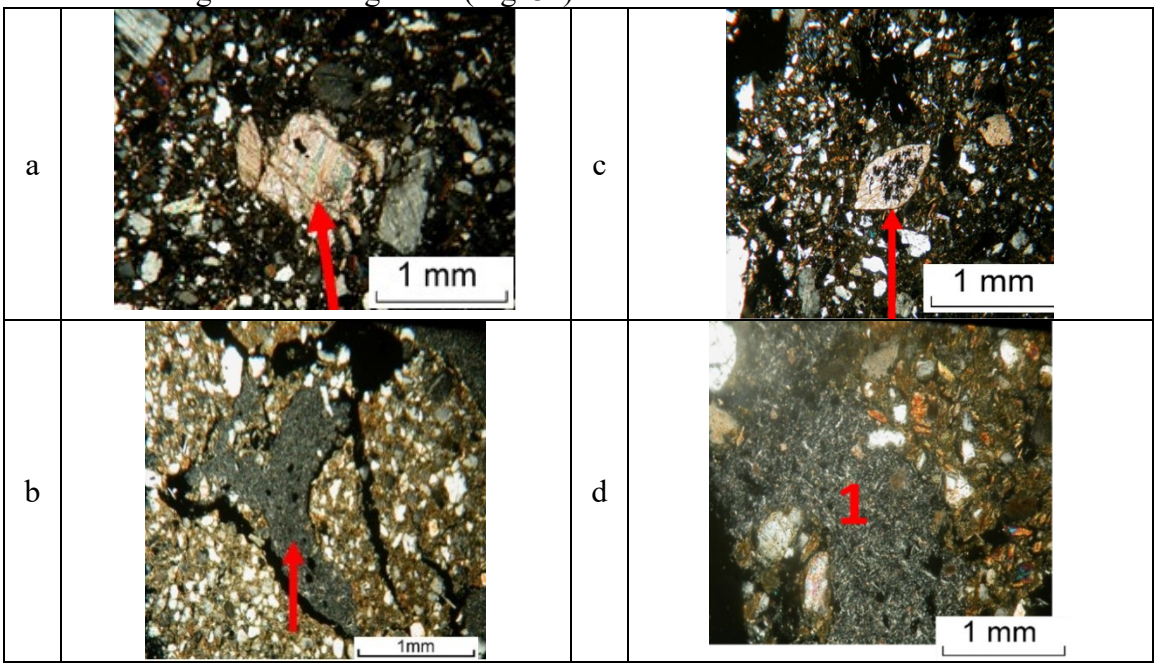


Figure 3. Microstructure of the crusty solonchak of the Priolkhonye area (pit 2): (a) dolomite fragment (red arrow); (b) salts in the pore (red arrow); (c) pseudomorphosis of calcite over gypsum (red arrow); (d) salts in large pores (1).

A specific feature of the microstructure of this solonchak is the high content of carbonates in the form of abundant cryptogranular calcite. In addition, analysis of the microstructure showed the absence of both individual crystals and accumulations of newly formed gypsum in the interaggregate pores. The presence of calcite pseudomorphs on gypsum is recorded (Fig. 3c). In the middle and lower parts of the soil profile, the accumulations of soluble salts in large pores are seen (Figs. 3b and 3d).

In the Priolkhonye area, there are soils containing gypsum in the profile. Figure 4a shows the salt profile of the meadow-marsh gypsum-bearing solonchak (pit 3). The salinity of the upper 20 cm is very strong, the amount of salts exceeds 2% reaching 30% in the crust. The salinity is of the magnesium–sodium sulfate type with gypsum. Below 30 cm, the degree of salinity drops to strong (total salts 1.7%, total toxic salts 1%) maintaining the same chemistry.

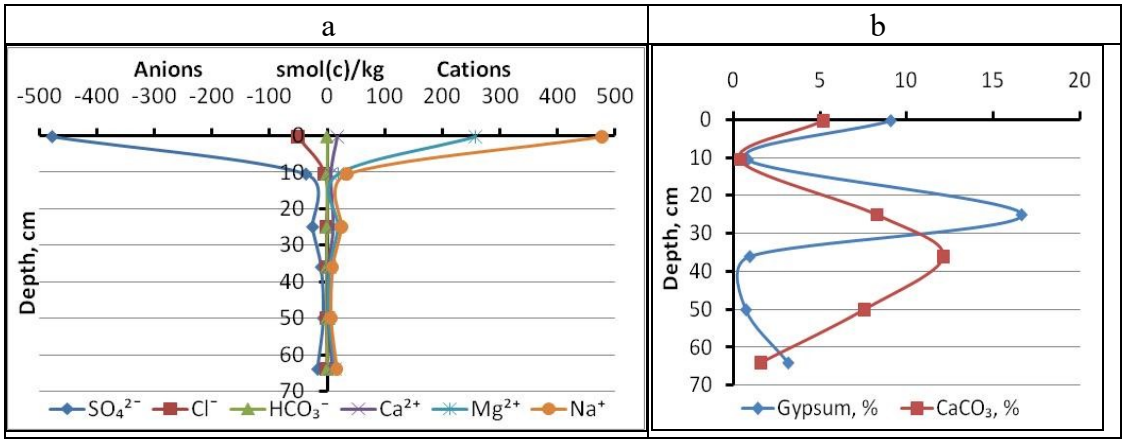
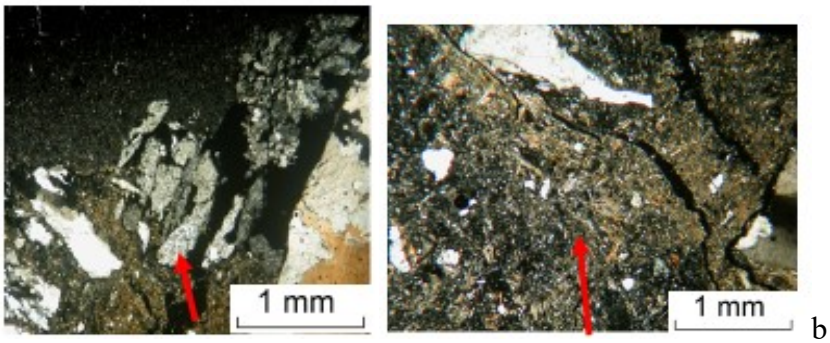


Figure 4. Salt composition of the meadow-marsh solonchak (a), contents of gypsum and carbonates (b) (pit 3, Priolkhonye area, Cis-Baikal region)

The gypsum content along the profile reaches 16.6%; the content of $CaCO_3$ is 12.1%. (Fig. 4b). The location of the maximum accumulation of gypsum is higher than the maximum of carbonates, which corresponds to the precipitation of salts from the solution according to the degree of their solubility and indicates their hydrogenic entry into the solonchak profile.

Micromorphological analysis of this solonchak (pit 3, fig. 5) demonstrated the presence of large corroded gypsum crystals (Fig. 5a), which excludes its modern origin.



a b

Figure 5. Microstructure of the meadow-marsh solonchak (pit 3, Priolkhonye area): (1) corroded gypsum crystals in a large interaggregate pore, (b) accumulations of salts in the plasma material.

The accumulations of soluble salts in large pores indicate the modern activity of soil salinization processes (Fig. 5b).

In the Trans-Baikal region, gypsum is much less common in soils. However, in the second study area in the center of the Selenga Mountains (Gusinoozersk Basin) gypsum is found among saline soils in a number of soil profiles.

Figure 6 shows the salt profile of sulfate-saline meadow-bog soil (pit 6). The soil is wet, and salts are clearly seen in it. Despite the fact that the amount ofsalts is more than 1% (1.2–1.8%), the amount of toxic salts is lower (0.8–1.3%), which is due to the presence of gypsum, non-toxic to plants. This corresponds to a strong degree of salinity [14].

The soil is classified as a strongly saline gypsum-bearing meadow-bog solonchak. The degree of salinity is strong throughout the profile, with some accumulation in the upper part. The salinity is of the sodium–magnesium sulfate type with gypsum. Magnesium predominates among the cations in the profile, which is observed in saline gypsum-bearing soils [4].

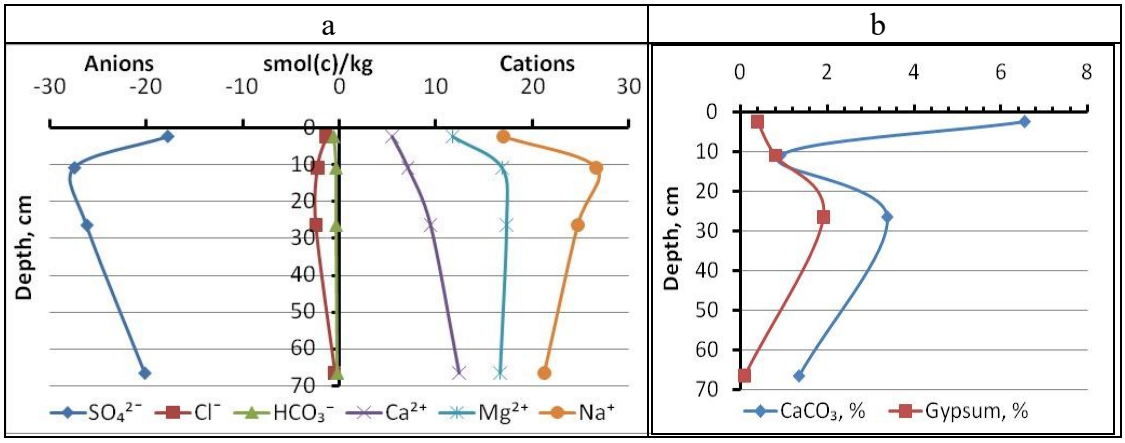
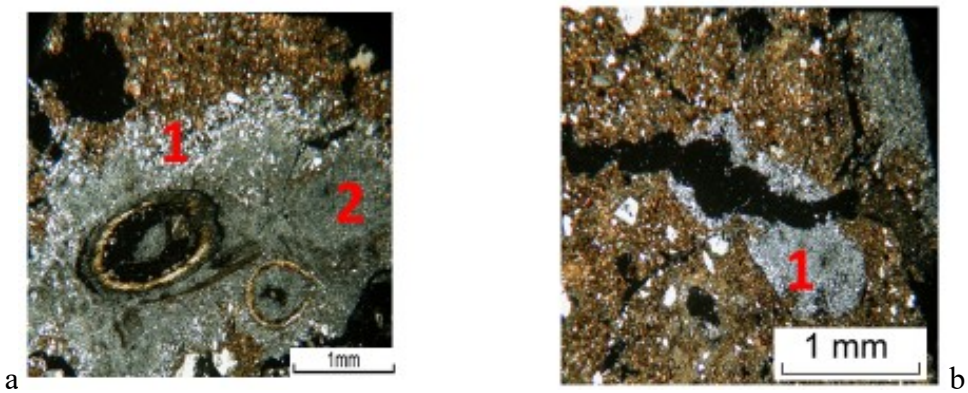


Figure 6. Salt composition of the meadow-bog solonchak (a), contents of gypsum and carbonates (b) (pit 6, Trans-Baikal region, Gusinoozersk Depression, Lake Sulfatnoe).

Micromorphological analysis of the soil profile of the meadow-bog solonchak showed the presence of newly formed gypsum and soluble salts in large pores (Fig. 7).



a b

Figure 7. Accumulations of newly formed gypsum (1) and soluble salts (2) in a large interaggregate pore of meadow-bog soil (pit 6).

Accumulations of gypsum fill the pores, either partially or completely (Fig. 7b), sometimes together with accumulations of soluble salts (Fig. 7a).

DISCUSSION

The chemistry of soil salinity is associated with the soil genesis. The genesis of soil salinization in the Priolkhonye area (Cis-Baikal region) is determined by the influence of strongly mineralized deep groundwater rising along a network of faults of different

directions and depths, and weathering of the rocks of the surrounding mountains composed of limestones and dolomites. The presence of dolomite and cryptogranular calcite is confirmed micromorphologically. In the Priolkhonye area, sulfate salinity (in some cases, with gypsum) predominates. However, toxic alkalinity is often present in the soil profile.

At the same time, the proportion of magnesium among the cations is high. In addition to the weathering of dolomite, the reason for the increase in the proportion of magnesium is associated with freezing processes, as a result of which calcium carbonates precipitate, and magnesium bicarbonates remain in the soil solutions [2]. It is magnesium bicarbonates that often determine increased alkalinity in gypsum-bearing soils of the Priolkhonye area. Freezing processes also increase the proportion of sulfates in the soils of the neighboring region [8]. Gypsum, whose presence can be supposed from data on the chemical analysis of soil water extract in pit 3, is micromorphologically visualized in the form of corroded crystals, which indicates the process of its introduction into the past stages of soil formation and destruction at the present time. Microsigns indicating the multi-temporal genesis of new gypsum formations, which have many morphotypes in the soil, are described in detail in the following works [1, 7, 13, 18, 19]. In the solonchak of pit 2 (Priolkhonye area), water extract data did not allow us to suppose the presence of gypsum. At the same time, the analysis of the microstructure of pit 2 made it possible to record the presence of pseudomorphs of calcite over gypsum, which indicates former presence of gypsum and its destruction at present. The presence of accumulations of soluble salts in the profile of both soils (pits 2 and 3) of the Priolkhonye area indicates the activity of modern soil salinization processes.

The genesis of soil salinization in Transbaikalia in the Gusinoozersk Basin (pit 6) is associated with the presence of sulfide pyrite-containing rocks in the coal seams of the deposit located here. During the oxidation of pyrite, calcium sulfate waters are formed. Sulfates in the groundwater appear during the circulation of water in coal seams and in some places are discharged onto the surface [9]. This determines the sulfate chemistry of soil salinity and the presence of gypsum in the profile. Gypsum in the soil profile stands represented by morphologically distinct crystals, which indicates its modern formation. The possible influence of mineralized groundwater on soil salinity is indicated by the presence of water springs on the surface. Micromorphologically, newly formed gypsum crystals and salt accumulations are diagnosed in pit 6, which indicates the ongoing processes of both gypsum formation and salt accumulation in the profile.

CONCLUSION

(1) A common feature of saline soils in the Cis-Baikal and Trans-Baikal regions is an unambiguous predominance of saline hydromorphic soils with the accumulation of salts in the upper part of the profile, which indicates the constant recharge of the profile from groundwater.

(2) Analysis of the composition of the water extract demonstrated the presence of gypsum and soluble salts in both studied areas of the Baikal region. However, this method does not allow us to determine the direction and stages of the salt accumulation process.

(3) The micromorphological method made it possible to clarify the genesis of concentrations of soluble salts and gypsum in the studied soils. Microfeatures attesting to the origin of these concentrations in different times were identified. Thus, gypsum pedofeatures in the solonchak of the Priolkhonye area (Cis-Baikal region) are specified by the presence of large corroded gypsum crystals indicating the origin of gypsum in the past stages of soil formation and its destruction at the present time. The modern process of soil salinization is indicated by the presence of accumulations of soluble salts in large pores. In the Trans-Baikal region (Gusinoozersk area), the meadow-bog solonchak contains distinct gypsans (gypsum coatings on pore walls) and accumulations of soluble salts in the pores. This microfabric indicates the activity of both processes - gypsum formation and salt accumulation - at the present stage of pedogenesis.

ACKNOWLEDGEMENTS

This work was supported in the framework of state assignment 0439-2022-0009 «To study the features of the genesis and distribution of saline soils in the steppe and dry steppe regions of Eastern Siberia using cartographic, chemical, micromorphological and mineralogical methods».

REFERENCES

[1] Álvarez D, Antúnez M, Porras S, Rodríguez-Ochoa R, Olarieta J. R and Poch R. M. Quantification of gypsum in soils: methodological proposal. Span. J. Soil Sci., vol. 12: 12:10669, 2022. DOI: 10.3389/sjss.2022.10669

[2] Anisimova N. P. Cryohydrochemical features of the frozen zone. Novosibirsk: Nauka. SO AS USSR. 153 p. 1981. (In Russian)

[3] Chernousenko G. Similarities and differences of soil salinization in Cis-Baikal and Trans-Baikal regions of Russia. Proc. 20th Intern. Multidiscipl. Sci. GeoConf. SGEM 2020, Albena, Bulgaria, 18–24 August. Sofia, vol. 20/issue 3.1, pp. 541–548, 2020. ISSN 1314-2704. DOI: 10.5593/sgem2020/3.1/s13.070

[4] Chernousenko G. I., Khitrov N. B., Pankova Ye. I. Magnesium in saline gypsum-bearing soils of Russia. Eurasian Soil Sci., vol. 56/issue 7, pp. 854–867, 2023. DOI: 10.1134/S1064229323600537

[5] Chernousenko G. I., Yamnova I. A. About the genesis of soil salinity in the western part of the Transbaikal region. Eurasian Soil Sci., vol. 37/issue 4, pp. 341–355, 2004.

[6] Dzyuba A. A., Tulokhonov A. K., Abidueva T. I., and Grebneva P. I. Distribution and chemistry of salt lakes in the Cis-Baikal and Trans-Baikal regions. Geogr. Prirodn. Resursy, issue 4, pp. 65–71, 1997. [in Russian].

[7] Gerasimova M. I., Kovda I. V., Lebedeva M. P., Tursina T. V. Micromorphological terms: the state of the art in soil microfabric research. Eurasian Soil Science, vol. 44/issue 7, pp. 739–753, 2011. DOI: 10.1134/S1064229311070052

[8] Kiyashko N. V., Komarov I. A., Golovanov D. L. Cryogenic transformation of soil solutions and the development of salt profiles in solonchaks of Mongolia according to the results of modeling. Eurasian Soil Sci., vol. 47/issue 5, pp. 353-359, 2014. DOI: 10.1134/S1064229314050068

[9] Kulikov A. I., Mangataev Ts.D. Changes in the salt regime of chernozem in Transbaikal region caused by irrigation with mineralized water. Eurasian Soil Science, vol. 33/issue 3, pp. 301-307, 2000.

[10] Lunina O. V., Gladkov A. S., Nevedrova N. N. Rift basins in Pribaikal'e: tectonic structure and development history. Novosibirsk: Geo. 316 p. 2009. [in Russian].

[11] Mats V.D., Yefimova I.M. Paleogeographic scenario of the late cretaceous – cenozoic for the central part of the Baikal region. Geodynamics & Tectonophysics, vol. 2/issue 2, pp. 175-193. 2011. [In Russian] DOI: 10.5800/GT-2011-2-2-0040

[12] Poch, R. M. Characteristics of the Sand Fraction of Two Hypergypsic Horizons of 'El Plad'Urgell' NE (Spain). Egypt. J. Soil Sci., vol. 31/issue 4, pp. 523–535, 1992.

[13] Poch R.M., Artieda O., Herrero J., Lebedeva–Verba M. Gypsic Features. In: Interpretation of Micromorphological Features of Soils and Regoliths. Amsterdam: Elsevier, pp. 259–280, 2018.

[14] Salt-Affected Soils of Russia. Moscow: Akademkniga, 2006. 854 p. ISBN 5-94628-198-4 [in Russian].

[15] Stoops, G., and Ilaiwi, M. "Gypsum in Arid Soils: Morphology and Genesis," in Proceedings of the Third International Soil Classification Workshop. The Arab Center for the Studies of Arid Zones and Dry Lands (acsad): Damascus. Editors F. H. Beinroth, and A. Osman, pp. 175–178, 1981.

[16] Ubugunov V. L., Khitrov N. B., Chizhikova N .P., Ubugunova V. I., Varlamov E. B., Zhambalova A. D., Chechetko E. S., Churilin N. A. The properties and the mineralogical composition of dark-humus-quasi-gley solonchak solonetzic cryoturbed Cryosols of Barguzin Hollow (Buryatia). Byull. Pochv. Inst. im. V.V. Dokuchaeva, vol. 92, pp. 62–94, 2018. DOI: 10.19047/0136-1694-2018-92-62-94 [in Russian]

[17] Ubugunov V. L., Ubugunova V. I., Zhambalova A.D. Diversity and classification of saline soils of the Barguzin Depression. Byull. K.I. Skryabin Kyrgyz National Agrarian Univ., vol. 2/issue 43, pp. 50–55, 2017. [in Russian]

[18] Yamnova I. A., Chernousenko G .I. Gypsiferous gazha soils of the subboreal zone of Eurasia. Eurasian Soil Sci., vol. 56/issue 1, pp. 1–15, 2023. DOI: 10.1134/S106422932260169X

[19] Yamnova I. A., Pankova E. I. Gypsic Pedofeatures and elementary pedogenetic processes of their formation. Eurasian Soil Sci., vol. 46/issue 12, pp. 1117–1129, 2013. DOI: 10.1134/S1064229313120089

MULTITEMPORAL SPECTRAL CHARACTERISTICS OF INTRAFIELD SOIL FERTILITY HETEROGENITY ZONES OF NORTHERN KAZAKHSTAN ARABLE LANDS

Vasily Rashkovich

Dr. Dmitry Rukhovich

Dmitri Borschev

Dokuchaev Soil Science Institute, **Russia**

ABSTRACT

New methods for assessing soil cover heterogeneity, based on the analysis of extensive satellite data using neural network filtering technologies, were implemented to evaluate the territory of northern Kazakhstan. A comparative analysis of the quality of soil cover structure (SCS) determination, using remote sensing data, was conducted using two different methods. The first method is indirect and involves determining the SCS by analyzing and aggregating multitemporal vegetation indices (MVI). The second method is unique and involves determining the spectral neighborhood of the soil line in RED-NIR space.

The soils in the study area are characterized by southern chernozems with varying thickness and humus content. The heterogeneity of the soil cover is largely influenced by the microrelief of the terrain. Soils on watershed and upland surfaces are typically eroded and less moist, resulting in reduced thickness and lower humus content compared to soils located on slopes and in depressions.

Field research established a relationship between SCS, MVI, and open soil surface (OSS). The reliability and accuracy of the developed OSS method, when applied to the soils of northern Kazakhstan, were confirmed.

The structure of the soil cover is crucial for agriculture, especially in conditions of moisture deficiency in the dry steppe zone. The determination of soil heterogeneity using the OSS method represents a powerful new tool for creating a cartographic basis for precision agriculture. Utilizing OSS maps as the basis for task maps, differentiated fertilizer application in the studied area demonstrated high effectiveness, resulting in a threefold increase in lentil yield.

Keywords: open soil surface, multitemporal vegetation index, precision planting, neural network satellite data filtration

INTRODUCTION

The doctrine of soil cover structure and soil heterogeneity on a microscale was established in the mid-20th century by V.M. Friedland [1,2]. He systematized and described the manifestations of soil cover heterogeneity based on different genesis, severity, and scale. The formation of soil cover structure is influenced by a comprehensive set of soil-forming factors: bioclimatic and lithological factors drive differences in soils on a macroscale,

https://doi.org/10.5593/sgem2024/3.1/s13.32

while local relief and lithological diversity influence heterogeneity on a microscale [1,3-5]. However, despite the robustness of Friedland's theory, it has not gained widespread adoption in agricultural production. This is primarily due to its complexity, which makes it challenging for the average farm specialist to apply, and the impracticality of implementing it without advanced tools. Additionally, traditional methods for compiling maps of soil cover structures, which do not involve remote sensing data, require immense labor, extensive sectioning, and prolonged post-processing of collected data, making them inefficient and time-consuming [6,7].

In recent years, technological advancements have revolutionized the field of agricultural production [6,8]. The advent of satellite data, including big satellite data, has opened new possibilities for soil analysis. This progress enables us to move towards automating the process of compiling maps of soil cover structures, which can serve as a crucial foundation for precision agriculture. The availability of large quantities of freely distributed satellite images allows for the development of sophisticated methods for assessing soil heterogeneity and creating detailed maps of soil fertility heterogeneity [9]. These maps are invaluable tools for generating task maps for farm equipment, enhancing the precision and efficiency of agricultural practices.

The territory of northern Kazakhstan was selected as the study area (Fig. 1). According to natural and agricultural zoning, this region belongs to the steppe zone, specifically the Kazakhstan province. This territory is a flat plain characterized by a weak microrelief, providing an ideal setting for studying soil cover heterogeneity.

The soils at the study site consist of southern chernozems with varying thickness and humus content. The heterogeneity of the soil cover is significantly influenced by the microrelief of the area. Soils on watershed and upland surfaces are typically eroded and less moist, resulting in reduced thickness and lower humus content compared to soils on slopes and in depressions. This variation plays a crucial role in the agricultural potential of the land.

The primary goal of the study is to determine the relationships between the soil cover structure, based on multitemporal vegetation indices, and the spectral characteristics of the open soil surface (OSS). By understanding these relationships, it is possible to develop more accurate and practical methods for soil analysis and management. This knowledge is essential for optimizing agricultural practices, particularly in regions facing moisture deficiencies like the dry steppe zone. Ultimately, the integration of these advanced methods



Fig. 1 – Location of the study area

into everyday agricultural production can lead to significant improvements in crop yields and soil management strategies, supporting the sustainability and productivity of farming operations in northern Kazakhstan and beyond.

MATERIALS AND METHODS

1. Neural network filtering of big remote sensing data.

2. Construction of soil fertility heterogeneity maps based on multitemporal vegetation indices (MVI).

3. Construction of the open soil surface map based on the soil line spectral neighborhood.

4. Field soil surveys based on MVI and OSS maps.

5. Measurement of biological productivity in different soil fertility heterogeneity zones.

MVI and OSS maps were constructed using data from Landsat and Sentinel satellite mission alongside with ALOS world DEM

RESULTS

Figure 2 displays an aggregation map of multitemporal vegetation indices for one of the fields in the study area. The map uses a red-yellow-green palette, where red indicates weak vegetation and green indicates strong vegetation. These maps are currently the primary tool for determining soil cover heterogeneity within agricultural land due to their ease of compilation and the availability of necessary source data. However, these maps have limitations as they indirectly represent soil heterogeneity through soil fertility, which is not a unique characteristic for a particular soil type.

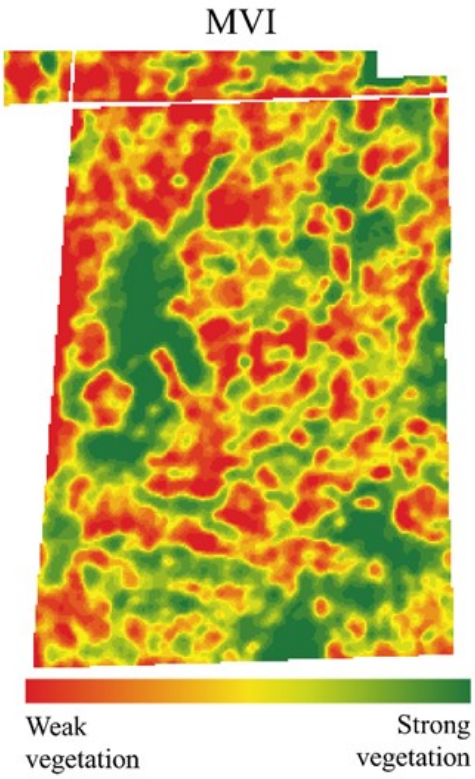


Fig. 2 – MVI map

Figure 3 illustrates a map of the open soil surface, colored in a blue-green-orange palette, where blue represents the darkest soils and orange represents the lightest. Since the technology for compiling such maps is relatively new, we currently lack models that directly relate spectral response data to specific soil differences. Nonetheless, it is well-established that darker areas on the map correspond to wetter or humus-rich areas in the field. Because these maps are based on images captured when vegetation is absent, they provide a direct assessment of soil heterogeneity. This method allows for a more accurate and detailed determination of soil cover structure both within and between fields.

Figure 4 presents a map overlaying the MVI on the OSS. Visually, it becomes evident that areas of increased fertility on the MVI map align with darker areas on the OSS map, while less fertile areas correspond to lighter areas. This relationship is further

https://doi.org/10.5593/sgem2024/3.1/s13.32

demonstrated in Figure 5, which shows that, even with high error levels, it is possible to reliably distinguish darker, fertile soils from lighter, infertile soils.

Figure 6 shows the results of field soil surveys. Testing points were established to investigate the causes of soil cover heterogeneity. Both soils examined are southern chernozems, but their profiles are quite different. The soil in the low-productive, lighter zone (Soil A) has a humus horizon thickness of 20 cm, whereas the soil in the highly productive zone (Soil B) has a humus horizon extending down to 110 cm. Additionally, soil A exhibits new formations of carbonates, which are absent in soil B. Previous agrochemical surveys by the farm also identified a high carbonate content, significantly affecting overall soil fertility. In the dry steppes of Kazakhstan, such differences are crucial and have a substantial impact on productivity, as shown in Figure 7.

Figure 7 highlights the actual difference in yield between different fertility zones as determined by various methods. The data clearly shows a significant variation in vegetation productivity. The actual yield was 127 kg/ha in the highly productive plot compared to 34 kg/ha in the low-productive plot.

DISCUSSION

The soil cover structure of northern Kazakhstan is closely linked to the microrelief conditions of the territory. The redistribution of moisture and its accumulation in relief depressions create favorable conditions for agricultural crop development. Erosion materials washed away from watershed surfaces are transported into these depressions, enriching the arable horizon with organic matter. Under increased moisture and organic matter conditions, plant roots can penetrate deeper, creating channels through which organic matter can flow further down, forming the soil profile B shown in Figure 6. This deep-flowing humus increases the total nutritional area for the root system, enhancing plant growth.

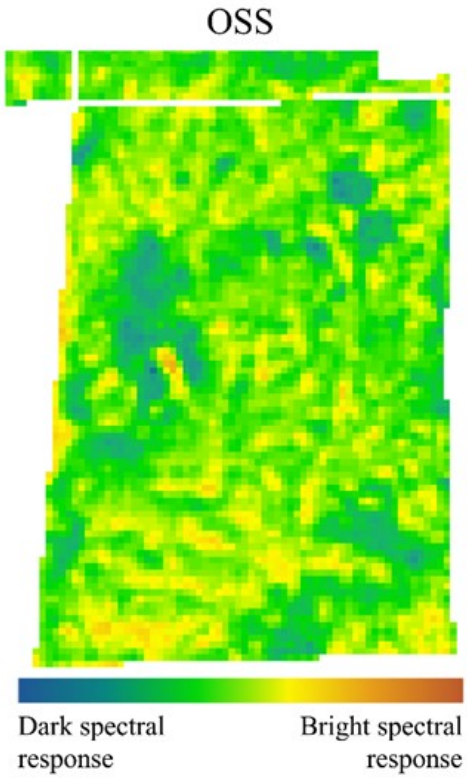


Fig. 3 – OSS map

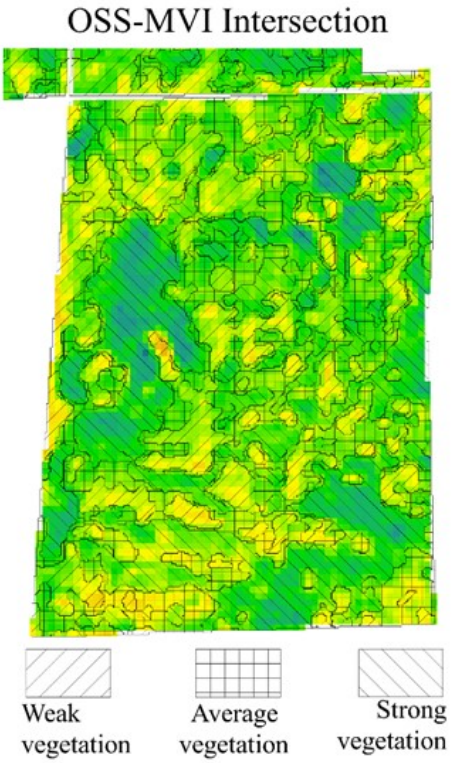


Fig. 4 – OSS-MVI intersection

These conditions result in a highly contrasting soil cover structure, with fertile, highly productive depressions and eroded, low-productive watershed surfaces. The contrasting levels of organic matter and moisture can be detected in soil images without vegetation, highlighting the potential of the OSS method. In images, soils in depressions appear darker due to the accumulation of moisture and organic matter, while eroded and plowed areas appear lighter. This spectral difference allows for the identification and differentiation of soils.

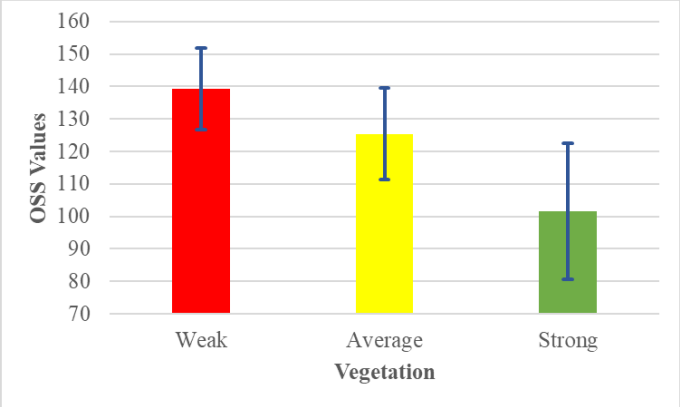


Fig. 5 – OSS-MVI intersection

Correlation analysis showed that OSS and MVI have a correlation level of -0.75; however, the precise functional dependence could not be established. As seen in Figure 5, with quantile grouping of MVIs, the difference between weak and strong vegetation is apparent, clearly delineating their boundaries.

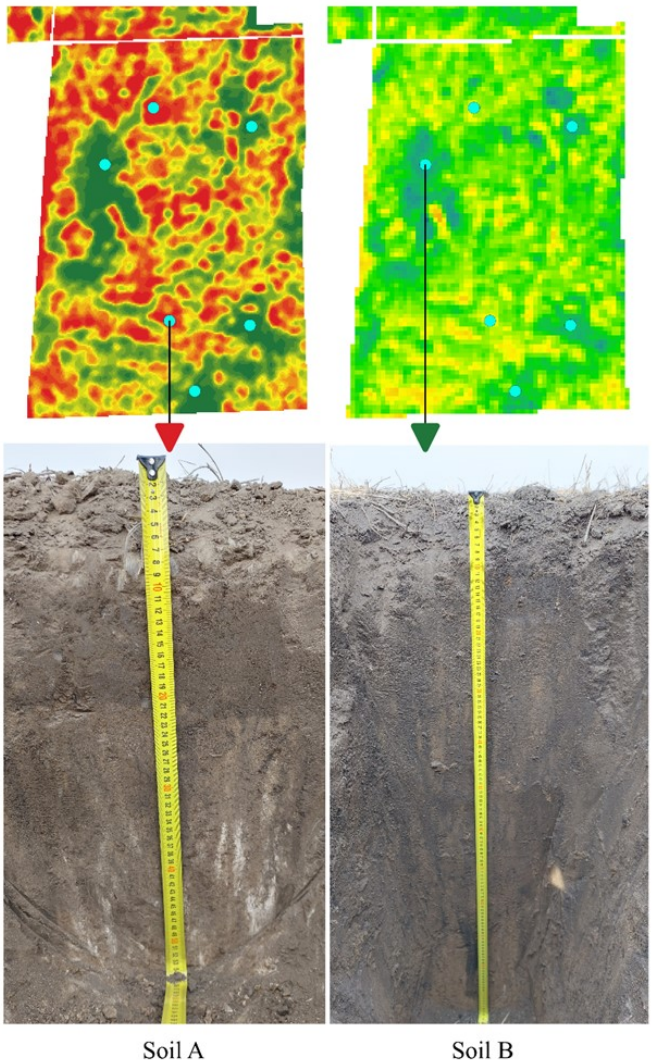


Fig. 6 – Difference in soils on the study site

From an applied perspective, constructing detailed SCS maps using the OSS method is highly valuable for precision agriculture. Because OSS maps are derived directly from soil images without vegetation, they offer greater detail and provide a direct assessment of soil conditions. This allows for the identification of issues such as salinity or sandiness, which may not be evident on MVI maps. This approach can help reduce costs and increase crop yields and margins through correct post-processing and proper redistribution of fertilizers in the field. To use OSS maps as a basis for task maps on fertilizer differentiation, ground surveys are necessary. These surveys

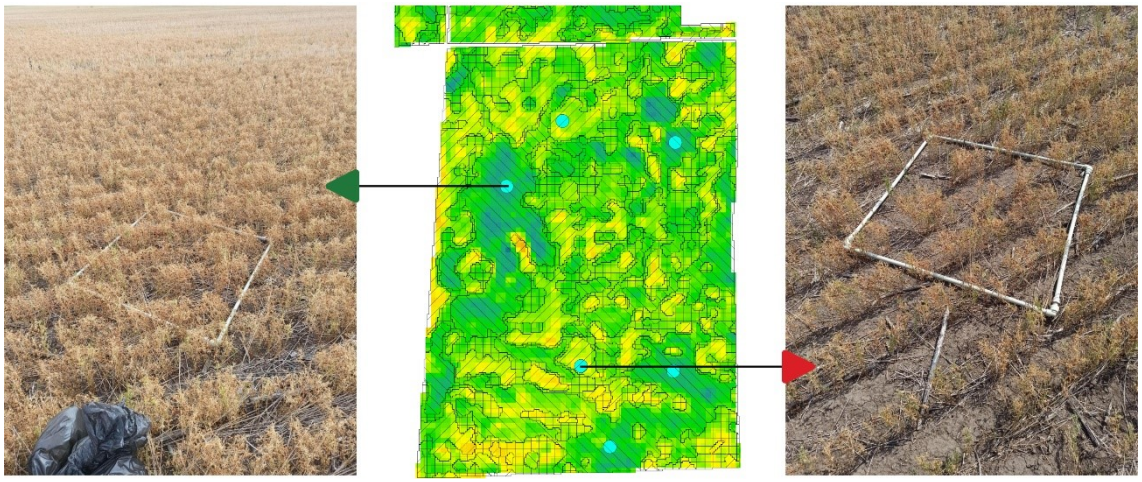


Fig. 7 – Difference in lentil vegetation

help assess the actual potentials and problems of each specific soil. Without this step, there is a risk of over-fertilizing low-productive areas (Figure 6, soil A) and under-fertilizing highly fertile areas (Figure 6, soil B).

According to farm data, the historical gross lentil yield in the studied field was 50 kg/ha. After implementing the technology of using OSS maps for differentiated fertilizer application, it became possible to determine the fertility limits of each soil within the soil cover structure, increasing the yield of productive areas to 127 kg/ha.

CONCLUSION

The accumulation of long-term datasets from the Landsat and Sentinel missions, along with the advancement of neural network and artificial intelligence technologies, has enabled the development and application of sophisticated technologies for agricultural mapping, particularly for compiling maps of soil cover structures.

Mapping soil patterns is a critical component in precision agriculture systems. Utilizing soil cover structure maps allows for a comprehensive assessment of soil problems and general characteristics. This facilitates the development of a differentiated plant nutrition program, aimed at achieving maximum productivity in each specific area of each field.

Traditional methods for compiling maps of soil cover structures based on multitemporal vegetation indices have several disadvantages. One significant drawback is the inability to compare the condition of adjacent fields due to varying vegetation states. In contrast, OSS is a direct method for assessing soil properties and does not depend on vegetation. This capability enables the mapping of large areas quickly and allows for the comparison of soils across different territories using a single resulting map.

REFERENCES

[1] Fridland V.M. Soil cover structure, Russia, 394p., 1972

[2] Fridland V.M. Structure of the soil mantle, Geoderma, vol. 12, pp. 35-42, 1974. DOI: 10.1016/0016-7061(74)90036-6

[3] V. I. Kiryushin. The Management of Soil Fertility and Productivity of Agrocenoses in Adaptive-Landscape Farming Systems, Eurasian Soil Science, vol. 52, pp. 1137–1145, 2019. DOI: 10.1134/S1064229319070068.

[4] V. I. Kiryushin. Methodology for integrated assessment of agricultural land. Eurasian Soil Science, vol. 53, pp. 960–967, 2020. DOI: 10.1134/S1064229320070066.

[5] Skryabina O.A. The structure of the soil cover, methods of its study. Perm, Perm State Agricultural Academy, 206 p, 2007.

[6] Kulyanitsa A.L., Rukhovich D.I., Koroleva P.V., Vilchevskaya E.V., Kalinina N.V. Analysis of the informativity of big satellite precision–farming data processing for correcting large–scale soil maps. Eurasian Soil Science, vol. 53/ issue 12, pp. 1709–1725, 2020. DOI: 10.1134/S1064229320110083.

[7] Kozlovsky F.I. Soil individual and methods for its determination. Patterns of spatial variation in soil properties and information and statistical methods for their study. Nauka, Moscow, pp. 42-59, 1970.

[8] Koroleva P.V., Rukhovich D.I., Kalinina N.V. Location of bare soil surface and soil line on the red–nir spectral plane. Eurasian Soil Science, vol. 50/ issue 12. C. 1375–1385, 2017. DOI: 10.7868/S0032180X17100045

[9] Yakusheva O.I. The influence of intra-field soil heterogeneity and the level of intensification of agricultural technologies on the yield of spring wheat. PhD dissertation of agricultural sciences, 2013.

PHYTOSTABLIZATION OF SULPHIDE MINE TAILINGS

Ph.D. candidate Raghad Soufan[1]

Prof. Dr. Antoine Karam[1]

Prof. Dr. Ahmed Aajjane[1]

[1]ERSAM, Department of Soils and Agrifood Engineering/Laval University, Quebec, **Canada**

ABSTRACT

Orphaned or abandoned sulphide tailing disposal sites pose significant environmental hazards, including eolian dispersion, water erosion, acid mine drainage, and heavy metal mobility. Phytostabilization, an eco-friendly strategy, entails the use of alkaline amendments alongside non-native plant species capable of thriving in environments with high concentrations of heavy metals. A greenhouse experiment was conducted to assess the effect of a commercial cement which contained 46.3% sand, applied alone or combined with three magnesium (Mg) reagents on the shoot dry yield (DMY) of ryegrass (*Lolium multiflorum* Lam.) grown on sulphide mine tailings (SMT) (pH 3.0). The 29 treatments evaluated were replicated three times in a randomized complete block design. All pots received N-P-K fertilizer. Treatments combining cement and Mg reagents significantly increased the pH of the cultivated tailings. Magnesium oxide (MgO) and magnesium hydroxide ($Mg(OH)_2$), when mixed with the cement, were more effective than magnesium carbonate ($MgCO_3$) in maintaining alkaline conditions in the cultivated tailings. The pH increase was notably higher in cultivated tailing samples treated with cement+MgO, reaching pH levels ranging from 4.93 to 7.58. Analysis of variance (ANOVA) revealed a highly significant effect of the cement+Mg reagents on the DMY of ryegrass. There was a strong correlation between substrate pH and DMY ($r = 0.853$, $p < 0.001$), with a quadratic regression equation providing the best fit to the data ($R^2 = 0.894$, $p < 0.001$). In conclusion, the study highlights the potential of an 8% cement combined with 2% MgO for tailing revegetation or cultivation purposes.

Keywords: revegetation, ryegrass, biomass production, cement, magnesium.

INTRODUCTION

Sulphide mine tailings (SMT) have extremely low pH, abundant Fe^{3+} ions, and high concentrations of hazardous heavy metals [1], [2]. These tailings are the materials left after the extraction and beneficiation of ores, copper (Cu), zinc (Zn), and other valuable metals [3]. Orphaned or abandoned sulphide tailing disposal sites pose significant environmental hazards, including eolian dispersion, water erosion, acid mine drainage, and heavy metal mobility [1], [4]. When exposed to air and water, sulphide-rich tailings form acid mine drainage [5-7], which causes the dissolution of heavy metals from tailings [8]. Therefore, responsible and sustainable management of SMT deposited in the tailing storage facilities is essential [6]. The aim of the present study, as part of a series of experiments to develop a phytostabilization program for sulphide mine tailings, was to promote the revegetation or cultivation of SMT, specifically by neutralizing active acidity using low-cost, locally accessible calcareous materials such as commercial cement, and by selecting fast-growing plants tolerant to hostile edaphic conditions. Phytostabilization [4], along with the revitalization, reuse, and valorization

of oxidized SMT, which have aged and become artificial soil-forming substrates (technosols) over time [8], for crop and biomass production [9], can significantly enhance current mine tailing and mine land management practices. A second objective was to evaluate the effect of commercial cement rich in calcareous products mixed with three chemical Mg reagents on the dry matter yield of ryegrass grown on acid SMT. The study was carried out in pot experiments.

MATERIALS AND METHODS

The sulphide mine tailing (SMT) used in the present study originated from the Solbec site at Thetford-Mines in the province of Quebec (Canada). The site surface characterization and the main geochemical characteristics of SMT are detailed elsewhere [10]. A greenhouse experiment was conducted using a randomized complete block design with three replications of 29 treatments. Three days before the experiment began, 1.0 kg of mine tailings was placed into each of the 87 polyethylene plastic pots. The amendments included: (i) commercial cement (C) obtained from the Quebec market, primarily composed of sand (46.3%) and cement (53.4%), with the latter containing 40.40% $CaCO_3$ and 1.44% $MgCO_3$; and (ii) three reagent-grade magnesium compounds: MgO, $Mg(OH)_2$, and $MgCO_3$. The 29 treatments were as follows: control (no lime, C-0); 2% cement (C-1); 4% cement (C-2); 6% cement (C-3); 8% cement (C-4); 2% cement + 1% MgO (CMO-1); 4% cement + 1% MgO (CMO-2); 8% cement + 1% MgO (CMO-3); 8% cement + 1% MgO (CMO-4); 2% cement + 2% MgO (CMO-5); 4% cement + 2% MgO (CMO-6); 8% cement + 2% MgO (CMO-7); 8% cement + 2% MgO (CMO-8); 2% cement + 1% $Mg(OH)_2$ (CMH-1); 4% cement + 1% $Mg(OH)_2$ (CMH-2); 8% cement + 1% $Mg(OH)_2$ (CMH-3); 8% cement + 1% $Mg(OH)_2$ (CMH-4); 2% cement + 2% $Mg(OH)_2$ (CMH-5); 4% cement + 2% $Mg(OH)_2$ (CMH-6); 8% cement + 2% $Mg(OH)_2$ (CMH-7); 8% cement + 2% $Mg(OH)_2$ (CMH-8); 2% cement + 1% $MgCO_3$ (CMC-1); 4% cement + 1% $MgCO_3$ (CMC-2); 8% cement + 1% $MgCO_3$ (CMC-3); 8% cement + 1% $MgCO_3$ (CMC-4); 2% cement + 2% $MgCO_3$ (CMC-5); 4% cement + 2% $MgCO_3$ (CMC-6); 8% cement + 2% $Mg(OH)_2$ (CMC-7); 8% cement + 2% $MgCO_3$ (CMC-8). Mineral fertilization based on nitrogen (N), phosphorus (P), and potassium (K) was added to each pot one week before sowing to facilitate the growth of ryegrass. This involved applying 10 g/pot of ammonium nitrate (33.5-0-0) as the N source, simple superphosphate (0-20-0) as the P source, and potassium muriate (0-0-60) as the K source. These quantities provided the equivalent of 1474 kg/ha of N, 880 kg/ha of P_2O_5, and 1320 kg/ha of K_2O, respectively. The plant chosen for phytostabilization and biomass production is Italian ryegrass (*Lolium multiflorum* Lam.), an annual grass in the *Poaceae* family. It is primarily used for quick cover in erosion control plantings and has been previously utilized in efforts to revegetate mining sites [11], [9]. Italian ryegrass is noted for its rapid regrowth ability [9] and its highly developed root system [12]. Steynberg et al. [13] found that Italian ryegrass can develop a deep root system when stressed. Ryegrass was sown at a rate of 2.4 g/pot. The greenhouse temperature was maintained at 24°C during the day and 18°C at night. Lighting was provided for 16 hours each day throughout the plant growth period. Watering was consistently performed once a day for all cases, using distilled water. Seven weeks after sowing, the shoot biomass was harvested, washed with distilled water, and dried to a constant weight at 70°C in a forced-air oven. The dried shoot biomass was weighed to determine the dry matter yield (DMY). After harvesting, subsamples of cultivated tailings from each pot were collected. These samples were air-dried and then sieved through a 2-mm

sieve. The pH of the cultivated tailing was measured in a 1:2 (w/v) tailing/distilled water mixture. Phytoavailable Ca (Ca_{M3}), Mg (Mg_{M3}), K (K_{M3}), Cu (Cu_{M3}), Fe (Fe_{M3}), Mn (Mn_{M3}) and Zn (Zn_{M3}) were assessed by the Mehlich-3 (M3) extraction method [14]. The M3 reagent composition was 0.015*M* NH_4F + 0.25*M* NH_4NO_3 + 0.2*M* CH_3COOH + 0.013*M* HNO_3 + 0.001*M* EDTA. This reagent proved to be useful for extracting various elements from coal mine soils in As Pontes, Spain [15]. Mehlich 3-extractable metallic micronutrients (e.g. Cu, Fe, Mn and Zn) are considered the most mobile and potentially phytoavailable forms in tailing substrates. The concentrations of Ca, Mg, K, Cu, Fe, Mn and Zn were determined using a flame atomic absorption spectrophotometer (Perkin Elmer AAnalyst 200, Perkin Elmer, Shelton, CT). All data were subjected to analyses of variance (ANOVA) using Statistix software (Analytical Software, Statistix version 10.0.0.9, User's manual, Tallahassee, Florida, 2017). Analyses of variance were performed on the following variables: shoot dry matter yield and cultivated tailing pH. Simple a priori contrasts were used to compare the different treatments at a significance level of $P = 0.05$. Additionally, Pearson correlation coefficients (r) were calculated using Statistix software to evaluate the linear relationships between variables. Both linear and non-linear regressions were used to relate Mehlich-3 extractable metallic micronutrients to the pH of the cultivated tailings.

RESULTS AND DISCUSSION

pH of Cultivated Tailings

Overall, the addition of cement mixed with high rates of Mg reagents to acidic SMT resulted in a marked increase in the pH of the cultivated tailings. Analysis of variance revealed a highly significant effect ($P < 0.001$) of the cement + Mg reagent treatments on the pH of the cultivated tailings (Table 1). The significance of Mg reagents in maintaining neutral to slightly alkaline conditions in cultivated tailings is clearly demonstrated. However, the *t*-test ($P < 0.05$) did not reveal significant differences between the control and the lower rates of cement (C-1, C-2, C-3 and C-4) and between the control and the following treatments: CMC-1, CMC-3 and CMH-1. Furthermore, the treatments involving cement combined with various magnesium materials showed significant differences from one another (Table 1). The pH values of the cultivated tailings increased in the following order: cement + $MgCO_3$ < cement + $Mg(OH)_2$ < cement + MgO (Fig. 1). The application of the highest rate of cement (8%) alone slightly increased the pH of the cultivated tailings from 3.63 (control) to 3.86 over 7 weeks of plant growth (Fig. 1). However, when 2% of MgO, $Mg(OH)_2$, or $MgCO_3$ was added to the cement-amended tailings, the pH values increased from 3.85 (with 8% cement) to 7.58, 7.35, and 6.03, respectively. The highest pH levels were recorded in the cultivated tailings that received 8% cement combined with 2% Mg reagents.

Notably, the increase in pH levels was generally more significant for the samples treated with cement + MgO, with pH values ranging from 4.93 to 7.58. Magnesium oxide and $Mg(OH)_2$ were more effective in maintaining alkaline conditions in the cultivated tailings than $MgCO_3$ or cement alone, likely due to the higher neutralizing capacity of MgO and $Mg(OH)_2$.

Table 1. Effects of treatments on the dry matter yield (DMY) of ryegrass and cultivated tailing pH.

Contrasts	*F* value	
	DMY	pH
Control vs cement	0.35 ns	0.56 ns
Control vs cement + MgO	64.33***	279.17***
Control vs cement + $Mg(OH)_2$	44.11***	155.93***
Control vs cement + $MgCO_3$	20.15***	40.18***
Cement vs cement + MgO	164.12***	760.50***
Cement vs cement + $Mg(OH)_2$	108.62***	410.70***
Cement vs cement + $MgCO_3$	44.81***	92.48***
Cement + MgO vs cement + $Mg(OH)_2$	8.56**	80.19***
Cement + MgO vs cement + $MgCO_3$	56.13***	483.87***
Cement + $Mg(OH)_2$ vs cement + $MgCO_3$	20.85***	170.10***

**, ***Significant at $P < 0.01$ and 0.001 respectively; ns not significant.

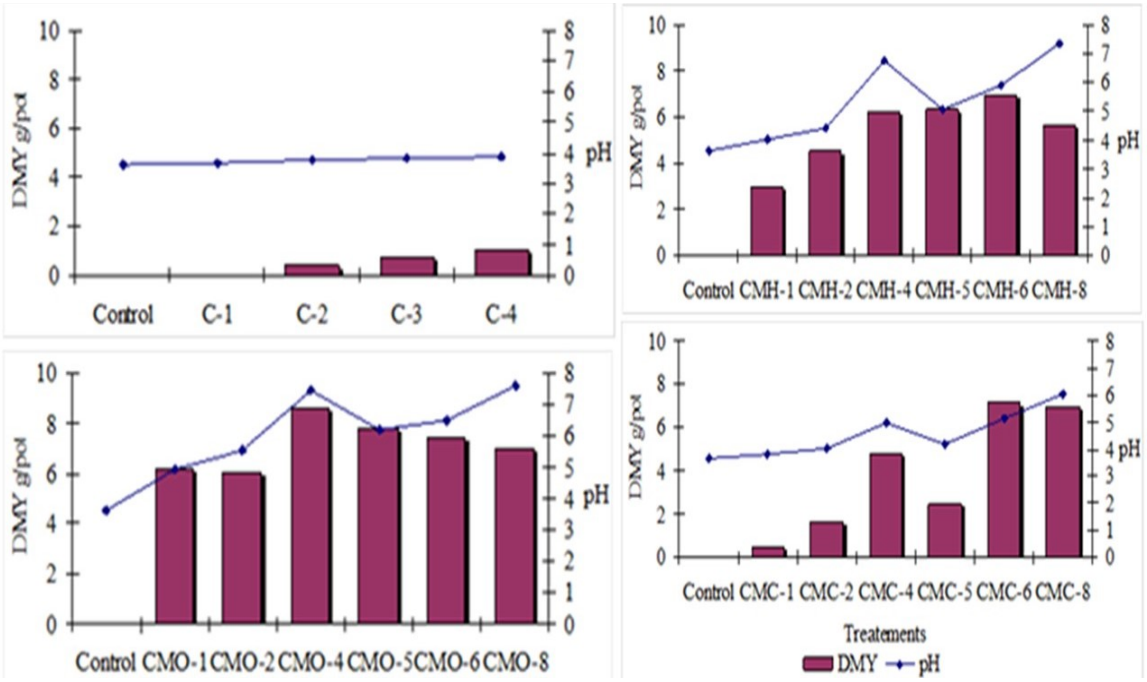


Figure 1. Effect of treatments on cultivated tailing pH levels and shoot dry matter yield (DMY) of ryegrass.

Indeed, the neutralizing capacities of the liming materials were 225% for MgO, 162% for $Mg(OH)_2$, 101% for $MgCO_3$, and 42% for commercial cement. At low rates, commercial cement has a notably low neutralizing capacity. This is likely due to its very low $Mg(CO_3)$ content, which has a higher neutralizing value compared to $CaCO_3$ [16].

Mora et al. [17] observed that the pH values of acidic Chilean soils treated with dolomitic lime [$CaMg(CO_3)_2$] were higher than those treated with calcitic lime ($CaCO_3$), due to the higher neutralizing capacity of dolomitic lime. As expected, liming materials increased Ca_{M3} and Mg_{M3} availability. All application rates of Mg reagents resulted in high levels of Mehlich-3 extractable Mg (Mg_{M3}), with the levels following this order: cement + $MgCO_3$ < cement + $Mg(OH)_2$ < cement + MgO (data not shown). The highest Mehlich-3 extractable Ca (Ca_{M3}) levels, ranging from 950 to 1040 mg Ca_{M3}/kg of cultivated tailings, were recorded in the cement-treated tailings. However, Mg_{M3} levels in the [cement + Mg]-treated tailings were generally higher than the Ca_{M3} levels. Furthermore, the pH of the cultivated tailings was very highly correlated with Mg_{M3} ($P < 0.001$) but showed a poor correlation with Ca_{M3} ($P > 0.05$). The pH values and Mg contents of the cultivated tailings were negatively correlated with Zn_{M3}, Cu_{M3}, Fe_{M3}, and Mn_{M3}. These results suggest that the presence of Mg reagents combined with commercial cement reduces the phytoavailability (i.e., labile fraction) of heavy metals in SMT.

Heavy Metal Availability

Liming an acidic soil is generally credited with reducing the availability of heavy metals, as illustrated by the regression data in Table 2. Heavy metal availability is highly pH-dependent. Mehlich-3 extractable iron (Fe_{M3}) decreased in cultivated tailings in the following order (mg Fe_{M3}/kg cultivated tailing): cement + $MgCO_3$ (3000) < cement + MgO (3238) < cement + $Mg(OH)_2$ (3374) < cement (4150) < control (5180). Shuman [18] also observed a reduction in available Fe following the addition of calcitic lime and various magnesium materials to agricultural soil. The same pattern was observed for Zn_{M3}, Cu_{M3}, and Mn_{M3} (data not shown). Doye [19] noted a reduction in Fe, Zn, and Cu leaching after adding alkaline materials such as kiln dust and red mud bauxite to reactive sulfide tailings. At low pH, metal availability can be high enough to be toxic to many plants.

Table 2. Polynomial regression model for selected Mehlich-3 extractable metals and cultivated tailing pH.

Extractable metals	Equation	R^2
Fe_{M3}	$Fe_{M3} = -15.64\ pH^3 + 304.6\ pH^2 - 1929.3\ pH + 4388.6$	84.4
Zn_{M3}	$Zn_{M3} = -1.26\ pH^3 + 22.2\ pH_2 - 127.79\ pH + 249.0$	70.0
Cu_{M3}	$Cu_{M3} = -0.96\ pH^3 + 18.4\ pH^2 - 117.63\ pH + 273.8$	69.4
Mn_{M3}	$Mn_{M3} = -0.44\ pH^3 + 8.1\ pH^2 - 49.29\ pH + 113.6$	45.1

Shoot Dry Matter Yield

The smallest dry matter yield (DMY) was observed in the cement-treated tailings, likely due to the very low pH of the growing media (pH 3.65 - 3.86). The leaves of the ryegrass grown on the cement-treated tailings turned almost entirely yellow. Very low biomass production was recorded in both the control (<0.01g/pot) and the 2% cement rate application (Fig. 1). According to [20], tailing pH values below 4 are unsuitable for

plant growth and survival due to the low availability of essential elements such as Ca and Mg and the high concentration of H^+ ions. In general, the application of magnesium reagents to cement substantially enhanced the growth of ryegrass (Fig. 1). Analysis of variance (Table 1) revealed a significant effect of the cement + Mg reagent treatments on DMY. However, no significant difference was observed between the control and the cement-treated tailings. Most of the treatments were significantly different from each other (Table 1). The application of MgO and $Mg(OH)_2$ to commercial cement substantially enhanced the growth of ryegrass, with the highest DMY recorded in tailings receiving the cement + MgO treatment (Fig. 1). Applying Mg reagents beyond 1% in combination with 8% cement did not further increase the growth of ryegrass (Fig. 1). The average shoot DMY of ryegrass grown with the various treatments followed this sequence: CMO (6.96 g/pot) > CMH (5.76 g/pot) > CMC (3.89 g/pot) > cement (0.54 g/pot) > control (<0.01 g/pot). The increase in the pH of the cultivated tailings associated with the application of Ca and Mg compounds likely contributed to increased nutrient uptake and DMY. A strong relationship was established between the DMY of ryegrass and certain chemical properties of the growing media. The pH of the cultivated tailings was the best-correlated property with DMY ($r = 0.853$, $P < 0.001$). The importance of pH in increasing the growth of ryegrass is clearly demonstrated. To better analyze the relationship between cultivated tailing pH and DMY of ryegrass, we examined four mathematical models: linear, quadratic, exponential, and logarithmic. Among these models, the quadratic regression equation provided the best fit to the data ($R^2 = 0.984$) (Fig. 2). This finding aligns with the observed trend where DMY levels off or decreases at the highest cement + Mg reagent rates.

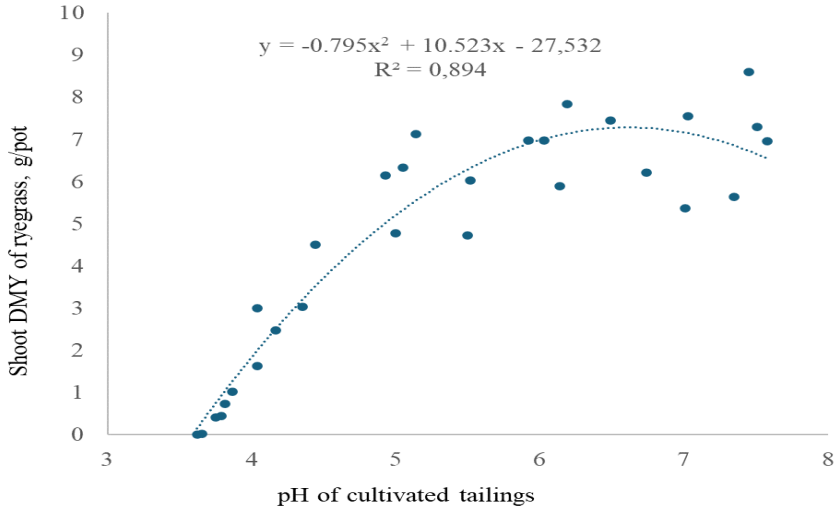


Figure 2. Relationship between the pH of cultivated tailings and the DMY of ryegrass.

The fitted curve can be divided into three distinct zones: a nearly horizontal part representing a zone of nutrient adequacy, a steeply descending part representing a zone of nutrient deficiency, and a transition zone between them. The DMY obtained for cement-amended tailings lies in the zone of deficiency. At high rates of Mg reagents, there was a decrease in yield, with values falling within the transition and deficiency zones of the curve.

CONCLUSIONS

This study underscores the promising potential of commercial cement concrete (Portland cement), particularly when enriched with calcareous products and combined with magnesium-based compounds like magnesium oxide, magnesium hydroxide, and magnesium carbonate. These materials have proven effective in increasing the pH of cultivated sulfide mine tailings (subsurface tailings material). These findings have practical implications for tailings management by reducing acid generation and trace metal lability in sulfide mine tailing profile, thereby minimizing the risk of water contamination. Additionally, these mixtures created favorable conditions for the establishment of ryegrass as a vegetation cover. Among the combinations examined, commercial cement + magnesium oxide yielded the most encouraging results. Given the beneficial role of Ca and Mg compounds in vegetation development and value-added aboveground biomass production on sulphide mine tailings, we recommend using Mg compounds in conjunction with commercial cement. However, future research could explore the efficacy of combining cement with other Mg amendments, such as dolomitic lime or industrial by-products containing Mg.

ACKNOWLEDGEMENTS

The authors wish to thank the Natural Sciences and Engineering Research Council of Canada for financial support.

REFERENCES

[1] Ritcey G.M., Tailings management. Problems and solutions in the mining industry. Process metallurgy 6. Elsevier Science Publishers B.V. The Netherlands, 1989.

[2] Zhang A., Bain J.G., Schmall A., Ptacek C.J., Blowes D.W., Geochemistry and mineralogy of legacy tailings under a composite cover. Applied Geochemistry, vol. 159, 105819, 2023.

[3] Sarathchandra S.S., Rengel Z., Solaiman Z.M., Remediation of heavy metal-contaminated iron ore tailings by applying compost and growing perennial ryegrass (*Lolium perenne* L.). Chemosphere, vol. 288, Part 2, 132573, 2022.

[4] Xie L., van Zyl D., The geochemical processes affecting the mobility of Cu, Pb, Zn during phytostabilization on sulfidic mine tailings revealed by a greenhouse study. Journal of Cleaner Production, vol. 418, 138119, 2023.

[5] Park I., Tabelin C.B., Jeon S., Li X., Seno K., Ito M., Hiroyoshi N., A review of recent strategies for acid mine drainage prevention and mine tailings recycling. Chemosphere, vol. 219, pp 588-606, 2019.

[6] Cacciuttolo C., Cano D., Custodio M., Socio-environmental risks linked with mine tailings chemical composition: Promoting responsible and safe mine tailings management considering copper and gold mining experiences from Chile and Peru. Toxics, vol. 11(5), 462, 2023.

[7] Martins N.P., Helser J., Plötze M., Snellings R., Habert G., Effect of sulfidic mine tailings used as mineral admixtures on the hydration of common and alternative cements. Materials and Struct vol. 57, 19, 2024.

[8] Fan L., Zhou X., Luo H., Deng J., Dai L., Ju Z., Zhu Z., Zou L., Ji L., Li B., Cheng L., Release of heavy metals from the pyrite tailings of Huangjiagou pyrite mine: Batch experiments. Sustainability, vol. 8(1), 96, 2016.

[9] Cross A.T., Lambers H., Young calcareous soil chronosequences as a model for ecological restoration on alkaline mine tailings. Science of The Total Environment, vol. 607-608, pp 168-175, 2017.

[10] Aajjane A., Karam A., Valorization of a sulphide mine residue for ryegrass production. Pollution, Bioremediation & Biodegradation Journal, vol. 1(1), 180001, 2018.

[11] Karam A., Guay R., Inondation artificielle du parc à résidus miniers Solbec-Cupra: études microbiologique et chimique. Rapport final. CANMET/DSS/MER 94, Ottawa, Canada, 1994.

[12] Gillet M., Les graminées fourragères. INRA, collection nature et agriculture. BORDAS, Paris, 1980.

[13] Steynberg R.E., Nel P.C., Rethman N.F.G., Soil water use and rooting depth of Italian ryegrass (*Lolium multiflorum* Lam.) in a small plot experiment, South African Journal of Plant and Soil, vol. 11, pp 80-83, 1994.

[14] Ziadi N., Tran T.S., Mehlich 3-extractable elements. in Carter M.R. & Gregorich E.G. (eds), Soil sampling and methods of analysis. Second edition. Canadian Society of Soil Science. CRC Press, Boca Raton, pp 81-88, 2008.

[15] Monterroso C., Alvarez E., Marcos M.L.F., Land degradation and development, vol. 10, pp 35-47, 1999.

[16] Donahue R.L., Miller R.W., Shickluna J.C., Soils: an introduction to soils and plant growth, Fourth edition. Englewood Cliffs, Prentice-Hall, New Jersey, 1977.

[17] Mora M., Venegas C., Lobos W., Demanet R., Dolomita una nueva alternative para suelos ácidos. Frontera Agrícola, vol. 1, pp. 54-62, 1993.

[18] Shuman L.M., Evaluation of liming and magnesium materials for increasing soil pH and available magnesium. Communications in Soil Science and Plant Analysis, vol. 16, pp 1053-1070, 1985.

[19] Doye I., Évaluation de la capacité de matériaux industriels alcalins à neutraliser des résidus et stériles miniers acides. Thèse de doctorat, Université Laval, Programme Interuniversitaire en Sciences de la Terre, Faculté des Sciences et de Génie, 2005.

[20] Lyle E.S.Jr., Surface mine reclamation manual. School of forestry, Auburn University, Elsevier Publishing Co. Inc., 1987.

QUALITY OF POST-HARVEST RESIDUES WHEN GROWING MAIZE IN THE SYSTEM OF MIXED CROPPING

Ing. Antonín Kintl[1]

Ing. Julie Sobotková[1]

Ing. Jakub Elbl [2]

Ing. Martin Brtnický[3]

Ing. Igor Huňady[1]

[1] Agricultural Research Ltd., **Czech Republic**
[2] Department of Agrosystems and Bioclimatology, Faculty of Agronomy, Mendel University in Brno, **Czech Republic**
[3] Department of Agrochemistry, Soil Science, Microbiology and Plant Nutrition, Faculty of Agronomy, Mendel University in Brno, **Czech Republic**

ABSTRACT

Potential environmental impacts of growing maize as monoculture lead to efforts focused on finding other potentially suitable crops or their combinations that could replace the pure maize cultures. The most frequent and most effective combination is a mixed crop of maize and legumes. The presented paper deals with the issue of the quality of post-harvest residues when growing maize in the system of mixed cropping. In the field experiment, yield and quality of post-harvest residues were studied during the growing season in the following variants: maize grown as monoculture and maize grown in the mixed culture with bean. Compared with the C:N ratio in the post-harvest residues of maize grown in monoculture (39:1), a benefit of mixed cropping was significantly reduced C:N ratio in the biomass of post-harvest residues that was approaching 30:1 which is considered optimal for their decay. The biomass of post-harvest residues from the mixed crop of maize and bean for silage contained by 70 kg/ha (54 %) more nitrogenous substances than the biomass of post-harvest residues from the pure maize culture.

Keywords: mixed cropping, maize, dry bean, legumes, maize yield, C:N ratio

INTRODUCTION

Maize is a crop of wide applications from bulky feeds for livestock and biogas plants to grain use. Exactly the maize grain is a commodity of versatile use, which is not good for feeding only but its use is increasingly gaining importance in food industry, too. Due to its high starch content, it is also much required for the production of bioethanol. Exactly the production of maize starch which is used in a number of industries such as paper manufacture, construction industry, chemical and pharmaceutical industries is another direction for using the maize grain [1].

However, Herrmann [2] mentioned some objections concerning the negative impact of growing maize on the environment. Other sources of biomass or their mixtures can have

a lower negative effect on the environment than the production of maize [3]. These facts lead to efforts to seek other potentially suitable crops or their combinations. Ofori and Stern [4] inform that the most frequent and the most effective crop combinations are mixed crops of maize and legumes. Compared with systems without legumes, the mixed intercropping system of maize and legumes is considered an alternative for saving nitrogen and higher productivity per unit time and area [5].

Brooker et al. [6] define the mixed cropping system as a system of growing two crops on one plot at the same time. The system makes use of legumes and other field crops. According to Stern [7], the success of mixed crop in the agricultural system depends first of all on the efficient biological fixation of nitrogen (BFN), and on the capability to provide the fixed N to non-leguminous plants. Legumes grown in the mixed cropping system can cover their need of nitrogen necessary for creating profitable yield from the BNF of atmospheric N_2. The yield of field crops depends on their ability to gain a sufficient amount of nutrients (particularly N in the form of N_{min}) and water from the soil. Exactly the effort to eliminate external input of nitrogen calls for cultivation measures that would optimize the process of utilizing atmospheric nitrogen fixation in the system of mixed cropping [8].

The need for incorporating legumes into the crop sequence in order to enhance soil fertility and sustainability of farming systems are topics that are often neglected in practice but their positive influence in the crop rotation is generally acknowledged [4];[6]. The effect of mixed culture on soil properties and soil fertility was described also by Van Kessel and Hartley [9] who confirmed the positive influence already after the first year of measurement. Mixed culture is evaluated on the basis of the economic efficiency of the whole cultivation system, i.e. also based on the value of pre-crop which affects the following crop.

Song et al. [10] inform about the positive effect of mixed cropping systems on increased yields claiming that compared with pure cultures, the cultivation of mixed cultures makes available larger amounts of soil N and P. The main advantage of mixed cultures is increased productivity from the use of solar radiation [6]. According to Cong et al. [11], the higher production of aboveground biomass reflects also in the increased production of underground biomass. The authors further inform that when the mixed cultures are included in the conventional crop rotation procedure, increased supply of soil organic matter is not the only benefit but, at the same time, a change occurs in the soil C:N ratio, which results in the better decomposability of organic matter and its further “turnover” in the soil. It is stated that post-harvest residues from the mixed cropping systems of cereals and legumes have a higher content of nitrogen than residues from cereals grown in monoculture thanks to the presence of legumes in the straw mixture [12].

The system of maize-legume mixed cropping is an important agronomic tool for increased efficiency of soil use as well as for the fixation of atmospheric nitrogen with the simultaneous restoration of soil fertility.

The research aimed to verify the effect of growing maize in the mixed culture with bean on the yield of maize grain and C:N ratio in post-harvest residues as compared with maize grown in monoculture.

MATERIALS AND METHODS

Localization of the field experiment

The field experiment was implemented near the village of Troubsko in the South-Moravian Region (49°10'25.909 "N, 16°29'47.081 "E). As to climate, it is a slightly dry and slightly warm zone with an average annual precipitation amount of 525.6 mm and mean annual temperature 8.95 °C. Geological basement is formed of loess and loess loam of the Bohemian Massif, soil type is Haplic Luvisol.

Experimental design

Stands of mixed cultures are currently established with the KINZE 3500 precision seed drill with the vacuum sowing device Model "Interplant Pro", which is equipped with 15 sowing units installed in two rows on the rotating frame, seeding into narrow lines 0.375 m.

The experiment was conducted during the growing season of year 2023. Maize was sown in the amount of 80 thousand seeds per hectare and grown in the system of monoculture and in the system of mixed culture with bean in the ratio of 1:1 (80 thousand seeds/ha and 80 thousand seeds/ha). Distance between the lines of bean and maize was 37.5 cm (Fig. 1) [13]. In order to assess the effect of bean in the mixed culture, mineral fertilizers were not used.

Grain yields, sampling of post-harvest residues and their analysis

Grain yields were evaluated of maize grown in the monoculture and maize grown in the mixed culture together with bean. Post-harvest residues were sampled from the maize monoculture as well as from the mixed culture of maize and bean. Then the effect of bean biomass on the amount of nitrogen in post-harvest residues was assessed and the resulting C:N ratio as compared with the maize monoculture.

The measured data were analysed in the software Statistica 14. ANOVA and Post-hoc Tukey HSD test were used to explore the data and to test potential differences at a level of significance $P < 0.05$.

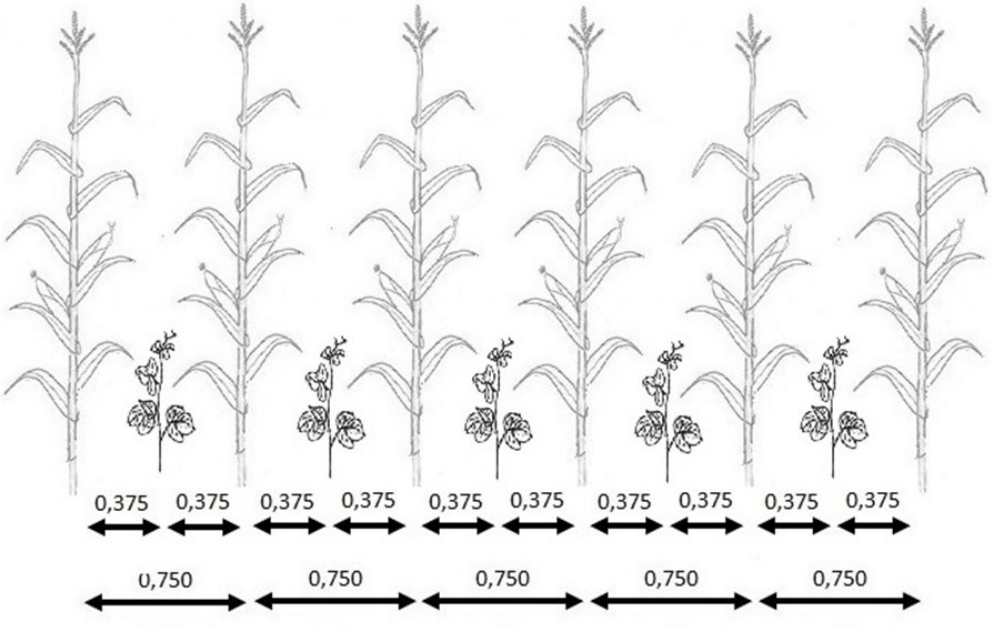


Fig. 1: The system of intercropping maize and bean [13].

RESULTS AND DISCUSSION

For a wider use of mixed cropping, its system should be as advantageous as possible in economic terms, which means that alternative cultivation systems should be developed that would ensure high yields of crops for their efficient production at low pressure on the soil and environment. Mixed cultures with legumes can be a suitable solution thanks to their capacity of biological fixation of nitrogen that would reduce consumption of inorganic nitrogenous fertilizers [14].

In the presented experiment, we assessed the yield of grain in maize grown alone and in maize grown in the mixed culture with bean. Further, the effect of bean biomass was evaluated on the amount of nitrogen in post-harvest residues and the resulting C:N ratio as compared with the pure culture of maize.

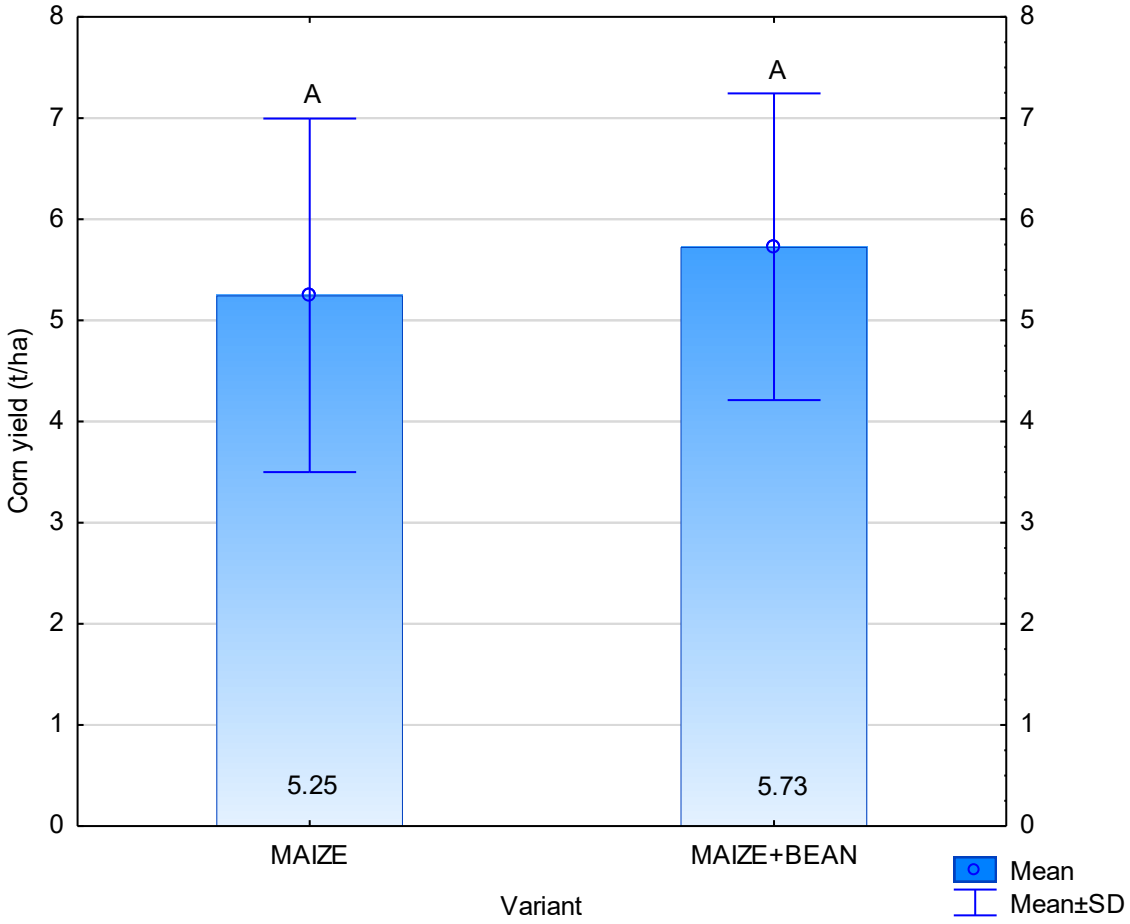


Fig. 2: Grain yields of maize monoculture and mixed culture of maize + bean.

The grain yield of maize grown in the monoculture was 5.25 t/ha whereas the grain yield of maize grown in the mixed culture reached 5.73 t/ha, thus being higher by 0.48 t/ha (9.14 %) (Fig. 2). This increase was however non-significant due to the high variability of measured values. It follows that compared with the yield of maize grown in the monoculture, the cultivation of maize in the mixed culture with bean had a beneficial influence on yield in spite of the fact that differences in yields were not statistically significant.

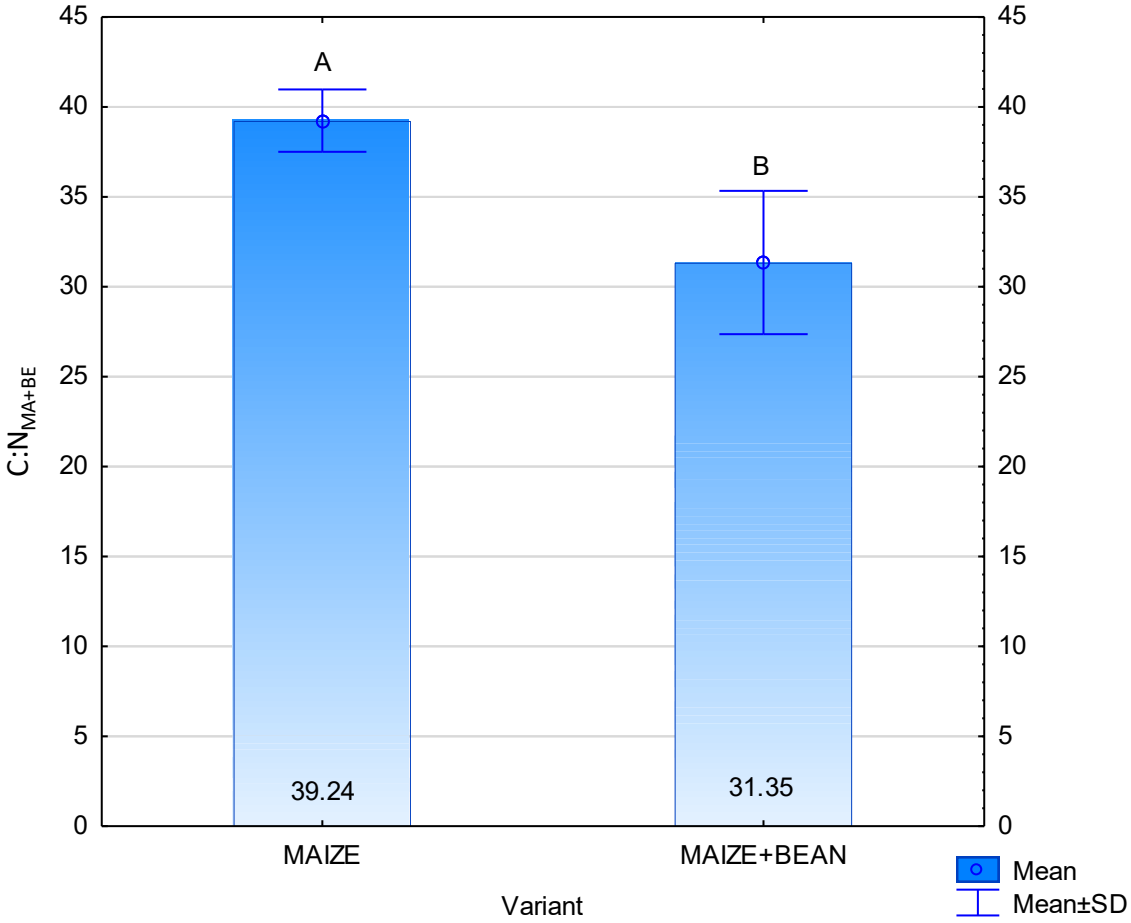


Fig. 3: Comparison of C:N ratio in post-harvest residues of maize grown in monoculture and in mixed culture.

Compared with the maize monoculture, growing maize in the mixed culture with bean had a demonstrably beneficial influence on the C:N ratio (Fig. 3). The presence of bean in the mixed crop, i.e. plant with the capability of symbiotic atmospheric nitrogen fixation, led to the increased representation of nitrogen in the biomass of post-harvest residues from the mixed culture nearly by 70 kg/ha (54 %) and hence also to the C:N ratio decreased from 39.2 in the monoculture to 31.4 in the mixed crop. The difference was statistically significant. These results indicate that as compared with post-harvest residues from the maize monoculture, post-harvest residues from the mixed crop of maize and bean feature better decomposition. An optimal C:N ratio for organic fertilization is considered 30:1 [15].

Bean had a demonstrable influence on the increased content of nitrogenous substances in biomass harvested from the mixed culture of maize and bean for the production of silage used for feeding farm animals. The content of N-substances was increased by 30.9 % compared with biomass from the maize monoculture. Average yields of N-substances (t/ha) in biomass obtained from individual variants were 2.36 t/ha (maize monoculture) and 3.09 t/ha (mixed culture of maize and bean) [13].

Information about the C:N ratio in post-harvest residues can help farmers avoid both overdosing with nitrogen and lack of nitrogen with all economic and environmental consequences. Knowing the C:N ratio is necessary to establish the rate of organic matter

decomposition by mineralization. If the ratio falls below 10, a negative phenomenon occurs, i.e. decrease of soil organic matter which is necessary for the formation of stable organic compounds. Stable organic compounds are important in creating soil fertility. If the topsoil is enriched with higher doses of mineral N fertilizers, the C:N ratio can be adversely affected. Excessive doses of nitrogen, nitrate forms in particular, may result in the increased leaching of N that can cause ecological and economic losses. On the other hand, the lack of available forms of nitrogen resulting from incorrect or erroneously interpreted analysis represents a significant yield factor of the cultivated crop. It is therefore useful to perform an analysis of post-harvest residues (straw) to determine total contents of C and N in order to be able to adapt the dose of applied N. The goal of N nutrition and its management consists in providing an optimal amount of N for crops in dependence on their physiological stage and actual need. Mobility of nitrogen within the soil profile makes its management and use one of the most complex agrotechnical measures both in the conventional and mixed cropping systems.

CONCLUSION

Based on the results of field experiments with growing maize in the mixed culture with bean we can state that although the intercropped maize had the yield of grain nearly by 10 % higher than maize grown in the monoculture, the difference was non-significant. On the other hand, a negative influence on yield of growing maize in the system of mixed culture was not demonstrated. Compared with the C:N ratio in the post-harvest of maize grown as pure culture (39:1), another benefit of mixed culture was a significant decrease of C:N ratio in the biomass of post-harvest residues from the mixed culture to 30:1 which is a value considered optimal for their decomposition. Bean in the post-harvest residues from the mixed culture with maize for silage production had a demonstrable influence on the content of nitrogenous substances increased by 70 kg/ha (54 %) as compared with biomass in the post-harvest residues from the maize monoculture. The use of crops with the capability of biological fixation of N in the cropping systems helps reduce emissions of glasshouse gases, carbon footprint of cereal products, thus enhancing environment sustainability and many other financially incalculable externalities.

ACKNOWLEDGEMENTS

The result was obtained within the framework of institutional support MZE-RO1724.

REFERENCES

[1] Bennetzen J.L., The Future of Maize, In: Bennetzen J.L., Hake S. (eds.) Handbook of Maize, Springer, New York, NY, 2009. ISBN 978-0-387-77862-4. doi:10.1007/978-0-387-77863-1_39

[2] Herrmann A., Biogas Production from Maize: Current State, Challenges and Prospects. 2. Agronomic and Environmental Aspects, BioEnergy Research, vol. 6/issue 1, pp 372–387, 2013. doi:10.1007/s12155-012-9227-x

[3] Wahid R., Feng L., Cong W.-F., Ward A.J., Møller H.B., Eriksen J., Anaerobic mono-digestion of lucerne, grass and forbs – Influence of species and cutting frequency, Biomass and Bioenergy, vol. 109, pp 199-208, 2018. doi:10.1016/j.biombioe.2017.12.029

[4] Ofori F., Stern W.R., Relative sowing time and density of component crops in a maize/cowpea intercrop system, Experimental Agriculture, vol. 23/issue 1, pp 41-52, 1987. doi:10.1017/S0014479700001113

[5] Seran T.H., Brintha I., Review on Maize Based Intercropping, Journal of Agronomy, vol. 9/issue 3, pp 135-145, 2010. doi:10.3923/ja.2010.135.145

[6] Brooker R.W., Bennett A.E., Cong W.-F., Daniell T.J., George T.S., Hallett P.D., Hawes C., Iannetta P.P.M., Jones H.G., Karley A.J., Li L., McKenzie B.M., Pakeman R.J., Paterson E., Schöb C., et al., Improving intercropping: a synthesis of research in agronomy, plant physiology and ecology, New Phytologist, vol. 206/issue 1, pp 107-117, 2014. doi:10.1111/nph.13132

[7] Stern W.R., Nitrogen fixation and transfer in intercrop systems, Field Crops Research, vol. 34/issue 3, pp 335-356, 1993. doi:10.1016/0378-4290(93)90121-3

[8] Geijersstam L.A., Mårtensson A., Nitrogen fixation and residual effects of field pea intercropped with oats, Acta Agriculturae Scandinavica, Section B — Soil & Plant Science, vol. 56/issue 3, pp 186-196, 2007. doi:10.1080/09064710510031222

[9] Van Kessel C., Hartley C., Agricultural management of grain legumes: has it led to an increase in nitrogen fixation?, Field Crops Research, vol. 65/issue 2-3, pp 165-181, 2000. doi:10.1016/S0378-4290(99)00085-4

[10] Song Y.N., Zhang F.S., Marschner P., Fan F.L., Gao H.M., Bao X.G., Sun J.H., Li L., Effect of intercropping on crop yield and chemical and microbiological properties in rhizosphere of wheat (Triticum aestivum L.), maize (Zea mays L.), and faba bean (Vicia faba L.), Biology and Fertility of Soils, vol. 43/issue 5, pp 565–574, 2007. doi:10.1007/s00374-006-0139-9

[11] Cong W.-F., van Ruijven J., Mommer L., De Deyn G. B., Berendse F., Hoffland E., Plant species richness promotes soil carbon and nitrogen stocks in grasslands without legumes, Journal of Ecology, vol. 102/issue 5, pp 1163-1170, 2014. doi:10.1111/1365-2745.12280

[12] Hauggaard-Nielsen H., Ambus P., Jensen S., The comparison of nitrogen use and leaching in sole cropped versus intercropped pea and barely, Nutrient Cycling in Agroecosystems, vol. 65/issue 3, pp 289-300, 2003. doi:10.1023/A:1022612528161

[13] Kintl A., Smeringai J., Sobotková J., Huňady I., Brtnický M., Hammerschmiedt T., Elbl J., Mixed cropping system of maize and bean as a local source of N-substances for the nutrition of farm animals, European Journal of Agronomy, vol. 154, 127059, 2024. doi:10.1016/j.eja.2023.127059

[14] Ladha J.K., Peoples M.B., Reddy P.M., Biswas J.C., Bennett A., Jat M.L., Krupnik T.J., Biological nitrogen fixation and prospects for ecological intensification in cereal-based cropping systems, Field Crops Research, vol. 283, 2022, 108541. doi:10.1016/j.fcr.2022.108541

[15] Procházková E., Kincl D., Kabelka D., Vopravil J., Nerušil P., Menšík L., Barták V., The impact of the conservation tillage “maize into grass cover” on reducing the soil loss due to erosion, Soil and Water Research, vol. 15/issue 3, pp 158-165, 2020. doi:10.17221/25/2019-SWR

SEASONAL DYNAMICS IN THE MICROBIOLOGICAL STATUS OF FOREST SOILS FROM THE TERRITORY OF VITOSHA NATURE PARK

Assist. Prof. Dr. Bilyana Grigorova-Pesheva[1]
Assoc. Prof. Dr. Boyka Malcheva[2]
Assoc. Prof. Dr. Biser Hristov[3]
[1,2,3]University of Forestry, Faculty of Forestry, Department of Soil science, Sofia, **Bulgaria**

ABSTRACT

The health, richness, and variety of microbial life in soil represent basic indicators for the evaluation and surveillance of forest ecosystem vitality. The vital role these microorganisms occupy in forest ecosystems underscores the necessity to in-depth assess and monitor their populations within soil habitats. Aiming to deepen our comprehension of microbial communities across different soils and soils horizons, we conducted an investigation of 22 soil profiles situated within the territory of Vitosha Nature Park. The investigation was carried out in one year period. We took samples from each of the studied soils during each of the seasons - spring, summer, autumn and winter. The following soil parameters were evaluated - pH, total nitrogen and humus for each soil horizon. From the microbiological indicators, the amounts of the main microbiological groups (non-spore-forming bacteria, bacilli, microscopic fungi and actinomycetes) were analyzed. Based on these data, the biogenicity of the soil was determined, as well as the percentage participation of individual groups compared to the total microbial number. Two clear peaks in the biogenicity of the studied soils were found - in spring and autumn. The dynamics of microorganisms in relation to change in altitude was reported. There is a correlation between the pH of the medium and the amount of microscopic fungi. Soils under broad-leaved vegetation stand out with higher biogenicity than soils under coniferous vegetation, in all seasons except winter.

Keywords: microorganisms, soil forest microflora, seasonal dynamics, soil biogenicity

INTRODUCTION

Forests cover a huge percentage of terrestrial ecosystems. Globally, forests are highly productive ecosystems that play a key role as a natural reservoir of carbon dioxide [1]. The functioning of forest ecosystems is impossible without the active participation of soil microorganisms. Microorganisms inhabit specific forest habitats such as fresh leaves, forest litter, dead wood, rocks, bark of living trees, etc. However, their diversity and quantity are greatest in forest soils [1]. As [2] points out Forest soil microorganisms are an indicator of the processes taking place in forest soils. According to this soil microorganisms take an active part in the transformation of organic matter and the ongoing biochemical processes in the soil [3]. The activity of soil microorganisms is of key importance for the biochemical cycles [4]. The composition of microbial communities in forest soils is influenced by factors such as nutrient availability and biotic interactions. Yu et al [5], also indicate that the activity of soil microorganisms is directly related to a number of environmental factors - amount of

humus, total nitrogen content, pH of the environment. There are studies that illustrate the changes in microbial communities occurring during different seasons [6]. When analyzing altitude as an environmental factor, López-Mondéjar et al [7] discovered certain changes occurring in the abundance of soil microorganisms. In Bulgaria, the main studies of soil microflora are focused on monitoring and analyzing the behavior of microorganisms in agricultural soils. The question of the biogenicity of forest soils and the influence of seasons change on forest soil microbial communities has been relatively poorly studied.

The main goal of the present study is to make a basic analysis of the main microbiological characteristics of soils from the territory of the Vitosha National Park in annual dynamics and to evaluate the interrelationships between seasons and the biogenicity of the studied forest soils.

MATERIALS AND METHODS

The object of the present study are soils from the territory of the Vitosha Natural Park. In order to achieve in deep analysis of the results, 22 soil profiles were examined. For the purpose of the study, 18 soil profiles were set in the spring of 2021, two more soil profiles were added in the summer and two more in the winter. The accumulation is due to the specificity of the permits for entry and scientific activity on the territory of the Park. Specific soil characteristics related to microbial communities were analyzed. For determination of humus (%) content the Turin method was used. Total nitrogen content was measured by the modified Kjeldahl method and ISO 10390 was used for $pH_{(H_2O)}$. For the purposes of microbiological analyses, soil material was collected on an annual basis. Microbiological analyzes include determination of the main microbiological groups. The Koch method was used to calculate the amount of the studied groups, including successive dilutions of the studied soil sample and subsequent inoculation of suitable nutrient media and cultivation. The results were calculated in colony forming units per gram of absolutely dry soil (CFU/g dry soil). To count the amounts of spore-forming bacteria, the samples were pasteurized. Inoculation is on mesopeptone agar (MPA). Cultivation for 48 hours at 28 °C. For determination of non-spore-forming bacteria we used mesopeptone agar (MPA) culture. Cultivation was made in 28 °C, for 48 h. For determination of actinomycetes, selective agar medium was used. Cultivation was carried out at 28 °C for 10 days. For determination of micromycetes Capek Dox agar medium was used. Cultivation was carried out at 25 °C for 7 days. Based on the obtained results, the total microbial number (biogenicity) of each of the studied soil samples was determined. The data were processed statistically. The StatSoft Statistics 12 program was used with set significance thresholds of 95%.

RESULTS

The results for the studied soil parameters are shown in Figure 1. Soils from soil profile 1,3,4,5,6,7,9,10,2,13,14,15,16,17,18 and 20 are defined as Cambisols. Soils from soil profiles 2, 8, 11 and 21 are Regosols according FAO. The soils of Profiles 19 and 22 are defined as Rendzinas. The soils of Profiles 1, 4, 8, 12, 13 and 18 are under coniferous vegetation of white pine (*Pinus sylvestris*). The remaining soil profiles are under broad-leaved plantations with a predominant species of European beech (Fagus sylvatica).

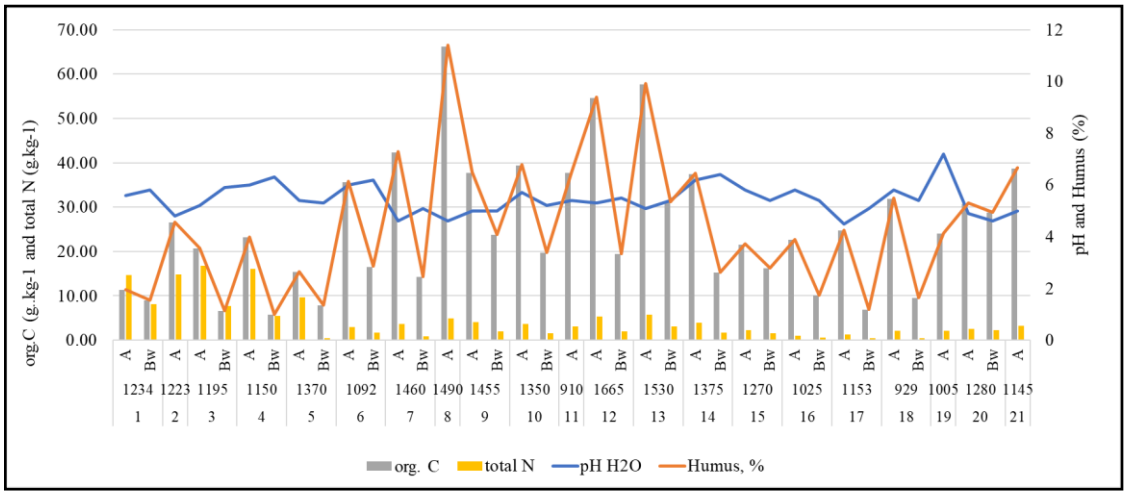


Figure 1. Studied soil parameters

In the A horizon of the studied profiles, the active soil acidity (pH_{H2O}) varies in the interval from 4.5 to 7.5. Soils with an acidic reaction prevail. The reaction in the A horizon of profiles 2, 7, 8 and 17 is very acidic. According to this we considered that free organic acids are present in these soils. Highly acidic is the soil reaction in profiles 3, 9, 13, 20 and 21. An increased intensity of destructive changes is present in these soils. The soil of the A horizon of profiles 1,4,5,6, 10, 12, 15, 16 and 18 is moderately acidic. The soils of sample plot (SP) 19 and 2 have a neutral reaction. For the investigated soils from the territory of the "Vitosha" Nature Park, an increase in the pH values in depth is established for profiles with numbers 1, 2, 3, 4, 6, 7, 8, 11, 12, 13, 14, 17, 19, 21 and 22. In the humus-accumulative horizon, the content of org. C is in the range from 11.31 $g.kg^{-1}$ (profile 1) to 66.18 $g.kg^{-1}$ (profile 13). It is rated as low to high, with high values formed at higher altitudes. This is explained by biogenic accumulation of less transformed organic matter in colder and wetter conditions. The decrease in the amount of org. C in depth is not characterized by large differences between individual soil profiles. The results for the "B" horizon show an organic carbon content in the range 5.79 $g.kg^{-1}$ (PP4) – 31.06 $g.kg^{-1}$ (PP13). The content of total nitrogen in A x-t of the investigated forest soils varies in a very wide range from 1.005 $g.kg^{-1}$ (profile 16) to 16.726 $g.kg^{-1}$ (profile 3). It is rated as low to very high. In the depth of the soil profiles (for B horizon), the content of total nitrogen naturally decreases. Values vary from very low - 0.37 $g.kg^{-1}$ in profile 17 to very high - 8.06 $g.kg^{-1}$ in profile 1.

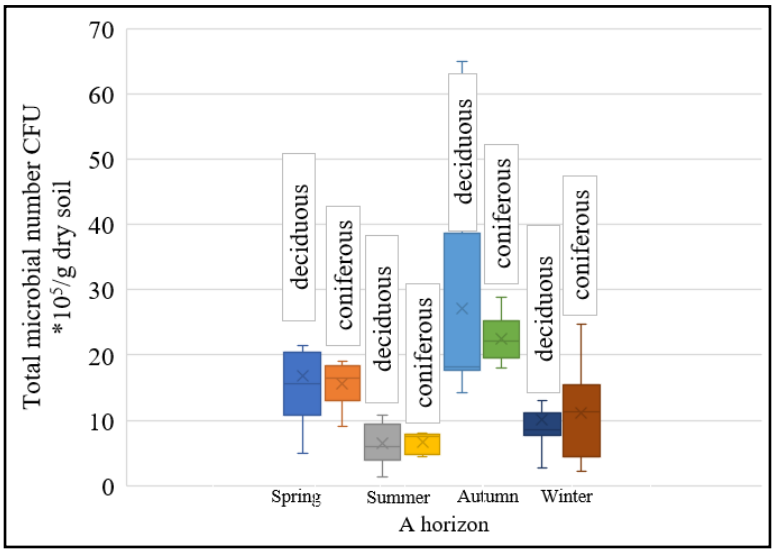


Figure 2. TMN in A horizon according seasons

The data on the reported microbiological indicators are shown in Figures 2 to 7. All the studied soils show two distinct peaks in the development of soil microorganisms - spring and autumn. The autumn season is characterized by the highest microbial abundance. In all studied profiles except PP13, soil biogenicity decreases with depth regardless of the considered season. However, the different seasons reflect a decrease in the amount of microorganisms at depth (Figures 3 – 4). During the peak season for the development of microbial biota (autumn), the average decrease in microbial abundance at depth was fivefold, while in spring it was sevenfold, in summer eightfold, and in winter sixfold. The data show greater microbial abundance under broadleaf vegetation compared to coniferous vegetation for spring, summer, and fall. The generated results for the studied soils during the winter season show a higher microbial abundance under coniferous vegetation (Fig. 2).

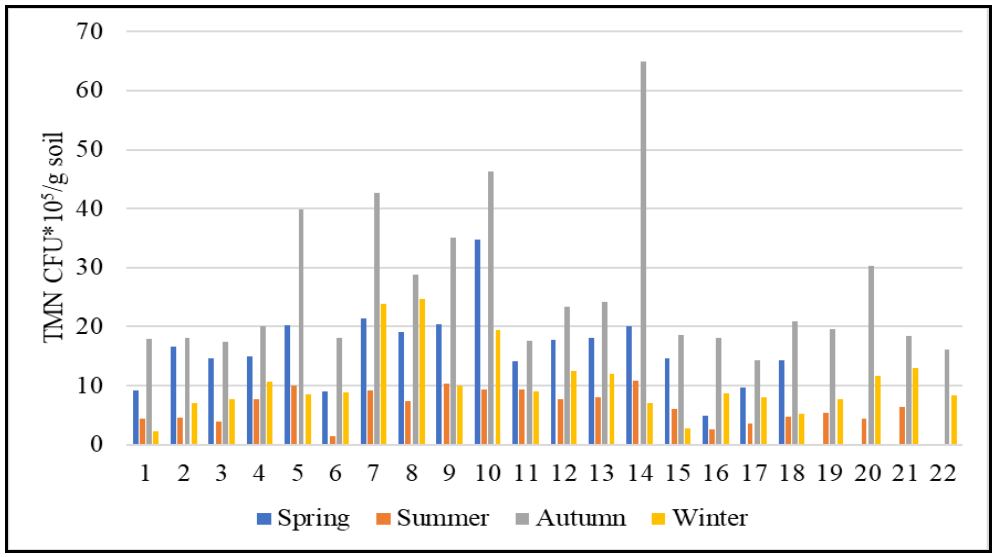


Figure 3. TMN in A horizon in annual dynamics

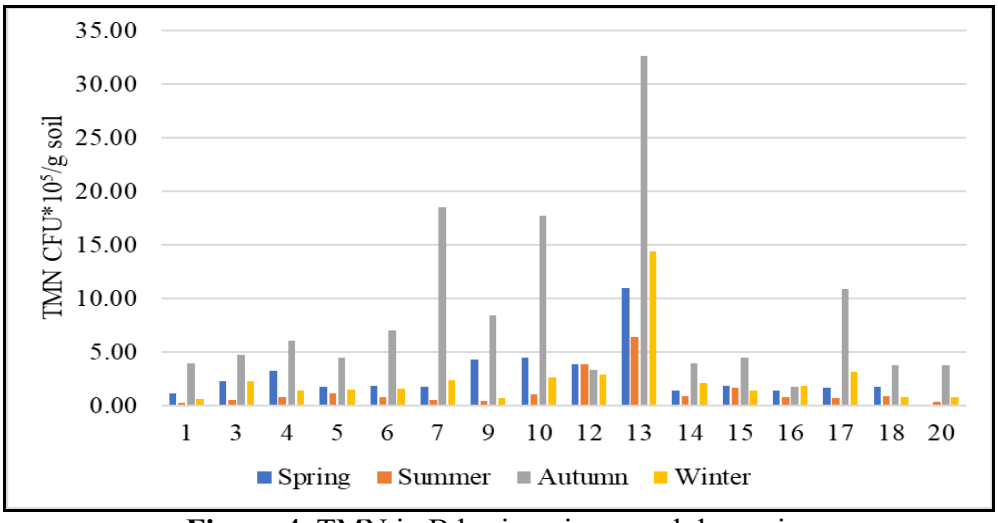


Figure 4. TMN in B horizon in annual dynamics

Figures 5 to 8 present data of the individual microbiological groups by seasons

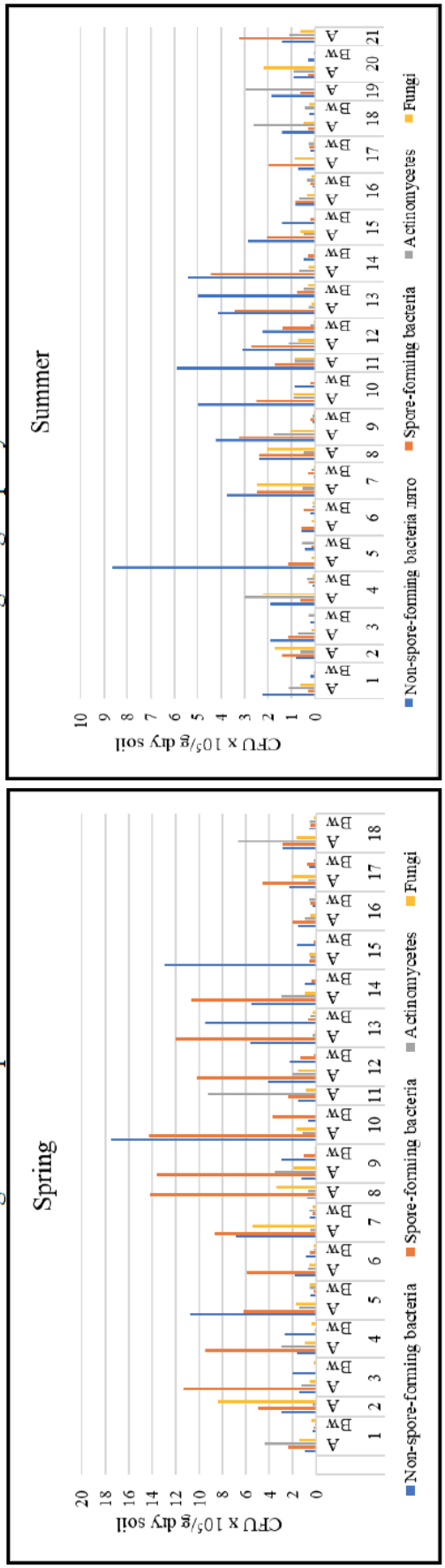


Figure 5. Individual microbiological groups in Spring

Figure 6. Individual microbiological groups in Summer

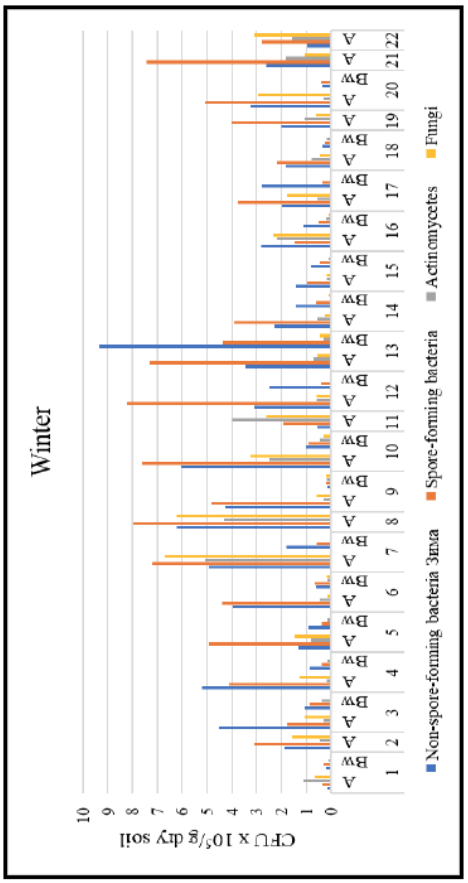


Figure 8. Individual microbiological groups in Winter

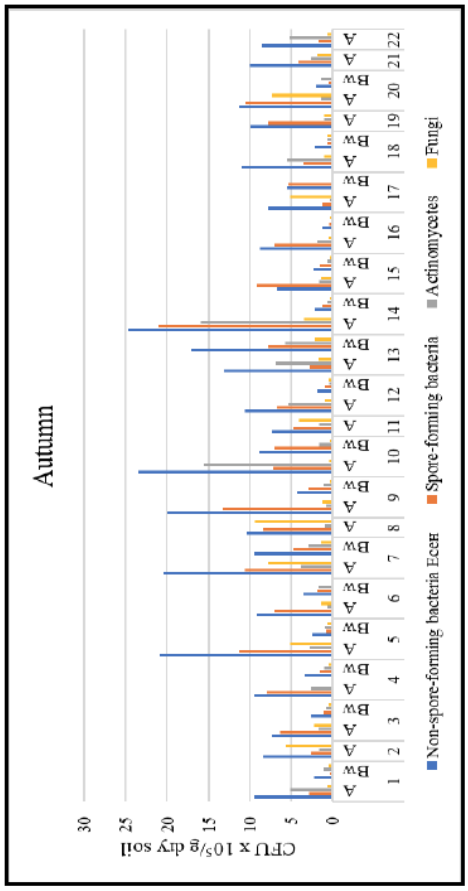


Figure 7. Individual microbiological groups in Autumn

https://doi.org/10.5593/sgem2024/3.1/s13.35

DISCUSSION

Soils under vegetation with a predominant broad-leaved component are characterized by a greater abundance of A horizon in spring, summer and autumn (Figure 2). During the winter season, the amount of microorganisms in the A horizon of the studied soils is greater under coniferous vegetation. These data point out that the specificity of the covering vegetation during the cold months when snow cover accumulates. Data so far show better temperature parameters for soil microorganisms under coniferous vegetation in winter. This is related to the accumulation of dead forest litter, which decomposes more slowly and provides better heat retention.

In all studied soils, two peaks in the development of the microbial community of the A horizon are observed - in spring and in autumn (Figure 3), confirming the conclusions reached by [8]. In the summer, the development of soil microorganisms has a low index, and the reported values are lower compared to the winter season. These data are related to the difficult adaptation of the microbial community to an increase in temperature and a decrease in soil moisture. In winter, the data indicate a significantly higher microbial abundance of the studied soils in the humus-accumulative soil horizon compared to the summer season. This is due to the increased humidity and the lack of sharp temperature fluctuations due to the presence of snow cover. Although the temperatures are low in the winter season, the humidity is increased compared to the summer season. The obtained data prove that the presence of moisture is one of the main factors for the development of soil microorganisms. Even if the soil temperature is within optimal limits, in the absence of water we have a depression in the microbial number in the upper soil horizons.

In the lower-lying B horizon, two distinct peaks in microbial development are again observed - spring and autumn. In contrast to the A horizon, here the results obtained for the total microbial number in summer and winter are roughly similar (Figure 4). As with some of the studied sample areas, we have lower values of the microbial abundance in the winter compared to the summer season (PP12, PP15 and PP18). These data indicate a worsening of the conditions for the development of soil microorganisms during the winter season in this horizon.

Increased involvement of microscopic fungi was observed in soils with lower pH levels. Similar to the data obtained by [9], the percentage share of fungi is greatest at the pH of the A horizon in the range 4.5 – 4.8. When analyzing the influence of altitude on soil microbial abundance, several main trends are observed. The maximum peak of microbial abundance varies with the season. For the spring season, the biogenicity of the studied soils is above the reported average for the season (16.33 CFU/g dry soil) at an altitude above 1300 meters. During the spring season, a higher microbial abundance is observed in the A horizon at a higher altitude than in the soils located in the lower mountain belt. This is due to the higher illumination and faster warming of the soil in the upper less dense vegetation areas. In summer, soil biogenicity in the A horizon is highest in the range 1300-1500 meters, after which a decrease in microbial abundance is observed. This is probably due to increased solar heating in the higher parts of the mountain, higher temperatures and reduced soil moisture. In autumn, again the highest values were recorded in the range of 1300-1500 meters. Again, below and above this altitude, microbial abundance declines. In the winter season, there is no clear trend, due to the different retention of the snow cover. These data show the dynamics in microbial communities and their response to environmental factors. There are no clear trends for the underlying soil horizon.

For additional information, a correlation between the microbial abundance of the studied soils and the organic carbon content was sought. After the analysis, no correlation was found between the microbial abundance of the A horizon and the organic carbon content for spring, summer and autumn (r=0.40, r= 0.35, r= 0.26). When analyzing the data for the winter season, however, we have a correlation coefficient between the two investigated parameters with a value of r=0.70. This shows that during the winter season the microbial abundance and microbial activity of the A horizon are more dependent on the available organic matter in the soil, compared to the other seasons. When analyzing the results for the B horizon as opposed to the A horizon, the greatest statistical correlation between the two studied parameters was observed in the spring season (r=0.77). This shows the different environmental conditions and the different requirements of the soil microorganisms in the individual soil horizons. During the spring season, due to plant vegetation and increased root exudate, the more exponential reproduction of soil microorganisms in the B horizon predetermines their dependence on a food base.

When analyzing the results, the group of bacilli is dominant in spring in the A horizon, while in summer and autumn, the group of non-spore-forming bacteria is dominant (Figure 5-8). There are no clearly expressed trends for B horizon. The large percentage participation of the group of bacilli in the A horizon in the spring season is associated with prevailing processes of advanced transformation of soil organic matter and presence of more stable forms of organic compounds. During the spring season, there is a destruction of the residual organic matter that was not transformed during last year's fall and winter. The dominant presence of non-spore-forming bacteria in summer and autumn in the A horizon indicates enhanced transformation processes of easily degradable organic matter. There is no clear trend for the winter season.

CONCLUSION

The present study aimed to analyze basic microbiological parameters of the studied forest soils in seasonal dynamics. The biogenicity of the studied soils decreases with depth of the soil profile. The generated results show two distinct peaks in the development of the soil microbial community - spring and autumn. The highest biogenicity is observed in autumn. Compared to the two seasons with lower reported amounts of soil microflora (summer and winter), summer emerges as the season with the worst conditions for the development of forest soil microorganisms and accordingly, has the lowest biogenicity. An analysis of the data revealed an increased participation of the group of microscopic fungi in soils with a pH in the range of 4.5-4.8. There are no clearly established correlational dependencies between the content of org. C and biogenicity of the A horizon in relation to seasonal dynamics. Only in winter there is an increased correlation dependence between the two parameters (r=0.70). The data for the B horizon show significant correlation values with respect to the organic carbon content and the total microbial number for the spring season (r=0.77). During the spring season, a higher microbial abundance is observed in the A horizon at a higher altitude than in the soils located in the lower mountain belt. In summer, the biogenicity of the soil in the A horizon is highest in the range 1300-1500 meters. In autumn, again the highest values were recorded in the range of 1300-1500 meters above sea level. Again, below and above this altitude, microbial abundance declines. There is no clear trend during the winter season. The group of bacilli predominates in the spring season, while the group of non-spore-forming bacteria predominates in summer and autumn. There are no clear

trends for the winter season. The findings from the research could establish a basic framework for future analyzes of the seasonal changes of soil microorganisms within the soil's layers. Given their high sensitivity and integral role in forest ecosystems, microorganisms offer valuable insights of the process occurring in them.

ACKNOWLEDGEMENTS

The current study was performed in the framework of Project– КП-06-Н56/7" funded by Research Fund of Ministry of Education and Science in Bulgaria.

REFERENCES

[1] Baldrian, P. Forest microbiome: diversity, complexity and dynamics. FEMS Microbiology Reviews, fuw040, 41, 2017, pp 109–130, doi: 10.1093/femsre/fuw040.
[2] Baćmaga, M., Wyszkowska, J., Borowik, A., Kucharski, J., Paprocki, L. Role of forest site type in determining bacterial and biochemical properties of soil, Ecological Indicators, 135 ,2022 ,108557, DOI: https://doi.org/10.1016/j.ecolind.2022.108557.
[3] Urbański, K. & Jakubiak, M. Impact of land use on soils microbial activity. J. Water Land Dev., 35 (10–12), 2017
[4] Aislabie J. & Deslippe J, Soil microbes and their contribution to soil services, In: Dymond John R, editor, Ecosystem services in New Zealand: Conditions and trends. Manaaki Whenua Press, Lincoln, 2013, pp 143–16.
[5] Yu, Z., Liang, K., Huang, G., Wang, X., Lin, M., Chen, Y., Zhou, Z., Soil Bacterial Community Shifts Are Driven by Soil Nutrient Availability along a Teak Plantation Chronosequence in Tropical Forests in China, Biology (Basel). 15;10(12):1329, 2021. doi: 10.3390/biology10121329.
[6] Yang, S., Tsai, S., Fan, H., Yang, C., Hung, W. & Cho, S., Seasonal variation of microbial ecology in hemloch soil of Tatachia Mountain, Journal of Microbiology, Immunology and Infection, 39(3), 2006, pp 195-205. 2006
[7] López-Mondéjar, R., Voříšková, J., Větrovský, T., & Baldrian, P, The bacterial community inhabiting temperate deciduous forests is vertically stratified and undergoes seasonal dynamics,Soil Biology and Biochemistry,Volume 87, 2015, pp 43-50, ISSN 0038-0717,https://doi.org/10.1016/j.soilbio.2015.04.008.
[8] Díaz-Raviña, M., Acea, J. & Carballas, T., Seasonal fluctuations in microbial populations and available nutrients in forest soils. Biology and Fertility of Soils, 16 (3), 1993, 205-210.
[8] Bååth, E., Brookes, P. C., Rousk, J. Contrasting Soil pH Effects on Fungal and Bacterial Growth Suggest Functional Redundancy in Carbon Mineralization. National Center for Biotechnology Information, 75(6), 2009, 1589-1596, DOI: 10.1128/AEM.02775-08. https://www.ncbi.nlm.nih.gov/pmc/articles/PMC2655475/

SELECTION OF CASE STUDY AREAS OF THE MOST BASIN FOR SOLVING RECLAMATION ISSUES OF EUROPEAN PROJECT REECOL

RNDr. Michal Řehoř, Ph.D.[1]
Eng. Pavel Schmidt[1]
Eng. Radka Dužeková[1]
Assoc. prof. František Helebrant[2]

[1]Brown Coal Research Institute j. s. c., Most, **Czech Republic**
[3]VSB – Technical University Ostrava, Ostrava, **Czech Republic**

ABSTRACT

Brown Coal Research Institute j. v. c. (VÚHU) from July 2023, together with scientific teams from several European countries, participates as part of the EU research program in the solution of the REECOL project, which deals with the reclamation of areas affected by mining in European coal basins. One of the important tasks of the first phase of the project solution is to find suitable case study areas in each country of the project solution. The selection of these areas in the Most Basin (CZ) is the subject of this paper. The selection of case study areas was based on the results of long-term research in the Most Basin. Areas with the occurrence of all main soil types, a long reclamation history and the application of various reclamation methods, including successional areas, were selected. The main part of the paper contains the characteristics and localization of the proposed case areas. The first of them is the Radovesice spoil heap with four experimental areas, two of which are left to natural succession and two are reclaimed using marls. The second area is the Střimice spoil heap with two experimental areas, one is left to natural succession and the other is reclaimed using bentonite. The paper describes the current situation of the areas, their reclamation history and long-term pedological development.

Keywords: soil, reclamation, case study areas

1 INTRODUCTION

Brown Coal Research Institute j. s. c. (VÚHU) participates for the first year in the solution of the European project of the Research Fund for Coal and Steel (RFCS) "Ecological rehabilitation and long - term monitoring of post mining areas" (acronym REECOL).

The first research package of the project is WP 3 "Identification of post-mining areas and approaches to ecosystem restoration", which deals with the characterization of different approaches to the reclamation of post-mining areas used in the countries of individual project partners. Currently, the research work of VÚHU focused on the first addressed task of WP 3, which is task T 3.4 "Selection of post-mining reclamation case study areas". The output of the T3.4 is this partial research report.

The paper deals with the research methodology, criteria and justification for the selection of case areas and a brief description of the selected areas, which is the main part of the paper.

2 MATERIALS AND METHODOLOGY

2.1 RESEARCH METHODOLOGY

When choosing a suitable case area in the Most Basin and its surroundings, the history of reclamation research, the geological and pedological diversity of the reclaimed soils and the planned reclamation use of the area were considered. The application of various reclamation methods, including natural succession [2], the occurrence of areas not yet reclaimed, and the presence of long-term monitored experimental areas were important [1].

The first stage of the research was the collection of available data from historical pedological surveys and research. It was primarily VÚHU's own data, as well as available data from stakeholders (mining organizations, regional universities, cooperating organizations dealing with pedological surveys of the region, etc.). The collection of archival materials was supplemented by our own research, during which the following laboratory analyses were used.

The selection of laboratory tests and analyses of their results was determined in the range of proven methodologies used in the Most Basin for a long time in reclamation activities [4]. For each sample, granularity determination, evaluation of mineralogical composition on Siemens X-ray diffractometer, determination of soil reaction, determination of CaCO3 content were carried out, determination of the content and quality of oxidizable carbon and humus, determination of nitrogen content, determination of sorption capacity and determination of the content of acceptable nutrients according to Melich III.

All performed laboratory analyses were carried out by testing laboratories VÚHU and VÚMOP v.v.i. accredited by ČIA according to ČSN EN 150/IEC 17025 based on internal methodological procedures based on the relevant standards [6].

3 RESULTS

3.1 PROPOSAL OF THE OPTIMAL CASE STUDY AREA IN THE MOST BASIN

After applying the research methodology described in chapter 2.1, the Radovesice - Střimice spoil heaps complex was selected as the main case study area. From the point of view of geology and pedology, most of the soil types of the Most Basin are represented here, reclamation additives were significantly used here, and the most important areas left to natural succession are located here. 6 long-term monitored experimental areas were established on these spoil heaps. On the Radovesice spoil heap there are 4 areas (2 reclaimed, 2 left to natural succession) and on the Střimice spoil heap there are 2 areas (1 reclaimed, 1 left to natural succession).

3.1.1 BRIEF DESCRIPTION OF THE RADOVESICE SPOIL HEAP

The Radovesice spoil heap has an elongated shape from the southeast to the northwest, and its territory belongs to the highlands of the České Středohoří Mts. itself. It is the most extensive spoil heap in the Moste Basin. Due to its scope, importance and the extremely unfavourable character of loose soils, local marlstones were used as a reclamation additive. These form the geological surface of the erosion valley in the bedrock of the landfill. The recultivation properties of marls are worse than in the case of bentonites, the application methodology was also based on research by VÚHU gradually adjusted, but overall, the event was successful. The characteristics of the created seasoning horizon are still used today by VÚHU monitored. 4 long-term monitored experimental areas were established on this spoil heap. The pedological parameters of the soils of the selected areas are shown in Tables No. 1 - 3.

Experimental area Radovesice XVIIA

The experimental succession area of Radovesice XVIIA with an area of approx. 20 ha was selected in the northern part of the landfill. The predominant soil type here is a heterogeneous dump mixture of brown clay, gray clay loam and gray sandy loam with an increased content of brown clay. Brown - gray kaolinitic - illitic clays also appear. The southern border of the area is the area of "sand dunes". There are also two large natural water reservoirs and several small bodies of water and wetlands in the area. Some small bodies of water turn into wetlands over the course of the year. The surface is approximately 32 years old. At present, it is already a fragmented, aesthetic area with several spontaneously formed, permanent bodies of water (see Figure No. 1).

Table No 1: Pedological parameters of soil profile - Radovesice XVIIA

Sampling interval (m)	Nc (%)	Cox (%)	$CaCO_3$ (%)	pH KCl	Acceptable nutrients ($mg.kg^{-1}$)			Sorption capacity		
					P	K	Mg	S	T	V (%)
								mmol/100 g		
2004										
0,00-0,60	0,05	2,1	0,4	6,8	2	184	724	15	15	100
2010										
0,00-0,60	0,08	2,5	0,5	6,8	3	330	860	17	17	100
2015										
0,00-0,60	0,06	2,4	0,6	6,9	3	325	844	16	16	100
2021										
0,00-0,60	0,11	2,8	0,6	6,8	8	361	880	17	17	100

Experimental area Radovesice XVIIB

The succession area of Radovesice XVIIB with an area of 32 ha was selected in the southern part of the landfill. The soil composition of the upper horizon is like to that of area XVIIA. In the eastern part of the area, sandy soils are more prominently represented, which form the natural boundary of the area. There are several of natural water bodies and smaller wetlands. The surface is approximately 22 years old. At present, it is also a fragmented, aesthetic area with numerous spontaneously formed, permanent bodies of water.

https://doi.org/10.5593/sgem2024/3.1/s13.36

Experimental area Radovesice I

The experimental recultivated area of Radovesice I, with an area of approximately 30 ha, was based on one of the first areas recultivated with the use of marls. This area was established in 1991 and is thus the oldest monitored experimental area in the Most Basin. The original landfill soil consisted of sandy clays and sands. This is the area where the original, unmodified method of applying saliva and slag was applied.

Experimental area Radovesice VI

The experimental recultivated area of Radovesice VI with an area of approx. 44 ha was established in the western part of the Radovesice spoil heap. A modified marls application methodology was already used here. A layer of 0.2 - 0.3 m thick silt was brought to the surface of the terrain and plowed to a depth of up to 0.5 m. The original fill soil consisted of sandy clays and sands. Currently, it is a very aesthetic area with a balanced share of forest reclamation, grass reclamation and hydric reclamation (Syčivka water reservoir – see Figure No 2).

Table No 2: Pedological parameters of soil profile - Radovesice VI

Sampling interval (m)	Nc (%)	Cox (%)	$CaCO_3$ (%)	pH KCl	Acceptable nutrients ($mg.kg^{-1}$)			Sorption capacity		
					P	K	Mg	S	T	V (%)
								mmol/100 g		
2010										
0,00-0,20	0,02	1,9	7,8	7,6	5	212	810	14	14	100
0,20-0,60	-	0,8	6,3	6,5	1	145	652	10	10	100
2015										
0,00-0,20	0,08	2,2	7,3	7,2	6	240	873	17	17	100
0,20-0,60	0,04	1,3	6,2	6,3	3	185	785	14	14	100
2021										
0,00-0,20	0,10	2,3	7,1	7,1	6	235	875	17	17	100
0,20-0,60	0,06	1,5	6,2	6,3	3	215	711	15	15	100

Table No 3: Pollutants content in experimental areas soils

Location sampling interval (m)	S %	Coal mass %	pH KCl	Sulfides Fe occurrence
Radovesice XVIIA	0,05	2,2	6,8	NE
Radovesice XVIIB	0,06	2,1	6,9	NE
Radovesice I				
0,00-0,20	0	2,2	6,9	NE
0,20-0,50	0	1,5	7,3	NE
0,50-1,00	0.11	1,8	6,8	NE
Radovesice VI				
0,00-0,20	0	2,1	6,9	NE
0,20-0,60	0,07	1,7	6,1	NE



Figure No 1: Succession area Radovesice XVIIA - overall situation



Figure No 2: Newly created reclamation landscape (Radovesice VI, Syčivka reservoir).

https://doi.org/10.5593/sgem2024/3.1/s13.36

3.1.2 BRIEF DESCRIPTION OF THE STRIMICE SPOIL HEAP

The Střimice spoil heap is located east of Most. It was established in the years 1959 – 1973. Due to the extremely phytotoxic properties of the surface zone of the spoil heap, the original forest reclamation practically died out. At the same time, a significant influence of erosion phenomena was manifested. At the suggestion of VUHU, bentonites from the Red Hill quarry were then used for reclamation [3], [5]. Recultivation was started in 1984. The layer of applied bentonite soil was set at 50 cm. After ploughing, weeding was carried out and forest reclamation was carried out later. In 1988, agricultural reclamation was started on the dump plain with a total area of 89 ha. At this reclamation event, VUHU has not yet participated, but has been monitoring for 30 years. 4 long-term monitored experimental areas were established on this spoil heap.

Experimental area Střimice I

The research experimental area Střimice I with an area of 2 ha was enclosed in a small, unreclaimed peripheral part of the Střimice landfill. The estimated age of the area is 45 years, research has been ongoing here since 1998 [3]. The predominant soil type here is a heterogeneous mixture of overburden soils from the coal seam formations of the Bílina open pit mine. Sandy clay loams and sands with a significant admixture of coal and siderite predominate. These are extremely acidic, phytotoxic soils (see Figure No 4). A unique development of erosion grooves with a depth of up to several meters can be observed on the surface. This phenomenon is probably the most prominently developed here in the entire area of the Most Basin. Considering the extremely acidic character of the area, minimal plant representation was found here, but rare acid-loving species may occur.

Experimental area Střimice II

The Střimice II experimental area with an area of 10 ha was defined on the top of the landfill reclaimed with the use of bentonite. The age of the area is approx. 30 years, research has been ongoing here since 1992. Bentonite was used on this area to meliorate the surface of unsuitable, phytotoxic landfill soils and to create a seasoning soil horizon (see Figure No. 3 and Table No 4). Forest reclamation was carried out on the area.

Table No 4: Pedological parameters of soil profile – Střimice II

Sampling interval (m)	Nc (%)	Cox (%)	$CaCO_3$ (%)	pH KCl	Acceptable nutrients ($mg.kg^{-1}$)			Sorption capacity		
					P	K	Mg	S	T	V (%)
								mmol/100 g		
2015										
[1]0,00-0,50	0,07	1,4	1,9	6,9	9	185	200	16	16	100
[2]0,50-0,90	0,07	0,7	9,9	8,2	3	215	939	31	31	100
[3]pod 0,90	0,05	2,9	0,2	4,5	1	101	299	4	8	50
2023										
[1]0,00-0,50	0,05	1,5	1,0	6,8	8	240	215	15	15	100
[2]0,50-0,90	0,04	1,0	8,6	7,8	3	260	986	32	32	100
[3]pod 0,90	0,01	2,4	0,5	4,8	1	100	190	3	8	39



Figure No 3: Soil profile with bentonite – Střimice II



Figure No 4: Succession area Střimice I

https://doi.org/10.5593/sgem2024/3.1/s13.36

4 CONCLUSIONS

This paper summarizes the current results of VÚHU in solving WP3 (Task 3.4). The research was devoted to the selection and brief characteristics of case study area in the Most Basin.

The paper describes the methodology for selecting the case study area. The history of reclamation research, the geological and pedological diversity of the reclaimed soils and the planned reclamation use of the area were considered. The application of various reclamation methods, including natural succession, the occurrence of areas not yet reclaimed, and the presence of long-term monitored experimental areas were important. Part of the methodology was the selection of the optimal set of pedological analyses.

The main part of the paper contains the characteristics of the selected case area, which is the Radovesice - Střimice spoil heaps complex. The Radovesice spoil heap represents a newer spoil heap, the main soil is sand and clay. The application of marls was used during the recultivation, part of the spoil heap was left to natural succession, and there are four experimental areas. Střimice spoil heap represents an old spoil heap, the main soil is phytotoxic coal clays and sands. Bentonite application was used during the recultivation, part of the spoil heap was not recultivated. Four test areas are located here.

ACKNOWLEDGEMENT

The article was published with the support and co-financing of the EU research program "Ecological rehabilitation and long-term monitoring of post mining areas", project no. 101112657 - REECOL - RFCS-2022.

REFERENCES

[1] HENDRYCHOVÁ M.: Reclamation success in post mining landscapes in the Czech Republic: a review of pedological and biological studies. Journal of Landscape Studies 1:63-78, 2008

[2] HODAČOVÁ D. et PRACH K., 2003: Spoil heaps from brown coal mining: technical reclamation versus spontaneous revegetation. Restoration Ecology 11: 385 – 391, 2003

[3] CHOCHOLOUŠKOVÁ S.: Development of soil quality at selected recultivated sites of the Střimice spoil heap. Bachelor thesis, Czech University of Life Sciences, Prague 2012

[4] PRACH K., PYŠEK P. et BASTL M., 2008: Spontaneous vegetation succession in human-disturbed habitats: a pattern across seres. Appl. Veg. Sci. 4 (2001) 83–88.

[5] HENDRYCHOVÁ M., ŘEHOŘ M. et ŠÁLEK M.: The methodology of the Střimice dump. SGEM Proceedings, p. 205-212, ISBN 10:954-91818-1-2, Albena, Bulgaria, 2010.

[6] Testing Laboratory No 1078: Internal methodological regulations of testing laboratory VÚHU, Testing laboratory No 1078 management, Most, 2022

SOIL PROTECTION AGAINST SOIL EROSION BY USING ANTI-EROSION METHODS IN THE HILL AREA OF BUZAU, ROMANIA

Assoc. Prof. Dr. Radu Alexandra Teodora[1]

Lecturer Ph. D. Burcea Mariana [1]

[1] University of Agricultural Sciences and Veterinary Medicine of Bucharest, **Romania**

ABSTRACT

The paper presents the results of research undertaken in 2023, in the perimeter of the Stationary for the Study of Soil Erosion located on the left side of the Slanic Hydrographic Basin in Buzau county, with a slope of 15-20 %.

Within the station are located 12 plots for the control of soil surface erosion cultivated differently. The amount of soil washed away by torrential rains during the growing season was different depending on the degree of soil cover given by agricultural crops [11]. From the plot cultivated conventionally with winter wheat it was observed that 3.8 t/ha of soil is washed, and on the soil cultivated with wheat sown in strips the amount of washed soil is 0 t/ha, compared to the uncultivated soil where the amount of soil washed is 41.9 t/ha. In conclusion, the role of agricultural crops and anti-erosion techniques, such as strip sowing is very important, thus the strip-sown wheat protected the soil better against erosion compared to conventional wheat, where the amount of washed soil increases by 9%.

Keywords: surface erosion, strip crops, wheat, uncultivated soil, hydrographic basin

INTRODUCTION

Erosion is a process of displacement of the surface layers of the soil located on the slope, under the influence of natural factors such as water from precipitation, its degree of torrentiality, the intensity and the amount falling in the unit of time [24]. This phenomenon can have significant negative consequences, such as loss of soil fertility, degradation of agricultural land with impact on natural or anthropogenic ecosystems [2], [18], [10], but also significant economic costs for society [19].

The capacity of agricultural ecosystems to function at normal parameters is directly related to the state of the soils and their functions. Thus, soil protection against erosion is mandatory for sustaining the capacity of agroecosystems, because soil sustainability is affected in cases where soil erosion rates are higher than soil formation rates. [23], [16]. Erosion causes the loss of nutrients, the decrease in the water retention capacity of the soil, the decrease in the thickness of the soil layer useful for plant growth and the reduction of soil fertility and biodiversity [8], [4].

Controlling and preventing soil erosion is important for the conservation of natural resources [17], [28]. Agricultural crops play an essential role in the prevention of erosion through the degree of coverage given to the soil, which reduces the impact of

raindrops and fixes the upper layers of the soil [21]. For example, the experimental data obtained at the Study Station for Soil Erosion, Aldeni-Romania, regarding the runoff water recorded in the fields cultivated with alfalfa, is 10.56 l/m^2 in the plot with a slope of 15 %, compared to the beet grown in strips (1.66 l/m^2) and wheat (1.31 l/m^2), regarding this protection of plants on the ground [20].

Research in China has shown that the rate of soil loss varies between 7.65 – 49.38 t/ha/year on agricultural land under conventional tillage. Land use types with permanent cover had the lowest soil loss rates, which were 0 – 1.89 t/ha/year for forest, 0.28–8.06 t/ha/year when the land was covered with shrubs, and 3.98 – 1.57 t/ha/year, when the land was covered with meadows [15].

There are various effective measures to control and combat soil erosion:

a) Soil conservation works through the implementation of techniques to reduce agricultural works that mobilize the active state of the soil with the reduction of surface erosion [22].

b) Creating grass strips between agricultural crops that can stop water runoff and prevent erosion [17], [1]. These buffer zones with vegetation can minimize erosion. For example, a 10 m wide buffer strip can reduce the phosphorus load from sediments by up to 95% and increase the diversity of flora and fauna in the immediate landscape [26].

c) Grass strips reduce the loss of sediment and nutrients from the soil. Barriers planted with stiff-stemmed plants reduced sediment losses by 91 %, while grassed strips reduced sediment by only 72%. Barriers provided by plants with rigid stems reduce sediment loss by 90 %, while grass strips reduce sediment by only 60 %. Stiff-stemmed plant barriers captured 4.9 times more organic N, 2.3 times more NH_4–N and 3.7 times more particulate P than grassed strips at 0.7 m [5].

d) Systems of organization and rotation of agricultural crops designed to prevent soil erosion. They are planned to maximize soil coverage and protection in a sustainable way [22], [12].

The study and monitoring of soil erosion processes in a controlled and systematic way is done in experimental fields, designed to collect accurate and detailed data by which different factors, such as rainfall, soil type, topography and agricultural practices influence soil erosion [25], [9].

Experimental fields are essential tools in scientific research for the development and testing of sustainable agricultural practices, as well as for understanding the mechanisms and factors that contribute to the intensification of soil erosion. Thus, medium- and long-term strategies can be developed to protect agricultural ecosystems affected by erosion in the conditions of current climate changes [25], [21].

MATERIAL AND METHOD

The studies and research undertaken in 2023 were carried out within the Stationary for the Study of Soil Erosion with an area of 840 m^2, located in the Valea cu Drum hydrographic basin, which has a total area of 7875 ha on the left slope with an average length of 375 m, in the Aldeni commune in Buzau County, Romania (fig. 1).

The type of soil in the premises of the station is Chernozem subtype argic, very strongly deep, eroded by water, formed on clay shales, medium clay/medium clay loam that

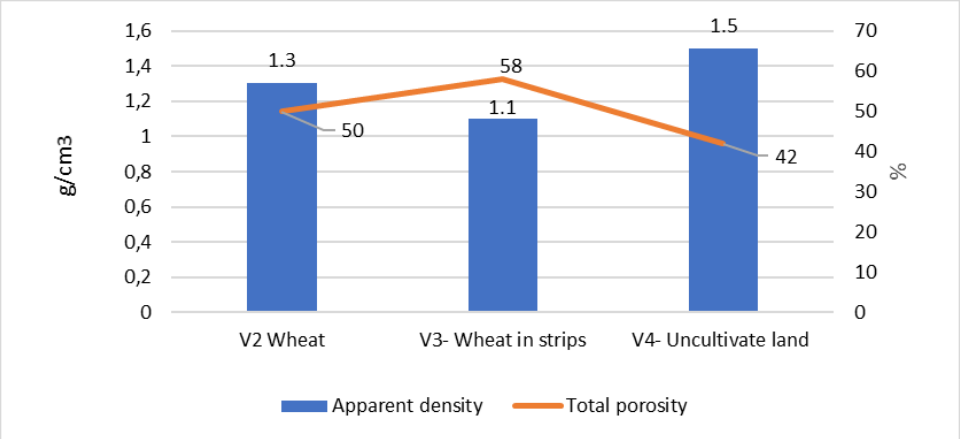
belongs to the class Cernisols, with the profile type ***Am - AB - Bt1 - Bt2 – Cn***, the Cn horizon being without carbonates [20].

Figure 1. **Stationary for the Aldeni Soil Erosion Study in the hilly area of Buzau County, Romania**



The texture of the soil is differentiated on the profile, it being loamy and clay loam, the apparent density is 1.3 g/cm^3 in the autumn wheat crop and 1.1 g/cm^3 in the variant with wheat grown in strips (fig. 2), and the soil reaction it is weakly acidic between 5.55 – 6.61, with a very small reserve of humus between 1.4% and 1.6%.

Figure 2. **The apparent density and total porosity values determined in the three variants, 2023**



Within the station, 12 plots are located for the control of surface runoff and soil erosion, 6 upstream and 6 downstream, as follows:

- the upstream plots are located on land with a 20% slope, each with an area of 100 m^2 (25m long x 4m wide);

- the downstream plots are located on land with a 15% slope, each with an area of 40 m^2 (10m long x 4m wide). These plots are included in long-term crop rotations involving rotation and diversification of agricultural crops combined with anti-erosion measures.

The 2023 crop rotation, which included plots on both slope categories, was made up as follows:

- plots V1 were cultivated with beans,

- plots V2 were cultivated with wheat, conventionally;

- on the V3 plots, the cultivation system was practiced with grassy strips of wheat, (the length of the plot was divided into equal strips that were cultivated alternately with wheat and perennial grasses)

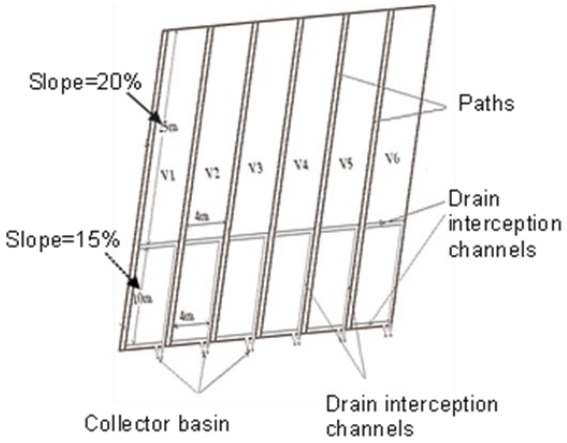
- the V4 plots were kept uncultivated, to highlight how agricultural crops protect the soil against erosion.

- plots V5 were grassed with fodder plants

- plots V6 were cultivated with corn.

Each plot has devices for capturing surface runoff, which make it possible to determine the amount of runoff water (As), as well as the amount of soil washed by torrential rains (Es) (fig.3), [7].

Figure 3. **Plots for erosion control Stationary Aldeni-Buzau, Romania, 2023**



Calculation of soil losses:

Obtaining soil loss data from experimental plots is influenced by factors that affect the variability of natural data and measurement of erosion processes on the plots [3].

The precise estimation of soil losses is made by direct measurements of the amount of washed soil and runoff water during rains [13].

The amount of washed soil (Es) from the control plots in the perimeter of the station was calculated with formula 1;

$$\mathbf{Es = (As^2 \times Mp):100 \quad t/ha \quad (1)}$$ [7]

Es – amount of washed soil (t/ha);

As – the amount of water drained from the control plots (l/m^2);

Mp – mass of drained soil (g);

100 – value for transformation into t/ha.

The amount of drained water (As) was determined by the volumetric method, using the collecting basins in the station premises, and the mass of the drained soil was determined gravimetrically by filtering, drying and weighing.

After each rain that produced runoff, the collected volume was determined by taking 1/2 liter of homogenized runoff, in three repetitions, from each collecting basin. After

decanting the samples, the following were performed: filtration, oven drying and the amount of drained soil was determined by weighing.

The degree of ground cover in the control plots was determined using the metric frame. The weather station within the station, equipped with a rain gauge and pluviograph, made it possible to measure and record precipitation, respectively other climatic events.

With the help of pluviograms, the structural characteristics of the rains that produced runoff and erosion were analyzed.

Of the six experimental variants, three were chosen for comparison (slope 15% and slope 20%), namely: variant V2 - cultivated with winter wheat; variant V3 - cultivated with wheat sown in strips and variant V4 - uncultivated land. Strip crops are techniques for managing agricultural land affected by erosion with the aim of improving the soil's ability to absorb water, reducing the risk of runoff and erosion.

RESULTS AND DISCUSSIONS

The county of Buzau is located in the south-eastern part of Romania, and includes hills and mountains with heights between 400 m and over 800 m, separated by wide valleys often with depression character. In the north, the peaks are higher and well wooded, and towards the south they gradually decrease in altitude, being made up of softer rocks (alternations of clays, sandstones, sands, etc.) which favor the production of landslides on the slopes, in the absence of forest terrain, mudslides, torrents, etc., [14].

The research located at the Soil Erosion Research Station in the Valea cu Drum area is a narrow valley with sills in the bed and steep slopes with landslides and torrents.

The climate of the area has a temperate continental character, under the influence of western, eastern, southern as well as northern and northwestern air masses [7]. Westerly (oceanic) air masses, which have the highest frequency, are generally cool and moist, resulting in a multi-year average temperature of 8.1 - 10°C. Precipitation values are between 501- 600 mm, in the Subcarpathian area, and higher values, of 601-700 mm, were individualized in the Subcarpathian hills.

Maintaining soil quality and increasing soil water availability is a major challenge for food production for the growing global population. Erosion degrades soil physico-hydric properties by decreasing soil organic matter content and consequently decreasing aggregate stability and water holding capacity, while increasing soil crust formation [27].

Practicing conservation agriculture is one of the best methods that contribute to keeping the soil in place, in case of water erosion of the soil. Thus, cover crops with natural vegetation can be used or the use of strip crops, which protect the soil thanks to the roots that strengthen it.

The results indicate that the root density of the studied cover crops varies between 1.02 kg/m^3 for *Phacelia tanacetifoli* and 2.95 kg/m^3 for ryegrass, therefore the distribution of root density with soil depth has a direct effect of reducing runoff erosion [6].

The precipitation during the vegetation period of 2023, recorded at the station, is shown in (fig.4). The total amount of water that fell as a result of the rains during 6 months was

332.6 mm, registering a surplus of 75.8 mm compared to the amount of water recorded at the Buzau weather station.

The analysis of the amounts of water falling registers positive deviations: in April with + 9.6 mm; in June with + 24.3 mm; in July with + 37.5 mm (rainiest month); in August with +15.1 mm Negative deviations were recorded in the months of May with - 8.9 m and September with -1.8 mm (the driest month).

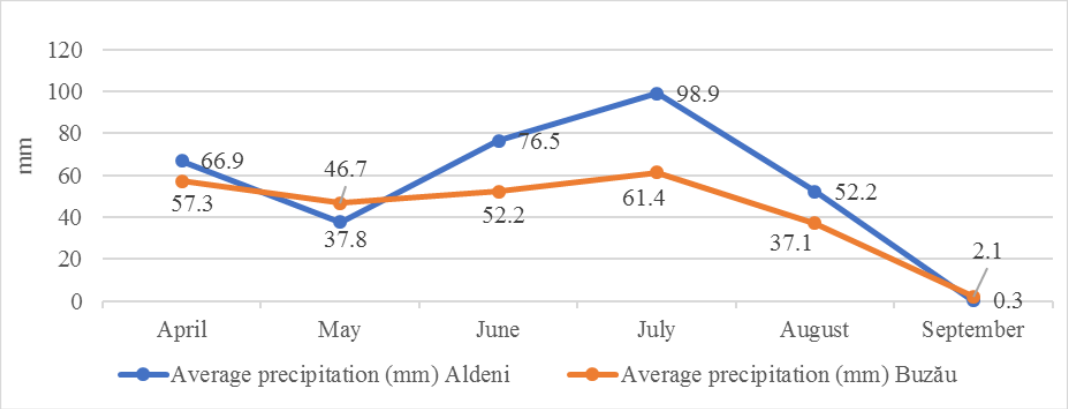


Figure 4. **Rainfall dynamics during the growing season recorded in 2023 at the Aldeni Station, Romania**

Table 1. **Grouping of rain during the vegetation period according to the amount of water, Aldeni-Romania, 2023**

Month	<5 mm	5,1-10 mm	10,1-20 mm	20,1-30 mm	30,1-40 mm	>40,1 mm	Total	%
April	2	2	3	-	-	-	7	41,3
June	-	1	2	-	1	-	4	23,5
July	-	-	1	-	-	1	2	11,9
August	1	1	1	-	-	-	3	17,4
September	1	-	-	-	-	-	1	5,9
Total	4	4	7	-	1	1	17	100
%	23,5	23,5	41,2	-	5,9	5,9		

The grouping of the rains that fell during the vegetation period, according to the amount of water, is presented in table 1, where it is found that of the 17 rains that fell during the mentioned period, 47% are rains less than 10 mm and 11.8% are rains greater than 30.1 mm.

The month of July should be mentioned, in which 98.9 mm of average precipitation fell (fig. 4) concentrated in two torrential rains, one of which exceeded 40.1 mm. A special feature of the precipitation recorded during the vegetation period of 2023 is the small number of rains that fell.

The comparative analysis of the total amount of water falling from precipitation during the vegetation period and torrential water highlights the months of June and July as follows: 22% of the total rainfall in June was torrential and 67% of the total rainfall in July was torrential (fig.5).

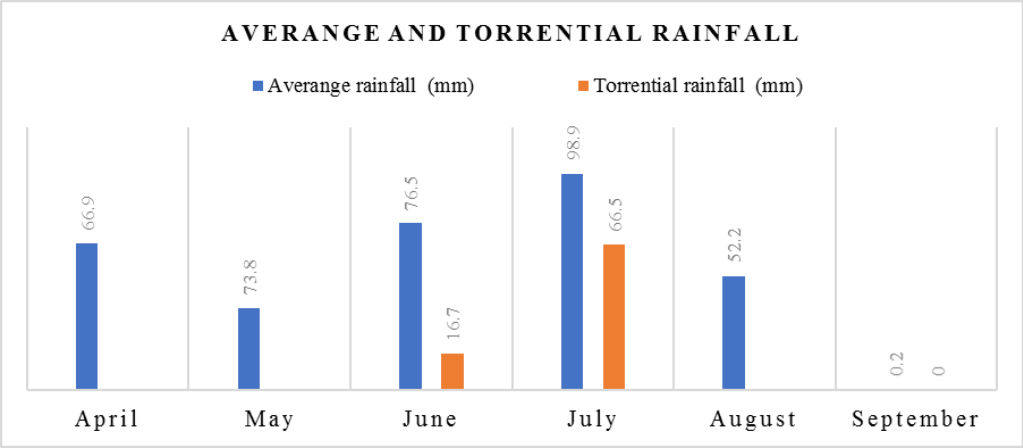


Figure 5. **Dynamics of total precipitation and torrential precipitation recorded during the vegetation period in 2023, at the Aldeni Station, Romania**

The data regarding the particularities of the torrential rains recorded at the Aldeni station are shown in figure 6. The three torrential rains have a water input of 83.2 mm of the 332.6 mm that were recorded during the observation period, which represents 29% of the total precipitation. Of note is the torrential rain on July 24 that lasted 60 minutes.

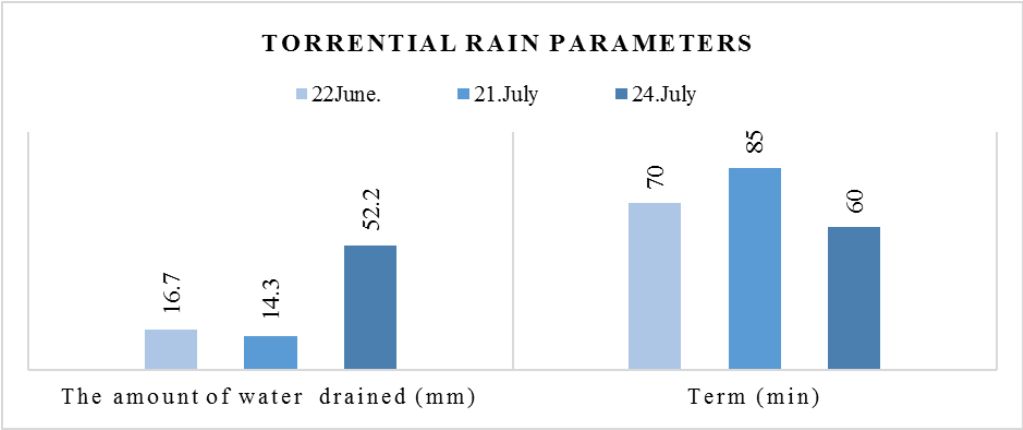


Figure 6. **The characteristics of the torrential rains recorded during the vegetation period of 2023, at the Aldeni Station, Romania**

Due ***The degree of soil coverage*** on the 15% slope, during the three torrential rains, by the autumn wheat from plot V2, the variant of wheat sown in strips from plot V3, to which is added the degree of coverage given to the soil by the perennial grasses sown between strips, compared to the uncultivated land in V4, is presented in figure 7.

There is an increase in the degree of soil coverage for wheat sown in the two variants V2 and V3 from the torrential rain of June 22 to that of July 24. The wheat sown in strips in the V3 variant has a higher degree of soil coverage (84.9%) compared to the autumn wheat in the V2 plot, where the degree of coverage is 39.8%.

In the most aggressive rain on July 24, the wheat sown in strips covers 99.2% of the soil in the V3 variant, compared to the autumn wheat in the V2 variant, which covers the soil in proportion to 50.5%. In the case of plot V4, the degree of coverage is zero during

the three torrential rains, this being the option to be avoided in this area with a slope greater than 15%.

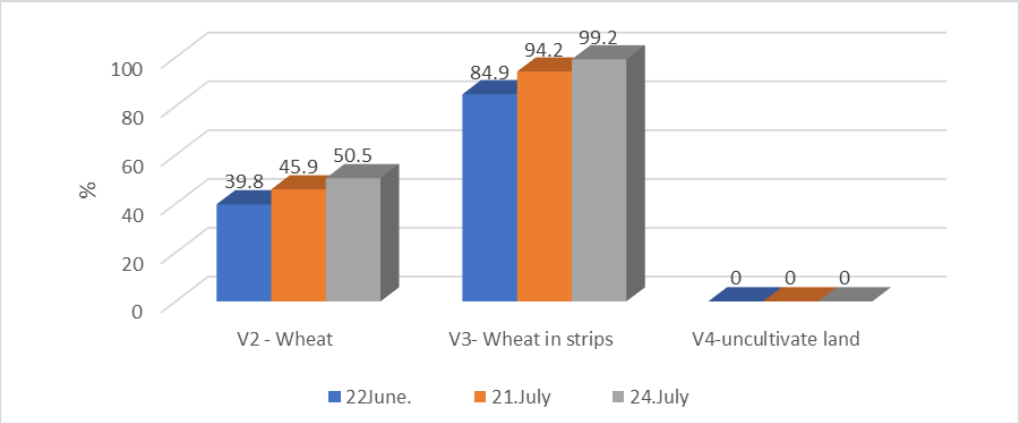


Figure 7. **The degree of coverage of the wheat crop on plots V2, V3 and V4 in the plot located on the slope of 15% at the Aldeni Station, Romania.**

The degree of coverage of the winter wheat from the V2 variant compared to the wheat sown in strips from the V3 variant and the V4 variant with the uncultivated land, located on a 20% slope, is presented in figure 8. Here, the increasing trend of the degree of soil coverage is maintained in the two cultivation variants, but shows lower values.

In the July 24 torrential rain, winter wheat in V2 has a coverage of 46.4% compared to strip-sown wheat in V3, which has a coverage of 93.9%. We note that even in this case the degree of coverage in plot V4 is null.

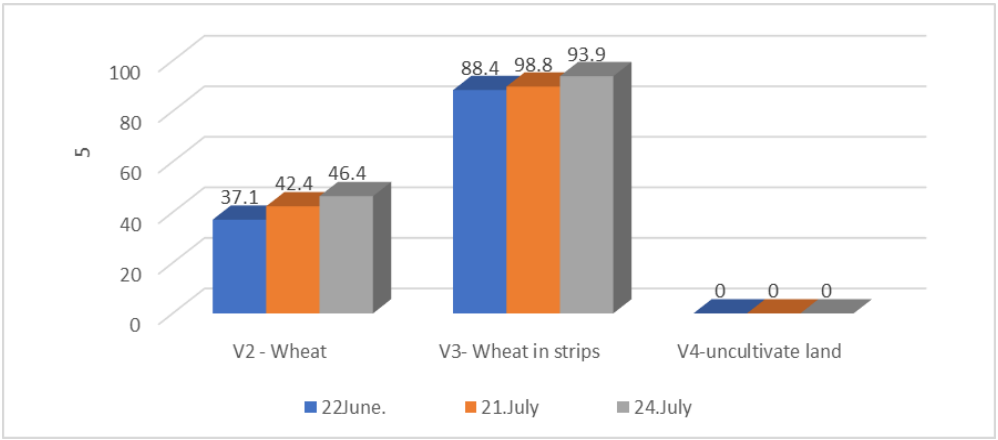


Figure 8. **The degree of coverage of the wheat crop on plots V2 and V3 in the plot located on the slope of 20% at the Aldeni Station**

The protection of the soil against erosion of the wheat sown in the two variants, on two categories of slope, depends on the vegetation phase at the time of the torrential rains, that is, on the degree of coverage given to the soil.

Analysis of soil losses, on the 15% slope land, caused by the torrential rains in the growing season of 2023, on the plots cultivated with winter wheat (V2) and strip-sown wheat (V3), compared to the unprotected soil in the plot V4, located are shown in figure 9.

In the winter wheat crop sown on plot V2, the amount of soil washed by the torrential rain of June 22 is 3.8 t/ha compared to the unprotected soil on plot V4, where the losses are 6.2 t/ha. During the rain of July 21, 15.2 t/ha of soil was washed from the unprotected soil, compared to the wheat in plot V2 where the losses are 1.9 t/ha. The torrential rain of 24 July washed away 41.9 t/ha of soil from the uncultivated plot (V4), compared to the amount of 0.83 t/ha for winter wheat in plot V2, when the degree of coverage was 50 %.

In total, 63.3 t/ha are lost from the unprotected soil located on the 15% slope compared to the soil covered with wheat (V2), when the total soil loss is 6.63 t/ha. On the plot cultivated with wheat sown in strips from the V3 variant, soil losses are non-existent, which indicates a very good protection of the soil for runoff on the 15% slope.

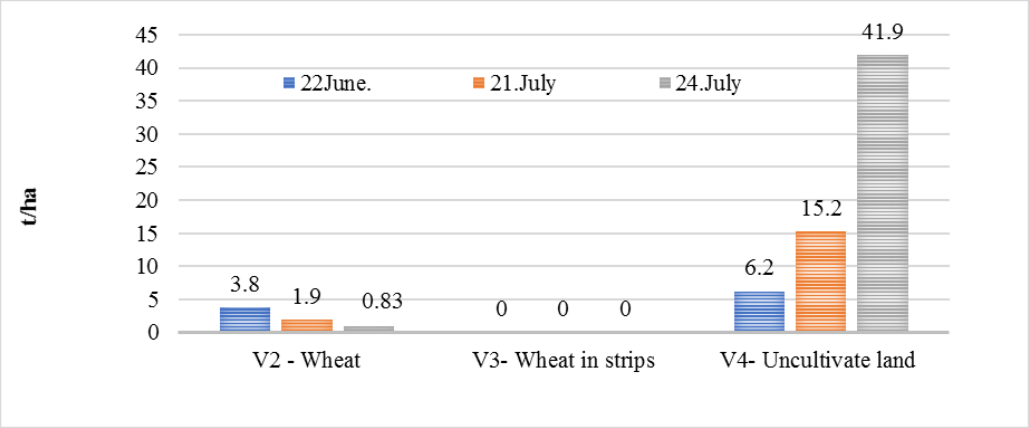


Figure 9. **Soil losses from the plot located on the slope of 15% at the Aldeni Station, t/ha.**

Soil losses on the 20% slope, caused by torrential rains in the growing season of 2023, from the plots cultivated with winter wheat, conventional method (V2) and strip-sown wheat (V3), compared to the unprotected soil in the plot V4, indicates the dynamics of recorded soil losses and are similar to the variants on the 15% slope (figure 10).

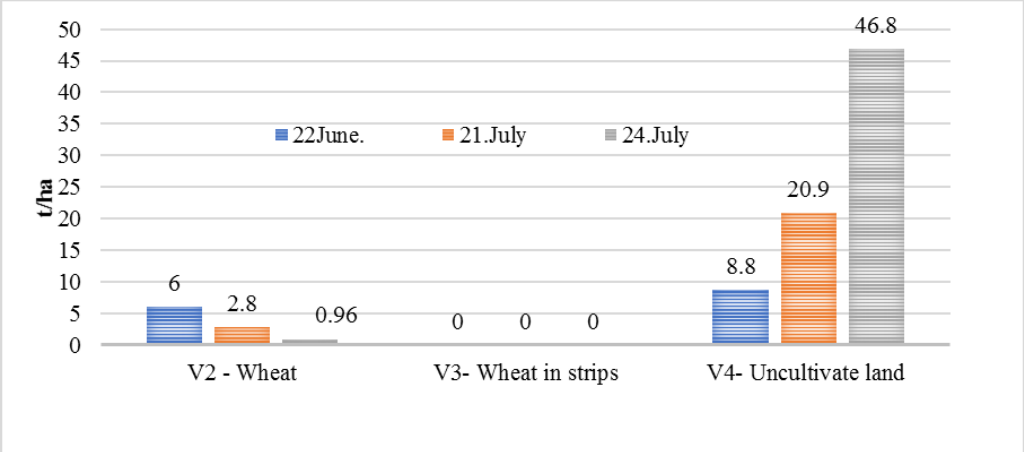


Figure 10. **Soil losses from the plot located on the slope of 20 % at the Aldeni Station, t/ha**

During the torrential rain of June 22.6 t/ha washed away from plot V2 with winter wheat, compared to the unprotected soil in plot V4, where the amount of washed soil was 8.8 t/ha.

In the rain of June 21, the amount of soil washed from plot V2 is 2.87 t/ha compared to 20.9 t/ha soil washed from variant V4 where the soil is uncultivated field. The biggest difference between the two variants was in the rain of June 24, where on the V2 plot with winter wheat 0.96 t/ha of soil was washed, compared to 46.8 t/ha of soil washed from the V4 variant where the soil is unprotected.

As in the case of the land with a slope of 15% and in the case of the land with a slope of 20%, on the plot V3 with wheat sown in strips no soil losses were recorded, these being zero, so it best protects the soil from runoff and sediment accumulations at the base of the slope.

In total, 76.5 t/ha is lost from the unprotected soil (V4) located on a 20% slope compared to the soil covered with wheat (V2) when the total soil loss is only 8.9 t/ha. In conclusion, a total of 139.81 t/ha is washed from the V4 plots with unprotected soil compared to 16.43 t/ha from the V2 plot cultivated with winter wheat.

CONCLUSION

The implementation of soil conservation measures slows water runoff on slopes, improves water infiltration on the profile and helps manage large water flows, reducing the chances of flooding and sediment deposition.

The total amount of water that fell in the hilly area of Buzau in Romania, as a result of the rains during the analyzed period, was 332.6 mm. During the vegetation period, 17 rains were recorded, of which 47% were rains smaller than 10 mm, which are not taken into account.

The comparative analysis of the total amount of water falling from precipitation during the vegetation period and torrential ones highlights 22% of the total precipitation in June as torrential and 67% of the total precipitation in July also torrential, which poses big erosion problems to the plots cultivated or in the field.

The strip-sown wheat in the V3 plot covered the soil better compared to the winter wheat in the V2 plot.

On the unprotected soil located on the 15% slope, a total of 63.3 t/ha is lost compared to the soil covered with wheat when the total soil loss is 6.63 t/ha. On unprotected soil located on a 20% slope, 76.5 t/ha are lost compared to soil covered with wheat when the total soil loss is 8.9 t/ha. In the V3 plots cultivated with wheat sown in strips, soil losses are zero. Wheat sown in strips practically cancels erosion under the climate conditions of the year 2023.

REFERENCES

[1] Aliyev, Z. H. "Scientifically based measures to combat erosion of slope lands in Azerbaijan." *GPH-International Journal of Applied Science* 6.08, 2023: pp 38-45, e-ISSN 2795-3248;

[2] Avezboyev, S., et al. "Issues concerning the use of anti-erosion measures in land management projects." *IOP Conference Series:Earth and Environmental Science*. Vol. 1138. No. 1. IOP Publishing, 2023.Online ISSN: 1755-1315;

[3] Bagarello, V., and V. Ferro. "Plot-scale measurement of soil erosion at the experimental area of Sparacia (southern Italy)." *Hydrological Processes* 18.1, 2004: pp 141-157. https://doi.org/10.1002/hyp.1318;

[4] Bennett, Hugh Hammond, and William Ridgely Chapline. "Soil erosion a national menace." *Environmental Geomorphology and Landscape Conservation*. Routledge, 2020, pp 57-83. ISBN 9780367460358;

[5] Blanco-Canqui, Humberto, et al. "Grass barriers for reduced concentrated flow induced soil and nutrient loss." *Soil Science Society of America Journal* 68.6, 2004: pp 1963-1972. https://doi.org/10.2136/sssaj2004.1963;

[6] De Baets, Sarah, et al. "Cover crops and their erosion-reducing effects during concentrated flow erosion." *Catena* 85.3, 2011, pp 237-244, https://doi.org/10.1016/j.catena.2011.01.009;

[7] Ene Alexandru, Radu Alexandra -Teodora, Impactul lucrărilor antierozionale asupra solurilor din zona inferioara a Bazinului Hidrografic Slanic - Buzau, Editura Bren, 2000. ISBN: 973-9493-43-2;

[8] García-Díaz, Andrés, et al. "Nitrogen losses in vineyards under different types of soil groundcover. A field runoff simulator approach in central Spain." *Agriculture, Ecosystems & Environment* 236, 2017, pp 256-267. https://doi.org/10.1016/j.agee.2016.12.013;

[9] Guobin, Liu. "Soil conservation and sustainable agriculture on the Loess Plateau: challenges and prospects." *Ambio 28(8)*, 1999: pp 663-668, http://www.jstor.org/stable/4314979;

[10] Gupta, Anil Kumar. "The Role of Soil Conservation in Plain and Hilly Areas." International Journal of Recent Research and Review, Vol. IX, Issue 4, December 2016, pp 48 – 52; ISSN 2277 – 8322, ISSN 2277 – 8322;

[11] Gyssels, Gwendolyn, Jean Poesen, Esther Bochet, and Young Li. "Impact of plant roots on the resistance of soils to erosion by water: a review." *Progress in physical geography* 29, no. 2, 2005, pp 189-217. https://doi.org/10.1191/0309133305pp443r;

[12] Hurni, Hans, et al. "Soil erosion and conservation in global agriculture." *Land use and soil resources*, 2008, pp 41-71. https://doi.org/10.1007/978-1-4020-6778-5_4;

[13] Hudson, Norman. *Field measurement of soil erosion and runoff*. Vol. 68. Food & Agriculture Org., 1993, ISBN 92-5-103406-0;

[14] Ielenicz, Mihai, Ileana-Georgeta Patru, and Mioara Ghincea. "Subcarpații Romaniei, Editura Universitara.", 2003, ISBN: 978-973-749-005-3;

[15] Issaka, Sakinatu, and Muhammad Aqeel Ashraf. "Impact of soil erosion and degradation on water quality: a review." *Geology, Ecology, and Landscapes* 1.1, 2017: pp 1-11. https://doi.org/10.1080/24749508.2017.1301053;

[16] Kril, T., & Havriluk, R., GEOSPATIAL ANALYSIS OF GEOLOGICAL FACTORS OF CHERNOZEM DEGRADATION IN THE SOUTHERN PART OF UKRAINE. *International Multidisciplinary Scientific GeoConference: SGEM*, *22*(3.1), 2022, pp 253-258. DOI: 10.5593/sgem2022/3.1/s13.31;

[17] Li, Changjia, et al. "Coupled Thorens and Soil Conservation Service Models for Soil Erosion Assessment in a Loess Plateau Watershed, China." *Remote Sensing* 15.3 (2023): 803. https://doi.org/10.3390/rs15030803;

[18] Montgomery, David R. "Soil erosion and agricultural sustainability." *Proceedings of the National Academy of Sciences* 104.33, 2007, pp 13268-13272, https://doi.org/10.1073/pnas.0611508104;

[19] RATTA, Raj; LAL, R. (ed.). *Soil quality and soil erosion*. CRC press, 1998. ISBN-13: 978-1574441000, ISBN-10: 1574441000;

[20] Radu, Alexandra Teodora, and Mariana Burcea. "The study of erosion processes in the hilly area of Buzău County (Romania) in the specific climatic conditions of year 2022." *Scientific Papers Series Management, Economic Engineering in Agriculture & Rural Development* 23.3, 2023, 756-767, PRINT ISSN 2284-7995, E-ISSN 2285-3952;

[21] Rajbanshi, Joy, Sharmistha Das, and Roni Paul. "Quantification of the effects of conservation practices on surface runoff and soil erosion in croplands and their trade-off: A meta-analysis." *Science of The Total Environment* 864, 2023, 161015. https://doi.org/10.1016/j.scitotenv.2022.161015;

[22] Silva, Thais Palumbo, et al. "Best management practices to reduce soil erosion and change water balance components in watersheds under grain and dairy production." *International soil and water conservation research* 12.1, 2024: pp 121-136. https://doi.org/10.1016/j.iswcr.2023.06.003;

[23] Steinhoff-Knopp, Bastian, Tinka K. Kuhn, and Benjamin Burkhard. "The impact of soil erosion on soil-related ecosystem services: development and testing a scenario-based assessment approach." *Environmental Monitoring and Assessment* 193. Suppl 1, 2021: 274. https://doi.org/10.1007/s10661-020-08814-0;

[24] Telles, Tiago Santos, Maria de Fátima Guimarães, and Sonia Carmela Falci Dechen. "The costs of soil erosion." *Revista Brasileira de Ciencia do solo* 35, 2011: pp 287-298. https://doi.org/10.1590/S0100-06832011000200001;

[25] Toy, Terrence J., George R. Foster, and Kenneth G. Renard. *Soil erosion: processes, prediction, measurement, and control*. John Wiley & Sons, 2002. ISBN 0-471-38369-4;

[26] Vought, Lena B-M., et al. "Structure and function of buffer strips from a water quality perspective in agricultural landscapes." *Landscape and urban planning* 31.1-3, 1995, pp 323-331. https://doi.org/10.1016/0169-2046(94)01057-F;

[27] Zhou, Xiaobo, et al. "Perennial filter strips reduce nitrate levels in soil and shallow groundwater after grassland-to-cropland conversion." *Journal of Environmental Quality* 39.6, 2010: 2006-2015. https://doi.org/10.2134/jeq2010.0151;

[28] Zuazo, VH Durán, et al. "Environmental impact of introducing plant covers in the taluses of terraces: Implications for mitigating agricultural soil erosion and runoff." *Catena* 84.1-2, 2011: pp 79-88. https://doi.org/10.1016/j.catena.2010.10.004;

SPECTRAL CHARACTERISTICS OF GROUPS AND TYPES OF LANDS, CONSTRUCTED BY AVERAGIN LONG-TERM SERIES OF VEGETATION INDECES

Dmitry Borshchev

Dr. Dmitry Rukhovich

Vasily Rashkovich

Dokuchaev Soil Science Institute, **Russia**

ABSTRACT

The optimal solution of intensification and ecologisation of agricultural production is achieved in adaptive-landscape farming systems. To solve the problems of adaptive landscape agriculture, classical methods of soil-landscape mapping and new methods of remote diagnostics of intra-field heterogeneity were combined to identify features that will further improve the efficiency of producing maps of groups and types of land and increase their accuracy. Identification of the spectral characteristics of groups and types of land has become possible due to neural network filtering of big remote sensing data. By intersecting the map of groups and types of lands with the bare soil surface map in geographical information systems, the median values of the 'C' coefficient for different land groups and types were calculated. Each agroecological group of lands has its own spectral characteristics, which are influenced by the granulometric composition, moisture regime and humus content. It was established for the first time that groups of lands differing in productivity have different reflectivity. Differences in spectral characteristics of land groups can be used for their remote diagnostics, quantitative assessment, and design of systems to improve low-productive areas.

Keywords: digital soil mapping, remote sensing data, neural network, multi-temporal soil line, adaptive-landscape farming.

INTRODUCTION

When the level of intensification of farming increases, problems related to the complexity of the soil cover structure (SCS) [1] and land degradation [2] are often manifested. The optimal solution of intensification and ecologisation of agricultural production is achieved in adaptive-landscape farming systems [3], which replaced zonal systems [4].

Adaptive-landscape farming system is a system of land use of a certain agro-ecological group, ensuring the sustainability of the agrolandscape and reproduction of soil fertility [5]. Agro-ecological groups of land are the determining link in the choice of agro-technology to it: crop rotation, soil treatment, plant protection means, applied fertilisers and ameliorants [6].

Intensive farming systems are currently designed in geographical information systems (GIS) of agronomic orientation, collected in various GIS shells [7, 8] based on the materials of special soil-landscape mapping, in the process of which the old soil maps

are refined, since the classical large-scale soil mapping of the USSR did not have a clear intra-field orientation [9, 10, 11, 12]. After field work, maps of agroecological groups of land types are created at a scale of 1:10000. It takes a lot of time to create such a map using traditional methods of ground mapping, which is why there is a need to search for and identify the signs of difference in lands belonging to different agroecological groups using remote sensing data [13].

New methods of processing large remote sensing data (LRDD) [14] using artificial intelligence [15] are actively applied to indicate different soils and spatial heterogeneity of the soil cover. The results of such processing are bare soil surface (BSS) maps [16] describing the spectral characteristics of the land surface, multitemporal vegetation indices (VI) [17], which reflect the multi-temporal vegetation state of crops within a production field. These maps are actively used in precision farming technology for applying seeds and fertilizers [18, 19, 20].

To solve the problems of adaptive landscape agriculture, classical methods of soil-landscape mapping and new methods of remote interpretation of intra-field heterogeneities were combined to identify features that will further improve the efficiency of compiling maps of groups and types of lands and increase their accuracy.

Aims of the work:

Identify the relationship between spectral characteristics of the bare soil surface and land groups constructed using averaged multiyear vegetation indices.

STUDY OBJECT, METHODS AND MATERIALS

Study area

The object of the study is located in the European part of the Russian Federation, in the forest-steppe zone of Bazarno- Karabulaksky district of Saratov region - Privolzhskaya upland. (Fig. 1). The average annual precipitation is 453 mm. The sum of active temperatures - 2236 C. Hydrothermal coefficient of moistening - 1. Agricultural lands with a total area of 3232 hectares were investigated.

Methods

1. Neural network filtering of big remote sensing data (BRDD);

2. Construction of a map of the bare soil surface (BSS) using the technology of the spectral neighbourhood of soil line (SNSL) containing ‘C’ coefficient information;

3. Construction of the map of stable intra-field heterogeneity (SIFH) of soil fertility based on averaging of multitemporal series of vegetation indices (VI);

4. Field soil surveys with determination of soil type and subtype on the basis of the map of stable in-field heterogeneity;

5. Construction of a map of groups and types of lands based on the map of stable intra-field heterogeneity for adaptive-landscape farming.

Materials

Landsat 4, 5, 7, 8 level 1 scene archives from 1984 to the present were used for calculations of the SIFH map and the BSS map. Atmospheric correction was performed using the ATCOR module of the ERDAS Imagine software package.

To create the map of groups and types of lands, the results of field soil survey with determination of soil type, subtype, humus horizon thickness, determination of granulometric composition and soil-forming rock were used.

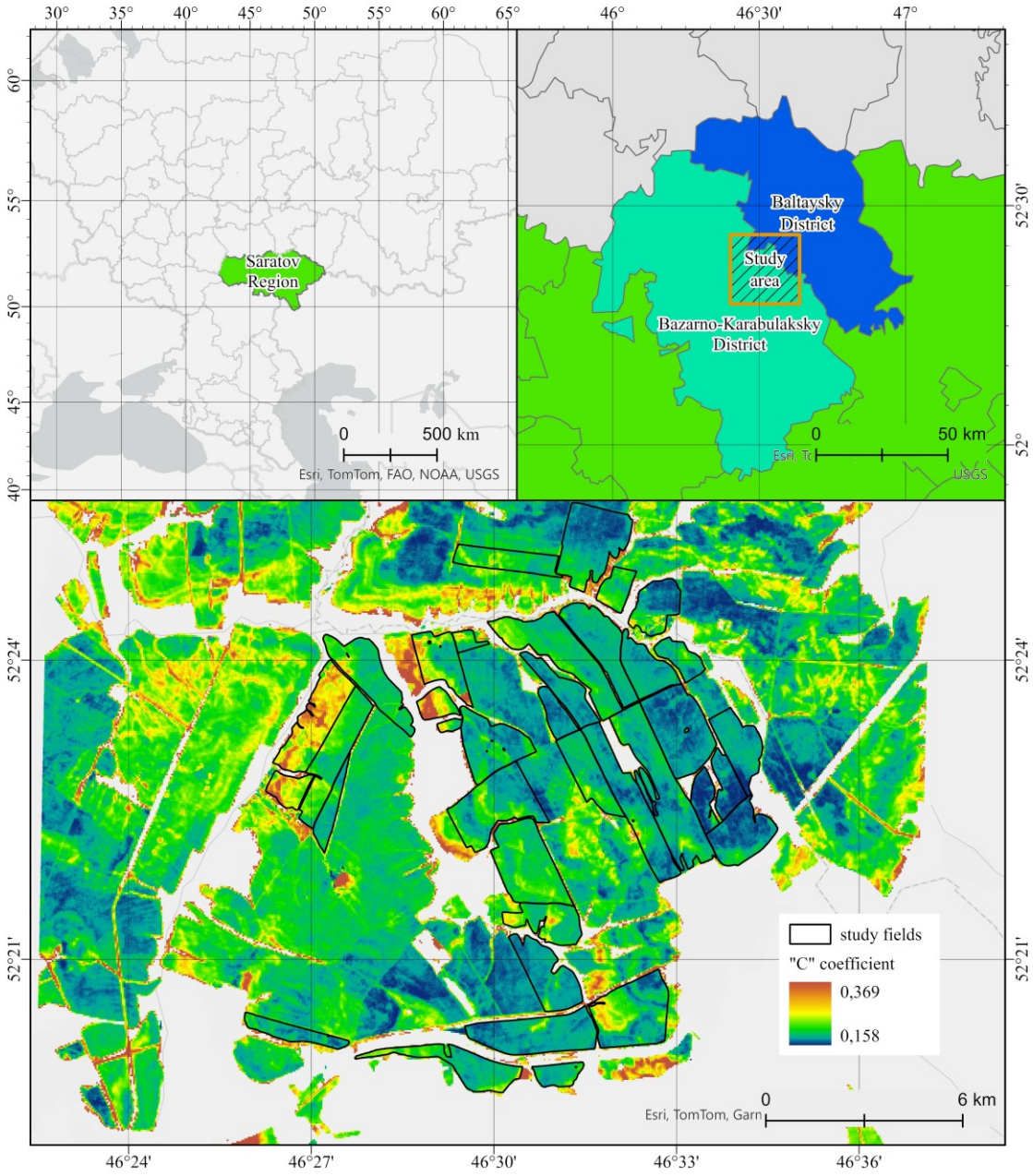


Figure 1. Location of study area and the map of the “C” coefficient of BSS.

RESULTS

BSS map - "C" coefficient map

Figure 1 shows a fragment of the ‘C’ coefficient map constructed for an area of 13,000 ha. of the Bazarno-Karabulaksky district of the Saratov region. The range of brightnesses varies from 0.15 to 0.32. Darker (shades of blue) colours are represented by more humusified leached chernozems with thick humus horizon, medium loamy and

https://doi.org/10.5593/sgem2024/3.1/s13.38

heavy loamy granulometric composition. Lighter (red and yellow) shades are weakly humusified, thin, sandy and light loamy leached chernozems.

The SIFH map

Figure 2 shows the SIFH map - the averaging map of multi-temporal VIs maps. Red shows zones of low fertility, yellow - medium, and green - high fertility. Since the SIFH map is a map of intra-field heterogeneity, the colour values are informative for each field. Thick and medium-thick leached chernozems of heavy loamy and medium loamy granulometric composition with high humus content are the most productive areas of the fields. At the same time, zones of low fertility of fields can be represented by medium-loamy thin chernozems and sandy soils. Also zones of low fertility can be represented by solonetz soils with different salinity degrees and solonetzic meadow-chernozem soils.

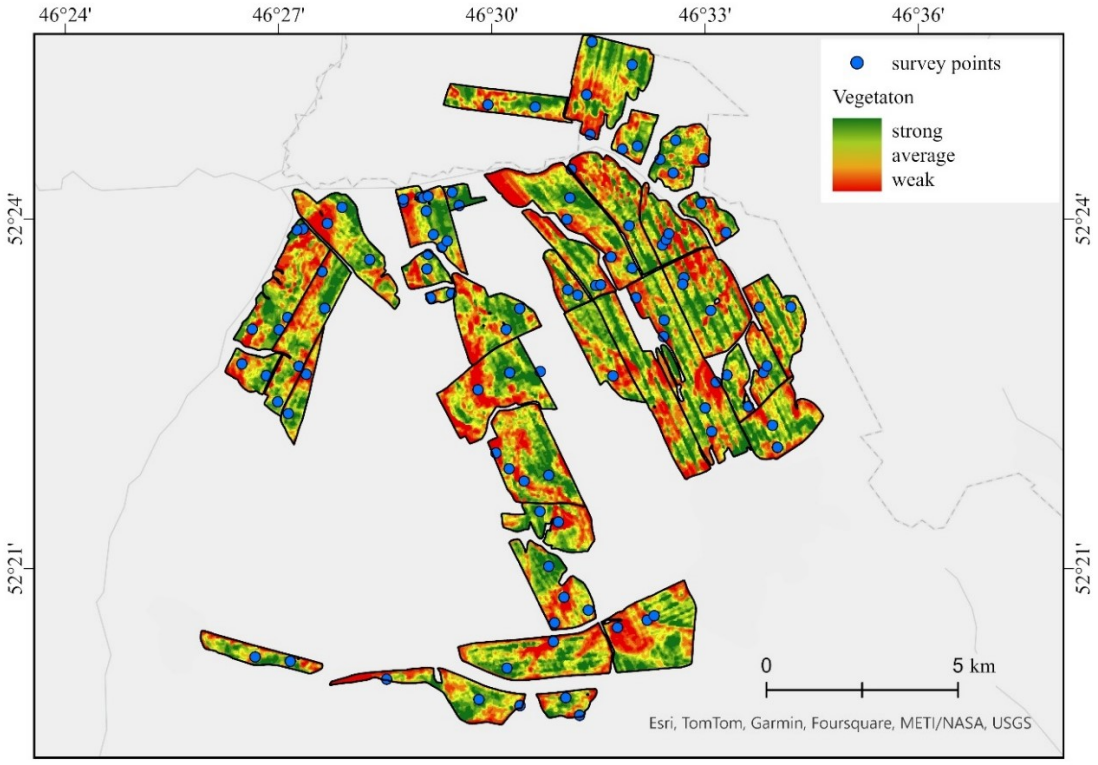


Figure 2. The map of the SIFH with field soil survey points.

Field soil survey

Field surveys (Fig. 2) were conducted on agricultural lands with a total area of 3232 hectares along a route crossing different relief elements, SIFH zones, areas with different spectral characteristics of BSS map. A total of 103 soil transects were laid out with identification of SCS. Also 103 soil samples were collected for humus content determination.

Map of groups and types of lands

Figure 3 presents a map of groups and types of lands - the result of the combined use of the SIFH map as a contour part and the results of soil survey as a source of information about the soil and the main limiting factors. Land groups are associations of homogeneous areas that were identified based on the prevalence of certain factors

limiting production and affecting crop cultivation. The following groups were identified:

1. Placor lands are drained plains with slightly undulating and convex watersheds, weakly dissected by a network of basins, and adjoining slopes of 1-3 degrees of cold exposures. This group is represented by leached chernozems of different thickness (60-120 cm), heavy and medium loamy on cover loams with a small share of meadow-chernozem soils.

2. Erosion lands. Erosion is the process of soil destruction under the action of water and wind. According to the degree of erosion the lands were classified into:

2.1. Slightly eroded lands. This group is represented by leached chernozems of medium thickness, slightly eroded, with a small share of medium eroded, medium loamy on different soil-forming rocks (cover loams and pre-Quaternary sediments).

2.2. Moderately eroded lands. This group is represented by chernozems leached medium-thick medium eroded, medium loamy.

2.3. Highly eroded lands. This group is represented by leached chernozems of different thickness (30-50 cm), highly eroded light loamy, medium loamy.

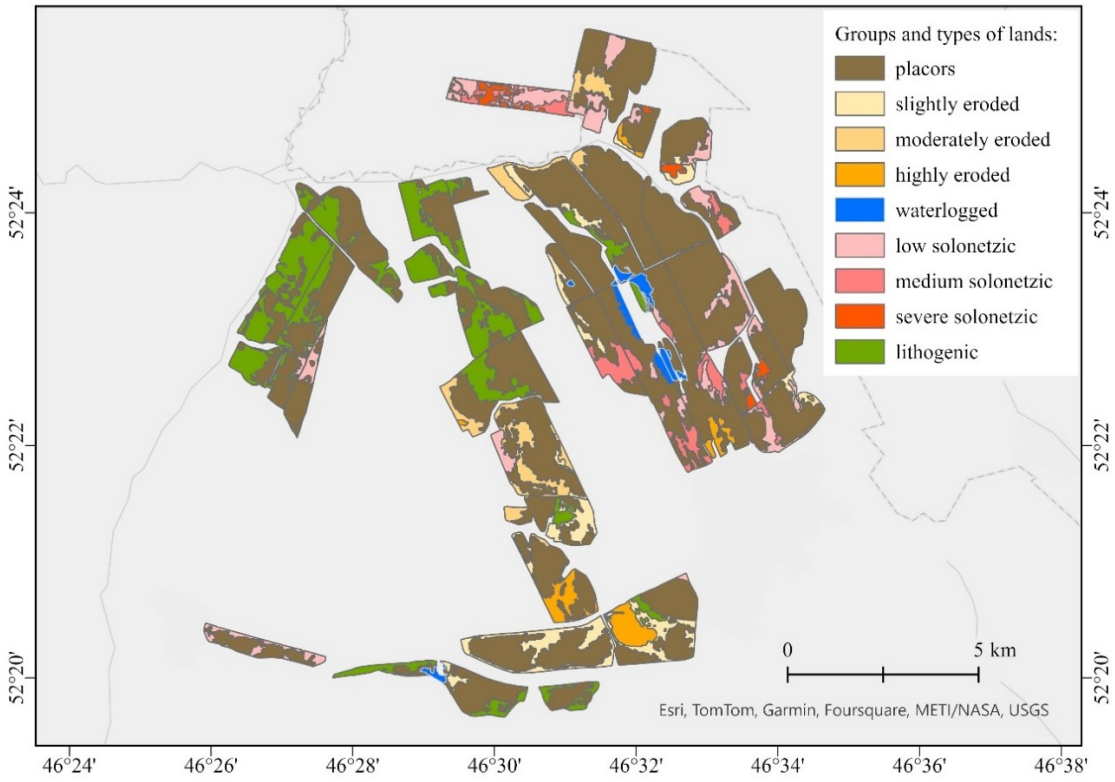


Figure 3. The map of groups and types of lands.

3.Waterlogged lands are formed in the conditions of excessive moistening. This group is represented by meadow-chernozem medium thick heavy loamy and clayey.

4. Solonetzic lands are developed in low relief elements with additional surface or ground moisture. They are formed on heavy granulometric composition of dense sediments. Contains carbonates, gypsum and often easily soluble salts.

https://doi.org/10.5593/sgem2024/3.1/s13.38

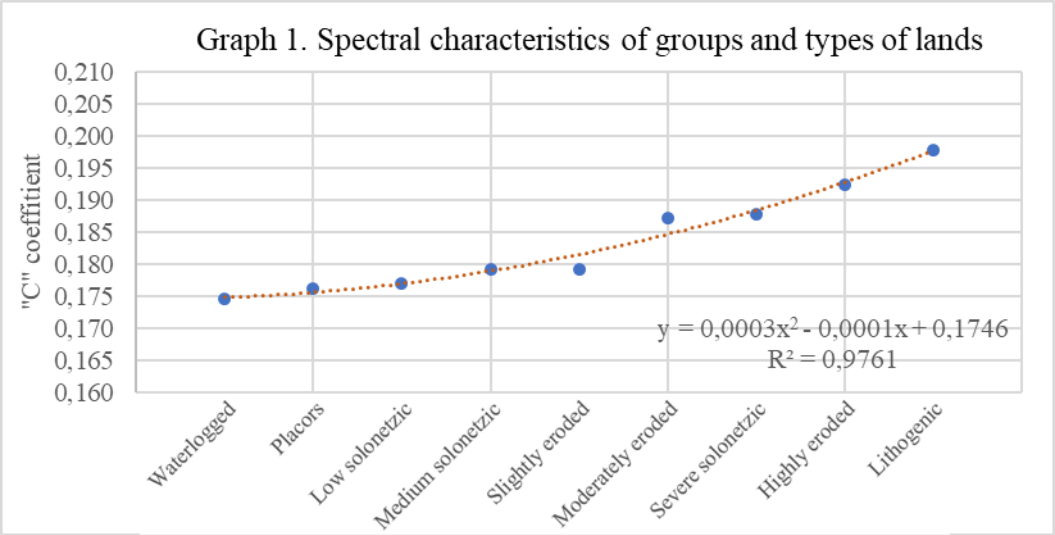
4.1. Low solonetzic lands. This group is represented by solonetz medium-saline medium-trick heavy loamy, clayey on pre-Quaternary clayey sediments.

4.2. Medium solonetzic lands. This group is represented by solonetz medium-saline, medium-thick, heavy loamy and clayey on pre-Quaternary sediments.

4.3. Severe solonetzic lands. This group is represented by severe saline, medium-thick, heavy loamy and clayey solonetzes on pre-Quaternary sediments.

5. Lithogenic lands. The lands that are hardly suitable for cultivation of agricultural crops due to irreversible limitations on the conditions of lithology of soil-forming rocks, relief, meliorative state and very limited adaptation possibilities. This group is represented by leached chernozems of different thickness (30-50cm), light loamy, sandy loam and sandy on pre-Quaternary sediments.

By intersecting the map of groups and types of lands with the BSS map in GIS, the median values of the 'C' coefficient for different land groups and types were calculated. The results of the calculations are presented in Graph 1.



Each agroecological group of lands has its own spectral characteristics, which are influenced by the granulometric composition, moisture regime and humus content.

The group of waterlogged lands is represented by soils of heavy loamy and clayey granulometric composition, which drain water poorly. Coefficient "C" – 0.174.

The highly productive group of placor lands is in conditions of optimal moisture, the granulometric composition is medium and heavy loam. On a map of the open surface has average reflectivity. Coefficient "C" – 0.176. Low solonetzic lands, whose moisture regime is similar to waterlogged lands, are located in the row after placor lands. Coefficient "C" – 0.177. Medium solonetzic and slightly erosion lands have the same spectral characteristics – 0.179. Groups of moderately eroded, severe solonetzic lands, like the previous groups, are in a similar range of spectral characteristics. The group of highly eroded lands has low humus content as a result of degradation. Coefficient "C" – 0.192. The lithogenic group of lands, being low-productive, has the highest reflectivity due to the low humus content and light granulometric composition. Coefficient "C" – 0.198.

DISCUSSION

Precision farming in adaptive landscape agriculture.

The complex structure of the soil cover and the large difference in yield within and between fields forces agricultural producers to look for new ways to optimize the farming process. Zones of stable intra-field heterogeneity in combination with soil and landscape surveys are a good tool for optimizing production: they allow identifying areas with different potential for further strategic planning of adaptive landscape farming systems. Reclamation of solonetzic lands is optimized by accurately identifying areas with varying degrees of solonetzization. It becomes possible to differentiate the method of basic soil cultivation to combat water erosion. In areas where reclamation is limited or impossible at all, the need for differentiated application of seeds and fertilizers increases. Applying an average rate of fertilizer to a field increases costs, which do not increase the productivity of low-productive areas and worsen the environmental situation. Fertilizers cannot compensate for moisture deficiency in sandy soils. They do not accumulate in eroded areas and do not help with the flooding of crops. Fertilizers released from low-productivity areas can be transferred to areas of high fertility, which will increase production efficiency. At the same time, the total fertilizer consumption on the field remains unchanged. The use of SIFH maps in combination with the BSS map makes it possible to solve the problem of how to redistribute fertilizers between fields as efficiently as possible.

CONCLUSION

New methods of processing BRSD for 40 years (1984-2024) using neural network filtering can improve the efficiency of soil mapping and soil difference interpretation methods, and reduce the number of ground-based soil survey samples. It was established for the first time that groups of lands differing in productivity have different reflectivity, which can be used in their detection. Differences in spectral characteristics of land groups can be used for their remote diagnostics, quantitative assessment, and design of systems to improve low-productive areas. Attempts to construct a map of groups of land types into unexplored territories have already been made previously. Using a digital relief model and soil survey points, for example, using the random forest method, it was possible to identify upland and eroded lands of varying degrees of erosion. In the study, we tried to cover an area with a more complex soil cover structure. As the result showed, to identify groups of lands with similar spectral characteristics it is necessary to improve the method.

REFERENCES

[1] Fridland V.M. Structure of the soil mantle, Geoderma, vol. 12, pp. 35-42, 1974. DOI: 10.1016/0016-7061(74)90036-6

[2] Krenz J., Greenwood P., Kuhn N.J. Soil Degradation Mapping in Drylands Using Unmanned Aerial Vehicle (UAV) Data. Soil Systems, vol. 3, pp. 33:1–33:19, 2019 DOI: 10.3390/soilsystems3020033

[3] V. I. Kiryushin. Methodology for integrated assessment of agricultural land. Eurasian Soil Science, vol. 53, pp. 960–967, 2020. DOI: 10.1134/S1064229320070066.

[4] The Application of Soil–Agroclimatic Index for Assessing the Agronomic Potential of Arable Lands in the Forest–Steppe Zone of Russia. Eurasian Soil Science, vol. 51, pp. 448–459, 2018. DOI: 10.1134/S1064229318040038.

[5] V. I. Kiryushin. The Management of Soil Fertility and Productivity of Agrocenoses in Adaptive-Landscape Farming Systems, Eurasian Soil Science, vol. 52, pp. 1137–1145, 2019. DOI: 10.1134/S1064229319070068.

[6] D. S. Bulgakov. A concept of agroecological assessment of soils of cultivated lands. Eurasian Soil Science, vol. 32. No.6, pp 630-633, 2002.

[7] URL: https://www.esri.com/ru–ru/home

[8] URL: https://qgis.org/ru/site/

[9] Kulyanitsa A.L., Rukhovich D.I., Koroleva P.V., Vilchevskaya E.V., Kalinina N.V. Analysis of the informativity of big satellite precision–farming data processing for correcting large–scale soil maps. Eurasian Soil Science, vol. 53/ issue 12, pp. 1709–1725, 2020. DOI: 10.1134/S1064229320110083.

[10] Ischenko T.A. All-Union instruction on soil surveys and the compilation of large-scale soil maps for land use. Kolos, Moscow, 1973.

[11] Soil map of the USSR. Scale: 1:16000000. 1983. Atlas of the USSR. Nature maps. Soil map / Main Directorate of Geodesy and Cartography under the Council of Ministers of the USSR. Moscow. 1983. P. 104-105.

[12] Simakova M.S. Soil maps. Cartographic knowledge of Russia (topographic and thematic maps). Publishing house of the Institute of Geography of the Russian Academy of Sciences, Moscow, pp. 113-133, 1999.

[13] Liu P. A survey of remote-sensing big data. Front. Environ. Vol. 3. Art. 45, 2015. DOI: 10.3389/fenvs.2015.00045.

[14] Rukhovich D.I., Koroleva P.V., Kalinina N.V., Vilchevskaya Y.V. Detecting degraded arable land on the basis of remote sensing big data analysis. Eurasian Soil Science. Vol. 54/ issue 2, pp. 161–175. 2021. DOI: 10.31857/S0032180X21020131.

[15] Rukhovich D.I., Koroleva P.V., Kalinina N.V., Rukhovich D.D. The use of deep machine learning for the automated selection of remote sensing data for determination of areas of arable land degradation prosses distribution. Remote Sensing. Vol. 13/ issue 1, pp. 2–4, 2021.

[16] Koroleva P.V., Rukhovich D.I., Kalinina N.V. Location of bare soil surface and soil line on the red–nir spectral plane. Eurasian Soil Science, vol. 50/ issue 12. C. 1375–1385, 2017. DOI: 10.7868/S0032180X17100045

[17] Kurbanov R.K., Zakharova N.I. Application of vegetation indexes to assess the condition of crops Sel'skokhozyaystvennye mashiny i tekhnologii, Vol. 14/ issue 2, pp. 4–11. DOI 10.22314/2073–7599–2020–14–4–4–11.

[18] URL: https://agronote.ru/en/

[19] URL: https://operations.cropwise.com/

[20] URL: https://onesoil.ai/en

TEMPORAL VARIATIONS IN GREENHOUSE GAS EMISSIONS FROM AGRICULTURAL SOILS

Ph.D. Kristine Valujeva[1]

PhD Candidate Jovita Pilecka-Ulcugaceva[1]

Bc.sc.ing. Kristaps Siltumens[1]

PhD Candidate Olga Skiste[1]

Ph.D. Inga Grinfelde[1]

[1] Latvia University of Life Sciences and Technologies, Scientific Laboratory of Forest and Water Resources, **Latvia**

ABSTRACT

Soil moisture, soil temperature, nutrient availability, and land use practices affect the GHG emissions from soils. In this study, the aim is to determine and analyse GHG emissions from agricultural soils in five monitoring sites. The mobile spectrophotometer Picarro G2508 is used for the quantification of N_2O, CH_4, and CO_2 soil flux across five monitoring sites used for agricultural production during the growing seasons from 2017 to 2023. Findings reveal significant variations in GHG emissions across the monitoring sites. Specifically, the average N_2O emissions at monitoring sites used form agricultural production varied from 3.73 to 46.54 g N_2O ha^{-1} day^{-1}, while the average CO_2 emissions ranged from 65.75 to 166.08 kg CO_2 ha^{-1} day^{-1}, and CH_4 assimilation ranged from 1.50 to 5.30 g CH_4 ha^{-1} day^{-1}. Meteorological conditions exert a considerable effect on soil microbiological activity within a growing season, further impacting GHG emissions. These findings highlight the complex interplay between soil dynamics, environmental factors, and GHG emissions in agricultural systems. This study contributes valuable insights into the understanding of GHG emissions from agricultural soils, providing essential information for policymakers, land managers, and stakeholders involved in developing sustainable agricultural practices and mitigating climate change.

Keywords: nitrous oxide, carbon dioxide, methane, Picarro G2508, land management

INTRODUCTION

The Member States of the European Union have committed to strengthening global action to prevent climate change by ratifying the UN General Convention on Climate Change and the subsequent Paris Agreement. The goals of the Paris Agreement are to keep global warming significantly below 2°C, improve adaptation to the negative effects of climate change, influence and promote climate resilience, and drive investments to ensure low-carbon and climate-resilient development [1]. The agricultural sector is one of the largest emitters of GHG emissions. Emissions of CH_4 from enteric fermentation and N_2O emissions from soils collectively account for 48% and 31% of overall agricultural greenhouse gas emissions, respectively [2].

Measuring greenhouse gas (GHG) emissions from soil is crucial for understanding their impact on climate change and informing mitigation strategies. Soil serves as both a source and a sink for GHGs, with emissions influenced by various factors [3]. Soil

https://doi.org/10.5593/sgem2024/3.1/s13.39

moisture levels affect microbial activity and gas diffusion rates, influencing GHG release [4, 5]. Soil temperature regulates microbial activity, with higher temperatures often leading to increased emissions [3, 5]. Nutrient availability influences microbial metabolism and organic matter decomposition, affecting GHG production [3]. Land use practices such as tillage, crop rotation, and fertilization can alter soil properties and microbial communities, consequently impacting GHG emissions [4, 6]. Accurate measurement and understanding of these factors are essential for effective climate change mitigation efforts. Therefore, the aim is to determine and analyse GHG emissions from agricultural soils in five monitoring sites.

MATERIALS AND METHODS

The measurement sites are located in Latvia, Northern Europe (Figure 1). GHG measurements are conducted at five monitoring sites where agricultural activities occur, including mineral soils (Berze, Mellupite, and Auce) as well as organic soils (Marupe and Laflora). The soil characteristics at the Berze monitoring site indicate its natural fertility and suitability for agricultural activities. It is identified as a *Calcic Cambisol* with a clay content of 28% at a depth of 0-25 cm and a pH range of 7.5-7.9. Meanwhile, the soil at the Mellupite monitoring site is classified as *Stagnic Luvisol*, with a clay content of 12.2% at a depth of 0-45 cm and a pH range of 6.7-7.0. Finally, the soil at the Auce monitoring site is categorized as *Gleyic Cambisol*, with a clay content of 0.6% at a depth of 0-30 cm. Marupe and Laflora represent organic soil used for agricultural production based on the definition of organic soils in 2006 IPCC Guidelines for National Greenhouse Gas Inventories [7].

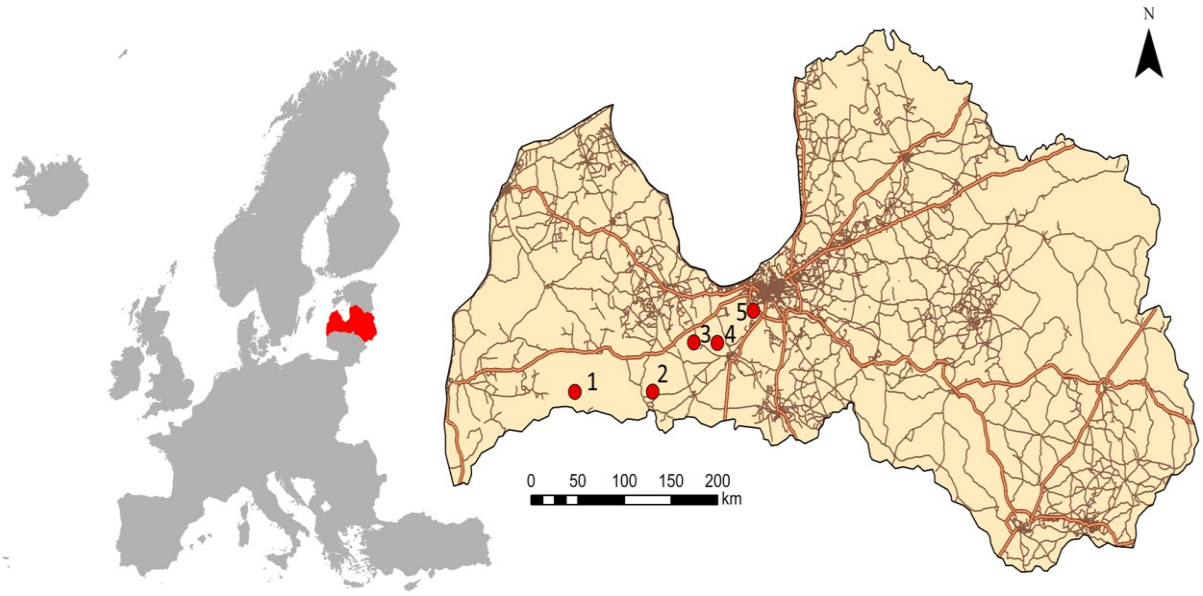


Figure 1. Locations of monitoring sites: 1, Mellupite monitoring site (56.493183, 22.229894); 2, Auce monitoring site (56.493935, 22.979702); 3, Berze monitoring site (56.713906, 23.375674); 4, Laflora monitoring site (56.711452, 23.603050); 5, Marupe monitoring site (56.853781, 23.948249).

Utilizing a portable spectrophotometer, namely the Picarro G2508 Gas Concentration Analyzer, concentration measurements of N_2O, CO_2, and CH_4 were carried out. A total of 852 measurements were conducted during the growing seasons of 2017, 2018, 2019, 2020, 2021, 2022, and 2023 from April to October, each spanning 400 seconds. For further details regarding the equipment and data transformation procedures, refer to Grinfelde et al. (2017) [8] and Valujeva et al. (2022) [9]. These concentrations of N_2O, CO_2, and CH_4 were employed in the computation of soil flux rates using a linear model [10] integrated into the Soil Flux Processor (SFP) software, developed by Picarro Inc. Following this, all flux rates were converted into either grams or kilograms per hectare per day.

According to the data from the Jelgava, Dobele, and Saldus meteorological stations of the Latvian Environment, Geology and Meteorology Centre, the lowest average air temperature (11.8°C) and the highest total precipitation (1451 mm) were recorded during the growing season of 2017. On the other hand, in the growing season of 2018, the highest average air temperature (14.9°C) and the lowest total amount of precipitation (964 mm) were observed. In other years, during the growing seasons, the average air temperature has varied from 13.1°C to 13.9°C, and total precipitation from 985 mm to 1118 mm.

According to the Shapiro-Wilk test, the values of GHG emissions from soils do not follow a normal distribution. Therefore, the Kruskal-Wallis test and Dunn's post hoc tests ($p < 0.05$) were used to determine the interrelationships between gases and the differences between years ($p < 0.05$), while Kendall's correlation coefficient was used to identify relationships between gases and soil moisture, as well as gases and soil temperature ($p < 0.05$). Statistical data analysis and graphical materials were prepared using IBM SPSS 22.

RESULTS

Comparing CH_4 emissions from soil across different measurement locations over the years, CH_4 emissions from soil are most stable at the Laflora measurement site. In Berze, however, there appears to be a trend of decreasing dispersion of CH_4 emission from soil every other year, with stable CH_4 levels observed for the past two years, approaching zero assimilation in the soil (Figure 2). Laflora is characterized by an extensive farming, where long-term land use, specifically the cultivation of bilberries, has ensured stable microbiological conditions in the soil. The results of the 2023 measurements show an increase in CH_4 assimilation in the soil. At the Mellupite measurement site, CH_4 emission from the soil has been increasing over the years.

There are statistically significant differences in CH_4 emissions from the soil between Berze and the other measurement sites, between Marupe and Mellupite, Laflora, Berze, and between Auce and Laflora ($p<0.05$). For CH_4 emission from soil, the largest differences are observed between years: 2019 and 2020, 2021, 2022, 2023, between 2017 and 2020, 2021, 2022, 2023, and between 2018 and 2020, 2022, 2023 ($p<0.05$), which means that since the beginning of the measurements, CH_4 assimilation in the soil tends to decrease in the measurement sites, except for the Laflora measurement site, where CH_4 assimilation in the soil increases.

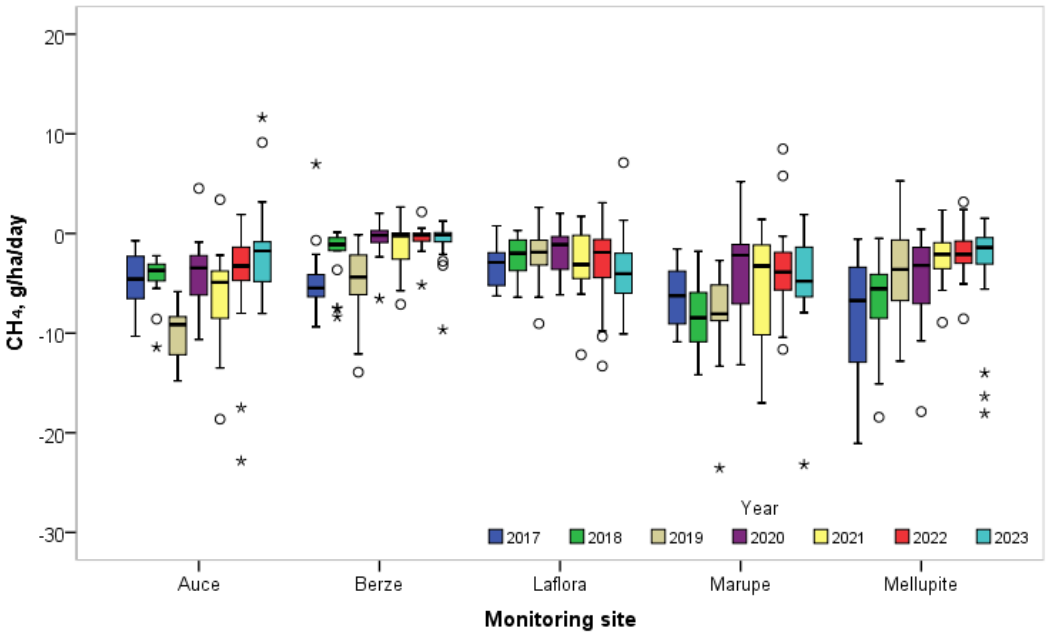


Figure 2. CH_4 emissions at five monitoring sites in the period from 2017 to 2023.

The CO_2 emissions from soils in 2023 at all measurement sites are lower compared to the previous year. This indicates that the dry and cool weather during the vegetation period has reduced the activity of microorganisms responsible for decomposition organic matter in the soil (Figure 3). There are statistically significant differences in CO_2 emissions from soils between Berze and the other measurement sites, as well as between Marupe and Auce, Mellupite, and Laflora ($p<0.05$). In 2023, CO_2 emissions from soils were significantly lower by about 35% compared to 2017 and 2022 ($p=0.004$ and $p=0.002$).

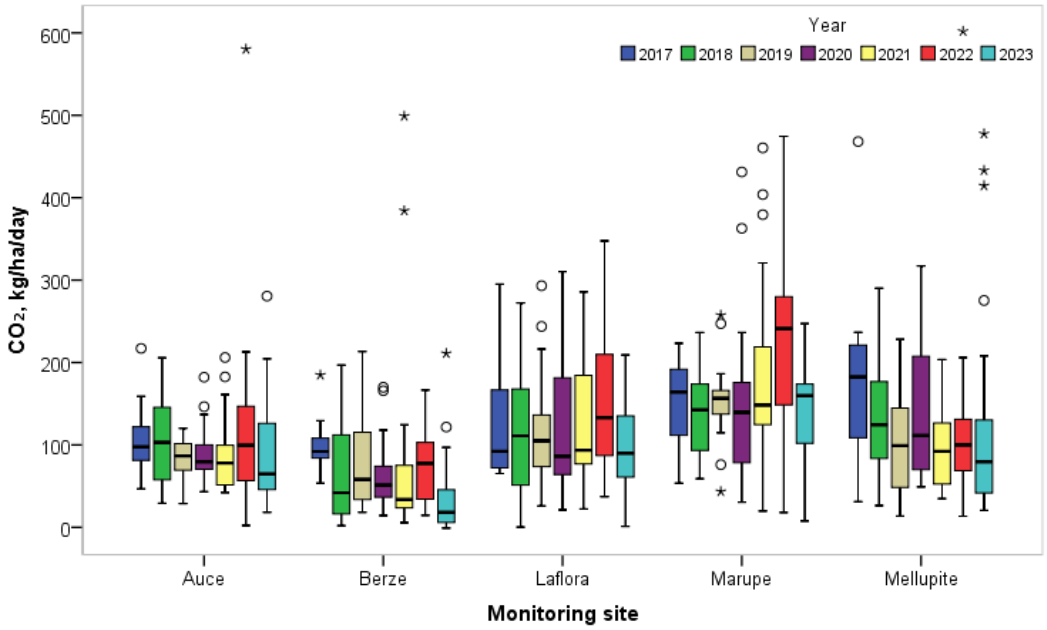


Figure 3. CO_2 emissions at five monitoring sites in the period from 2017 to 2023.

The N_2O emissions from soil exhibit significant variation in emission volumes from year to year when analysing the observed maximum N_2O values (Figure 4). The measurements in Laflora show relatively stable results, with soil emissions exhibiting the smallest fluctuation amplitude throughout the year. Pronounced extreme values were observed in 2020, attributed to the extensive farming practices and long-term bilberry planting, which have fostered highly stable soil conditions in the organic soil. In all measurement sites, there is an increase in N_2O emissions from soils in 2023 compared to previous years, except for Laflora, where the 2023 emission level remains approximately the same as that of 2022. Each measurement site has experienced extreme values in certain years. For example, in Auce, extreme values were observed in 2019; in Berze, in 2021; in Mellupite, in both 2020 and 2023; in Laflora, in 2020; and in Marupe, in both 2019 and 2021.

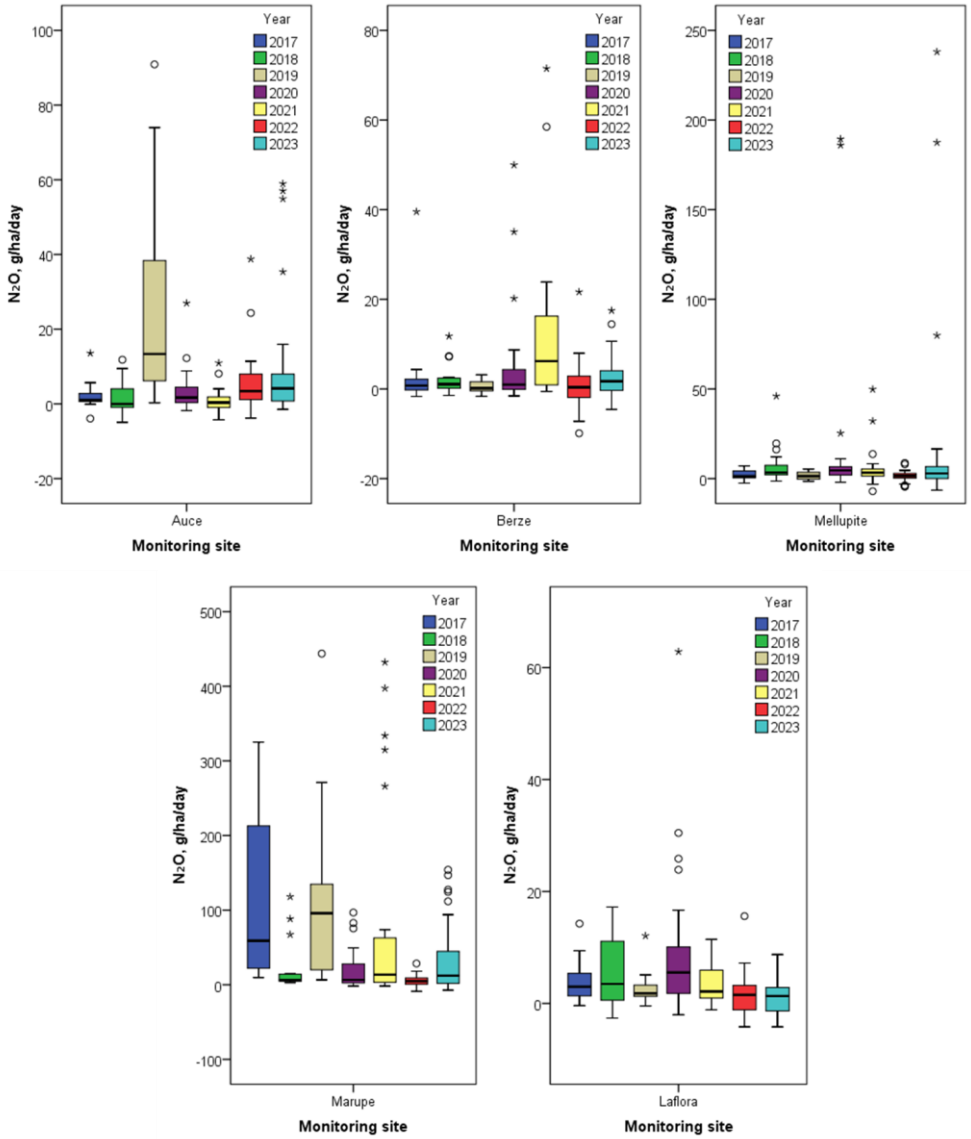


Figure 4. N_2O emissions at five monitoring sites in the period from 2017 to 2023.

Statistically significant differences in N_2O emissions from soils have been observed between Marupe and the other measurement sites ($p<0.05$), as well as between Berze and Mellupite ($p=0.044$). The difference between Marupe and the other measurement sites indicates significant variations in N_2O emissions from soils. This can be attributed to the intensive tillage and agricultural production practices on organic soils at the Marupe measurement site. At the Laflora measurement site, the soil cultivation and agricultural production practices are extensive, resulting in no significant differences observed between the N_2O emissions from soils at Laflora and the other measurement sites. When comparing across years, significant differences are evident between the average values of N_2O emissions from soil in 2022 and those in 2019, 2020, and 2021 ($p=0.017$, $p=0.001$, $p=0.005$ respectively). In 2022, the average N_2O emission value is 3.61 g N_2O ha^{-1} day^{-1}, whereas in other years, it ranges from 13.20 to 60.33 g N_2O ha^{-1} day^{-1}.

From 2017 to 2023, soil temperature has shown a positive effect on CO_2 emissions from soil, while soil moisture has been found to increase N_2O, CH_4, and CO_2 emissions from soil. The emission of CH_4 from the soil exhibits a negative correlation with other gases, while the emission of CO_2 from the soil shows a positive correlation with the emission of N_2O from the soil (Table 1). Correlation analysis suggests that soil moisture has a significant influence on the emission formation processes in the soil.

Table 1. Kendall correlation coefficients for the period 2017-2023

Coefficients	Soil temperature, °C	Soil moisture, %	N_2O, g ha^{-1} day^{-1}	CH_4, g ha^{-1} day^{-1}	CO_2, kg ha^{-1} day^{-1}
Soil temperature, °C	**1.000**	-0.034	-0.042	0.009	**0.113****
Soil moisture, %	-0.034	**1.000**	**0.082****	**0.130****	**0.054***
N_2O, g ha^{-1} day^{-1}	-0.042	**0.082****	**1.000**	**-0.057***	**0.092****
CH_4, g ha^{-1} day^{-1}	0.009	**0.130****	**-0.057***	**1.000**	**-0.307****
CO_2, kg ha^{-1} day^{-1}	**0.113****	**0.054***	**0.092****	**-0.307****	**1.000**

** $p<0.01$; * $p<0.05$

DISCUSSION

Our study demonstrates significant variations in GHG emissions from soil across diverse measurement sites over a seven-year span. Notably, CH_4 emissions showed distinct patterns, with Laflora displaying stability and Berze indicating cyclic decreases. Extensive farming in Laflora, particularly bilberry cultivation, facilitated stable soil microbiological conditions, thereby improving CH_4 assimilation, while Mellupite experienced consistent CH_4 emission increases. Statistically significant differences in CH_4, CO_2, and N_2O emissions between sites and years underscore the influence of meteorological conditions and agricultural practices. The decrease in CO_2 emissions in 2023, resulting from dry and cool conditions, highlights the influence of climate variation on soil microbial activity and organic matter decomposition. Conversely, research by Mühlbachová et al. (2023) suggests that the lowest average CO_2 emissions

occurred during a hot and dry year [11]. Variations in N_2O emissions between Marupe and other sites emphasise the effect of tillage on organic soils, contrasting with stable conditions in Laflora. Correlation analysis highlights the complex relationship between soil temperature, moisture, and GHG emissions, as described in Chalco et al. (2020) [5], underscoring the need for ongoing long-term monitoring to inform effective mitigation strategies in agricultural ecosystems.

CONCLUSION

The emissions of greenhouse gases from soils are closely linked to the microbial activity within the soil, which is heavily impacted by the meteorological conditions of any given year. To discern trends in greenhouse gas emissions associated with particular agricultural practices or soil types, sustained long-term monitoring is essential.

CH_4 assimilation and CO_2 emission observed at the Berze monitoring site are significantly lower from those observed at the other monitoring sites, while N_2O emissions were significantly higher at the Marupe comparing to other monitoring sites. This can be explained by the intensive agricultural activity occurring on organic soil in Marupe.

The results of seven years of measurements demonstrate that CH_4 uptake predominates in both mineral and organic soils utilized in agriculture. Observations suggest that methane uptake remains stable, with mean and median values showing a negative trend, indicating prolonged and consistent methane absorption in agricultural soils. Through further measurements, this aspect, influenced by anthropogenic activities, can be utilized in future evaluations of nitrogen and methane balances in the agricultural sector.

ACKNOWLEDGEMENTS

The research was funded by ‘Assessment of the Impact of Land Reclamation on the Reduction of Climate Change (Flood Risk)’, of the Ministry of Agriculture of the Republic of Latvia.

REFERENCES

[1] EC. Regulation (EU) 2023/857 of the European Parliament and of the Council of 19 April 2023 amending Regulation (EU) 2018/842 on binding annual greenhouse gas emission reductions by Member States from 2021 to 2030 contributing to climate action to meet commitments under the Paris Agreement, and Regulation (EU) 2018/1999. European Commission, 2023, 26.04.2023

[2] EEA. Greenhouse gas emissions from agriculture in Europe. European Environment Agency, 2023. Available from: https://www.eea.europa.eu/ims/greenhouse-gas-emissions-from-agriculture.

[3] Oertel, C., Matschullat, J., Zurba, K., Zimmermann, F., Erasmi, S. Greenhouse gas emissions from soils—A review. Chemie Der Erde 2016, 76 (3), 327–352.

[4] Wilson, D., Blain, D., Couwenberg, J., Evans, C.D., Murdiyarso, D., Page, S.E., Renou-Wilson, F., Rieley, J.O., Sirin, A., Strack, M., Tuittila, E. S. Greenhouse gas emission factors associated with rewetting of organic soils. Mires and Peat, 2016, Volume 17, Article 04, p. 1-28.

[5] Chalco Vera, J., Curti, R. N., Acreche, M. M. Integrating critical values of soil drivers for mitigating GHGs: An assessment in a sugarcane cropping system. Sci. Total Environ 2020, 704, 135420, https://doi.org/10.1016/j.scitotenv.2019.135420

[6] Shakoor, A., Shakoor, S., Rehman, A., Ashraf, F., Abdullah, M., Shahzad, S. M., et al. Effect of animal manure, crop type, climate zone, and soil attributes on greenhouse gas emissions from agricultural soils—A global meta-analysis. J. Clean. Prod. 2021, 278, 124019. doi:10.1016/J.JCLEPRO.2020.124019

[7] Bickel, K., Richards, G., Köhl, M., Vianna, Rodrigues, R.L. 2006 IPCC Guidelines for National Greenhouse Gas Inventories, Chapter 3: Consistent Representation of Lands.

[8] Grinfelde, I., Valujeva, K., Zaharane, K., Berzina, L. Automated cavity ring down spectroscopy usage for nitrous oxide emission measurements from soil using recirculation system. Engineering for Rural Development, Jelgava, Latvia, 24.-26.05.2017, DOI: 10.22616/ERDev2017.16.N235

[9] Valujeva, K., Pilecka-Ulcugaceva, J., Skiste, O., Liepa, S., Lagzdins, A., Grinfelde, I. Soil tillage and agricultural crops affect greenhouse gas emissions from Cambic Calcisol in a temperate climate, Acta Agriculturae Scandinavica, Section B — Soil & Plant Science 2022, 72:1, 835-846, DOI: 10.1080/09064710.2022.2097123

[10] Wagner, S.W., Reicosky, D.C., Samuel Alessi, R. Regression models for calculating gas fluxes measured with a closed chamber. Agron. J. 1997, 89, 279-284.

[11] Mühlbachová G, Růžek P, Kusá H, Vavera R. CO_2 emissions from soils under different tillage practices and weather conditions. Agronomy. 2023; 13(12):3084. https://doi.org/10.3390/agronomy13123084

STATISTICAL AND CHEMICAL ANALYSIS OF SOIL POLLUTION FROM KOSHTOVA LANDFILL MITROVICË - KOSOVO

MSc. Bahri Sinani[1],
Prof. Dr. Blazo Boev[2],
Prof. Dr. Arianit Reka[3],
Prof. Dr. Ivan Boev[2],
Berat Sinani[4],
MSc. Elida Lecaj[5],
MSc. Adelina Haskaj[5]
1 Directorate of Environmental and Forest Protection - Municipality of Mitrovica, **Kosovë**
2. University "Goce Delcev", Faculty of Natural and Technical Sciences, **North Macedonia**
3. Faculty of Natural and Technical Sciences, State University in Tetovo, **North Macedonia**
4. University "Isa Boletini", Faculty of Geo-Science, Mitrovicë, **Kosovë**
5. Alma Mater Europaea Campus College "REZONANCA", Prishtine, **Kosovë**

ABSTRACT:
The purpose of this research is to conduct a research on soil pollution in the village of Koshtovë (Mitrovica/Kosovo), from the sanitary landfill, in this landfill all waste from the cities of Mitrovica, Vushtria and Skenderaj are collected.
The growth of population and industry also increases the amount of waste, this study aims to study the level of soil pollution from the sanitary landfill of Koshtova, the village in the western part of the city of Mitrovica.
This area has been clean, by the river Ibër, the construction of the landfill has started to pollute the water flowing from the landfill where the soil is also polluted by this water.
Through this research we have taken 6 soil samples which we have processed, analyzed, from this research we will see a distribution of some polluting elements in this area. Samples were taken at a depth of 25 to 40 cm, in quantities of approximately 200 g, which were placed in Zip bags, writing number of samples, date of sampling, X, Y and Z coordinates in KosovaREF coordinate system, and filling the notebook with the description of the area where it was taken samples.
From the results presented, we see that Pb has a large distribution in this area with an average of 32.68 ppm, as well as Fe has a fairly large distribution with an average of 49775 ppm, which represents a high degree of distribution despite that in the sediments of the river Ibër there is a rather small distribution compared to this. Likewise, the distribution of Cu is quite large and this study shows us that we are dealing with a very serious and dangerous pollution.
So, from this study we can distinguish the degree of pollution, the source of pollution of the river sediment and the soil under the dump where we have a high occurrence of pollution.
Keywords: Waste, Landfill, Heavy Metals, Risk, Public, Koshtova, Kosova

INTRODUCTION

Viewed from a geographical point of view, the landfill is built in the upper part, and in addition to this, any atmospheric changes such as rain, precipitation, winds, etc., will all have their impact and spill over into the surrounding villages, and especially into the Ibër River with in which case they create negligible pollution.

The landfill is located in a more sensitive part, by the river Ibër, as well as less than 50m from the Ibër - Lepenci canal, which supplies drinking water to the region of Mitrovica, Vushtria and Skenderaj, and also to industrial purposes, almost the entire territory of Kosovo is supplied by this canal, which comes from Lake Ujman.

The Koshtova landfill is a regional sanitary landfill that collects waste from the cities of Mitrovica, Vushtria and Skenderaj, unfortunately this landfill has two very high-risk points such as the Ibër-Lepenci Canal, a canal that sends water to the factory water where these three cities are processed and supplied with drinking water as well as the Ibër river, one of the largest rivers of the city of Mitrovica and Kosovo.

So in both directions potential pollution represents a potential risk for a Iber-Lepenc canal and also for soils of Koshtova villages, especially in the windy season, stinks a lot, but the purpose of this study is to see how polluted the land is under the parts of this dump exactly in the direction of the Ibër River. So, this study aims to study soil pollution from the landfill, if there is a soil polluted or not, if there is polluted, at what levels is the pollution, is it within the allowed limits according to the international standards or not.

MATERIALS AND METHODS FOR THIS RESEARCH

In order to carry out this research, it is necessary to take samples and analyze them, due to the short distance from the landfill to the river Ibër, a total of 6 samples were taken since it is a fairly short distance (Fatos Rexhepi – 2010).

Sampling has been done according to all norms and standards necessary for testing, samples have been taken through adequate sampling tools, they have been placed in the bag for taking samples attached with the sample number, sample coordinates and description of the area with necessary information which will help to verify the area.

The samples were sent to the laboratory to be analyzed, where they were first dried at a temperature of 105°C, to remove the presence of water and to dry the samples. After that, the samples were ground in order to analyze them, after grinding the samples were put into bags with maximum care to preserve identification and their contents were sent to be analyzed

X-ray fluorescence (XRF) spectrometry is a well-known, well-established and widely applied technique in the determination of many major elemental compositions of earth materials. XRF confers the ability to analyse solid samples non-destructively through X-radiation (Oyedotun, 2018)

The samples were first analyzed with a hand-held XRF, Handheld Thermo Scientific NITON energy-dispersive X-ray fluorescence (EDXRF) analyzers (“portable XRF analyzers”) are able to perform fast and non-destructive analysis of environmental samples, including soils, dust collected on air monitoring filters or wipe samples, rocks, and metal samples. Providing simultaneous analysis of up to 25 elements, this technique significantly cuts the time required for sample characterization. The instrument can operate in several measurement modes, including bulk sample, thin sample and lead in paint testing (Radu & Diamond, 2009)

After that, they were analysed and processed in Microsoft Excel, also through the statistical tools in Microsoft Excel, the descriptive statistics for each element identified in

this study were found and after that the conclusions and recommendations derived from this research were given (Viola Vambo et al.,)

METHODOLOGY OF SAMPLING

Maintaining and accuracy of data during field work is just as important as the samples to be taken (Zeqir Veselaj, 201). To conduct such research we have done a very detailed study by sampling and analysing, where a total was taken 8 samples as explained in figure 4.

Samples are taken in deepth from 25 to 40cm based on Horizon B standard, samples are added to the Zip Bags, and sent to the laboratory.

All samples were taken and dried at 105°C, after drying they were ground and prepared for chemical and mineralogical analysis (“Milaim Musliu – 2023”).

In the picture below we will present the sampling and analyzing process up to the results which are presented in Fig. 1, based on methodology of sample prepairing (Sinani et al., 2018) .

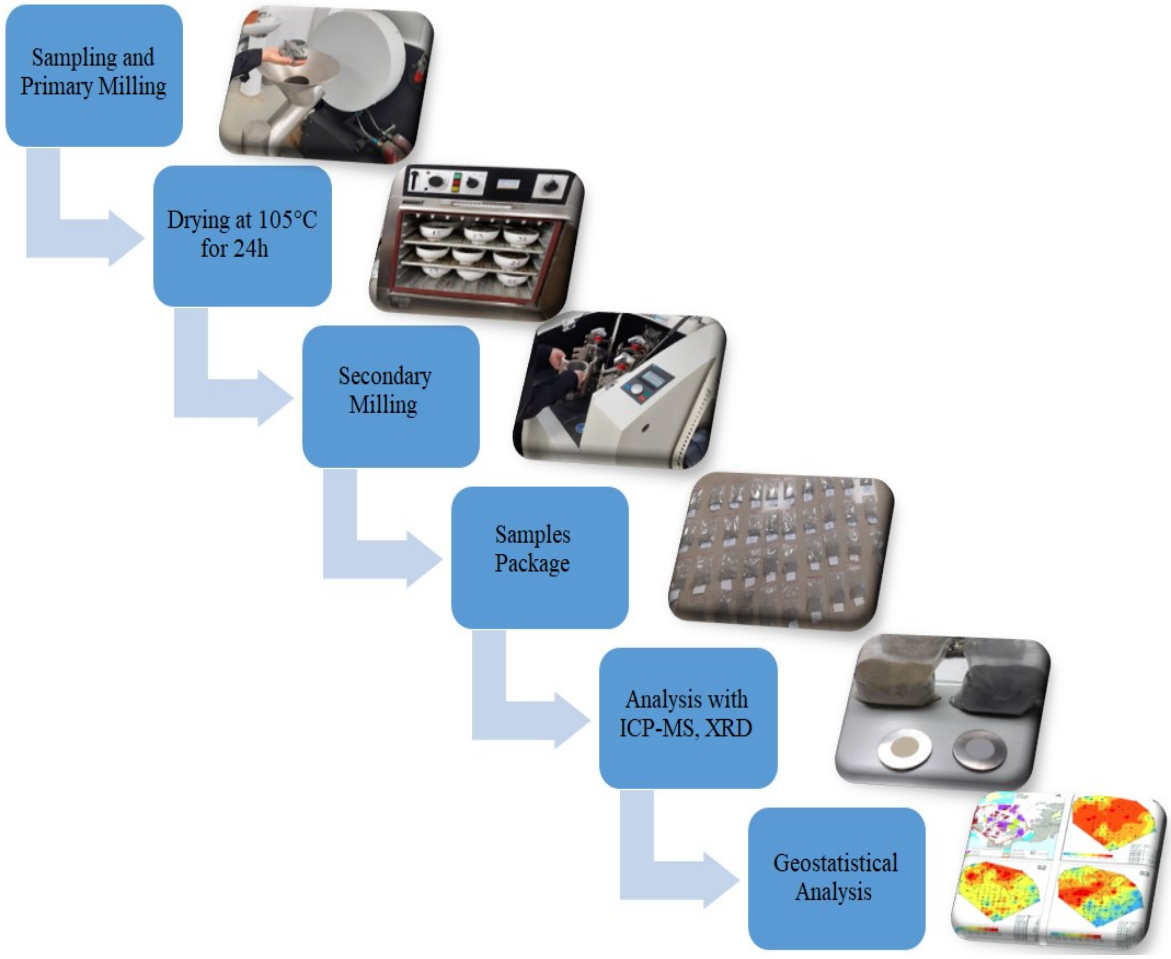


Fig. 1. Methodology of sampling preparation

SAMPLING LOCATION AND ANALYSING

In order to obtain the most accurate results on the impact of landfill pollution on soil and water, we have chosen some key points that will give us the correct impact results. As they are: by the river Ibër, on the restaurants near the river, on the houses of the village of Koshtovë, on the main road to the landfill, points under the water plants as well as on both sides of the landfill.



Fig. 2. Mitrovica Landfill

Evaluation of the impact of landfills on the environment(Vaverková, 2019). Landfill have a very large impact on the process of environmental pollution So, by means of this research, almost all possible points have been touched to highlight the pollution from the Germova landfill in the Koshtovë village of Mitrovica. So, in order to analyse in detail, all the samples were taken, to see every point on the possibilities of changing the physical and chemical parameters (Milaim Musliu – 2023).



Fig. 3. Sampling location

RESULTS AND THEIR DISCUSSIONS

After taking the samples and their processing, analysis, we have extracted the obtained results, which we will present as follows.

Table 1. Results from the samples analysis

Mostra	X	Y	Z	Pb [ppm]	Zn [ppm]	Ni [ppm]	Fe [ppm]	Mn [ppm]	Cr [ppm]	Cu [ppm]
BS1	4747620	7484460	536	33.80	64.40	394.00	23700.00	249.70	4242.00	0.00
BS2	4747514	7484386	531	61.40	167.50	2043.00	45000.00	1059.00	1725.00	16.30
BS3	4747401	7484318	543	36.70	92.40	2273.00	46500.00	5716.00	1672.00	69.30
BS4	4747260	7484255	554	22.20	116.00	2019.00	53000.00	1182.00	1264.00	121.70
BS5	4746960	7484288	576	29.80	60.40	2715.00	59000.00	1964.00	0.00	0.00
BS6	4746802	7484297	602	39.80	77.70	2671.00	55000.00	1318.00	2480.00	71.60
BS7	4746811	7484354	611	18.34	61.30	2041.00	68000.00	1276.00	1675.00	129.30
BS8	4746811	7484469	614	37.70	111.90	1490.00	48000.00	933.30	1554.00	143.20

Now, after the presentation of the results, we will do a short statistical analysis related to the detected parameters, thus elaborating whether their distribution is in the limited ranges or not. There are a large number of statistical and geostatistical methods for their analysis, but in particular are the methods of descriptive statistics ("ESS L.L.C - 2022"). Statistical methods have been widely applied to interpret geochemical data sets and define anomalies (Kastrati P et al., 2023).

Descriptive statistics and appropriate visual representations of scores are important for all test developers, whether they are experienced testers working on large-scale projects, or novices working on small-scale local tests. Many teachers put in charge of testing projects do not know why they are important, however, and are utterly convinced that they lack the mathematical ability to address the matter anyway (Carr, 2008).

In the table presented below we have the descriptive statistics for each analyzed element.

Table 2. Descriptive Statistics for each analyzed element

Numri	8	8	8	8	8	8	8
Minimumi	0.00	60.40	394.00	23700.00	249.70	0.00	0.00
Maksimumi	61.40	167.50	2715.00	68000.00	5716.00	4242.00	143.20
Shuma	261.40	751.60	15646.00	398200.00	13698.00	14612.00	551.40
Mesatarja	32.68	93.95	1955.75	49775.00	1712.25	1826.50	68.93
Devijimi Standard	17.34	36.93	742.92	12936.85	1685.77	1197.95	58.83
Varianca	300.61	1364.19	551936.79	167362142.86	2841836.50	1435084.57	3460.73

Based on the table presented above, we see that almost all elements exceed the allowed values in the research area. Prandaj, this area requires special treatment and study.

CONCLUSSIONS AND RECCOMENDATION

The presence of heavy metals has been shown by sampling in the Municipal Warehouse in Germove, such as lead (Pb), zinc (Zn), nickel (Ni), iron (Fe), manganese (Mn), chromium (Cr) and copper (Cu).) in addition to their presence can have different implications, depending on their concentrations and the context of the location.

Lead (Pb): Lead is highly toxic and is often associated with contamination from discarded materials, old paint, batteries, and electronic materials that are dumped in that landfill.

Zinc (Zn): Zinc is essential for plant growth in small amounts, but is highly reactive and toxic in high concentrations.

Nickel: Nickel is commonly found in this environment due to the deposition of metal parts containing Zn, such as metal coatings and battery production.

Iron (Fe): Iron is naturally abundant in soil due to the geological composition of the terrain and the amount of deposited material.

Manganese (Mn): Manganese is also an essential natural element, but in these cases it exceeds the values due to the deposition of materials that have Manganese.

Chromium (Cr): In our case, coma can be presented to us by natural causes because half of the landfill area is built in ultrabasic formations with fine chromium presence, but we also have amounts of waste with the presence of chromium.

Copper (Cu): Copper is another essential trace element for plants and animals, but high levels can be toxic. The increase in copper in this landfill comes as a result of agricultural waste (eg pesticides).

Based on the data obtained from going out into the field and taking samples, the current condition of the field as well as the results obtained from laboratory analyses, we see that the area is quite contaminated.

In the whole area we see that we have soil pollution and this is a consequence of not treating the water properly, the flow of polluted water has caused the soil to become polluted as shown in the diagrams above.

During the preparation and testing, we went in the direction of the water flow in the landfill, where the pollution of the soil and water becomes higher as we approach the landfill, but also the smell of the air is felt to a great extent. , indicating the high degree of pollution.

Also, in addition to these, a skin burn was observed during sampling, which also shows the high degree of pollution and the problems that can be presented to the inhabitants of that region during the cultivation of their lands and daily life in the lands of theirs. gardens and yards.

REFERENCES

[1] Carr, N. T. (2008). Using Microsoft Excel® to Calculate Descriptive Statistics and Create Graphs. Language Assessment Quarterly, 5(1), 43–62. https://doi.org/10.1080/15434300701776336

[2] Oyedotun, T. D. T. (2018). X-ray fluorescence (XRF) in the investigation of the composition of earth materials: a review and an overview. Geology, Ecology, and Landscapes, 2(2), 148–154. https://doi.org/10.1080/24749508.2018.1452459

[3] Kastrati P .Gashi A (2023). Determining the composition of types of municipal waste through physical analysis of waste in the municipality of Pristina, Gjilan, Prizren and Gjakova

[4] & Diamond, D. (2009). Comparison of soil pollution concentrations determined using AAS and portable XRF techniques. Journal of Hazardous Materials, 171(1–3), 1168–1171. https://doi.org/10.1016/J.JHAZMAT.2009.06.062

[5] Zeqir Veselaj, Behxhet Mustafa2 (2015, June 20). Overview of Nature Protection Progress in Kosovo, DOI 10.3097/LO.201545

[6] Sinani, B., Peci, N., Elezaj, Z., & Sinani, B. (2018). STATISTICAL ANALYSIS OF DISTRIBUTION OF Ag, Au, Pb AND Zn IN TREPCA MINE. International Multidisciplinary Scientific GeoConference: SGEM, 18(1.1), 497–503.

[7] Vaverková, M. D. (2019). Landfill Impacts on the Environment—Review. Geosciences 2019, Vol. 9, Page 431, 9(10), 431. https://doi.org/10.3390/GEOSCIENCES9100431

[8]"ESS L.L.C - 2022" Waste Composition Analysis Report South Mitrovica Municipality

[9] “Milaim Musliu, Astrit Bilalli, Halil Ibrahimi, Nusret Berisha – 2023” Analysis of the Quantity and Composition of Waste in the Peja District, Kosovo. doi.org/10.12911/22998993/166391

[10] “Fatos Rexhepi, Ardian Rugov,Tahir Arbnesh2 - 2010”- Assessment of Heavy Metal Pollution in Ibër River Sediment, Kosova - BALWOIS- 25, 29 May 2010

[11] “Viola Vambo, lsergij Vambolnadeem A. Khannastaran Mozaffariniloofar Mozaffari” - Advances in Energy from Waste, SBN: 978-0-443-13847-8

SECTION

FOREST ECOSYSTEMS

A COMPARATIVE STUDY OF CARBON SEQUESTRATION IN DIFFERENT TYPES OF FOREST

PhD Ress. Nodar Khujadze[1]

Prof. Dr. Lia Matchavariani[1]

[1] Ivane Javakhishvili Tbilisi State University, **Georgia**

ABSTRACT

This study aimed to investigate carbon storage dynamics in pure pine, oak, and mixed forests within a one-hectare area. Tree samples were collected to measure their weight, size, and density. Each type of forest was estimated how much carbon is hold per hectare. The findings revealed significant differences in carbon storage capacities among them. Pure oak forests emerged as the top carbon reservoirs, with 57% of their trees' mass comprising carbon. Pure pine forests followed closely with 51% carbon storage. Interestingly, mixed forests, hosting both pine and oak trees, exhibited a considerable carbon storage potential of about 53%. This finding highlights the ecological advantages of mixed forests over pure ones. Mixed forests stand out for their biodiversity, benefiting from the complementary strengths of multiple tree species. While oak trees tend to store more carbon in their dense wood, pine trees excel in capturing carbon through their rapid growth and expansive root systems. This diverse composition creates a synergistic effect, enhancing carbon capture and storage capabilities within mixed forests. The superiority of mixed forests in carbon storage has significant implications for forest management and climate change mitigation efforts. Protecting and promoting mixed forests can maximize carbon sequestration potential while fostering resilient and sustainable ecosystems. Recognizing the value of mixed forests, policymakers, conservationists, and land managers can prioritize conservation efforts and implement strategies to safeguard these invaluable carbon sinks. In summary, this research highlights the significance of forest composition in carbon storage dynamics. By emphasizing the ecological benefits of mixed forests over pure ones, our study contributes to informed decision-making and sustainable forest management practices aimed at preserving and enhancing carbon sequestration in natural landscapes.

Keywords: Carbon sequestration, Pure forests, Oak forests, Mixed forests

INTRODUCTION

In the present era, climate change and global warming represent pressing challenges for our planet. Experts anticipate a significant rise in average temperatures, ranging from 1.1 to 2.9 degrees Celsius, by the latter half of this century [1]. This warming trend, against the backdrop of natural factors, is significantly provoked also by human activities, notably the extensive use of carbon-based fossil fuels and widespread deforestation, leading to a surge in greenhouse gas emissions, particularly carbon dioxide, and triggering the well-known "greenhouse effect." Numerous high-profile summits and conferences have been convened to address this critical issue [2], including

the landmark Paris Summit of 2015 and the XXI Climate Change Conference, during which participating nations committed to reducing greenhouse gas emissions [3].

The consequences of climate change are observable worldwide, with Georgia experiencing an uptick in extreme weather events such as storms, floods, and landslides, directly linked to climate change [4], [5]. This ongoing warming trend poses a significant threat to forest expansion and diversity, with detrimental effects already underway.

Forests play a crucial role in mitigating climate change, serving as vital carbon sinks and combatting global warming. Expanding forested areas through afforestation and reforestation presents a viable strategy for climate change mitigation [6]. Within afforestation and reforestation efforts, two primary approaches are utilized: pure forests and mixed forests. Mixed forests, characterized by their diverse ecosystem structure and functionality, are considered more resilient than pure forests [7], [8]. However, there remains debate regarding whether mixed forests outperform pure forests in terms of carbon sequestration. Some argue that mixed forests can effectively reduce competition for resources, thereby enhancing carbon sequestration abilities [9]. To study annual carbon sequestration patterns in trees, a case study was also conducted from scots pine monospecific stands and mixed stands with sessile oak [10], etc.

The primary objective of this study is to investigate the differences in carbon sequestration between pure forests (e.g., pine or oak) and mixed forests.

MATERIALS AND METHODS

The study area is located in country Georgia specifically in Samtskhe-Javakheti, Akhaltsikhe municipality, where the city of Akhaltsikhe is the administrative center. The municipality is bordered by Borjomi and Aspindza to the east, Adigeni to the west, Imareti to the north and Turkey to the south. The city of Akhaltsikhe is located at an altitude of 989 meters above sea level (Fig.1), has a cold and temperate climate. Akhaltsikhe has abundant precipitation, notably higher compared to other regions even during the dry seasons, the average temperature in January is -4,2°C and in July 18.6°C. The average annual average precipitation is about 680 mm.

In the Samtskhe-Javakheti region, specifically within the Akhaltsikhe municipality, three distinct plots were carefully selected for study. Each plot represents a different forest type: two plots consist of pure oak (Quercus petraea subspecies iberica) and pine forests (Pinus sylvestris), one plot is characterized by a mixed forest populated by both pine and oak trees of the same species. The geographical data for these plots is summarized in Table 1.

Table 1. The summarized geographical data for study plots

Plot Type	Longitude (°, ', '')	Latitude (°, ', '')	Exposition	Inclination (°)	Altitude (m)
Mixed Forest	41.6077	42.9771	E	7	1559
Pure oak Forest	41.6071	42.9780	E	15	1450
Pure pine Forest	41.6078	42.9769	E	6	1499

This data provides a geographical snapshot of each plot, including longitude and latitude coordinates, exposition, inclination, and altitude. Such information is crucial for understanding the environmental conditions under which each forest type thrives and its potential impact on carbon sequestration capabilities.

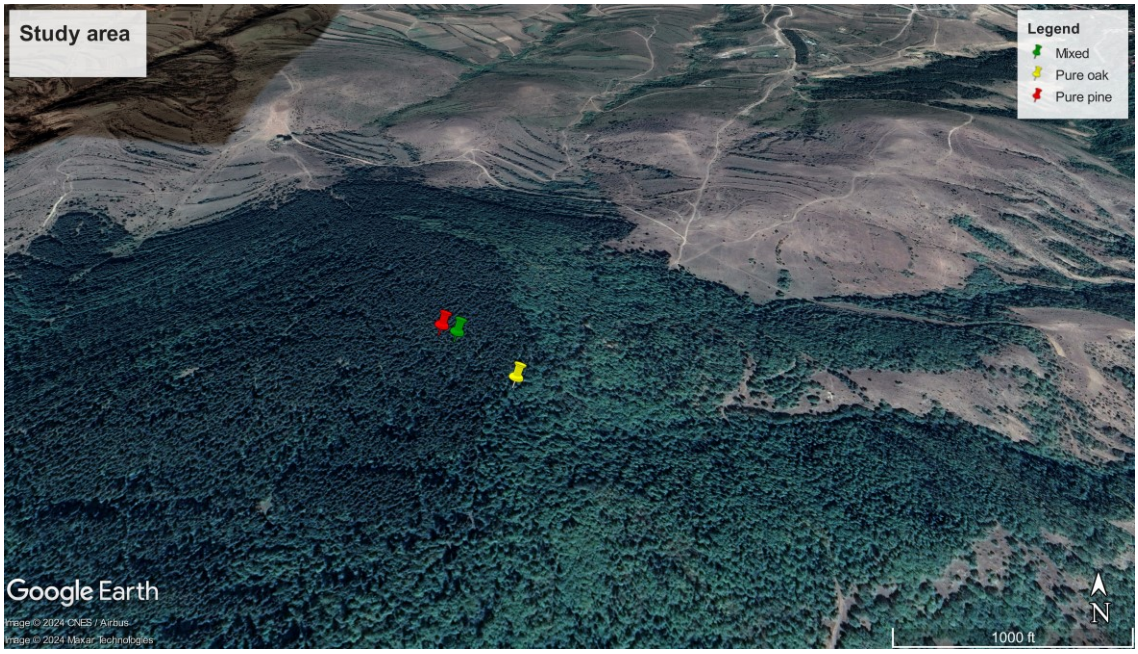


Fig. 1. Study area with the three explored plots located in Akhaltsikhe http://www.earth.google.com [11].

Sample analyzes.

Morphological characteristics of trees were taken from all three plots and listed in data sheet recorded for each tree included tree species, DBH (diameter at breast height), tree height and angle. Mainly, trees whose diameter at breast level was 8 cm or more were included, the reason for this was that the research and selection of materials was guided by the standards adopted by FAO.

In addition, wood samples necessary for further laboratory analyzes were collected using a 5.15 mm increment borer. The comprehensive database obtained from these field measurements forms the basis for a detailed ecological analysis of the study area. The collected wood samples were subjected to comprehensive analysis to understand various parameters such as mass, volume and wood density. The samples were weighed after over-drying at 105 C until it reached constant weight. Mass of the samples was measured using a Lab Analytical Digital Balance Scale, while the volume was determined using the water displacement method. wood density (ρ) were calculated using Equations (1).

$$\rho = \frac{m}{v} \quad (1)$$

Here, P is density; m is oven dried mass; V is volume [12].

To determine the carbon content in the samples, the loss on ignition (LOI) method was employed. According to this method, the samples were subjected to heating at 400°C for a duration of 16 hours. A high-temperature oven, provided by the Science-Research Center of Agriculture, was utilized for this purpose. After heating, the tree cores were weighed to determine any changes in weight. The resulting loss in weight after heating represents the loss of organic matter, primarily carbon, from the burned bore cores.

Stem Volume, Mass, and Carbon Content: Calculation and Analysis.

In our study for finding stem volume was used Bettinger's formula for finding basal area and Leveret's formula for finding volume [13], [14].

Basal area formula (2):

$$G = \frac{\pi \times (DBH/2)^2}{10000} \quad (2)$$

Here, G is basal area at single tree breast height; DBH is diameter at breast height.

Volume formula (3):

$$V = F \times H \times G \quad (3)$$

Here, G is basal area at single tree breast height; F is form factor; H is tree height.

Stem biomass was determined using formula (4):

$$m = \rho * v \ (4)$$

Here, M is weight (kg); V is volume (m^3); P is density (kg/m^3).

The carbon content of the stem was calculated using the formula for finding stem carbon content, we are using formula mentioned bellow (5):

$$C_{stem} = \frac{C_{core}}{M_{core}} * M_{tot} \ (5)$$

Here, C core is carbon content of the core sample; C stem is carbon content of the stem; M core is dry weight of the core sample; M tot is total stem mass.

To estimate the carbon sequestration by the entire tree stem on both total and yearly bases, the carbon content of the stem is multiplied by 3.67 [15].

To assess the carbon storage in one hectare of forest, various calculations and adjustments were made based on the data collected from sample plots within the forest.

Subsequently, an expansion factor was applied to extrapolate the tree count from the sample plot to one hectare, considering the difference in area.

$$EF = \frac{10000m^2}{Area}$$

Additionally, a correction factor was applied to adjust for variations in slope within the sample plots [16].

$$CF = \frac{1}{Cos\alpha}$$

Following these adjustments, the density of trees per hectare was estimated. This involved multiplying the corrected expansion factor by the number of trees counted in the sample plot. The resulting density provided a basis for further calculations.

With the density of trees per hectare established, the total volume of trees per hectare was estimated. This estimation was derived by multiplying the average plot volume by the tree density per hectare. Subsequently, the stem biomass per hectare was determined by multiplying the tree stem volume per hectare by the average plot density.

Finally, the carbon content of the entire hectare was estimated by multiplying the stem biomass by the average carbon content percentage obtained from laboratory analyses of wood samples. This calculation provided insights into the carbon storage potential of the researched forest ecosystem, crucial for understanding its role in carbon sequestration and climate change mitigation efforts.

RESULTS

The comparative study of carbon sequestration in different types of forests—pure pine, oak, and mixed – revealed significant variations in their carbon storage capacities. Here are the key findings shown in Table 2 and 3.

Table 2. Summary of carbon sequestration by study plots.

Forest Types	Average DBH, cm	Average above ground biomass, kg/tree	Average Carbon, %	Average Carbon, kg/tree	Average CO_2 sequestered, kg/tree
Mixed	21.04	169.36	53.67	91.03	334.08
Pine	25.24	274.96	51.71	147.38	540.87
Oak	16.12	85.12	57.10	48.52	178.06

Table 3. Summary of carbon sequestration by hectare.

Forest Types	Tree count per ha	Average Total biomass, kg/ha	Average Carbon, kg/ha	Average CO_2 sequestered, kg/ha	Average CO_2 sequestered, in year, kg/ha
Mixed	720	121671.56	65444.43	240181.07	3431.16
Pine	787	216298.45	115935.98	425485.00	6078.36
Oak	1602	136347.83	77718.26	285226.02	4074.66

These results underscore the importance of forest composition in carbon storage dynamics. While pure oak forests demonstrated the highest carbon storage capacity per tree, pure pine forests exhibited slightly lower but still significant carbon sequestration potential. Remarkably, mixed forests, comprising both pine and oak trees, showcased

considerable carbon storage capabilities, outperforming pure pine forests in terms of carbon retention. This emphasizes the ecological advantages of mixed forests and suggests their potential role in climate change mitigation efforts.

DISCUSSION

The present study examined carbon sequestration in three randomly selected plots with different forest types: Pine, Oak, and Mixed (a combination of pine and oak). The table provided (Table 2;3) illustrates the amount of carbon stored in each forest type. The data suggests that oak trees have a higher carbon-to-tree-body ratio, indicating that they store more carbon relative to their size compared to other tree species. This phenomenon can be attributed to the fact that denser trees tend to store more carbon through absorption and sequestration processes. However, despite the higher carbon concentration in oak trees, the data reveals that trees with higher density have less carbon sequestration. This is primarily due to the significantly higher tree count per hectare in oak forests compared to pine forests. Densely packed forests might compete for resources such as sunlight, water, and nutrients, which can limit their individual growth. This competition can lead to smaller trees and less overall biomass compared to forests with lower tree density where individual trees have more access to resources and can grow larger Similarly, the Mixed Forest, which comprises both pine and oak trees, demonstrates a balance between the two species' characteristics. Furthermore, it's important to acknowledge methodological disparities between our study and similar research in Georgia, particularly in the Aspindza-Sagarejo region for oak and the Samtskhe-Javakheti region for pine [17], [18]. Foreign studies rely on a coefficient to convert tree attributes into carbon content [19], While the previous study relied on a coefficient to convert tree attributes into carbon content, we opted for a more mechanical approach, such as the loss on ignition method. However, it's recognized that utilizing an elemental analyser would offer more precise data. Additionally, the consistency in tree age across studies, with an average age of around 70 years, underscores the comparability of findings. This consistency bolsters the validity of conclusions drawn regarding carbon sequestration dynamics. In summary, while tree density is a significant influencer of carbon sequestration, it's crucial to note that while tree density is a significant factor influencing carbon sequestration, other variables such as tree species, soil conditions, and climate also play crucial roles [20].

CONCLUSION

To calculate the current CO_2 sequestered in trees on the study plots in Akhaltsikhe, a non-destructive method was employed. The diameter at breast height (DBH) and height of trees on three different plots, situated in the same ecological locations, were measured. This allowed for an estimation of the amount of carbon these trees currently store in their stems. The average carbon ratio for all three plots was found to be 51.71% for pine, 57.1% for oak, and 53.67% for mixed forests. Additionally, the carbon sequestration and yearly carbon sequestration per hectare were determined providing a consistent basis for comparison across the different forest types. It's worth noting that factors such as belowground tree roots, leaves, needles, branches, and other components contributing to carbon sequestration were excluded from the analysis due to the immense effort and time required to obtain such data.

REFERENCES

[1] Climate Change 2013: The Physical Science Basis – The Working Group I Contribution to the Fifth Assessment Report of the Intergovernmental Panel on Climate Change (IPCC), Switzerland, pp 27, 2013.

[2] Report of the Conference of the Parties on its Sixteenth Session, Held in Cancun from 29 November to 10 December 2010, Framework Convention on Climate Change, Cancun, Mexico, 2010.

[3] Paris Agreement under the United Nations Framework Convention on Climate Change, Climate Change Conference, Paris, pp 33, 2015.

[4] Barrett S. Climate treaties and approaching catastrophes, J. Environ. Econ. Management 66, pp 235-250, 2013.

[5] Gibson R., Habib M.A., Ziegler A. Reinsurance securitization: the case of natural catastrophe risk, J. Math. Econ. 53, pp 79-100, 2014.

[6] Arora V., Montenegro, A. Small temperature benefits provided by realistic afforestation efforts. Nature Geosci., 4, pp 514-518, 2011.

[7] Pretzsch H., Schütze G. Tree species mixing can increase stand productivity, density, and growth efficiency and attenuate the tradeoff between density and growth throughout the whole rotation. Annals of Botany, 2021.

[8] Rodriguez de Prado D., Vazquez Veloso A., Quian Y.F., Ruano I., Bravo F., Herrero de Aza C. Can mixed forests sequester more CO_2 than pure forests in future climate scenarios? A case study of Pinus sylvestris combinations in Spain. Europian Journal of Forest Research, Springer. Vol. 142(1), pp 91-105, 2023

[9] Chomel M., Desrochers A., Baldy V., Guittonny M., Gauquelin T. Non-additive effects of mixing hybrid poplar and white spruce on aboveground and soil carbon storage in boreal plantations. Forest Ecology and Management, 328, pp 292-299, 2014.

[10] Giberti G.S., Wellstein C., Giovannelli A., Bielak K., Uhl E., Aguirre-Ráquira W., Giammarchi F., Tonon G. Annual carbon sequestration patterns in trees: A case study from scots pine monospecific stands and mixed stands with sessile oak in central Poland. Forests, 13(4), p.582, 2022

[11] Google earth V 7,3. (December 1, 2020). Akhaltsikhe, Georgia. 41° 36’ 30.31” N, 42° 58’ 43.57” W, Eye alt 1000 feet. Maxar technologies 2024, CNES/Airbus 2024. http://www.earth.google.com [April 26, 2024].

[12] Chave J., Sabatier U.P. Measuring wood density for tropical forest trees, 2006.

[13] Bettinger P., Boston K., Siry J., Grebner D. Forest Management and Planning: Second Edition, pp 21-63, 2017.

[14] Leverett R.T. Rejuvenated White Pine Lists and Volume Modeling. November 11, 2008.

[15] Güttler B., Bettin H., Brown R., Davis R., Mester Z., Milton M., Pramann A., Rienitz O., Vocke R., Wielgosz R. Amount of substance and the mole in the SI. Metrologia, 2019.

[16] Kleinn C., Traub B., Hoffmann C. A note on the slope correction and the estimation of the length of line features. Canadian Journal of Forest Research 32(4), pp 751-756, 2002.

[17] Vachnadze G.S., Tiginashvili Z.T., Tsereteli G.V., Aptsiauri, B.N., Nishnianidze Q.G. Carbon stock sequestered from the atmosphere by coniferous forests of Eastern Georgia in conditions of global warming. Annals of Agrarian Science, 2016.

[18] Vachnadze G., Tiginashvili Z., Tsereteli G., Aptsiauri B., Basilidze L. Carbon Stock Sequestered in the phytocenosis of oak forests in Georgia. Annals of Agrarian Science, 2018.

[19] Holtmann A., Huth A., Pohl F., Rebmann C., Fischer R. Carbon sequestration in mixed deciduous forests: The influence of tree size and species composition derived from model experiments. Forests, 12(6), 726, 2021

[20] Osei R., Titeux H., Bielak K., Bravo F., Collet C., Cools C., Cornelis J.T., Heym M., Korboulewsky N., Löf M., Muys B. Tree species identity drives soil organic carbon storage more than species mixing in major two-species mixtures (pine, oak, beech) in Europe. Forest Ecology and Management, 481, p.118752. 2021.

BIOMETRIC MEASUREMENTS AND DEMOGRAPHIC STRUCTURE OF DUCKS HUNTED ON LAKE ENGURE IN THE PERIOD 1993-2022

Dr. Linards Sisenis[1]
Prof. Irina Pilvere[1]
Bc. Toms Endziņš[1]
Ph. D. Baiba Jansone[1]
Dr. Oskars Keišs[2]

[1]Latvia University of Life Sciences and Technologies, **Latvia**
[2]Latvia University, **Latvia**

ABSTRACT

The research aims to identify changes in the biometric measurements and demographic structure of game ducks living on Lake Engure.

Game management in Latvia as well as the entire Northern Europe is an important segment of the economy, which has rich and ancient traditions. Although a small segment of society perceives game management as the killing of animals, which is not the case, it should be understood that it represents an economic activity resulting in limiting the animal population, which can increase rapidly because of anthropogenic factors. Therefore, the functioning of an ecosystem modified by humans is unthinkable today without hunting. Waterfowl hunting is a kind of hunting that is important to hunters, and the hunters are often those who also create artificial nesting sites to increase the population of ducks, thereby increasing the success of nesting in their hunting grounds. Ducks have many natural enemies, as well as there are other abiotic and anthropogenic factors that can sometimes significantly affect the local population of ducks.

The research was conducted in Latvia, on Lake Engure, which is one of the richest lakes in ducks and where research on waterfowl has been conducted for several decades. Censuses of nesting waterfowl on the islands of Lake Engure and on grass and reed swamps as well as other censuses are taken every year. The research analysed hunted waterfowl by taking biometric measurements, identifying their wing length and weight and collecting demographic data on their sex and age. The changes were analysed by the regression analysis method; an independent parameter was the number of days from the beginning of the year, while dependent parameters were wing length and body weight, which were calculated for each hunted waterfowl species during the year/season. To identify the overall health condition of hunted waterfowl, the body mass index was calculated for each species.

The research found that the number of hunted ducks on Lake Engure significantly decreased in the period 1993-2022 ($r=0.54$; $p=0.002$). The number of days from the beginning of the year to the beginning of the waterfowl hunting season did not significantly affect the wing length of ducks living on Lake Engure. For ducks nesting in Latvia on Lake Engure: northern shovelers ($r=0.23$; $p=0.51$), Eurasian teals ($r=0.24$; $p=0.46$), mallards ($r=0.23$; $p=0.46$), garganeys ($r=0.28$; $p=0.47$), gadwalls ($r=0.19$;

p=0.57) and common pochards (r=0.46; p=0.18), the body mass index has not significantly changed in the period 1993-2022.

Keywords: biometric measurements, demographic structure, body mass index, ducks

INTRODUCTION

In Europe and around the world, hunting is a popular way of spending leisure time in nature, with 6.7 million hunters in Europe representing a variety of professions. To become a hunter, the individual needs to undergo training and pass some tests. Although hunting is aimed at limiting the animal population, the role of hunters in nature is also positive. Hunting is a kind of wildlife management, and the hunter is not interested in depleting the animal population. Global progress has a negative impact on nature, yet hunters are those who try to create a better living environment for game animals, which is an important measure for the animal population to be stable or even increase. In many European countries, hunters represent a valuable source of information for scientists, which significantly facilitates the acquisition of data for various research studies on game animals [1], thereby making a significant contribution to counting animal populations, setting hunting limits and other measures [2].

There are various kinds of hunting, and one of them is waterfowl hunting, which is a popular kind of hunting in Europe. Waterfowl hunting involves a variety of tactics, e.g. pass shooting and jump shooting from the boat. A less popular method is to hunt with decoys, but it has been found that usually weaker birds are hunted this way [3].

The beginning and duration of the waterfowl hunting season varies widely in Europe. Latvia is a country where the waterfowl hunting season is one of the shortest – three and a half months [4], in the neighbouring countries – Lithuania and Estonia – the duration is very similar [2]. However, there are countries, e.g. France and the Netherlands, which hunt waterfowl for almost twice as long as in Latvia, namely 6 months, the hunting season begins on 1 August and lasts until 31 January. It is also interesting that the hunting season ends on different dates. For example, in Malta, which has one of the longest hunting seasons, waterfowl are hunted until March [2]. In Latvia, waterfowl hunting is allowed in public and private areas. The relevant regal regulation for hunting in protected areas, such as the water body where this research was conducted, is different, setting various limits from a complete prohibition of hunting to hunting of various intensities.

In Latvia, a total of 16 species of waterfowl are allowed to be hunted, of which four species represent geese: Anser fabalis, Anser albifrons, Branta canadensis and Anser anser. The following 11 duck species may be hunted: Anas crecca, Anas strepera, Anas clypeata, Anas platyrhynchos, Anas querquedula, Anas penelope, Anas acuta, Aythya fuligula, Aythya marila, Melanitta nigra and Bucephala clangula, as well as one non-duck species – Fulica atra [4].

Eastern European duck populations have experienced changes in both distribution and size in recent years, and the reasons for this were global climate change as well as the consequences of land management policies. The availability of suitable habitats is a factor limiting the existence of any species. For waterfowl, habitats are associated with water bodies or wetlands. Wetlands are a habitat that is important for waterfowl to survive, i.e. for nesting, feeding and resting during migration. In many areas, humans have transformed part of wetlands by draining, degrading and destroying them to obtain

agricultural land or land for industrial construction, and this is one of the factors in the decrease in waterfowl species populations [5]. It could be observed that certain species of ducks are particularly sensitive to changes in suitable living environments and the eutrophication of shallow lakes and ponds is a serious problem, which significantly affects the survival of duck species in the region [6]. In Europe, various measures for protecting waterfowl are actively taken; however, there is no unified system that would set, for example, the end of the hunting season and hunting limits by uniformly imposing them on each country. Of course, there is a lot of data on the sizes of nesting waterfowl populations as well as information on hunted waterfowl and nesting success, which have been collected over a long period; however, some data are missing or there are problems with the flow of information, which does not reveal the real situation. There are populations of several species of waterfowl whose size is still unknown. Overall, European duck populations experience changes that are, unfortunately, negative in many areas.

Latvia is located on the Eurasian-African bird migration path, and it is known that some duck species make longer or shorter migrations from nesting to wintering sites and vice versa, which means that if considering this fact from the perspective of hunting, the waterfowl are hunted on their migration path between many European and African countries, thereby posing high risks for overhunting the species. The protection of migratory waterfowl on the Eurasian-African migration route is governed by the Agreement on the Conservation of African-Eurasian Migratory Waterbirds (AEWA) under the auspices of the Bonn Convention, which is legally binding on all the parties involved [7].

Sustainable waterfowl population management is based on data obtained in various ways: 1) censuses of nesting birds; 2) records of wintering birds and 3) records of hunted birds [8]. Nesting bird censuses, which are taken during the nesting period, count nests and nesting pairs. Nest counting is done mainly on the ground. In contrast, nesting pairs are counted from the air over wetlands and other nesting habitats suitable for waterfowl. Wintering waterfowl are counted similarly because there is a high density of waterfowl in their wintering areas, which allows scientists to get more accurate information about the population in an easier way [9]. Hunters count their hunted waterfowl to report the data (species and the number of hunted birds); of course, the data are less reliable as well as incomplete, but this procedure is still in place. It should be mentioned that the reliability of such data might differ, depending on the country. In Denmark, for example, hunters are obliged to send in bird wings [8], while in Latvia the number of hunted birds by species must be reported [4]. The positive aspect is the comprehensive nature of reported data, i.e. the data, although not entirely accurate, are obtained from different areas, which at least theoretically better indicate the overall situation in regions of different sizes [10].

Another method to mention is bird ringing to obtain data on bird migration as well as their survival abilities. Rings are attached to waterfowl legs. Coloured neck rings are attached to larger waterfowl such as geese and swans, while coloured leg rings are used for ducks; of course, there are also metal leg rings. Information about birds is obtained from the rings during their lifetime or at the end of their lives when they are hunted or found dead [11].

For analysis of the condition of a waterfowl population, the body mass index is widely used in research as an indicator that shows their survival and reproductive abilities as well

as behaviour and also provides the knowledge necessary for wild animal management and nature protection [12]. For birds, the body mass index represents the ratio of weight to beak length or width, leg length, body length, tail length or wing length, which are measured linearly. A wide range of body mass index formulas is used because there is no universal formula that works equally well for all birds. The main factor that determines the best formula is the size of the bird. The most popular formula for calculating the body mass index for waterfowl is the ratio of weight to the length of the wing because it is one of the formulas resulting in the highest correlation coefficient [13]. The body mass index as an indicator employed in research on waterfowl populations or individual waterfowl allows for a better assessment of their physical characteristics as well as the overall condition of their health. Of course, there are a number of factors affecting the body mass index, e.g. feeding conditions, precipitation, air temperature, the season, diseases etc. [14]. Interestingly, the body mass index changes over time and across areas for each species, depending on sex and age, because of the usual order in nature, i.e. nesting and migration, but mainly due to the change of feathers.

The reproductive success index, which is the ratio of young birds to adult females, is also used to analyse the condition of a bird population. This indicator shows the reproductive output and the survival of waterfowl up to the time of being flight-capable in autumn [15].

MATERIALS AND METHODS

Lake Engure lies in the north-western part of Latvia; the lake and the Gulf of Riga are separated by a strip of dunes about 2 km wide. It is one of the lagoon-type lakes that formed in coastal lowlands and is also the largest lake of this type in Latvia. The area of the lake is 3500 ha. When a canal was dug in 1842 to connect Lake Engure and the Gulf of Riga, the water level in the lake decreased by about one meter and fifty centimetres, while in some areas the water line receded by three kilometres, forming vast meadows where livestock can graze. The lake has nine large and small islands, as well as grass and reed swamps, which create particularly favourable conditions for nesting birds. The lake is shallow, on average 0.4 m deep (the deepest level is 2 m), which is a very good feeding ground for both waterfowl and waders. Migratory birds also use the lake for feeding and recreation during their migration from nesting to wintering grounds. Since there are not many such habitats in Latvia, the nature park Lake Engure was established in 1998.

The data used by the research were collected in the period from 1993 to 2022 as part of the census of waterfowl hunted in the coastal lakes of Latvia as well as in the ecosystem of the largest lake in Latvia – the Lubana wetland. Full-time and freelance employees from the Institute of Biology of the University of Latvia take part in counting waterfowl, which is done on the opening day of waterfowl hunting and the day after it, i.e. for two days, as approximately 70% of the data registered in the season are obtained on the first two days after the opening of the hunting season. The rest of the data are collected later during the hunting season by hunters themselves according to the public monitoring manual, and the data are submitted throughout the waterfowl hunting season.

Since the lake is a protected area, hunting takes place in areas where it is allowed and only lead-free ammunition is used. Although access to the lake is possible in several places, hunters enter the lake from boat piers, where they return after the hunt. Both the biometric and demographic parameters of birds hunted by hunters are recorded: the species and sex, as well as some measurements are also taken: wing length and weight. In addition, the following data are recorded: the number of hunters in the boat, whether a hunting dog was used for hunting, as well as whether there were ducks that had not been found after the shot and had fallen into the vegetation. The data on each hunted bird are recorded in a registration card for hunted waterfowl (Table 1).

Table 1 **Registration card for hunted waterfowl**

Species	Age	Sex		Wing length, mm	Weight, gr	Number of hunters	Dog
		♂	♀				
Anas platyrhynchos	young	X		275	1300	2	no
Anas platyrhynchos	old		X	284	1410	1	1

The weight of hunted birds is measured by scales suitable for field use. The measurement accuracy is 10 grams.

The wing length of a hunted bird is measured from the last joint of the unstretched wing to the tip of the longest primary feather. A 300-millimeter ruler with a ninety-degree stop at the zero mark is used for wing length measurements, with the wing being pressed against the ruler to measure its length with an accuracy of 1 mm.

The sex of ducks is identified using wing secondary feathers. If necessary, hunters use a waterfowl handbook which describes differences in plumage between females and males of the particular species.

A feature specific to all goose-like birds – the tips of tail feathers – is used to identify the age of a duck. If the bird is young and hatched in the current year, there are slits and notches at the ends of tail feathers, while if the ends are pointed, the bird is one year older. For birds hunted later in autumn, especially mallards, after the change of feathers, this method is no longer applicable; therefore, the age of a hunted duck is identified using the wing plumage pattern.

To identify the general health condition of hunted waterfowl, a body mass index was calculated for each species according to the following equation:

$$BMI = \frac{m}{wl}, \tag{1}$$

where BMI – body mass index;

m – weight, g;

wl – wing length, mm.

Potential changes in the body mass index for hunted waterfowl were calculated using regression analysis, where the independent parameter was years and the dependent parameter was the body mass index.

Demographic data collected on waterfowl hunted were as follows: species, sex and age. The data were summarized by species, age and sex. To identify the changes in the reproductive output for waterfowl, the reproductive success index R for each species was initially calculated if there were sufficient data. The reproductive success index R was calculated according to the following equation:

$$R = \frac{o}{y}, \tag{2}$$

where R - reproductive success index;

o – number of old females;

y – number of young birds.

The potential changes were determined using regression analysis, where the independent parameter was years, while the dependent parameter was the mentioned reproduction success index. The changes were calculated for each species if sufficient data were available.

The research identified potential changes to biometric measurements, which in this case were the wing length and body weight of hunted waterfowl. The changes were identified using regression analysis, where the independent parameter was the number of days from the beginning of the year, while the dependent parameters were wing length and body weight. The changes were calculated for each of the species of waterfowl hunted during the year/season.

EVALUATION OF RESULTS AND DISCUSSION

In the period from 1993 to 2022, in the first two days of the opening of hunting season, 5063 waterfowls had been hunted, a total of 17 species (Table 2).

Table 2. Age and gender structure of species hunted in a first two days of the opening of the bird hunting season in lake Engure in years 1993 to 2022.

Species	Young birds				Old birds				Total
	Gender			Total	Gender			Total	
	♂	♀	Un-identified		♂	♀	Un-identified		
Fulica atra	1		1285	1286			418	418	1704
Anas platyrhynchos	322	246	8	576	733	164	2	899	1475
Anas crecca	238	163	8	409	142	64	1	207	616
Aythya ferina	181	145	12	338	11	35	1	47	385
Anas clypeata	135	78	3	216	78	38		116	332
Anas querquedula	68	74		142	12	11		23	165
Aythya fuligula	11	22	44	77	10	49	1	60	137
Anas strepera	28	37	1	66	48	14		62	128
Anas penelopegar	11	9		20	17	10		27	47
Anas acuta	20	15		35	1	8		9	44
Bucephala clangula	13	11	6	30				0	30
Total	1028	800	1367	3195	1052	393	423	1868	5063

In the period from 1993 to 2022, a significant reduction of hunted waterfowl can be observed in lake Engure (Fig. 1). This indicates the deterioration of the living environment, the factors affecting it can be various, for example, eutrophication of the water body, the increase in the number of natural enemies (predators, or lack of suitable food. In order to determine the most likely cause, body mass index had been assessed for all the species. It demonstrates significant influence of the species and similar trend (example in Fig. 2): substantial inter-annual variation with notable changes over longer (assessed) time period. Therefore, most likely not the reduced quality of environment, but rather the increase in predator populations has to be blamed for the outcome. This conclusion if further supported by no changes in the index of breeding success.

Results might have been affected by different flight capacity of bird species at the specific days when the opening hunting season is opened each year. However, this statement had been rejected by analysis of wing length at this moment: the number of days between the beginning of the year and the opening of the waterfowl hunting season does not significantly affect this trait of any duck species and they all are able to fly at the time of assessment.

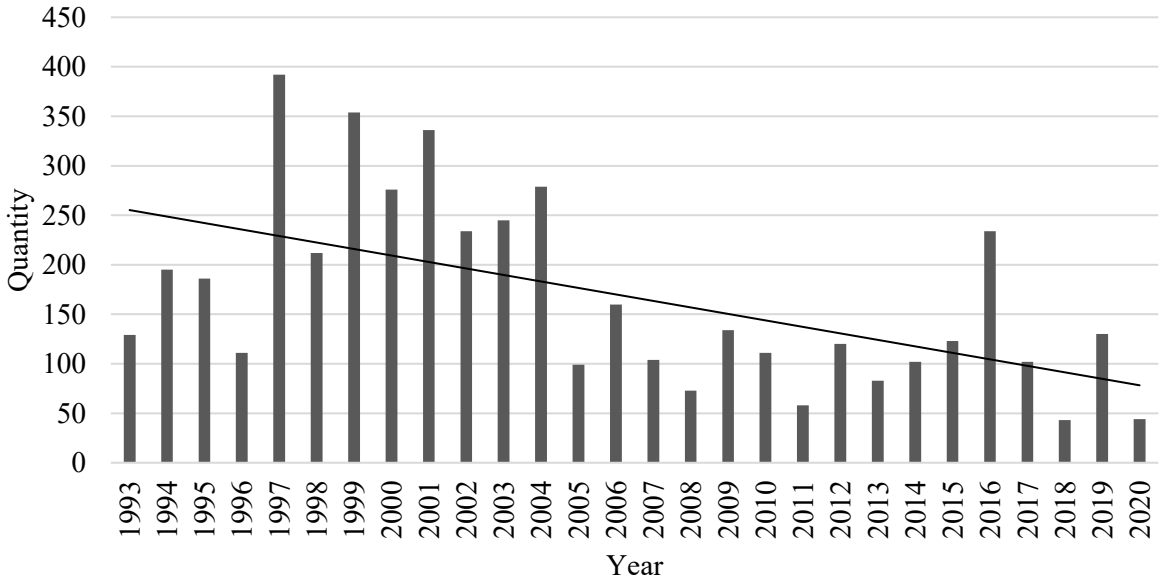


Figure 1. Species hunted in a first two days of the opening of the bird hunting season in lake Engure.

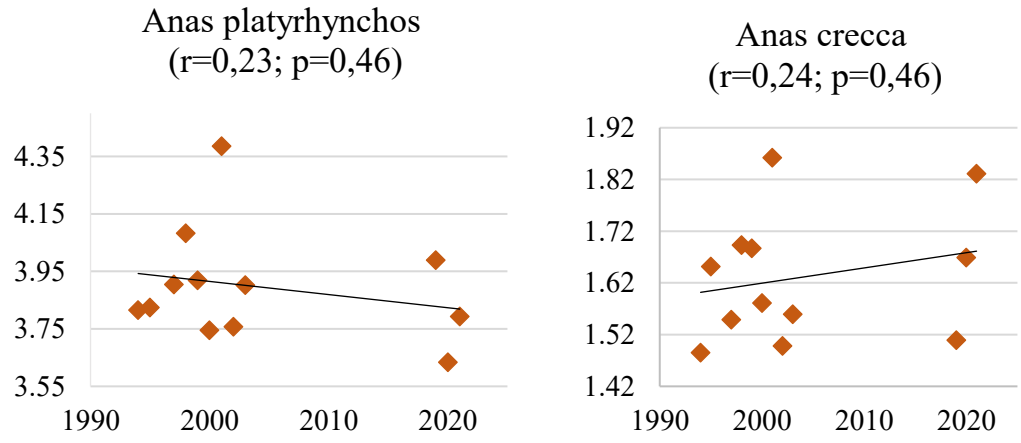


Figure 2. Body mass index of two most common duck species in lake Engure from 1993 to 2022.

CONCLUSION

Body mass index – a measure of health of birds – of assessed species has not significant changed in the period from 1993 to 2022. Even so, the number of ducks hunted in fist two days of the opening of the bird hunting season has significantly (r=0.54; p=0.002) decreased from 1993 to 2022. Combined, this suggests a suitable environment for birds, but increased pressure, most likely from predators, leading to reduced population densities of assessed birds.

REFERNCES

[1] Helle, P., Ikonen, K., & Kantola, A. (2016). Wildlife monitoring in Finland: Online information for game administration, hunters, and the wider public. *Canadian Journal of Forest Research*, *46*(12), 1491–1496. https://doi.org/10.1139/cjfr-2015-0454

[2] Mooij, J. (2005). Protection and use of waterbirds in the European Union. *Beiträge Zur Jagd- Und Wildforschung*, 49–76.

[3] Guillemain, M., Fritz, H., Johnson, A. R., & Simon, G. (2007). What type of lean ducks do hunters kill? Weakest local ones rather than migrants. *Wildlife Biology*, *13*(1), 102–107. https://doi.org/10.2981/0909-6396(2007)13[102:WTOLDD]2.0.CO;2

[4] Ministru kabineta noteikumi Nr. 421, Medību noteikumi, 22.07.2014. Pieejams: https://likumi.lv/ta/id/267976-medibu-noteikumi

[5] Beatty, W. S., Kesler, D. C., Webb, E. B., Raedeke, A. H., Naylor, L. W., & Humburg, D. D. (2014). The role of protected area wetlands in waterfowl habitat conservation: Implications for protected area network design. *Biological Conservation*, *176*, 144–152. https://doi.org/10.1016/j.biocon.2014.05.018

[6] Viksne, J., Svazas, S., Czajkowki, A., Janaus, M., Mischenko, A., Kuresoo, A., & Serbryakov, V. (2010). *Atlas of Duck Populations in Eastern Europe*. Akstis.

[7] *Agreement on the Conservation of African-Eurasian Migratory Waterbirds (AEWA)*. (2018).

[8] Holopainen, S., Arzel, C., Elmberg, J., Fox, A. D., Guillemain, M., Gunnarsson, G., Nummi, P., Sjöberg, K., Väänänen, V. M., Alhainen, M., & Pöysä, H. (2018). Sustainable management of migratory European ducks: Finding model species. *Wildlife Biology*, *2018*. https://doi.org/10.2981/wlb.00336

[9] Elmberg, J., Nummi, P., Pöysä, H., Sjöberg, K., Gunnarsson, G., Clausen, P., Guillemain, M., Rodrigues, D., & Väänänen, V. M. (2006). The scientific basis for new and sustainable management of migratory European ducks. In *Wildlife Biology* (Vol. 12, Issue 2, pp. 121–127). https://doi.org/10.2981/0909-6396(2006)12[121:TSBFNA]2.0.CO;2

[10] Johnson, F. A., Boomer, G. S., Williams, B. K., Nichols, J. D., & Case, D. J. (2015). Multilevel learning in the adaptive management of waterfowl harvests: 20 years and counting. *Wildlife Society Bulletin*, *39*(1), 9–19. https://doi.org/10.1002/wsb.518

[11] Sanders, T. A., & Trost, R. E. (2013). Use of capture-recapture models with mark-resight data to estimate abundance of Aleutian cackling geese. *Journal of Wildlife Management*, *77*(7), 1459–1471. https://doi.org/10.1002/jwmg.59

[12] Frauendorf, M., Allen, A. M., Verhulst, S., Jongejans, E., Ens, B. J., van der Kolk, H. J., de Kroon, H., Nienhuis, J., & van de Pol, M. (2021). Conceptualizing and quantifying body condition using structural equation modelling: A user guide. *Journal of Animal Ecology*, *90*(11), 2478–2496. https://doi.org/10.1111/1365-2656.13578

[13] Labocha, M. K., & Hayes, J. P. (2012). Morphometric indices of body condition in birds: a review. *Journal of Ornithology*, 1–22.

[14] Arsnoe, D. M., Ip, H. S., & Owen, J. C. (2011). Influence of body condition on influenza a virus infection in mallard ducks: Experimental infection data. *PLoS ONE*, *6*(8). https://doi.org/10.1371/journal.pone.0022633

[15] Holopainen, S., Christensen, T. K., Pöysä, H., Väänänen, V. M., Rintala, J., & Fox, A. D. (2018). Associations between duck harvest, hunting wing ratios and measures of reproductive output in Northern Europe. *European Journal of Wildlife Research*, *64*(6). https://doi.org/10.1007/s10344-018-1227-5

ASSESSMENT OF THE QUALITY AND PRODUCTIVITY OF LODGEPOLE PINE GROWN IN THE WESTERN PART OF LATVIA

Prof. Linards Sisenis[1]

Prof. Irina Pilvere[1]

Ph. D. Baiba Jansone[1]

Dr. Dace Brizga[1]

Mg. Edgars Dubrovskis[1]

[1]Latvia University of Life Sciences and Technologies, **Latvia**

ABSTRACT

The research aims to examine the pace of growth of lodgepole pine, the amount of damage caused by biungulates and the quality of trunks for lodgepole pine provenances growing in the western part of Latvia in the areas around Ugale and Kuldiga, identifying the most damage-resistant and promising provenances for cultivation in Latvia.

In Latvia, foresters and plant breeders have been working for years to increase the quality and productivity of local tree species, while assessing various forest stand management patterns and trying to reduce the rotation period of stands. Nowadays, because of climate change, i.e. with the climate becoming warmer, it is clear that in the future in Latvia not only a management strategy for the dominant tree species have to be changed but also the possibilities of introducing new tree species suitable for the conditions in Latvia need to be considered to reduce the forest rotation period. At the same time, introducing new tree species requires considering that the tree species must have economic potential, i.e. the wood has prospects for being processed and consumed (e.g. construction) in the local region, as carbon is sequestrated during the growth of the trees and stays in Latvia. Lodgepole pine is one of the tree species that could have prospects for cultivation on an industrial scale in plantations, which was introduced in Latvia at the beginning of the last century. Based on the experience of Swedish foresters in growing lodgepole pine on an industrial scale in the 1980s, experimental lodgepole pine plantations were established in Latvia by using both domestic seeds and those from the natural range in Canada and the United States, as well as from Sweden.

The research analysed the following tree inventory data collected from the experimental plantations of lodgepole pines at the ages of 27 and 43 years in the western part of Latvia: the height and diameter of the trees and compared the data for Scots pine grown in identical conditions. In addition, the proportions of trees damaged by deer etc. as well as the proportions of trees with multiple tops and branch-to-stem attachments because these defects significantly reduce the chances of producing quality roundwood assortments in the future were analysed for both species. The data were processed using parametric methods.

In an experimental plantation in the area near Ugale, 43-year-old lodgepole pines demonstrated a performance similar to that of Scots pines, with average heights of 18.2 and 18.4 meters and diameters of 19.1 and 19.0 cm, respectively, i.e. the differences were

insignificant. In the plantation near Kuldiga, the differences were found significant, as the average height difference between the species was 1.3 m, while the diameter difference was 1.3 cm. It was concluded that lodgepole pines had lower trunk quality and were more damaged by deer. It was also found that the least productive lodgepole pine provenances were more damaged by deer.

Keywords: lodgepole pine, productivity, trunk quality, damage by deer

INTRODUCTION

The impacts of climate change are increasingly faced by the world, as well as many industries, but especially agriculture and forestry, which are most directly exposed to meteorological extremes [1]. Because of climate change and an increase in the average air temperature during the autumn and spring periods, the vegetation period has overall become longer in Latvia, winters are shorter and warmer [2], which, from the perspective of forestry, is positive because it extends the period of wood production; however, summers have more frequent long periods of drought, alternating with intense rains as well as wind extremes [3]. Although climate change can have a positive effect on forestry, not only the above-mentioned abiotic risks but also biotic risks should be considered, as their nature and intensity could also change as the climate becomes warmer [4,5]. Another problem that foresters faced in Latvia in the 1970s and 1980s and very seriously today is the very high density of large ungulates: Cervus elaphus, Alces alces and Capreolus capreolus, as the animals seriously damage forest plantations and young trees [6]; therefore, the foresters have to seek solutions to this problem: either tree species used less intensively by biungulates for feed need to planted or forest plantations and young stands need to be protected because otherwise, it is impossible to grow forests and produce commercially important roundwood assortments in the future [7].

In Latvia, the most common tree species are Pinus sylvestris, Betula sp. and Picea abies, which are also the most economically significant [8]; however, when establishing forest plantations, depending on the purpose, other tree species, including introduced ones, are also allowed to be planted [9]. In Latvia, forest plantations began to be established in the 1970s-1980s [10,11] for experimental purposes to identify the suitability of foreign species for domestic conditions from the perspective of plant breeding. The species that have been introduced in Latvia not only in experimental plantations but also in economic forests are larch of various species (*Larix* sp.) [9], while from among the Pinus genus, the North American species (lodgepole pine (Pinus contorta Dougl.), variety Latifolia), which has been introduced in many places in Europe, especially in Sweden, was considered to be the most suitable for the conditions in Latvia. The natural range of lodgepole pine is between 30 and 64º north latitude and covers the western part of the North American continent. The initial results of the introduction of this pine species and foreign research proved that in Europe, the variety Latifolia is characterized by a high survival rate, high productivity and slender trunks, as well as resistance to negative biotic and abiotic factors [12]; besides, the species is suitable for cultivation in poor growing conditions. Therefore, Pinus contorta is considered to be a good alternative to the local Pinus sylvestris, as the mechanical wood properties of both species are also similar [13].

Although it is not allowed to grow lodgepole pine in forest stands according to the legal framework of Latvia, it may be done by setting up plantations outside forest lands, e.g. in

unused agricultural lands. The proportion of plantations constantly increases in Latvia because of an increase in the demand for both industrial and energy wood as well as the fact that the timing and volumes of wood harvesting in plantations are not governed by the legislation, i.e. the plantations are not subject to the regulatory requirements for felling trees, which are in force and must be complied with in forest lands. Since research has confirmed the suitability of the species for the conditions in Latvia, as certain provenances demonstrated significantly higher productivity than Scots pine did [12], it is recommended to continue research in the experimental lodgepole pine plantations established in Latvia to analyse not only the pace of tree growth but also the quality of wood. Despite the fact that Latvia is not a large country, the climatic conditions in its eastern and western parts are different, which should also be taken into account concerning forestry [14]. The western part of Latvia has a typical seaside climate, while the eastern part is more continental.

Therefore, the research aims to examine the pace of growth of lodgepole pine, the amount of damage caused by biungulates and the quality of trunks for lodgepole pine provenances growing in the western part of Latvia in the areas around Ugale and Kuldiga, identifying the most damage-resistant and promising provenances for cultivation in Latvia.

MATERIALS AND METHODS

The research collected data from two lodgepole pine plantations located in the western part of Latvia near the urban areas of Ugale and Kuldiga. Both experiments were conducted approximately 40 km from the Baltic Sea.

The experimental plantation near Ugale was established in 1980. An area in the former plant nursery was selected for the experiment. The growing conditions were appropriate for the Vacciniosa forest type; however, since the area has previously been used for plant nursery purposes, the soil has been tilled by applying the continuous ploughing method. The experiment established four Scots pine parcels for control purposes. The total experimental area was 0.5 ha. The experiment used one-year-old lodgepole pine and Scots pine seedlings grown in a nursery, germinated in a greenhouse, and then transplanted into the field. A total of 12 lodgepole pine provenances were used in the experiment, and their characteristics are given in Table 1. The experiment had four replications. The experiment used 10 provenances originating from Canada and the USA (No. 1-10 in Table 1) as well as the planting material of two provenances grown from the seeds of lodgepole pines previously introduced in Latvia. Scots pine seedlings from locally sourced seeds were also used in the experiment.

Table 1**. Toponyms and geographical coordinates of Ugale experiment provenances according to the WGS 84 coordinate system**

No.	Provenance	North latitude	West longitude	Height above sea level, m
1	Teslin, Yukon	60º 15'	132º 50'	750
2	Moberly Lake	55º 40'	121º 25'	750
3	Pink Mountain	57º 00'	122º 32'	900
4	Fort St.James	54º 30'	124º 10'	900
5	Lac le Jeune	50º 29'	120º 29'	1250
6	Falkland	50º 32'	119º 40'	1300
7	Rocky Mountain House	52º 37'	155º 20'	1000
8	Nordegg	52º 20'	116º 25'	1400
9	Monashee	50º 08'	118º 30'	950
10	Smithers	54º 15'	127º 00'	650
11	Skriveri	56º 40'	25º 10'	29
12	Bukulti	56º 55'	24º 25'	12
13	Scots pine	56º 50'	23º 00'	30

The Kuldiga experimental plantation was established in 1995 in forest lands, Vacciniosa forest type, and its area was 0.6 ha. The soil was prepared in strips using a rotary tiller designed for forest soil tillage. The experiment used two-year-old lodgepole pine seedlings, a total of 9 provenances from Canada and the USA, one provenance represented previously introduced lodgepole pines in Latvia as well as one provenance whose origin was unknown. The characteristics of the provenances are given in Table 2. A total of 55 lodgepole pines were planted in each parcel, with a 2 m distance between rows and a 1 m distance between the trees in a row. The experiment had four replications, except for the parcels with lodgepole pines of unknown origin (X), which had two replications. A Scots pine control plantation was established as part of the lodgepole pine experiment.

Table 2. **Toponyms and geographical coordinates of Kuldiga experiment provenances according to the WGS 84 coordinate system**

No.	Provenance	North latitude	West longitude	Height above sea level, m
1	Beatton River	56º 50'	121º 25'	750
2	Dease Lake	58º 15'	129º 50'	850
3	Pink Mountain	57º 00'	122º 30'	850
4	Buick Creek	56º 53'	121º 32'	850
5	Wonowon	56º 36'	121º 30'	850
6	Haifway River	56º 37'	122º 15'	900
7	Bukulti	56º 55'	24º 25'	12
8	Cassior	58º 50'	129º 25'	880
9	Mackensia	58º 50'	129º 25'	880
10	Hudson Hope	56º 02'	122º 45'	650
11	X – unknown origin	-	-	-
12	Scots Pine	56º 50'	23º 00'	30

The data were collected in the autumn of 2023 after the vegetation period, as well as in the experimental area near Ugale in 2006 after the end of the vegetation period, and in the experimental area near Kuldiga in 2012. The following measurements were made for

all trees for each provenance: 1) the height of the tree (m) was identified by a Vertex electronic altimeter. The measurements were made according to the standards adopted for forest inventory with an accuracy of 6 cm; 2) the diameter of the tree was measured at a height of 1.3 m from the neck of the roots by a metal calliper with a centimetre-millimetre scale. The diameter was measured with an accuracy of 0.5 cm, making one measurement and orienting the calliper in the east-west direction; 3) the height of damage caused by biungulates was measured by a metal measuring tape, from the neck of the roots with an accuracy of 1 cm. The height of damage allows the species of biungulates that caused the damage to be identified. If the damage is up to 1 m high, it is caused by Capreolus capreolus, the height of damage caused by Cervus elaphus is on average 1.3 m, while Alces alces can damage the tree up to 2 m high; 4) to calculate the damaged area on a trunk, the height and width of the damaged area were measured with an accuracy of 0.5 cm. If the damage was irregularly shaped, the widest and longest spot was measured because it is the width of the damage that determines how much of the trunk perimeter has damaged the tree's vascular tissue, thereby affecting the flow of nutrients in the trunk. However, the height of damage in the vertical direction affects the growth of the scar and, therefore, the quality of the trunk wood in the future; 5), branch-to-stem attachments were visually identified for all the trees. A branch that grows at a narrow angle relative to the trunk and whose diameter is smaller than the diameter of the trunk is considered a branch-to-stem attachment. The occurrence of branch-to-stem attachments significantly affects the quality of wood in the future because the roundwood assortment with branch-to-stem attachments cannot be used for high-quality sawn timber; 6) the existence of several tops was also identified for the trees. Double tops are roughly the same diameter and length and, just like branch-to-stem attachments, reduce the chance of getting valuable roundwood assortments in the future.

The research calculated the average characteristics for the forest inventory for provenances, the average height and area of damage caused by Cervidae as well as the proportion of damaged trees (%) for provenances, as well as a correlation between a provenance and the incidence of damage. The proportion of trees with double tops and branch-to-stem attachments (%) for provenances as well as a correlation between a provenance and the occurrence of the particular characteristic was calculated. The t-test was used to identify the significance of differences

EVALUATION OF RESULTS AND DISCUSSION

1. Quality and productivity of experimental lodgepole pines in Ugale

An analysis of the average height of experimental lodgepole pines revealed that it was 11.0 m in 2006, while in the autumn of 2023, it was on average 18.2 m. The average heights of Scots pines were 11.7 m and 18.4 m, respectively, performing overall better than the lodgepole pines. It should be noted that the average tree height of none of the lodgepole pine provenances exceeded the height of Scots pines. An analysis of the average annual height increase revealed that for lodgepole pines it was on average 42 cm during the growing season, while for Scots pines it was on average 45 cm per year. However, an analysis of height differences between lodgepole pine provenances revealed that in 2006, the average tree height was between 10.2 m and 11.7 m, and the differences were statistically significant ($p<0.05$), while in 2023 when the forest stand was measured again, it was found that the tree heights were in the range of 17.9-18.4 m, and the

difference decreased between the provenances, although it was still statistically significant ($p<0.05$). The largest annual height increases were found for provenances 6 and 7, 7.9 m and 7.7 m, respectively, and the lowest increase was found for provenance 11.

An analysis of tree diameters revealed that in 2006, lodgepole pines had an average tree diameter of 12.4 cm, with annual growth averaging 0.48 cm per year, while in 2023, the pines had an average tree diameter of 19.1 cm and an average annual increase of 0.45 cm. Compared with Scots pines, the difference in diameter was 0.1 cm and was not statistically significant ($p>0.05$). A comparison of diameter differences between the species revealed that in 2006, Scots pines exceeded lodgepole pines by on average 1.1 cm, and this difference was statistically significant ($p<0.05$). In 2023, however, the average diameter of Scots pines was 19 cm, which did not statistically significantly lag behind lodgepole pines ($p>0.05$). An analysis of average diameter differences for lodgepole pines by provenance revealed that in 2006, the differences were statistically significant ($p<0.05$) in the range from 11.6 cm to 13.5 cm, while in 2023 the average diameters were in the range of 19.1- 19.3 cm, and the difference was not statistically significant ($p>0.05$). The average diameter increase for lodgepole pines was in the range of 5.6-7.4 cm during the period analysed. The largest average increases were for provenances 6 and 8, 7.4 cm and 7.5 cm, respectively, whereas the smallest was for provenance 11 at 5.3 cm.

An analysis of the intensity of damage caused by biungulates to lodgepole pines found that, when the experiment took measurements for the first time, the proportion of damaged trees in 2006 ranged from 19% to 53%, or on average 36%, which could be considered a very high percentage; this might be explained by a very high Cervus elaphus population density in the region. In contrast, the damage to experimental Scots pines was relatively small in 2006, which indicated that the deer chose the introduced tree species for feed, which was not typical for local conditions. It was found that the intensity of damage was significantly different between provenances ($p<0.05$). An analysis of damage caused by biungulates in 2023 found that the intensity of damage decreased and was in the range of 4-41%. This could be explained by the fact that as the tree grows older, the thickness of its bark also increases, and the bark becomes woodier, so the interest of biungulates in eating it decreases. It was found that biungulates repeatedly damaged the same trees that they damaged before ($r=0.78$). Besides, a relatively strong correlation ($r=0.86$) was found between the damaged trees and trees with multiple trunks, i.e. the biungulates more intensively (willingly) damaged the lodgepole pines that had multiple trunks.

An analysis of the quality of lodgepole pine trunks found that trees with branch-to-stem attachments and multiple tops were common for this pine species. The proportion of trees with multiple tops, depending on the provenance, ranged from 11 to 32%, or on average 22%. An analysis of the proportion of branch-to-stem attachments for provenances found that it was in the range of 14-34%; besides, a tree might had both defects: multiple tops and a branch-to-stem attachment. The proportion of Scots pines with multiple tops was 2%, while 14% of trees had branch-to-stem attachments.

2. Quality and productivity of experimental lodgepole pines in Kuldiga

An analysis of changes in tree height in the Kuldiga experiment found that in 2012, the average height of lodgepole pines was 4.1 m, statistically significantly ($p<0.05$) lower than that of Scots pines whose height was 5.3 m, while in 2023 the average height of lodgepole pines was 9.7 m and 11.0 m for Scots pines, the difference was statistically significant ($p<0.05$). This means that in this experiment, the average height of Scots pines increased more than that of introduced lodgepole pines. An analysis of the average increase in tree height by provenance found that at the age of 17, the average height was in the range of 3.4-4.7 m, the difference between provenances was statistically significant (($p<0.05$). A similar trend was also observed in 2023 when the differences were still significant ($p<0.05$) and were in the range of 8.1-9.5 m. The best performance was demonstrated by provenances 5 and 10, with an average height increase of 0.54 m at 0.56 m per year, whereas the lowest increase of 0.48 m per year was found for provenances 2 and 8. Scots pines had an average height increase of 0.56 m per year, similar to that for lodgepole pines.

An analysis of changes in average diameter revealed that the average diameter of lodgepole pines was 4.5 cm in 2012, while in 2023 it was 9.7 cm, which was significantly ($p<0.05$) smaller than for Scots pines whose average diameters were 5.3 cm and 11.0 cm, respectively. In the period analysed, the average height increase for lodgepole pines was 5.2 cm and 5.7 cm for Scots pines, or 0.31 cm and 0.33 cm, respectively, during the growing season. An analysis of differences in average diameter for lodgepole pines found that in 2012, the diameter ranged from 3.5 to 5.1 cm, and the differences were statistically significant ($p<0.05$), thereby lagging behind Scots pines by 0.2 cm. In 2023, the differences in diameter were significant ($p<0.05$) between lodgepole pine provenances, ranging from 9.0 to 10.6 cm and lagging behind Scots pines whose average diameter was 11.0 cm. The largest diameters were found for provenances 7 and 10, 10.2 cm and 10.6 cm, respectively, as well as the average diameter increases of 0.31 cm and 0.32 cm, respectively, during the vegetation period. However, the average diameter of Scots pines was 11 cm, while the average increase in diameter during the vegetation period was 0.33 cm. The smallest diameter and also the smallest increase in diameter were found for provenances 2 and 8, as the average diameter was 9.0 cm, while the increase in diameter was 0.30 cm during the vegetation period.

An analysis of the damage caused by biungulates found that on average, it was more intense near Kuldiga than near Ugale because the proportion of damaged trees was on average 39%, exceeding 30% for most provenances. It could be concluded that a trend was observed that biungulates preferred to eat the trees of less productive provenances. For provenance 2, the proportion of damaged trees reached 60%, it was also very high for provenance 1. The experiment near Kuldiga, just like that near Ugale, found a strong correlation ($r=83$) between the intensity of damage in 2012 and 2023 for the same provenances because as the age of the tree increases, the intensity of damage decreases. An analysis of the intensity of damage to Scots pines revealed that it was minimal, only 3%, in 2012, while in 2023, any damage caused by biungulates to Scots pines was not detected.

An analysis of the proportion of trees with multiple tops in the experiment near Kuldiga found that, compared with that near Ugale, it was similar, i.e. in the range of 14-34% and on average 23%, while the proportion of trees with branch-to-stem attachments varied

from 20 to 34% or on average 27%. For Scots pines, the figures were 2% and 15%, respectively.

3. Assessment of the quality and productivity of Lodgepole pines in the western part of Latvia

The best growth performance was demonstrated by the Falkland and Rocky Mountain House provenances from Canada and the USA in the Ugale experiment and the Hudson Hope provenance from Canada in the Kuldiga experiment. In contrast, the lowest productivity in the Ugale experiment was found for the provenance of local origin, the original seed origin of which was unknown, while in the Kuldiga experiment the provenance Cassior demonstrated the lowest productivity. In the Ugale experiment, both pine species had a similar pace of growth ($p>0.05$); however, if considering the quality of trunks and the intensity of animal damage, local Scots pines were still superior to lodgepole pines. In the Kuldiga experiment, Scots pines demonstrated significantly better growth performance ($p<0.05$) than Scots pines did.

A comparison of differences in height and diameter between the experiments and the two species found that the average diameter and height in the Ugale experiment were similar for both species ($p>0.05$), whereas in the Kuldiga experiment, Scots pines showed superiority over the other species in terms of height and diameter across all the provenances ($p<0.05$). This means there is an opportunity to select lodgepole pine provenances equal to or superior to Scots pine.

An analysis of the proportions of trees damaged by biungulates in both experiments found that the trees of the introduced tree species were damaged significantly more ($p<0.05$). In the Ugale experiment, the proportion of trees damaged by biungulates was found to be 36% in 2006 and 23% in 2023, and the difference between the species was significant, as the proportion of damaged Scots pines in the survey years was 13% and 0%, respectively. A similar situation was also observed in the Kuldiga experiment, as the proportions of lodgepole pines damaged were 39% in 2012 and 28% in 2023, while for Scots pines it was only 3% and 0%, respectively.

An analysis of the height of damage caused by biungulates found that it was in the range of 1.15-1.53 m, which indicated that the damage to the pines was caused by Cervus elaphus, and the calculation revealed that there was no difference in the average height of damage between the two experiments, lodgepole pine provenances and individual trees ($p>0.05$). This indicated that the damage was caused by animals of the same species in both experiments.

An analysis of the damaged area of lodgepole pine bark revealed similar trends in both experiments. The total area of damage to a lodgepole pine, including both old damage and recent damage, ranged from 100 to 1210 cm^2 or on average 720 cm^2. The average area of damage to a Scots pine was 200 cm^2, which was significantly ($p<0.05$) smaller than that for lodgepole pines.

An analysis of the quality of trunks found that the occurrence of multiple trunks and branch-to-stem attachments was similar in both experiments. The proportion of trees with multiple tops was 23% for lodgepole pine, while trees with branch-to-stem attachments represented 26% of the total, as the occurrence of this trait is determined by heredity. For Scots pines, the figures were significantly lower, as the proportion of trees with multiple

tops was only 3%, while the trees with branch-to-stem attachments made up 15% of the total.

CONCLUSION

Overall, the research proved that after considering several biotic and abiotic factors, lodgepole pine could be suitable for being grown in short rotation plantations in the western part of Latvia as energy wood or wood for pulp production by selecting the most productive provenances. However, given the high proportion of double tops and branch-to-stem attachments as well as the interest of ungulates in this tree species as feed, lodgepole pine has no future as an economically valuable tree species to be grown in the current conditions in the western part of Latvia.

REFERENCES

[1] Matisons, R., Krišāns, O., Jansone, D., Jansons, Ā. and Zeltiņš, P. (2024) The genetic and environmental variance of radial increment in Scots pine of south-eastern Baltic provenances in response to weather extremes. Baltic Forestry 30(1), https://doi.org/10.46490/BF719

[2] Kitenberga M., Matisons R., Jansons A., Donis J. (2018). Teleconnection between the Atlantic sea surface temperature and forest fires in Latvia and Estonia. Silva Fennica, 52 (1), article id 7771. 8 p. https://doi.org/10.14214/sf.7771

[3] Donis J., Saleniece R., Krisans O., Dubrovskis E., Kitenberga M., Jansons A. (2020) A financial assessment of windstorm risks for Scots pine stands in hemiboreal forests. Forests, 11, 566; doi:10.3390/f11050566

[4] Bāders E., Jansons, Ā., Matisons R., Elferts D., Desaine I. (2018) Landscape diversity for reduced risk of insect damage: a case study of Spruce bud Scale in Latvia. Forests, 9, 545; doi:10.3390/f9090545

[5] Siliņš I.; Kārkliņa A.; Miezīte O., Jansons Ā. (2021) Trends in Outbreaks of Defoliating Insects Highlight Growing Threats for Central European Forests, and Implications for Eastern Baltic Region. Forests 2021, 12, 799. https:// doi.org/10.3390/f12060799

[6] Prieditis A., Howlett S.J., Baumanis J., Bagrade G., Done G., Jansons Ā., Neimane U., Ornicāns A., Stepanova A., Šmits A., Žunna A., Ozoliņš J. (2017) Quantification of deer browsing in summer and its importance for game management in Latvia. Baltic Forestry, 23(2), 423-431.

[7] Donis, J.; Šņepsts, G.; Zeltiņš, P.; Jansons, J.; Zālītis, P.; Jansons, Ā. (2024) Sawlog Recovery in Birch, Black Alder, and Aspen Stands of Hemiboreal Forests in Latvia. Forests 15, 326. https://doi.org/10.3390/f15020326

[8] Gailis A., Kārkliņa A., Purviņš A., Matisons R., Zeltiņš P., Jansons Ā. (2020) Effect of breeding on income at first commercial thinning in silver birch plantations. Forests 2020, 11, 327; doi:10.3390/f11030327

[9] Jansons Ā., Matisons R., Šēnhofa S., Katrevičs J. Jansons J. (2016) High-frequency variation of tree-ring width of some native and alien tree species in Latvia during the period 1965–2009. Dendrochronologia, 40, 151–158.

[10] Lībiete Z., Matisons R., Rieksts-Riekstins J., Priedītis A., Jansons J., Smilga J., Done G., Jansons Ā. Aboveground biomass equations of 40-year-old Norway spruce in Latvia. Baltic Forestry, 23(2), pp 515-521, 2017.

[11] Vuguls, J.; Dubra, S.; Garanča, A.; Zute, D.; Jansons, Ā. Management of Birch Spruce Mixed Stands with Consideration of Carbon Stock in Biomass and Harvested Wood Products. Forests 2023, 14, 57. https://doi.org/10.3390/f14010057

[12] Jansons A., Sisenis L., Neimane U., Rieksts-Riekstiņš J. (2013) Biomass production of young lodgepole pine (Pinus contorta var. latifolia) stands in Latvia. iForest – Biogeosciences and Forestry, 6, 10-14

[13] Irbe I., Sable I., Treimanis A., Jansons A. (2013) Variation in the Tracheid Dimensions of Scots Pine (Pinus sylvestris L.) and Lodgepole Pine (Pinus contorta Dougl. var. latifolia Engelm) Trees Grown in Latvia. Baltic Forestry, 19(1), 120 – 127.

[14] Lībiete Z., Jansons Ā., Runģis D., Donis J. (2023) Forest resources and sustainable management. In: Fred O. Asiegbu and Andriy Kovalchuk (eds.) Forest Microbiology: Tree Diseases and Pests. Elsevier, pp. 3-32. ISBN 978-0-443-18694-3

FIRE SAFETY IN PEAT EXTRACTION SITES IN LATVIA

Assoc. Prof. Dr. Dace Brizga[1]

Mg. silv.Edgars Dubrovskis

Prof. Dr. Olga Miezīte[2]

Prof. Dr. Linards Sisenis[3]

Mg. Kristīne Kiršbauma [4]

[1; 2; 3;4;5] Latvia University of Life Sciences and Technologies, **Latvia**

ABSTRACT

Today about 10% of Latvia's territory is occupied by peatlands (645,100 ha), but the extraction of peat happens in only 4% (25,739 ha) of the total. In regulatory documents peat bogs are mentioned as having a very high probability of flammability (in the context of climate change and other natural elements: drought, heat, lightning and deliberate or unintentional human activity). This indicates the need to improve fire safety by conducting research and improving regulatory frameworks. The aim of the study was to analyse the impact of forest fires on the forest ecosystem, to find out the causes of peat fires and the possibilities of reducing them. In order to analyse the situation in eight peat objects in Latvia, expert interviews were used as a qualitative data collection method and object evaluation in the context of fire safety. The results of the study show that existing fire extinguishing equipment meets regulatory requirements. On average 1-3 cases of fire occur in facilities every year, which are extinguished by the efforts of facility personnel. The three most important risk factors were found to be careless behaviour by employees and by third parties, and natural ignition of peat dust. Technical measures to minimize risks include monitoring the territory and providing sufficient water resources for more operative action in the event of a fire, including the installation of a deep well water intake point.

Keywords: forest ecosystems, peat fire, risk factors

INTRODUCTION

In Latvia, as well as in the world in general, drastic climate changes are observed - natural elements: drought, heat, lightning and conscious or unconscious human activity-as a result of which the number of fires continues to increase. The impact of fires plays a significant role in forest ecosystems, with special emphasis on coniferous forests. This is evidenced by several studies in Latvia, the main purpose of which was to analyse the effect of fires on the structure of the forest stand and the characteristics of the vegetation succession [1], because as the biological properties of soil at the level of microorganism species and population dynamics change, pest species multiply. Characterizing the soil regeneration and successional vegetation after a fire in boreal and to some extent also hemiboreal forests over several years [2], it was found that habitats and species have

continuously developed and regenerated. In Latvia, peat fires are analysed in the context of forest fires, characterizing *Sphagnos* forests, which occupy 1.4% of the total forest area of Latvia, and which are characterized by a peat layer at least 30 cm thick and an unsuccessful regime of soil moisture and aeration. The publication [3] states that as a result of fires, trees wither and fall two or three years after burning, but natural regeneration with pubescent birch (*Betula pubescens Ehrh*.) is allowed. A similar study [4] indicated that fire is extinguished in drained bogs and peat fields faster and more easily due to better access. There, fire ignites quickly and does not burn deeply (only 2-3 cm). Groundwater levels also affect the spread of fire. Burning and smouldering at the deepest layers of peat (up to 50 cm deep) occurs less often and usually in bogs with a low groundwater level. However, scientists have pointed out that each bog and peatland is different, so individual surveys and research are required. An extensive study [5] concluded that the activity of forest fires in the European boreal zone is still closely related to annual climate variability, which is characteristic specifically of April and May with a significant positive correlation (r=0.53). The study [6] mentions human-caused risk factors (for example: burning grass, careless handling of fire), as fire-increasing risk factors in the boreal region, regardless of climate change. The 2020 Order of the Cabinet of Ministers of Latvia No. 696 "Guidelines for sustainable use of peat 2020-2030 for the year", spells out that swamps or peatlands play an important role in the national economy and occupy 10% - 15% of Latvia's territory (6782 km2 - 9700 km2) [7], which indicates the need to attend to and prevent the destructive effects of fires on the forest ecosystem in a timely manner. The aim of the study was to analyse the impact of forest fires on the forest ecosystem, to find out the causes of peat fires and how to reduce them.

MATERIALS AND METHODS

As part of the study, the influence of climatic conditions on the forest ecosystem was analysed, as well as statistical data on the causes of fires in Latvia.

The circumstances in 8 peat objects located in different regions of Latvia were surveyed and analyzed: Pierīga, Zemgale, Vidzeme, Latgale, with a combined mining area of over 100 to 1000 ha. An expert interview and data analyses were conducted with the aim of finding out the impact of climate change on the forest ecosystem and the possibilities of mitigating the impact of risk factors caused by fires.

In order to conduct an in-depth study, 5 experts were interviewed (Table 1), who are identified with codes for the purpose of anonymity [8].

Table 1**. List of experts**

Experts	Position, scope	Length of service, years	Education
A	Ensures and monitors fire safety measures at the peat facility. Consultant or author of several studies related to forest fire safety.	13	Higher
B	Manager of the peat facility and responsible for fire safety	16	Higher
C	Ensures and monitors fire safety measures at the peat facility	17	Higher
D	Ensures and monitors fire safety measures at the peat facility	11	Higher
E	Ensures and monitors fire safety measures at the peat facility	10	Higher

RESULTS AND THEIR ANALYSIS

Analysing statistical data [9] for the period from 2018 to 2022 (Table 2), it was concluded that the largest area burned in 2018. Also in that year the most destructive fire in recent years, "Lielsalas purvs", broke out in Valdgales Parish of Talsu County, and also hit the "Stiklu Purva" nature reserve. On the other hand, analysing the number of forest fires, it can be seen that 2018 was also the year with the highest number of forest fires overall in Latvia. Analysing the causes , it became clear that in 2018 "other" fires predominated, which in this specific case are related to the fire in the peat deposit "Lielsalas purvs" and in the nature reserve "Stiklu purvi", while the second leading cause of forest fires was the careless actions of forest visitors. Although the number of fires tends to decrease after that year, the statistical data of 2022 indicate that the main cause for the fires cannot be determined.

Table 2. Forest fires in Latvia in 2018-2022

Causes of forest fires	Number of fires					Area of fires, ha				
Year	2018	2019	2020	2021	2022	2018	2019	2020	2021	2022
Arson	31	48	25	275	19	12.2	42.7	10.2	6.6	20.5
Careless handling of fire by forest visitors	281	330	174	15	130	187.0	182.5	119.6	155.6	118.8
Those related to human economic activity	23	59	27	30	22	14.2	74.6	19.5	30.0	13.2
Others (including power line short circuits, caused by lightning)	504	28	15	133	22	2529.7	10.6	6.5	15.7	8.6
The reason for the emergence cannot be determined	0	495	287	13	198	0.0	257.9	76.5	297.3	59.9
Total	972	1110	581	466	391	2863.9	821.7	309.0	505.2	220.9

The successful organization of forest fire prevention and extinguishing [6] requires information on the causes of ignition, size distribution and relationship with weather conditions. In order to clarify this information, in the fall of 2022 a survey of 8 facilities and 5 face-to-face expert interviews were conducted, in which competent specialists of peat facilities were interviewed in order to find out the main causes of fires.

When surveying the peat objects, it became clear that the minimum distance between water intake points is ensured in all objects. A territory survey is carried out in seven objects; in two objects, additional observation is carried out from the fire tower. In three objects, an unmanned aerial vehicle is used as an additional way of surveying. In one facility, the territory is monitored using high-visibility binoculars.

In one of the facilities, to ensure that water does not flow out of the firefighting reservoir, a measure was implemented - covering the water intake area with a film. The technical solution can be seen in Figure 1. In the specific case of water outflow, it is related to the characteristics of the soil in the specific part of the mining facility.



Fig. 1 Water supply solution in special soil conditions.

The main findings that became clear in the expert interviews:

Expert A - natural ignition really is a significant risk factor, so it is necessary to carry out timely assessments of the risk factors of forest fires in order to minimize the impact on the forest ecosystem as much as possible. Meteorological conditions - average air temperature and humidity level play a significant role in the development of fire. Careless handling of a fire by a third party (for example, when moving with a motorcycle or quad bike through the forest or peat mining areas, especially relevant in the Pieriga region) causes peat dust to ignite. The fire spreads in the swampy forests adjacent to the peat fields, as a result of which the entire ground cover is burned.

Expert B – the main causes of forest fires are the careless handling of fire by a third party and natural ignition. Natural ignition can also occur during a lightning discharge; this is a factor that cannot be influenced by human actions. Such a fire occurred in a peat object, the extinguishing work was carried out in the initial stage, and it was successfully extinguished by one's own efforts. If preventive measures for fire localization are not taken in a timely manner, then it will cause damage to the forest ecosystem.

Expert C – the main risk factor for forest fires is the careless handling of fire by a third party, because in logging, including peat objects, if all preventive measures are implemented, the probability is about 1%. When staying in the forest during the high flammability period, all civilians must comply with fire safety requirements in order to reduce the risk of fire and damage to the forest ecosystem.

Expert D – self-ignition of peat dust can be mentioned as one of the risk factors, but this risk factor can be significantly reduced by careful and regular temperature control. With peat fires, an average of 1-3 fires are found every year and are extinguished by direct attack if they occur in peat objects, reducing the impact on the forest ecosystem.

Expert E – as one of the factors, one can mention damage to wiring, which results in a short circuit and a fire, especially in places where logging equipment is operating. If sufficient preventive measures have been taken, peat fires will most often be noticed in their first stage and be immediately extinguished, preventing their further spread.

In the question of fire mitigation options and preventive measures, the experts recommended the following:

- To include an unmanned aerial vehicle equipped with a thermal camera as firefighting equipment in peat objects. The thermal camera provides an opportunity to detect not only ignition, but also to detect whether smouldering of peat (underground peat fire) is still taking place. Unmanned aerial vehicles can be used both for inspection and surveying the territory. The cost of one unmanned aerial vehicle equipped with a thermal camera and made in the EU in the summer of 2022 is on average from 5000.00-6500.00 EUR.
- In peat mining facilities, where the amount of water in the firefighting basins is partially sufficient due to the characteristics of the ground, they should be covered with a special, one-sided film, in order to independently ensure an adequate water level. The average cost of such a 1mm thick film in the summer of 2022 is 8.00-11 EUR/m2
- Evaluate the installation of a borehole as an additional water intake for both fire protection and production purposes, especially in facilities where peat extraction fields border the peat processing plant. The cost of installing a borehole in the summer of 2022 is on average EUR 55-70.00/m, which constitutes the most important overall cost. Agreements with the competent institutions and necessary materials for the installation of a deep well make up the costs of approximately EUR 2376.61

CONCLUSION

As a result of the study, it was concluded that in the period from 2018 to 2022, the number of fires in Latvia had a tendency to decrease, thus reducing the damage caused to the forest ecosystem. When inspecting the peat objects, it was found that the fire extinguishing equipment meets the requirements of the regulatory framework. On average, 1-3 cases of fire are found in facilities every year, which are extinguished by their own efforts. The three most important risk factors are careless behaviour by employees, by third parties, and natural ignition of peat dust. As a preventive measure, monitoring of the territory is implemented in the facilities, and various solutions for securing the water resource are sought for more operative action in the event of a fire. Installation of a deep well as a water intake is possible, its cost depends on the required water flow rate and geological factors - at what depth the well should be installed.

REFERENCES

[1] Kviatkovskis E., Dubrovskis E., Zaļkalns O., Miezīte O. Priežu audžu vitalitāte pēc meža ugunsgrēka sausieņu un slapjaiņu meža tipos dabas liegumā "Stiklu purvi" (Vitality of pine stands after a forest fire in dry and wet forest types in the nature reserve "Stiklu purvi") LU 78th international scientific conference. Environmental science, Paper theses, 2020. (In Latvian)

[2] Freimane L., Čakša L., Kārkliņa A., Elferts D, Bērziņa B. Post fire ground vegetation development over 25 years. Research for Rural Development, 36, pp. 44–50

[3] Miezīte O., Indriksons A., Dreimanis A., Freimane l. The Consequences of the Forest Fire in Sphagnosa Forest Site Type Ecosystem. The sixth international scientific conference proceedings "Rural development 2013", Aleksandras Stulginskis University, 28-29.november, 2013, pp 356-365. https://www.vdu.lt/cris/entities/publication/3ac562dd-c40a-4430-a823-0f6466703f17/details

[4] Silamiķele, I., Kalniņa, L., Ivanovs, N., Purmalis, O., Ozols, V., Ceriņa, A., Krūmiņš, G. Evidence of fires reflected by the changes of peat properties in Saklaura Bog. LU 79. starptautiskā zinātniskā konference, sekcija "Ecosystems and fires", 28.01.2021, pp190-193.
https://www.geo.lu.lv/fileadmin/user_upload/LU.LV/Apaksvietnes/Fakultates/www.gzzf.lu.lv/LU_79_konferece_tezes_kopaa_2021.pdf

[5] Drobyshev, I., Ryzhkova, N., Eden, J., Bergeron, Y., Kryshen, A. Trends and patterns in annually burned forest areas and fire weather across the European boreal zone in the 20th and early 21st centuries. August 2021Agricultural and Forest Meteorology 306, 108467, 15 August 2021.

[6] J Sjöström,·2023, Human activity and demographics drive the fire regime in a highly developed European boreal region, Fire Safety Journal.

[7] Par kūdras ilgtspējīgas izmantošanas pamatnostādnēm 2020. – 2030.gadam. Ministru Kabineta 2020.gada 24.novembra rīkojums Nr.696.

[8] Paura, L., & Arhipova, I. (2002). Neparametriskas metodes: SPSS datorprogramma. Jelgava: LLKC.

[9] PxWeb - Select database. https://stat.gov.lv/lv/statistikas-temas/noz/mezsaimnieciba/tabulas/meu010-meza-ugunsgreku-celoni

MACROMYCETES OF BEECH FOREST IN MTIRALA NATIONAL PARK, GEORGIA

Assoc. Prof. Dr. Inga Diasamidze[1],

Researcher Dr. Gia Bolkvadze[2],

Assoc. Prof. Dr. Natela Varshanidze[1]

Assoc. Prof. Nana Zarnadze[1]

Master's Ress. Nino Varshanidze[1]

[1] Batumi Shota Rustaveli State University, **Georgia**
[2] Phytopathology and Biodiversity Institute, Batumi Shota Rustaveli State University**, Georgia**

ABSTRACT

This review provides an overview of the diversity of macromycetes (fungi with visible fruiting bodies) in Mtirala national park beech forests, highlighting their ecological roles and significance within these ecosystems. Mtirala National Park is a protected area in Adjara region, Western Georgia. It is part of the Colchic Rainforests and Wetlands, a UNESCO World Heritage Site. Mtirala National Park Colchic broad-leaved and mixed forests include sweet chestnut and Oriental beech woods. Mount Mtirala is one of the most humid areas in the country.

The fungal community in beech forests encompasses a wide range of taxa, including edible mushrooms, wood-decay fungi, mycorrhizal associates, and decomposers. Hypsizygus tessellatus (Beech Mushroom), Armillaria mellea (Honey Fungus), and Fomes fomentarius (Tinder Fungus) are among the common species found in these forests, contributing to nutrient cycling and decomposition processes.

Furthermore, mycorrhizal fungi such as Ganoderma spp. (Reishi Mushrooms) and Phellinus spp. (Cracked-cap Polypore) form symbiotic relationships with beech trees, enhancing their nutrient uptake and overall health. The presence of Laetiporus sulphureus (Chicken of the Woods) and Xylaria polymorpha (Dead Man's Fingers) on decaying wood further highlights the dynamic interactions between fungi and their substrates in beech forests.

Understanding the diversity and ecological roles of macromycetes in beech forests is crucial for conservation efforts and sustainable forest management practices. Continued research into these fungi will provide valuable insights into the functioning and resilience of beech forest ecosystems in the face of environmental changes and anthropogenic disturbances.

Keywords: macromycetes, beech forests, Mtirala National Park, biodiversity conservation.

INTRODUCTION

Mtirala National Park(MNP) is a protected area in Adjara region, Western Georgia. It is part of the Colchic Rainforests and Wetlands, a UNESCO World Heritage Site. Mtirala National Park Colchic broad-leaved and mixed forests include sweet chestnut and Oriental beech woods. Mount Mtirala is one of the most humid areas in the country [1]. The pressures exerted by visitors to parks, along with other human activities such as urban growth, logging, and forest fires, can indeed have significant impacts on forest ecosystems, including those dominated by beech trees. These impacts often manifest as habitat fragmentation, alteration of land use patterns, and direct damage to vegetation and soil. The Colchic Rainforests and Wetlands are part of the Caucasus Ecoregion, a global biodiversity hotspot[2,3]. The "System of Biogeographical Provinces of the World" established by Udvardy (1975) [4] does not capture this ecoregion well: Geographically, the Colchic region overlaps with the provinces "Mediterranean Sclerophyll" and "Caucaso-Iranian Highlands" of the Palaearctic Realm, but these categories do not reflect its peculiarities. In the more recent classification of terrestrial ecosystems of Olson et al.[5], the Colchic forests are part of the neighbouring ecoregions of Euxine-Colchic Broadleaf Forests and Caucasus Mixed Forests within the Temperate Broadleaf and Mixed Forests Biome of the Palaearctic Realm. Olson & Dinerstein [6] include them in the Global 200 Priority Ecoregion Caucasus-Anatolian-Hyrcanian Temperate Forests. The colcheti refugium, along with the Hyrcanian refugium, represents a unique natural phenomenon in Eastern Eurasia, where thermophilic broad-leaved forests have persisted continuously for hundreds of thousands of years. These factors contribute to the special biological importance of Colchic forests, where the proportion of relict, relict-endemic, and endemic species is particularly high [See fig 1] [7].

MNP beech forests are unique ecosystems characterized by their dominance of beech trees (*Fagus orientalis)* and their associated flora and fauna. These forests are not only significant for their ecological importance but also for their cultural and economic value. Within these ecosystems, macrofungi, also known as macromycetes, play a crucial role in nutrient cycling, decomposition, and symbiotic relationships with other organisms.

The macromycetes of beech forests encompass a diverse array of fungal species belonging to various taxonomic groups, including Basidiomycota and Ascomycota. These fungi exhibit a wide range of forms, colors, and ecological roles, contributing to the richness and complexity of beech forest ecosystems. Some macromycetes form mycorrhizal associations with beech trees, facilitating nutrient uptake and enhancing the trees' resilience to environmental stresses. Others are saprotrophic, decomposing organic matter such as leaf litter and woody debris, thereby contributing to nutrient cycling and soil formation.



Fig.1 Caucasus Ecoregion https://www.caucasus-naturefund.org/ecoregion/caucasus-hotspot/

Understanding the diversity and ecological functions of macromycetes in beech forests is essential for ecosystem management, conservation, and sustainable use. Moreover, these fungi have garnered increasing attention due to their potential medicinal, culinary, and biotechnological applications. Studying their distribution, abundance, and interactions with other organisms can provide insights into ecosystem dynamics and inform conservation strategies aimed at preserving the biodiversity and ecological integrity of beech forests.

In this review, we explore the diversity, ecological roles, and significance of macromycetes in beech forests. We discuss their taxonomy, distribution patterns, habitat preferences, and interactions with beech trees and other organisms. Furthermore, we highlight the importance of preserving these fungi and their habitats and suggest avenues for future research to deepen our understanding of their biology and ecological functions in beech forest ecosystems. By elucidating the role of macromycetes, we aim to foster appreciation for the intricate web of life within beech forests and promote their conservation in the face of environmental change and anthropogenic pressures.

MATERIALS AND METHODS

To study the diversity and distribution of macromycetes species known and their distribution in the beech forest of MNP. The mycological studies were conducted in 2022-2024 with the tracking method, and the permanent study plots, mainly throughout the most widespread local plant communities [8].

- *Fagus orientale* woodland (*Fagetum rhododendronosum)*. The study area is spread across slopes facing the sea, ranging from 600-800 m to 2000 m above sea level. The soil is wetland, and the annual precipitation amount is 3000 mm.

This statement outlines a mycological study aimed at understanding the diversity and distribution of macromycetes species within the beech forest of MNP (presumably a national park).

Study Objective: The primary objective of the study is to investigate the diversity and

distribution of macromycetes species within the beech forest ecosystem. By focusing on macromycetes (large fungi such as mushrooms), the researchers likely aim to explore their ecological roles, interactions, and overall importance within the forest ecosystem.

Methodology: The study utilized the tracking method, which likely involves systematic surveys and observations of fungi within the study area [see Fig 2]. Additionally, the use of permanent study plots suggests a long-term approach to monitoring fungal populations and their changes over time. By selecting study plots within the most widespread local plant communities, the researchers aim to capture a representative sample of fungal diversity across different habitats within the beech forest.



Fig 2. Mtirala National Park is a sample area rich in fungal species.

Temporal Scope: The mycological studies were conducted over the period of 2022-2024, indicating a recent and relatively comprehensive assessment of fungal diversity. This timeframe allows for the observation of seasonal variations in fungal fruiting patterns and provides a snapshot of fungal communities during the study period.

Significance: Understanding the diversity and distribution of macromycetes species in the beech forest is crucial for ecosystem management and conservation efforts. Fungi play vital roles in nutrient cycling, decomposition, and symbiotic relationships with plants, making them integral components of forest ecosystems. By elucidating fungal diversity patterns, the study contributes to broader conservation goals and informs management strategies for maintaining ecosystem health and biodiversity.

The following monographs and keys were utilized for fungi identification: Nakhucrishvili I. [9], "Mushrooms of Georgia Field Guide"[10], Gorlenko [11], and Bolkvadze [12]. Standard methods for studying macrofungi, involving microscopic analyses, were employed for species identification (hand-made sections or squash preparations mounted in water, 3-5% KOH, Melzer's reagent; light microscope). Nomenclature adheres to Nakhucrishvili (2006)[9] and Index Fungorum[13]. Threat categories are classified according to the IUCN Red List. Specimens are deposited in the Herbarium Universitatis BSU.

Habitats of Mtirala National Park: Nearly 100% of the territory is covered by forests and impenetrable thickets. Hypsometrically, the forests are distributed as follows:

a) 500-600 m above sea level: mixed broad-leaved forests of the foothills and hilly belt, known as Colcheti forests;

b) 500 (600)-1000 (1200) m above sea level: chestnut belt (*Castanea sativa* Mill*)* of the lower mountain zone;

c) 1000 (1200 m): the beech belt (*Fagus orientalis* Lipsky,) of the middle and upper (>1500 m) mountain zones.

The largest part of the park's territory is occupied by forest communities dominated by beech. In the lower zone, there are chestnut-beech forests, where *Carpinus caucasica* Grossh, Fraxinus excelsior, and others are frequent in the first tier. In the undergrowth, Colchis bladdernut (*Staphylea colchica* Steven), boxwood (*Buxus colchica* Pojark), pontic rhododendron (*Rhododendron ponticum* L.), yellow azalea (*Rhododendron luteum* C.K.Schneid.), cherry laurel (*Prunus laurocerasus* L), and others are common.

Within the same belt, there are common communities dominated by chestnut, which do not differ much from beech forests in composition.

RESULT

Presented list contains first mycological data from Mtirala National Park beech forest.

In total, 98 taxa of macomycetes (species and forms) including 10 Ascomycota and 88 Basidiomycota were identified.

his analysis provides valuable insights into the fungal diversity and ecological roles within the studied habitat:

Dominance of Saprotrophic Fungi: The fact that saprotrophic fungi comprise 70% of the studied material suggests that the habitat provides ample organic matter for decomposition. This could indicate a healthy ecosystem with a diverse array of decaying plant material such as leaves, needles, cones, and small branches.

Diverse Substratum: The presence of diverse substrata for fungal growth, including leaves, needles, cones, and small branches, further supports the idea of ecological richness and complexity within the habitat. Different fungal species are likely to specialize in decomposing specific types of organic matter, contributing to nutrient recycling and ecosystem functioning.

Mycorrhizal Fungi: The presence of 34 mycorrhizal fungi species indicates a symbiotic relationship with plants, where the fungi form associations with plant roots. Mycorrhizal fungi play crucial roles in nutrient uptake and exchange with plants, contributing to plant health and ecosystem stability.

Parasitic Fungi: The occurrence of three parasitic fungi species highlights potential ecological interactions where certain fungi exploit living organisms for their own growth and reproduction. Understanding the presence and impact of parasitic fungi is essential for assessing ecosystem dynamics and the health of host populations.

Fruit Body Production: The distribution of fruit bodies above ground and on wood suggests different ecological niches and preferences among the fungi. This variation in

fruiting habits likely reflects adaptations to different environmental conditions and substrate availability.

Overall, this analysis underscores the importance of fungi in ecosystem functioning, including nutrient cycling, decomposition, and symbiotic relationships with other organisms. It also emphasizes the ecological diversity and complexity of the studied habitat, as reflected by the diverse array of fungal species and their ecological roles.

CONCLUSION

To summarize, the intricate web of relationships between fungi and beech trees exemplifies the complexity and importance of forest ecosystems. Mycorrhizal fungi like Ganoderma spp. (Reishi Mushrooms) and Phellinus spp. (Cracked-cap Polypore) play a crucial role in enhancing nutrient uptake and overall health of beech trees through their symbiotic associations. Additionally, the presence of saprophytic fungi such as Laetiporus sulphureus (Chicken of the Woods) and Xylaria polymorpha (Dead Man's Fingers) on decaying wood underscores the dynamic interactions and vital processes of decomposition and nutrient cycling in these environments. These fungi not only contribute to the health and sustainability of beech forests but also highlight the interconnectedness of living and decaying components within these ecosystems. Understanding and preserving these relationships is essential for maintaining the ecological balance and biodiversity of beech forests.

In conclusion, understanding the diversity and ecological roles of macromycetes in beech forests is crucial for conservation efforts and sustainable forest management practices. Continued research into these fungi will provide valuable insights into the functioning and resilience of beech forest ecosystems in the face of environmental changes and anthropogenic disturbances.

ACKNOWLEDGEMENTS

Thanks to the BSU University administration for their financial support, as well as the Rustaveli National Science Foundation for the master's grant.

REFERENCES

[1]. https://whc.unesco.org/en/list/1616/

[2]. Mittermeier, R.A., Turner, W.R., Larsen, F.W., Brooks, T.M., Gascon, C. (2011). Global Biodiversity Conservation: The Critical Role of Hotspots. In: Zachos, F., Habel, J. (eds) Biodiversity Hotspots. Springer, Berlin, Heidelberg. https://doi.org/10.1007/978-3-642-20992-5_1

[3]. Williams JW, Jackson ST, Kutzbach JE (2007) Projected distributions of novel and disappearing climates by 2100 AD. Proc Natl Acad Sci USA 104:5738–5742

[4]. Udvardy , M. D. F. 1975 . A classification of the biogeographical provinces of the world . IUCN Oceasional Papers No. 18 ,

[5]. Olson DM, Dinerstein E, Wikramanayake ED, Burgess ND, Powell GVN, Underwood EC, D'amico JA, Itoua I, Strand HE, Morrison JC, Loucks CJ, Allnutt TF, Ricketts TH, Kura Y, Lamoreux JF, Wettengel WW, Hedao P, Kassem KR. 2001. Terrestrial ecoregions of the world: a new map of life on earth. BioScience 51:933.

[6]. Olson, D. M., & Dinerstein, E. (2002). The Global 200: Priority Ecoregions for Global Conservation. Annals of the Missouri Botanical Garden, 89, 199-224. https://doi.org/10.2307/3298564

[7]. https://www.caucasus-naturefund.org/ecoregion/caucasus-hotspot/

[8]. Khvachakidze R. 2009. Sakartvelos mcenareuloba= Vegetation of Georgia / Tbilisi Botanical Garden, ISBN: 9789941012068, Georgian National Academy of Science. 154p

[9].Nakhucrishvili I. 2006 sakartvelos sokoebi=Geoargian Fungy, bunebaprnt.ge Tbilisi ISBN 99940- 856-1-1 256pg

[10]. Mushrums of Georgia The Field Guide.2022, CENN ISBN 978-9941-8-4547-5

[11].Gorlenko M. Bondartsev M. Garibova L.1980. Gribi CCCR =Mushrums USSR. Maskva. 303 pg Russian

[12]. Bolkvadze G, Diasamidze I. 2013 Fungal Biodiversity of Adjara (South Colch) International Caucasian Forestry Symposium, Artvin, Turkey Abstarct book, 61-62pp, 2013

[13] https://www.indexfungorum.org/

NATURAL REGENERATION OF *PINUS SYLVESTRIS* L. FROM SEED TREES IN POOR MINERAL SOILS

Prof. Dr. Olga Miezite[1]

Mg.silv. Edgars Dubrovskis

Dr. Dace Brizga[2]

Mg. Aija Bērziņa[3]

[1,2,3,4] Latvia University of Life Sciences and Technologies, **Latvia**

ABSTRACT

In economic forests, the productivity of forest stands should be increased as much as possible, because the global demand for timber is growing every year. Planted forest trees can be realized using the advantages of selection, naturally regenerated - faster growth can be achieved by improving the growing conditions and limiting factors that reduce or delay the formation of growth. Data were collected in 6-year-old P.sylvestris forest stands Cladinoso-callunosa and Vacciniosa. The plots were established in an area of 17.2 ha (R=7.98 m; S=200 m2), each with a seed tree in the center. The aim of the study is to evaluate the effects of left seed trees and soil preparation in furrows on the natural regeneration of Pinus sylvestris in poor mineral soils Cladinoso-callunosa and Vacciniosa. Pine trees that reached a height of 10 cm were measured for height and annual growth, diameter at the root neck, and a specific location in the plot (in the furrow or in unprepared soil and under or outside the canopy of seed trees). The diameter, height, number of seed trees, as well as the importance of the effect of the crown of seed trees and soil preparation on the natural regeneration of pine were calculated The dendrometric indicators of seed trees were calculated, the significance of the influence of the crown of seed trees and soil preparation on the natural regeneration of pine was determined. It has been established that when restoring a forest stand from left seeds of seed trees, soil preparation is necessary for both Cladinoso-callunosa and Vacciniosa, because the number of trees in the furrows is significantly higher, as well as the annual and average growth of tree height both under the crown of the seed tree and outside it ($p<0.05$) than in untreated soil. Compared to under the crown of the seed trees, the annual height increases of the Scots pine are significantly lower, therefore the seed trees should be cut down sooner up to the age of 6 than in the current practice, so as not to interfere with natural regeneration.

Keywords: preparation of soil, *Cladinoso-callunosa*, *Vacciniosa,* increment, number of trees.

INTRODUCTION

Trees grown from seeds of local origin are the most suitable for Latvia. The Scots pine belongs to the Pinus genus of the Pinaceae family. Only one species of this genus, Pinus sylvestris L., is found in its natural range in Latvia [1], which, according to the data of the State Forest Service, occupies 32% (~0.99 million ha) of the total area of Latvian forests. P.sylvestris is a widespread species in Eurasia, but its natural range can be significantly changed by various risk factors [2]. Current European Scots pine forest management strategies focus on the application of natural regeneration processes to

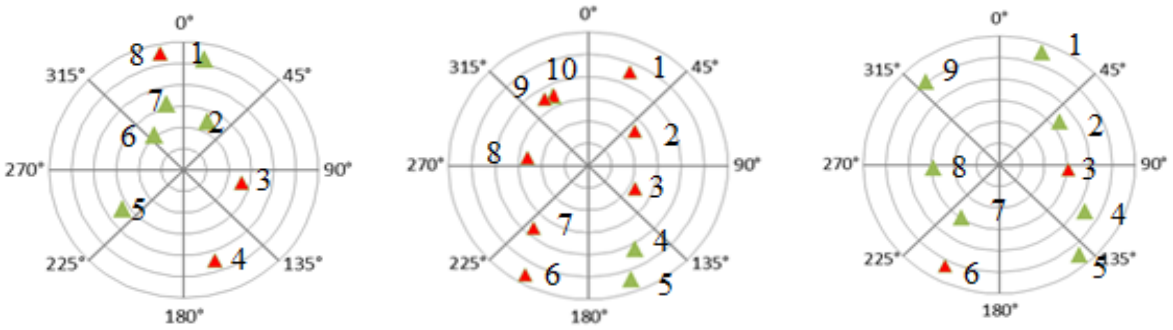
preserve the continuity of the stand structure by maintaining seed-bearing and ecological trees at different densities. Soil scarification can be used to promote the natural regeneration of Scots pine [3]. Natural regeneration is the main regeneration method for Scots pine on poor soils, and is preferred under extreme conditions with high seedling mortality. Scots pines are less tall and have lower retention rates under seed trees than in the open after clearcutting. In clearings, soil scarification in strips has been used to promote natural regeneration. Soil scarification contributes to the increase in the number of trees due to the increase in the area of exposed mineral soil [4], while larger cultivated areas have a negative effect on the annual growth of tree height [5]. The natural regeneration of Pinus sylvestris L. is successful in soils poorer in nutrients, because in fertile soils it cannot compete with evergreens and other tree species [6]. In very poor soils,typical of Cladinoso-callunosa, the natural regeneration of pine is slow, reaching 40% of the desired number of trees within 10 years, while the composition of naturally regenerated stands of Vacciniosa is affected by competition from birch (Betula spp.) Cladinoso-callunosa and Vacciniosa are types of dry mineral soils. The Cladinoso-callunosa stand consists of low-yielding pure stands of IV and V bonita pines, which grow in dry, nutrient-poor sandy soils. The soil is covered by a very thin layer of litter -. poor mineral soil, very acidic sandy soil with good bearing capacity, and pronounced podzolization process. The Vacciniosa stand is made up of grade III pine stands. The soil is poor podzol soils formed from sandy forest with a thin layer of litter. Natural regeneration is influenced by seed yield, type of soil preparation and rainfall: In favorable conditions, 20-30 pcs. ha^{-1} is sufficient for ensuring successful regeneration of seed trees within a year [7]. Under the conditions present in Latvia, a successful natural recovery of seed yield can be ensured within 3-4 years, depending on the pine seed yield [1]. A higher number of seed trees reduces the risk of being damaged or blown over by wind [8], but significantly reduces the growth rate of regenerated trees mainly due to competition for growth resources [9]. Soil preparation also has a beneficial effect on the development of mycorrhizal fungi, which form a symbiosis with plant roots [10]. After successful regeneration, attaining the desired number of trees, it is recommended to remove seed trees as soon as possible, because in the long term, pines growing under seed trees lose one meter in height by 15 years of age [11]. Seed trees are cut down when the average height of the dominant tree species reaches at least 30 cm [5]. On average, 11.7% of regenerated trees are damaged during cutting and removal of seed trees [12]. In order to keep the amount of damaged trees as small as possible, cutting of seed trees should be done before the average height of the regenerated forest stands reaches one meter. Depending on the conditions of a specific place, seed trees can be left in the forest for 8-16 years [5]. The opinions of scientists differ on the period of time for felled seed trees after felling a forest stand. Therefore, the goal of the study was to assess the effect of seed trees and soil preparation in furrows on the natural regeneration of Scots pine (Pinus sylvestris L.) in poor mineral soils Cladinoso-callunosa and Vacciniosa, thereby assessing the possible age at which seed trees can be harvested after forest regeneration.

MATERIALS AND METHODS

The investigated forest areas are characterized by hilly terrain, which has made it difficult to prepare the soil in some places. The arrangement of seed trees is uneven and clustered.

In the *Cladinoso-callunosa* ground cover, sedge (*Calluna vulgaris* L.), common lingonberry (*Vaccinium vitis-idaea* L.), deer cladina (*Cladina rangiferina* L.) and star-shaped cladina (*Cladina stellaris* Opiz) etc. are mainly found. On the other hand, common bilberry (*Vaccinium myrtillus* L.), common lingonberry, cypress heather, various mosses such as Schreber's rust (*Pleurozium schreberi* Mitt.), shiny splendens (*Hylocomium splendens* Hedw.) etc. are mostly found in the ground cover of Vacciniosa. [7]. The data were collected in *P.sylvestris* forest stands *Cladinoso-callunosa* and *Vacciniosa* in the Vidzeme region of Latvia, which have naturally regenerated from the seed trees left after soil scarification in the furrows. In the forested area, all seed trees are listed, measured and their location determined. Sample plots have been set up for the assessment of regeneration (hereinafter referred to as PL). Their location is selected depending on the area of the section, the shape and the location of the remaining seed trees. PL are set in each forest stand on the longest diagonal, choosing the most characteristic places for the forest area and forest type. Deviations from the diagonal arrangement are in forest stands where there is an uneven arrangement of seed trees and characteristic conditions. PL was installed in forest stands with an area of S=200 m^2 and a radius of R=7.98 m. 5 PLs were installed in each forest stand. Each PL is set up in such a way that there is a seed tree in its center, the diameter of which is measured 1.3 m from the root neck with a measuring tape (accuracy ±0.1 cm), the height with the VERTEX laser altimeter (accuracy ±3 cm), the length and width of the crown, and the position of the crown against the sky. If there are several seed trees in PL, the distance between them was measured, and the impact on the course of pine regeneration and growth was also evaluated. All conifers that have reached a height of at least 10 cm are listed in each PL. The height of the pine is determined by measuring the heights of the branches [13] with the help of a measuring tape (accuracy ±1 mm). The diameter was measured with a mechanical caliper (accuracy ±2 mm) at the root neck. For the measured trees, the location under the crown of the seed tree or outside its projection, as well as the location in tillage furrows or unprepared soil, was noted. Coordinates are determined for each PL center with GPS device LKS-92, determining geographical coordinates in the XY system. Each tree is located in PL by the polar method, determining its azimuth from magnetic north and the distance to the PL center. Magnētiskais azimuts mērīts ar busoli (precizitāte ±1°). Magnetic azimuth measured with a compass (accuracy ±1°). The distance from the PL center to the measured tree is determined with a measuring tape (accuracy ± 1 cm).

In order to evaluate the state of health of the pines as well as the placement of viable trees in each PL, a visual assessment of the trees was performed in points as follows: 0 points, if the pine has no signs of weakening and growth disorders; 1 – with economically insignificant damages (small bark abrasions, broken off individual branches); 2 – with economically significant damage (at least one small injury to the trunk, less than ½ of the trunk circumference, double top); 3 – with significant damage (damage to the central shoot, signs of withering, the trunk is bent and unable to assume a vertical position, adhesions along the entire length of the trunk or at least one trunk injury exceeding ½ of the trunk circumference); 4 – the pine has withered in the current year (yellow or brown needles have remained); 5 – if the pine has withered in previous years [14].



A **B** **C**

Fig. 1 Placement of trees in PL and assessment of the state of tree health:

A - uneven tree placement in PL; B – risk of PL opening formation; C – PL uniform arrangement of trees; In the center of PL, a seed tree, red triangle – assessment of a tree with economically significant damage, green triangle – tree without economically significant damage.

The empirical data obtained as part of the fieldwork was compiled into Microsoft Excel for further processing. The volume of the trunk of common pine seed trees is calculated according to formula 1 of I. Liepas (1996) [14], the average increase in tree height according to formula 2 [13]:

$$V = \psi \cdot L^{\alpha} \cdot D^{\beta lgL+\varphi}, \quad (1)$$

where V – pine stock, m^3; L – trunk length, m; D – tree diameter at a height of 1.3 m above the root neck, cm; ψ – coefficient, for pine 1.6541·10-4; α – coefficient, for pine 0.56582; β – coefficient, for pine 0.25924; φ – coefficient, for pine 1.59689.

$$z_h^v = \frac{h_A}{A}, \quad (2)$$

where z_h^v – average height increase of pine, cm; h_A – pine height, cm; A – pine age, years. The incidence of damaged trees (P, %) and damage intensity (R, %) were also determined. The incidence of tree damage was calculated using formula 3:

$$P = \frac{n \cdot 100}{N}, \quad (3)$$

where P – incidence of tree damage, %; n – number of damaged trees, trees per ha; N – total number of surveyed trees, trees per ha. Formula 4 was used to determine the intensity of tree damage:

$$R = \frac{\sum_{i=1}^{6} n_i b_i \cdot 100}{N \cdot k}, \quad (4)$$

where R - damage intensity, %; n_i – number of damaged trees, trees per ha; b_i – damage degree; N – total number of surveyed trees, trees per ha; k - highest damage degree, points [14].

A t-test was performed to determine the annual and average height growth and diameter at the root neck of the regenerated pine depending on its location either under the seed tree or outside its crown projection, as well as thegrowth depending on its location in untreated soil and in treated (furrows). A t-test was used to check whether there are significantly more viable trees in furrows after tillage than in untreated soil. Correlation and univariate regression analysis were used to examine the dependence of height growth on the distance to the seed tree, the influence of seed tree dendrometric indicators on the

height growth of regenerated trees. Using Microsoft Excel 2018, the confidence interval method was applied to determine whether the incidence and intensity of damage to damaged trees has a significant impact on the growth of the stand.

RESULTS AND THEIR ANALYSIS

Common pine seed trees. Theselected trees were straightand slender without visual faults or trunk defects. The age of the seed trees of *Cladinoso-callunosa* (forest stands of IV rating) is 121-140 years, and of Vacciniosa (forest stands of III rating) 101-120. On average, 29 pcs. of seed trees were left per ha^{-1} *Cladinoso-callunosa* and 32 pcs. ha^{-1} *Vacciniosa*. The number of seed trees left is sufficient in all areas, except for area 277/32 (tab. 1), but this does not interfere with natural regeneration in this area, because a larger number of seed trees significantly reduces the growth of regenerated trees [9]. However, the number of trees that have been restored is higher in forest plots with the largest number of seed trees left. The average height of seed trees – 25.2±1.3 m Cladinoso-callunosa is 0.6 m higher than tree height – 24.6±2.2 m Vacciniosa. The diameter at a height of 1.3 m above the root neck is 1.2 cm larger, respectively, than Cladinoso-callunosa 38.6±2.5 cm and Vacciniosa 37.4±1.5 cm and the average volume of one tree is 0.1170 m3 higher (formula 1). Dendrometric indicators of seed trees do not show differences in the growth of forest types, as they are not intended to reflect growing conditions. In the areas with the forest type *Cladinoso-callunosa,* significant differences in growth conditions have been found depending on changes in the relief (hilliness), and this may also be a decisive factor in the occurrence of higher dendrometric indicators of pine. In the researched forest stands, the distribution of seed trees varies, both evenly throughout the area and in part of the area, and separate groups of seed trees are also found. So that leaving seed trees in groups, where possible, facilitates logging and mechanized soil preparation, as well as less risk of tree damage during machinery movement.

Table 1 The location of the studied stands and the average dendrometric indicators of the seed trees left behind

Quarter / district	Coordinate		H±SE, m	D±SE, cm	V, m^3	Number of seed trees, pcs. ha^{-1}	Area, ha
	X	Y					
198 / 21	609150.6530	394714.7984	24.5±1.8	36.0±2.8	1.1228	30	4.37
290 / 19	609460.8700	390459.0134	25.2±1.2	39.3±1.2	1.3703	29	4.43
317 / 28	609185.8577	389067.2721	25.9±0.8	40.5±1.0	1.4932	27	1.91
Average *Cladinoso-callunosa*	-	-	25.2±1.3	38.6±2.5	1.3288	29	-
245 / 5.1	610020.4281	392513.6977	24.5±0.9	38.0±1.1	1.2481	50	2.60
245 / 8.1	609996.7374	392388.0646	22.8±2.1	36.7±1.8	1.0872	44	1.98
277 / 13	605958.2916	390566.5215	25.3±0.7	35.7±2.3	1.1395	28	0.98
277 / 32	606233.9410	390566.5217	25.7±0.6	39.3±0.8	1.3969	8	0.93
Average *Vacciniosa*	-	-	24.6±2.2	37.4±1.5	1.2118	32	-

Denotations: H±SE – mean height and standard deviation of seed tree; D±SE – average diameter and standard deviation of seed tree; V – the average volume of the seed tree.

Effect of seed trees on the heights, diameters and number of trees of regeneration trees

The height of a tree is one of the components of volume growth, which is determined by various factors: tree species, age, growing conditions, etc. [13]. In evaluating the annual height increases of the Scots pine and the dendrometric indicators of the seed trees, it was found that there are no significant correlations between the height of the seed tree (r=0.09 and r=0.05) and the diameter of the seed tree (r=0.02 and r=0.07) in *Cladinoso-callunosa* or in *Vacciniosa*. There is no significant correlation between the annual growth of the pine and the number of regenerated trees between the positions facing the sky.

The annual height increase and the tree numbers increase markedly at a distance of 2 m from the seed tree in *Cladinoso-callunosa* (Fig. 2). Further from the center, the maximum values of the annual height increase increase linearly. The regenerating trees of *Vacciniosa* closer to the PL center have higher annual increases than *Cladinoso-callunosa*, and at a distance of 1.2 m there is a pronounced increase in the number of trees and maximum values of annual height increase of 10 cm. A weak positive correlation exists between annual height growth and distance from PL central seed tree, r =0.15 *Cladinoso-callunosa* and r =0.25 *Vacciniosa*, respectively, explaining part of the variation in annual height growth of regenerating trees.

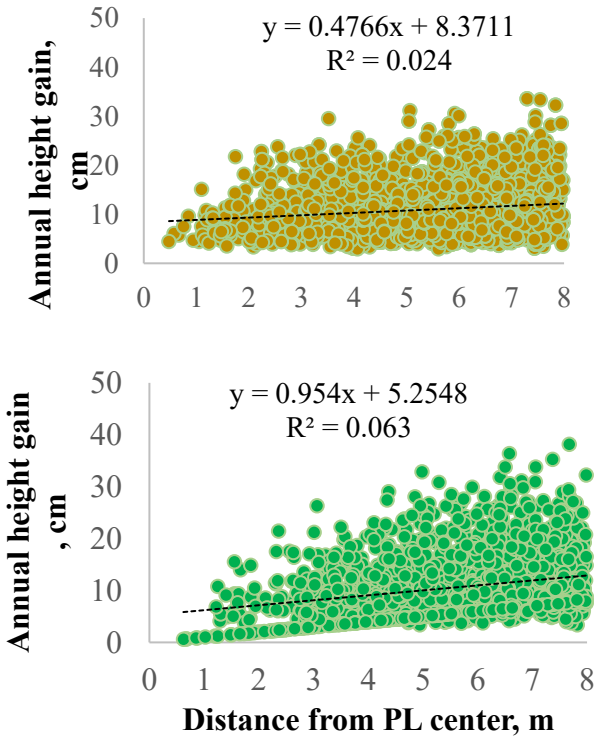


Fig. 2 Relationship between distance from PL center (seed tree) and annual height growth of regenerated Scots pine: A – *Cladinoso-callunosa* un B – *Vacciniosa.*

Partial tillage and the effect of risk factors on the natural regeneration of pine.

The effect of soil preparation is examined, comparing the growth rates of regenerated trees to trees growing in unprepared soil. It was found that for trees growing in furrows, the distance from the PL center has less effect on growth than in unprepared soil. Prepared soil also contributes to the increase in the number of trees [4]. Part of the variation in

height growth can be explained by the distance to the seed tree, a linear regression model that statistically significantly ($p<0.05$) explains the variation in annual height growth in *Cladinoso-callunosa* and *Vacciniosa*. The annual growth of pine height increases with each year of growth for both in-furrow and out-of-furrow regenerated trees (Fig. 3), however, the annual and average growth of the pine height outside the furrows is lower than for the trees regenerated in the furrows, as well as being significantly lower under seed trees than outside the crown deck in both *Cladinoso- callunosa* and *Vacciniosa* ($p<0.05$). There are significant differences between forest types, as edaphic and lighting factors play a special role in the process of pine growth formation [13]. Under the crown of seed trees, the average height increase of Cladinoso-callunosa pine in furrows regenerated is 11.5±1.6 cm (formula 2), which is 2.7 cm (18.4%) less than that of trees located outside the crown of seed trees, while outside the furrows under the crown in unprepared soil there is 10.4±1.2 cm less growth than outside the crown by 2.3 cm (17.9%). Accordingly – Vacciniosa under the seed tree crown in furrows of 12.5±1.2 cm, which is 3.3 cm (20.6%) less than outside the crown, and under the tree crown in untreated soil is10.7±1.5 cm, which is 3.9 cm (27.1%) less than outside the crown. The annual increase in pine height in the first year is not significantly higher ($p>0.05$) for regenerated trees measured outside furrows, while from the second to sixth year inclusive, it is significantly higher for trees growing in furrows than in unprepared soil ($p<0.05$).

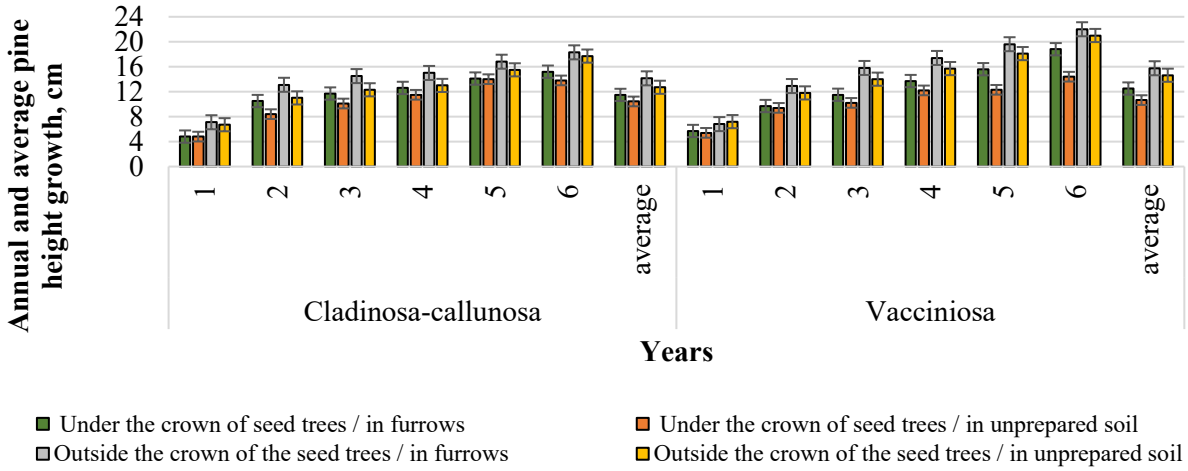


Fig. 3 Annual and mean height growth (±standard error) of Scots pine in Vacciniosa.*Cladinosa-callunosa* un *Vacciniosa* forest types.

The diameter of regenerated pines is significantly smaller ($p=0.001$) below the seed tree 9.8±1.4 mm (by 23%) than the average diameter of the crown projection outside the seed tree 12.7±1.6 mm. The average diameter of pine trees growing in furrows is 13.8±1.7 mm, which is 1.1 mm (8%) higher than that of trees growing in unprepared soil. The distribution of naturally regenerated trees, unlike planted trees, cannot be obtained evenly [7]. In *Cladinoso-callunosa*, it can be observed that there are significantly fewer regenerated trees in the center of the PL than further away from the center, and at the PL scale this means an uneven density of regenerated trees. A smaller number of regenerated trees can be observed where there is another seed tree closer than 10 m from the PL center. A high risk of opening formation was found in groups of seed trees where there was anabsence of new trees, when one or more seed trees are located at a distance of 7 to 14 m from the PL center. Groups of trees form in areas more suitable for growth, but there is a risk of openings forming in less suitable areas. In both types of forest, it can be

observed that there are significantly fewer regenerated trees in the center of PL than further away from the center. On the other hand, due to the damage caused by various risk factors, the formation of openings is not observed, as the damaged trees were found uniformlyGroups of trees form in areas more suitable for growth, but there is a risk of openings forming in less suitable areas. In both types of forest, it can be observed that there are significantly fewer regenerated trees in the center of PL than further away from the center. On the other hand, due to the damage caused by various risk factors, the formation of openings is not observed, as the damaged trees were found uniformly. *Vacciniosa* regenerated trees are prominently located in furrows in three areas (245/5.1, 277/13, 277/32), due to careful tillage up to the seed tree. *Vacciniosa* tillage is thus an important factor in ensuring even tree placement. The formation of openings is facilitated not only by the effect of the crown of seed trees, but also by the exposure of the slope towards the south, which reduced the success of natural regeneration.
Occurrence of damaged trees (formula 3) in *Vacciniosa* was found less often than *Cladinoso-callunosa*, and their arrangement was random (tab. 2). It is precisely due to the damage by risk factors that the formation of openings is not observed, because the damaged trees are distributed evenly and not in one place. Forest management aims to obtain a straight and slender trunk, but this is threatened by any damage to the central shoot and top bud. Threats to the health statuss and viability of pine in the surveyed stands are mainly damage by hoofs, pine-aspen rust (Melampsora pinitorqua (A.Br.) Rostr.) and conifers (*Laphodermium sp*.). The average incidence of damaged trees is 22% and their intensity (formula 4) is 9%, respectively in *Cladinoso-callunosa* forest types, 31%, 11% and in *Vacciniosa* – 13% and 7%. The incidence and intensity of damaged trees is significant (p=0.03). Damage by hooves occurs mainly in *Cladinoso-callunosa* pine, and besides hoof damage, significant damage by pine-aspen rust occurs in *Vacciniosa*. The regenerated pines are treated with repellents to protect against significant hoof damage.

Table 2. Incidence of regenerated P.sylvestris damaged trees (P, %) and their damage intensity (R, %) in the researched stands

District / quarter	Type of Forest	Number of trees (N±SE), pcs. ha^{-1}	Number of damaged trees (n±SE), pcs pcs. ha^{-1}	P, %	R, %
198 / 21	*Cladinoso-callunosa*	6440±187	1980±129	30.8	15.0
290 / 19		3980±175	870±82	21.9	13.1
317 / 28		5050±92	1980±201	39.2	5.6
245 / 5.1	*Vacciniosa*	3970±106	190±43	4.8	2.7
245 / 8.1		6930±154	590±87	8.5	3.8
277 / 13		9350±179	2500±144	26.7	12.2
277 / 32		8380±132	1140±76	13.6	7.6

The number of regenerated trees in furrows was found to be 68% Cladinoso-callunosa on average, while in unprepared soil 1,663 pcs. ha^{-1} or 32%. The total average number of trees was found to be 5,156. ha-1. Vacciniosa was found on average in 69% and outside the furrows, 2,210 pcs. ha^{-1}. *Vacciniosa* konstatēti vidēji 69% un ārpus vagām atjaunojušies vidēji 2 210 gab. ha^{-1}. On average, there are 7,158 pieces of naturally regenerated Scots pine in the area ha^{-1}. The number of trees in the furrows is significantly higher in both types of forest: both *Cladinoso-callunosa* (p=0.02) and *Vacciniosa* (p=0.01), therefore the soil must be partly cultivated for successful natural regeneration. The significant number of regenerating trees and their annual height increases indicate that the seed trees should be cut down earlier than in the current practice in young stands

of common pine - it should be done before the age of 6 years. Forest stands have regenerated, and further preservation of seed trees would significantly reduce the height gains of regenerated trees [15]. It is recommended that seed trees that are to be felled be left undisturbed if permitted by the intended method of felling the seed trees and the risk of wind damage. Seed trees left in groups reduce the number of regenerated trees below them and there is a risk of openings.

CONCLUSION

In regenerating stands, groups of seed trees contribute to the formation of openings. There is no significant correlation ($p>0.05$) between the annual height growth of the regenerating *Scots* pine and the dendrometric indicators of the seed trees Under the crown of seed trees, the regenerating pine *Cladinoso-callunosa* in furrows has a lower average height increase than trees outside the crown of seed trees by 18.4%, while there is a smaller increase outside the furrows under the crown in the unprepared soil than outside the crown by 17.9%, Vacciniosa 20.6% and 27.1 % respectively.Under the crown of seed trees, the regenerating pine *Cladinoso-callunosa* in furrows has a lower average height increase than trees outside the crown of seed trees by 18.4%, while there is a smaller increase outside the furrows under the crown in the unprepared soil than outside the crown by 17.9%, *Vacciniosa* 20.6% and 27.1 % respectively. The annual height increase of pine is significantly lower ($p=0.01$) under the crowns of seed trees than for trees that grow outside the crowns. In regenerating forest stands, tillage is a significant factor in ensuring the number of trees and their even distribution in both low-fruited forest types: both *Cladinoso-callunosa* ($p=0.02$) and *Vacciniosa* ($p=0.01$). In pine, damage caused by biotic factors occurs without creating openings. A significant number of regenerating trees and their annual height increases show that the seed trees in young growth should be cut down before the age of 6 years. Forest stands have regenerated, and further retention of seed trees would reduce height gains for regenerated trees.

REFERENCES

[1] Baumanis I., Jansons Ā., Neimane U. *Priede. Selekcija, ģenētika un sēklkopība Latvijā.* (Pine tree. Breeding, genetics and seed production in Latvia), Salaspils, Latvian State Forestry Institute "Silava", 325 p., 2014.

[2] Przybylski P., Konatowska M., Jastrzębowski S., Tereba A., Mohytych V., Tyburski Ł.; Rutkowski P. The possibility of regenerating a pine stand through natural regeneration. *Forests,* Vol. 12(8), 2021.

[3] Huth F., Wehnert A., Wagner S. Natural Regeneration of Scots Pine Requires the Application of Silvicultural Treatments such as Overstorey Density Regulation and Soil Preparation. *Forests*, Vol.13, 817, p. 1-24, 2022.

[4] Saursaunet M., Mathisen K., Skarpe C. Effects of Increased Soil Scarification Intensity on Natural Regeneration of Scots Pine Pinus sylvestris L. and Birch Betula spp. L. *Forests*, Vol. 9, p. 262, 2018.

[5] Simonsen R. Optimal regeneration method – Planting vs. natural regeneration of Scots pine in northern Sweden. *Silva Fennica*, Vol. 47(2), p. 1-23, 2013.

[6] Aleksandrowicz-Trzcińska M., Drozdowski S., Studnicki M., Zybura H. Effects of site preparation methods on the establishment and natural-regeneration traits of scots pines (*Pinus sylvestris* L.) in Northeastern Poland. *Forests*, Vol. 9 (11), 2018.

[7] Mangalis I. (2004) *Meža atjaunošana un ieaudzēšana*. Monogrāfija. Rīga: Et Cetera. 455 lpp., 2004. (In Latvian).

[8] Béland M., Agestam E., Ekö P., Gemmel P, Nilsson U. Scarification and Seedfall affects Natural Regeneration of Scots Pine Under Two Shelterwood Densities ans a Clear-cut in Southern Sweden. *Scandinavian Journal of Forest Research*, Vol. 15, 2000.

[9] Tishler M., Tullus T., Tullus A., Jäärats A., Lutter R., Lundmark T., Tullus H. Effects of shelterwood method and plant stock type on the early growth and survival of pine seedlings in regeneration stands under hemiboreal conditions. *Scandinavian Journal of Forest Research*, Vol. 35:1-2, p. 85-95, 2020.

[10] Orlander G., Gemmel P., Hunt J. *Site Preparation: a Swedish Overview*. Southern Swedish Forest Research Station, Swedish University of Agricultural Sciences, BC Ministry of Forests, Victoria, 60 p., 1990.

[11] Hyppönen M., Alenius V., Valkonen S. Models for the establishment and height development of naturally regenerated Pinus sylvestris in Finnish Lapland. *Scandinavian Journal of Forest Research*, Vol. 20, p. 347-357, 2005.

[12] Akczell L. A comparison of planting, sowing and natural regeneration for Pinus sylvestris (L.) in boreal Sweden. *Forest Ecology and Management*, Vol. 61(3-4), p. 229-245, 1993.

[13] Liepa I. Latvijas skujkoku mežu krājas pieaugums (Annual Volume Increment of Coniferous). *LLU raksti*, 20 (315), Jelgava, 46-52 lpp., 2008. (In Latvian).

[14] Miezite O., Okmanis M., Indriksons A., Ruba J., Polmanis K., Freimane L., Assessment of Sanitary Conditions in Stands of Norway Spruce (Picea abies Karst.) Damaged by Spruce Bud Scale (Physokermes piceae Schrnk.), iForest, vol. 6, pp 73-78, 2013.

[15] Rautio P., Hallikainen V., Valkonen S., Karjalainen J., Puttonen P., Bergsten U., Winsa H., Hypponen M. Manipulating overstory density and mineral soil exposure for optimal natural regeneration of Scots pine. *Forest Ecology and Management* 539, 2023.

STOCHASTIC SIMULATION OF SELF-THINNING

Prof. Dr. Petras Rupšys[1]

[1] Vytautas Magnus University, **Lithuania**

ABSTRACT

Understanding the principles of self-thinning forest ecosystems is essential for taking modern management techniques into practice. The spatial distribution of the surviving trees in a stand is influenced by a variety of factors, including tree mortality. In young forests, competition has a major role in determining spatial mortality; in older forests, random changes in the environment have a major role. The dynamics of the number of living and dead trees in the forests of central Lithuania will be addressed in this study. The Gompertz type mixed effect parameters univariate stochastic differential equations of the tree diameter, height, and occupied area combined with the normal copula function are used to derive new models for the number per ha of living and dead trees. The mean values of the dead tree size variables had much lower trajectories, which is especially apparent in mature stands, as demonstrated by the study of the individual tree size variables (height and diameter). The results are illustrated using experimental field studies carried out in Lithuania, in the municipality of Kazlu Ruda. The following information was gathered using 48 permanent test plots placed in mixed-species, uneven-aged stands: age, diameter at breast height (58,829 trees), tree position (58,829 trees), and height (10,796 trees). All results were implemented using the symbolic algebra system Maple.

Keywords: self-thinning, occupied area, diameter, height, stochastic differential equation, copula function.

INTRODUCTION

The occurrence of tree death is a major driver of changes in the geographic heterogeneity of stands. The literature has provided a thorough description of the rates and causes of mortality at various phases of stand evolution; however, little research has been done on the dynamics of the number of dead trees, or how this process changes over mean stand age. One of the most crucial elements for the appropriate use, preservation, and restoration of forest ecosystems is evaluating the causes and dynamics of tree mortality. The primary factors influencing tree mortality in boreal forests include age, disease, competition, and stochastic fluctuations in the forest environment. When a forest starts growing, competition is especially intense as young trees fight intensely for resources like water, sunshine, and nutrients. Competition between neighboring trees grows when the quantity of tree size variables in a stand goes up in tandem with the need for resources to support the process of growth. This results in the simultaneous occurrence of two processes: the process of tree mortality and the process of accumulating live tree size variables. The output of a stand at a given age consists of the production of living trees and dead trees since mortality causes regular losses of trees. The output of a stand at a given age consists of the production of living trees and dead trees since mortality causes regular losses of trees. Numerous fixed and random environmental factors, such as location, species composition, air quality, and climate, affect the prediction of a given tree's mortality time. The logistic regression model is the most often used statistical tool

for analyzing individual tree and whole stand mortality. A stand's tree mortality is a very dynamic phenomenon that is influenced by the age of the trees as well as their size (diameter, height, crown base height, etc.).

Individual tree mortality occurs when a tree is regarded as dead but its precise cause and exact time of death are unknown. Repeated measurements of experimental plots—which tend to be relatively small—are necessary for an accurate mathematical explanation of the dynamic process of mortality. Most models of the dynamics of forest mortality are based on databases that integrate dendrochronologically generated information on individual tree radial development with static data on the structure and composition of the forest. This work suggests a fully dynamic model that is described by stochastic differential equations with mixed-effect parameters and unknown parameters that are inferred from longitudinal observations on long-term experimental plots. The majority of mortality process models now in use, however, are basically discrete since they assume that the process is discrete in time and require continuous remeasurement cycle intervals over the period of the time interval. Therefore, these models have two key limitations: (i) they can incorrectly identify relationships due to their tendency to inaccurately represent the actual underlying process, which is actually continuous in time; and (ii) they can be difficult to adapt to irregular intervals in the remeasurement cycles. Many phenomena that are regularly observed over time in disciplines like forestry, biology, ecology, and finance are inherently uncertain. Under these circumstances, stochastic differential equation models perform better than deterministic models because they deal with stochastic processes [1] that can reflect both the deterministic trend and the uncertain nature of the underlying trajectory. Complex structures that depend on a number of tree and forest stand variables [2], including the nature of interaction [3], local and global properties associated with fluctuations [4], emergent characteristics of the local specific characteristics [5], etc., can be seen in forest growth systems. The extraction of such dynamic enclosed information is still a major problem, unfortunately. However, there aren't many studies in the literature that use stochastic differential equation models to solve issues concerning the dynamic of the number of dead and living trees. In order to better understand the effects of stand size variables on the number of dead trees per hectare, this study will use an Itô [6] stochastic differential equation model that is based on an underlying deterministic model for analyzing tree or stand growth processes [7].

MATERIALS AND METHODS

Tree growth models make it possible to predict the development of forest ecosystems by defining the size variable of each simulated tree in the forest as a function of age. The growth models used are often called "individual tree models" because they are based on the growth and death of individual trees, but linking the development of individual trees by analogy with diffusion processes yields generalized stochastic differential equations (SDEs) models that describe the whole stand. We will use Gompertz-type SDEs to determine the dynamics of tree diameter, occupied area and height over time, with the additional inclusion of random factors that determine the effect of individual plots on growth trajectories. In the following, we assume that the tree diameter trajectory $X_1^i(t)$, the occupied area trajectory $X_2^i(t)$ and the height trajectory $X_3^i(t)$ over time for each plot i =1, ..., M (M is the number of different plots) are defined by SDE:

$$dX_j^i(\mathrm{t})=\left(\left(\alpha_j+\phi_j^i\right)-\beta_j ln\left(X_j^i(t)-\gamma_j\right)\right)\left(X_j^i(t)-\gamma_j\right)dt$$

$$+\sqrt{\sigma_j}\left(X_j^i(t)-\gamma_j\right)\cdot dW_j^i(t),\ X_1^i(t_0)=x_{10}, X_2^i(t_0)=x_{20}=\delta, X_3^i(t_0)=x_{30}, \quad (1)$$

where δ is an unknown fixed-effect parameter to be estimated, $W_j^i(t)$, j = 1, …, 3 are independent one-dimensional Brownian motions, the random effects ϕ_j^i, j = 1, …, 3 are independent and normally distributed random variables with zero mean and constant variances ($\phi_j^i \sim N\left(0;\sigma_{j\phi}^2\right)$), and the unknown fixed effect parameters $\theta_0 = \left\{\alpha_j,\beta_j,\gamma_j,\sigma_j,\sigma_{j\phi}, j=1,\dots,3,\delta\right\}$ must be estimated.

Using the process transformation, we obtain that the conditional stochastic processes $(X_j^i(t)|X_j^i(t_0)=x_{j0}), j = 1, \dots, 3$ take the lognormal distribution $LN_1\left(\mu_j^i(t);\ v_j(t)\right)$, with mean $\mu_j^i(t)$, variance $v_j(t)$, and probability density function $f_j^i(x_j,t|\Theta_j,\phi_j^i)$defined as:

$$\mu_j^i(t) = ln\left(x_{j0}-\gamma_j\right)e^{-\beta_j(t-t_0)} + \frac{1}{\beta_j}\left(1-e^{-\beta_j(t-t_0)}\right)\left(\alpha_j+\phi_j^i-\frac{\sigma_j}{2}\right), \quad (2)$$

$$v_j(t) = \frac{1-e^{-2\beta_j(t-t_0)}}{2\beta_j}\sigma_j, \quad (3)$$

$$f_j^i(x_j,t|\theta_j,\phi_j^i) = \frac{1}{\sqrt{2\pi v_j(t)}(x_j-\gamma_j)}exp\left(-\frac{\left(ln(x_j-\gamma_j)-\mu_j^i(t)\right)^2}{2v_j(t)}\right), \quad (4)$$

$\theta_1=(\alpha_1,\beta_1,\gamma_1,\sigma_1)$, $\theta_2=(\alpha_2,\beta_2,\gamma_2,\sigma_2,\delta)$, $\theta_3=(\alpha_3,\beta_3,\gamma_3,\sigma_3)$.

The copula function is a multivariate cumulative distribution function in which the marginal probability distribution of each variable is uniform over the interval [0,1] [8]. The copula function method is commonly used to model the dependence structure of a multidimensional distribution [9]. In this context, this method can be used in forestry to reflect the dependence structure of several tree size variables. In the following study, we use a three-dimensional normal copula function to combine three different probability density functions defined by equations (2)-(5). This study uses a three-dimensional normal copula function to join three different probability density functions defined by equations (2)-(5). The normal copula is completely determined by the correlation matrix P [10]. For a given correlation matrix P, the normal three-dimensional copula $C_{1,2,3}$: $[0,1]^3 \to R$ is:

$$C_{1,2,3}(u_1,u_2,u_3|P) = \Phi_3(\Phi^{-1}(u_1),\Phi^{-1}(u_2),\Phi^{-1}(u_3)), \quad (5)$$

where Φ^{-1} is the inverse cumulative distribution function of the standard normal distribution, and Φ_3 is the three-dimensional normal cumulative distribution function with a mean vector *0* and correlation matrix *P* [11]. Copula's probability density function can be written as:

$$c_{1,2,3}(u_1,u_2,u_3|P) = \frac{1}{\sqrt{|P|}}exp\left(-\frac{1}{2}\begin{pmatrix}\Phi^{-1}(u_1)\\ \Phi^{-1}(u_2)\\ \Phi^{-1}(u_3)\end{pmatrix}^T\cdot(P^{-1}-I)\cdot\begin{pmatrix}\Phi^{-1}(u_1)\\ \Phi^{-1}(u_2)\\ \Phi^{-1}(u_3)\end{pmatrix}\right), \quad (6)$$

where I is the identity matrix, $F_j\left(x_j,t\right)=\int_{\gamma_j}^{x_j} f_j(z,t|\hat{\theta}_j,\hat{\phi}_j)dz$, $u_j = F_j\left(x_j,t\right)$ 'hat' is the parameter estimate, and P takes the following form:

$$P = \begin{pmatrix} 1 & \rho_{12} & \rho_{13} \\ \rho_{12} & 1 & \rho_{23} \\ \rho_{13} & \rho_{23} & 1 \end{pmatrix}. \quad (7)$$

There are many methods for estimating the copula parameters of a given data sample. In this study, we used a semiparametric maximum pseudo-likelihood estimator for the copula parameters. The semi-parametric maximum likelihood parameter estimation introduced by Ai [12] is characterized by a two-step approach, i.e. estimating the parameters of the marginal distributions and the copula parameters separately. For a given discrete set of three-dimensional measurements consisting of tree diameter (x_1), occupied area (x_2) and height (x_3)) $\{(x_{11}^i, x_{21}^i, x_{31}^i), (x_{12}^i, x_{22}^i, x_{32}^i), \ldots, (x_{1n_i}^i, x_{2n_i}^i, x_{3n_i}^i)\}$ at discrete times (ages) $\{t_1^i, t_2^i, \ldots, t_{n_i}^i\}$ (n_i is the number of trees observed in the ith stand, i = 1, ..., M), the semi-parametric maximum-likelihood copula parameter estimate is defined as follows:

$$LL(\rho_{12}, \rho_{13}, \rho_{23}) = \sum_{i=1}^{M} \sum_{j=1}^{n_i} ln\left(c_3\left(\Phi^{-1}\left(F_1\left(x_{1j}^i, t_j^i\right)\right), \Phi^{-1}\left(F_2\left(x_{2j}^i, t_j^i\right)\right), \Phi^{-1}\left(F_3\left(x_{3j}^i, t_j^i\right)\right) | (\rho_{12}, \rho_{13}, \rho_{23}), t_j^i\right)\right). \quad (8)$$

The parameters for the marginal distributions of fixed and random effects are estimated using an approximate maximum likelihood procedure [13].

The field studies were carried out in Lithuania, in the municipality of Kazlų Rūda. Most of the municipality of Kazlų Rūda is located in the fertile lowlands of Užnemunė and is among the most forested areas of Lithuania. Plots were remeasured between two and seven times every five or more years. After 48 permanent experimental plots were installed, the following data were obtained: age, diameter at breast height (58,829 trees), tree position (58,829 trees) and height (10,796 trees). Figure 1 shows the dynamics of the number of measured trees per ha, the mean diameter, the mean occupied area, and the mean height as a function of the mean age of the stand.

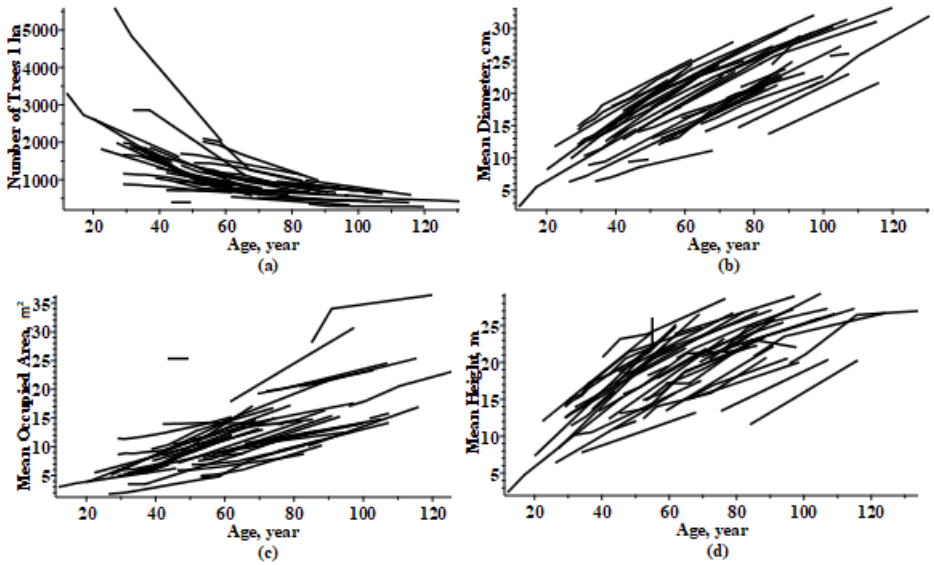


Figure 1. Dynamics of the number of trees per ha, diameter at breast height, occupied area, and height: **(a)** the number of trees per ha; **(b)** the mean diameter at breast height; **(c)** the mean occupied area; **(d)** the mean height.

RESULTS

Dead wood is generally classified into standing and fallen wood. In this presentation, dead trees and fallen trees in the stand are combined into one class and called dead trees. As the stand increases in age, it naturally enters a phase of spontaneous stem reduction called self-thinning. Next, we use the SDE (2), which is designed to model the dynamics of the area occupied by a tree, to define the dynamics of the number of dead, $Nl^i(t)$, i = 1, 2, …, M (M – is the number of different stands), and living trees, $Nd^i(t)$, per hectare according to this equation, respectively:

$$Nl^i(t) = \frac{10000.}{m_2^i(t|\widehat{\Theta}_2,\widehat{\varphi}_2^i)}, \quad (9)$$

$$Nd^i(t) = -10000.\cdot \frac{d}{dt}\left(\frac{1}{m_2^i(t|\widehat{\Theta}_2,\widehat{\varphi}_2^i)}\right), \quad (10)$$

where the estimates of the fixed effect parameters, $\widehat{\Theta}_2$, are obtained from the semiparametric maximum likelihood procedure by taking measurements of the 'living trees' section, the random effects, $\widehat{\varphi}_2^i$, are calibrated accordingly, and the trend of the mean of the occupied area, $m_2^i\left(t|\widehat{\Theta}_2,\widehat{\varphi}_2^i\right)$, is derived from a lognormal distribution, $LN_1\left(\mu_j^i(t);\ v_j(t)\right)$. Figure 2 shows the simulated trajectories of living and dead trees along with observations for the fixed effect scenario.

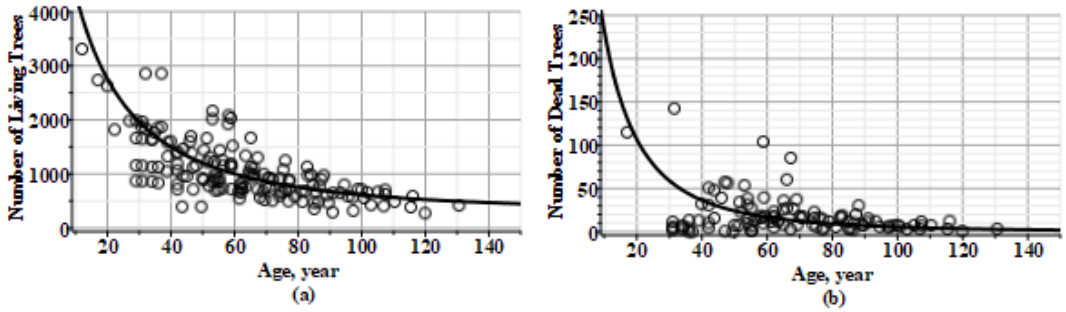


Figure 2. Trajectories of the number of trees per ha of living and dead trees: **(a)** living trees; **(b)** dead trees; observed values in circle.

Tree mortality per hectare is often characterized in different ways. In this paper, relative mortality, or in other words the instantaneous dynamics of relative mortality, is defined as the ratio of the decrease in the number of trees per hectare to the current number of trees (using a percentage scale), in the following form:

$$Mr^i(t) = -\frac{d}{dt}\left(\ln\left(Nl^i(t)\right)\right) = -\frac{d}{dt}\left(\frac{1}{m_2^i(t|\widehat{\Theta}_2,\widehat{\varphi}_2^i)}\right)\cdot m_2^i\left(t|\widehat{\Theta}_2,\widehat{\varphi}_2^i\right),\ i = 1, 2, \ldots, M. \quad (11)$$

Figure 3 shows the simulated relative mortality trajectory presented on a percentage scale.

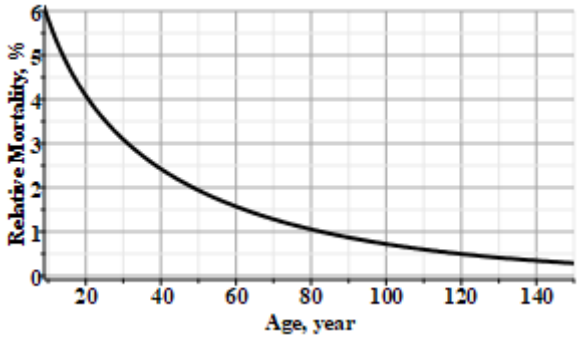


Figure 3. Dynamic of the relative mortality.

Figure 4 shows the simulated number of living and dead trees on three different stands for the mixed effect scenario. Figure 5 shows the simulated relative mortality on three different stands for the mixed effect scenario.

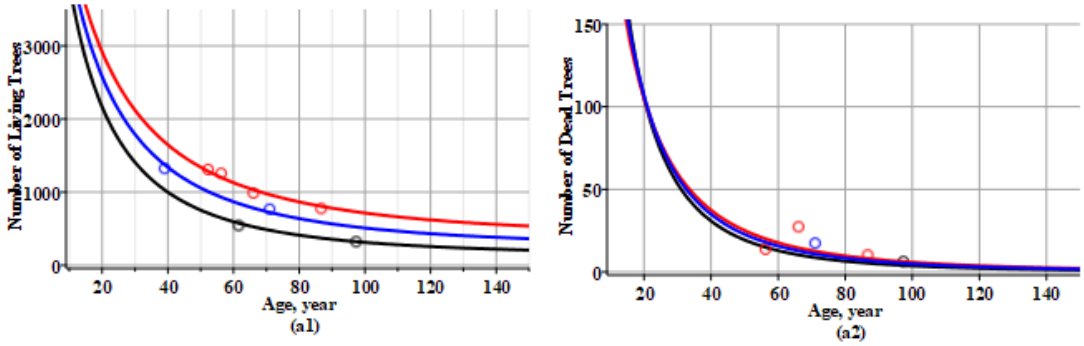


Figure 4. Trajectories of the number of trees per ha of living and dead trees on three different stands (the first stand in black, the second stand in red, the third stand in blue): (a) living trees; (b) dead trees; observed values in circle.

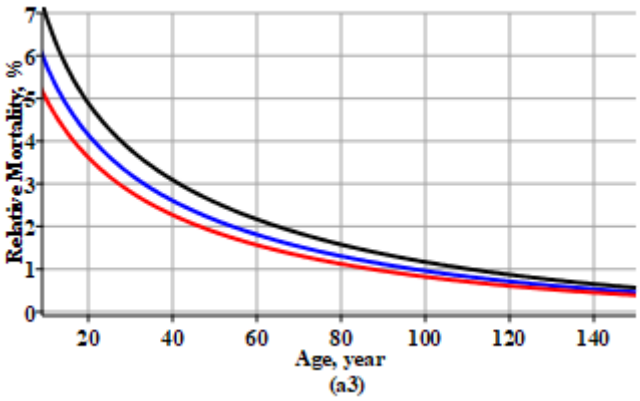


Figure 5. Dynamic of the relative mortality on three different stands (the first stand in black, the second stand in red, the third stand in blue).

DISCUSSION

Self-thinning of tree populations refers to a steady gradual decrease in the number of trees per unit area in a stand due to competition-induced mortality, with individual tree size variables increasing and accumulating more biomass overall, while on the other hand the intensity of competition increases [14] and local resources become limited for everyone to survive [15,16]. Figure 2 (fixed effect scenario) and Figure 4 (mixed effect scenario) show that the self-thinning process is particularly intense in stands up to 30 years old, with at least 50 trees falling per year. Figure 3 (fixed effect scenario) and Figure 5 (mixed effect scenario) show that relative mortality decreases to 2% when the mean age of the stand reaches approximately 50 - 60 years and relative mortality decreases to 1% when the mean age of the stand reaches approximately 80 - 100 years.

CONCLUSION

The main objective of this paper is to present a new mathematical model of stand growth and to demonstrate its ability to simulate the self-thinning process of trees. Modelling the self-harvesting process helps foresters to more accurately assess stand productivity, plan management operations and assess changes in CO_2 concentrations. The diffusion

processes used in this work are described by stochastic differential equations, which are widely used in various scientific fields [17]. In the future, the analysis of the process of self-thinning of stands will be carried out for individual tree species, and diffusion processes of another form will be discussed.

ACKNOWLEDGEMENTS

I thank the Edmundas Petrauskas research group for their help with sampling in the field. This research paper has received funding from Horizon Europe Framework Programme (HORIZON), call Teaming for Excellence (HORIZON-WIDERA-2022-ACCESS-01-two-stage) - Creation of the centre of excellence in smart forestry “Forest 4.0” No. 101059985”. This research was co-funded by FOREST 4.0 - Ekscelencijos centras tvariai miško bioekonomikai vystyti" (Nr. 10-042-P-0002).

REFERENCES

[1] Di Crescenzo A., Iuliano A., Mustaro V., Verasani G. On the Telegraph Process Driven by Geometric Counting Process with Poisson-Based Resetting, Journal of Statistical Physics, vol. 190, 191, 2023.

[2] Rupšys, P. Understanding the Evolution of Tree Size Diversity within the Multivariate Nonsymmetrical Diffusion Process and Information Measures, Mathematics, vol. 7, 761, 2019.

[3] Balandier P., Mårell A., Prévosto B., Vincenot L. Tamm review: Forest understorey and overstorey interactions: So much more than just light interception by trees, Forest Ecology and Management, vol. 526, 120584, 2022.

[4] Rupšys P. Univariate and bivariate diffusion models: computational aspects and applications to forestry, Stochastic Differential Equations: Basics and Applications, New York, pp 1-77, 2018.

[5] Haq S.M., Khoja A.A., Lone F.A., Waheed M., Bussmann R.W., Mahmoud E.A. Elansary H.O. Floristic composition, life history traits and phytogeographic distribution of forest vegetation in the Western Himalaya, Frontiers in Forests Global Change, vol. 6, 1169085, 2023.

[6] Itô K. On stochastic processes, Japanese Journal of Mathematics, vol. 18, pp 261–301, 1942.

[7] Visalga G., Rupšys P., Petrauskas E. Influence of Noise on Decay Predictions in Standing Trees, AIP Conference Proceedings, vol. 1895, 030006, 2017.

[8] Bai Z., Wei H., Xiao Y., Song S., Kucherenko S. A Vine Copula-Based Global Sensitivity Analysis Method for Structures with Multidimensional Dependent Variables, Mathematics, vol. 9, 2489, 2021.

[9] Nelsen R.B. An Introduction to Copulas, Springer, New York, 1999.

[10] Eklund J., Kim J.-M. Examining Factors That Affect Movie Gross Using Gaussian Copula Marginal Regression, Forecasting, vol. 4, pp 685-698, 2022.

[11] Sklar A. Random variables, distribution functions, and copulas – a personal look backward and forward, IMS Lecture Notes – Monograph Series, vol. 28, pp 1–14, 1966.

[12] Ai C. A Semiparametric Maximum Likelihood Estimator, Econometrica, vol. 65, pp 933–63, 1977.

[13] Rupšys P., Mozgeris G., Petrauskas E., Krikštolaitis R. (2023). A Framework for Analyzing Individual-Tree and Whole-Stand Growth by Fusing Multilevel Data: Stochastic Differential Equation and Copula Network. Forests, vol. 14, 2037, 2023.

[14] Tian D., Bi H., Jin X., Li F. Stochastic frontiers or regression quantiles for estimating the self-thinning surface in higher dimensions? Journal of Forestry Research, vol. 32, pp 1515–1533, 2021.

[15] Diao S., Sun H., Forrester D.I., Soares A.A.V., Protásio T.P., Jiang J. Variation in Growth, Wood Density, and Stem Taper Along the Stem in Self-Thinning Stands of *Sassafras tzumu*, Frontiers in Plant Science, vol. 13, 853968, 2022.

[16] Lu L., Zeng F., Zeng Z., Du H., Zhang C., Zhang H. Diversity and soil chemical properties jointly explained the basal area in karst forest. Frontiers in Forests and Global Change, vol. 6, 1268406, 2023.

[17] Shao Y. Dynamics of an Impulsive Stochastic Predator–Prey System with the Beddington–DeAngelis Functional Response, Axioms, vol. 10, 323, 2021.

TAXONOMIC AND ECOLOGICAL STRUCTURE OF FREE-LIVING AND PLANT PARASITIC NEMATODES IN POTATO FIELDS IN KHULO (AJARA, EASTERN GEORGIA)

Assoc. Prof. Dr. Lali Jgenti[1]

Prof. Dr. Eka Tskitishvili [2,3]

Tengiz Vadachkoria[1]

[1] Batumi Rustaveli State University **Georgia**
[2] Ilia State University, Institute of Zoology, **Georgia**
[3] Georgian Technical University, **Georgia**

ABSTRACT

The aim of this study is to determine the prevalence of plant parasitic nematodes in the main potatoe growing area in Ajara and to show whether altitu-dinal gradient affects nematode diversity and community structure along three contrasting altitudinal localities of Ajara: Kobuleti (10 m.a.s.l), Shuakhevi (450 m.a.s.l) and Khulo (950 -1800 m.a.s.l). The first part of this study is to assess for the first time the taxonomic and ecological structure of plant parasitic and free-living nematodes in agroecosystems of Khulo in this territory. Fauna of soil nematodes was studied in three villages of Khulo municipality: Dekanashvilebi, Okhropilauri and Uchkho. Sampling was conducted in six sites in early spring, in middle summer and in late fall. The 3 composite soil samples collected from each field (weighing 300-500g) consist of 50 individual sub-samples of soil and roots. Nematodes were extracted by a modified Baermann's method from a sample of 50 g, and exposition time was 48 h. The fauna consists of 109 forms of free-living and phytoparasitic nematodes, with up to species identified. The majority of the unidentified nematodes are in larval forms. 2 forms have been identified down to the family level. Registered nematodes belong to 8 orders and one suborder (*Enoplida; Filipjev, 1929*, *Araeolaimida De Coninck & Schuurmans Stekhoven 1933*, *Dorylaimida; Pearse, 1942*, *Mononchida Jairajpuri, 1969*, *Rhabditida; Chitwood, 1933*, *Tylenchida Thorne, 1949; Aphelenchida; Siddiqi, 1980*), encompassing 33 families and 53 genera. The largest abundance of nematodes was observed in the village Uchko, with 86 specimens/ 50 g soil, and the smallest was in the village Dekanashvili, with 37 specimens/50g. Plant-parasitic nematodes from 7 genera (*Ditylenchus, Xiphynema Tylechus, Tylenchorhynchus, Helicotylenchus, Pratylenchus, Aphelenchus*) were found in soil and (or) potato root samples. All these nematodes can be divided into five groups according to their feeding habits. The omnivore group, with 23 species (45,9%) in Spring, 38 species (34,2%) in Summer and 41 species (40,2%) in Autumn, constitut the core of nematode community. Investigations reveal that nematode populations and communities vary seasonally, with their maximum numbers observed during harvest. The number of identified phytoparasitic nematodes does not exceed a certain limit, which causes measurable economic damage. The obtained data are very significant for studying the biodiversity of the nematode population in Georgia.

Keywords: Soil nematodes, species community, agrocenosis, Khulo, Georgia

INTRODUCTION

Potato is a highly important crop with versatile uses and valuable nutritional properties. However, economic losses caused by phytopathogens are significant worldwide. This problem also affects Georgia, as the climatic conditions in the region are highly conducive to the development, reproduction, overwintering, and spread of microorganisms responsible for causing plant diseases.

Potato production plays a crucial role in ensuring food security and income for small peasant farms in the Autonomous Republic of Adjara. Taking the Khulo region as an example, it can be noted that across an area of 1272 hectares, approximately 7000 small farms operate, with an average size of landholding not exceeding 0.2-0.4 hectares. It is easy to understand the significance of potato cultivation on these farms considering the prevailing climatic conditions that limit the production of alternative crops.

In 2018, with the support of the European Commission, multi-profile complex studies were conducted in the Khulo region under the auspices of "Promoting Rural Development and Diversification in the Khulo Municipality," focusing primarily on agricultural soil analysis. This initiative was prompted by the detection of potato cancer in the Khulo region during 2016-2017, resulting in significant economic losses for the municipality. However, this comprehensive study did not encompass nematological research. We think that phytohelminthological studies are being carried out in the Khulo municipality for the first time.

MATERIALS AND METHODS

To identify pathogenic nematode diseases, the study was carried out in the agrocenoses of the Khulo municipality in the Autonomous Republic of Adjara. Three villages were selected: **Dekanashvili** (N41.3906, E42.1757), **Okruashvili** (N41.3856, E42.827), and the village **Uchkho (**N 41°40'46.6" E 42°18'52.1")**.** Within the villages, two potato agrocenoses (each covering an area of 0.5 hectares) with distinct ecological conditions were chosen for stationary research, focusing on edaphic factors, temperature regime and humidity. To determine the maximum total number and species composition of the nematode population, three composite (mixed) samples were collected from each selected station using the zigzag and diagonal method. Each composite sample weighed between 400-500 grams and comprised 50 primary samples. The research depth for each sample was 25-30 cm. Four expeditions were conducted. Samples were collected to encompass the complete vegetation cycle: before planting the seed material (in March), during the vegetation period (in April and September), and after harvesting (at the end of November). Approximately 1000 primary soil samples were collected throughout the entire research period.

For the extraction of nematodes from soil, Baermann's funnel technique was used [1], [2], [3]. Exposition term was 5 days. TAF (triethanolamine 2 ml (40 %) formalin 7 ml and distilled water 91 ml) was used for fixation of the nematodes [4]. Temporary microscope slides preparation and nematodes staining were done by standard techniques [5]. Species identification was carried out with using the microscopes OMAX 14 Mp Digital USB3.0 Microscope Camera with Stage Micrometer A35140U3. We used the monographs by [6], [7], [8], [9], [10] [11], [12], Frequency of detection and the average quantity of nematodes were counted for the 50 cm^3 of soil.

RESULTS

In total, 109 forms of nematodes belonging to 8 orders, 33 families, and 53 genera are registered in the fauna. Among these, 65 forms have been identified down to the species level, 3 forms to the family level, and 40 forms to the genus level [13]. Some specimens could not be identified to the species level due to being in larval forms or being damaged. (Table 1.)

Table 1. Distribution of genus of nematodes

Order	Familie	Genus	Trophic groups	Sp.N
Enoplida	Alaimidae	Alaimus	B	2
		Amphidelus	B	2
	Tripilidae	Tripyla	B	2
		Tripilina	B	1
	Tobrilidae	Tobrilus	B	1
Monhisterida	Monhisteridae	Geomonhistera	B	1
Areolaimida	Plectidae	Anaplectus	B	1
		Plectus	B	4
	Cylindrolaimidae	Cylindrolaimus	B	1
Dorylaimida	Dorylaimidae	Dorylaimus	O	1
		Sicaguttur	O	1
		Mesodorylaimus	O	6
	Qutsianematidae	Eudorylaimus	O	13
		Discolaimus	O	2
		Ecumenicus	O	1
	Aporcelaimidae	Aporcelaimellus	O	5
		Paraxonchium	O	1
	Nordiidae	Longidorella	Ph	1
	Longidoridae	Xiphinema	Ph	5
	Belondiridae	Belondira	O	1
	Axonchidae	Axonchium	O	1
	Tylencholaimellidae	Tylencholaimellus	M	2
	Tylencholaimidae	Tylencholaimus	O	1
	Leptonchidae			
	Actinolaimidae	Actinolaimus	Pr	1
	Nigolaimidae	Nigolaimus	Pr	2

		Nigolaimus (paravulvus)	Pr	2
Mononchida	Mononchidae	Clarcus	Pr	2
		Comansus	Pr	1
		Prionchulus	Pr	2
	Anatonchidae	Anatonchus	Pr	1
	Mylonchulidae	Mylonchulus	Pr	1
Rhabditida	Rhabditidae	Rhabditis	B	2
		Mesorabditis	B	1
		Pelodera	B	1
	Cephalobidae	Cephalobus	B	2
		Eucephalobus	B	3
		Heterocephalobus	B	2
		Chiloplacus	B	1
		Acrobeloides	B	1
	Panagrolaimidae	Panagrolaimus	B	1
Sub.Ord. Diplogasterina	Diplogasteridae	Mesoipologaster	B	2
Tylenchida	Tylenchidae	Filenchus	Ph	1
		Tylenchus	Ph	3
		Psilenchus	Ph	1
	Anguinidae	Ditylenchus	Ph	1
	Hoplolaimidae	Helicotylenchus	Ph	5
		Rhotylenchus	Ph	2
	Tylenchorinchidae	Tylenchorinchus	Ph	1
	Neotylenchidae	Neotylenchus	Ph	1
	Pratylenchidae	Pratylenchus	PH	1
Aphelenchida	Aphelenchidae	Aphelenchus	M	1
	Aphelenchoididae	Aphelenchoides	M	1
		Seinura		2

(B)bacterivorous, (F) fungivorous, (O) omnivorous, (P) predators (Ph)phytohelminthes**.**

DISCUSSION

According to the percentage of species composition, the order Dorylaimida (44.95%) leads the count, with the family Qutsianematidae being the most prominent within it. The diversity of species within this order is attributed to a wide range of adaptations. Following closely, the second and third places are occupied by representatives of the

Rhabditida; Chitwood, 1933 (18.5%) and Tylenchida (17.44%) groups, respectively. The order Monchisterida Filipjev, 1929 is represented by only one species (Fig 1).

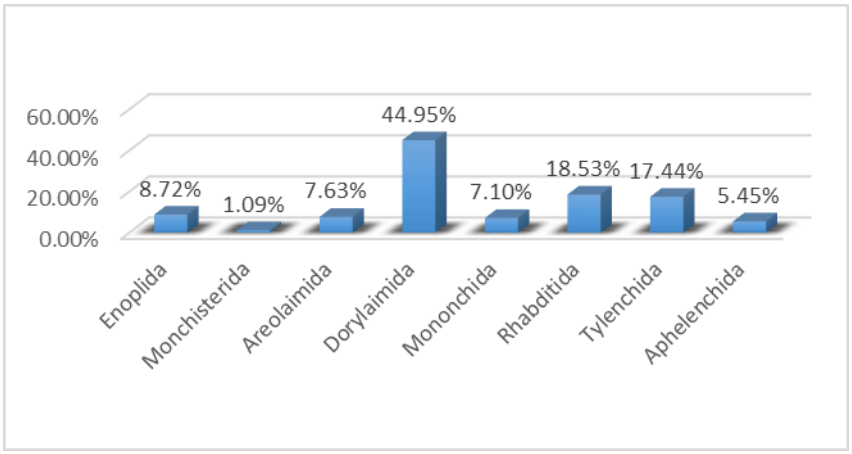


Fig. 1. Percentage of species in orders

19 eudominant and dominant soil-nematode genera constituting the basis of the community structure were identified. They constitute 54.3–66.4% of the total number of the registered genera in spring, 49.4–58,2% in summer, 57.7–69.6% in fall, and 39.3–43.6% in winter.

We studied the number dynamics of the potato pathogenic nematode Ditylenchus destructor Thorne, 1945 (Fig. 2). [14],[15][16] . Before planting, its percentage in the soil compared to the total amount did not exceed 6%. However, after planting and throughout the entire vegetation period, this indicator increased to 12% and then to 40%. After harvesting, this indicator decreased again, reaching 24%. Such fluctuations in numbers suggest the utilization of invasive seed material.

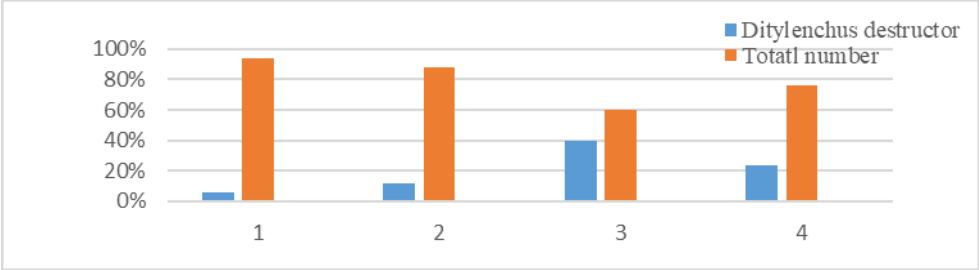


Fig.2. Percentage of *Ditylenchus destructor Thorne, 1945* . 1- Before planting; 2-3 – Entire vegetation period; 4 - After planting

The ecological characteristics of nematode populations are determined by the nature of their adaptation within the biocenosis. We classified the identified species into 5 ecological groups based on their trophic nature: bacterivorous, fungivorous, omnivorous, predators and plant parasitic nematodes. [17]

Representatives of *Dorylaimida*; *Pearse, 1942* which are prominent order in almost all agro and natural ecosystems, were leading from a taxonomic perspective. True predators took the second place from a trophic standpoint (25 species- 26,4% of species composition). Slightly behind them were omnivores and bacteriovores (27 species - 24,7% of specis composition and 25 species-22,9% respectively). True plant parasites are represented by 21 species (19,2% of species composition). *Ditylenchus destructor*

Thorne,1945, Longidorus elongatus (de Man, 1976) Thorne et Swanger, 1936 and *Xiphinema brevicolle Lordello & Da Costa, 1961* were the most coomon species. Among fungivorous nematodes (which accounted for 7,33% of species composition- 8 species) the most common species was *Aphelenchus avenae Bastian, 1865.*[18]

CONCLUSION

Our investigations reveal the frequency of encountering the most common nematodes in the soil of six agro-ecosystems within Khulo region. At least one free-living or one phytoparasitic nematode was found in all agroecosystems. The highest abundance of nematodes was observed in the village Uchko, while the lowest was recorded in the village Dekanashvili. Additionally, Uchkho demonstrates the highest species diversity among the studied areas. 19 eudominant and dominant soil-nematode genera constituting the basis of the community structure were identified. They constitute 54.3–66.4% of the total number of the registered genera in spring, 49.4–58,2% in summer, 57.7–69.6% in fall, and 39.3– 43.6% in winter. 21 species of phytonematodes were identified, although the number did not exceed 5-6 individuals per 50 grams of soil. The abundance was slightly higher in *Ditylenchus destructor Thorne, 1945*. This increase can be attributed to the utilization of invasive seed material. Therefore, it is imperative to exercise caution when implementing agro-engineering measures to prevent the spread of this harmful pathogen in potato cultivation.

ACKNOWLEDGEMENTS

This work was carried out within the framework of the Project "**Fauna of Georgia – current trends and conservation**", funded by the Ministry of Science and Education of Georgia. Authors gratefully acknowledge support of all members of Department of Nematology at Institute of Zoology of Ilia State University.

REFERENCES

[1] Baermann, G. Eine einfache Methode zur Affi ndung von Ankylostomum (Nematoden) larven in Erdprobem // Geneesk. Tijdschr. Ned. (1917) Ind. 57. — S. 131–137.

[2] Decker, H. (1972). Plant nematodes and their control. (Phytonematology). Kolos, Moscow, 444 p.(In Russ)

[3] Kirjanova, E. S., Krall, E. L. (1969). Plant-parasitic nematodes and measures of their control. Moscow : Nauka, Vol. 1-477 p.(In Russ)

[4] Courtney WD, Polley D, Miller VL. TAF: An improved fixative in nematode technique. Plant Disease Reporter. 1955; 39:570–571.

[5] Decker, H. Plant nematodes and their control. (Phytonematology). — Moscow : Kolos, 1972. 444 p. Russian

[6] Siddiqi, M. R. (2000). Tylenchida: parasites of plants and insects. Norfolk : CABI,. 834 p

[7] Stirling, G., Nicol, J., Reay, F. Services for Nematode Pests : Operational Guidelines // Rural Industries Research and Development Corporation. — Canberra, 2002. —120 p

[8] Mai, W. F., Mullin, P. G. Plant-parasitic nematodes. A pictorial key to genera. — New-York : Cornell University Press, 1996. — 278 p

[9] Ryss, A. Yu. (1988) Parasitic root nematodes of the family Pratylenchidae (Tylenchida) of the world fauna. Leningrad : Nauka, 368 p. Russian

[10] Goodey, T. (1963) Soil freshwater nematodes. London : Methuen 544 p.

[11] Eliava, I. J. (1988) Free-living nematodes of the family Dorylaimidae.. Nauka Leningrad, 264 p. (In Russ)

[12] Kirjanova, E. S., Krall, E. L. Plant-parasitic nematodes and measures of their control. — Moscow : Nauka, 1971. Vol. 2. 522 p. Russian

[13] Ferris Howard (1999). University of California. http://nemaplex.ucdavis.edu/index.htm

[14] EPPO.(2017) Diagnostics. PM 7/87 (2). Ditylenchus destructor and Ditylenchus dipsaci. Bulletin OEPP/EPPO Bulletin 47 (3): 401–419

[15] Shesteperov, A.A (1985)., The dynamics of the number of phyonematodes in various natural and climatic zones and its importance in ecological studies, in Printsipy i metody ekologicheskoi fitonematoloii (Principles and Methods of Ecological Phytonematology). Petrozavodsk, pp. 51–77

[16] Brzeski M.W. (1991). Review of the genus Ditylenchus Filipjev, 1936 (Nematoda: Anguinidae). Revue de Nématologie (14) 9–59.

[17] Yeates G.W., Bongers T., De Goede R.G.M. [et al.]. (1993). Feeding habits in soil nematode families and genera. An outline for soil ecologists. Journal of Nematology.;25:315–331

[18] Yeates, G.W., Bongers, T., (1999) Nematode diversity in agroecosystems. Agriculture, Ecosystems and Environment 74, pp.113–135

THE CHANGES OF FOREST GROUND VEGETATION CAUSED BY GRAZING, LATVIA

Prof. Dr. Inga Straupe[1]

Bac.silv. Alise Dimane[1]

[1] University of Life Sciences and Technologies, **Latvia**

ABSTRACT

The aim of the research is to find out how the forest ground vegetation changes in forest pasture where wild horses are allowed to graze, and what impact their grazing in the forest have on the vegetation and how the situation changes in a forest stand where animals are allowed to graze and, in a forest, stand of the same type without grazing. So far forest pastures practically have not been studied, but forest management using animals especially in private forestry is becoming more and more relevant. Almost no similar study has been conducted in Latvia on the impact of large herbivores (wild horses) on forest ground vegetation. Forest stand is divided into two parts – one where the animals graze, the other behind the fence in the same forest stand where they are not grazed, so it is possible to objectively assess the changes between the two territories and how the ground vegetation changes under the influence of animals. The study compares changes between forest pasture and ungrazed forest area: the number, the occurrence and the projective coverage of plant species, as well as other vegetation indicators. It has been established that the ground cover of forest pastures does not differ significantly to compare with ungrazed forest area.

Keywords: forest pasture, forest grazing, wild horses, forest ground vegetation

INTRODUCTION

Wild horses (tarpans) *Equus ferus ferus* and wild cows (tauruses) *Bos taurus primigenius* are large herbivores that inhabited the territory of Latvia in ancient times, as evidenced by archaeological excavations. Forest pastures have a long history, where large herbivores have shaped the landscape by grazing in meadows and forest stands. It is known that until 1940 cattle grazing in the forest was common throughout Latvia and over-grazed sparsely stocked forests or park-like situations with ground vegetation characteristic of grasslands. They were often found in the fifties of the past century, in some cases appropriately managed biotopes were found already in the 1980s, and after a few years of management discontinuation they still exist today [1].

Large herbivores have learned to co-exist well together and each species plays an important role in shaping the overall ecosystem [2]. Wild cows *Bos taurus primigenius* prefer to feed on taller grass without plucking it to the ground, therefore they need large, extensive pastures in order to survive. They are classified as ruminants, just like today's domestic cows. These herbivores use the grass which was not consumed during the summer season as food in the winter season. They need fertile and extensive pastures to be able to provide themselves with all the necessary nutrients. As for wild horses, they are not ruminants, so they need more feed than wild cows. They mainly feed on newly grown short grass which is much juicier. Horses tend to make "toilets", where the animals do not eat the regrown grass composed mostly of nitrogen-loving plant species or nitrophilous plants. Both species of animals are perfectly able to co-exist, since their

feeding patterns only complement each other. Animals of both species also tend to browse on the bark of trees, as well as mechanically affect the trunks by rubbing their bodies against them. There are places which are not grazed at all, thus mosaic grazing pattern is formed [1].

Among the large wild animals none can replace wild horses and cows, which are the only large herbivores. For example, moose and deer are typical wild animals that inhabit the forest, but they are classified as shrub and grass eating animals. Depending on the eating habits of herbivores, the vegetation in the forest also changes [2].

In most part of Europe, forests and meadows have become two different ecosystems due to forestry and agriculture. Cultivating or grazing meadows does not create an opportunity for young trees to grow, while open areas in the forest are planted, preventing the formation of glades. Under natural conditions, the formation of forests is facilitated by meadows and vice versa, this means that the meadow and the forest can be considered as one whole, which ensures free movement of wild animals [1].

Overgrazing causes damage to the growth and development of trees, therefore it is important to keep close watch on animal density by dividing them into several herds during the growing season, but without separating family divisions or, if possible, graze animals in younger stands where the trees are less susceptible to damage.

In order for plants to obtain all the necessary nutrients, they need to absorb them from nature with the help of roots and green mass. Manure, including also horse manure, is a form of fertilization with the help of which plants can take up some of the necessary nutrients. They contain potassium, phosphorus, nitrogen, etc. A positive aspect of animal manure is that it not only provides the plant with nutrients, but also forms a fertile layer. Over time, it becomes humus, which forms the upper layer of the soil, and it has a positive effect on the mechanical and physical properties of the soil. Another point to consider is that the nutrients contained in fresh manure are mostly difficult to absorb [3].

Horse manure is considered to be very valuable since it contains much more nutrients compared to cow manure. An approximate chemical composition of horse manure per kg of manure is as follows: calcium - 3.5 g, potassium - 2 g, nitrogen - 4.7 g and phosphorus - 3.8 g. The role of nitrogen in plant life is very important. The presence of nitrogen ensures the formation of green mass for the plant during its growth. Animal manure has a high level of nitrogen, which serves as a good fertilizer for plants in the spring, promoting plant growth and development. The nitrogen present in manure remains in the soil for a long time. Phosphorus is important for protein synthesis and transfer of genetic information. It is also part of the metabolism and energy exchange as well as an intermediate product in the reactions of photosynthesis and respiration. Most of phosphorus is found in seeds. In the case of phosphorus deficiency, the reproductive organs and their development are affected, the amount of seeds decreases, growth is hindered and dark coloured spots are observed on the leaves. In the presence of potassium, more nitrogen is taken up by plants, and it also reduces soil acidity. Potassium deficiency can affect plant respiration and interfere with the use of phosphorus and nitrogen. Older plants can more easily use the compounds that are less soluble, but younger plants can easily take up potassium. Calcium is present in all plant cells. The aboveground parts of the plant contain more calcium than the roots, however the presence of calcium is also important for the development of the root system. Calcium affects the utilization and uptake of other elements in the plant [3].

As a result of grazing, the habitat protected by the European Union is formed in Latvia *9070 Forest pastures* - a vegetation complex consisting of dispersed trees or groups of trees and shrubs that alternate with open meadow glades in a mosaic pattern. The most characteristic tree species are common oak *Quercus robur* L., small-leaved lime *Tilia cordata* Mill., wych elm *Ulmus glabra* Huds., European white elm *Ulmus laevis* Pall., and European ash *Fraxinus excelsior* L. Today, only a small part of this habitat is managed. This is a species-rich vegetation complex with rare or endangered meadow species and a rich flora of epiphytic mosses and lichens. Many endangered species are found on old trees growing in semi-open conditions. This habitat type has a high aesthetic and cultural-historical importance as a feature of the traditional rural landscape of Latvia, which was widespread during the formation of the Latvian state. The biotope is considered one of the oldest landscape forms in our climatic zone, having formed by the interaction of man and nature and existing until today, at least since the Bronze Age (3500 years ago). Perhaps the appearance and importance of forest pastures in maintaining biodiversity is quite close to the primitive – untouched by man – conditions maintained by wild large herbivores in ancient times [4, 5].
Animals prefer to stay closer to the edge of the forest, as forest pastures are usually located adjacent to open pasture grasslands. In general, a structure promoting diversity can be observed in forest pastures where permanent grazing takes place. Animals tend to walk on trails or leave hoof prints in the soil. There are places where they prefer to stay, and there the ground vegetation contains fewer plants while in other places there are more of them. In the autumn season, if there are fruit trees in the area of forest pastures, animals gather around them, trampling down the layer of herbaceous plants, thus hindering the introduction of competing species. In places which are more frequented by animals, there is more animal excrement. This means that in such places there will be more uneaten grass and nitrogen-loving species will be found more frequently – *Urtica dioica* L. or *Stellaria media* (L.) Vill. [4]. The aim of the study is to assess the changes in the ground vegetation in forest pastures.

MATERIALS AND METHODS

The research area is located in Rauna county farm 'Jaun-Ievinas', Latvia. Grazing started in 2003, and a forest area (20.9 ha) and meadows (5.1 ha) are available for grazing animals. In total, 7 tarpans and 14 cattle graze here. Only horses inhabit the pasture throughout the year, but during the vegetation season cows are also allowed to graze in the area.
The forest type is *Mercurialiosa mel*., the soil is rich, formed from the residues of deciduous trees. The forest stand is composed of silver birch *Betula pendula* L., Norway spruce *Picea abies* L.H. Karst., grey alder *Alnus incana* (L.) Moench., some aspen *Populus tremula* L. The undergrowth is composed of Norway spruce, grey alder, common oak *Quercus robur* L., bird cherry *Padus avium* Mill, common hazel *Corylus avellana* L., glossy buckthorn *Frangula alnus* Mill., Norway maple *Acer platanoides* L., wild cherry *Prunus cerasus*, mountain ash *Sorbus aucuparia* L. and plum *Prunus spp*. The forest stand is divided by a fence, forming sample plots on both sides of the fence - in the forest pasture and in the ungrazed area - it is possible to objectively compare the effect of particularly these large herbivores on the changes in the ground vegetation.
Three sample plots of 20 x 20m (area 400 m^2) were established in each forest stand area. The data were collected in August – during the vegetation season, when the plant species of ground vegetation are clearly identifiable. For each vegetation layer and for

each species, the projective coverage was assessed in percentage: in the tree layer E3 (trees and shrubs higher than 7 m), in the shrub layer E2 (undergrowth shrubs and advanced growth trees 0.5 - 7 m), in the herbaceous plant layer E1 (herbaceous plants, also young trees and shrubs not exceeding 0.5 m in height) and in the moss layer E0. Microsoft Office Excel programme was used for calculations. T-test was used to determine whether significant differences exist between the forest pasture and the ungrazed area. According to the Raunkiaer formula, an occurrence coefficient was calculated for each species of vascular plants, which reflects the frequency of the species representation in the sample plots [6]. Constancy classes were also determined for the species, by referencing the number of the plots where the species was found against the total number of sample plots: I (< 21 %), II (21 – 40 %), III (41 – 60 %), IV (61 – 80 %) and V (81 – 100 %) [7]. The Jaccard similarity coefficient was calculated to compare changes in vegetation stands in the forest pasture and in the ungrazed forest area. The value of the Jacquard coefficient can be from 0 - 1. The closer the value is to 1, the greater the similarity between the two compared sites. Ecological indicators were determined for the species of vascular plants present in the herbaceous plant layer according to the Ellenberg's standard scale. Ecological indicators of the species were determined for the following environmental factors: light, temperature, soil reaction, moisture and nutrients content [8].

RESULTS AND DISCUSSION

Number of species. The total number of species in all sample plots is 84. There are 8 species in the tree layer, 10 species in the shrub layer, 64 species in the herb layer and 8 species in the moss layer. The total number of species found in the forest pasture area is 70 plant species, while in the ungrazed area there are 65 plant species. It can be concluded that the number of species found in the forest pasture is greater than in the ungrazed forest area, which confirms the fact that forest pasture, where large herbivores graze, have a greater species diversity [4]. In the area of forest pasture, 7 plant species are found in the tree layer and the same number of plant species is found in the ungrazed area. The shrub layer includes 6 plant species in the forest pasture area and 9 plant species in the ungrazed area. There are 59 plant species in the layer of herbaceous plants in the area of forest pasture, whereas in the ungrazed area there are 53 species. In the moss layer of the area of forest pasture there are 6 species, in the ungrazed area there are 7 species. Using the t-test, it was determined that the differences by layers between the number of plant species found in the forest pasture and in the ungrazed area were not significant (p-value 0.8 > 0.05). In 1930, a study by H.J. Lutz, a professor of forestry in Pennsylvania, examined the effect of cattle grazing on forest vegetation. The total number of species of shrubs and herbaceous plants was higher in the forest pasture than in the ungrazed area, and the species that had not been found in the ungrazed area appeared in the forest pasture [9].

Plant occurrence using the Raunkiaer's occurrence coefficient and constancy classes. By summarizing the data on the occurrence of species and belonging to constancy classes (Table 1), it is possible to determine how frequently a species is found in a particular area.

The more often a plant species is found, the more stable it is and the better it characterizes the site. On the other hand, if a species is found rarely or quite rarely, it may have entered the area accidentally and may also quickly disappear.

Table 1
Occurrence of plant species in forest pasture and ungrazed areas

Constancy class	Number of species in forest pastures	Species proportion in forest pasture %	Number of species in ungrazed area	Species proportion in ungrazed area %
V	36	45.6	25	32.5
IV	18	22.8	15	19.5
III	0	0	0	0
II	25	31.6	37	48.0
I	0	0	0	0

The largest number of species in forest pasture in total by layers is right at the constancy class V (most frequently) - 36 species (45.6 %). 18 plant species (22.8 %) belong to class IV (frequently) and 25 plant species (31.6 %) belong to class II (quite rarely), but no plant species is found belonging to class I (rarely) and class III (quite frequently) constancy index. It can be concluded that in this territory, the conditions for the growth of the majority of plants (68.4 % in total) are favorable and stable under the specific conditions, despite the disturbance caused by animal grazing. However, 31.6 % of the plants here are found temporarily, due to grazing disturbances - trampling, improvement of light conditions, etc. In the ungrazed area, there are 25 plant species (32.5 %) belonging to constancy class V (frequently), 15 species (19.5 %) to class IV (frequently), and 37 plant species (48.0 %) to class II (quite rarely), found to be of greatest prevalence exactly in the ungrazed area. No plant species are found belonging to constancy class III (quite frequently) and I (rarely). One of the affecting factors could be climatic conditions or various disturbances in the forest that are not related to livestock grazing, but windthrown trees create more light, which temporarily allows the development of light-loving species. Evaluating the proportion of species by layers in the forest pasture and in the ungrazed forest area, no significant changes were found – in the tree layer (p-value $0.8 > 0.05$), shrub layer (p-value $0.3 > 0.05$) and herbaceous plant layer (p-value $0.8 > 0.05$).

Changes of plant species by vegetation layers. In order to compare changes in vegetation layers in the forest pasture and in the ungrazed forest area, the Jaccard similarity coefficient was used in the study, which is identical for tree, herbaceous plant and moss layers - 0.3, and 0.1 for shrub layer. In this case, the similarity between the grazed and ungrazed site is small. This means that the differences in vegetation between the two sites are visible and there is a diversity of plant species between them. There are species that occur more frequently in the ungrazed area, but the growth conditions are less suitable for them in the forest pasture, for example *Corylus avellana*, *Frangula alnus* or *Quercus robur*. The animals which graze in the forest pasture have thinned the shrub layer by nibbling it, and due to their movement, the disturbance to the species is too great in this layer, and they cannot grow under such conditions.

Vegetation projective cover. The average projective cover of the forest pasture in the tree layer is 70%, and in the ungrazed area – 51.7%. The average projective cover in the shrub layer of forest pasture is 38.3%, in the ungrazed area - 50%. In the herbaceous plant layer of forest pasture, it is 88.3%, while in the ungrazed area it is 56.7%. The

average projective cover in the moss layer of forest pasture is 6.3%, but in the ungrazed area it is 5% (Figure 1).

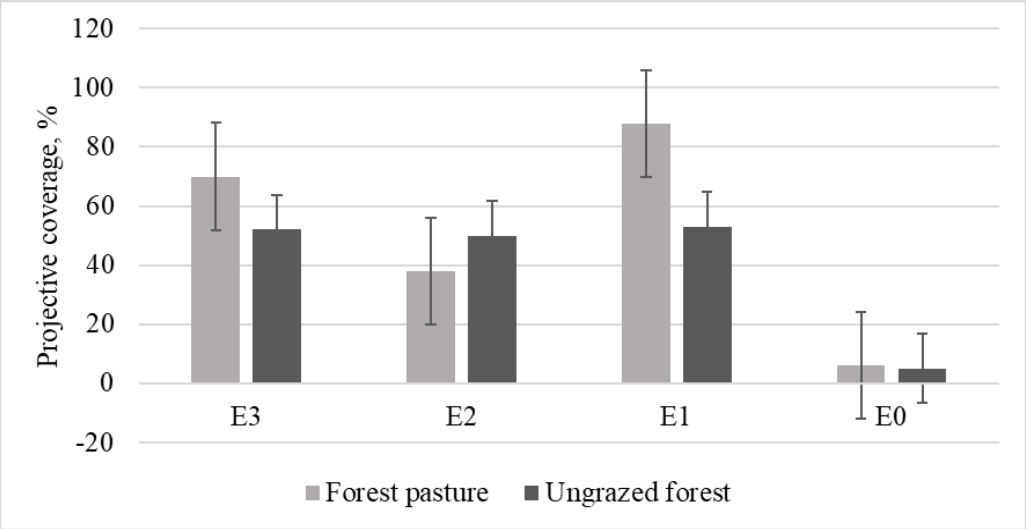


Fig.1 Projective cover by layers in forest pasture and in ungrazed area

Betula pendula has the highest projective cover in the tree layer, both in the forest pasture and in the ungrazed area, and no significant differences between the sites were found (p-value 0.06 > 0.05). *Padus avium* forms the largest projective cover in the shrub layer in the forest pasture, while in the ungrazed area it is *Picea abies*, and no significant differences were found between the sites (p-value 0.4 > 0.05). The largest projective cover is composed of a layer of herbaceous plants. *Oxalis acetosella* L., *Poa trivialis* L. and *Padus avium* form the largest projective cover in the herbaceous plant layer in the forest pasture. In the ungrazed area in the herbaceous layer they are *Padus avium*, *Poa trivialis* and *Geum rivale* L. In the herbaceous plant layer, the difference between the forest pasture and ungrazed area (respectively 88.3 % and 50 %) is significant (p-value 0.003 < 0.05). The most important affecting factor here is light. As a result of animal grazing, small openings have formed in the forest, the shrub layer has become thinner as well. Thus, the access of light to the ground vegetation increases and an there is an opportunity for sun-loving species to develop. In the moss layer of forest pasture *Plagiomnium undulatum* (Hedw.) T. Kop. and *Dicranum polysetum* Sw. are the most common, while *Rhytidiadelphus triquetrus* (Hedw.) Warnst. is found in the ungrazed area, and no significant differences have been found (p-value 0.4 > 0.05).

Characterization of environmental factors. Ellenberg's indicator values were used to describe environmental factors. These values determine the requirement of plant species for specific climatic and edaphic factors (Figure 2). In the forest pasture, the average value of the light index is 5.7, but in the ungrazed area it is 5.4. This indicates that the plant species in the forest pasture are more light-demanding compared to the ungrazed area. Since more light reaches the ground vegetation as a result of animal grazing in the forest pasture, more sun-loving species grow there. The requirement of plants for the edaphic environmental conditions has also been studied. Plant requirements for moisture are the identical in the forest pasture and in the ungrazed forest area - 5.9. The demand for nutrients (soil reaction) is higher in the forest pasture – 6.1, while in the ungrazed forest area it is – 5.8. This can be attributed to the presence of animals in the area. The requirements of plant species for nitrogen are the identical in both sites (nitrogen value - 4.8). In the forest pasture, plants obtain part of nitrogen from

excrement left by animals, in which the nitrogen content is high, in the ungrazed area the demand for nitrogen has the same value, which indicates a similar chemical composition of the soil [3]. There are found significant differences between the shrub layers (p value 0.03 < 0.05) in both areas.

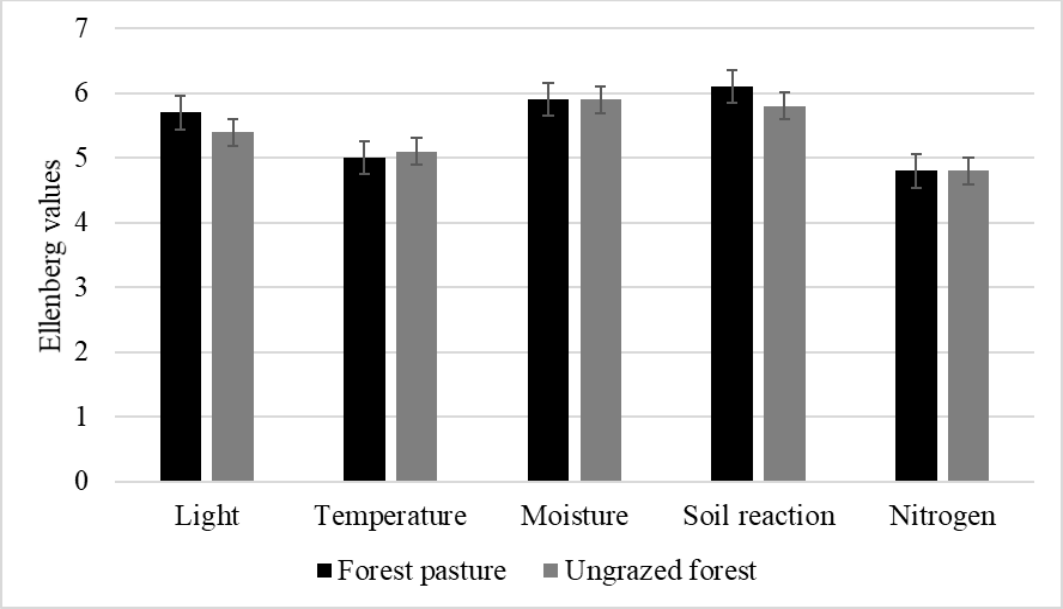


Fig.2 Ellenberg's indicator values of environmental factors

A greater diversity of vegetation can be found in the forest pasture area than in the ungrazed forest area due to the ability of animals to free trees and bushes from the lower branches and foliage, thus ensuring more light for the topsoil. When cattle graze in the forest pastures, it has been established that a horizon free of foliage has formed, at a height of about 1.5 - 2 m, because the undergrowth and the lower branches of the trees have been browsed or broken off by the cattle rubbing against them. This means that more light reaches the ground vegetation - about 15.8%, but only 9.5% of the light reaches the ungrazed areas [4].

CONCLUSIONS

A total of 78 plant species have been found in the forest pasture throughout all layers, and 76 plant species in the ungrazed area. The differences between them in terms of the number of species are not significant. The most common plants in the forest pasture belong to constancy class V (most frequently), but in the ungrazed area, the largest number of species is found exactly at the constancy class II (quite rarely). In both areas, the largest projective cover is occupied by the herbaceous layer, and the differences between the two areas are significant. No significant differences were found between the tree and shrub layers in the forest pasture and in the ungrazed area. When comparing the requirements of plant species for specific climatic (light) and edaphic (moisture, soil reaction, nitrogen) factors in the forest pasture and in the ungrazed area, there are significant differences between the shrub layers. A future task would be to study how vegetation changes over a longer period of time.

ACKNOWLEDGEMENTS

This study was funded by Latvia University of Life sciences and Technologies' Z72 project 'Influence of meteorological factors on radial increment of introduced tree species in Latvia'.

REFERENCES

[1] Lielo savvaļas zīdītāju dabiskā ganīšanās (Natural grazing of large herbivores), Latvia, WWF, 2004. Available: https://wwflv.awsassets.panda.org/downloads/lielo_savvalas_zaledaju_gramata.pdf (in Latvian)

[2] Vermeulen R., Natural grazing: Practises in rewilding of cattle and horses, Netherlands, 2015. Available: https://rewildingeurope.com/app/uploads/2015/07/Natural-grazing-%E2%80%93-Practices-in-the-rewilding-of-cattle-and-horses.pdf

[3] Mauriņa H., Augu fizioloģija (Plant physiology), Latvia, Riga, Zvaigzne, 357 pp., 1987. (in Latvian)

[4] Larmanis V., 9070 Meza ganibas (Forest pastures). Latvia, Dabas aizsardzibas parvalde, 2015. Available: https://www.daba.gov.lv/lv/media/4670/download (in Latvian)

[5] Vera F., Grazing Ecology and Forest History, USA, Wallingford: CABI Publishing, 506 pp., 2000.

[6] Markovs M., Vispārējā ģeobotānika (General geobotany), Latvia, Riga, Liesma, 434 pp., 1965. (in Latvian)

[7] Mueller-Dombois D., Ellenberg H., Aims and methods of vegetation ecology, USA, New York, Wiley, 547 pp., 1974. DOI: 10.2307/213332

[8] Ellenberg H., Weber H. E., Dull R., Wirth V., Werner W., Paulbent D., Zeigerwerte von Pflanzen in Mitteleuropa, Germany, Göttingen, Verlag Erich Goltze, 248 pp., 1992.

[9] Lutz H.J., Effect of cattle grazing on vegetation of a virgin forest in Northwestern Pennsylvania, USA, Journal of Agricultural Research, vol. 41, pp. 561-570, 1930.

THE EFFECT OF TRAIL PATHS IN GRASSLAND ECOSYSTEMS USING A SWOT-AHP HYBRID METHOD

Dr. Aimilia Lempesi[1]

Christodoulos Daoutis[1]

[1]Department of Forestry and Management of the Environment and Natural Resources of the Faculty of Agriculture and Forestry of the Democritus University of Thrace, **Greece**

ABSTRACT

In recent years, the use of trail paths for recreation and tourism has seen remarkable growth in many countries. Trail paths have several benefits for the local community, people's physical and mental health, and for offsetting degraded grassland ecosystems. The objective of the study was to assess the effect of trail paths on grassland ecosystems in the Prefecture of Xanthi in northern Greece. The SWOT-AHP hybrid method was used. The criteria of the SWOT (Strengths, Weaknesses, Opportunities, and Threats) method were recorded based on the literature review. Data were collected using questionnaires and analyzed using the AHP (Analytic Hierarchy Process) method, and the criteria were compared pairwise. The study found that the Strengths group occupied the largest percentage (40.3%), immediately after the Weaknesses group occupied 26.7%, followed by the Opportunities group at 21.0% and the Threats group which had the smallest percentage (12.0%). The results also showed that in the comparisons of the Strengths group, the largest percentage (43.4%) held the (Increase biodiversity along trail paths) criterion. In the comparisons of the Weaknesses group, it was observed that the (The construction and use of trail paths cause soil erosion and compaction) criterion gathered a large percentage of 39.6%. In the comparisons of the Opportunities group, the largest percentage (41.1%) held the (Trail paths can be used as a passage for rescuers) criterion and (Visiting the trail paths can increase the risk of fire) criterion from the comparisons of the Threats group was the biggest threat with a percentage that exceeds 50.0%.

Keywords: trail paths, grasslands, recreation, SWOT-AHP

INTRODUCTION

Trail paths provide access to traditional settlements and tourist attractions [1]. For hikers, walking the trail paths is a way of pleasure, an economical way to socialize, physical activity and improve health [2]. For the local community, nature-based tourism attracts visitors and enables local economic development, generating economic revenues and employment [3]. On the other hand, campfires and smokers are two of the biggest causes of fires [4]. Therefore, the risk of fire by trail paths visitors can be increased [5]. The increase in visitors to forest and mountainous areas increases accidents caused by hikers, but trail paths can be important points of assistance for rescuers [6].

Several studies report that biodiversity increased along the trail paths [7]. This could be due to seed dispersal as hiking trails act as dispersal corridors for some plant species [8], due to the movement of people and animals along the trails [9]. According to Klug et al. [10] The number of seeds was greater near the trail paths because grasses are more

resistant to trampling than other functional plant types [11]. In addition to grass species, some orchid and flowering species have been recorded to benefit from pathway-related disturbances, including rare species [12].

Trail paths disrupt communities through their construction and maintenance [13] and can cause changes in plant succession [14]. In cases where trail paths pass through forests, there may be adverse effects on the root system of trees subject to frequent trampling [15]. Trampling from hiking trails can cause changes in composition, vegetation structure and vegetation cover and causes soil erosion and compaction [16]. According to Wolf and Croft [17] on high-traffic trails, soil compaction increased. In addition, trampling can contribute to vegetation changes through mechanical destruction of plants, loss of species [5], and habitats [18]. Habitat loss, introduction of invasive species and change in vegetation composition led to reduced biodiversity [18]. The trail paths also contribute directly to increasing illegal plant harvesting, especially in biodiversity hotspots and developing countries [13]. It is also widely known to increase the dominance of woody [19] and invasive species near trail paths [8]. The increase in light and space caused by clearing and construction along the trail paths alters the structure and increases the growth of invasive species [17].

Investing in trail paths can have many benefits for the local community, for hikers themselves, and for compensating for degraded grassland ecosystems [3]. Hiking trails are inextricably linked to the environment, and to the grasslands studied in this paper.

MATERIALS AND METHODS

STUDY AREA

The research area (Figure 1) was the Prefecture of Xanthi (41°8′0″N 24°53′0″E). Administratively, it belongs to the Region of Eastern Macedonia and Thrace (Greece). The area of the prefecture is 495 km². According to the data obtained from the Greek Mountaineering Club of Xanthi (https://www.eosx.gr) 22 trails with a total length of 191.26 km are recorded. According to Corine 2018, the area has grassland ecosystems with an area of 7127.15 ha, through which many trails pass.

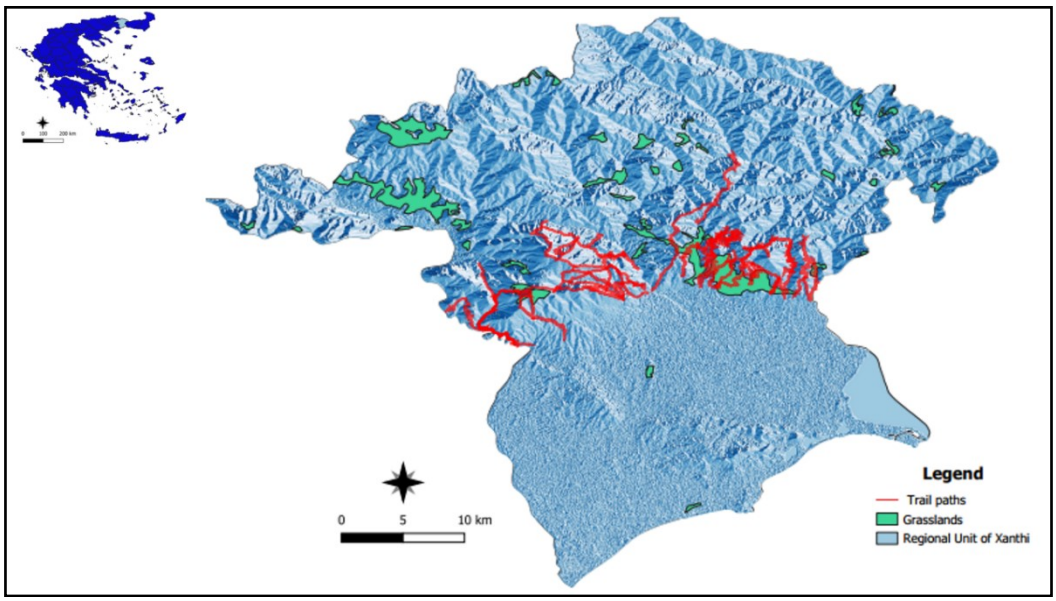


Figure 1: Study area (Prefecture of Xanthi)

METHODOLOGY

In this study, the SWOT-AHP method was applied to evaluate the criteria regarding the effect of trail paths in grassland ecosystems using a SWOT-AHP hybrid method. The hybrid SWOT–AHP method interprets the SWOT criteria (Table 1) with quantitative values and makes them comparable [20]. For collecting data, a structured questionnaire was constructed, and 100 closed-ended questionnaires were distributed to hikers for the comparison of the SWOT criteria (Strengths, Weaknesses, Opportunities and Threats).

Table 1: SWOT (Strengths, Weaknesses, Opportunities, Threats)

Strengths	S1. Increase biodiversity along trail paths S2. Grasses are resistant to trampling S3. Trail paths act as distribution corridors for certain plant species S4. Trail paths help local economic development	W1. The construction and use of trail paths cause soil erosion and compaction W2. Trampling can alter the composition and structure of vegetation W3. Trail paths cause changes in plant succession W4. Increase dominance of woody and invasive species near trail paths	Weaknesses
Opportunities	O1. Trail paths can be used as a passage for rescuers O2. Trail paths can be used to observe sights and nature O3. Trail paths can benefit the growth of rare species O4. Hikers' contact with the natural ecosystem can benefit health and social contacts	T1. Trail paths can cause habitat and species loss T2. Facilitate access to illegal plant collection T3. The construction of trail paths can affect the root system T4. Visiting trail paths can increase the risk of fire	Threats

AHP Analysis

The information derived from pairwise comparisons can be summarized in a table of weights, where the relative weight enters the table as element aij and the inverse of the preference ratio 1/aij goes on the opposite side of the main diagonal.

$$A = (a_{ij}) = \begin{bmatrix} W_1/W_1 & W_1/W_2 & \dots & W_1/W_n \\ W_2/W_1 & W_2/W_2 & \dots & W_2/W_n \\ \vdots & \vdots & & \vdots \\ W_n/W_1 & W_n/W_2 & \dots & W_n/W_n \end{bmatrix} \quad (1)$$

When we multiply the matrix A by the permutation of the vector of weights (w), we get the resulting vector nw.

$$(A_w - \lambda_{max} I)W = 0 \quad (2)$$

For consistency to exist, λmax=n otherwise λmax>n. Therefore, array A must be checked for consistency using the formula:

$$CI = \frac{(\lambda \max - n)}{(n-1)} \quad (3)$$

The CI consistency index is determined by normalizing the difference below. The consistency index RI is the random index generated for a random matrix of order n and CR is the consistency ratio [21]. The general rule is that CR should be CR≤0.1 for the table to be consistent.

$$CR = \frac{CI}{RI} \quad (4)$$

RESULTS

Four criteria (Strengths, Weaknesses, Opportunities and Threats) and their sub-criteria were rated by hikers using a questionnaire. With the SWOT analysis method, the most important internal (Strengths and Weaknesses) and external (Opportunities and Threats) factors affecting human activities and the plant community were recorded. With the contribution of the AHP method, the factors of SWOT were compared pairwise to analyse the factors for developing strategies. The degree of importance after the pairwise comparison of (Strengths, Weaknesses, Opportunities and Threats) (Figure 2) exhibited that the Strengths group occupied the largest percentage (40.3%). This is followed by Weaknesses with 26.7% and Opportunities with 21.0%. Threats ranks last with a percentage of 12.0%.

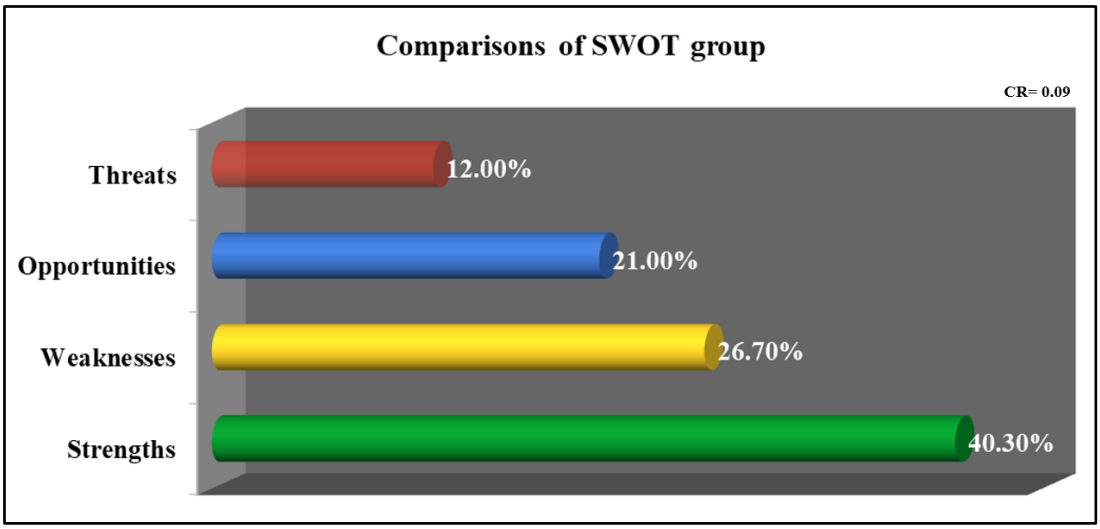


Figure 2: Comparisons of SWOT group

In the comparisons of the Strengths group (Figure 3a), it was observed that the sub criteria "increase biodiversity along trail paths (S1)" and "grasses are resistant to trampling (S2)" had the highest percentages of 43.4% and 31.3% respectively. In third place with a percentage of 19.2% was the sub criterion "trail paths act as distribution corridors for certain plant species (S3)". The last of the sub-criteria was "trail paths help local economic development (S4)". In the comparisons of the Weaknesses group (Figure 3b), it was observed that the first place with a percentage of 39.6% occupied the sub criterion "the construction and use of trail paths cause soil erosion and compaction (W1)". This was followed by the sub criterion "increase dominance of woody and invasive species near trail paths (W4)" with a percentage of 22.7%. In third and fourth place by a small margin (19.2% and 18.5%) were the sub criteria "trampling can alter the composition and structure of vegetation (W2)" and "trail paths cause changes in plant succession (W3)". (Figure 3c) shows the ranking of sub-criteria by Opportunities. The sub-criterion "trail paths can be used as a passage for rescuers (O1)" gathered 41.1% and held the first place, followed by the sub-criteria "trail paths can benefit the growth of rare species (O3)" (25.3%) and "trail paths can be used to observe sights and nature (O2)" (21.1%). Finally, the sub-criterion "hikers' contact with the natural ecosystem can benefit health and social contacts (O4)" (12.5%) was identified. In the comparisons of the Threats group (Figure 3d) it was observed that the sub criterion "visiting trail paths can increase the risk of fire (T4)" received a percentage of 58.2%. The second-largest threat was the sub criterion

"facilitate access to illegal plant collection (T2)" (29.4%). The threats with the lowest percentages were "trail paths can cause habitat and species loss (T1)" and "the construction of trail paths can affect the root system (T3)" with percentages of 6.8% and 5.6%.

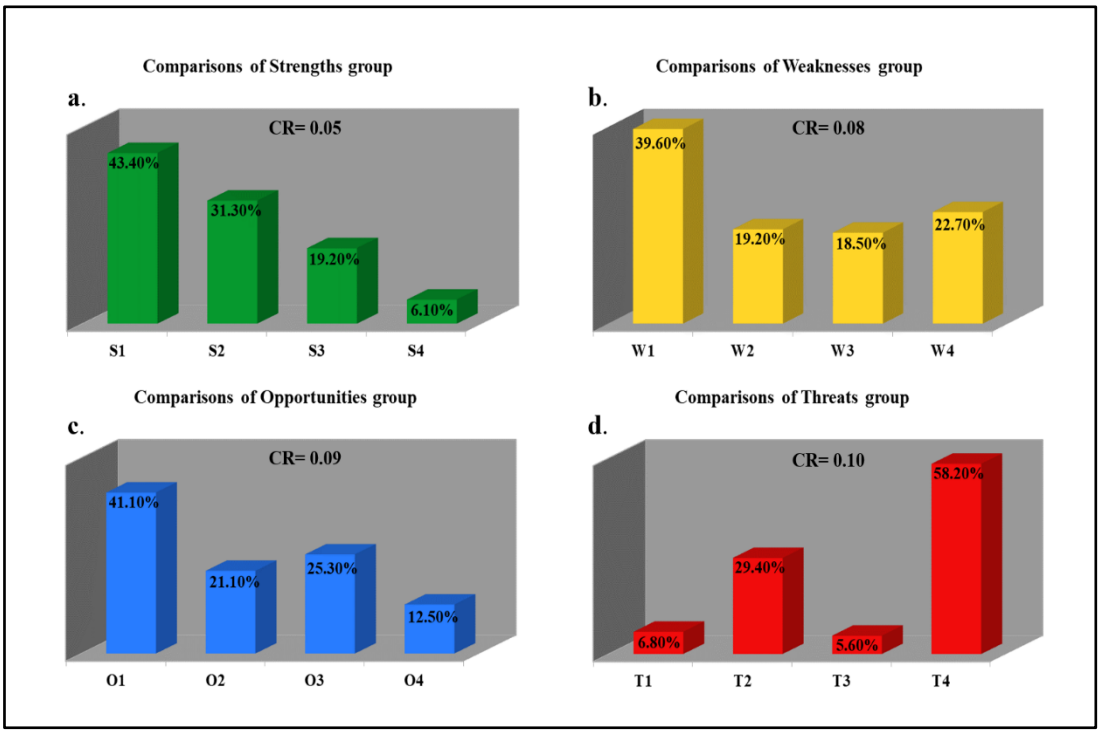


Figure 3: a. Comparisons of Strengths group, b. Comparisons of Weaknesses group, c. Comparisons of Opportunities group, d. Comparisons of Threats group

CONCLUSION

The trail paths can bring hikers into contact with the natural environment, especially with grassland ecosystems. Trail path management should encompass strategies such as construction, upkeep, repair, control of type and duration of use, and educating trail path visitors. Managers and decision-makers, through the SWOT-AHP method, could apply a strategic plan for the construction or maintenance of trail paths in a grassland ecosystem. According to the SWOT-AHP hybrid method, it was observed that the Strengths gathered the most preference of the respondents after comparing with the rest of the criteria. The Weaknesses and the Opportunities followed, and Threats occupied the last place. Regarding the sub-criteria of SWOT, Strengths highlighted the sub-criterion "Increase biodiversity along trail paths". In Weaknesses, "the construction and use of trail paths cause soil erosion and compaction" was considered the weakest point. The opportunity that had a first place was "trail paths can be used as a passage for rescuers» and the biggest threat was «Visiting trail paths can increase the risk of fire". These results make planners aware of the problems in the natural environment and biodiversity if trail paths exist, or new ones are built.

REFERENCES

[1] Tomczyk A. M., Ewertowski M. W., White P. C. L., Kasprzak L., A new framework for prioritising decisions on recreational trail management, Landscape and Urban Planning, vol. 167, pp 1-13, 2017. https://doi.org/10.1016/j.landurbplan.2017.05.009

[2] Kaczynski A. T., Henderson K. A., Environmental correlates of physical activity: A review of evidence about parks and recreation, Leisure Sciences, vol. 29/issue 4, pp 315-354, 2007. https://doi.org/10.1080/01490400701394865

[3] Maria Raya J., Martínez-Garcia E., Celma D., Economic and social yield of investing in hiking tourism: The case of Berguedà, Spain, Journal of Travel and Tourism Marketing, vol. 35/issue 2, pp 148-161, 2018. https://doi.org/10.1080/10548408.2017.1350252

[4] González-Olabarria J. R., Mola-Yudego B., Coll L., Different factors for different causes: analysis of the spatial aggregations of fire ignitions in Catalonia (Spain), Risk analysis, vol. 35/issue 7, pp 1197-1209, 2015. https://doi.org/10.1111/risa.12339

[5] Kolodziejczyk K., Networks of hiking tourist trails in the Krkonoše (Czech Republic) and Peneda-Gerês (Portugal) national parks—comparative analysis, Journal of Mountain Science, vol. 16/issue 4, pp 725-743, 2019. https://doi.org/10.1007/s11629-018-5228-3

[6] Ciesa M., Grigolato S., Cavalli R., Analysis on vehicle and walking speeds of search and rescue ground crews in mountainous areas, Journal of Outdoor Recreation and Tourism, vol. 5-6, pp 48-57, 2014. https://doi.org/10.1016/j.jort.2014.03.004

[7] Jolivet A., MacDougald A. C., Graae B. J., Klanderud K., Wedegärtner R. E. M., Sticking to the trail: Seed rain, seed bank and seedling density are elevated along hiking trails in the scandes mountains, Journal of Vegetation Science, vol. 33/issue 4, 2022. https://doi.org/10.1111/jvs.13144

[8] Potito A. P., Beatty S. W., Impacts of recreation trails on exotic and ruderal species distribution in grassland areas along the Colorado front range, Environmental Management, vol. 36/issue 2, pp 230-236, 2005. https://doi.org/10.1007/s00267-003-0177-0

[9] Suárez-Esteban A., Fahrig L., Delibes M., Fedriani J. M., Can anthropogenic linear gaps increase plant abundance and diversity?, Landscape Ecology, vol. 31, pp 721-729, 2016. https://doi.org/10.1007/s10980-015-0329-7

[10] Klug B., Scharfetter-Lehrl G., Scharfetter E., Effects of trampling on vegetation above the timberline in the eastern alps, Austria, Arctic, Antarctic, and Alpine Research, vol. 34/issue 4, pp 377-388, 2002. https://doi.org/10.1080/15230430.2002.12003508

[11] Jägerbrand A. K., Alatalo J. M., Effects of human trampling on abundance and diversity of vascular plants, bryophytes and lichens in alpine heath vegetation, northern Sweden, SpringerPlus, vol. 4/issue 1, 2015. https://doi.org/10.1186/s40064-015-0876-z

[12] Sinclair A., Catling P. M., Ontario goldenseal, hydrastis canadensis, populations in relation to habitat size, paths, and woodland edges, Canadian Field-Naturalist, vol. 114/issue 4, pp 652-655, 2000. https://doi.org/10.5962/p.364034

[13] Ballantyne M., Pickering C. M., Tourism and recreation: A common threat to IUCN red-listed vascular plants in Europe, Biodiversity and Conservation, vol. 22/issue 13-14, pp 3027-3044, 2013. https://doi.org/10.1007/s10531-013-0569-2

[14] McDougall K. L., Wright G. T., The impact of trampling on feldmark vegetation in Kosciuszko national park, Australia, Australian Journal of Botany, vol. 52/issue 3, pp 315-320, 2004. https://doi.org/10.1071/BT03145

[15] Pelfini M., Santilli M., Dendrogeomorphological analyses on exposed roots along two mountain hiking trails in the central Italian alps, Geografiska Annaler, Series A: Physical Geography, vol. 88/issue 3, pp 223-236, 2006. https://doi.org/10.1111/j.1468-0459.2006.00297.x

[16] Kostrakiewicz-Gierałt K., Pliszko A., Gmyrek-Gołab K., The effect of visitors on the properties of vegetation of calcareous grasslands in the context of width and distances from tourist trails, Sustainability (Switzerland), vol. 12/issue 2, 2020. https://doi.org/10.3390/su12020454

[17] Wolf I. D., Croft D. B., Impacts of tourism hotspots on vegetation communities show a higher potential for self-propagation along roads than hiking trails, Journal of Environmental Management, vol. 143, pp 173-185, 2014. https://doi.org/10.1016/j.jenvman.2014.04.006

[18] Leung Y. F., Newburger T., Jones M., Kuhn B., Woiderski B., Developing a monitoring protocol for visitor-created informal trails in Yosemite national park, USA, Environmental Management, vol. 47/issue 1, pp 93-106, 2011. https://doi.org/10.1007/s00267-010-9581-4

[19] Nemec K. T., Allen C. R., Alai A., Clements G., Kessler A. C., Kinsell T., Major A., Stephen B. J., Woody invasions of urban trails and the changing face of urban forests in the great plains, USA, American Midland Naturalist, vol. 165/issue 2, pp 241-256, 2011. https://doi.org/10.1674/0003-0031-165.2.241

[20] Kurttila M., Pesonen M., Kangas J., Kajanus M., Utilizing the analytic hierarchy process (AHP) in SWOT analysis—a hybrid method and its application to a forest-certification case, Forest policy and economics, vol. 1/issue 1, pp 41-52, 2000. https://doi.org/10.1016/S1389-9341(99)00004-0

[21] Saaty, R. W., The analytic hierarchy process—what it is and how it is used, Mathematical modelling, vol. 9/issue 3-5, pp 161-176, 1987. https://doi.org/10.1016/0270-0255(87)90473-8

SECTION

MARINE AND OCEAN ECOSYSTEMS

ROLE OF UNACCOUNTED SOURCES OF TOTAL NITROGEN AND PHOSPHORUS IN THE NEVA BAY ANTHROPOGENIC EUTROPHICATION

Assoc. Prof. Dr. Victor Tretyakov[1, 2]

Postgraduate Stepan Klubov[2]

Prof. Dr. Vasiliy Dmitriev[1]

Ress. Anna Nikulina[1]

[1] Saint Petersburg State University, **Russia**
[2] Russian State Hydrometeorological University, **Russia**

ABSTRACT

There is a worldwide ecological problem of anthropogenic eutrophication. The problem is especially serious one for the ecosystems of lakes, water-storage basins, and closed seas, such as the Baltic Sea. The eastern part of the sea is the Neva Bay. The water area is totally located within the administrative border of St. Petersburg and is influenced by the megacity. There is monitoring of the total nitrogen and phosphorus inflow into the Neva Bay with water of the Neva River and its spill streams. Nevertheless, there are watercourses entering the bay without points of monitoring. We presented the methodology for evaluation of the total nitrogen and substances outflow from the catchment areas without the monitoring points into the Neva Bay and the eastern part of the Finnish Gulf, and the evaluation results at the previous conferences SGEM2023 and SGEM Vienna GREEN 2023 “GREEN Science for GREEN Life”. However, there is the problem: “What is the unaccounted income influence on the bay ecosystem life?” If the influence is negligible, the authorities have not to organize monitoring points on the unaccounted watercourses. Otherwise, the authorities have to organize the monitoring points. The paper presents methodology for the problem solution by means of the ecosystem functioning computer simulation and some results of the numerical experiments. The influence significance is evaluated by modification of the Nash–Sutcliffe criterion.

Keywords: estuary ecosystem anthropogenic eutrophication

INTRODUCTION

Estuaries are wide river mouths. Any estuary is a former river valley, which was flooded in the result of the sea level increase. It could be caused by the World Ocean level increase after the last Ice Age, or by the local sinking of the earth's crust. Therefore, the estuaries ecosystems are affected by the seas and the entering rivers. The rivers are large ones with vast drainage areas. For this reason, the rivers gather contaminants over the catchment areas. In addition, megacities are usually located near the estuaries or on the shores, for example, London and Hamburg. Due to the factors, the estuaries ecosystems are the most contaminated ones. Consequently, there are a number of researches of the estuaries ecological state. Thus, the research of the Elba River estuary reviews the nitrogen cycling in Elbe estuary [1]. The researchers used model hind-casts of the years 2012 and 2013 that provided a detailed reconstruction of nitrogen recycling with ammonium appearing as the key species of the remineralisation

process. The simulations proved that the nitrogen cycling in the Elbe estuary could be tackled with a robust NPZD model coupled to a high-resolution 3D hydrodynamic model. The simulations revealed high relevance of the Hamburg harbor for heterotrophic degradation. The Sishili Bay is located in Yantai City in the northeastern Shandong province, China. The estuary is deeply influenced by human activities, such as population growth, industry, shipping, and fertilizer usage and sewage discharge [2]. There is importance of managing freshwater inflows to estuaries for their conservation and sustainable use [3]. Estuaries are dynamic ecosystems where freshwater from rivers mixes with seawater, creating a unique environment that supports diverse flora and fauna. However, alterations in freshwater flow can have significant impacts on the ecological balance and health of estuaries. Changes in freshwater inputs can disrupt delicate balances of the salinity gradient, nutrient cycling, and overall ecosystem function within estuaries, leading to shifts in species composition, habitat degradation, and loss of biodiversity [3]. Estuaries are affected by incomes of anthropogenic biogenic elements and organic matter. Estuaries, as sensitive and valuable ecosystems, are facing a myriad of environmental problems, primarily due to organic pollutants that are being discharged into them on a daily basis [4]. There is alarming amount of wastewater, along with plastic waste and pollutants they may carry, being emptied into South African estuaries. This has significantly increased pollution pressure in these regions, particularly in cool temperate and subtropical areas where the largest volumes of wastewater are being discharged. The use of persistent organic pollutants (POPs) in South Africa poses a significant threat to the health of estuarine ecosystems and the organisms that inhabit them [4]. Turbidity significantly influences on estuarine ecosystems. The research of the Pearl River Estuary during the 2020 dry season revealed distribution of the suspended particulate matter (SPM) [5]. River discharge emerges as a key driver influencing the distribution of SPM, with elevated concentrations observed during periods of increased freshwater input. Moreover, seawater intrusion exerts its own influence on SPM levels, underscoring the intricate interplay between riverine and marine factors in shaping suspended particle dynamics within estuarine environments [5]. Earth remote sensing can be used for turbidity evaluation. Thus, a new algorithm to the evaluation is used in the highly turbid Guadalquivir estuary using Sentinel-2 satellite data [6]. The results showed correlation between the satellite-derived turbidity and in situ measurements, indicating the algorithm's effectiveness in monitoring and assessing turbidity in the estuary. The focused attention to estuarine ecosystems requires wide usage of computer simulation. We can point at a number of such researches. A simulation model provides a comprehensive analysis of the dynamics within salt-plug estuaries, particularly focusing on the interplay between density gradients and tidal forcings [7]. It highlights the presence of positive longitudinal estuarine circulation landward of the salinity maximum zone, with an inverse circulation cell seaward of it. There is an ecosystem model for size-structured phytoplankton dynamics in coastal bays [8]. The model includes state variables: major inorganic nutrients, size classes of phytoplankton, zooplankton, and organic matters. The model was integrated with STELLA 7.0 using Runge-Kutta method to study phytoplankton dynamics in the pelagic coastal ecosystem. A model-based assessment approach for evaluating the health of estuary ecosystems was applied on the Richibucto estuary (Canada) as a case study [9]. The assessment method, termed Latent Health Factor Index (LHFI), integrates various health metrics and environmental covariates into hierarchical generalized linear mixed models. A

computational scheme has been developed and tested to simulate property exchange by advection and dispersion in estuaries at time and space scale that are well suited to ecological and management simulations, but are coarse relative to the demands of physical hydrodynamic models [10]. In addition, there is such direction, as trophic state simulation. For example, the results of the trophic model for the Cross River estuary (Nigeria) reveal Ecotrophic Efficiency (EE) values, with the highest found in species like bonga shad and Macrobrachium spp., indicating high exploitation rates [11]. The Tagus Estuary in Portugal is a complex ecosystem where fresh water from rivers meets the saltwater ocean. The estuary provides valuable services like filtering pollutants and supporting marine life. However, human activities are putting a strain on the estuary. Scientists use computer models to simulate how the estuary works. These models can help predict how the estuary will respond to future changes, like increased pollution or climate change. This information can be used to make decisions about how to manage the estuary in a sustainable way [12]. Estuarine systems are among the most valuable and endangered ecosystems in the world. The main threats to estuaries include discharges of pollutants and nutrients that degrade water quality, as well as changes in geomorphology (for example, dredging of canals, construction of dams and hydraulic structures). These changes directly affect hydrodynamic conditions (for example, flow velocity, flooding pattern, residence time, salinity penetration), posing a threat to numerous species that may be unable to adapt to survive in various conditions. The rapid degradation of estuarine ecosystems highlights the need to develop and implement comprehensive and intensive monitoring methods and tools capable of predicting them natural evolution, as well as to assess the consequences of the aggravation of climatic and anthropogenic threats. The above-mentioned processes are researched by computer simulation [13]. A 3D coupled hydrodynamic-ecological model “Production and Destruction of Organic Matter Model” was applied to the whole Baltic Sea and the subregion of the Gulf of Gdansk. It describes nutrient cycles (phosphorus, nitrogen, silicon) through the food web with 15 state variables, oxygen conditions and the parameterization of water-sediment interactions [14]. The Neva Bay is a true estuary for the reason that traces of an ancient riverbed was found on the bottom. However, there are differences with majority of estuaries. Thus, the majority is characterized by periodical tides. The factor does not affect the Neva Bay ecosystem. It was impacted by non-periodical floods because of a long anemobaric wave from the Baltic Sea. After 2011, Saint Petersburg Dam protects the ecosystem and St. Petersburg against the floods. The majority of estuaries are zones of river fresh and marine saline waters interflow. The Neva Bay is practically fresh water area.

MATERIALS AND METHODS

Special aspects of the Neva Bay ecosystem functioning have been examined by means computer simulation. We used the zero-dimensional model of a flowing water area ecosystem, which was realized by Assoc. Prof. Dr. Victor Tretyakov as the computer program “EVTOX” [15]. The research essence consists in comparison results of the numerical experiments with the model without and with substances income from the unaccounted catchment areas into the Neva Bay. The Nash–Sutcliffe criterion modification was applied for the results difference evaluation [15]. The generalized annual dynamics of the simulated ecosystem components in the Neva River and the river run-off, and the water temperature in the Neva Bay were determined on the base of

data of Northern-Western Department of Hydrometeorology and Environmental monitoring. The components annual dynamics in the stream flow from the unaccounted watersheds and the total run-off from the watersheds were also calculated on the base of the data according to the methodology, which was presented at Conference SGEM Vienna GREEN 2023 “GREEN Science for GREEN Life” [16].

RESULTS

The generalized annual dynamics of the nitrogen and phosphorus inflow into the Neva Bay according to the research results are demonstrated in figures 1 and 2.

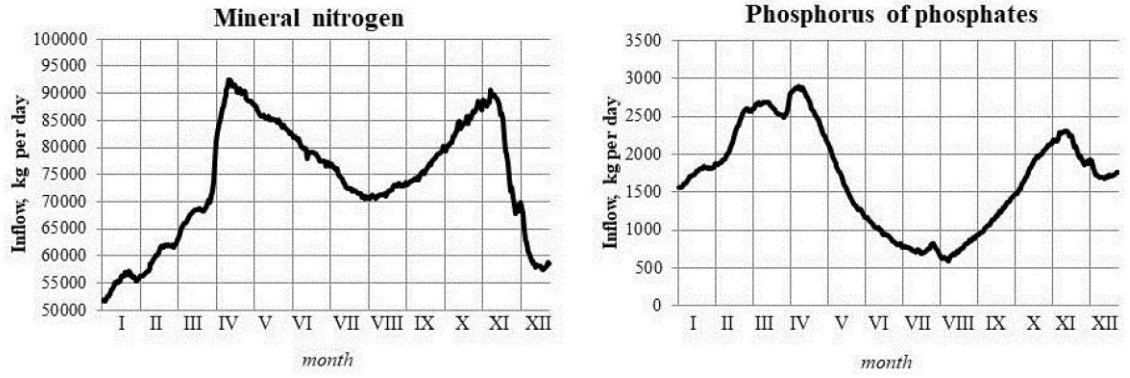


Fig. 1. The generalized annual dynamics of the nitrogen and phosphorus inflow with the Neva River runoff

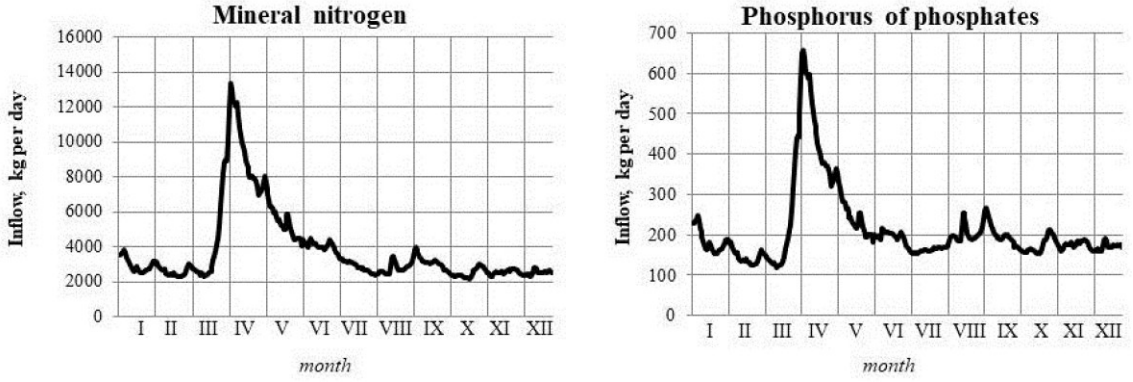


Fig. 2. The generalized annual dynamics of the nitrogen and phosphorus inflow from the Neva Bay catchment area

The figures show that the spring peaks of the substances inflow with the Neva River runoff and from the Neva Bay watershed coincide. The average share of the annual water inflow into the Neva Bay with the Neva River runoff is greater than 99% of the total water inflow into the water area. Concentrations of the nitrogen and phosphorus compounds in the outflow from the Neva Bay catchment area are significantly greater ones in the Neva River runoff. Thus, the phosphates concentration in the outflow from the Neva Bay watershed is greater than one in the Neva River runoff at average more than in 26 times. Nevertheless, average increase of the mineral phosphorus concentration in the common inflow into the Neva Bay compared to one in the Neva

River runoff is equal to 13.7%. According to the computer simulation the additional inflow of the substances into the Neva Bay ecosystem influences over the ecosystem functioning. Thus, there is some increase of the plankton biomass. The increase of the diatoms increase average annual biomass is equal to 42.5%. The analogous increase of the blue-green algae is equal to 11.0%, and one of the remaining phytoplankton biomass is equal to 2.4%. The modified Nash–Sutcliffe criterion also demonstrates changes of the ecosystem functioning. Thus, it is revealed significant difference between the annual dynamics of the diatoms biomasses in the numerical computer experiments with and without simulation of the Neva Bay catchment area impact. Otherwise, the criterion shows negligible differences between the annual dynamics of the biomasses of the blue-green algae and the remaining phytoplankton. Annual dynamics of the phytoplankton primary production intensity also demonstrates significant difference of the temporal variability of the parameter in the numerical experiments with and without the catchment area influence only for the diatoms.

DISCUSSION

Of course, the obtained results are ones of the computer simulation rather than results of field survey. However, the catchment area influence on the Neva Bay ecosystem may be really greater due to increasing urbanization of the Neva Bay watershed.

CONCLUSION

It is evident that there is significant influence of the Neva Bay catchment area on the water area ecosystem functioning. Therefore, precise determination and forecasting of the Neva Bay ecosystem trophic and ecological state demands to take into account the nitrogen and phosphorus inflow into the ecosystem from the watershed. Any aquatic ecosystem adapted to some amounts of the biogenic elements. The adaptations demand long temporal periods with the duration of hundreds or even thousands years. Although the Baltic Sea anthropogenic eutrophication began only in the second half of the twentieth century, we cannot say that before the period the biogenic elements income into the Baltic Sea was suitable to the outflow from natural watersheds because the sea catchment area was for a long time used for agriculture. However, the old growth of the biogenic elements income was very slow, and the sea ecosystems had enough time for the adaptation. Otherwise, abrupt growth of the biogenic elements income leads to the aquatic ecosystems destruction. Determination of level of the biogenic elements income, which corresponds the former stable state of an aquatic ecosystem can be made with computer simulation of the biogenic elements outflow from various catchment areas and calculation of the biogenic elements unit discharges. The results of the determination define objectively value of the necessary decrease of the biogenic elements income. Thus, the Neva Bay has four sources of the biogenic elements income. They are: 1) income with the Neva River and its spill streams runoff, 2) the outflow from the municipal sewage treatment plants, 3) the outflow from the partial catchment areas, 4) income with the atmospheric precipitation. The sources have the following proportion of the amounts for 1979-2022: 1) the incomes with the runoff are equal to 86% of the summarized income of the total nitrogen and 72% of the total phosphorus one, 2) the outflows from the plants are equal to 10% of the total nitrogen summarized income and 22% of the total phosphorus one, 3) the outflows from the partial watersheds are in 3% of the total nitrogen income and 4% of the total phosphorus one, 4) and the incomes with the atmospheric precipitation are only in 1% of the total nitrogen income and 2%

of the total phosphorus one. Transformation of the biogenic elements from organic matter into mineral substances in the municipal sewage treatment plants intensifies the anthropogenic eutrophication. Therefore, for the process prevention it is necessary full taking out of the biogenic elements from the sewages, and disposability of the substances in landfills.

ACKNOWLEDGEMENTS

The research was funded by Russian Science Fund, grant No 23-27-10011, and by Saint Petersburg Science Fund.

REFERENCES

[1] Pein J. et al., Nitrogen cycling in the Elbe estuary from a joint 3D-modelling and observational perspective, Biogeosciences Discussions, Germany, pp 1-34, 2019, DOI: 10.5194/bg-2019-265

[2] Zhang B. et al., Variation characteristics of ocean sediment Fe levels and their relationship with grain sizes in culture areas over a long period, Helgoland Marine Research, Germany, vol. 75/issue 9, pp 1-34, 2021, DOI: 10.1186/s10152-021-00554-z

[3] Adams J., Determination and implementation of environmental water requirements for estuaries, Ramsar Technical Report No. 9 / CBD Technical Series No. 69, Switzerland/Canada, 2012, https://www.researchgate.net/publication/270573861_Determination_and_implementation_of_environmental_water_requirements_for_estuaries

[4] Olisah C., Adams J.B., Rubidge G., The state of persistent organic pollutants in South African estuaries: A review of environmental exposure and sources, Ecotoxicology and Environmental Safety, Great Britain, vol. 219, art. 112316, 2021, DOI: 10.1016/j.ecoenv.2021.112316

[5] Deng L. et al., Vertical distribution of suspended particulate matter and its response to river discharge and seawater intrusion: a case study in the Pearl River Estuary during the 2020 dry season, Frontiers in Marine Science, France, vol. 10:1239649, pp 01-12, 2023, DOI: 10.3389/fmars.2023.1239649

[6] Chowdhury M. et al., Monitoring turbidity in a highly variable estuary using Sentinel 2-A/B for ecosystem management applications, Frontiers in Marine Science, France, vol. 10:1186441, pp 01-15, 2023, DOI: 10.3389/fmars.2023.1186441

[7] Hosseini S.T. et al., Longitudinal and lateral circulation and tidal impacts in salt-plug estuaries, Frontiers in Marine Science, Portugal, vol. 10:1152625, pp 01-20, 2023, DOI: 10.3389/fmars.2023.1152625

[8] Bach Q.D., Dynamical estuarine ecosystem modeling of phytoplankton size structure using STELLA, Vietnam Journal of Hydrometeorology, Vietnam, vol. 02, pp 35-44, 2019, DOI: 10.36335/VNJHM.2019(2).35-44

[9] Chiu G.S., Wu M.A., Lu L., Model-Based Assessment of Estuary Ecosystem Health Using the Latent Health Factor Index, with Application to the Richibucto Estuary, PLoS ONE, International, vol. 8(6), art. e65697, pp 1-12, 2013, DOI: 10.1371/journal.pone.0065697

[10] Kremer J.N. et al., Simulating property exchange in estuarine ecosystem models at ecologically appropriate scales, Ecological Modelling, France, issue 221, pp 1080-1088, 2010, DOI: 10.1016/j.ecolmodel.2009.12.014

[11] Otogo G.A., Enin U.I., Ndome C.B., Trophic modelling of the Cross River Estuary, Nigeria, Journal of Marine Science Research and Oceanography, International, vol. 6, issue 1, pp 01-18, 2023, DOI: 10.33140/JMSRO, ISSN: 2642-9020

[12] Vaz N. et al., The Tagus Estuary as a numerical modeling test bed: A review, Geosciences, France, vol. 10(1), issue 4, pp 01-21, 2020,
DOI: 10.3390/geosciences10010004

[13] Lopes C.L. et al., Advances in monitoring and modelling spatial and temporal dynamics of estuarine ecosystems, Frontiers in Marine Science, Australia, vol. 11:1367378, pp 01-03, 2024, DOI: 10.3389/fmars.2024.1367378

[14] Ołdakowski B. et al., Ecohydrodynamic model of the Baltic Sea. Part 1. Description of the ProDeMo model, Oceanologia, Poland, vol. 47 (4), pp 477–516, 2005, http://www.iopan.gda.pl/oceanologia/

[15] Tretyakov V., Dmitriev V., Sergeev Y., Kulesh V., Monitoring of an aquatic ecosystem ecological status and assessment of its resistance to anthropogenic impacts by results of simulation, 19th International multidisciplinary scientific geoconference SGEM2019/Conference Proceedings. Volume 19. Ecology, economics, education and legislation. Issue 5.1. Ecology and environmental protection, Albena, Bulgaria, pp 485-492, 2019. DOI: 10.5593/sgem2019/5.1

[16] Tretyakov V., Klubov S., Dmitriev V., Nikulina A., Methodology of total phosphorus and nitrogen outflow unit discharges evaluation for watersheds without monitoring points, 23rd International multidisciplinary scientific geoconference SGEM 2023. Conference proceedings of selected papers. Water resources. Forest, Marine and Ocean Ecosystems. Volume 23. Issue: 3.2. DOI: 10.5593/sgem2023V/3.2/s12.20